PNC TN941 85-56
~~PNC SN941 85-56~~

~~NOT FOR PUBLICATION~~

Sodium Boiling Experiments at Decay Power Levels (4)

Summary Assessment of the Low-Flow and Low-Heat-Flux Sodium Boiling Experiments at PNC

本資料はH13年8月16日付けで
登録区分変更する。
大洗工学センター管理部技術情報室

No.
60.6.17

March, 1985

OARAI ENGINEERING CENTER
POWER REACTOR AND NUCLEAR FUEL DEVELOPMENT CORPORATION

本資料の全部または一部を複写・複製・転載する場合は、下記にお問い合わせください。

〒319-1184　茨城県那珂郡東海村大字村松4番地49
核燃料サイクル開発機構
技術展開部　技術協力課

Inquiries about copyright and reproduction should be addressed to:
Technical Cooperation Section,
Technology Management Division,
Japan Nuclear Cycle Development Institute
4-49 Muramatsu, Tokai-mura, Naka-gun, Ibaraki, 319-1184
Japan

© 核燃料サイクル開発機構 (Japan Nuclear Cycle Development Institute)

of

登録区分
91. 8. 16
変更表示

~~配 布 限 定~~
PNC TN941 85-56
~~PNC SN941 85-56~~

1985 年 3 月

崩壊熱沸騰試験（4）

動燃における低流量・低熱流束ナトリウム沸騰試験の総合評価

山口勝久*, 磯崎 正*, 青木忠雄*

要 旨

崩壊熱沸騰試験は，高速炉の配管破損事故や崩壊熱除去系機能喪失事故などを想定した場合に問題となる沸騰による炉心燃料集合体の除熱に関して，実験的に検討することを目的としている。試験に先立ち，低流量時の沸騰事象の推移を評価するにあたって補強すべき情報の摘出を行った。崩壊熱沸騰試験に関係深い既存の試験として，SIENA装置で実施された一連の低熱流束・低流量試験をとり上げ，特に除熱限界（ドライアウト）データの整理という観点で総合評価を行った。評価に当っては，既在の水に関する知識も参考にした。主要な結果は以下の通りである。

(1) 比較的高流量で再現される環状流流動様式でのドライアウトは熱流束に依存せず，出口クォリティ＝0.5というクライテリヤで良く説明できる。

(2) 低流量になると，熱出力／流量のミスマッチが増加しても，不安定な流動振動と気泡の拡大・縮小を繰返すスラグ流流動様式が持続され，除熱能力は周囲のヒートシンクに助けられ，飛躍的に向上する。

環状流でのドライアウト・クォリティのデータ傾向は，水のデータと酷似しており，その知識の外挿から，流動様式が環状流となるなら従来のドライアウト評価方法は妥当であろうと結論できる。したがって，今後の試験では流動様式を支配する要因の調査，および除熱性能の劣る環状流での除熱限界の追加調査に重点を置くべきといえる。

* 大洗工学センター，高速炉安全工学部，高速炉工学室

登録区分
01. 8. 16
変更表示

PNC TN941 85-56
~~NOT FOR PUBLICATION~~
~~PNC SN941 85-56~~
Mar. 1985

SODIUM BOILING EXPERIMENTS AT DECAY POWER LEVELS (4)

Summary Assessment of the Low-Flow and Low-Heat-Flux Sodium Boiling Experiments at PNC

K. Yamaguchi*, T. Isozaki* and T. Aoki*

Abstract

The objective of the Sodium Boiling Experiments at Decay Power Levels is to examine the heat removal capability of reactor fuel subassemblies under sodium boiling condition, which is a matter of arguments in analyzing the accidents like the loss of piping integrity and the loss of shutdown heat removal system. Prior to progressing the test program, a survey study was conducted to fix the scope within which an advanced investigation should be required to analyze the event sequence following after sodium boiling at low flow. The study focused on the results of the past low-flow and low-heat-flux boiling tests performed with the SIENA Facility, with special attension to summarizing the critical (dryout) conditions of the two-phase flow heat transfer. The corresponding data for water cases were also examined. The topical results are as follows:

(1) The dryout phenomenon reproducible under annular flow condition at relatively high flow is well predicted to occur by the criterion that the exit quality equals to 0.5.

(2) Even if the mismatching ratio of power to flow is increased at low flow range, the slug flow pattern is sustained, repeating the void expansion and contraction synchronized with the unstable flow oscillation. In this case, the extra-superior heat removal capability is expected due to strong heat sink around the voided region.

The tendencies of the dryout quality data at annular flow on several parameters are resembled to those of water data, from which one can reach the conclusion that the dryout criterion confirmed here would be reasonable for the sodium flow cases. The forthcoming experiment should be, therefore, concentrated on examining the factors influential to the flow pattern transition and on generalizing the dryout data base at annular flow having less coolable nature.

---

* Reactor Engineering Section, FBR Safety Engineering Division, O-arai Engineering Center, Power Reactor and Nuclear Fuel Development Corporation.

CONTENTS

LIST OF TABLES

LIST OF FIGURES

NOMENCLATURES

A	:	flow area
c_p	:	specific heat at constant pressure
d	:	pin diameter
d_h	:	equivalent diameter
E_b	:	imaginary deposition rate of entrained droplets to compensate for the lack of deposition rate under the presence of counter current film evaporation
E_d	:	deposition rate of entrained droplets in the absence of film evaporation
E_e	:	entrainment generation rate
E_v	:	evaporation rate of liquid film
G_e	:	total mass flow rate of entrainment
G_f	:	total mass flow rate of liquid film
G_o	:	total mass flow rate of coolant
p	:	pin pitch
P	:	pressure
r	:	radial distance
q''	:	heat flux
t	:	time
T	:	temperature
U_o	:	inlet velocity
x	:	quality
z	:	axial distance from the upper end of heated section
α	:	void fraction
ρ	:	density
λ	:	heat conductivity

Subscripts

in	:	inlet
out	:	outlet
exit	:	upper end of heated section
max	:	maximum
cr	:	critical
sat	:	saturation
sub	:	subcooling

1. INTRODUCTION

In the cases of Loss of Piping Integrity (LOPI) and Loss of Shutdown Heat Removal System (LSHRS) accidents in a Liquid Metal Fast Breeder Reactor (LMFBR), the process of decay heat removal may lead to sodium boiling. It has been mentioned that the low-heat-flux boiling is strongly influenced by the transient change of the buoyancy force induced by the changes of local coolant temperature and density. Also pointed out is the presence of the thermal heat conduction between adjacent coolant subchannels, which tends to homogenize flow and temperature patterns. The compounded complexities are, however, not well known from past sodium boiling experiments conducted under relatively high heat flux and high flow conditions. The sophisticated coupling between thermohydraulics within a subassembly and hydrodynamics around a primary loop is an associated important subject to be solved to account for the emergency cooling during the LOPI and LSHRS transients.

From these general needs, the Research and Development (R&D) program, "Decay Heat Sodium Boiling Test", was initiated in 1978 at the Reactor Safety Section of O-arai Engineering Center, Power Reactor and Nuclear Fuel Development Corporation (OEC/PNC). The first series experiments used a 37-pin bundle test section named "37F"[1],[2]. The complex behavior of "natural circulation" sodium boiling was examined there, including seven dryout runs. The present report is addressed to describing the results of the second series experiments conducted in 1980 with a similar 37-pin bundle test section, "37G". The main purpose of the present experiments lies in obtaining and supplementing a knowledge on the critical condition of decay heat removal by "steady-state" sodium boiling.

Besides these efforts at PNC, several experiments relevant to the low-heat-flux boiling have been carried out, such as those conducted at Oak Ridge National Laboratory (ORNL) with the Thermal-Hydraulic Out-of-Reactor Safety (THORS) and Sodium Boiling Test (SBT) facilities[3]-[8] and at Kernforschungszentrum Karlsruhe (KfK) with the Natrium Siede Kreislanf (NSK) facility[9],[10]. There existed many differences in every experimental conditions, bundle configurations, test procedures and so on (see Table 1); they naturally caused the observed dryouts to fall into rather disconnected results. However, fundamental consequences of the low-heat-flux boiling might be pictured with the results of these experiments. For instance, the PNC three natural circulation dryout runs[1],[2] showed drastic changes of flow patterns from bubble flow to slug flow and then to annular or annular-mist flow in keeping with the increase of operating power. The similar transitions of flow patterns were identified in the ORNL natural circulation boiling test with SBT facility[5],[6], where two dryout runs revealed the presence of the insecure transition phase where the dryout and rewetting were repeated in turn prior to the permanent dryouts. One data point issued from the KfK natural circulation boiling test with NSK facility[10] also implies the similar feature of the high-quality dryout.

On the other hand, the THORS facility at ORNL provided for the Loss-of-Flow (LOF) type transient sodium boiling experiments. A total of three dryout runs[3],[4] was conducted with rather high power conditions. Since dryout was reached at the end of the LOF-induced short-period transient boiling of less

than one minute each, an inevitable incoherency of the boiling behavior by the wrapper tube thermal inertia and by the other retaining traces of the flow coast seemed to force the flow pattern to remain unstable (i.e. the slug flow and/or oscillatory boiling). However, the order of the magnitudes of exit equilibrium qualities, if calculated using the mean values of oscillating variables, are close to those of the steady high-quality dryout experiments.

There is a long history of the burnout experiments in water. The effects of various parameters on the boiling crisis have been extensively discussed (11)-(16), while we cannot find so much data obtained at decay heat power levels. Even in this area, the discussion of importance must be, therefore, based on the extrapolation of the data tendencies identified at the middle power range. The extrapolation leads to the prospects that the generated decay heat must be removed by the liquid film evaporation and convective heat transfer of the vapor and droplet mixture, viz. if the liquid film vanishes completely, dryout would eventually occur. Based on this dryout model, it has been pointed out that the effective parameters on the boiling crisis are the quality (enthalpy), boiling length, flow pattern, entrainment generation rate, film thickness, vapor pressure, coolant flow rate and so on(11),(12),(16) (see Appendix A). The weak dependency on the local heat flux is worth noting for a high-quality dryout. In general, it would be too hasty to apply the conclusions obtained from water to sodium, because there is a large difference in thermal properties between these two working fluids and a distinct gap between the tested pressure and flow conditions in water and those interested in the LMFBR emergency cooling. Nevertheless, we can gain the essential knowledge of the high-quality dryout from water to achieve a better understanding of the possible correlations of dryout conditions in sodium.

Meanwhile, all the published data of critical heat flux in sodium, summarized in Table 1, can be traced against exit equilibrium qualities at the onsets of permanent dryouts(2),(4),(6),(10); the result is shown in Fig. 1. A glance at the figure reveals the insufficiency of the number of data points around the decay heat level(17) from which one can examine the similar items to those suggested for the high-quality dryout in water. Therefore, the effort of the present work was focused on obtaining dryout data as many as possible under low-heat-flux conditions covering decay heat power levels of 5 to 20 W/cm^2. The test method should be selected so that we can widely alter several operating parameters to examine the sensitivities of them on the boiling crisis. The natural circulation operation of the test facility is inadequate for this aim. Therefore, the forced convection method with very tight initial settings of the inlet valve throttlings was adopted to suppress unintentional flow acceleration by the induced buoyancy force of two-phase flow. Better simulations of the test conditions and the geometrical ones in respect to the LMFBR accidents, e.g. the simulations of pin bundle size, axial power shape, heated length and primary loop hydrodynamics, are the subjects of the forthcoming studies. Due to the technical difficulties in performing transient experiments, the present study was, in addition, restricted within the frame of steady-state boiling. Transient experiments simulating LOPI accidents like those conducted at Argonne National Laboratory (ANL) and Hanford Engineering Development Laboratory (HEDL) with in-pile Sodium Loop Safety Facility (SLSF), i.e. the test series "P1"(18)-(20) and "W1"(21)-(23) (see Appendix B), are far beyond the capability of our aged facility.

Table 1. Summary of the high-quality dryout experiments under low heat flux conditions.

Tester	Pin bundle	Heated length	Heat flux	Exit quality
PNC	37-pin wire-wrapped bundle***	450 mm	39-52 W/cm^2 (uniform)	0.6-0.7
ORNL	Tube	965 mm	17 W/cm^2 (uniform)	(1.0-1.5)*
KfK	Equivalent 37-pin bare bundle with central 24-subchannel blockage**	400 mm	12 W/cm^2	0.8
ORNL	19-pin wire-wrapped bundle	914 mm	39-92 W/cm^2 (Chopped-cosine)	0.3-0.7

* There is some uncertainty in the heat balance of the test section heated by a radiant furnace.
** Central equivalent 7 pins and outermost equivalent 6 pins are not heated.
*** One or three pins are not heated.

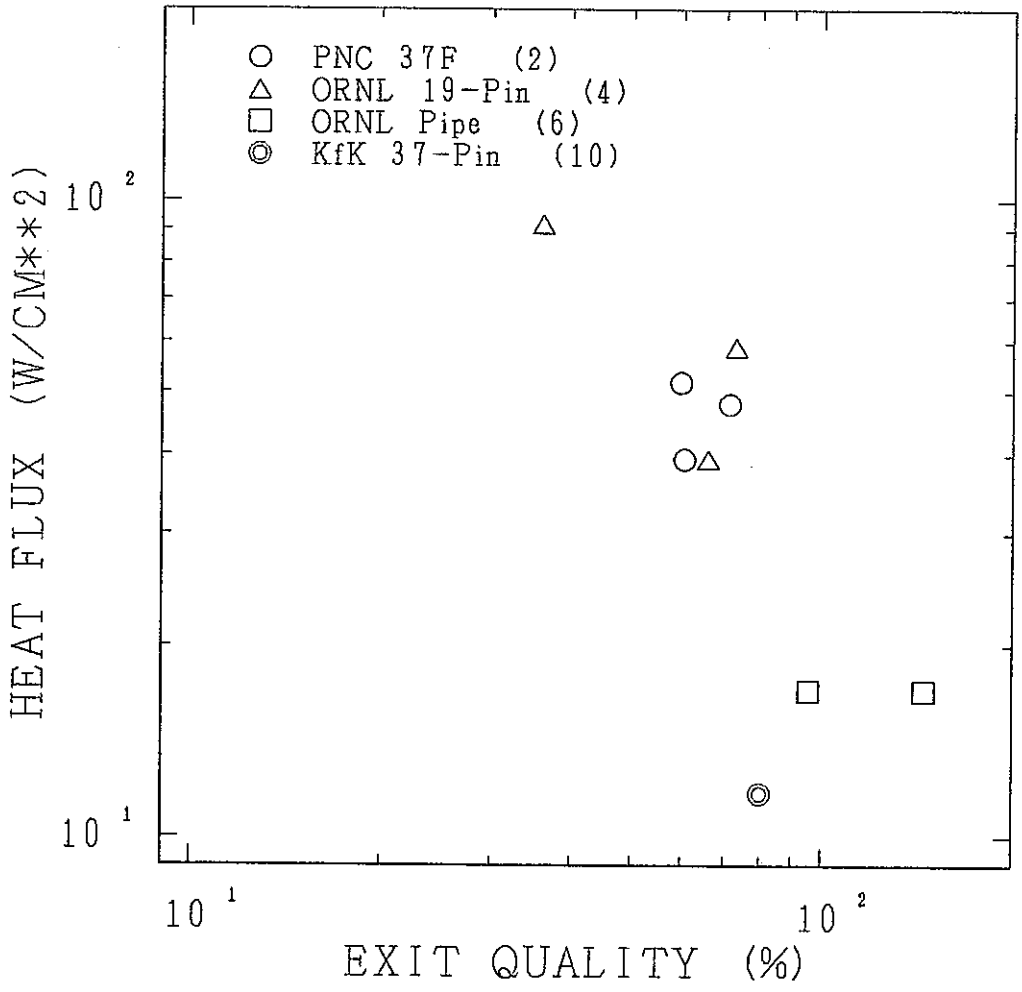

Fig. 1 High-quality dryout data under low heat flux conditions

2. SIENA FACILITY AND 37G TEST SECTION

2.1 Sodium loop

The schematic diagram of the SIENA facility is shown in Fig. 2. The present experiments were conducted with the FPL (right hand side of the illustrated diagram), in which the 37G test section was mounted on the attachment ports of the T-3 test section. The SBL is mainly used to purify the charged sodium. The plugging temperature was around 120°C. This means that the desolved O_2 concentration is around 1 ppm (by Eichelberger).

The main line of the SIENA facility which is used in the present experiments consists of two inches (2B) and three inches (3B) pipes, two tanks (expansion tank; ETK, and separator tank; STK), air cooler, pump, 37G test section, and several valves. They are shown in Fig. 3, where the pipe lengths and the elevations are also written with [mm] units. The datum plane defined for the 37G experiments is equal to the EL-6643 mm plane, which corresponds to the top plane of the heated section. The sodium driven by the main pump enters the test section, flows up through the pin bundle, being heated up to cause sodium boiling and dryout. Although the voided region can extend toward downstream unheated sections, it takes very long time for the cold sodium in the outlet piping to be replaced by the two-phase hot sodium due to nearly stagnated coolant flow. During the present experiments, the sodium temperature entering the expansion tank was always below the boiling point. The sodium coming out of the expansion tank moves to a subsequent separator tank. In the cases of gas release runs, sucked gas bubbles in sodium can be completely separated by these coupled tanks. After leaving these tanks, the sodium enthalpy is lowered, if required, by an air cooler to maintain the cold-leg sodium temperature constant.

The FPL has the other two passes from the main pump to the expansion tank, i.e. a line through the T-2 test section and a bypass line. The attachment ports of the T-2 test section are designed to have a capability of receiving only a pin bundle of size up to a 7-pin bundle. Therefore, it was not used in the present experiments, but was replaced by a 1B Sch20s (O.D. = 34.0 mm, I.D. = 28.0 mm) stainless steel (SUS-316) pipe. An auxiliary heater is in the bypass line so that the loop sodium temperature condition can be regulated prior to the experiments. During the loop operation, flow conditions through three parallel passages from main pump to expansion tank are independently controlled by throttling the inlet valves or by changing the main pump power. The layouts of these bypass lines are drawn in Fig. 4. The air cooler has its bypass line. The bypass line is often used for such experimental runs as conducted with a small amount of pin power which is well removable by the heat loss from the surfaces of pipes and plena.

The normal sodium level of the FPL is designed to be EL-9200 mm (±50 mm), while the sodium charge into the loop was frequently ceased by attaining the level of EL-9100 mm. The total sodium inventory in the dump tank is about 1,300 kg and its half amount is charged to the loop. There are two free surfaces of sodium: one is in the expansion tank and another in the separator tank. During the operation of the loop, free surfaces of sodium in these tanks are covered with the argon gas supplied through a connecting line: the separator tank is

directly connected with the expansion tank via the 6015 mm long 3B Sch20s (O.D. = 89.1 mm, I.D. = 81.1 mm) sodium line and the 2675 mm long 1B Sch20s cover gas line. At a middle point of this cover gas line (1465 mm from expansion tank and 1210 mm from separator tank), the pipe is branched and is connected with a large surge tank via the ~11.1 m long 1B Sch20s gas surge line. The vacuum and vapor trapping systems are equipped at the SBL side of this gas surge line. Besides these cover-gas lines, the FPL has a high-temperature gas supply system. It can be used to inject argon gas into the flowing sodium from the inlet piping of the test section with nearly the same gas temperature with that of sodium.

2.2 37-pin bundle test section

An LMFBR fuel subassembly was simulated by an electrically heated 37-pin bundle, 37G, illustrated in Fig. 5. The geometrical configuration is summarized in Table 2, where the scales of every items are contrasted with that of the 37F test section and the MONJU fuel subassembly. The pin bundle is installed in a hexagonal wrapper tube made of 10 mm thick Inconel-600 so that the nominal gap between the peripheral pins and the inner wrapper tube wall is 1.43 mm (it is 1.34 mm for MONJU). These subchannel characteristics are summarized in Table 3.

Figure 6 shows the pin used for the 37G test section. The heated section and the lower unheated section of all test bundles have been fabricated thus far with the universal specification, i.e. the diameter of each pin is 6.5 mm and the pin pitch of the triangularly located pins is 7.9 mm. The pin spacing specified by the pitch to diameter ratio of 1.216 is maintained by wrapping a spacer wire (SUS-316) of 1.3 mm diameter around each pin with a helical pitch of 265 mm, while it is replaced by the same diameter thermocouple for some pins. The bundle has a 450 mm length heated section, both ends of which are connected to a lower and an upper unheated sections of 248 and 849 mm long, respectively. The design of the upper unheated section is often changed for different bundles. For the 37G test bundle, 10 mm long pellets of SUS-304 are inserted in a hollow pipe located next to the heated section. There is an inert helium gas (atmospheric pressure at room temperature) in the gaps of the pipe wall and pellets.

A small plenum is attached at the bottom of the hexagonal wrapper tube of the test section. It is shown in Fig. 7. The inlet pipe is conected to it. The bottom plate of the inlet plenum serves as a flange for the pin extraction. A total of 37*2 lead wires from the pins is distributed in the electrode box which is filled with the helium gas with the pressure of about 0.15 MPa. The upper structure of the 37G test section is shown in Fig. 8. There is no bundle-exit structures at the downstream region except for a sleeve of the eddy-current flow/temperature probe of PNC Mark-II type, although a simulated neutron shield was attached to the 37F test section.

2.3 Heat balance

There is no thermal insulator around the electrode box attached to the bottom of the inlet plenum of the test section. Therefore, the heat conduction through the flange and the heat penetration across the box would be a major fraction of the heat loss from the inlet plenum. The heat loss would be up to a few kW order in magnitude, while no detailed evaluation has been conducted thus far. The inlet temperature denoted usually in this report means the sodium

temperature measured at the 285 mm upstream point from the plenum center. Hence, the sodium is cooled before entering the hexagonal test section to yield a lower inlet temperature especially for low-flow runs.

The hexagonal tube of the 37G test section is wrapped with the fine-flex (glass fiber) thermal insulator of 112 mm in outer diameter. The steady heat loss under boiling condition is roughly predicted as 0.5 $kW/m^{(2)}$. The thermal properties of the insulator and structure materials are summarized in Table 4, where T is a temperature denoted by [°C] unit.

The simulation of the transient heat sink of the wrapper tube is beyond the scope of the present experiments, because the thick wrapper tube is used to endure the severe condition of boiling experiments. One of the typical values of the maximum transient heat sink is around 5 kW/m in such a case that the temperature ramp ratio of the wrapper tube is 1 °C/s.

2.4 Instrumentation

Figures 9 and 10 show the external instruments of the test section used for the present experiments. There are four flow-meters (F-101, F-102, F-103 and F-106) in the SIENA facility, and one (F-107) at the 37G test section. Their specifications and locations are listed in Table 5. The flow-meters F-101, F-102 and F-103 (total flow, inlet flow of T-2 test section, and inlet flow of T-3 test section) are fabricated by a fabricator with a sufficient knowledge on utilization in sodium. Still, some of them are calibrated also in the SIENA facility by checking the enthalpy balance of the heated sodium flow. The F-103 signal is usually used as an inlet flow of the T-3 test section. The F-106 and F-107 are flow-meters provisionally installed. Parmanent magnets are fastened on the thin covers of the thermal insulator of inlet pipe and wrapper tube, respectively, with no pretensions to artifice.

There are four pressure sensors (P-201, P-103, P-106 and P-108) in the SIENA facility, and three (P-109, P-110 and P-111) at the 37G test section. Their specifications and locations are listed in Table 6. The P-201 signal is used as a system pressure (over-pressure of the gover-gas volume) and the P-108 signal is as an inlet pressure of the test section. The inlet pressure P-106 was not in operation during the present experiments. There are many acoustic sensors. They are used for the boiling detection.

The sodium temperature at the inlet of the test section is measured by the 3.2 mm diameter thermocouple T-003. T-003 is inserted into sodium flow through the pressure guide tube for P-106 and P-108 (see Fig. 7). It was often changed into a new one and was carefully calibrated prior to its attachment in the SIENA facility. It has been customarily used as a standard temperature throughout all experimental runs.

Five thermocouples of 1.6 mm in diameters (T-101 through T-105) monitor surface temperatures of the hexagonal wrapper tube and the inlet plenum (see Fig. 10). They are mainly used to control preheater powers added to the test section materials during the preheating operation of the SIENA facility. Hence, some of them are not connected to any data logging devices except for the power controllers.

Around 130 thermocouples are distributed at 25 horizontal planes of the test

section. The axial locations of them (and Chen-type void probes) are noted in Fig. 10 by the horizontal plane names labeled in alphabetical order. The top views of their locations at A though Y planes are illustrated in Fig. 11(a) thgough Fig. 11(i), where the definitions of sensor marks and the detailed views of their attachments are shown in Fig. 12. The number of sensors at every planes is summarized in Table 7. About 30 thermocouples are embedded in the pin claddings to measure the pin surface temperatures. Sodium temperatures are observed by about 100 thermocouples located at the subchannel centers. In the sensor allocation scheme, emphasis lies in obtaining the axial growth of boiling region during the experiment at the upper region of the heated section. In addition, the thermocouples at M plane are attached so as to measure the radial temperature distribution at the upper end of the heated section.

The outlet thermocouple T-004 whose diameter is 4.8 mm is inserted through the pressure guide tube of P-109 at a plane 50 mm downstream from the bundle exit (EL-7560 mm, z = 917 mm). It is illustrated in Fig. 8. Three thermocouples of 0.3 mm in diameters are fastened on the sheath of T-004 in a manner that the hot junctions are located at an upstream plane by 1 mm from the T-004 surface. So, the precise elevations of T-004 and the fine thermocouples T-014, T-024 and T-034 in order from the center zone to the outer zone differs by 3.4 mm.

There are 19 Chen-type void probes in the bundle. They also serve as spacer wires. The sensitive part against void attack (top end of the probe) is lifted up by around 1.3 mm to catch the flowing bubbles (see Fig. 12). The void attack can be detected by an on/off singnal superposed on a temperature drift component. From this signal, the time averaged void fraction can be estimated roughly as shown in Appendix C.

There are about 20 pairs of void taps on the wrapper tube surfaces. The layout of them is illustrated in Fig. 10. One pair is made of two taps located at 0° and 180° directions (the definition of the angle is shown in the same figure). To measure the axial voltage drop between two tap-planes, a constant electrical current of about 45 A is supplied between two electrods located at the 50 mm upstream and downstream planes from the first and last planes for tap mounting, respectively. After completing the experiments, the time series data of the voltage drops between arbitrary two pairs of void taps are analyzed to yield qualitative data of volume averaged void fractions between two planes distinguished by the void taps.

The pin power can be supplied by two DC power supplies. They are customarily called as the SBL and FPL power supplies. The heat flux of the heater pin is estimated from the readings of the voltage and current meters of the power supply, whose accuracies are around ±1 %. The time series signal of the current meter is available. It gives the timing sequence of power changes. The transient change of temperatures forced the pin power to fall gradually keeping with the increasing electrical resistance of the heater element (tantal), viz. the power supplies used were of voltage stabilization type. The actual pin power shape can be estimated by the empirical method shown in Appendix D. In general, the axial power shape becomes a trapezoidal form whose maximum point is located at the top end of the heated section. The transient change of radial power shape was not known precisely, because the electrical current fed to each pin was not measured. The uniform profile of the radial power shape is assumed in the present study.

2.5 Data acquisition

A grobal view of the SIENA data acquisition system is shown in Fig. 13. Around 200 signals are gathered from the SIENA facility and the 37G test section by case-by-case manners. Some of them required for the plant operation are directly connected to the wide-use pen recorders, indicators and micellaneous plant control devices.

As a main force of the data acquisition system, a digital data logger, the HP-2116C computer system, is used. As shown in Fig. 14, the HP-2116C system is made of double multiplexers, a 12-bit AD converter, a mini-computer HP-2116C, and an MT device. The signals of 128 channels are chosen from the board of (128 + 6) inputs. The gain of each channel is separately fixed by a data logging program. The recording density of the produced MT is 800 bpi at first. Then the data set is condensed into a 1600 bpi MT by the other computer system (FACOM M-190/200) together with the file and sensor information required for the data reproduction.

The other devices, such as the YODAC, pen recorders and so on, back up mainly the insufficient capability of the channel numbers of HP-2116C system. Among all, the YODAC, a low-speed multi-channel digital data sampler and printer, play an important role in obtaining the sensor information required for the reduction of the HP-2116C data, viz. the gain accuracies and offset values of flow and temperature signals are carefully checked with the YODAC calibration data to recover the grade of the measured data by the HP-2116C system even if the measurement circuits fall in mismatching situations by a certain bad device coupled in the signal branch network. The sensor selection scheme of the HP-2116C system is, in general, modified prior to each SIENA operation, where the serial SIENA operation number in which the present experiments are included are 139 through 146. An example of the list of the selected signals and their information is shown in Table 8. Only the monitor recorders mounted on the control pannels of the SIENA facility have fixed signal wirings.

The timing sequence of the data loggings is shown in Fig. 15. The monitor recorders are continuously running during the SIENA operation. YODAC samples the initial data only once before starting the HP-2116C system and performing the test.

2.6 Accuracies of the data

F-103 has been treated as a standard flow-meter. The unit conversion factor and the gain accuracy of F-103 are evaluated as 7.843E+2 (m/s)/(V) and ±0.002 m/s, respectively. The other flow-meters were calibrated by the relative check method: The output signals from F-101, F-106 and F-107 were compared with that from F-103 under single-phase flow condition to obtain the sensitivity curves against flow rate. The results are shown in Appendix E. It should be noted that the accuracies of F-106 and F-107 are not high enough to give quantitative results.

The pressure sensors can give plausible signals of the transient changes of static pressures. However, their base values upon which any spikes are superposed are sometimes unreliable because of the highly sensitive drifts by the inevitable temperature changes around the sensors. All of the in-bundle pressure sensors were, therefore, calibrated against the P-201 signals using the data of sequential pressure reduction runs as shown in Appendix E, where the accuracy of P-201 is evaluated as ±0.001 MPa. After fixing the gains of every

sensors, their offsets were estimated by the head calculation method, i.e. certain constant values were canceled out from the measured data so that the reference data obtained prior to the experiments under stagnated flow condition became in agreement with the calculated static heads at the sensor elevations. Naturally, this calculation may introduce small errors which are partly ascribed to the calculation errors of the reference static heads and to the inconsistency between the temperature fields attained during the calibration runs and the experimental runs. The maximum errors of P-103, P-108 and P-110 are evaluated as ±0.005 MPa. However, the outlet pressures P-109 and P-111 have unacceptable large errors caused by the temperature drift.

Most of the thermocouples are 0.3 mm in sheathed outer diameters. Their source impedances are very high (for instance, the DC resistance is around 1.7 kΩ at 900 °C level). Therefore, some confidential signal conditioners should be required to keep the thermocouples away from possible mismatchings with the HP-2116C system and the other devices having not so high input impedances. The thermocouple leads were, however, connected to plural devices without signal isolations until the 142th SIENA operation. An active circuit for a burn-out detection of heater pin fed small drain current to the thermocouple connected. The resultant voltage drop and imposed offset introduced large error for the data logging. In addition, the temperature measurement circuits had no devices to fix the cold-junctions of the thermocouples to be zero degree C, i.e. the HP-2116C system measured only the temperature difference between the truth and a certain cold-junction temperature.

Besides these insufficiencies in constructing the instrumentation system, the quality of the thermocouple fabrication becomes in question, because the thermocouples equipped are of 0.75 % class (maximum error of ±7.5 °C at 1000 °C level) and sometimes deteriorate under heavy utilization beyond allowable temperature range of about 600 °C. The integrities of the thermocouples were examined roughly by drawing the multi-channel signal traces and by finding the anomalous behavior of the failed thermocouples. When the failed thermocouples were identified by this work, subsequent data measured without noticing the deteriorations were made unavailabe by forcing the unit conversion factors of the failed thermocouples to be zero.

To solve these problems in temperature measurement, the calibration was conducted by fixing T-003 as the standard thermocouple and the others in the test section were treated as the thermocouples being tested. From the fitting equation of the data of tested thermocouple against those of the standard thermocouple, we can estimate both the degree of global mismatching and the over-all offset unique to each thermocouple tested. The results of the calibration are summarized in Appendix E. The calibration work revieled that the standard deviation of the calibration data from the fitting line was very small (±2 °C, for instance) for many thermocouples. Only small numbers of thermocouples connected to many devices at once yielded scatterings of data points around the fitting lines. The corresponding maximum error is about ±5 °C. The error of the common offset corresponding to the cold-junction temperature was not so precisely evaluated, because the practical utilization of the calibration results to the data reproduction was expected to suffice a requirement of accuracy enough to analyze the boiling data from the engineering standpoints.

2.7 Operation record

Prior to the 139th SIENA operation, the 37G test section was installed on the attachment ports of T-3 test section, and was detached after terminating the 146th operation. The low-heat-flux boiling experiments were carried out at the 139th through 145th operations. The single-phase flow tests and the LOF boiling tests were also conducted during the 139th through 141th operations and 145th through 146th operations, respectively, while they are not examined in the present study. The record of each operation is summarized as follows and is shown in detail in Appendix F.

139th operation: (Nov. 20 to Nov. 22, 1979)	• Single-phase flow runs	
	Run 37(37)H-260-10 through Run 37(37)H-100-20	... 15 cases
	Run 37(37)HA-100-25-A through Run 37(37)HA-50-25-A	... 6 cases
	• Low-heat-flux boiling runs	
	Run 37(37)LHF-200 through Run 37(37)LHF-203	... 4 cases
140th operation: (Dec. 4 to Dec. 6, 1979)	• Single-phase flow runs	
	Run 37(37)HA-260-25-A through Run 37(37)HA-260-25-C	... 3 cases
	Run 37(37)H-260-40 through Run 37(37)H-260-50	... 8 cases
	Run 37(37)HA-150-25-A through Run 37(37)HA-260-35-C	... 21 cases
	• Low-heat-flux boiling runs	
	Run 37(37)LHF-210 through Run 37(37)LHF-219	... 10 cases
141th operation: (Jan. 16 to Jan. 18, 1980)	• Single-phase flow runs	
	Run 37(37)HB-260-20 through Run 37(37)HB-260-10	... 24 cases
	• Low-heat-flux boiling runs	
	Run 37(35)LHF-220 through Run 37(35)LHF-228	... 9 cases
142th operation: (Jan. 30 to Feb. 1, 1980)	• Low-heat-flux boiling runs	
	Run 37(36)LHF-230 through Run 37(36)LHF-232	... 3 cases
	Run 37(34)LHF-233 through Run 37(34)LHF-239	... 7 cases
143th operation (Feb. 26 to Feb. 28, 1980)	• Single-phase flow runs	
	Run 37(33)NCT-1 and Run 37(33)NCT-2	... 2 cases
	• Low-heat-flux boiling runs	
	Run 37(33)LHF-240 through Run 37(33)LHF-248	... 9 cases
144th operation (Mar. 17 to Mar. 19, 1980)	• Low-heat-flux boiling runs	
	Run 37(29)LHF-250 through Run 37(29)LHF-253	... 4 cases
	• Single-phase flow runs	
	Run 37(25)H-001 through Run 37(25)H-010	... 10 cases
	Run 37(25)H-101 through Run 37(25)H-103	... 3 cases
145th operation (Apr. 8 to Apr. 10, 1808)	• Low-heat-flux boiling runs	
	Run 37(26)LHF-260 and Run 37(26)LHF-261	... 2 cases
	Run 37(24)LHF-262	... 1 case
	Run 37(20)LHF-263	... 1 case

	• LOF boiling runs	
	Run 37(20)FC-102 through Run 37(20)FC-107	... 6 cases
	Run 37(16)FC-108 and Run 37(16)FC-109	... 2 cases
146th operation (May. 7 to May. 8, 1980)	• LOF boiling run	
	Run 37(11)FC-111	... 1 case

The low-heat-flux boiling experiments were carried out sequentially by changing the flow and pin power conditions in turn with an appropriate time intervals required to attain steady conditions in every steps. The main line of the loop was used with relatively high sodium temperature levels. After observing sodium boiling, the power supplies were cut off by either a manual or an auto-scram method to terminate each run. The total number of the 37G low-heat-flux boiling runs is 50. Depressurization boiling runs were conducted several times. The over-pressure of the cover gas volume of FPL was reduced by combining the gas line with the gas surge volume in SBL which was preparatively exhausted to nearly 0 MPa.

Earlier runs were conducted successfully under favorable condition where all pins were integral. However, the electrical insulators of the heater pins became deteriorated as the boiling runs were repeated many times. The failed pins were disconnected from the power supplies to carry out the subsequent runs with residual pins being heated. The change of the heating patterns of the 37G bundle is shown in Fig. 16.

Table 2. Summary of the test section geometries

Item	unit	37G test section	37F test section	MONJU assembly
Number of pins	--	37	37	169
Diameter of pins	mm	6.5	6.5	6.5
Pin pitch	mm	7.9	7.9	7.87
Total length of pins	mm	1749	1515	2818
Length of unheated entrance region	mm	248	148	398
Heated length	mm	450	450	930
Length of unheated downstream region	mm	849	715	1490
Heat flux	W/cm^2	(max. 250)	(max. 250)	av. 101.9 max. 176.0
Heat flux profile	--	(flat)	(flat)	(chopped-cosine)
Material of cladding	--	SUS-316	SUS-316	SUS-316
Thickness of cladding	mm	0.55	0.55	0.47
Diameter of wire spacer	mm	1.3	1.3	1.32
Helical pitch of wire spacer	mm	265	265	307
Cross sectional flow area	mm^2	924	924	3636
Equivalent hydraulic diameter	mm	3.43	3.43	3.22
Hexcan inner flat-to-flat distance	mm	50.4	50.4	104.6
Thickness of hexcan	mm	10	10	3
Material of hexcan	--	Inconel-600	Inconel-600	SUS-316
Gap between outermost pins and inner wall of hexcan	mm	1.43	1.43	1.34

Table 3. Summary of the subchannel specifications

Item	37G & 37F bundles			MONJU fuel assembly		
	central	edge	corner	central	edge	corner
Flow area without spacer wire mm^2	10.43	20.54	7.22	10.23	19.53	6.63
Cross section of spacer wire mm^2	1.33			1.37		
Flow area mm^2 (fraction of spacer wire)	9.77 (1/2)	19.88 (1/2)	7.00 (1/6)	9.55 (1/2)	18.85 (1/2)	6.40 (1/6)
Wetted perimeter mm (fraction of spacer wire)	12.25 (1/2)	20.15 (1/2)	9.51 (1/6)	12.28 (1/2)	20.15 (1/2)	9.39 (1/6)
Heated perimeter mm	10.21	10.21	3.40	10.21	10.21	3.40
Hydraulic diameter mm	3.19	3.95	2.94	3.11	3.74	2.73
Heated perimeter/flow area mm^{-1}	1.05	0.51	0.49	1.07	0.54	0.53

Table 4 Thermal properties of the insulator and structure materials

item	material	note
density (kg/m^3)	fine-flex	50
	sodium	$950.1 - 0.22976\ T - 1.46E\text{-}5\ T^2 + 5.638E\text{-}9\ T^3$
	SUS-316	7820
	Inconel-600	8430
	BN	1800 ~ 1870 (av. 1850)
thermal conduc. ($W/m°C$)	fine-flex	$0.051 + 0.00014\ T$
	sodium	$93.979 - 3.25E\text{-}2(1.8T+32) + 3.619E\text{-}6(1.8T+32)^2$
	SUS-316	16.25 at 100 °C, 21.44 at 500 °C
	Inconel-600	$17.5 + 1.4876E\text{-}2\ T + 6.1227E\text{-}6\ T^2$
	BN	8.37 ($\pm$0.3) at 600 ~ 800 °C
specific heat ($kJ/kg°C$)	fine-flex	0.84
	sodium	1.256
	SUS-316	0.502
	Inconel-600	$0.435 + 2.937E\text{-}4\ T - 1.589E\text{-}7\ T^2$
	BN	1.85 at 727 °C, 2.10 at 1727 °C

Note: The properties of boron-nitride (BN) are actually measured ones under the same condition with that used in the heater pins.

Table 5 Specifications and locations of the flow-meters attached to the SIENA facility

name	object	maximum flow rate (l/min)	location		
			component	EL (mm)	note
F-101	total	400	pump exit	4232	see Fig. 3
F-102	bypass	100	T-2 inlet	4737	see Fig. 4
F-103	inlet	400	T-3 inlet	5875	see Fig. 3
F-106	inlet	400	T-3 inlet	5932	500 mm upstream from the inlet plenum
F-107	outlet	400	37G bundle	7143	z = 500 mm

Table 6 Specifications and locations of the pressure transducers attached to the SIENA facility

name	object	span (kgf/cm^2g)	location		
			component	EL (mm)	note
P-201	gas	-1 to 2	ETK	(9100)	
P-103	sodium	-1 to 5	pump exit	4203	660 mm downstream from the pump
P-106	sodium	-1 to 9	T-3 inlet	5938	see Fig. 7, item [18]
P-108	sodium	-1 to 13	T-3 inlet	5938	see Fig. 7, item [18]
P-109	sodium	-1 to 13	37G bundle	7560	z = 917 mm
P-110	sodium	-1 to 6	37G bundle	6118	z = -525 mm
P-111	sodium	-1 to 6	37G bundle	7410	z = 767 mm

Table 7 Summary of the locations and numbers of in-bundle sensors

plane			thermocouple			void probe
name	z (mm)	θ_w (deg)	sodium area	pin surface	wrapper tube	
A	-507.3	180	1	0	0	0
B	-397.8	120	4	0	0	0
C	-353.6	60	3	0	1	0
D	-309.4	0	4	0	0	0
E	-243.1	270	4	0	0	0
F	-154.7	150	4	0	1	0
G	-132.6	120	4	0	0	0
H	-110.5	90	4	0	0	0
I	-88.4	60	4	0	0	0
J	-66.3	30	4	0	0	0
K	-44.2	0	4	1	0	3
L	-22.1	330	4	1	0	4
M	0	300	4	31	1	4
N	22.1	270	4	1	0	4
O	44.2	240	4	0	0	4
P	66.3	210	4	0	0	0
Q	88.4	180	4	0	0	0
R	110.5	150	4	0	0	0
S	132.6	120	4	0	0	0
T	154.7	90	4	0	0	0
U	176.8	60	4	0	0	0
V	198.9	30	4	0	0	0
W	221.0	0	4	0	0	0
X	243.1	330	4	0	1	0
Y	839.8	240	2	0	0	0
total			94	34	4	19

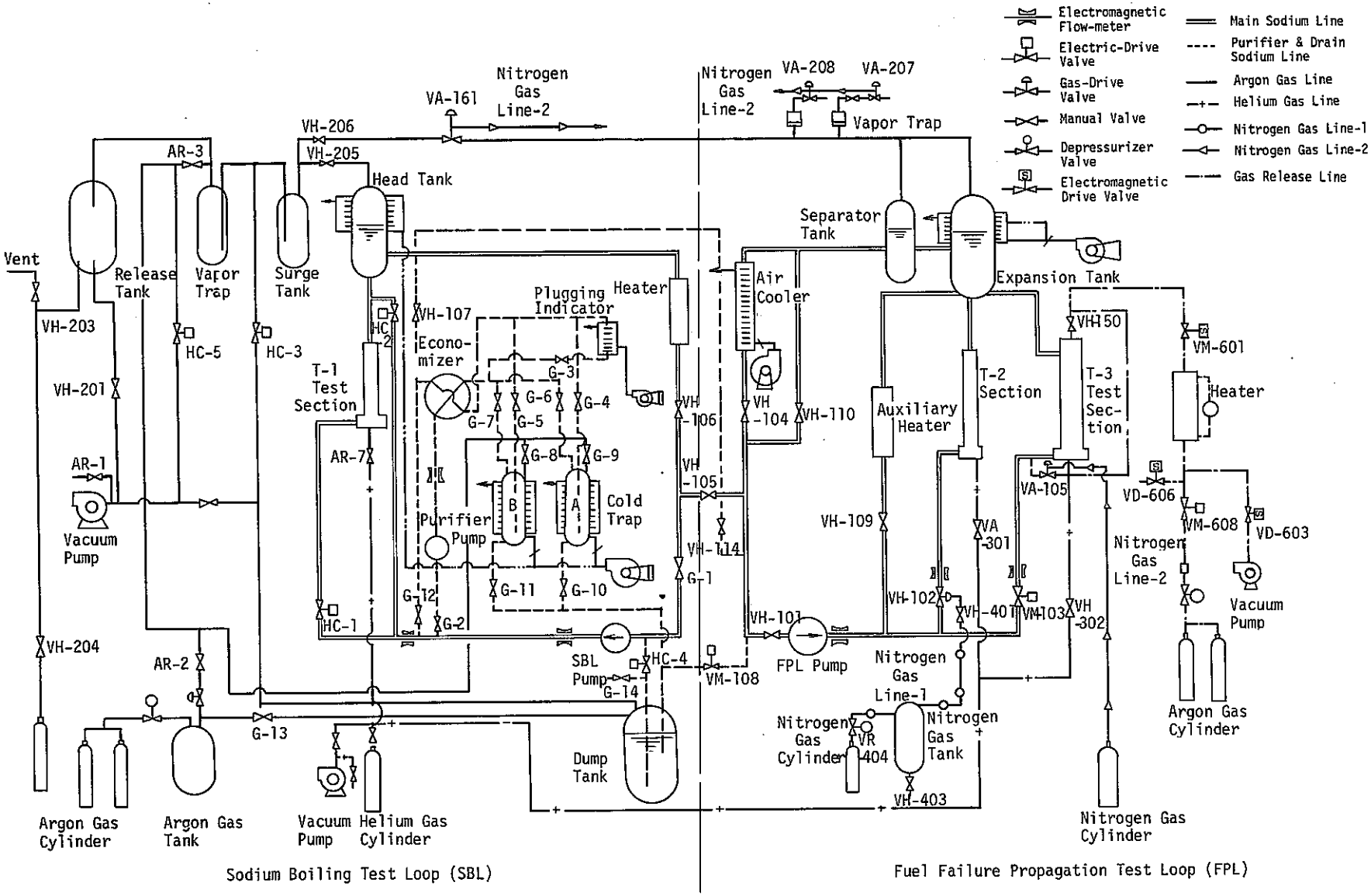

Fig. 2 Schematic diagram of the Sodium Boiling and Fuel Failure Propagation Test Facility, SIENA

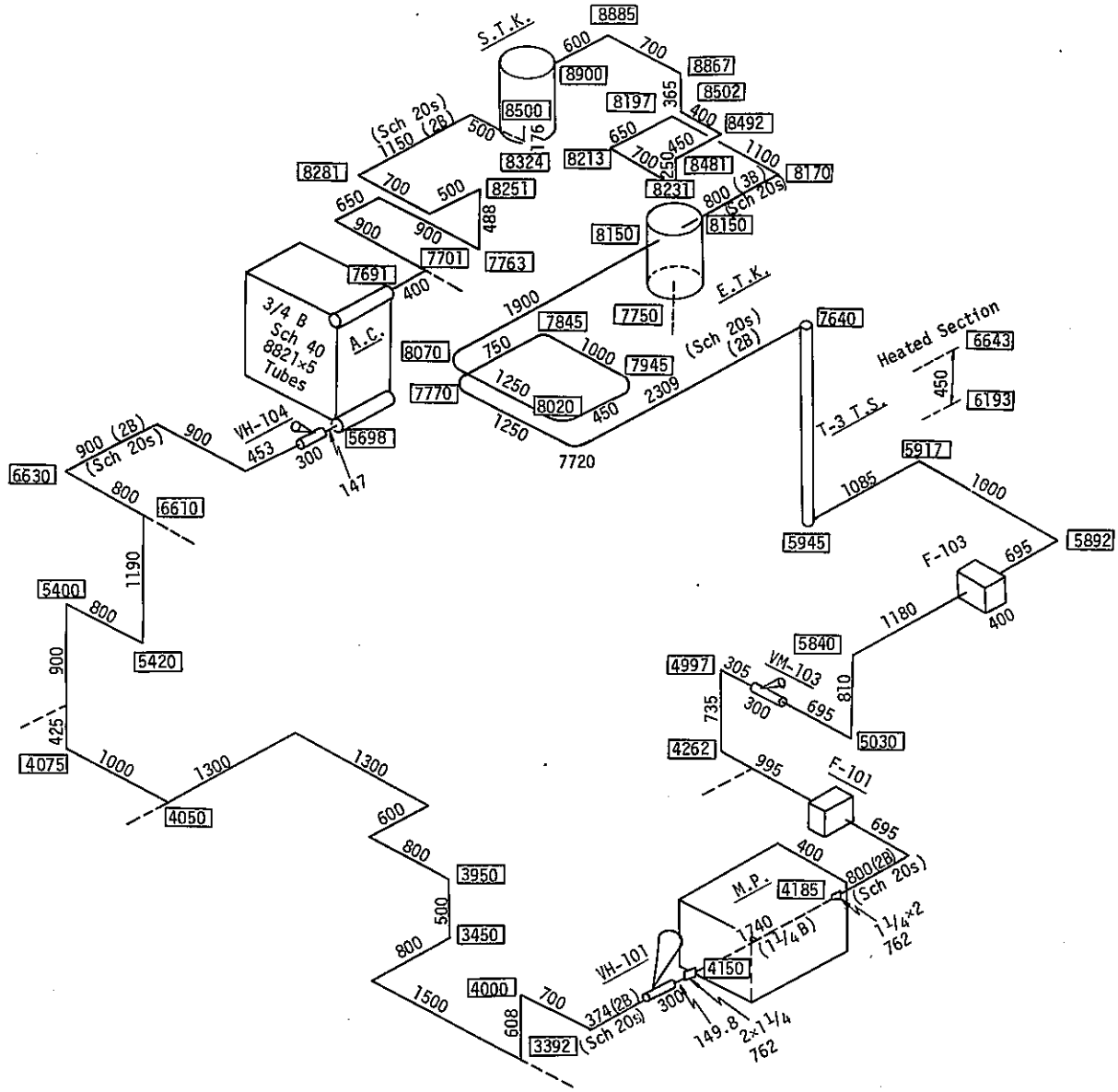

Fig. 3 Bird's-eye view of the main line of SIENA facility used for the 37G experiments

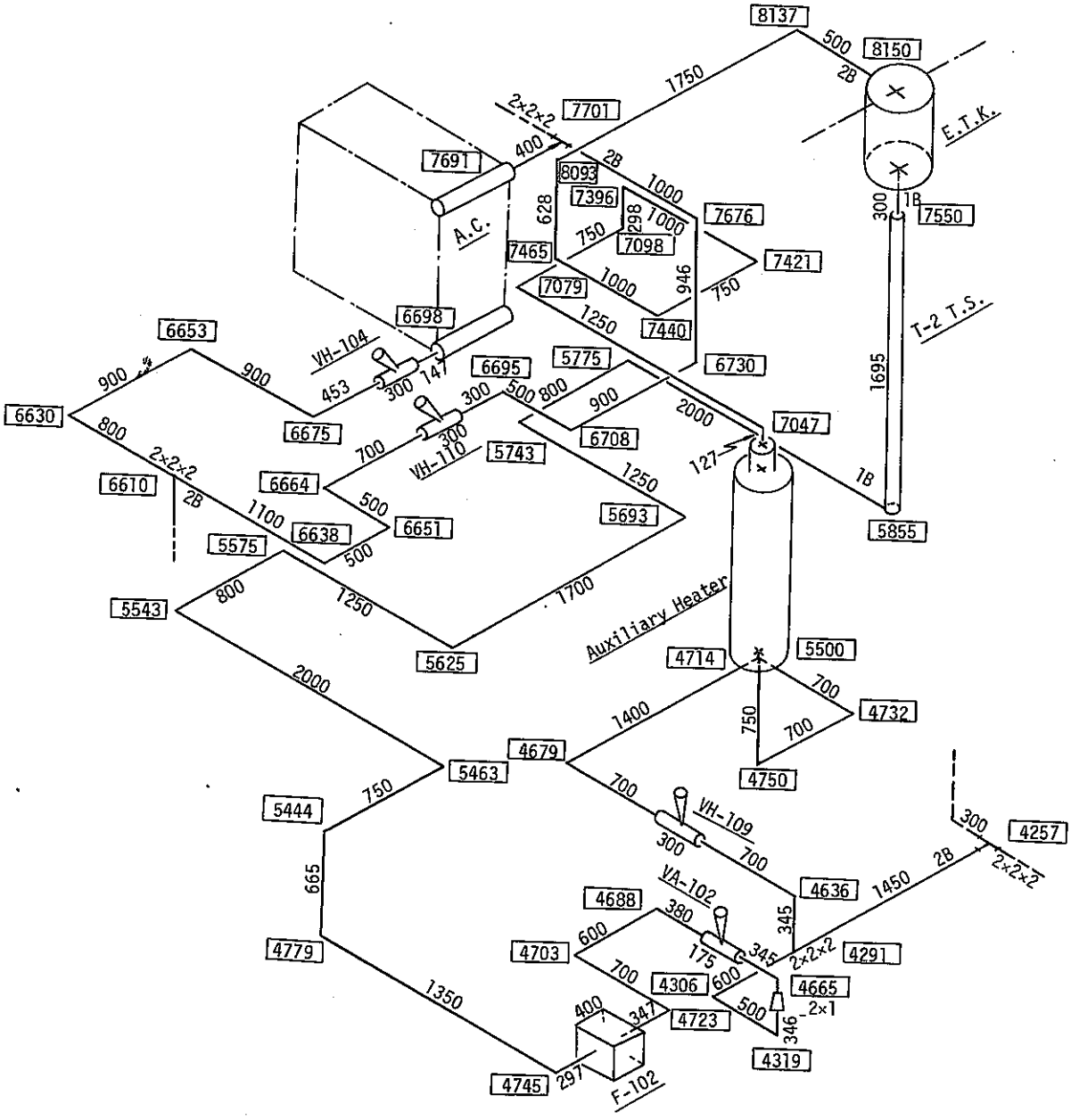

Fig. 4 Bird's-eye view of the bypass lines of SIENA facility used for the 37G experiments

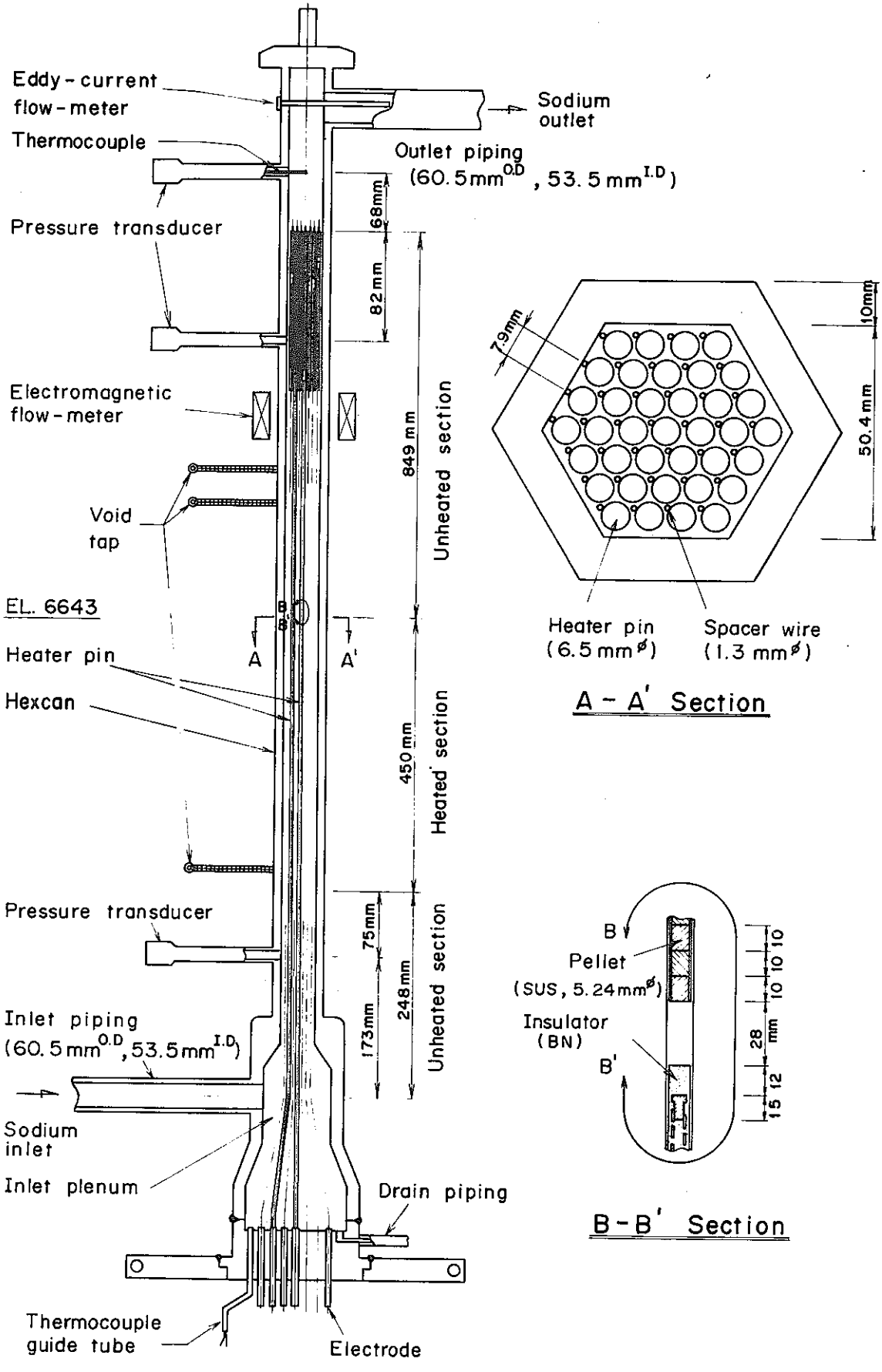

Fig. 5 Wire-wrapped 37-pin bundle test section, 37G

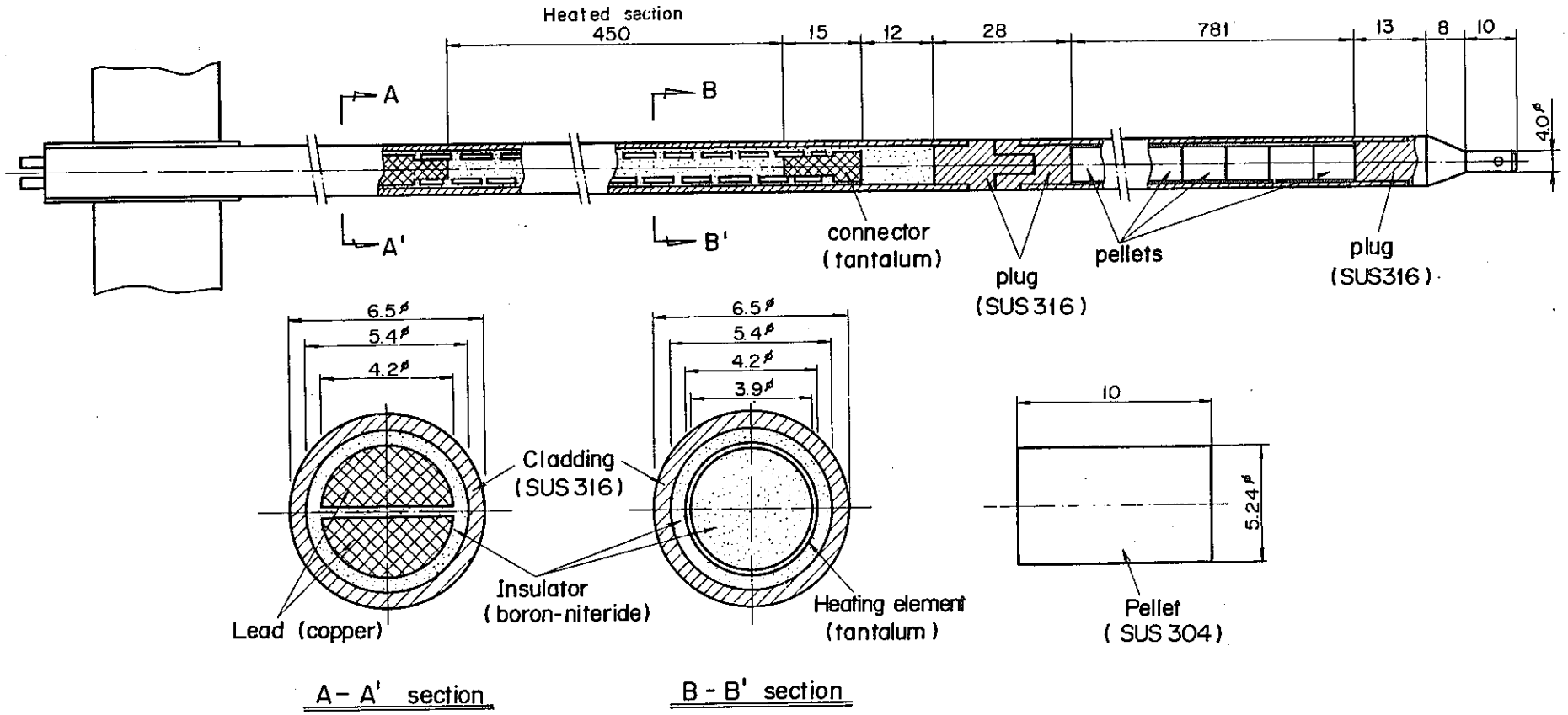

Fig. 6 Design specification of the heater pin used for the 37G test section

Item	Description	No.	Material	Note
1	End plate	1	SUS 316	φ406.4, t=70
2	Electrode box	1	SUS 304	OD. φ406.4, t=6
3	Ceramic terminal	40	$A\ell_2O_3$	
4	Flange	1	SUS 304	φ540, t=15
5	Cover plate	1	"	φ540, t=20
6	Maintenance cover	1	"	φ280, t=15
7	Helium gas nozzle	1	"	3/4B, OD. φ272, t=2.5
8	Compression fitting	5	"	
9	Harmonica terminal	22		12P TH-212
10	Electrode	74	Cu	
11	Lead wire	74	"	14 mm^2
12	Wrapper tube	1	Inconel	t=10
13	Heater pin	37		OD. φ6.5
14	Inlet plenum	1	SUS 316	
15	Inlet nozzle	1	"	2B, OD. φ60.5, t=3.5
16	Drain nozzle	1	"	3/8B, OD. φ17.3, t=2
17	Gas release nozzle	1	"	φ27, φ6.5, φ0.5 hole
18	Pressure guide tube	1	"	1/2B, OD. φ21.7, t=2.5
19	Inlet thermocouple	1		φ3.2 (T-003)

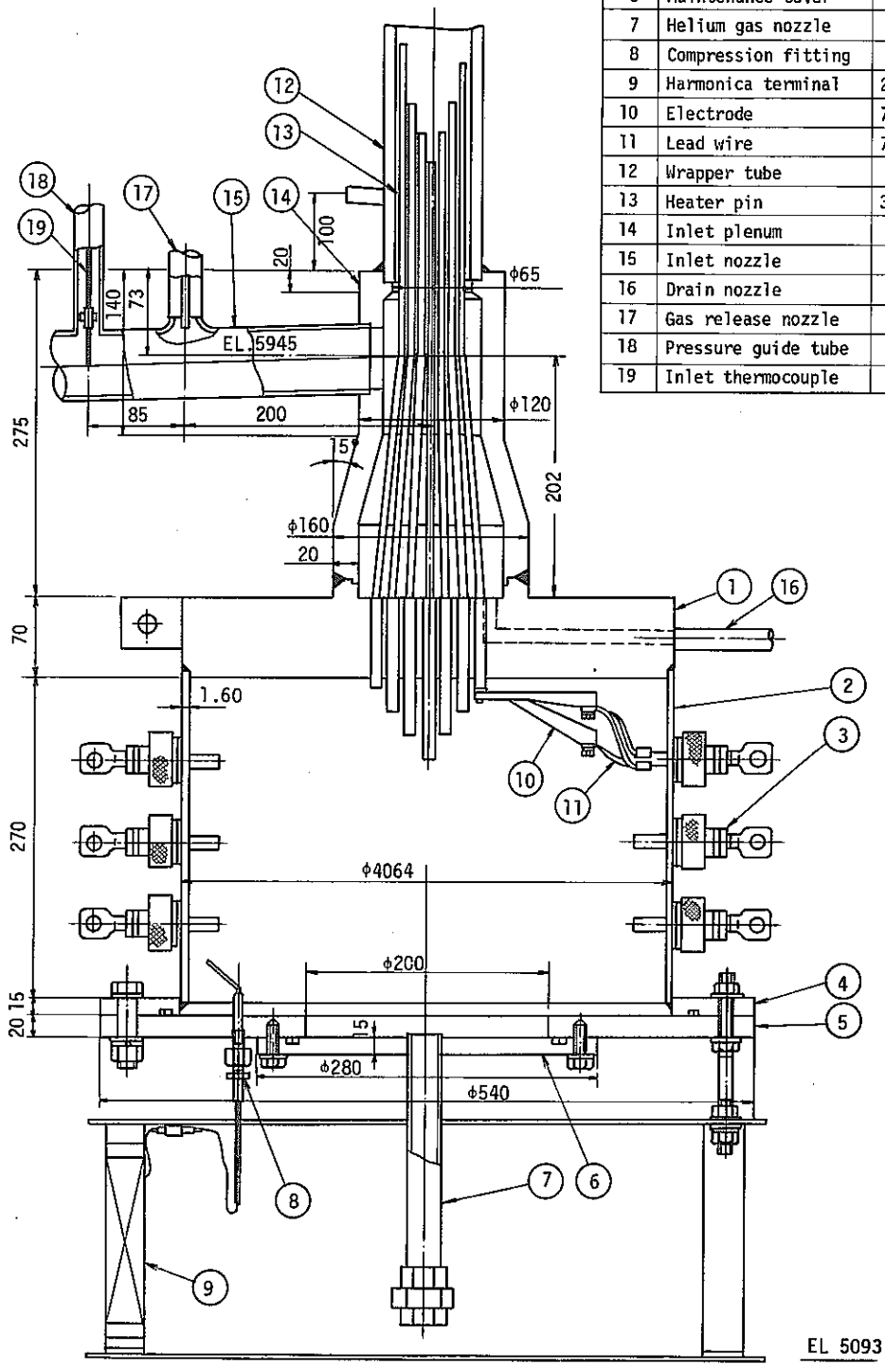

Fig. 7 Sketch of the lower structure of the 37G test section

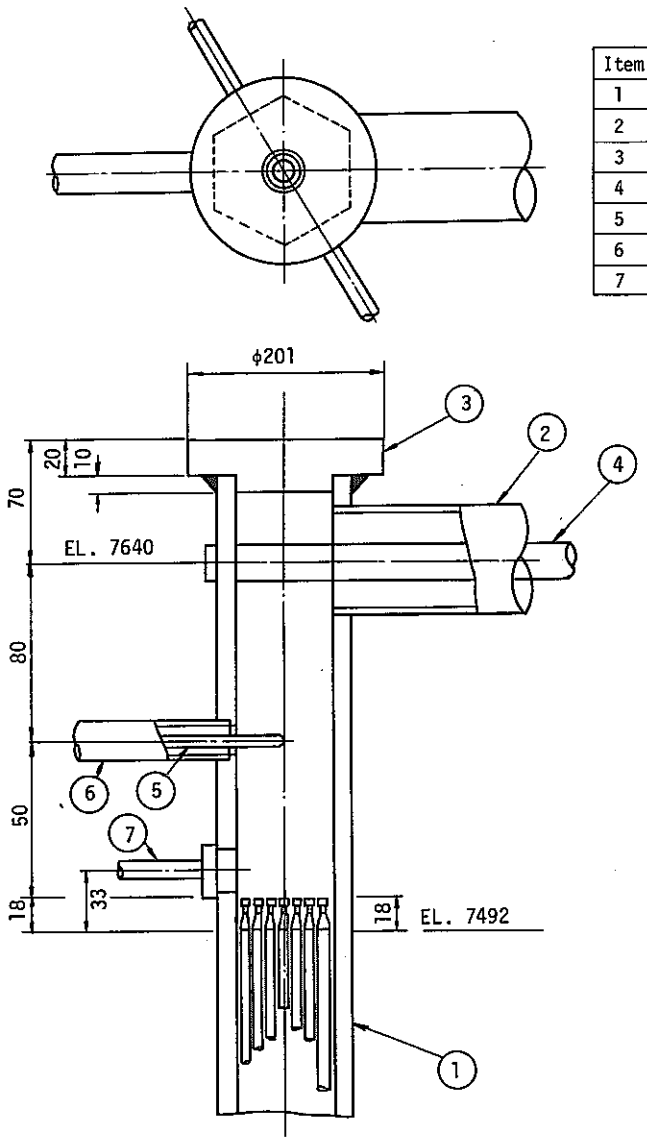

Item	Description	No	Material	Note
1	Wrapper tube	1	Inconel	
2	Outlet nozzle	1	"	2B, OD. φ60.5, t=3.5
3	Plug	1	"	
4	Flow-meter sleeve	1	SUS 316	1/4 B, OD. φ13.8, t=1.2
5	Outlet thermocouple	1		φ4.8 (T-004)
6	Pressure guide tube	1	Inconel	1/2 B, OD. φ21.7, t=2.5
7	Thermocouple sleeve	2	"	φ9.0, t=1.0

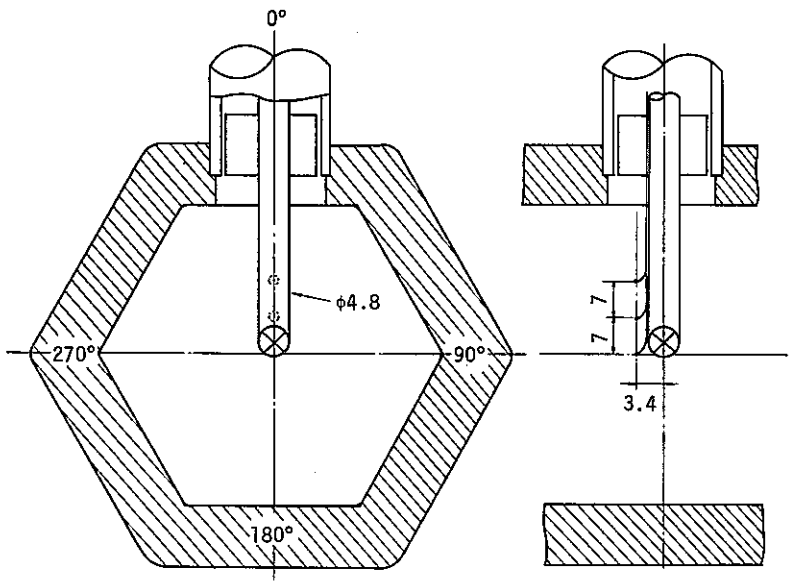

K section (z=997.0)

Fig. 8 Sketch of the upper structure of the 37G test section

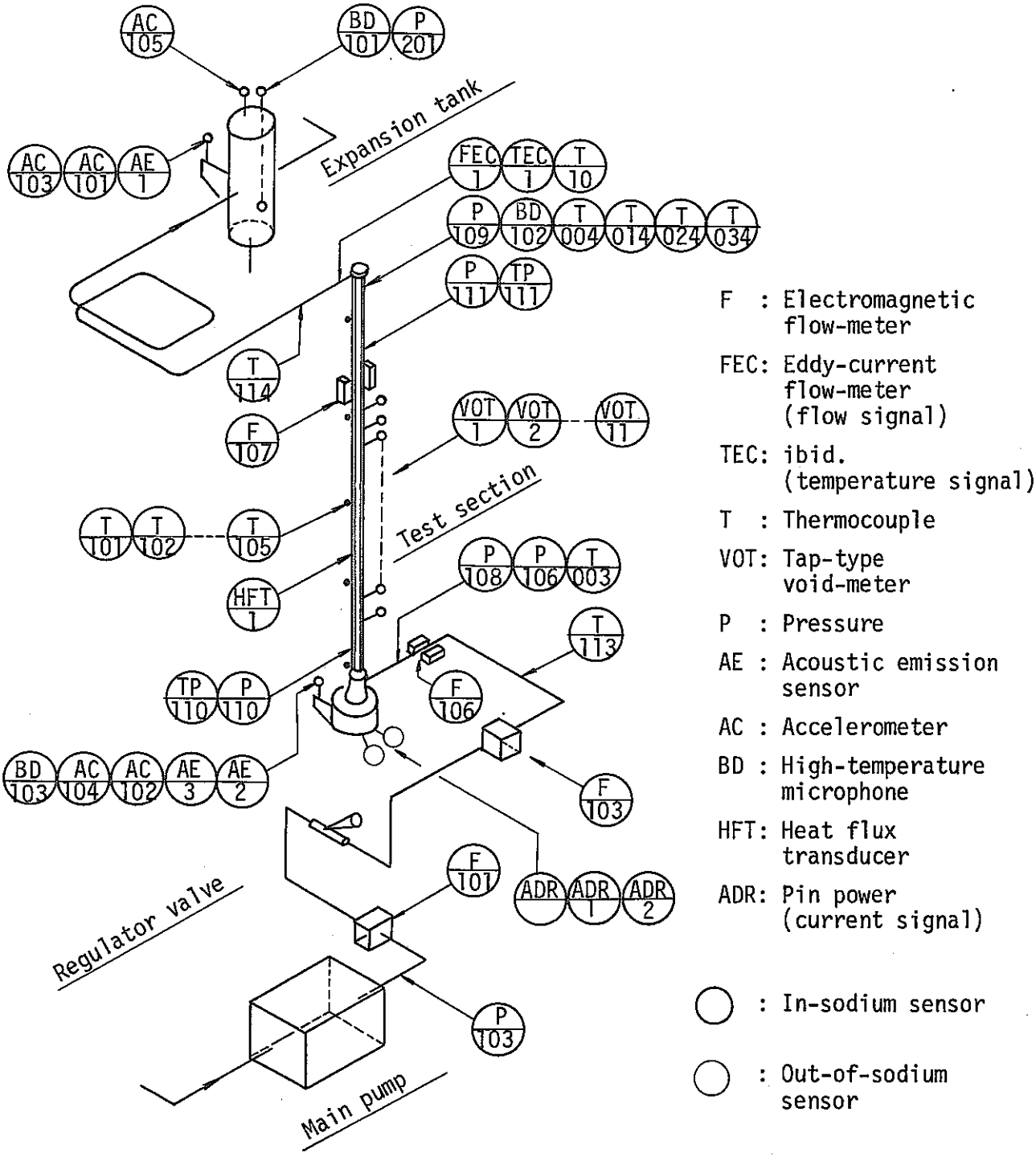

Fig. 9 Plant instrumentation of the SIENA facility and the external instrumentation of the 37G test section

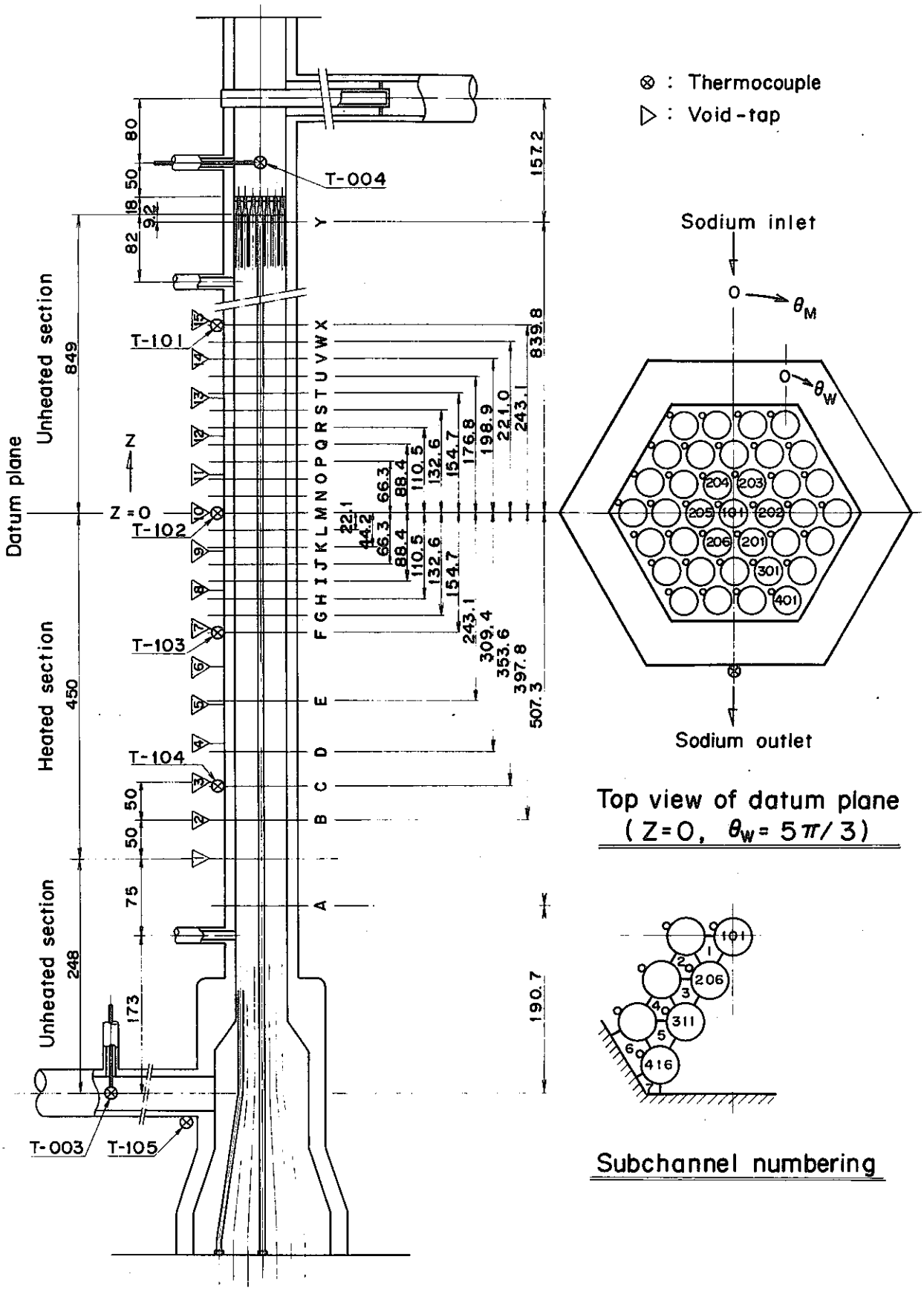

Fig. 10 Locations of the test section instrumentation in the 37G test section

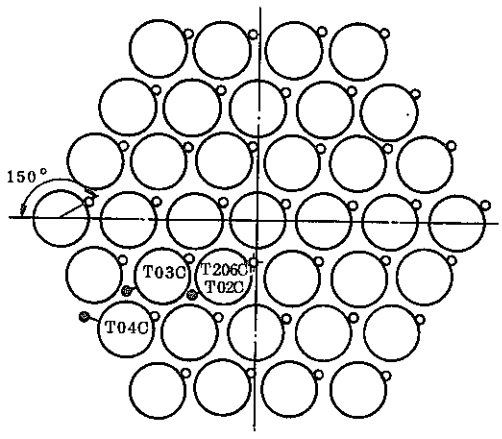

C Section (z=-353.6mm)

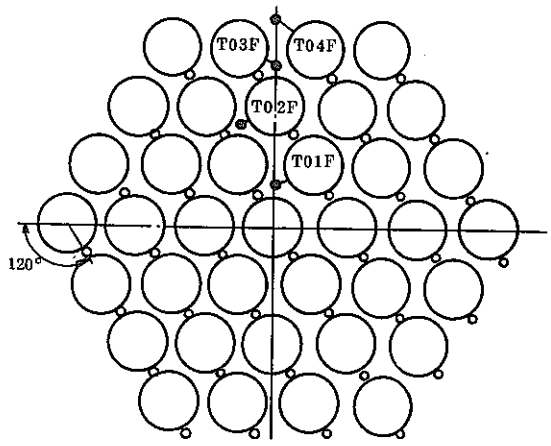

F Section (z=-154.7mm)

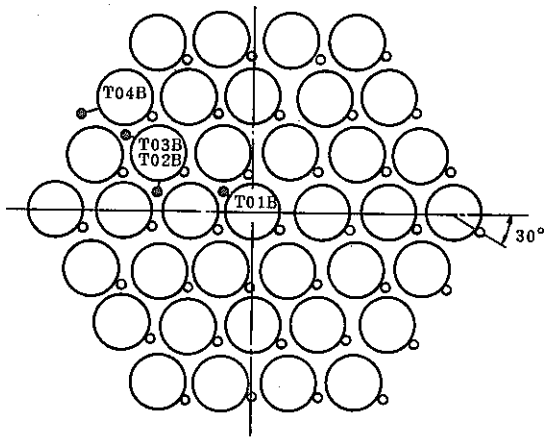

B Section (z=-397.8mm)

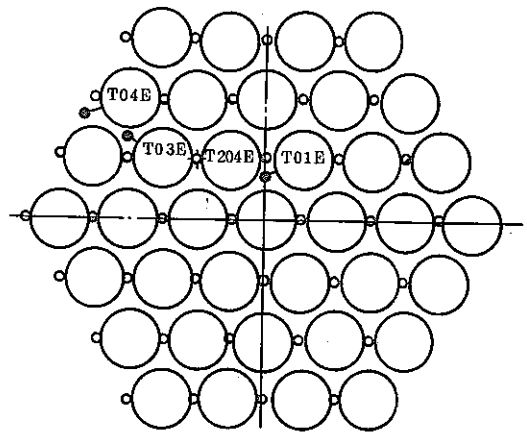

E Section (z=-243.1mm)

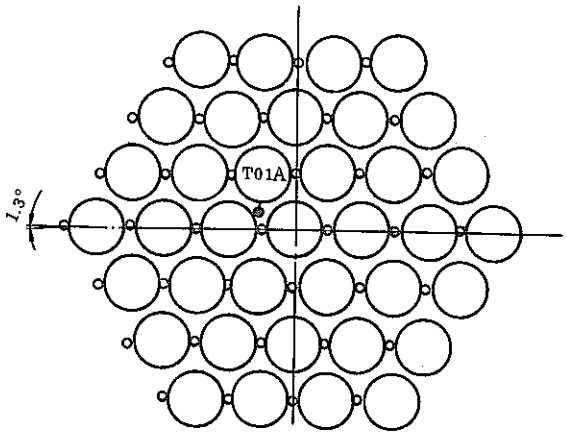

A Section (z=-507.3mm)

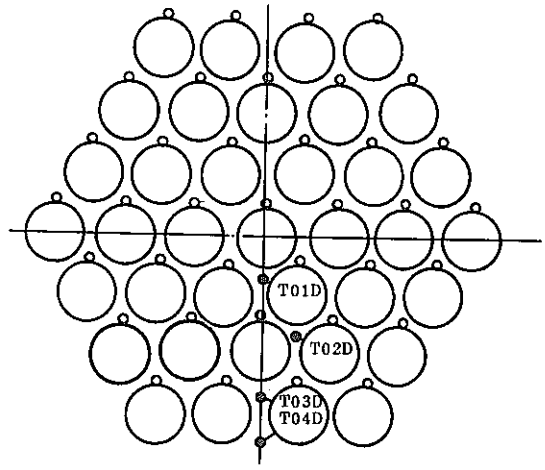

D Section (z=-309.4mm)

Fig. 11 Locations of the thermocouples and Chen probes in the 37G test section (1)

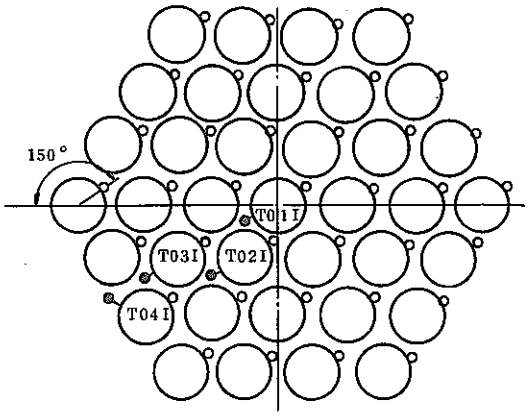

I Section (z=-88.4mm)

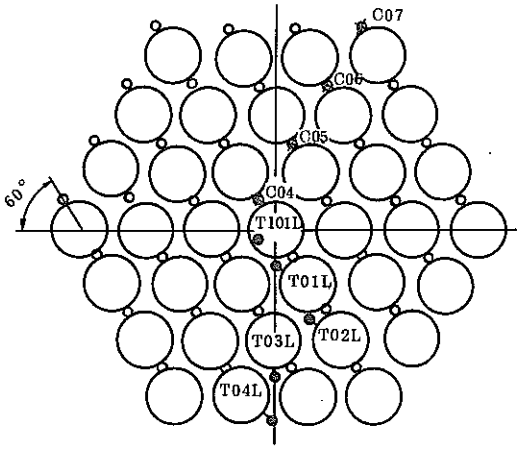

L Section (z=-22.1mm)

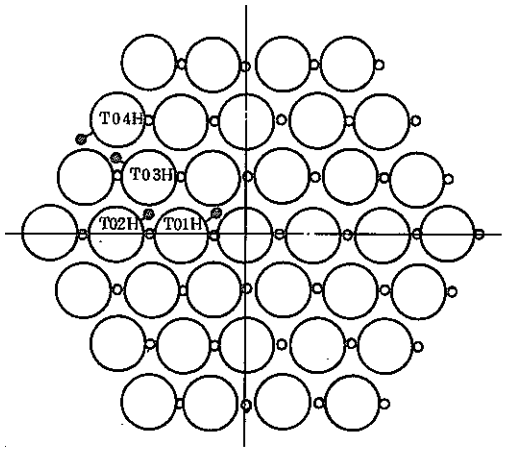

H Section (z=-110.5mm)

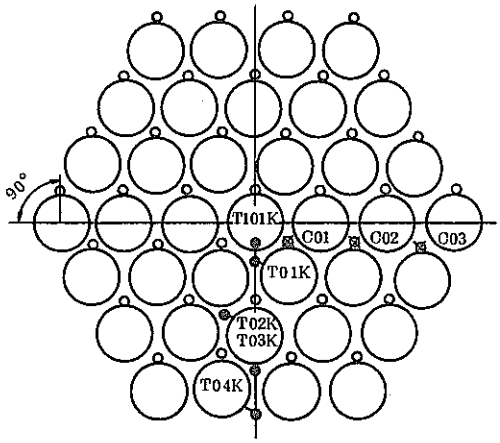

K Section (z=-44.2mm)

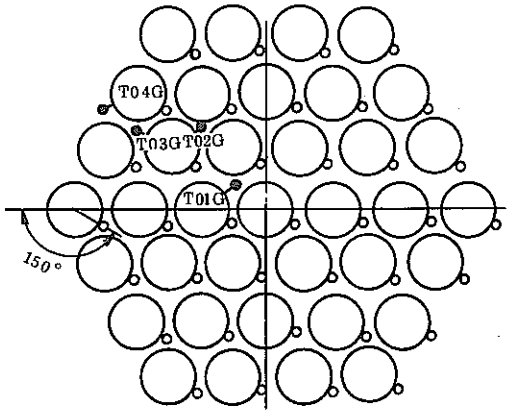

G Section (z=-132.6mm)

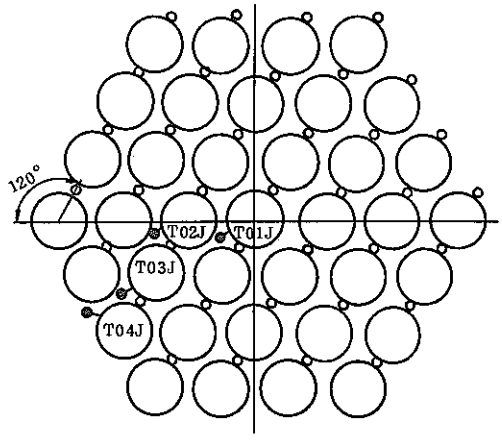

J Section (z=-66.3mm)

Fig. 11 Locations of the thermocouples and Chen probes in the 37G test section (2)

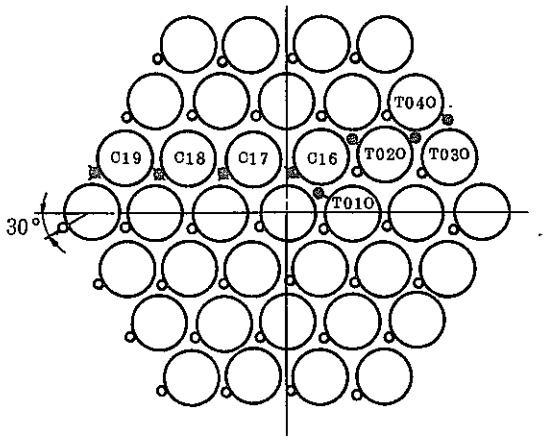

O Section (z=44.2mm)

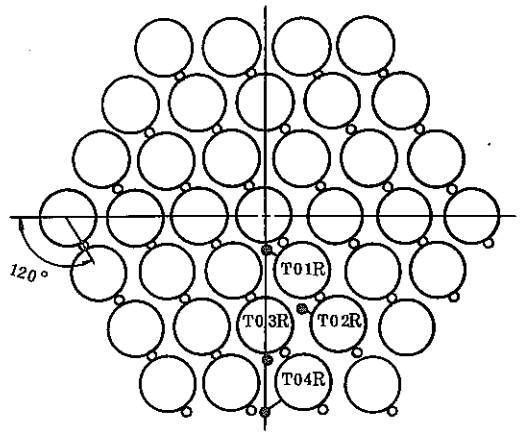

R Section (z=110.5mm)

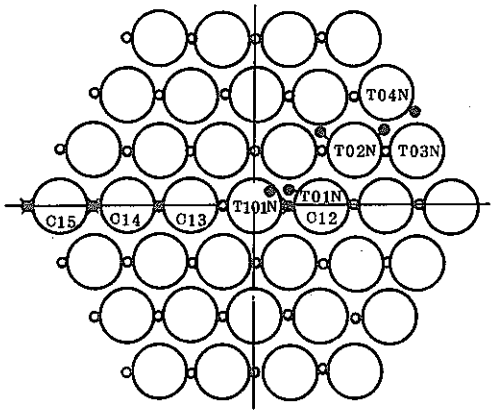

N Section (z=22.1mm)

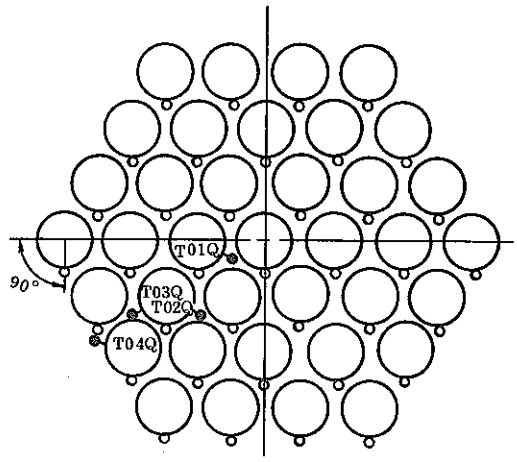

Q Section (z=88.4mm)

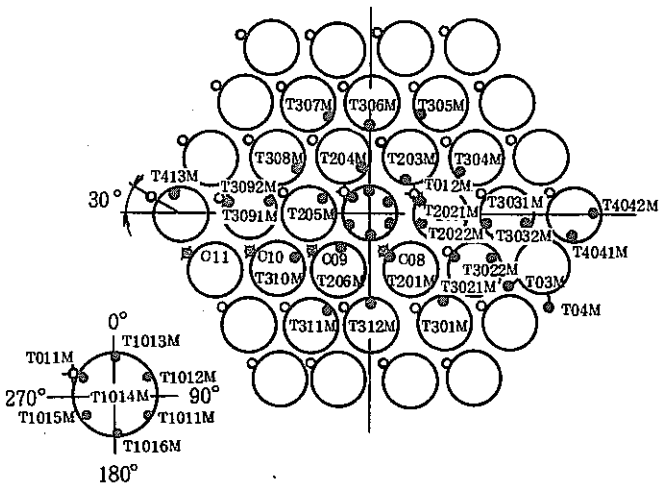

M Section (z= 0mm)

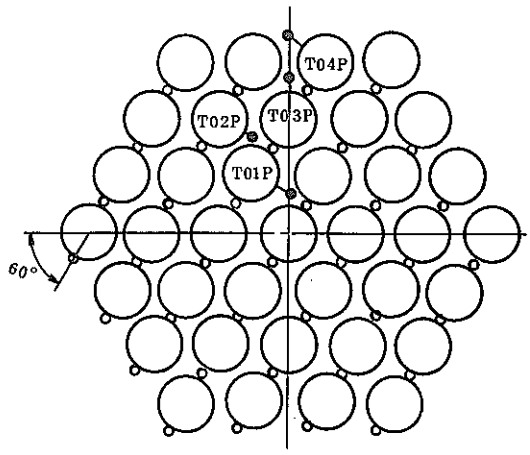

P Section (z=66.3mm)

Fig. 11 Locations of the thermocouples and Chen probes in the 37G test section (3)

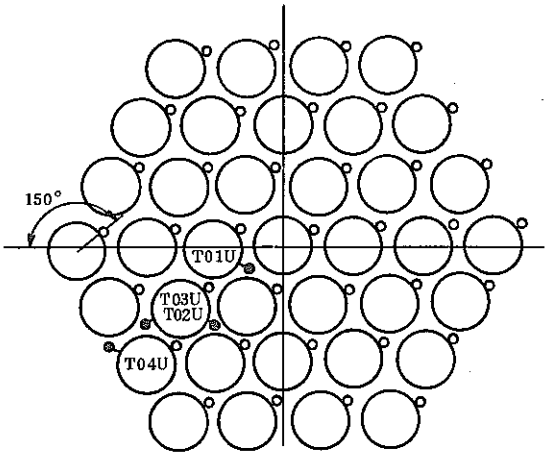

U Section (z=176.8mm)

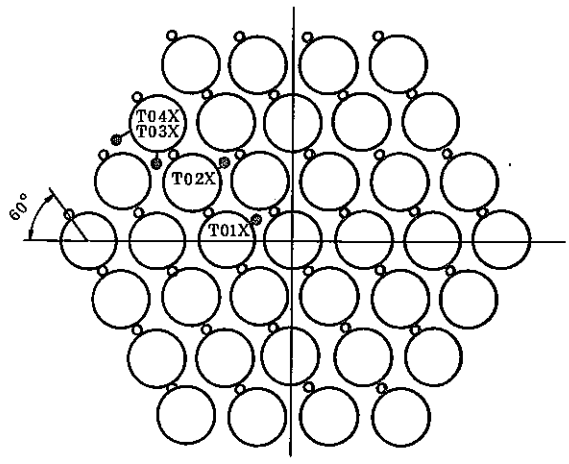

X Section (z=243.1mm)

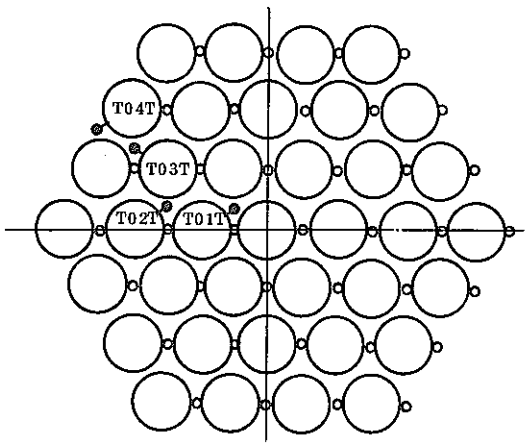

T Section (z=154.7mm)

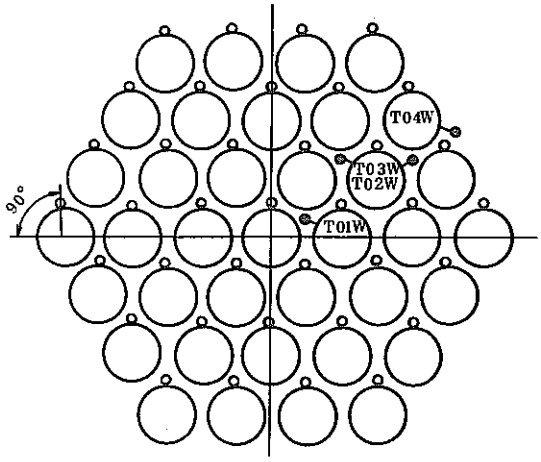

W Section (z=221.0mm)

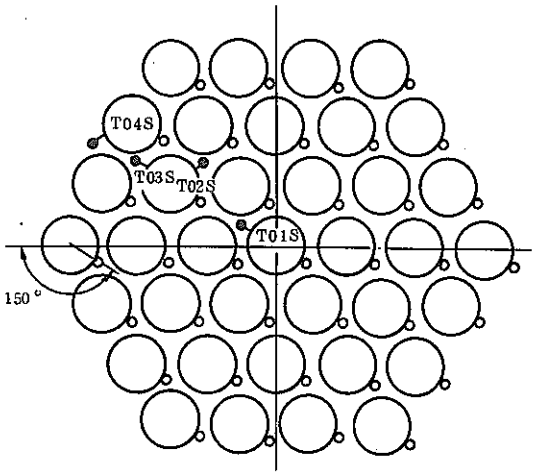

S Section (z=132.6mm)

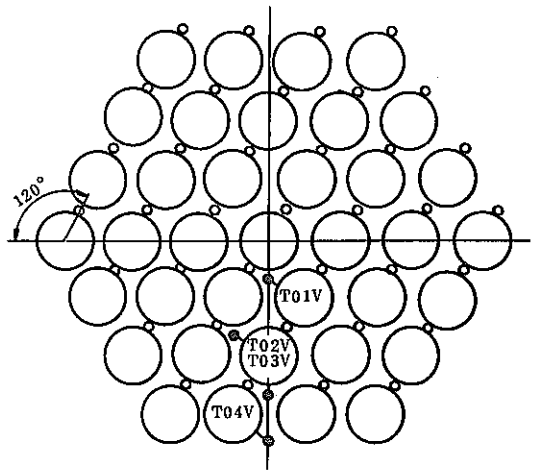

V Section (z=198.9mm)

Fig. 11 Locations of the thermocouples and Chen probes in the 37G test section (4)

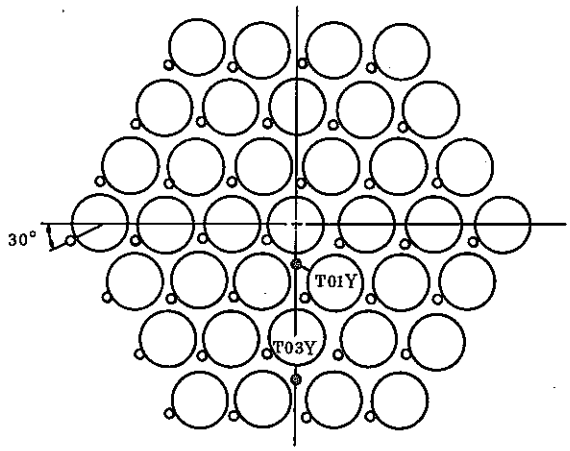

Y Section (z=839.8mm)

Fig. 11 Locations of the thermocouples and Chen probes in the 37G test section (5)

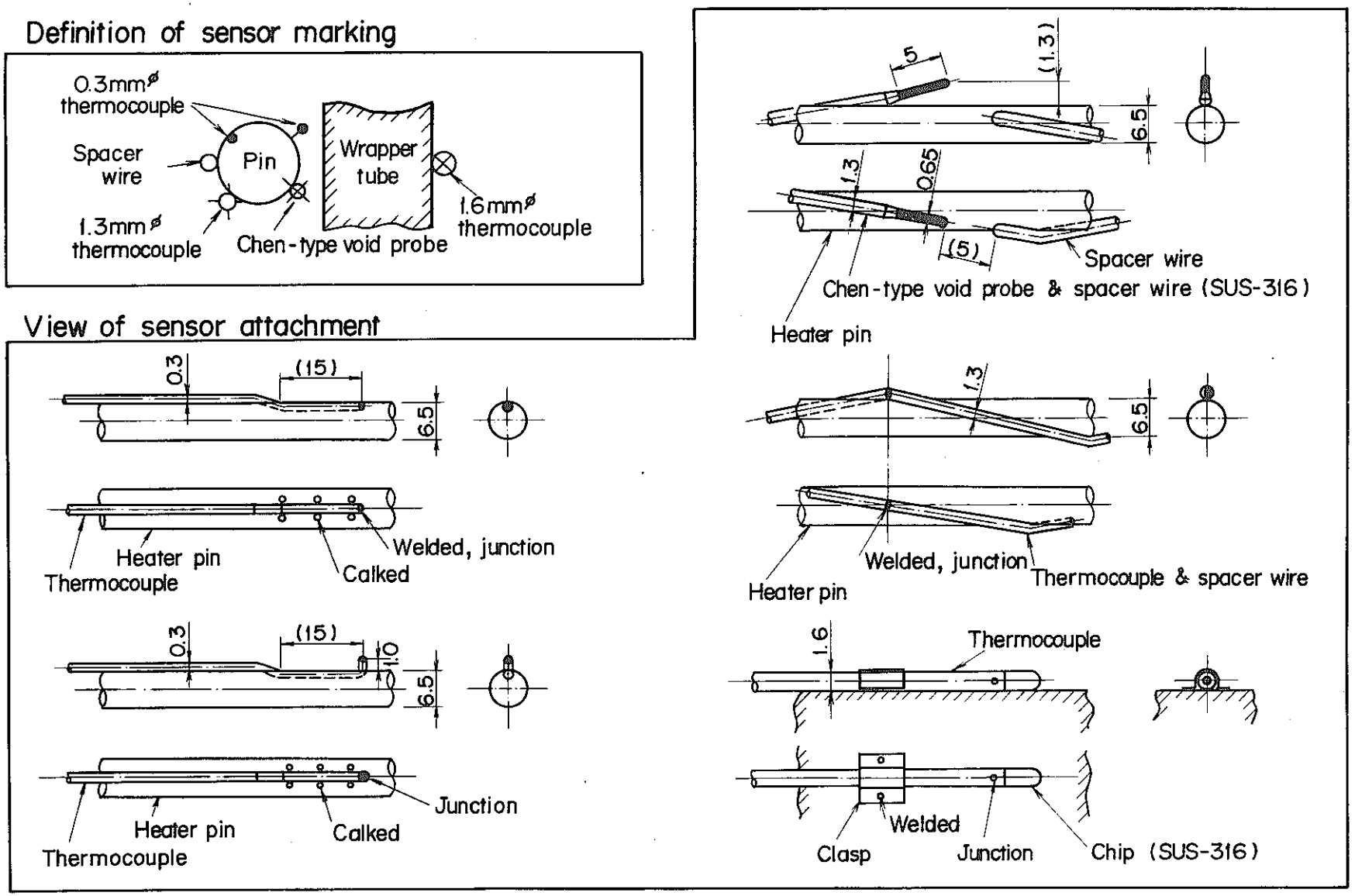

Fig. 12 Difinitions of sensor markings and views of sensor attachements

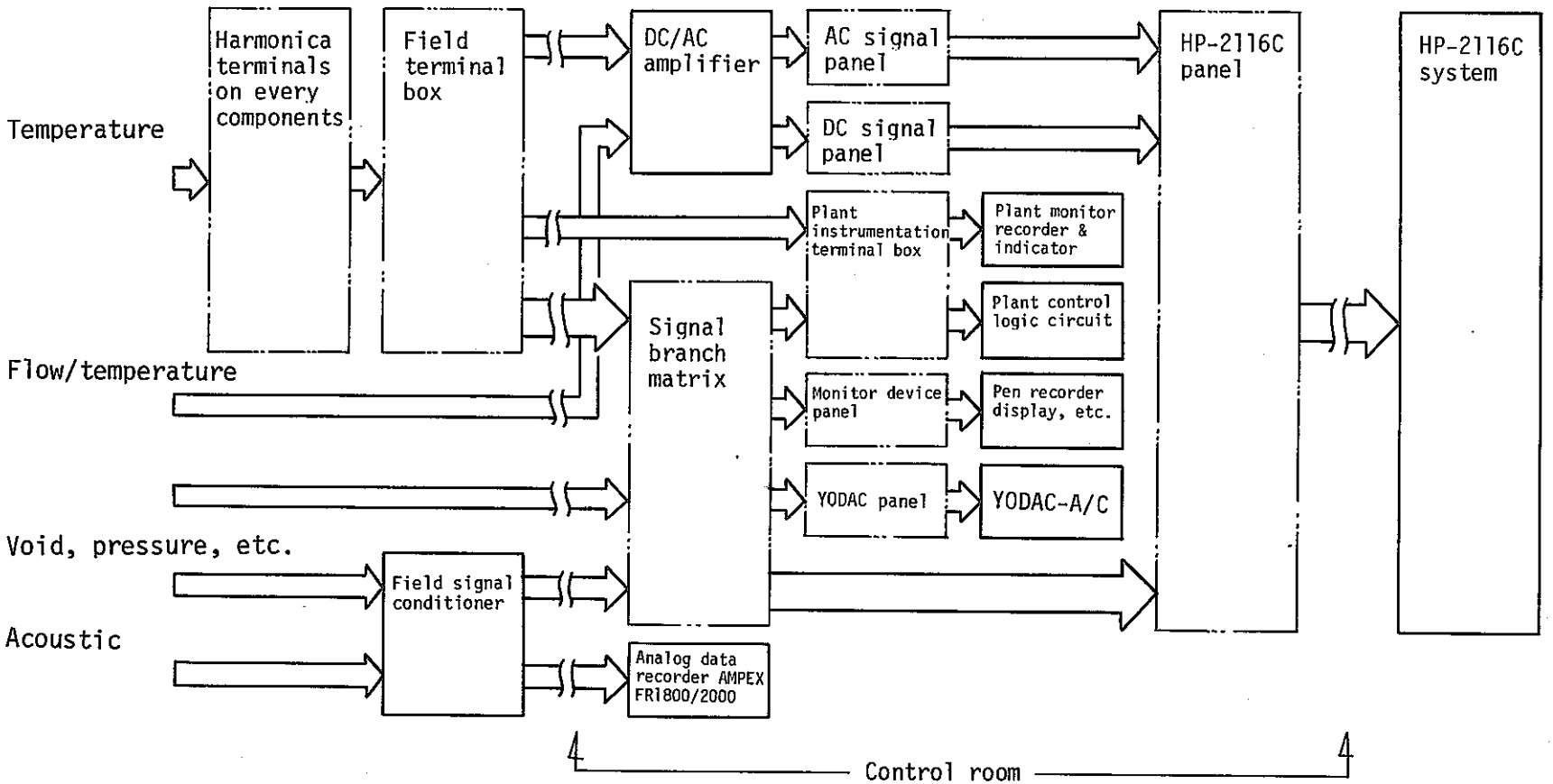

Fig. 13 Signal flow diagram of the SIENA data acquisition system for the 37G experiments

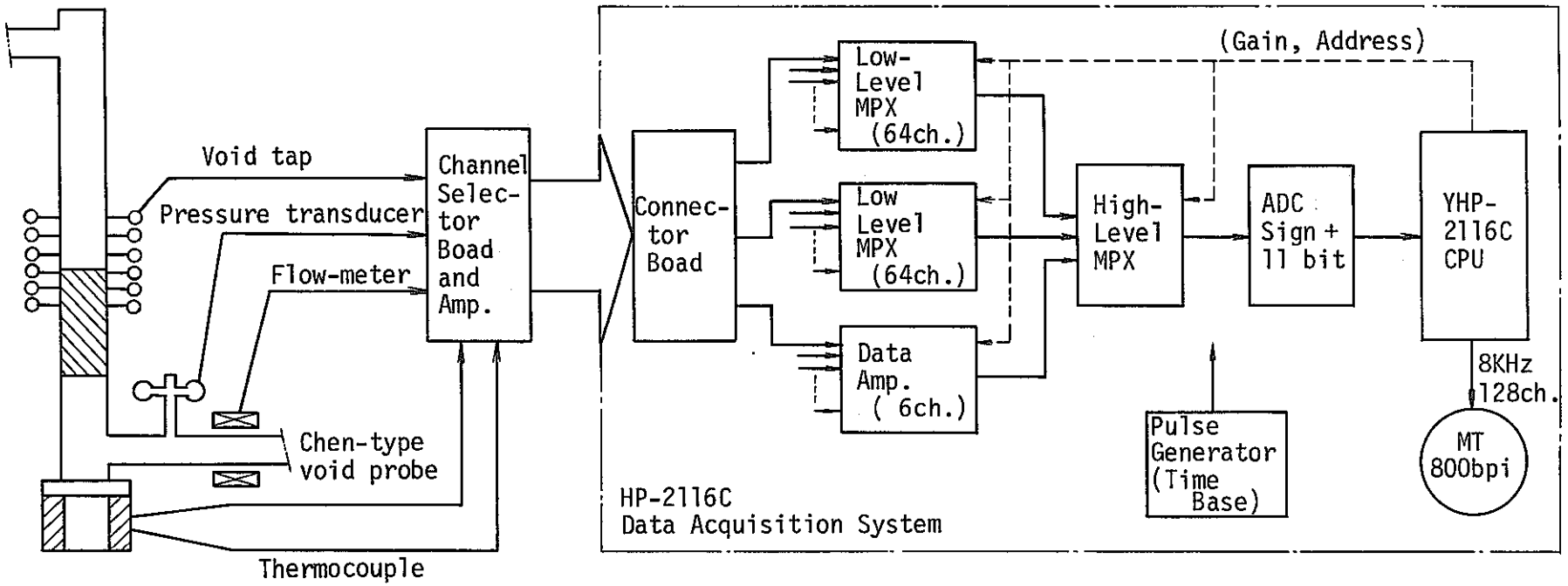

Fig. 14 SIENA digital data acquisition system

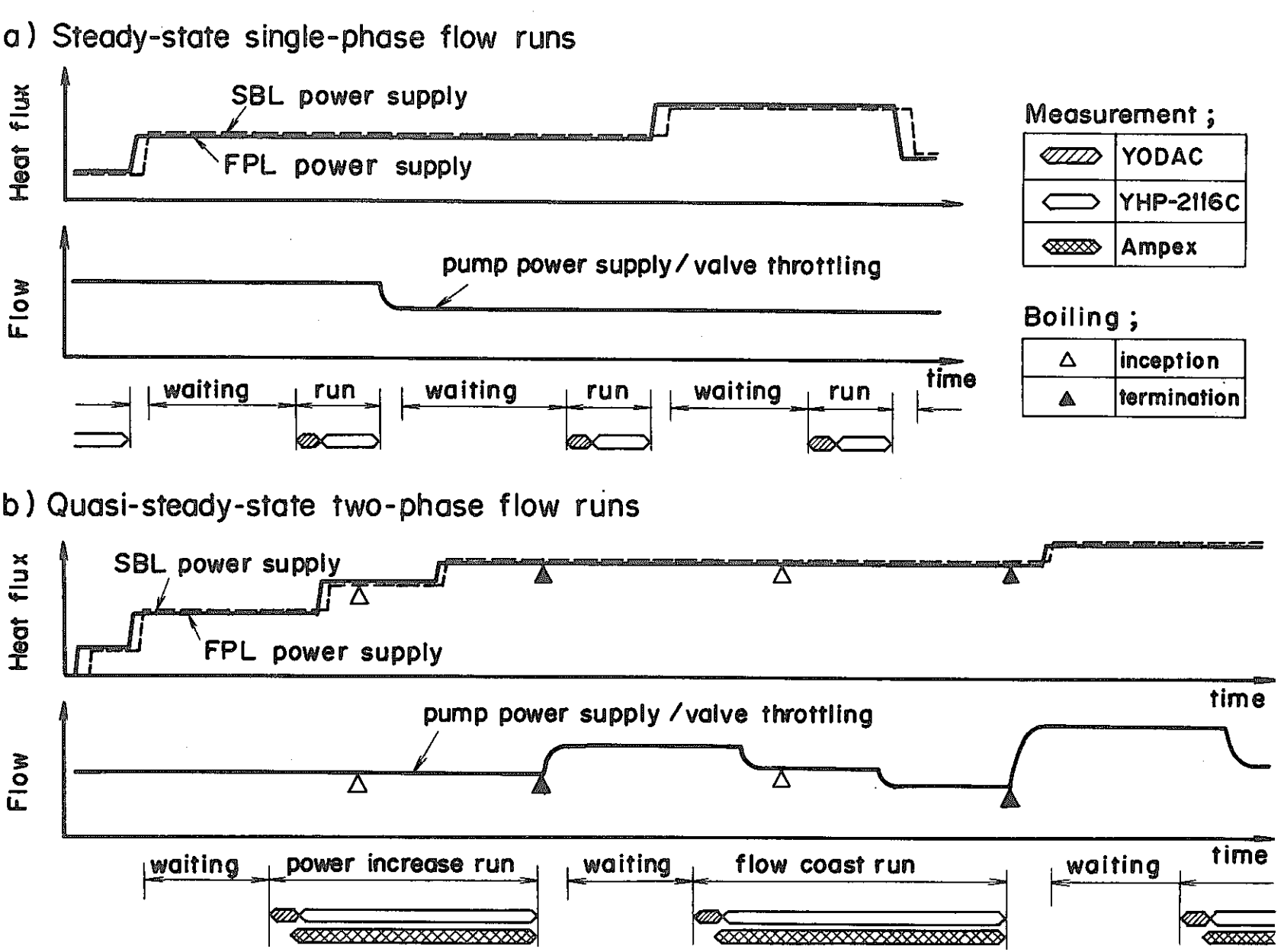

Fig. 15 Experimental procedures and timing sequences of measurements

Normal pin used for experiments

Unused pin due to its dielectric breakdown

Unused pin due to its melting or pair connection of molten pin

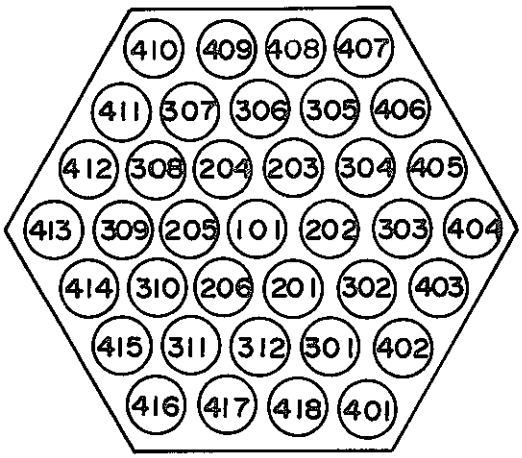

Initial run to 141th operation, 37HB-260-10

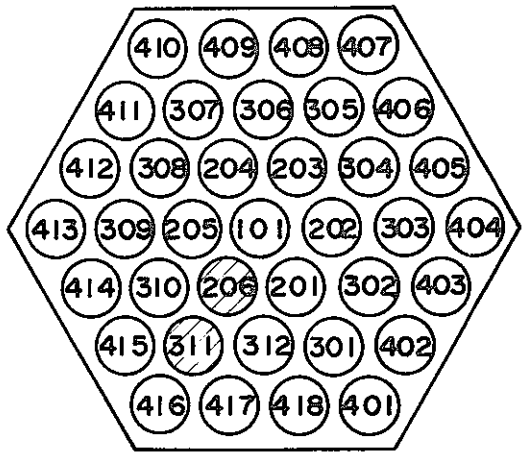

141th operation, 37(35)LHF-220 to 37(35)LHF-228

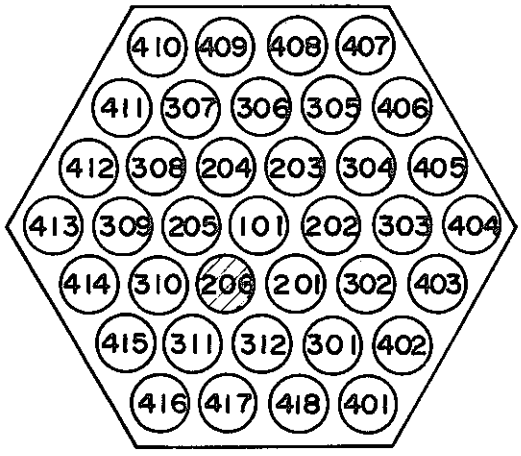

142th operation, 37(36)LHF-230 to 37(36) LHF-232

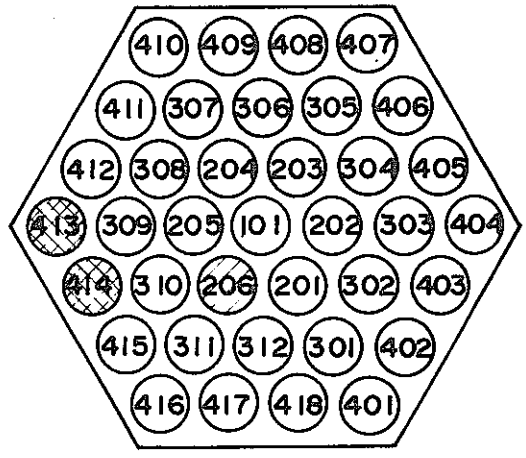

142th operation, 37(34)LHF-233 to 37(34)LHF-239

Fig. 16 Transition of the heating patterns of the 37G test pins (1)

Normal pin used for experiments

Unused pin due to its dielectric breakdown

Unused pin due to its melting or pair connection of molten pin

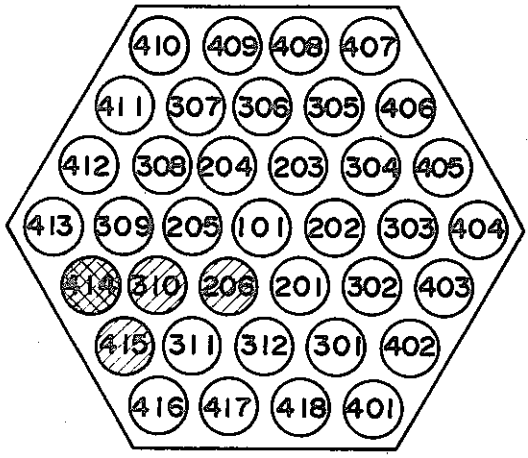

143th operation, 37(33)NCT-1 to 37(33) LHF-248

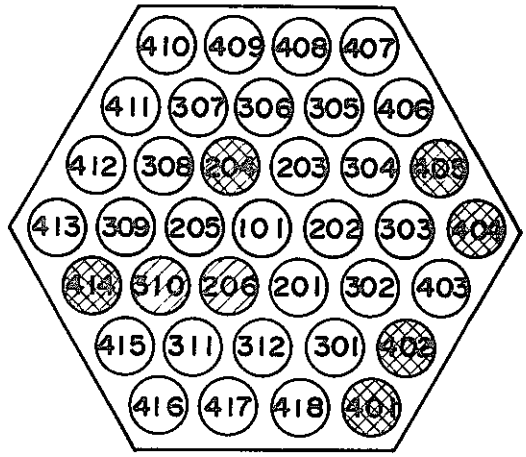

144th operation, 37(29)LHF-250 to 37(29) LHF-253

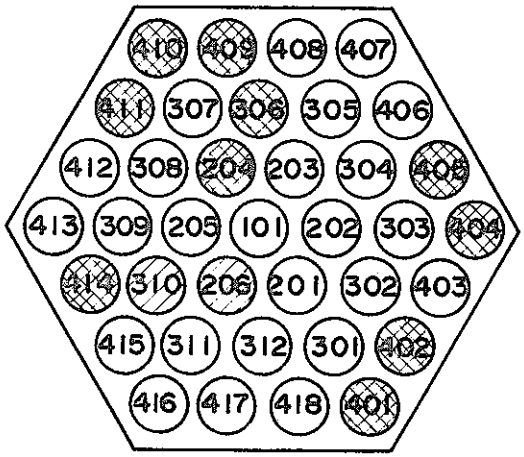

144th operation, 37(25) H-000 to 37(25) H-103

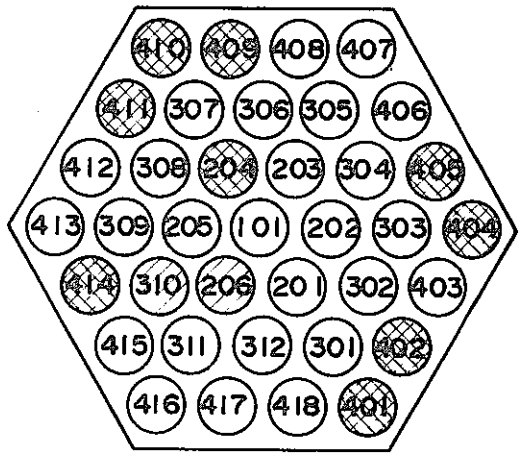

145th operation, 37(26)LHF-260 to 37(26) LHF-261

Fig. 16 Transition of the heating patterns of the 37G test pins (2)

Normal pin used for experiments

Unused pin due to its dielectric breakdown

Unused pin due to its melting or pair connection of molten pin

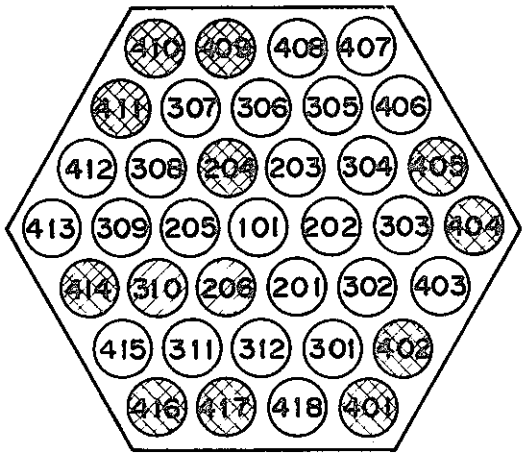

145th operation, 37(24)LHF-262

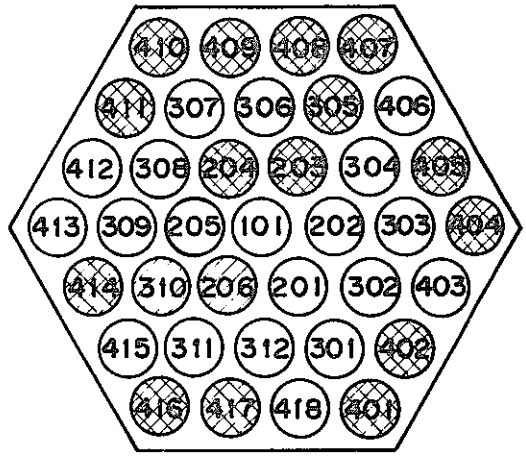

145th operation, 37(20)LHF-263 to 37(20) FC-107

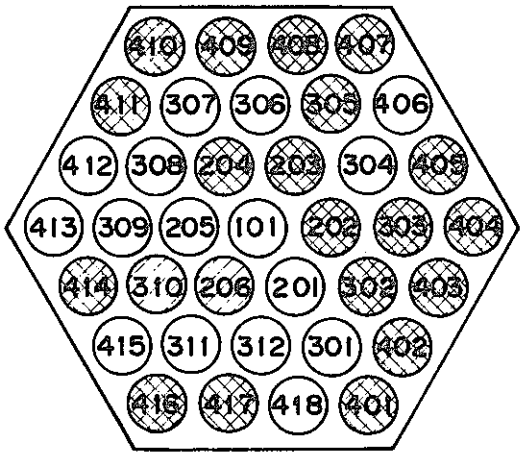

145th operation, 37(16) FC-108 to 37(16) FC-109

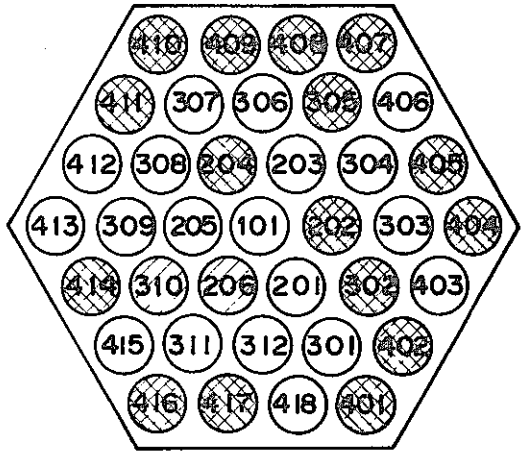

146th operation, 37(19) FC-110

Fig. 16 Transition of the heating patterns of the 37G test pins (3)

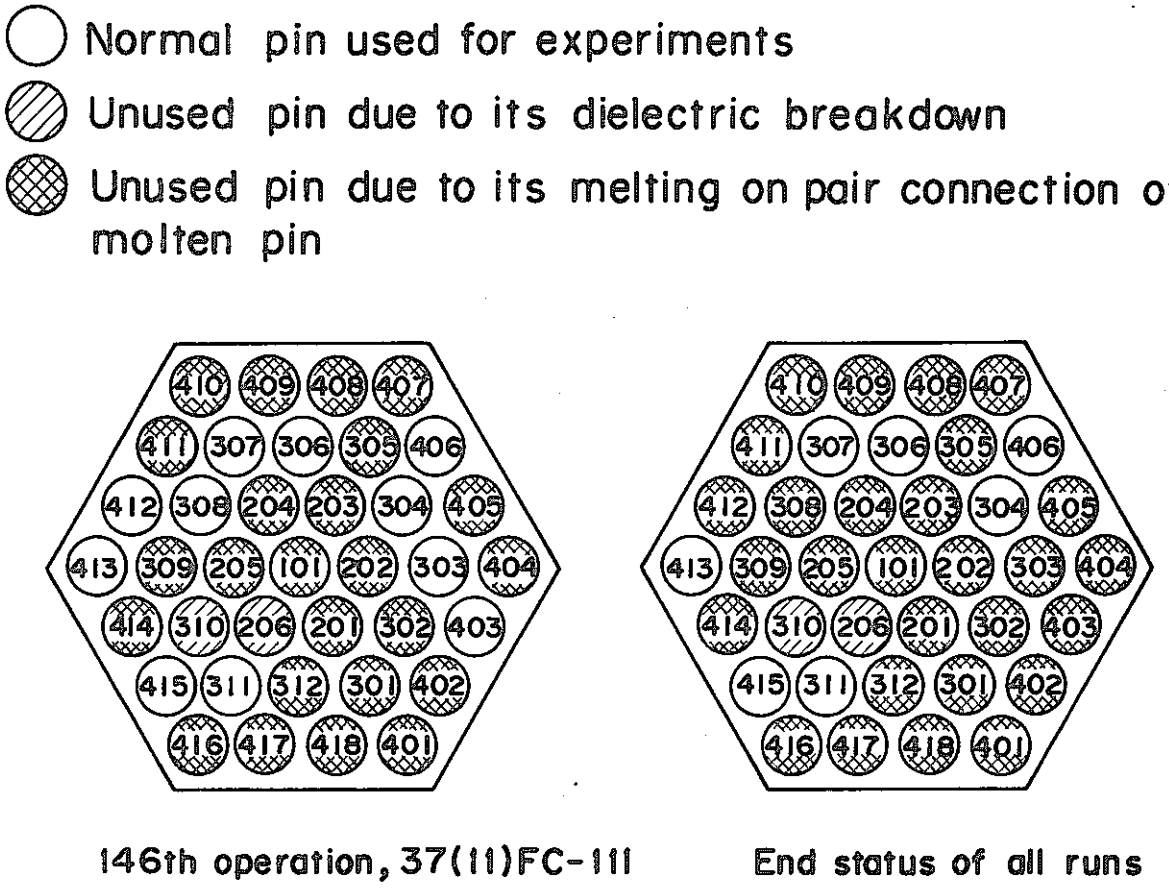

Fig. 16 Transition of the heating patterns of the 37G test pins (4)

3. EXPERIMENTAL RESULTS AND DISCUSSIONS

3.1 Typical runs

Run 37(37)LHF-200

This is the first low-heat-flux boiling run conducted with the 37G test section. Figure 17 show the result of this run, where the temperatures, pressure, flow and power are traced to see the relations among them. The T-2 line (bypass line) was left open. The inlet valve was throttled, as a first action into transient, from 100 % to 15 %, and then the pump power was gradually decreased. The heat flux of the central 13 pins was adjusted to be 25 W/cm^2, which is higher than that of peripheral 24 pins by about 25 %, to obtain the radial convex temperature profile during this run. Confirming that the thermal-hydraulic properties were all settled stationarily under the slightly subcooled condition, the pump power was reduced stepwise to see incoherent sodium boiling around the central region of the pin bundle. The subsequent increase of the inlet flow due to the mixed-convection sodium boiling forced the initial boiling to terminate in about 30 s.

The pump power was reduced again to observe a little more intensified boiling phenomenon under the same incoherent condition. The inlet flow began to oscillate after attaining the second boiling condition. The flow signal became quite similar to that observed at the 37F natural circulation boiling runs (the characteristic points relevant to this boiling phenomenon will be described in section 3.2). The experiment was terminated by increasing the pump power (inlet flow).

Run 37(37)LHF-201

A quite similar experiment to the last one was carried out as shown in Fig. 18. The difference lies in the heating pattern: all pins were heated uniformly to attain a wider boiling boundary toward peripheral direction than the last case. Boiling was initiated like the earlier phase of the second boiling step of the last case. The inlet flow oscillated as before. However, the oscillation began to decay in keeping with the increasing mean inlet flow. A new stage was reached naturally next to the decay of the oscillation, where the boiling intensity became moderate suggesting the backing to the bubble flow condition. Whether or not the special aspect like this depends on the difference in the heating pattern is not known. Meanwhile, this case has been used for the validation study of the REDNEC code at PNC[36].

Run 37(35)LHF-220

Before conducting this run, the electrical insulation of the #206 pin was broken to force the following 9 runs to be conducted with two pins (forming an internal parallel wiring to a common pair of electrodes in the electrode box shown in Fig. 7) being unheated, while one pin (#311) was made usable again prior to the Run 37(36)LHF-230. In the following 9 runs, the heating pattern was changed to obtain laterally skewed thermal field, i.e. the 12 pins located at the 300° side of the bundle were over-heated by 17 % than the 13 pins located

at the 120° side, and the residual 10 pins were heated to have an averaged heat flux.

In this case, the sodium boiling was reached by the pressure reduction method. The over-pressure of the cover gas volume of FPL was reduced stepwise by opening for a short time the stop valve which combines FPL with the gas surge volume of SBL exhausted to nearly 0 MPa beforehand. The experimental result is shown in Fig. 19, indicating a quite different boiling behavior like a slow-motion. The system pressure was decreased twice during the boiling phase. It can be identified from the P-201 signal. At the midway of the first boiling step, the inlet flow fell drastically once probably because the boiling region extended toward the wrapper tube wall. After that, the pressure and the saturated temperature oscillated slowly with quite resembled manner each other.

The second pressure reduction led to a fall of saturation temperature by around 30 °C. It would be reasonable to consider that the boiling region extended very widely up to the outlet piping section. The thermal-equilibrium quality at the top of the heated section exceeds far beyond 1.0, when calculated with the condition at the end of this run. An undoubted permanent dryout (temperature excursion) was initiated at the wide region of the heated section without any violent events. Monitoring such a temperature excursion, this run was terminated by decreasing the pin power.

Run 37(36)LHF-231

The effort of the experiment was focused on obseving the dryout phenomena in detail under the condition of uniform heating. Accordingly, the earlier steps for increasing the boiling intensity were passed from one state to another with short waiting time. The power increase method was adopted in such a hurried approach until a certain vigorous boiling condition was reached, preparing for the settled examination of the dryout phenomena. However, we had little knowledge on the boiling behavior at a decay power level from which we can catch a sign of ending the power increase approach. This run was, therefore, terminated in the midway of the power increase approach by the automatic power scram operated by the temporary dryout.

Figure 20 shows the test result. The inlet flow was maintained below 0.01 m/s on average. The power levels of higher than 8.78 W/cm^2 brought about severe thermal conditions where the exit quality exceeded beyond 1.0. Nevertheless, the pin powers of less than 19.10 W/cm^2 were removed without the occurrence of permanent dryout. It means that the concept based on the normal heat balance within the heated section does not hold at all when the flow pattern is slug flow like that attained in this run. Since the flow velocity was slow, the temperature at the T-004 measurement point could not rise up to saturation point. Therefore, it would be reasonable to consider that the fairly subcooled liquid column fell into the heated section and evaporated there to pump out the decay heat repetitively. As the power was increased, the growing speed of the vapor slug also increased to yield a more compressed slug just before it was ejected upward together with the liquid column located next to the slug. This phenomenon can be seen from the diverging hights of the cyclic pressure pulses.

Run 37(34)LHF-234

When the Run 37(36)LHF-232 was finished, the electrical insulation of the pair pins #413 & #414 (the peripheral pins!) was broken due to dryout. So, this

run was conducted with the residual 34 pins being heated uniformly. The pin power was increased up to 20 W/cm^2 level, as shown in Fig. 21, and left intact thereafter for about 6.5 min. until it was cut off by the automatic scram circuit triggered by the dryout. Since the flow velocity was adjusted to a level little higher than the previous runs, the upper part of the test section became covered with the saturated sodium at an earlier power up steps. In this case, the flow pattern changed from bubble flow to slug flow and further to annular flow, as was usually found at the dryout runs of 37F experiments.

After going into the annular flow stage, the temporary dryouts were frequently observed especially by the thermocouple T-4042M which was located at the corner of the pin bundle, while the other parts were also dried to some extent. The first temporary dryout looks having a different nature from the residual ones succeeded a few minutes later: it appeared at the flow pattern transition phase. It would be ascribed (from the knowledge of the 37F dryout data) to a short term flow instability occasioned sometimes during the flow stabilization process, and will be discussed again in sections 3.3 and 3.4. The dryout quality at the end of this run was 0.61.

Run 37(34)LHF-235

The experimental result is shown in Fig. 22. This is one of the most important runs attained with special effort: the dryout data was obtained under the annular flow condition at decay power levels. The heat flux was maintained at 12 W/cm^2 level. Then, the pump power was decreased three times, while the flow reduction was not clearly observed except for the last time.

The flow pattern transition from slug flow to annular flow occurred when the outlet thermocouple T-004 reached the saturation point. The first temporary dryout lasted for about 5 to 10 s like that observed in Run 37(35)LHF-220. The exit quality was 0.32 at this stage. The final pump operation led to a sudden flow reduction by which a violent dryout was induced at the wide region of the test section including the lower part of the heated section. The pin power was decreased since it was very dangerous. The tentatively estimated quality from the final step condition exceeded 2.0. However, this is a similar condition to that attained in Run 37(36)LHF-231 at 12 W/cm^2 power level, which was coolable under the slug flow situation.

Run 37(34)LHF-239

The experimental result is shown in Fig. 23. This is one of the typical runs which were terminated without observing the flow pattern transition from slug flow to annular flow. The regular oscillation of the pressure signal was observed. The peak value of the pressure pulse increased monotonously with increasing pin power. Being synchronized with the pressure oscillation, the pin surface temperatures oscillated also to reach a climax where the automatic scram circuit of the power supply became in operation due to dryout.

At the earlier power step of 9.85 W/cm^2, there appeared a special event that the flow pattern was probably going to be changed once or twice from slug flow to annular flow, viz. the pressure oscillation had a tendency of damping a little. However, such a tendency was broken soon by a certain unspecified reason and led to a disconnected pressure perturbation which was switched to a diverging pressure oscillation. The averaged exit quality at this setp was 0.22. It was very low, yet the temporary dryout began to be seen after this special event.

Residual runs

There are many interesting runs which are not shown here. The time series data of these runs are compiled in Appendix G.

3.2 Buoyancy controlled boiling behavior

The temperature and flow signals measured during the slug flow stage of Run 37(37)LHF-200, for instance, enable us to understand the buoyancy controlled characteristic behavior of the flowing vapor slug (since the 37G data were not rearranged into an appropriate form for the interpretation, the similar result of Run 37(36)LHF-123, i.e. the 37F series run, shown in Fig. 24 is used for discussions below).

Figure 24 shows the relation between the transient movement of boiling boundary at a specified horizontal plane near the top of the heated section and the transient behavior of the inlet flow oscillation. The void expansion phase and the void contraction/streaming phase are examined in detail of which the one cycle of the oscillatory boiling is composed. The event sequence can be broken down as follows:

(1) Flow stagnation
(2) Intensive vapor generation yielding rapid and almost isotropic void expansion
(3) Increase of natural circulation (mixed convection) flow
(4) Slow contraction of the void due to promoted convective heat transfer
(5) Slow streaming of the void to meet with an effectively cooled condition due to heat sink
(6) Vigorous vapor condensation yielding rapid void contraction and re-entry of the liquid column
(7) Flow oscillation with the mean flow being kept around a small positive value

These events seem to be repeated for a long time until the strong heat sink disappears from the test section.

For the dynamic movements of the vapor slug in the test section and the liquid columns located at the upper and lower positions of the test section, the flow inertia and the pressure drop characteristics of the loop play very important role. Nevertheless, the effects of the heat generation and heat sink are most important at an early stage of the slug flow, because the required time for a vapor slug to reach the effectively cooled condition, i.e. the inverse of the frequency of thermal-hydraulic oscillation, is thought to be dominated by these parameters. The oscillation frequency becomes constant, on the contrary, under the condition of loss of strong heat sink at the wide part of the test section. The constant value would be specified then by the loop characteristics. The detailed analysis of the results of depressurization boiling runs, the Run 37(35)LHF-220 for instance, would lead to a better understanding on this point.

3.3 Flow pattern transition

An accurate assessment of the flow regimes under given power and flow conditions is very important because the heat removal capability depends strongly on the flow pattern attained. As was suggested in the model of the buoyancy

controlled heat transfer, the heat transport is promoted in the case of slug flow comparing that in the case of annular flow by the factors: (1) the slug flow leads to the entrainment enriched condition owing to the repetitive turbulences of the liquid film around the pin surfaces; (2) the extra convective cooling is expected by the re-entering liquid column and by its evaporation both of which are synchronized with the oscillative behavior of the boiling boundary.

Using the limited mumbers of the operational data of those runs which were terminated after observing all patterns of bubble flow, slug flow, annular flow and dryout, the flow regime map was drawn. The result is shown in Fig. 25, where the inlet flow velocity at the bundle section and the total pin power are taken for horizontal and vertical axes, respectively, and the operational conditions reached at every boiling steps are plotted with several symbols defined to identify the observed flow patterns. The dash line connecting each symbol means the history of the operational steps of each run. The data from the 37F series runs are also added together with the data from the present experiments. The identification to each flow regime is based on the following:

(1) The transition from single-phase flow to bubble flow is identified by the appearance of irregular fluctuations in the measured pressure signals, and by the attainment of the saturation point in a certain temperature signal.
(2) The transition from bubble flow to slug flow is identified by the onset of the regular and cyclic oscillations in the pressure, flow and temperature signals, and by the appearance of the characteristic behavior that the temperature at the non-boiling region decreases to a certain extent during the flow pattern transition because of the promoted heat removal capability.
(3) The annular flow is easily distinguished by the decay of the oscillatory boiling to yield a stabilized and quiescent boiling. All kinds of signals become undisturbed like those at the single-phase flow. However, this transition sometimes takes long time until the developed annular flow condition is reached. Accordingly, for those steps whose operational conditions are changed in the midway of the slow transient, a new category "transition" is used for the flow pattern identification.
(4) The dryout, which is equivalent to the transition from annular flow to mist flow in the present case (see Appendix A and the discussions in section 3.4), is identified by the sudden temperature excursion beyond saturation point due to the inferior heat removal performance of the mist flow. Only when the automatic power scram circuit was triggered by the instant temperature rise up to 1000 °C, such a dryout was categolized into the permanent dryout, while the other cases were into the temporary dryout.

In Fig. 25, the flow regimes at the decay power levels (2 to 7 % rated powers of the full power of 580 kW) are not so definitely categolized, viz. the lower flow and lower power side of the figure was overlaid with various symbols. However, we shall note that there are many unplotted data at the region in question whose runs were terminated without observing the transition from slug flow to annular flow like the Runs 37(36)LHF-231 and 37(34)LHF-239. With the help of further investigation, the operational data and related information (the estimated exit quality, boiling onset point, and the observed flow pattern) of all dryout runs are summarized in Table 8 including those of 37F experiments. Here, the exit quality and the boiling onset point are estimated by the following bundle-averaged heat balance equations:

$$x_{exit} = 0.2388\ Q_B/U_o A\rho L$$
$$Q_B = Q_T - Q_{NB}$$

$$Q_{NB} = 4.187\ (T_{sat} - T_{in})\ U_o A \rho c_p$$
$$Q_T = Sq''$$
$$z_B = 450\ (Q_{NB}/Q_T - 1)$$

and the simplified equations of the sodium properties:

$$L = 3571.64\ T_{sat}^{-0.1991}$$
$$\rho = 950.1 - 0.22976\ T - 1.46E\text{-}5\ T^2 + 5.6E\text{-}9\ T^3$$
$$T = (T_{in} + T_{sat})/2$$

where,

- A : flow area = 9.24E-4 [m^2]
- S : heated surface area [m^2]
- q'' : heat flux [kW/m^2]
- U_o : inlet flow velocity [m/s]
- ρ : density [kg/m^3]
- L : latent heat [kcal/kg]
- c_p : specific heat = 0.3 [kcal/kg°C]
- Q : heat [kW]
- z : axial distance [mm]
- T : temperature [°C]

subscripts;

- B : boiling
- NB : non-boiling
- T : total

Judging from the data shown in Table 8, an intuitive conclusion may be reached that the flow pattern at the decay power levels is more likely to be slug flow rather than the annular flow. At least from the data of depressurization boiling runs, i.e. Runs 37(35)LHF-220 and 37(33)LHF-241 through 243, one can point out that the flow pattern is influenced by the pressure field and that the annular flow is reproduced easily under low pressure conditions.

The reason why the flow pattern transits from slug flow to annular flow has been considered within the frame of the stability problem of the large vapor slug generated within the pin bundle under low flow condition[2]. For both cases of slug and annular flows, the large voided core (vapor slug) in the pin bundle illustrated in Fig. 26 chokes major parts of the flow passages. The upper liquid column looks to be supported by the pressure of the voided core and the entering fluid at the inlet. It would be needless to say that the system like this is essentially unstable, especially when the inlet flow is very low to make effective the void surfacing force due to its buoyancy. In consequence, the stable annular flow would be allowable only under a certain restricted condition in the case of low flow.

From the scenario of the natural circulation boiling shown in section 3.2, one can understand that the important thermal-hydraulic factor to keep the two-phase flow within the slug flow regime is the presence of the axial distance between two regions: one is the heated region and another is the effectively cooled region. The void moved one-way only between these two regions. Meanwhile, a larger void can be created by a certain operational method which can connect these two regions directly by itself even if it does not stream like the flowing slug. At such a situation, and if the pressure field allows the large void to stay quiescently, it can be said that all conditions are sufficed and the flow pattern changes to the annular flow. From this sense, it would be reasonable to say that the key thermal-hydraulic properties for the void

stabilization would be heat generation within the void, heat sink (subcooling) of the surrounding sodium, and the pressure profile around the slug. When these parameters does not suffice the stationary heat and mass balance of the voided core, the slug would fall into oscillation to satisfy it on average. This is the similar idea to that introduced in the discussions of the stabilization of a single void trapped behind the planar blockage(37).

The present experiments apparently show that the flow pattern easily becomes stable (annular flow) under the condition of smaller mismatching of power to flow ratio when the flow rate is relatively high. The outlet sodium temperature is close to the saturation point at that stage. On the contrary, it does not rise to such a high temperature condition when the flow rate is low and the boiling pattern is oscillatory. Therefore, the reason why the annular flow is reached during the depressurization boiling runs even when the flow is very low may be ascribed to the non-existance of the strong heat sink at the upper unheated section of the pin bundle. In any way, the quantitative interpretation of the flow pattern transition problem is beyond the capability of the present study.

3.4 Annular-flow dryout model

The above discussions suggest that the instantaneous picture of the large vapor slug does not differ each other without regard to whether the flow pattern is slug flow or annular flow. The main carrier of the generated heat at the heated section would be entrained droplets. The mass balance of the liquid film would be also maintained through entrainment generation and deposition. This model is extensively analized for the usually working fluid as summarized in Appendix A and in the paper by Andreussi(38), for example. The situation is basically identical to the present sodium case. This model inevitably leads to the understanding that the dryout is equivalent to the transition of flow pattern from annular flow to mist flow, i.e. the enthalpy burn-out or the high-quality dryout. Therefore, a prediction of such a dryout should be based on the criteria tightly related to the enthalpy balance of the two-phase flow.

All of the annular-flow dryout data are correlated in Fig. 27 from the standpoint of using the thermal-equilibrium exit quality for the dryout prediction. The inlet flow velocity or the pin power is taken as the horizontal axis to see its possible relation with the dryout quality. As is implied from the high-quality dryout hypothesis (see Appendix A), the dryout quality does not depend directly on the pin power. Therefore, it would be logical to conclude that the local nonuniform power shape brings about no influence on the dryout quality. However, there still remains a possibility that the inlet flow velocity might be an influential parameter to the dryout quality. The experimental data is so densely gathered within the low flow region that it would be impossible to draw a definite conclusion on this point. From the present knowlege, it looks appropriate to recognize that the annular flow dryout would be predictable by a criterion which is expressed by $X_{exit} = 0.5$ on average for the power and flow ranges of interest. We shall note that the correlation $X_{exit} = 0.5$ is not necessarily a universal one for all bundles having different geometrical configulations, but might be a restricted one for the present experimental conditions.

A detailed look at the Fig. 27 indicates that there are excpetional cases of dryout conditions. There are a lot of temporary dryout data which are located around the flow pattern transition curve from slug flow to annular flow. The

dryout of this kind is induced by the short term flow instability occasioned during the flow stabilization process to the annular flow[2]. However, the temperature excursion resulted from this flow instability seems to be limited to low unless the exit quality does exceed the critical value of 0.5, while the short term flow instability occasioned under the condition of exit quiality being greater than 0.5 often leads to the onset of permanent dryout. In consequence, the high-quality dryout induced by the flow instability need not be distinguished from the annular flow dryout which appears under constant flow conditions.

3.5 Radial incoherency of dryout

At the stage where the exit quality is close to the critical value, almost all parts of the top plane of the heated section are highly dried to yield irregular temperature rises and falls over the saturated temperature level. However, the radial distribution of the excess temperature over saturation point does not remain constant during the dried time interval. In the case of the final step of Run 37(34)LHF-235, the dryout was initiated at the central region at the time 12.5 s before power scram, and the peak temperature increased monotonously for about 4.3 s to reach up to about 970 °C, with the dried region being expanded toward outer pin rings. The partial cooling of the central region and the further over-heating of the outer region occurred thereafter until the power scram was triggered. The most dried point was located around the pins three to five subchannel distance apart from the bundle center.

There was a tendency that the peripheral pins were damaged at the earlier operations than the central pins (see Fig. 16). It seems difficult to interpret this experimental fact in terms of local pin twist alone. These phenomena suggest the importance of the distribution and redistribution of entrained droplets for the prediction of dryout in a different bundle.

3.6 Post-dryout cooling

The examination of the heat transfer performance under the mist flow condition is also very important. The heat transfer coefficient becomes very low of course comparing that at the annular flow. The qualitative formulation cannot be obtained on this subject at present, while the effort will be directed to see how is the post-dryout cooling in the forthcoming study.

Table 8 Summary of the average exit quality and the boiling inception points estimated under steady heat balance assumption

Run No.	Q_T (kW)	U_o (m/s)	T_{in} (°C)	T_{sat} (°C)	x_{exit} (-)	z_B (mm)	Flow pattern	Dryout pattern
37(36)LHF-116	32.89	0.054	430.0	920	0.057	-117.9	NB	
	37.78	0.034			0.236	-268.0	bubble	
	40.25	0.100			-0.017	---	slug	
	49.97	0.109			0.003	- 9.1	"	
	58.49	0.036			0.419	-325.5	"	
	67.25	0.096			0.090	-161.4	"	temporary
	72.74	0.069			0.216	-258.2	"	"
	81.89	0.138			0.051	-109.2	transit.	
-117	40.91	0.069	394.8	942	0.032	- 68.5	slug	
	50.11	0.076			0.056	-106.9	"	temporary
	56.91	0.042			0.304	-283.0	"	"
	64.33	0.076			0.123	-182.7	"	"
	71.79	0.094			0.093	-153.7	"	"
	81.95	0.073			0.221	-248.4	transit.	"
-120	43.30	0.081	395.4	922	0.017	- 41.5	NB	
	49.45	0.045			0.218	-251.3	bubble	
	56.55	0.101			0.026	- 59.9	slug	
	72.46	0.144			0.006	- 15.9	"	
	86.98	0.137			0.053	-106.0	"	
	98.83	0.138			0.082	-145.0	"	temporary
	113.73	0.139			0.118	-183.1	transit.	
-121	65.10	0.119	385.7	922	0.018	- 42.9	NB	
	73.17	0.145			0.003	- 8.6	bubble	
	86.45	0.104			0.119	-182.0	slug	
	99.90	0.146			0.067	-124.5	"	
	110.96	0.160			0.070	-128.8	transit.	temporary
	129.07	0.182			0.076	-135.9	annular	
	144.98	0.121			0.249	-264.1	"	
	153.82	0.063			0.690	-358.8	"	temporary
-122	91.82	0.169	381.2	924	0.015	- 34.8	NB	
	101.50	0.178			0.024	- 54.5	bubble	
	115.34	0.192			0.035	- 74.6	slug	
	129.02	0.184			0.071	-128.4	"	
	140.25	0.098			0.329	-292.4	transit.	
	150.50	0.058			0.742	-363.1	annular	temporary
-123	104.00	0.205	369.9	921	-0.001	---	NB	
	113.37	0.226			-0.003	---	bubble/NB	
	131.10	0.233			0.019	- 42.2	bubble	
	146.74	0.262			0.018	- 40.3	slug	
	161.94	0.234			0.064	-118.4	"	
	171.60	0.078			0.597	-345.7	annular	permanent
37(34)LHF-124	19.12	0.039	454.1	920	0.023	- 58.5	NB	
	21.55	0.038			0.050	-111.7	bubble	
	29.14	0.032			0.173	-239.3	"	
	37.15	0.043			0.157	-227.8	"	
	48.34	0.083			0.056	-120.4	slug	
	61.29	0.069			0.165	-234.0	"	
	72.81	0.060			0.282	-291.8	"	temporary
	86.93	0.080			0.236	-273.4	transit.	"
	106.57	0.075			0.356	-314.9	annular	
	122.83	0.058			0.605	-359.4	"	permanent

Table 8 (continued)

Run No.	Q_T (kW)	U_o (m/s)	T_{in} (°C)	T_{sat} (°C)	x_{exit} (-)	z_B (mm)	Flow pattern	Dryout pattern
37(34)LHF-125	39.60	0.072	362.7	922	0.012	- 26.0	NB	
	43.16	0.075			0.020	- 44.8	bubble	
	56.24	0.069			0.105	-164.0	"	
	65.48	0.116			0.016	- 37.1	slug	temporary
	82.28	0.124			0.051	- 98.6	"	"
	97.94	0.097			0.174	-219.2	"	"
	110.00	0.112			0.164	-212.7	transit.	"
	128.30	0.096			0.289	-275.6	annular	
	149.84	0.059			0.714	-358.2	"	permanent
37(35)LHF-220	15.46	0.067	440.8	810	-0.039	---	NB	
	12.80	0.012		"	0.247	-305.0	annular	
	11.29	0.002		808	1.813	-422.7	"	permanent
37(36)LHF-230	7.20	0.016	410.5	918	-0.006	---	NB	
	9.65	"			0.049	-102.0	bubble	
	13.10	0.012			0.222	-257.5	"	
	16.38	"			0.319	-296.0	slug	
	19.63	"			0.415	-321.5	"	
	23.19	0.008			0.863	-377.5	"	
	26.39	"			1.006	-386.3	"	
	29.57	0.009			1.001	-386.1	"	temporary
	33.06	0.007			1.510	-405.5	"	"
	34.92	0.009			1.212	-395.9	"	"
	36.40	0.008			1.449	-403.8	"	"
	39.77	0.007			1.851	-413.0	"	"
	41.12	0.009			1.456	-404.0	"	"
	44.70	0.007			2.099	-417.1	"	"
-231	10.06	0.006	409.5	912	0.430	-325.7	NB	
	12.99	0.008			0.412	-321.8	bubble	
	19.20	"			0.686	-363.2	"	
	22.65	"			0.839	-376.5	"	
	29.06	0.007			1.306	-399.8	slug	
	32.88	0.006			1.777	-412.0	"	temporary
	36.11	0.005			2.395	-421.2	"	"
	39.31	"			2.620	-423.5	"	"
	43.33	"			2.906	-426.0	"	"
	45.87	"			3.087	-427.3	"	"
	49.71	0.004			4.239	-433.2	"	"
	52.63	"			4.497	-434.2	"	"
	57.71	"			4.948	-435.6	"	"
	63.18	"			5.431	-436.8	"	"
	69.20	0.003			8.007	-441.0	"	"
-232	9.18	0.016	456.7	911	0.057	-124.7	bubble	
	12.76	0.015			0.155	-230.4	"	
	17.69	0.011			0.426	-333.8	"	
	22.73	0.010			0.662	-367.7	slug	
	29.16	0.007			1.338	-405.1	"	
	35.92	0.008			1.453	-408.4	"	temporary
	43.08	"			1.772	-415.3	"	"
	45.16	0.009			1.641	-412.7	"	"
	49.64	0.007			2.382	-423.6	"	"
	53.93	0.005			3.698	-432.7	"	"
	62.08	0.008			2.620	-425.9	"	"
	66.10	0.011			1.996	-418.9	"	"

Table 8 (continued)

Run No.	Q_T (kW)	U_o (m/s)	T_{in} (°C)	T_{sat} (°C)	x_{exit} (-)	z_B (mm)	Flow pattern	Dryout pattern
37(34)LHF-233	18.71	0.050	462.5	918	-0.015	---	NB	
	24.67	0.048			0.035	- 86.2	bubble	
	27.59	0.046			0.066	-138.1	"	
	30.77	0.048			0.081	-158.2	slug	
	37.13	0.056			0.088	-167.7	"	
	46.18	0.055			0.152	-227.2	"	
	54.73	0.050			0.243	-279.1	"	
	61.70	0.055			0.253	-283.2	transit.	
	69.08	0.059			0.270	-290.2	annular	
	77.58	"			0.322	-307.7	"	
	83.88	0.055			0.397	-327.3	"	temporary
	92.57	0.050			0.514	-349.0	"	permanent
	(102.30)	(0.048)			(0.614)	(-362.2)	(")	(permanent)
-234	17.96	0.035	460.6	917	0.034	- 84.6	NB	
	24.99	0.039			0.080	-157.4	bubble	
	30.38	0.040			0.123	-203.2	slug	
	36.72	0.041			0.171	-240.6	"	
	43.62	"			0.231	-273.7	"	
	48.83	0.045			0.239	-277.2	"	
	55.43	"			0.291	-297.7	"	
	61.34	0.029			0.607	-361.3	annular	permanent
-235	12.58	0.034	456.6	915	-0.017	---	NB	
	19.27	0.035			0.047	-107.7	bubble	
	24.26	0.037			0.085	-162.6	"	
	29.82	0.038			0.131	-209.9	slug	
	36.75	0.040			0.178	-244.7	"	
	37.46	0.037			0.212	-263.8	"	
	36.79	0.025			0.376	-321.8	"	
	36.65	0.028			0.318	-306.0	annular	temporary
	"	0.006			2.032	-419.1	"	permanent
-236	15.60	0.046	499.7	914	-0.013	---	NB	
	18.25	0.044			0.014	- 41.8	bubble	
	21.51	0.038			0.068	-150.7	"	
	24.06	0.028			0.174	-253.0	slug	
	25.08	0.029			0.176	-254.3	"	
	24.56	0.028			0.180	-257.0	"	temporary
	24.15	0.027			0.186	-260.7	"	"
	24.40	0.026			0.202	-269.6	"	"
	24.31	0.029			0.166	-248.0	"	"
	28.01	0.031			0.190	-262.7	"	"
-237	14.00	0.031	459.9	915	0.013	- 35.7	NB	
	18.45	0.033			0.051	-115.1	bubble	
	22.39	"			0.094	-174.4	"	
	25.44	"			0.127	-207.2	slug	
	30.53	0.032			0.192	-253.9	"	
	36.16	0.033			0.243	-279.2	"	temporary
	37.33	0.029			0.312	-304.7	"	"
	37.20	0.022			0.456	-339.4	"	"
	37.06	0.017			0.630	-364.2	"	"
	37.10	0.016			0.680	-369.3	"	"
	36.82	"			0.674	-368.7	"	"
	36.65	0.015			0.725	-373.4	"	"
	"	0.012			0.943	-388.7	"	"
	40.65	"			1.062	-394.8	"	"
	43.82	0.010			1.417	-407.3	"	"

Table 8 (continued)

Run No.	Q_T (kW)	U_o (m/s)	T_{in} (°C)	T_{sat} (°C)	x_{exit} (-)	z_B (mm)	Flow pattern	Dryout pattern
37(34)LHF-238	16.37	0.037	457.0	916	0.008	- 23.44	bubble	
	19.60	"			0.039	- 93.51	"	
	27.69	0.041			0.091	-170.5	"	
	33.77	0.040			0.151	-226.5	slug	
	39.04	0.033			0.273	-290.5	"	
	44.79	"			0.335	-311.0	"	temporary
	52.66	0.039			0.332	-310.2	transit.	"
	58.53	0.041			0.360	-317.8	annular	"
	61.72	0.028			0.638	-364.4	"	permanent
	(65.40)	(0.026)			(0.749)	(-375.0)	(")	(")
-239	15.10	0.046	455.0	915	-0.033	---	NB	
	20.25	0.037			0.045	-104.2	bubble	
	24.62	0.033			0.116	-196.3	slug	
	30.78	0.030			0.216	-265.5	transit.	temporary
	34.70	0.026			0.326	-308.1	slug	"
	37.84	"			0.369	-320.0	"	"
	40.66	0.031			0.318	-305.7	"	"
	46.72	0.031			0.388	-324.4	"	"
	52.90	0.030			0.479	-342.7	"	"
	59.10	0.033			0.490	-344.4	"	"
37(33)LHF-240	13.35	0.039	481.4	914	-0.019	---	bubble	
	20.19	0.030			0.100	-186.7	slug	
	27.38	0.025			0.251	-288.2	"	
	29.90	0.023			0.325	-313.6	"	
	29.75	0.016			0.525	-354.7	"	
	29.60	0.012			0.743	-378.1	"	temporary
	29.00	0.009			1.013	-395.0	"	"
-241	9.16	0.031	456.1	809	-0.011	---	NB	
	17.73	0.032			0.078	-183.9	bubble	
	25.66	0.028			0.202	-289.0	slug	
	35.17	0.026			0.352	-341.0	"	
	44.75	0.031			0.383	-347.8	annular	temporary
	44.00	0.021			0.606	-379.6	"	permanent
-242	8.16	0.039	453.9	809	-0.042	---	NB	
	17.53	0.033			0.069	-170.4	bubble	
	25.82	0.008			0.994	-404.0	annular	permanent
-243	9.16	0.039	447.6	809	-0.035	---	NB	
	14.52	0.018			0.161	-262.6	bubble	
	24.49	0.014			0.484	-363.6	annular	permanent
-244	13.00	0.039	463.2	915	-0.028	---	NB	
	20.85	0.037			0.054	-120.8	bubble	
	26.09	0.033			0.135	-215.1	slug	
	34.50	0.034			0.215	-267.1	"	
	37.28	0.031			0.282	-295.6	"	
	35.56	0.024			0.382	-324.6	"	temporary
	35.23	0.022			0.425	-334.0	"	"
	35.16	0.020			0.481	-344.4	annular	permanent

Table 8 (continued)

Run No.	Q_T (kW)	U_o (m/s)	T_{in} (°C)	T_{sat} (°C)	x_{exit} (-)	z_B (mm)	Flow pattern	Dryout pattern
37(33)LHF-245	11.69	0.039	447.7	915	-0.045	---	NB	
	19.21	0.033			0.055	-119.7	bubble	
	30.16	0.032			0.184	-245.9	"	
	38.54	"			0.277	-290.2	slug	
	48.70	0.038			0.305	-299.8	"	temporary
	49.13	0.028			0.473	-340.3	"	"
	48.01	0.016			0.918	-385.9	"	"
	"	0.010			1.560	-409.9	"	"
	47.52	0.007			2.273	-421.7	"	"
	47.93	0.005			3.265	-429.9	"	"
	57.86	0.003			6.727	-440.0	"	"
-247	16.48	0.023	444.4	915	0.102	-179.6	NB	
	20.22	0.020			0.207	-258.3	bubble	
	27.65	0.018			0.394	-323.8	"	
	30.09	0.018			0.442	-334.0	slug	temporary
	29.80	0.008			1.173	-397.9	"	"
	27.42	0.004			2.460	-423.5	"	"
	27.69	-0.001					"	"
	27.26	-0.002					"	"
-248	11.89	0.039	474.0	916	-0.035	---	NB	
	23.61	0.036			0.091	-173.7	bubble	
	33.62	0.035			0.200	-261.3	slug	
	43.87	0.034			0.318	-309.5	"	
	53.32	"			0.418	-334.5	"	
	62.73	"			0.517	-351.8	annular	
	72.11	0.037			0.554	-357.0	"	
	71.50	0.029			0.739	-376.5	"	permanent
37(29)LHF-252	7.51	0.047	488.9	915	-0.082	---	NB	
	12.84	0.052			-0.050	---	bubble	
	19.14	0.050			-0.002	---	"	
	24.74	0.054			0.025	- 69.6	slug	
	30.18	0.042			0.119	-207.2	"	
	33.10	0.049			0.103	-191.8	"	temporary
	"	0.052			0.089	-176.0	"	"
	33.00	0.055			0.076	-159.3	"	"
	33.20	"			0.077	-161.2	"	"
	33.10	0.057			0.069	-149.7	"	"
	"	0.059			0.062	-139.2	"	"
-253	7.99	0.008	416.0	915	0.192	-243.3	NB	
	14.52	0.010			0.353	-307.8	bubble	
	19.78	0.009			0.617	-356.0	slug	
	24.94	"			0.821	-375.5	"	
	31.66	0.005			2.085	-417.4	"	temporary
	32.95	0.006			1.787	-412.4	"	"
	33.00	"			1.790	-412.5	"	"
	33.10	"			1.797	-412.6	"	"
37(26)LHF-261	9.14	0.009	479.6	915	0.222	-274.3	NB	
	18.24	0.010			0.512	-352.2	slug	
	28.53	0.014			0.588	-362.4	"	
	37.45	0.015			0.753	-378.5	"	temporary
	38.37	"			0.775	-380.2	"	permanent

Table 8 (continued)

Run No.	Q_T (kW)	U_o (m/s)	T_{in} (°C)	T_{sat} (°C)	x_{exit} (-)	z_B (mm)	Flow pattern	Dryout pattern
37(24)LHF-262	7.69	0.014	429.9	915	0.037	- 85.3	NB	
	12.99	"			0.172	-234.1	bubble	
	18.95	"			0.323	-302.0	"	
	25.06	0.015			0.436	-330.1	slug	
	29.79	0.014			0.599	-355.9	"	
Gas	"	0.012			(0.725)	(-369.3)	annular	
"	28.80	0.009			(0.980)	(-387.4)	"	temporary
"	28.36	0.004			(2.364)	(-421.7)	"	"
"	27.91	0.001			(9.770)	(-442.8)	"	permanent
37(20)LHF-263	20.88	0.019	390.2	915	0.217	-251.6	NB	
	24.95	0.016			0.380	-310.2	bubble	
	30.55	0.028			0.214	-250.2	slug	
Gas	30.73	0.035			(0.139)	(-201.7)	annular	
"	29.91	0.016			(0.508)	(-336.5)	"	
"	29.34	0.010			(0.886)	(-377.1)	"	
"	28.97	0.008			(1.125)	(-390.5)	"	
"	28.52	0.005			(1.877)	(-412.4)	"	permanent

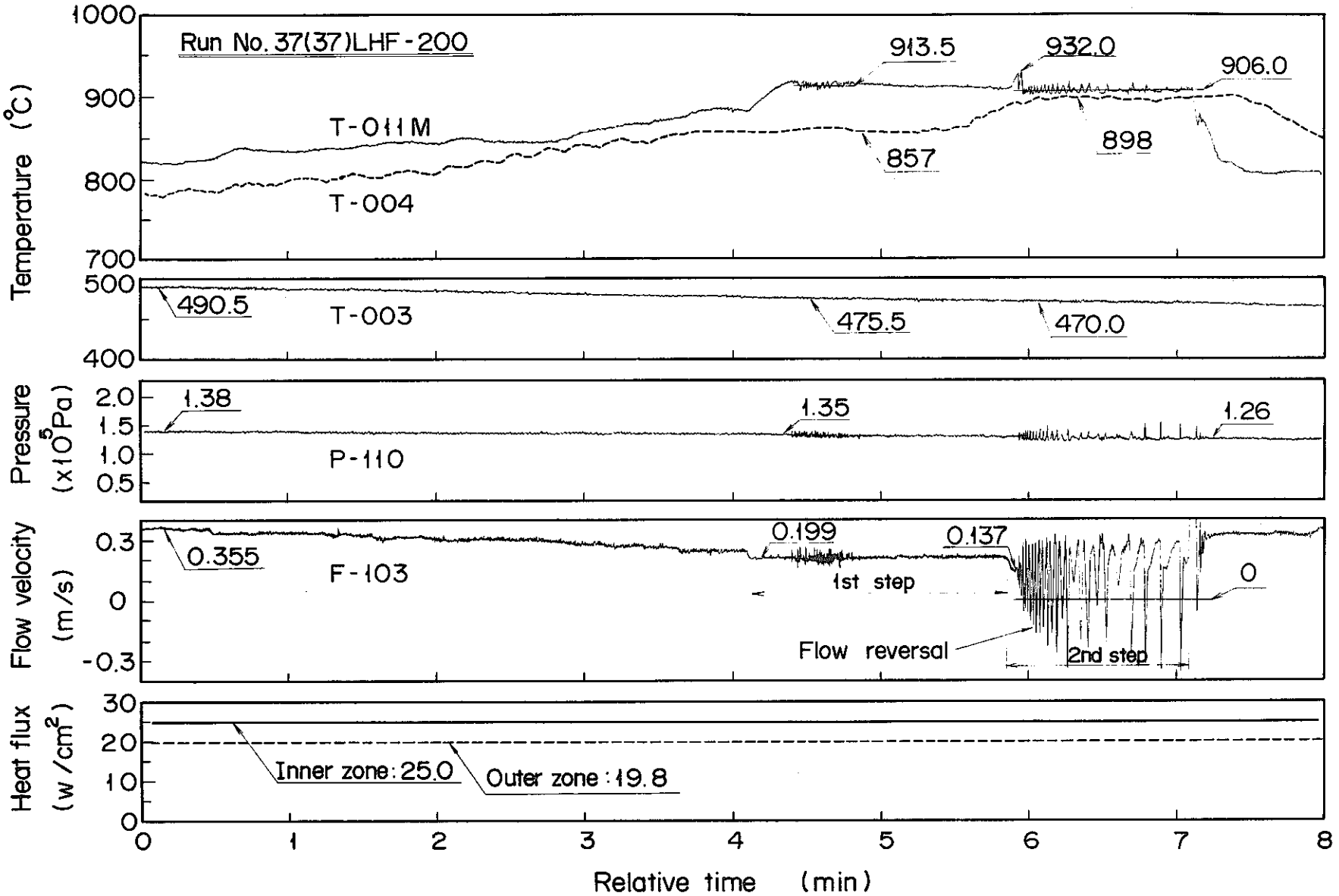

Fig. 17 Outline of the 37G low-heat-flux boiling experiments, Run 37(37)LHF-200

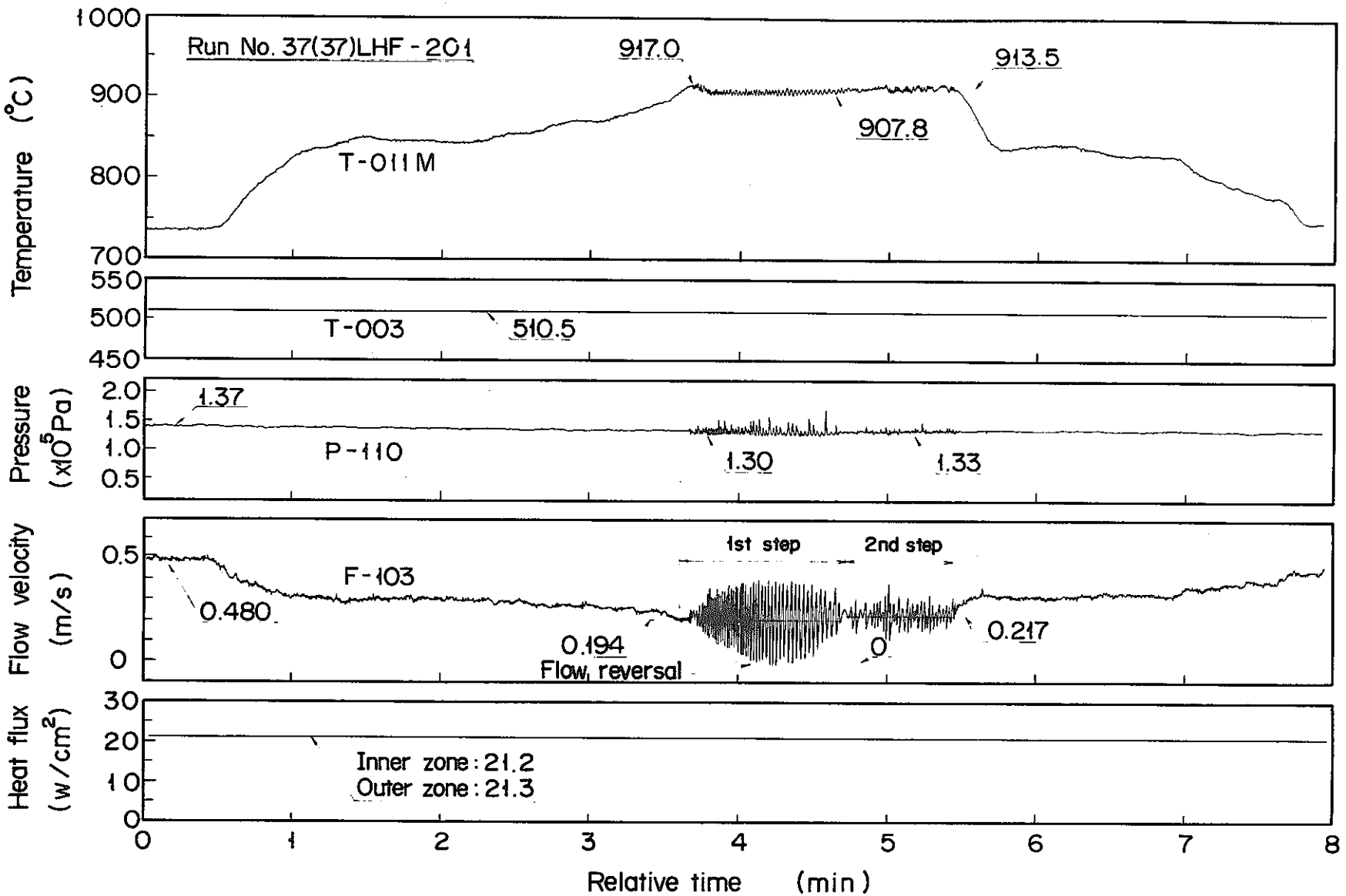

Fig. 18 Outline of the 37G low-heat-flux boiling experiments, Run 37(37)LHF-201

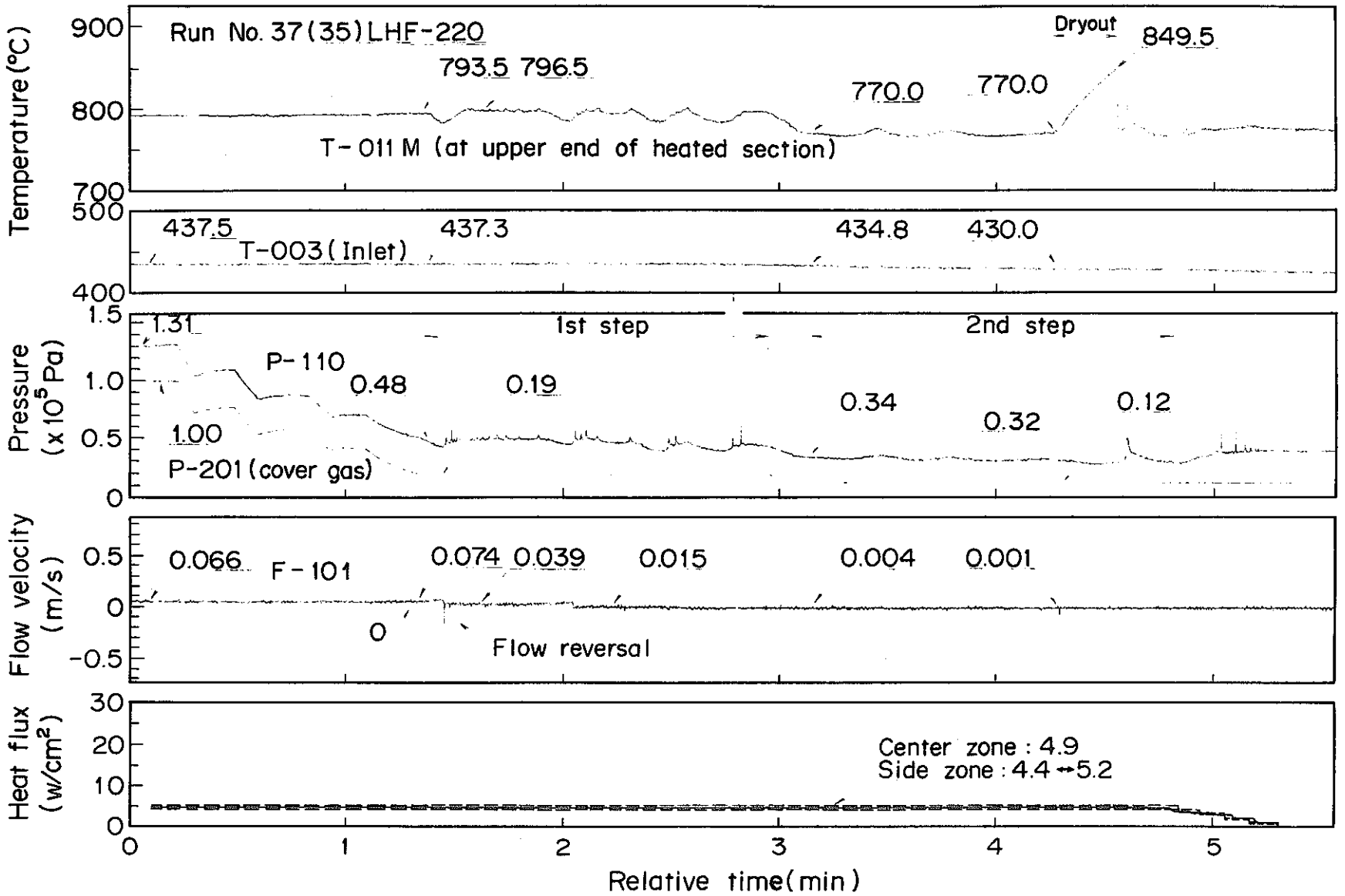

Fig. 19 Outline of the 37G low-heat-flux boiling experiments, Run 37(35)LHF-220

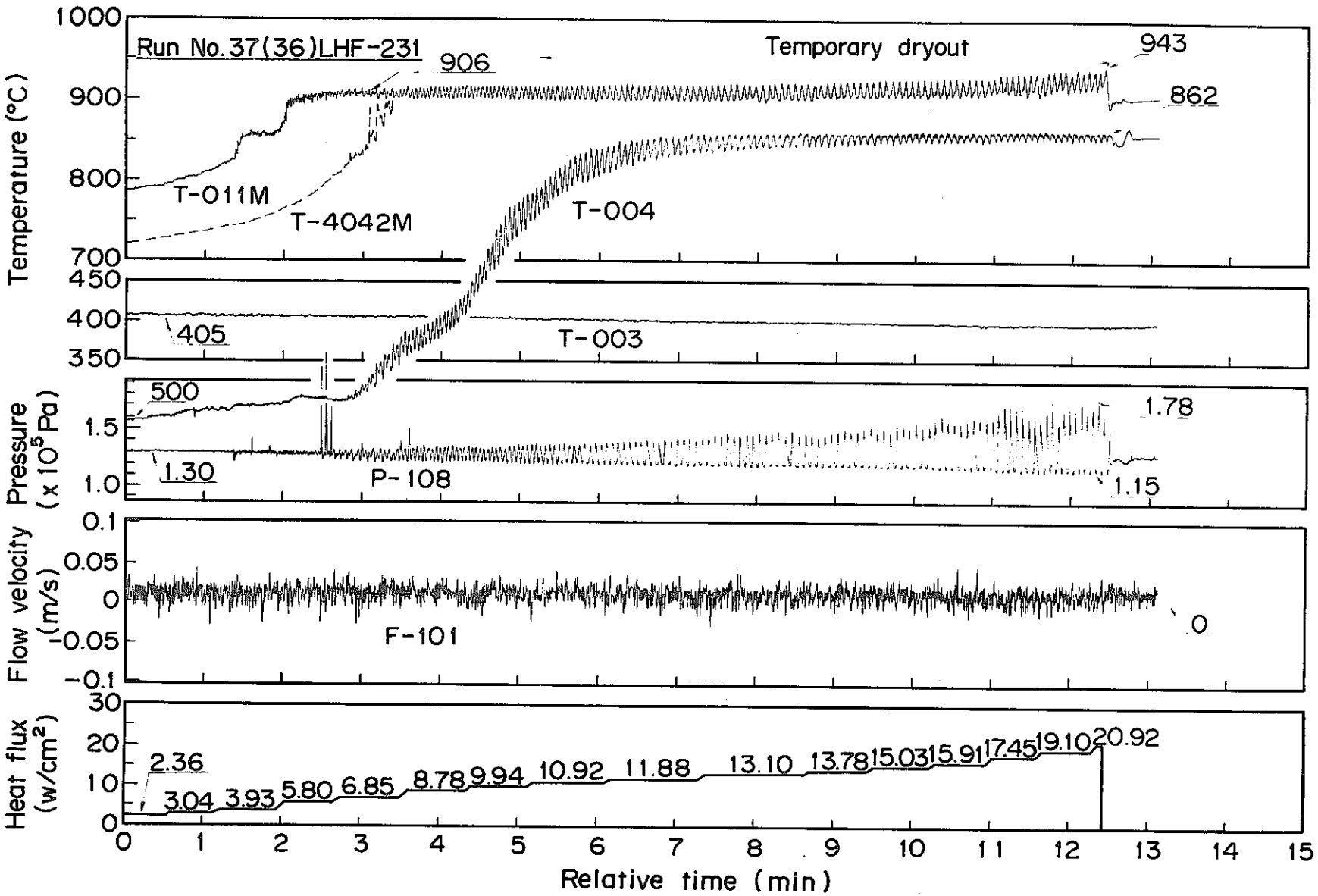

Fig. 20 Outline of the 37G low-heat-flux boiling experiments, Run 37(36)LHF-231

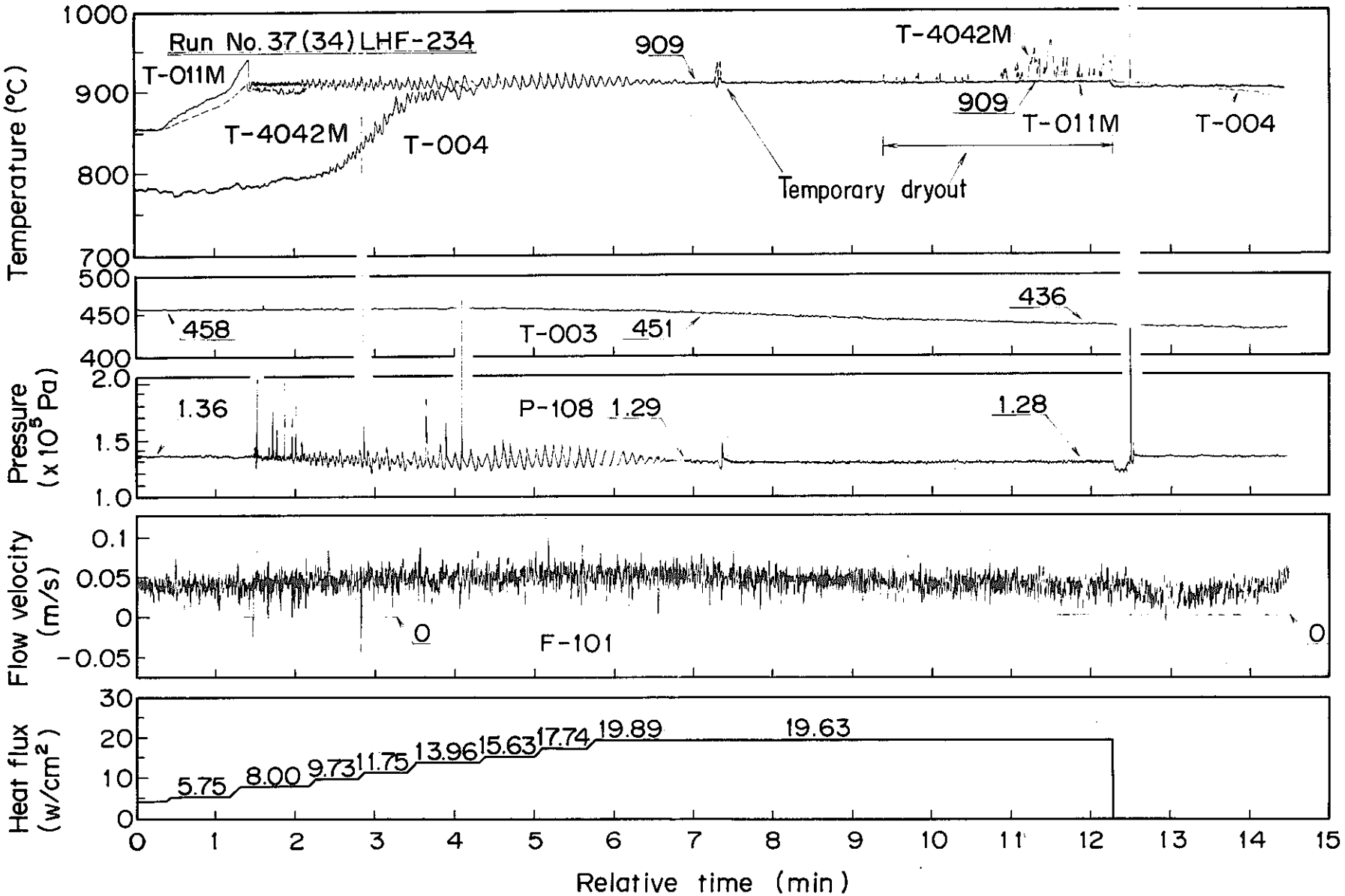

Fig. 21 Outline of the 37G low-heat-flux boiling experiments, Run 37(34)LHF-234

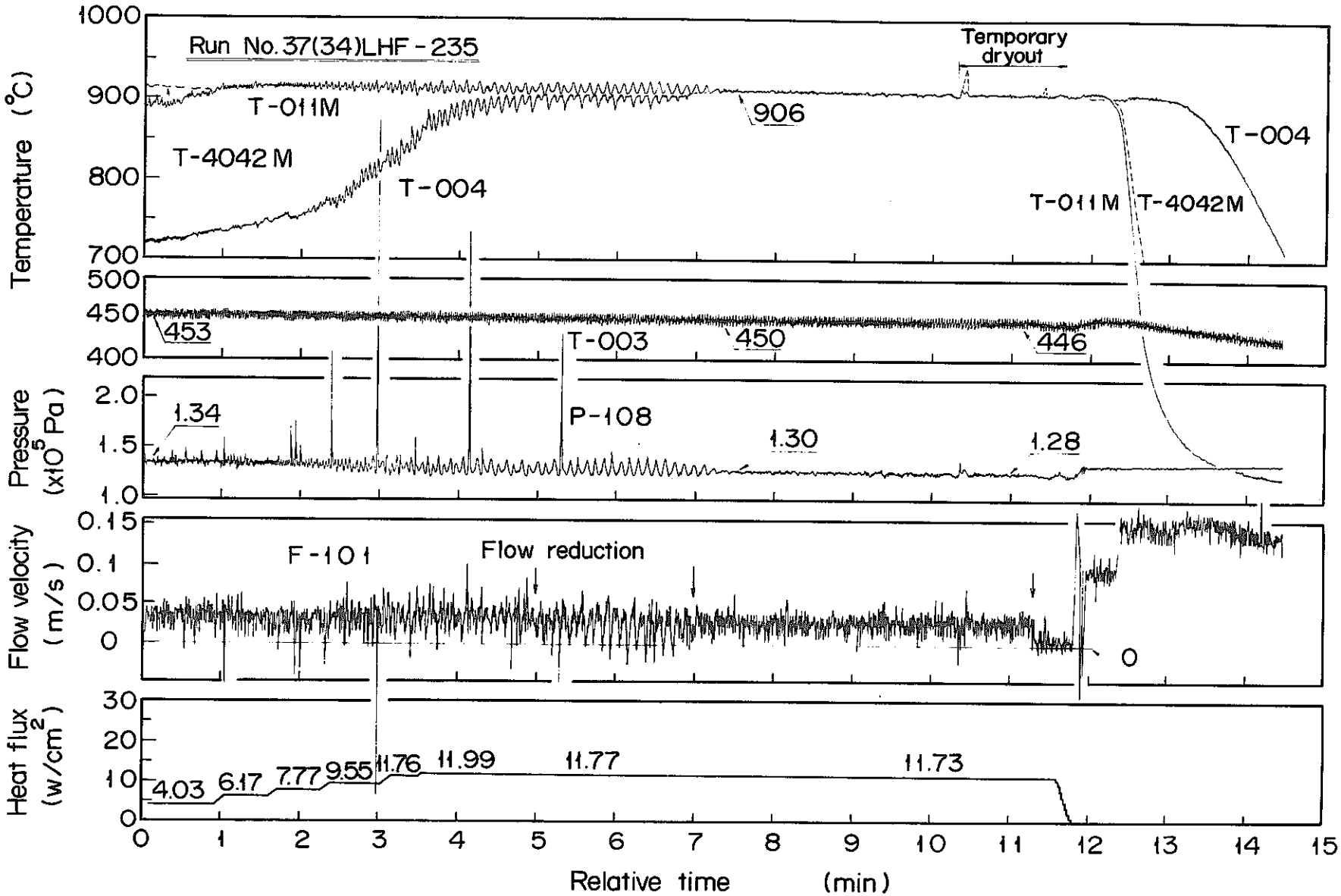

Fig. 22 Outline of the 37G low-heat-flux boiling experiments, Run 37(34)LHF-235

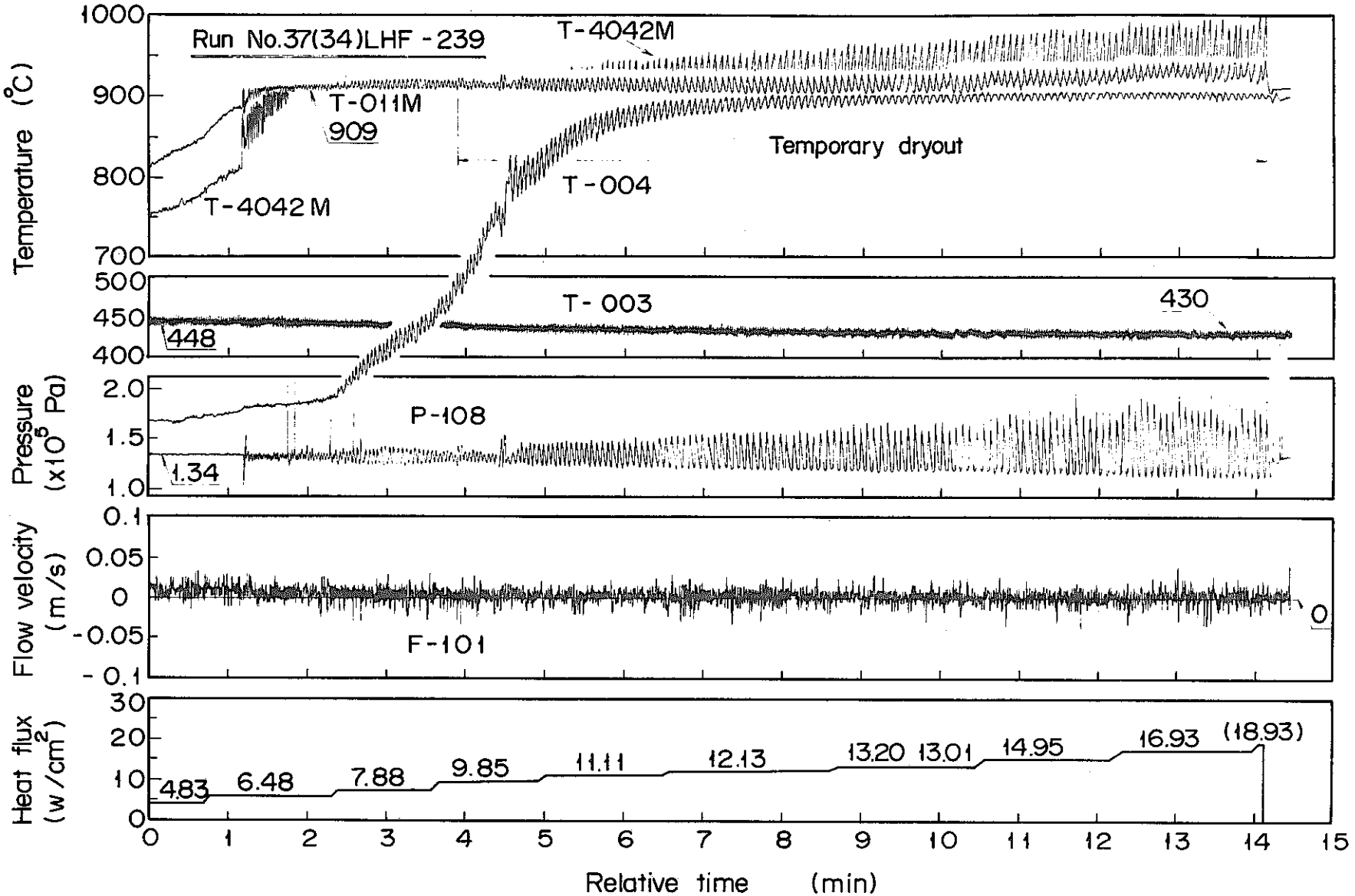

Fig. 23 Outline of the 37G low-heat-flux boiling experiments, Run 37(34)LHF-239

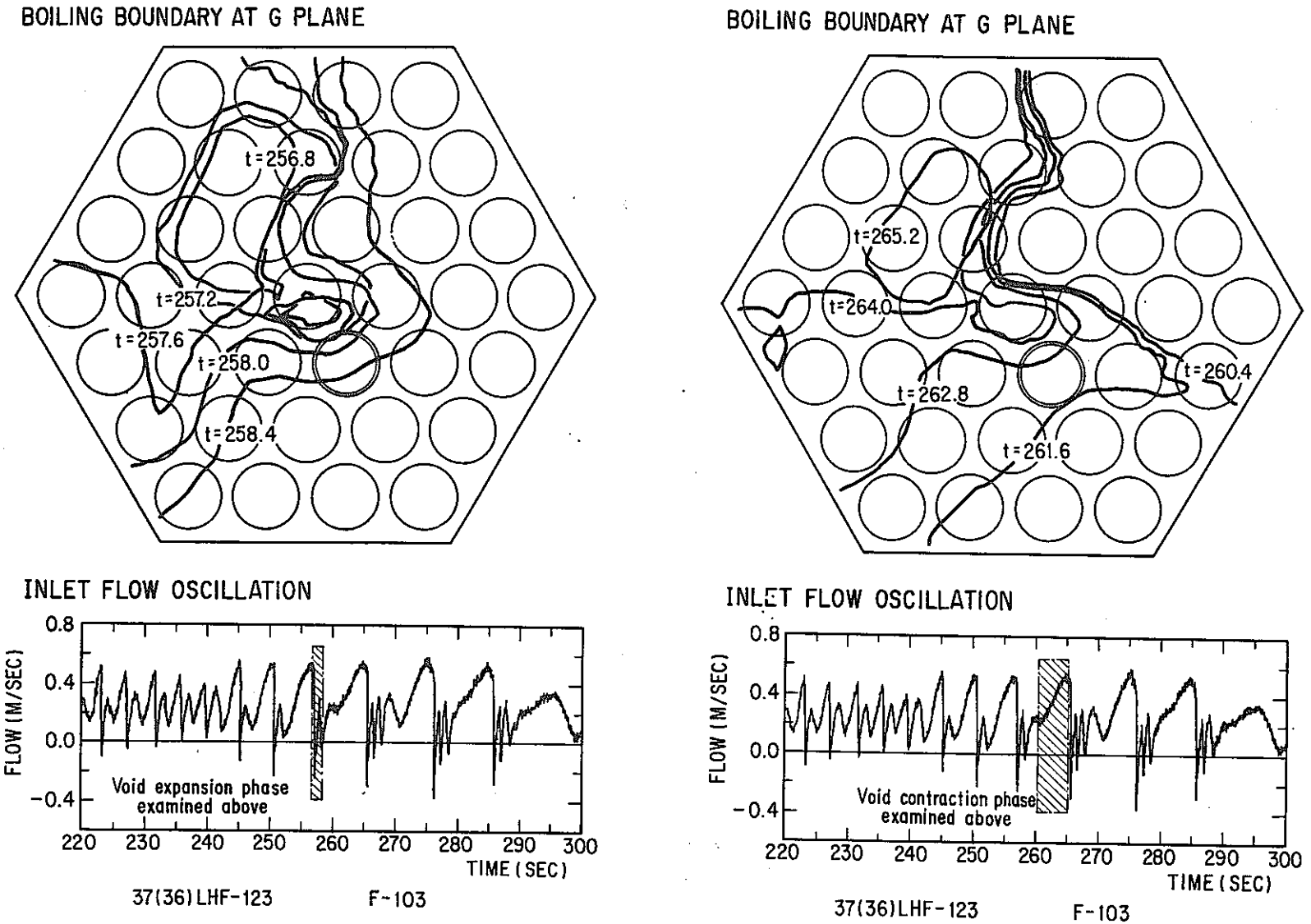

Fig. 24 Oscillation of the boiling boundary and the inlet flow velocity observed during the slug flow

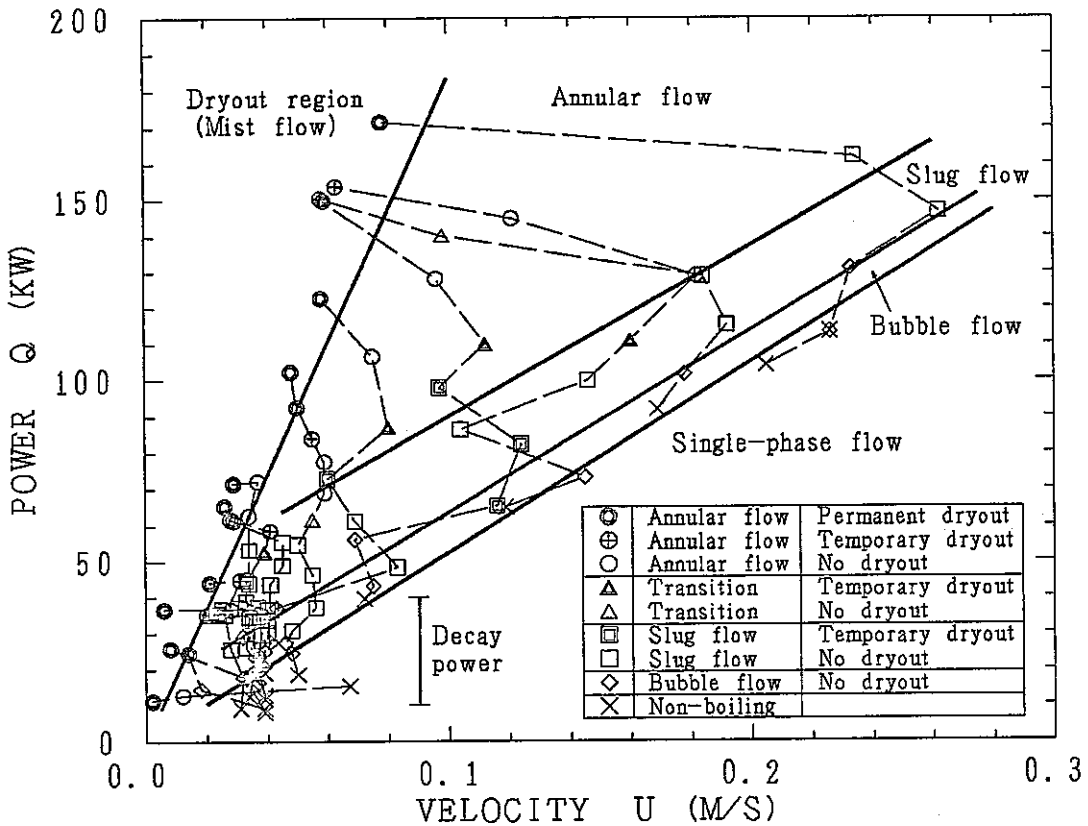

Fig. 25 Experimental conditions and flow pattern transitions

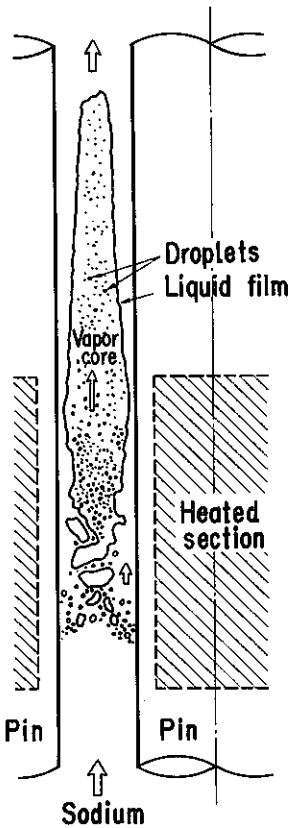

Fig. 26 Annular flow model

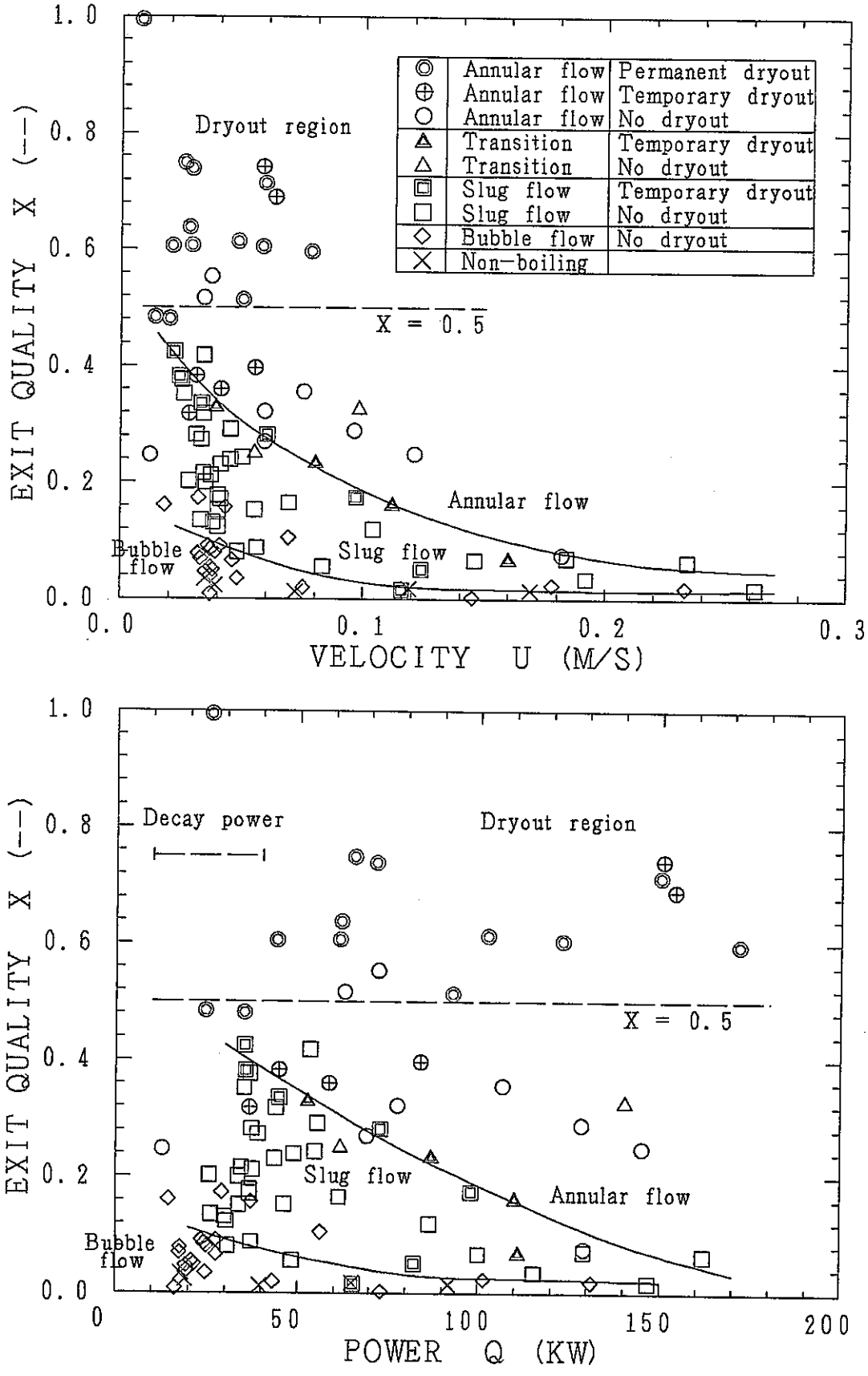

Fig. 27 Dryout criterion for 37F/37G configuration

4. CONCLUSIONS AND PROSPECTS FOR THE FUTURE

To examine the fundamental phenomena relevant to the low-heat-flux boiling and to obtain the knowledge on the decay heat removal capability are the objectives of the Decay Heat Sodium Boiling Test Program. The first item was focused in the 37F series experiments which were conducted under natural circulation condition. The second item was examined here with emphasis on the quasi-steady-state low-heat-flux boiling experiments conducted under weak forced convection condition using the SIENA facility and the 37G test section. The general views of these experiments and the special aspects of individual runs were examined based on the knowledges obtained from the 37F experiments.

Our efforts were directed to the derivation of the dryout data by which we can scope the critical condition of the decay heat removal. Dryout phenomena were recorded during 24 runs. The brief summary of these data revealed that the dryout conditions differed much depending on the two-phase flow pattern attained at the boiling crisis. Therefore, the flow regimes were first categolized using the map whose horizontal and vertical axes were flow rate and pin power, respectively. The flow patterns were simply classified there into bubble flow, slug flow, annular flow and dryout.

For the cases where the dryouts come into question, typical two flow regimes were identified, i.e. slug flow and annular flow. They were essentially equivalent to the unstable boiling and stable one, respectively. It was reasonable to consider that the dryout with stable boiling correspondeds to the transition from annular flow to mist flow. On the other hand, the dryout with unstable flow pattern appeared at the slug flow stage or the transition stage from slug flow to annular flow, where the brief dried condition was repetitively observed at pin surfaces covered by the vapor slug. For both cases, the dryout was ascribed to the lack of the deposition of entrained droplets which played an important role for the heat removal capability.

It was shown that the stable boiling had a coolability margin smaller than that of unstable boiling due to the shortage of the entrainment generation and to the absence of the extra convective cooling by the falling liquid column. For this case, a simplified dryout criterion was made available that the dryout would appear in the situation where the exit quality exceeds 0.5 in a 37-pin bundle.

Besides the interpretation of the experimental results, the effects of several key parameters on the dryout condition were studied using the available data of both sodium and the other working fluids. This exercise revealed that a prediction of dryout in terms of exit quality would hold in any case. This concept was based on the enthalpy balance in which the total power per unit flow area of a specified channel was a dominant parameter for the heat removal. Hence, the flow channel having a longer axial heated length in a larger pin bundle with smaller hydraulic diameter will eventually meet with severer condition than that tested in the present study. The above initial conclusion means that the effect of differing these parameters is well predictable in terms of exit quality only, for which further parametric studies should be conducted.

ACKNOWLEDGEMENT

The review work of the past 37F series experiments and the summary work of the present 37G series experiments have been conducted to meet with the increasing needs for the reliable data base which covers the area of low-flow and low-heat-flux sodium boiling. The authors wishe to express his acknowledgement to Drs. A. Watanabe, Y. Mimoto, K. Takahashi, and K. Haga for their efforts on executing the Decay Heat Sodium Boiling Test Program. The present experiments were completed with the help of Mr. A. Satoh. The data reproduction was supported by Messrs. T. Hasebe and M. Yoshino. The authers are deeply indebted to these contributors.

This report was prepared not only for the interium use in fast breeder reactor project programs in PNC but also for the information exchange between PNC and foreign organizations.

REFERENCES

(1) Haga, K. et al., "Sodium Boiling Experiment-13; Decay-Heat Level Boiling Experiment in a 37-Pin Bundle (in Japanese)," PNC SN941 79-84, Aug. 1979.

(2) Yamaguchi, K. and Haga, K., "Low-Heat-Flux Sodium Boiling Experiments with a 37-Pin Bundle (37F)," PNC SN941 83-129, Aug. 1983.

(3) Wantland, J. L. et al., "Dynamic Boiling Tests in a 19-Pin Simulated LMFBR Fuel Assembly", Transactions of the American Nuclear Society, Vol. 27, 1977, pp. 567-569.

(4) Wantland, J. L. et al., "Sodium Boiling Incoherence in a 19-Pin Wire-Wrapped Bundle," Proceedings of the International Meeting on Fast Reactor Safety Technology, Seattle, Aug. 1979.

(5) Garrison, P. W., Morris, R. H., and Montgomery, B. H., "Natural Convection Boiling of Sodium in a Simulated FBR Fuel Assembly Subchannel," Proceedings of the International Meeting on Fast Reactor Safety Technology, Seattle, Aug. 1979.

(6) Klein, G., and Dunn, F., "SAS3D Analysis of Natural-Convection Boiling Behavior in the Sodium Boiling Test Facility," Transactions of the American Nuclear Society, Vol. 33, 1979, pp. 517-518.

(7) Hinkle, W. D. et al., "LMFBR Safety and Sodium Boiling", Proceedings of ENS/ANS International Topical Meeting on Nuclear Power Reactor Safety, Brussels, Oct. 1978.

(8) Edit. Fast Reactor Safety Technology Management Center, Argonne National Laboratory, "U.S. Department of Energy Fast Reactor Safety Program, Progress Report Oct.-Dec. 1979," ANL/TMC 80-1, 1980.

(9) Kaiser, A., Peppler, W., and Straka, M., "Decay Heat Removal from a Pin Bundle," CONF-761005-517-7, 1976, pp. 1578-1586.

(10) Kaiser, A., Peppler, W., and Straka, M., "Investigations into FBR-Emergency Decay Heat Removal under Natural Convection and Boiling Conditions," ENS/ANS International Topical Meeting on Nuclear Power Reactor Safety, Brussels, Oct. 1978.

(11) Bergles, A. E., "Burnout in Boiling Heat Transfer, Part III: High-Quality Forced-Convection Systems," Nuclear Safety, Vol. 20, No. 6, 1979, pp. 671-689.

(12) Roko, S., "Flow Pattern and Heat Transfer of Gas-Liquid Two-Phase Flow, Part 2: Thermohydraulics and Dryout at High Quality Region (in Japanese)," 31th Lecture Conference of the Kansai Branch of the Japanese Society of Mechanical Engineers, 1977, pp. 19-33.

(13) Leung, J. C. M., "Critical Heat Flux under Transient Conditions: A Literature Survey," NUREG/CR-0056, ANL-78-39, June 1978.

(14) Katto, Y., "A Generalized Correlation of Critical Heat Flux for the Forced Convection Boiling in Vertical Uniformly Heated Round Tubes," International Journal of Heat and Mass Transfer, Vol. 21, 1978, pp. 1527-1542.

(15) Katto, Y., "A Generalized Correlation of Critical Heat Flux for the Forced Convection Boiling in Vertical Uniformly Heated Round Tubes -- A Supplementary Report," International Journal of Heat and Mass Transfer, Vol. 22, 1979, pp. 783-794.

(16) Katto, Y., "On the Heat-Flux/Exit Quality Type Correlation of CHF of Forced Convection Boiling in Uniformly Heated Vertical Tubes," International Journal of Heat and Mass Transfer, Vol. 24, 1981, pp. 533-539.

(17) Sheriff, N., "Possible Features of Sodium Boiling at Low Power," 9th Meeting of the Liquid Metal Boiling Working Group, Rome, June 1980.

(18) Gartside, C. H. et al., "Heat Transfer, Sodium Boiling and Fuel Pin Integrity after a Severe LMFBR Piping Failure", Symposium on the Nuclear Reactor Safety Heat Transfer, 1977 ASME Winter Annual Meeting, Atlanta, Nov. 1977.

(19) Gartside, C. H. et al., "Final Report on SLSF In-Pile Experiment P1, Volume I: General Operations and Post-Test Examination, Volume II: Simulation of an FTR Piping System Failure," ANL/RAS 77-29, 1977/1978.

(20) Gartside, C. H. et al., "The Sodium Loop Safety Facility," Nuclear Safety, Vol 19, No.3, 1978, pp. 339-355.

(21) Henderson, J. M., Rothrock, R. B., and Wood, S. A., "HEDL W-1 SLSF Experiment LOPI Transient and Boiling Test Results," Transactions of the American Nuclear Society, Vol 34, 1980, pp. 544-545.

(22) Henderson, J. M., Wood, S. A., and Rothrock, R. B., "HEDL W-1 SLSF Experiment LOPI Transient and Boiling Test Results," HEDL-SA-2012-FP, CONF-800607-74, 1980.

(23) Edit. Hanford Engineering Development Laboratory, "W-1 SLSF Experiment," USDOE/PNC Seminar, Tokyo, Nov. 1978.

(24) Dwyer, O. E., "Boiling Liquid-Metal Heat Transfer," American Nuclear Society, 1976.

(25) Akagawa, H., "Gas-Liquid Two-Phase Flow (in Japanese)," Korona-sha, 1974.

(26) Hewitt, G. F., "Critical Heat Flux in Flow Boiling," Proceedings of the 6th International Heat Transfer Conference, Vol. 6, Tronto, Aug. 1978, pp. 143-171.

(27) Bari, R. A. et al., "Accident Progression for a Loss of Heat Sink with Scram in an LMFBR," NUREG/CR-0427, BNL-NUREG-50910, 1978.

(28) Additon, S. L., and Bouchey, G. D., "Natural Circulation in FFTF," US/USSR Exchange Meeting on Fast Reactor Safety, HEDL-SA-1945, 1979.

(29) Perkins, K. R., Bari, R. A., and Pratt, W. T., "In-Vessel Natural Circulation during a Hypothetical Loss-of-Heat-Sink Accident in the Fast Flux Test Facility," ASME Winter Annual Meeting, 79-WA/HT-66, 1979.

(30) Khatib-Rahbar, M., Guppy, J. G., and Agrawal, A. K., "Hypothetical Loss-of-Heat-Sink and In-Vessel Natural Convection: Homogeneous and Heterogeneous Core Designs," Specialists' Meeting on Decay Heat Removal and Natural Convection in FBRs, BNL Upton, Feb. 1980.

(31) Agrawal, A. K. et al., "Dynamic Simulation of LMFBR Plant under Natural Circulation," CONF-790808-8, 18th ASME National Heat Transfer Conference, San Diego, Aug. 1979.

(32) Ribando, R. J., "A Comparison of Numerical Results with Experimental Data for Single-Phase Natural Convection in an Experimental Sodium Loop," CONF-790808-13, 18th ASME National Heat Transfer Conference, San Diego, Aug. 1979.

(33) Stevenson, M. G., et al., "Current Status and Experimental Basis of the SAS LMFBR Accident Analysis Code System," Proceedings of the Fast Reactor Safety Meeting, Beverly Hills, Apr. 1974, CONF-740401-p3, NTIS, Apr. 1974, pp. 1303-1321.

(34) Chen, J. C., Kalish, S., and Schoener, G. A., "Probe for Detection of Voids in Liquid Metals," The Review of Science Instruments, Vol. 39, No. 11, Nov. 1968, pp. 1710-1713.

(35) Isozaki, T., and Satoh, A., "Temperature Compensation Type Void Meter (in Japanese)," Letter of Patent, 55-p-6 (Japan), Aug. 1980.

(36) Ozaki, O, and Kimura, T., "REDNEC: Low Flow Sodium Voiding Analysis Code; Characteristics and Problem (in Japanese)," PNC SN941 81-204, Sep. 1981.

(37) Yamaguchi, K., Hakamura, H., and Haga, K., "Boiling and Dryout Conditions in Disturbed Cluster Geometry anf Their Application to the LMFBR Local Fault Assessment," Proceedings of the 2nd International Topical Meeting on Nuclear Thermalhydraulics, Santa Barbara, Jan. 1983.

(38) Andreussi, P., "Droplet Transfer in Two-Phase Annular Flow," Int. J. Multiphase flow, Vol. 9, No. 6, 1983, pp. 697-713.

Appendix A: Literature Survey on the High-Quality Dryout in Water

The status of the studies of dryout in high-quality convection systems of ordinary working fluid is reviewed to summarize the recent developments in this area. From a considerable numbers of literatures on this subject, only limited numbers of summary papers by Bergles[11], Roko[12], Leung[13], Katto[16], Dwyer[24], Akagawa[25], and Hewitt[26] were chiefly reviewed in this study.

A.1 Burn-out and dryout

The term "burn-out" is widely used to represent a sudden drop in boiling heat transfer coefficient due to a change in heat transfer mechanism, as indicated by an excursion of the heating surface temperature. The burn-out is characterized by "annular flow" and "lower critical heat flux". At a critical condition, the liquid film on the heated wall breaks down or is consumed for evaporation. Most of the past studies highlighted the information on burn-out in high-power system. The discussions on nuclear applications were, for instance, directed to the "unprotected" accidents such as the loss of flow (LOF) without scram accident and the transient over-power (TOP) accident. However, recent progresses in the studies of nuclear reactor safety relevant to the "protected" accidents, e.g. the loss of piping integrity (LOPI) accident and the loss of shut-down heat removal system (LSHRS) accident, have made clear the importance of the second less emphasized area.

A.2 General feature of heat transfer

The critical heat flux of burn-out has been correlated to the local heat transfer parameters having strong connections to heating surface conditions. This "local conditions hypothesis" means the disconnection between burn-out and two-phase flow regime. The situation is just in reversal for the high-quality dryout: the two-phase flow regime governs the phenomena.

As shown in Fig. A.1, the flow regime in a vertical evaporator channel changes widely from liquid single-phase flow to vapor single-phase flow. Depending on the transitions of flow regimes, specific parameters such as the heat transfer coefficient, quality, coolant temperature and wall temperature behave like those illustrated in Fig. A.1. The break down or disappearance of the liquid film on the heating surface is a possible event for the annular and annular-mist flow regimes, where the thin liquid film receives heat from wall and evapolates from its surface to remove the added heat. Naturally, the generated vapor streams toward the channel center to form a high-speed vapor core flow due to the abrupt volume change associated with the phase change. When the vapor velocity exceeds a certain critical value, the shear stress acting at the film surface forces the film to become wavy, i.e. the onset of film instability. After that, the wave front is mechanically sheared off to form fine liquid droplets in the vapor core, i.e. the entrainment generation. This situation is identical to the regime transition from annular flow to annular-mist flow. In the annular-mist flow region, the entrained droplets can partly deposit onto the film surface. However, the film thickness will be further

reduced and will become zero at last.

Several appoaches have been taken to obtain further detailed information on the heat transfer mechaism at the onset of dryout. Bergles et al. examined the film thickness by the resistive probe method and related it to the quality and the appearance of dryout. Bennet et al. measured the flow patterns by the X-ray and drawn a flow regime map. Doroshchuk et al. correlated the appearance of dryout with the measured quality. Hewitt et al. made an extensive examination on the relations between multi-variables such as the film flow rate, heat loading amount, film break point and appearance of dryout. Roko et al. also examined the transition of flow regime. The results of these studies are summarized in Fig. A.2 from the standpoint of correlating the onset of dryout with the transition of flow regime from annular-mist flow to mist flow.

In Fig. A.2, the solid line represents the transition condition of flow regime from annular-mist flow to mist flow (disappearance of the liquid film) drawn by Bennet et al., the broken line is an empirical formula by Doroshchuk et al. expressing the relation between flow rate and dryout quality, and the data shown by various symbols are the experimental results of the disappearance of liquid film obtained by Bergles et al.. From these results, it seems reasonable to correlate the onset of dryout with the disappearance of liquid film. In addition, the argument of correlating it with the condition that the film flow rate becomes zero is prevalent, on the basis of the experimental results by Hewitt et al..

The liquid film flow rate is theoretically formulated by means of the mass balance which takes into account the generation of liquid droplets, their re-deposition and the evaporation of liquid film. The generation rate of droplets E_e is derived from the analysis of the stability of waves existing on the film surface. The evaporation rate of liquid film E_v is calculated by dividing the heat loading rate by the latent heat of film evaporation. The deposition rate of droplets E_d is obtained as a solusion of the turbulent diffusion equation of free droplets, where the radial distribution of droplet concentration and the diffusion coefficient of the free droplets are assumed, on the basis of experimental data, as expressed by a certain function (the radial distribution of the droplet concentration at the upstream region of the annular-mist flow is a concaved one having a minimum concentration at the channel center, while the minimum value tends to rise gradually as the coolant flows downstream). The factor that the diffusion of droplets is not free but is directed opposite to the evaporating vapor stream from the film surface toward the channel center must be taken into account (the droplet deposition rate is thereby reduced from that in the absence of vapor evaporation). It has been tried to formulate this factor by introducing a hypothetical generation rate of droplets E_b into the mass balance equation. The above discussion leads to the following expressions for the balance equations of the mass flow rates of film flow G_f and entrainment G_e.

$$dG_f/dz = - \pi D \ (E_e - E_d + E_b + E_v)$$

$$dG_e/dz = \pi D \ (E_e - E_d + E_b)$$

where, πD means the heating surface length normal to the axis of the flow channel. Figure A.3 illustrates the result of an example calculation conducted by Yanai for the evaporation channel, i.e. the system having increasing quality in the downstream axial direction, in which typical tendencies in variations of

the entrainment generation rate, deposition rate, film flow rate and entrainment flow rate in the core flow are clearly identified. In the cited case, dryout appears at x = 0.62. The flow regime at the downstream region next to the dryout point is a mist flow, where the total entrainment flow rate is formulated by $G_e = (1 - x)\ G_o$ and decreases monotonously. Incidentally, in the case of the analysis of tansient phenomena such as a pipe break accident, a correction term for the transient change in film thickness δ proposed by Kirby et al. is occasionally introduced in the balance equation of the film flow rate. This modification is employed in interpreting the experimental information that the application of the steady dryout condition to a transient case leads to a conservative assessment as compared with a direct evaluation from the experimental data (there are also opposite data, in this connection, which show that the dryout condition does not differ from each other in both the steady and the transient cases).

Apart from the above model, there are different models proposed by Belda et al. and Whalley et al., respectively. These are the other expressions oriented from different approaches, owing to the fact that the means of evaluating key variables, i.e. the entrainment generation rate, for instance, are not established yet. Therefore, these models are not explained here.

A.3 Factors influencing the high-quality dryout

On the basis of the studies for the causes of the high-quality dryout and the nature of the thermal-hydraulic phenomena at dryout, the following factors are conceivable as influencing the high-quality dryout: the quality, flow pattern, entrainment generation rate, liquid film thickness, boiling section length, inlet subcooling (inlet quality), channel geometry, heat flux distribution, pressure and flow rate. The local heat flux, though it is related to the evaporation rate of liquid film, may not be so significant in the range of low heat flux. This is readily seen in the relationship between critical heat flux and quality shown in Fig. A.4 after Levitan et al. for an evaporation channel. In the figure, the region where the critical heat flux does not depend on the quality means a high-quality dryout region in question. In such a region, the critical heat flux must be predicted by a roundabout way as follows: It must be first grasped how the dryout quality x_d (which becomes constant over the wide range of heat flux) is influenced by various key parameters, e.g. the mass flow rate, system pressure and so on. Then, based on the derived information, the quality which gives rise to the dryout under a certain operating condition can be estimated. Finally, the value of heat flux leading to such a dryout quality condition is known from the thermal equilibrium calculation for the boiling channel. In the region of local heat loading burn-out, however, such a heat flux is ordinarily obtained from an empirical formula giving directly the critical heat flux. So, there are some empirical formulae, by Macbeth and Biasi et al., for instance, which also correlate the critical heat flux for high-quality dryout with key variables like those for the local heat loading burn-out.

In Fig. A.4, the pressure and flow rate are treated as parameters influencing the dryout quality x_d. The effects of such parameters on the dryout quality are described below qualitatively. For those factors which cannot be correlated with the dryout quality, the description will be treated later based on how they directly influence the critical heat flux.

(a) Effect of the flow rate

At higher flow rates, the dryout quality becomes low. In this case, the critical heat flux becomes of course high. This fact means that the transition from annular-mist flow to mist flow occurs under relatively low enthalpy condition. Typical data obtained by Roko et al. are shown in Fig. A.5. The general tendency of x_d against G_o can be explained in terms of the relation between the dryout and the stability of the annular liquid film or the amount of generated entrainments: At higher flow rates, the relative speed of the liquid film and the vapor flow becomes larger. Consequently, the shearing force at the film-vapor interface grows larger, increasing the amount of entrainments which are dispersed from the liquid film into the vapor core. On the other hand, the amount of the deposition of entrained droplets does not increase pronouncely comparing with the growing generation of entrainments. With the total entrainment flow rate thus being large (i.e. with low quality), there occurs, therefore, the break down of the liquid film. In various empirical formulae, the dependency of the dryout quality on the flow rate is expressed by the exponential decay functions in the range of about $G_0^{-0.3}$ to $G_0^{-0.7}$.

(b) Effect of the pressure

The dryout quality becomes to take a maximum value at a certain value of system pressure. It decreases at both higher and lower presssures from this maximum level. The experimental data by Roko et al. are shown in Fig. A.6. A similar explanation to that in item (a) is possible for the effect of pressure on the dryout quality. When the pressure rises, both of the kinematic viscosity and the surface tension of the liquid film decrease to enhance the instability of the liquid film. On the other hand, the relative speed of the liquid film and vapor decreases corresponding to the increasing density of the vapor. This factor helps to increase the stability of the liquid film. These two opposite effects co-exist in mutual competition. In consequence, the dependency of the dryout quality upon the pressure becomes complex, as indicated in the figure. Therefore, the expressions of this dependency are widely varied in various empirical formulae.

(c) Effect of the length of boiling section

In general, the transition from annular-mist flow to mist flow in an evaporation channel takes place under higher quality condition than in the case of the unheated channel. This is probably because all parts of the evaporation channel are equivalent to the "entrance" region of the developing convection system, while the flow is a fully developed one in the case of unheated tube, viz. the experiments are conducted under developed flow condition. If it is assumed that the similar consideration is permitted also for the length of the boiling section, i.e. short or long, the dryout quality should be higher in a short boiling section where the two-phase flow cannot be grown sufficiently as in the case of low flow. However, the empirical formula by Tong et al. shows that the tendency is even the reverse. Judging from the data, the effect of the length of the boiling section on the dryout quality can be concluded as being negligible.

(d) Effect of the inlet subcooling (inlet quality)

In the empirical formula by Biasi et al., there is a description concerning the inlet subcooling. The results of trial calculations reveal, however, that

the resulting differences in dryout qualities are essentially negligible. Furthermore, the effect of the inlet subcooling is not observed in most of the experimental data. Only in a special case of two-phase flow having high inlet quality which is already close to or higher than the dryout quality of a subcooled flow, the dryout quality becomes larger than that in inlet subcooling case. As an example, the experimental data by Doroshchuk et al. are shown in Fig. A.7. The reason for the appearance of the effect of inlet quality may be as follows: Even when the two-phase flow having high quality is fed to the inlet of the heated channel, there would be a microscopoic liquid film of extremely small thickness in the vicinity of the inlet. This thin film would disappear after passing over a certain length of the heated section, giving rise in the dryout quality.

(e) Effect of the channel geometry

A larger diameter channel lowers the dryout quality to some extent, while, according to the empirical formula, the dryout quality is inversely proportional to the 0.07 to 0.15 power of the channel diameter. The effect is, therefore, negligible practically.

The experiments with the tubes of a steam generator also indicate that the dryout data do not depend on the heat loading rate. Figure A.8 shows the data at GE (General Electric Co.) and at ANL (Argonne National Laboratory) which are reported by Wolf et al.. In the figure, the broken line is a correlation for the dryout in an evaporation channel shown in Fig. A.4 by the vertical line by Levitan et al., and the solid line is a correlation for tubes by Wolf et al.. A glance at the figure reveals the presence of an evident difference between two correlations without regard to whether or not the data scattering is taken into account. The reason for the difference is, however, unknown. These two correlations are considered to be valid in the region of high flow. For the region of low flow, on the contrary, the validity is questioned by Roko et al., for instance. Therefore, it is not elucidated yet whether the difference between the cases of single tube and multi-tubes also holds in the region of low flow.

Many experiments are conducted with an annular channel, i.e. the simplest configuration which can give a prospect of applying the results to a pin-bundle system. However, the experiments are few which show the tendencies described in items (a) through (d) as a characteristic nature of the high-quality dryout, i.e. the experiments are mostly directed to examining the heat loading burn-out. Ivashkevich et al. found that the dryout quality for the case of annular channel in which a central pin is heated is about 1/1.5 of that evaluated for the evaporation tube. For the annular channel in which the wall is also heated, Jensen et al. and Becker et al. reported that the dryout quality varries with the percentage of heat loading rate to the wall, and that there is such a radial heat flux distribution as gives a maximum dryout quality under specific conditions. Yücel et al. and Collier et al. conducted experiments with rectangular ducts heating one, two, or four walls presumably to examine the essential effects of unheated walls on the dryout quality. It is already pointed out that there is a tendency that the dryout occurs under less severe thermal condition when there exist unheated walls in the channel than when the walls are all heated. The classical burn-out experiments at GE, i.e. the 3 x 3 pin bundle experiments by Polomik et al. are very familiar. However, pin bundle experiments confirming this tendency in the area of high-quality dryout (the steady-state dryout experiments at low flow and low pressure) are not performed yet as far as the scope of the present review work is concerned.

In the pin bundle experiments, there are complicated factors which are probably influencial on the dryout, such as a spacer, pin displacement and radial distribution of heat loading rate. They are taken into consideration for the case of heat loading burn-out i.e. in a W-3 correlation, a Babcock/Wilcox-2 correlation, and so on. However it has not been settled yet whether or not the following findings for the case of heat loading burn-out are also applicable to the high-quality dryout: the displacement of pins gives essentially no influence on the dryout condition up to the extent where the pins fall nearly in mutual contact; the radial power grandient of up to ten percents or more gives also no effect.

(f) Effect of the heat flux distribution

The relation with the radial power distribution was described above. It is, therefore, examined here how the dryout quality is in the case of chopped-cosine axial power shape, comparing with the case of uniform heat loading. Figure A.9 shows typical data reported by Doroshchuk et al. for an evaporation channel (single tube), where the broken lines represent predictions from an empirical formula by Levitan et al. for the uniformly heated tube. Evidently, the heat flux which defines the boundary between heat loading burn-out and high-quality dryout is extremely lower than in the case of the uniform heating by about 50 to 60 % according to the data by Doroshchuk et al.. Nevertheless, the dryout quality at high-quality dryout region is essentially the same as in the uniform heating case. The similar results are obtained in many other experiments including those by Remizov et al.. The experiments by Becker et al. conducted with an annular channel whose central pin is heated nonuniformly also give no effect of the heat flux distribution. Incidentally, the pin bundle experiments by Hill et al., in which the heat loading is changed for a short time as a spike, did not lead to the dryout. These findings would be resonable from the fact that the high-quality dryout is governed mainly by the cumulative results of phenomena taking place at the upstream region from the dryout point (i.e. by the entrainment generation and its deposition), and is free from local disturbances.

(g) Effect of the other factors

An important factor to be considered first is the problem of the flow instability. We cannot discard the possibility that this problem, which has confused the interpretation of the past burn-out data, might also affect the interpretation of the high-quality dryout data through introducing such phenomena as a carry-over or carry-under of the liquid droplets (these phenomena brought about bad effect on the heat loading burn-out by lowering largely the critical heat flux). Up to the present, the problem of the flow instability has not been studied much for the low flow and low pressure system enough to be discussed in this review study.

The information of dryout conditions at transients should be summarized. In connection with the safety evaluation of a Loss-of-Coolant Accident (LOCA) of light water reactor, the pin bundle experiments and mock-up experiments of a full-scale assembly are conducted with empases. Numerous analyses of the experimental results have been conducted using the codes such as RELAP and COBRA. In conclusion, the view is prevalent by the analytical workers that it is possible to predict the occurrence of dryout in respective subchannels of a pin bundle system by means of empirical formulae for steady state (e.g. the W-3 correlation), while there are uncertainties in the evaluation of cross flow

mixing or turbulent flow mixing by the calculation code. However, we must further consider the transient behavior of the flow configuration itself, such as the concept of the transient change of film thickness by Kirby et al., in cases as follows: the causes of the misleadings are to be explained that the code predicts fairly earlier occurrence of dryout than observed in the experiment, or the dryout did not take place while the occurrence is anticipated by the calculation; the situations of the flow stagnation and some reversal flow conditions are to be examined. The results of the evaluations by the codes are more or less conservative when various empirical formulae derived on the basis of steady-state data are applied in the analyses of the transients.

A.4 Range of the application of high-quality dryout data

The dryout data examined so far are mostly rather in the ranges of high pressure and high flow. Figure A.10 is a parameter map of typical experiments for examining high-quality dryout. It is the same figure as prepared by Roko et al.. The region of interest is a lower pressure and lower flow region, i.e. about one order of magnitude below the tested region by Roko et al.. Consequently, the problem still remains how the conclusions given already will be in such a lower region (in the present survey study, the description of the empirical formulae were, therefore, limited only to the required ones in order to evade needless confusion). On the other hand, the volume of documents in this area is increasing remarkably in recent years. So, it is expected that the data under lower flow and lower pressure conditions will be available in the future. If such data are concerned with the flow construction, the phenomena of high-quality dryout will be grasped in more detail and clearly.

In the present study, the fluid models intending for the extrapolation of the results with water to different fluids (for example, approaches by Ahmad based on a classical dimensional analysis and by Katto who introduced quite different dimensionless quantities in his correlation scheme) were not taken up. Under the present situation of little experimental data on sodium, it would be, however, epoch-making if the knowledge and information on water can be utilized quantitatively through such models. Much is, therefore, expected in advance in this field of fluid models.

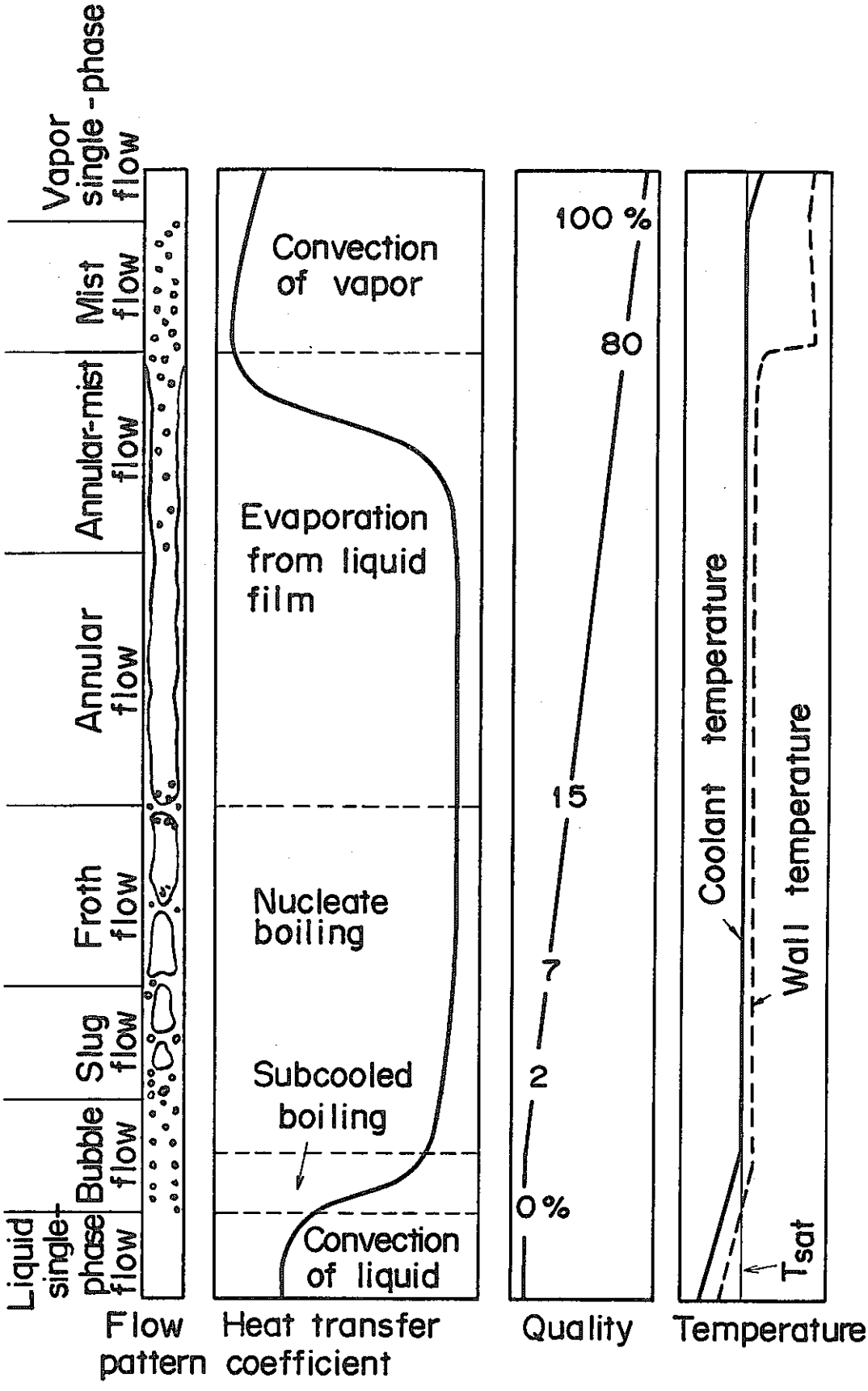

Fig. A.1 Conceptual figure for the relation between flow pattern and heat transfer

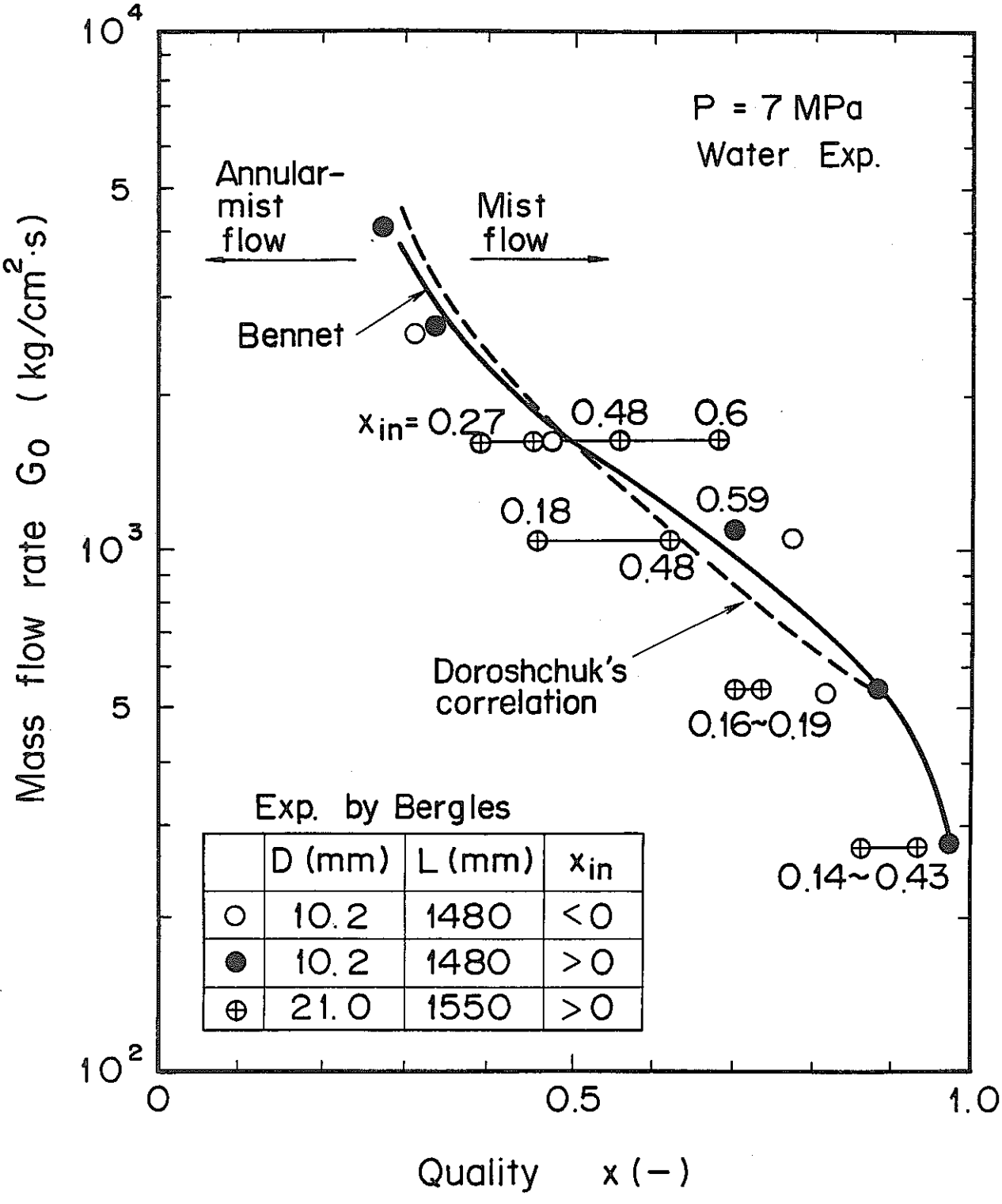

Fig. A.2 Boundary of annular-mist flow and mist flow (after Akagawa)

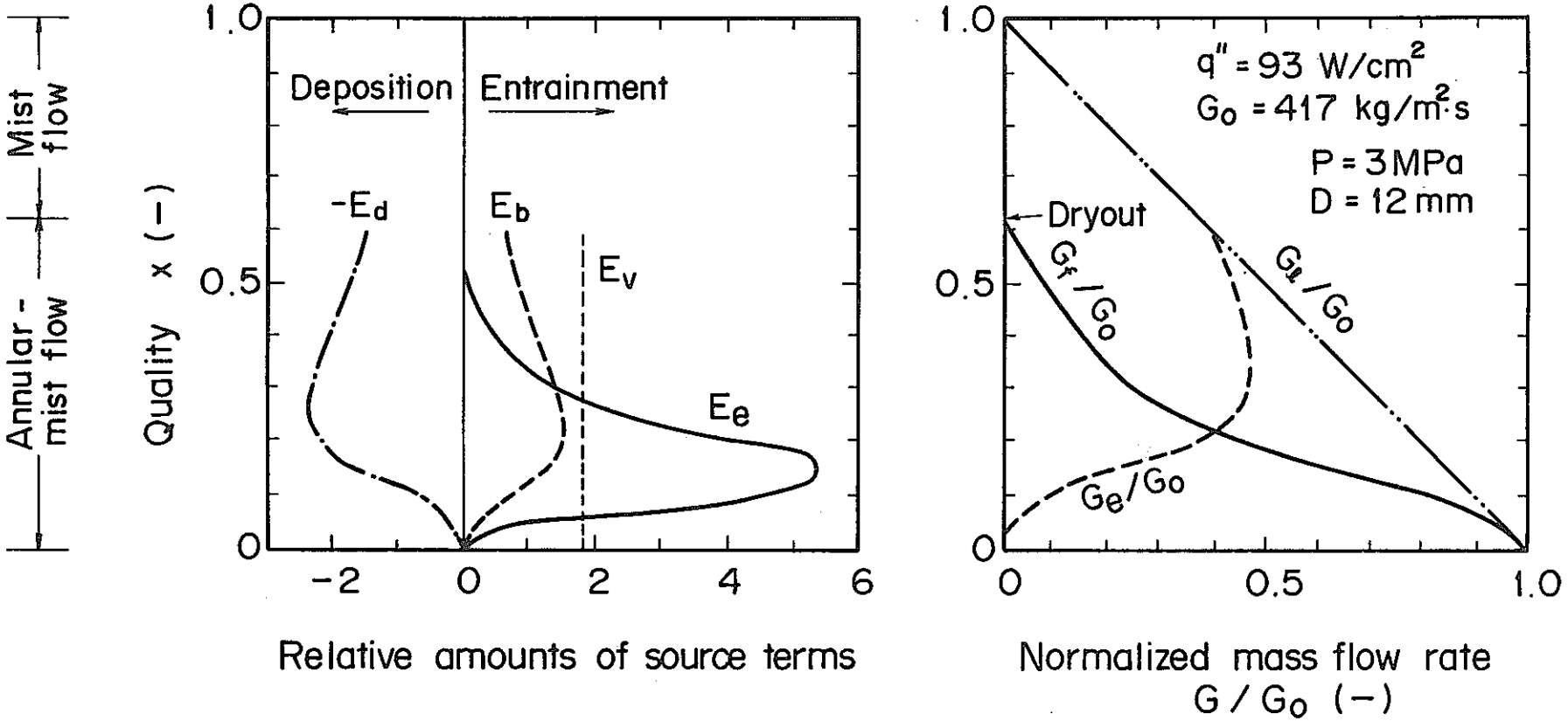

Fig. A.3 Typical result of the calculation of mass balance equation (after Yanai)

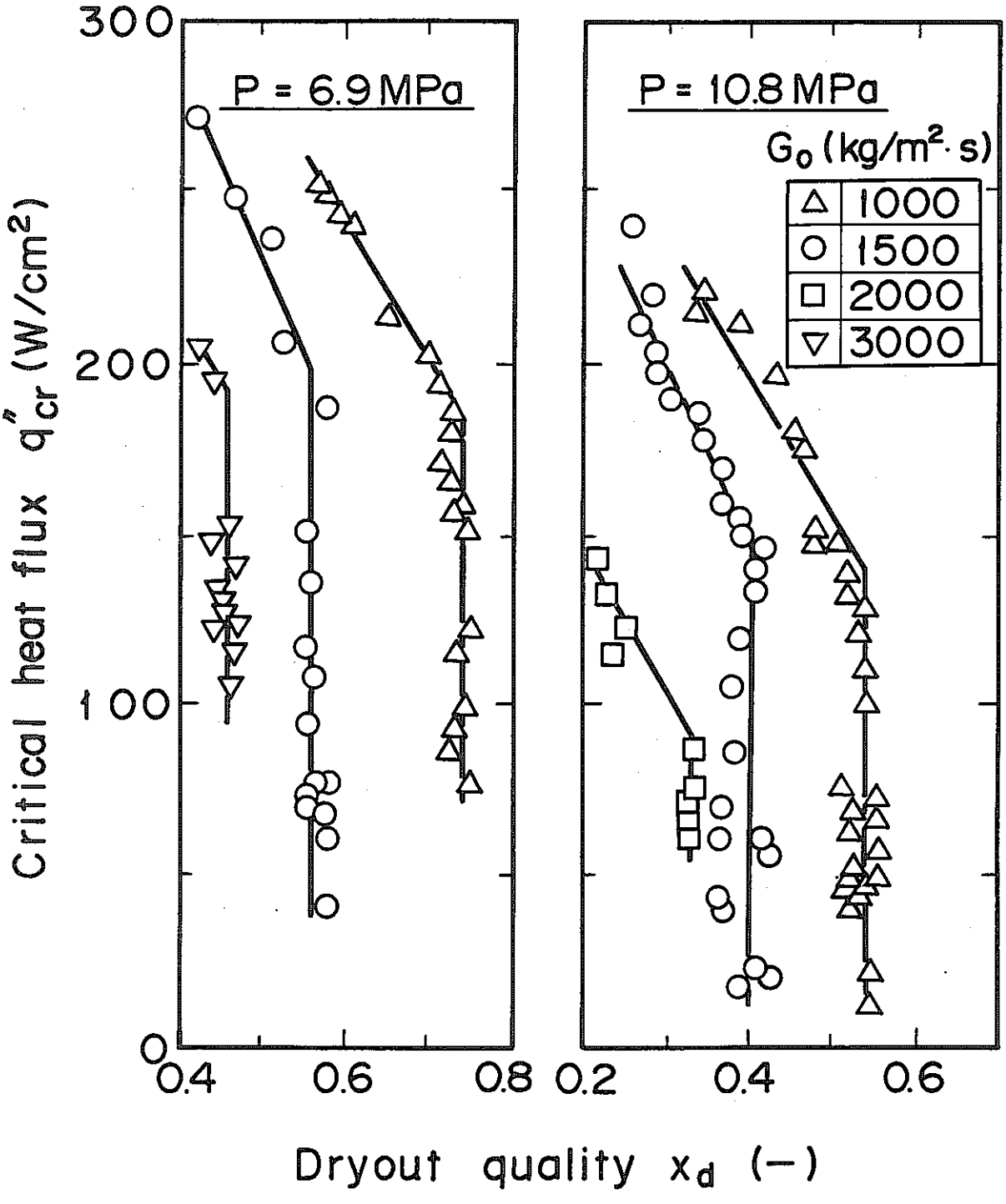

Fig. A.4 Typical high-pressure critical heat flux data for uniformly heated tubes (after Levitan et al.)

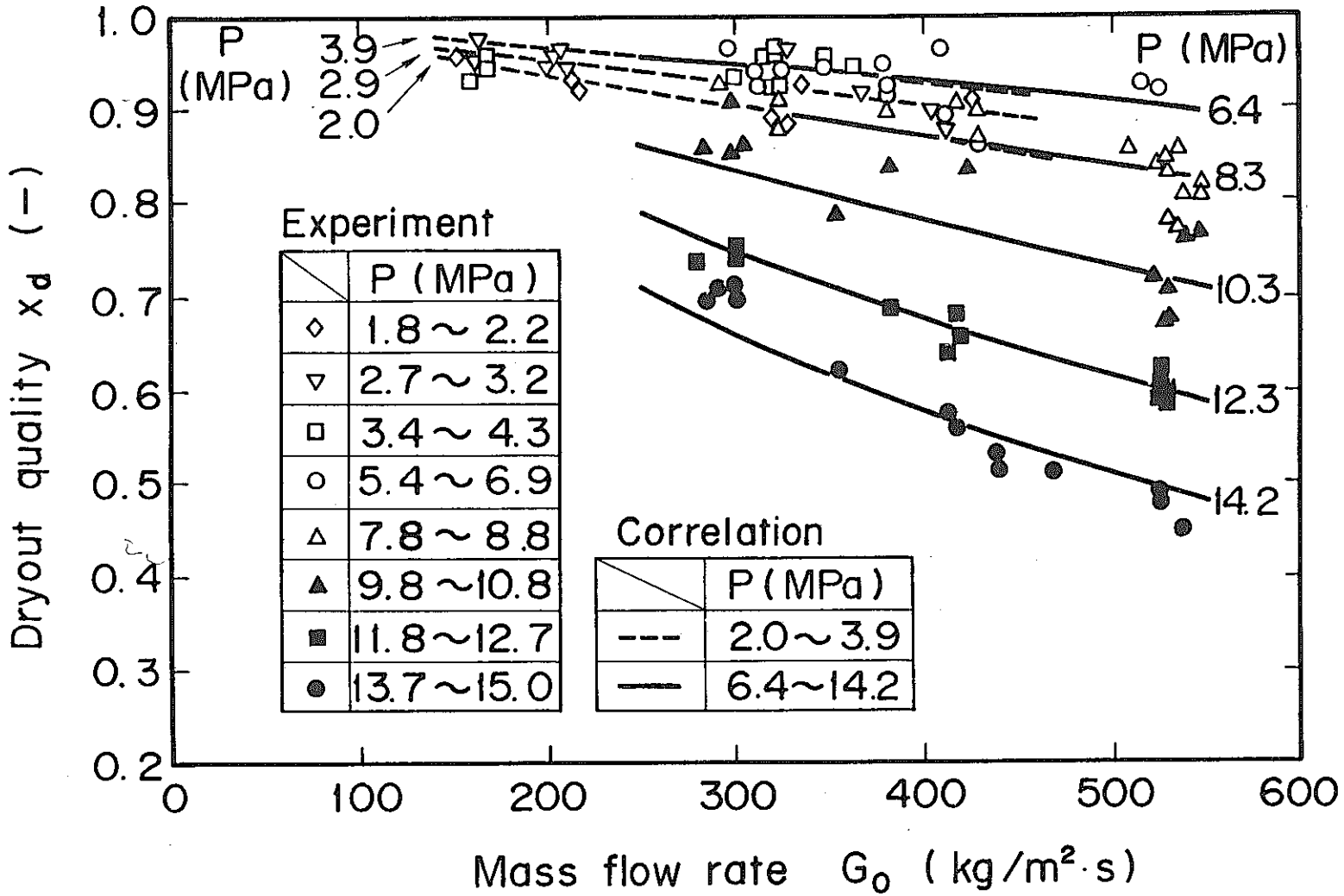

Fig. A.5 Effect of mass flow rate on the dryout quality (after Roko)

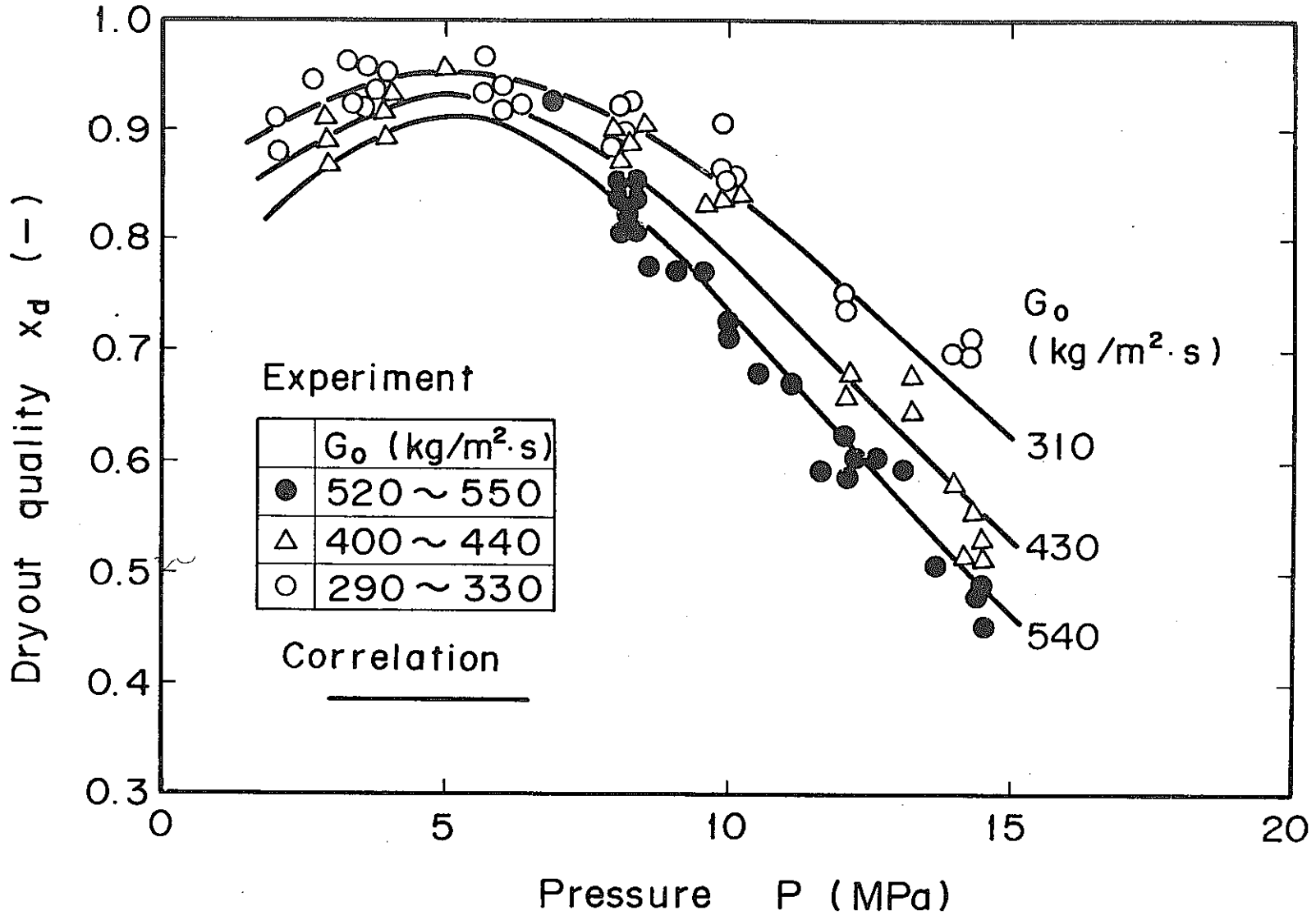

Fig. A.6 Effect of pressure on the dryout quality (after Roko)

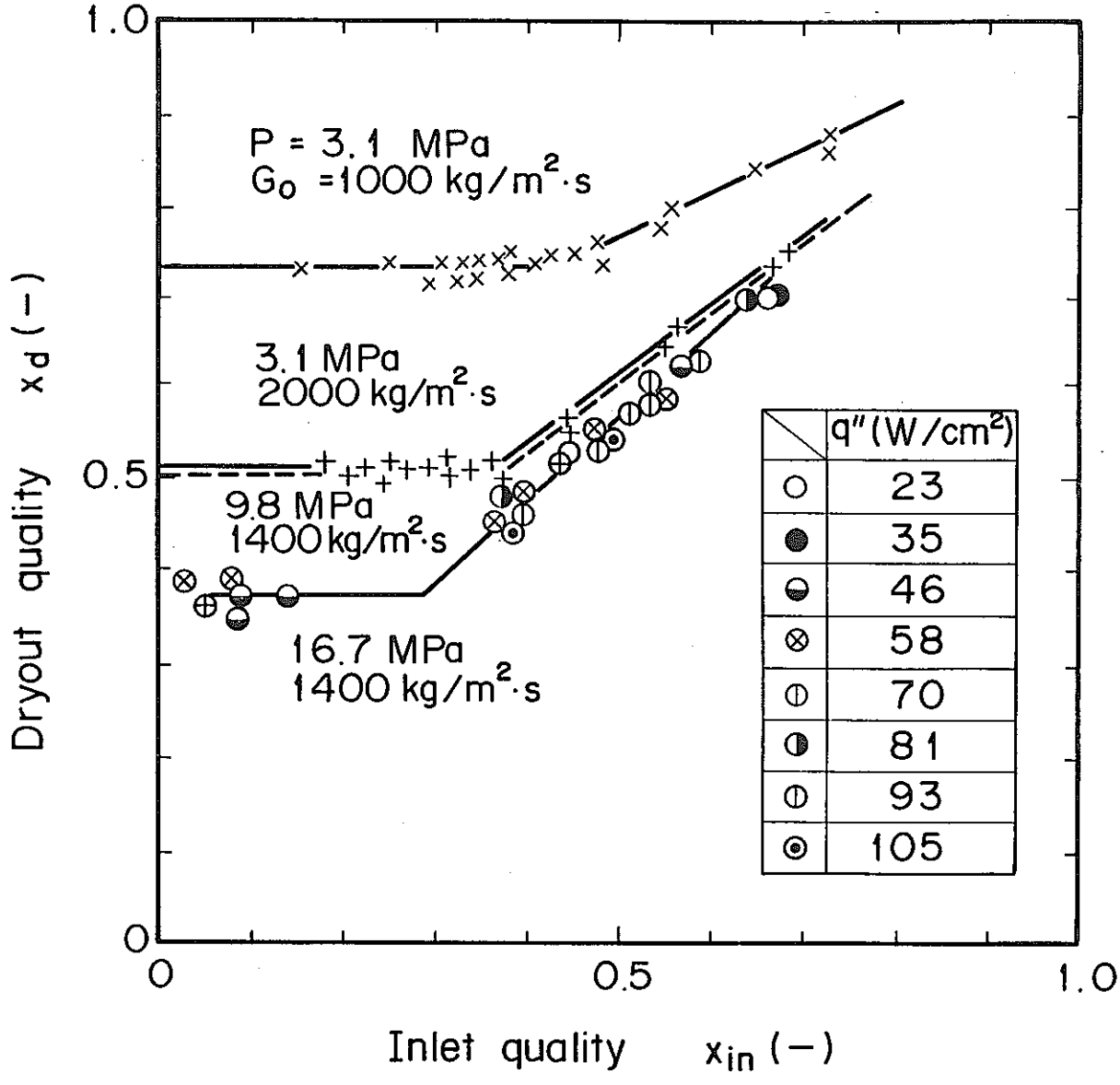

Fig. A.7 Effect of inlet quality on the dryout quality (after Doroshchuk et al.)

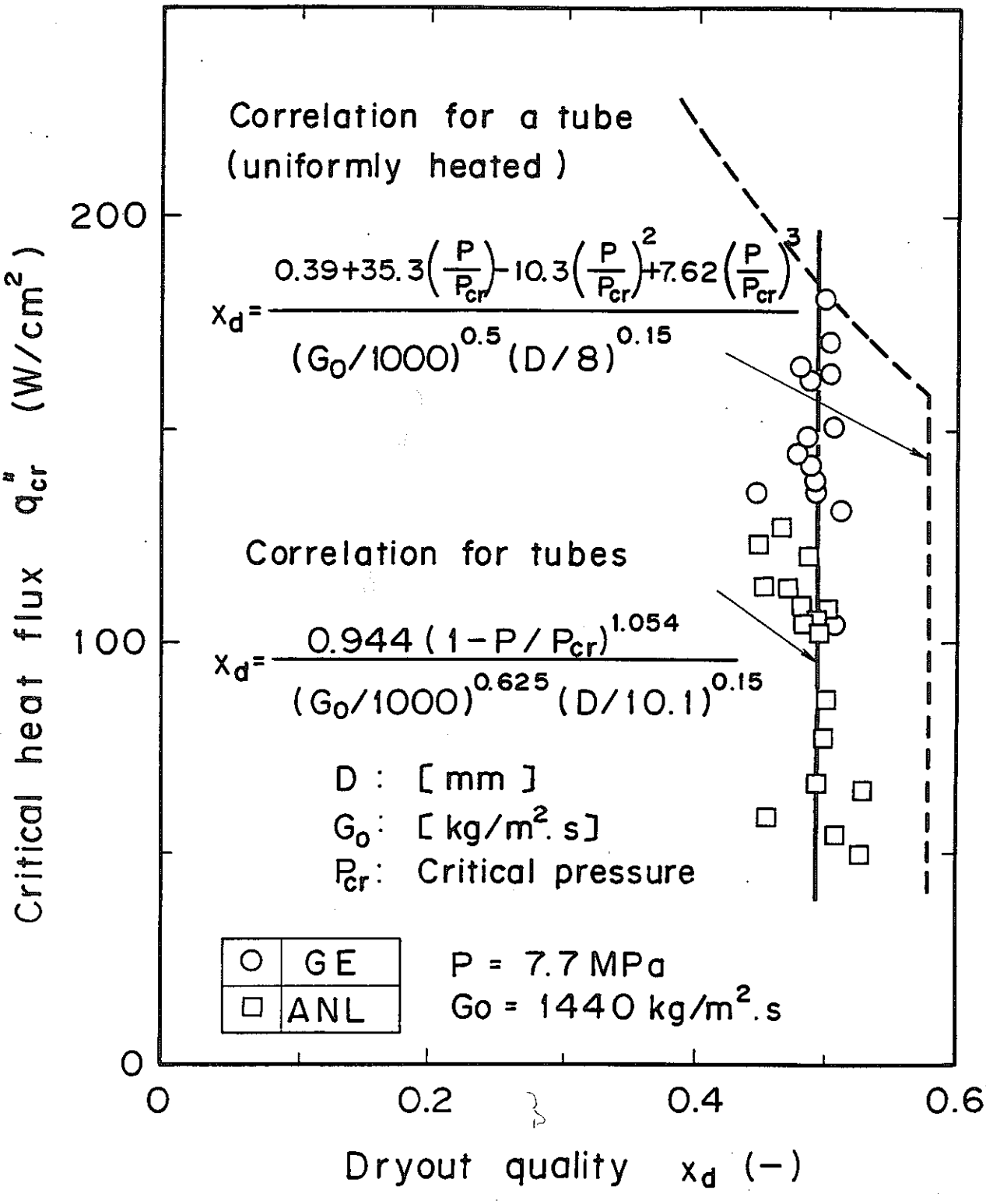

Fig. A.8 Comparison of correlations for a tube and tubes (after Wolf et al.)

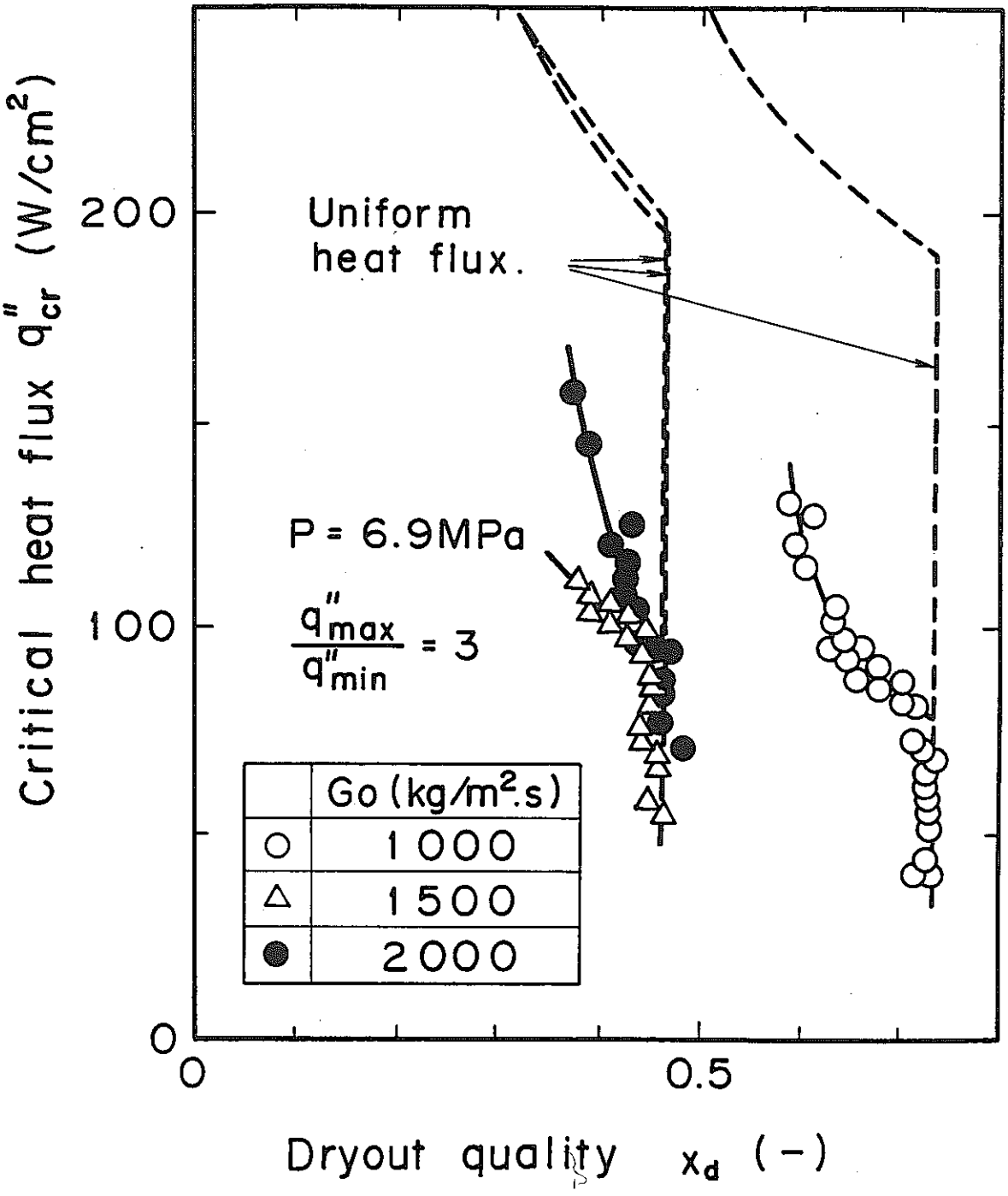

Fig. A.9 Effect of chopped cosine axial heat flux on the dryout quality (after Doroshchuk et al.)

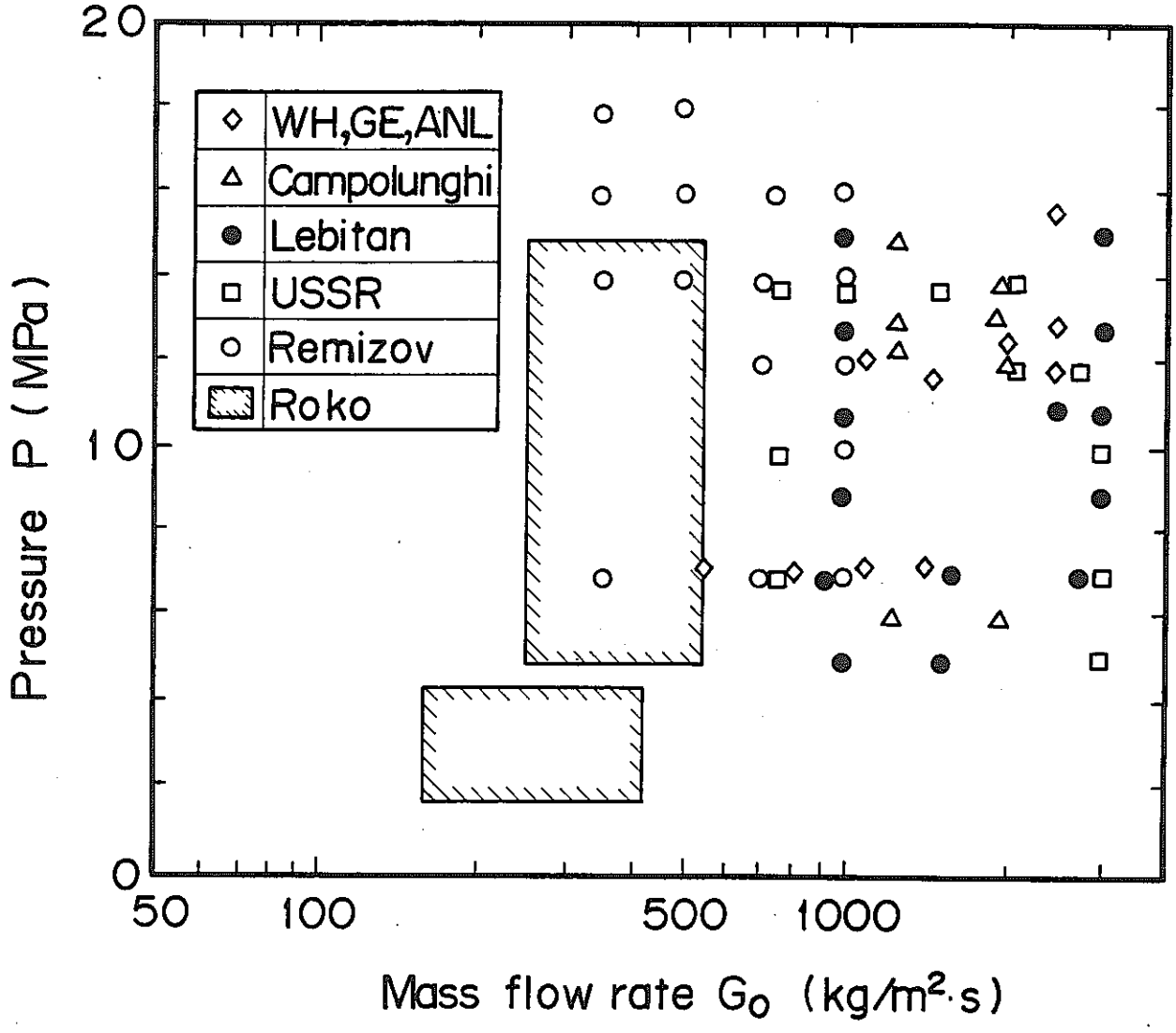

Fig. A.10 Parameter map of typical experiments for high-quality dryout (after Roko)

Appendix B: Summary Review of the SLSF LOPI Simulation Tests

SLSF is a sodium loop inserted in ETR (Engineering Test Reactor)[20],[23]. A mock-up test assembly containing a bundle of up to 61 pins can be settled in a loading/unloading machine located at a center of the loop. Bundles of 19 fuel pins were used for the test series of SLSF-P1[18],[19],[20] and SLSF-W1[21],[22],[23]. The difference in the objectives of these two series tests are as follows: the P1 series simulated the LOPI condition of FFTF (Fast Flux Test Facility) in FTR (Fast Test Reactor) and the W1 series simulated that of CRBR (Clinch River Breeder Reactor). A double-ended guillotine rupture in the primary system inlet pipe of the respective reactor was examined in these test series. The results of these experiments are summarized here only briefly.

B.1 Conditions of the SLSF-P1 and SLSF-W1 tests

The flow rate was projected to be reduced to 21 % in 0.2 s and kept constant thereafter. The delay time of reactor scram after flow reduction is 0.5 s in the P1 test, and is 0.65 s in the W1 test while it is 0.55 s in the case of CRBR plant (since it was impossible to simulate the power decay curve of CRBR exactly with ETR, the delay time of reactor scram was set as given in order to simulate the total heat amount generated during the time interval between the initiation time of the accident and the estimated time of the onset of sodium boiling). The fuel pins simulated the severe conditions: a 15 % over-power of the maximum power of each reactor core, the thickness of fuel cladding corresponding to that at the end of fuel burn-up, the FP gas pressure equivalent to that at the maximum fuel burn-up, and so on.

The geometrical specifications of the fuel pins of P1 and W1 test assemblies are: the outer diameter is 5.84 mm, heating length (excluding the blanket section) is 914 mm, pins pitch is 7.26 mm, spacer -wire outer diameter is 1.42 mm (only the peripheral pins are wrapped with special wires which are 0.71 mm in outer diameters and partly swelled with 1.42 mm diameter sleeves), and spacer-wire winding pitch is 305 mm. The blanket sections of both assemblies did not necessarily simulate the reactor condition. The coolant conditions of P1 and W1 tests are: the inlet temperatures are 422 °C and 388 °C, respectively, being fairly different between both tests, while the estimated saturation temperatures at the boiling onset points are around 956 °C in both tests.

The P1 test was the first one conducted with SLSF. Therefore, its primary purpose was to confirm functions of the loop and ETR and to establish experimental techniques. In part of this series, several runs were carried out simulating LOPI conditions. Except for the final case, many cases were, however, trial operations at low power levels for the purpose of conducting the final run successfully. In the W1 test, five runs were carried out to obtain information on the followings: (1) the heat release characteristics of the FBR fuel pins at the LOPI accident, (2) the boiling inception condition and the void expansion characteristics, and (3) the boiling condition leading to fuel pin failure, and so on. In the respective runs, the parameters changed were pre-irradiation and pre-melting conditions of the fuel, while the LOPI accident cnditions were the same in all runs. Accordingly, the same test assembly was used throughout, viz.

starting with the state of fresh fuel, the test assembly experienced the simulated LOPI accidents succeedingly, being changed its fuel conditions from one state to another.

The P1 series run had a long duration time. On the contrary, the W1 series run was terminated within 3 to 4 s by raising the flow rate to its initial state. The series of tests covered the part of LOPI accident scenario up to a point corresponding to a primary peak in the behavior of coolant temperatures, and left intact such a loss-of-coolant condition as lead to a subsequent secondary peak. The reason for this is that even where the failure in the start-up of a pony motor of primary pump, for instance, is introduced in the scenario of the LOPI accident of FTR or CRBR, the high temperature sodium generated during the primary peak phase is already away from the assembly at the subsequent natural circulation step, and the whole of assembly is in cooled condition like the initial state or even lower. The tests for the secondary peak phase have been conducted together with the R&D on safety evaluation of LSHRS accidents[27]-[32].

B.2 Results of the SLSF-P1 test

The pre-test analyses by SAS-3A and the other codes for the SLSF-P1 test[20],[23],[33] predicted the following: At 0.5 s after start of flow reduction, boiling will take place at a point 127 mm upstream from the top of the heated section. At 0.9 s after, the void region will extend over the whole of assembly, resulting in violent melting of the caldding material to yield channel blockage. However, the results of the P1 test were as follows:

(1) The temperature increase at the single-phase region was about 1/2 of the predicted value.
(2) At 1.2 s after start of flow reduction, three thermocouples set on the plane 25 mm upstream from the top of the heat section detected the boiling inception (the adjoining measurement planes to this plane are 152 mm away). Of the three thermocouples, one is located in the first subchannel from the central pin, and the other two are in the second subchannel. A thermocouple located in the fourth subchannel was in the subcooled region.
(3) Boiling continued for 0.8 s. The bubble region was confined stationarily to a narrow region enclosing the seven central pins in the vicinity of the top of the heated section. The saturation temperature was also measured in the upper blanket region, meaning that the two-phase region extended axially over 152 mm.
(4) There were no signs of phenomena such as the flow reversal, coolant ejection and violent flow oscillation. The integrity of the cladding tubes was retained.

The typical test data cited from reference (19) are shown in Fig. B.1.

The test results were examined as to whether the discrepancy between prediction and experiment was due to error in the setting of the test conditions, or to inadequacy in the analysis, or due to both. In consequence, the following were pointed for the experiment: The flow reduction curve was more gradual than the planned curve, and its asymptotic value stayed at 26 % rated flow. The rated heat output exceeded the planned level by 19 %. For the analysis, it was concluded that the boiling phenomena in a LOPI accident cannot be evaluated by the single-channel slug model of the SAS-3A code, while the thermal-hydraulics of the single-phase flow can be well explained by putting the asymptotic value of

the inlet flow to 30 % rated flow and duplicating the heat conductance through the gap between fuel and cladding from its nominal value in COBRA-3M or SAS-3A codes (the validity of these modifications is not established yet). It appears impossible to evaluate the data of P1 test any further because of the uncertainties of the in-pile test and various troubles ascribed to the first experience and some trivial errors.

B.3 Results of the SLSF-W1 test

The pre-test analysis[23] of the SLSF-W1 test indicated the following: At 0.9 to 1.0 s after start of flow reduction, boiling will take place at a point about 7 mm upstream from the top of the heated section, and at 1.6 to 1.8 s after, it will be terminated (the boiling duration time will be 0.75 to 0.8 s) with the pins being not damaged. In contrast to this prediction, the test results were as follows: No boiling took place under the LOPI condition of CRBR, while the maximum sodium temperature reached up to 15 to 20 °C subcooling level. In the final case, which was started erroneously with the higher heat output by 5 % over the planned rating, i.e. about 20 % over power of CRBR, boiling for 0.5 s was observed. The test results cited from reference (22) are shown in Fig. B.2. Any more details on the analysis of the test data will be shown on another opportunity.

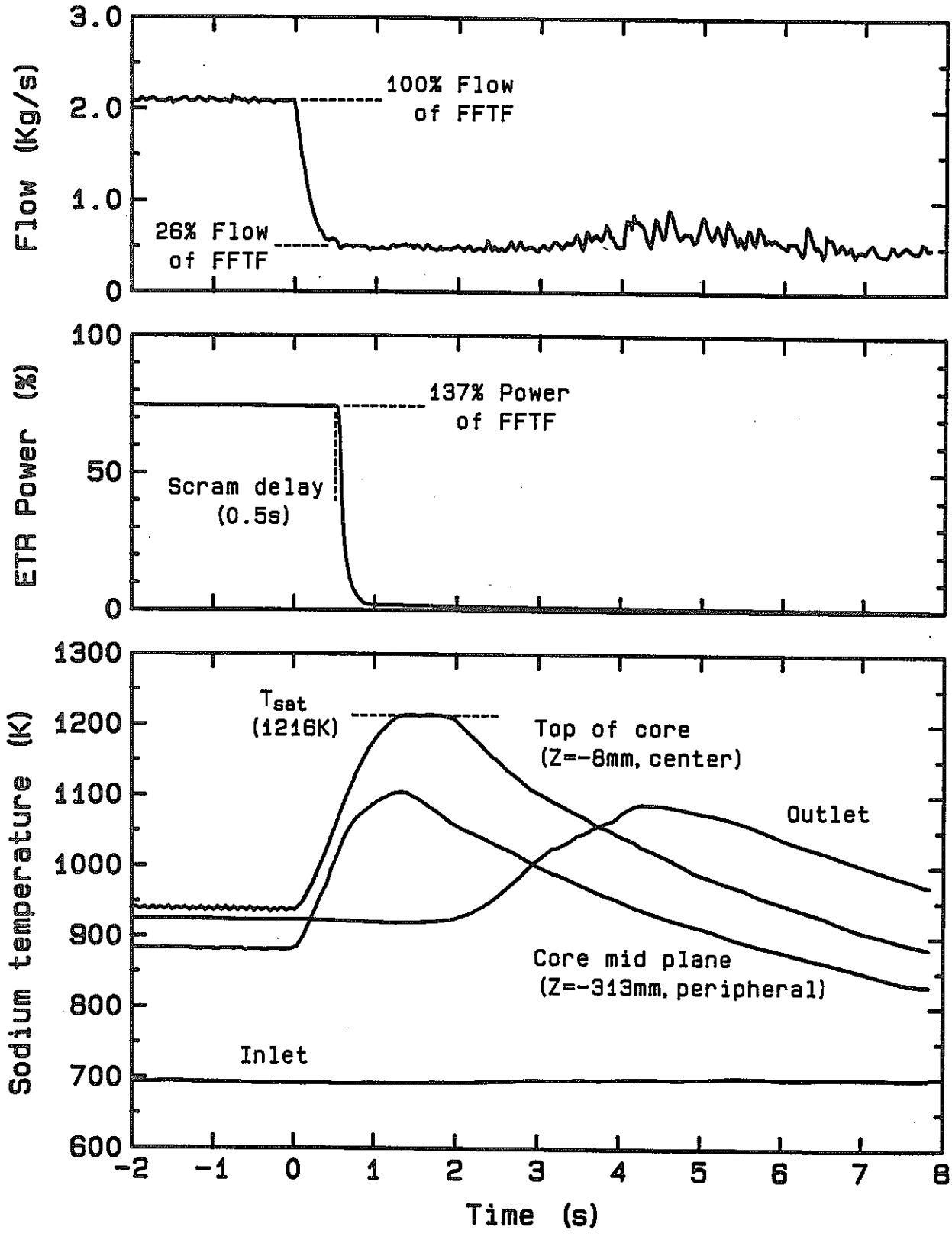

Fig. B.1 P1 SLSF experiment LOPI transient

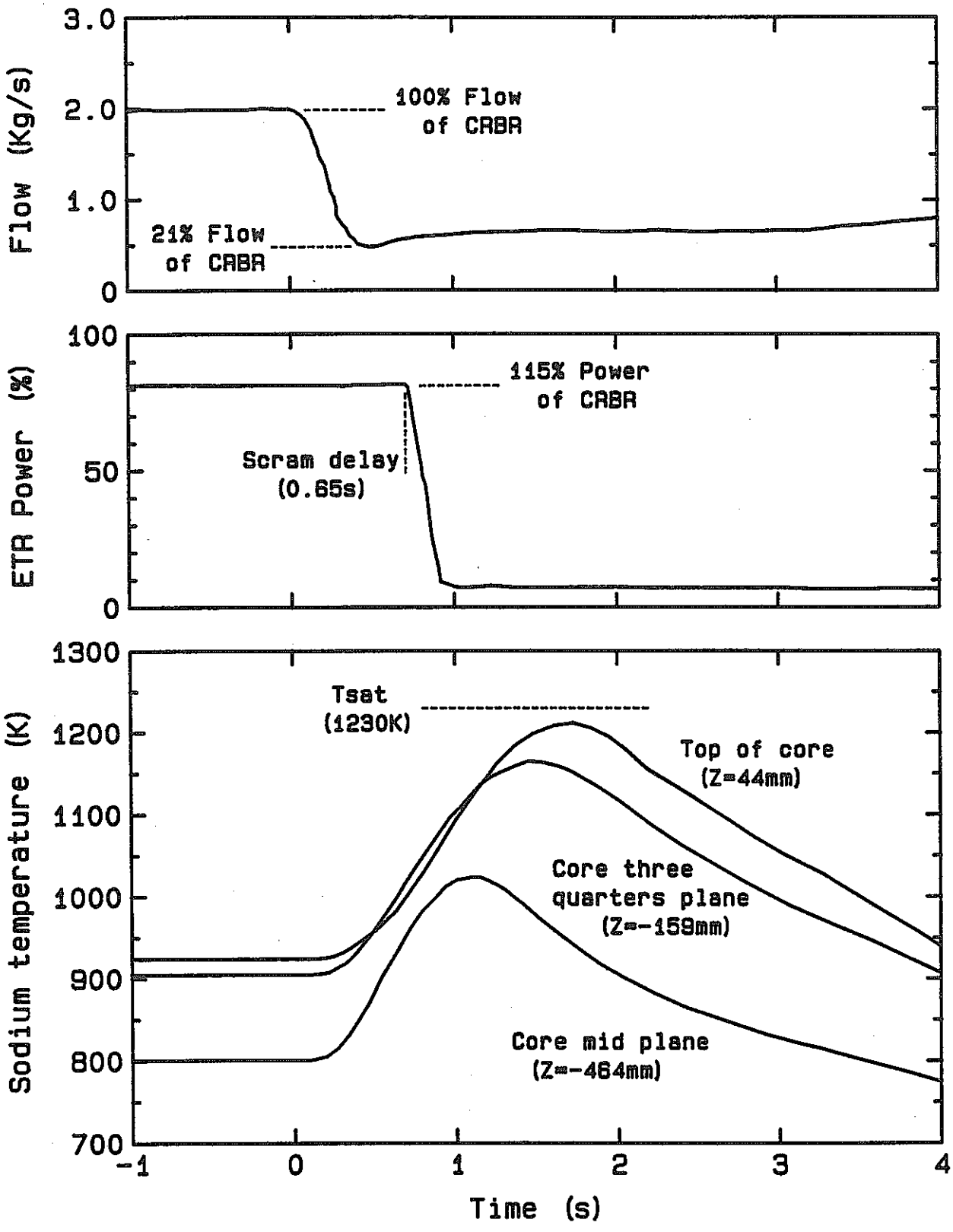

Fig. B.2 W1 SLSF experiment LOPI transient 2A

Appendix C: Principle of Void Fraction Measurement

To attain measurements of void fraction profile in a boiling two-phase flow, many Chen-type void probes are inserted in a pin bundle. The void probe consists of two parallel lead wires of stainless steel and a cladding tube. The outer surface is 1.3 mm in diameter for most of its length and is squeezed into a fine tube of 0.65 mm diameter for about 5 mm long from its pointed end, where two internal wires are welded to the cladding. The tightened part surves as a void sensor. The specially fabricated electrical circuit, i.e. the void meter, picks up the delicate change of electrical resistivity between the cladding and one of the internal wires, so that the attachment and departure of sodium void around the void probe yields an on/off type output signal. At the data reproduction, the on/off signal is further intergrated by the void fraction analyzer for a short time period to deduce a time averaged void presence ratio which is treatable as a local void fraction when the two-phase flow attains a stationary condition. The following describes the principles of the data processing methods relevant to the void fraction measurement.

C.1 Chen-type void probe and its void meter

The basic idea of the Chen-type void probe and its circuit was proposed by Chen[34]. Following his idea, a conventional void meter circuit named Mark-I void meter was devised and used for two series of experiments with the 37F and 61A test sections. In addition, an improved circuit named Mark-II void meter was introduced at the present experiments with the 37G test section. The major difference in these two circuits lies in wheather it has a function of compensating for an output drift due to a change of sodium temerature around void probe.

Figure C.1 shows the circuit design of the Mark-I void meter. The upper and lower figures are drawn based on the sensor image and on an equivalent DC bridge balance circuit, respectively. Let the bridge balance resistance R_B and a constant voltage power supply E_o be connected between one of the internal wires (R1) and the cladding ($R_3+\Delta Rs$), the electrical potential between the contact point of the divider of R_B and another internal wire (R_2) gives the void signal e_o. In this case, the DC bridge circuit is made of the first wire (R1), cladding ($R_3+\Delta R_s$), one part of the bridge balance resistance (R_4), and another part ($R_5 = R_B-R_4$), where the resistance of cladding includes the changeable component ΔR_s depending on the void attachment and departure. The bridge balance is initially settled so as to suffice the relation: $R_5 \cdot R_1 = R_4 \cdot R_3$

The Mark-I void meter gives unfavorable ouptut drift when the resistances of wires and cladding are changed drastically. This problem was solved in fabricating the Mark-II void meter. The details are shown in the letter of patent by Isozaki and Satoh[35]. The superior performance of the Mark-II void meter is indicated by an example output shown in Fig. C.2, where the similar result by the Mark-I void meter is also shown for comparison. Though the LOF-induced sodium boiling can be sensed by both void meters, the Mark-II void meter has a better performance against the temperature drift and easily enables us to direct the data processing to a further interesting stage.

C.2 Void fraction analyzer

Provided the output of the void meter can give regular time series pulses, a conventional pulse analyzing technique is applicable to the void meter signal. The void fraction analyzer was thus deviced as a typical single-channel pulse analyzer/monitor. Figure C.3 shows its full view. The main specification is listed in Table C.1. The input pulse from the void meter is reformed by the comparator and is fed to the pulse counter circuit. The clock pulses passed through by the comparator pulse windows are counted under the control of the integration time controller. The counted number is then normalized by the total number of clock pulses generated during the time of the integration control gate being open. These processes are repeated to obtain a time series void fraction signal, while it is smoothed over with an appropriate combination with a low-pass filter.

The void fraction analyzer was tested by an off-line method with a recorded void meter signal. First of all, the smoothing technique of the output singnal is checked as shown in Fig. C.4. The recommended cut-off frequency of the low pass filter is decided as an inverse of the integration time interval. Using the filter thus specified, the void fractions were then calculated. Figure C.5 shows typical results of the void fractions calculated under various integration time which can be arbitrarily chosen based on the required frequency response.

Table C.1 Specifications of the void fraction analyzer

Item	Specification
Input voltage Detectable minimum amplitude Trigger level	-5 to +5 V (floating differential) 50 mV p-p movable in -5 to +5 V span by 10-turn potentiometer
Output voltage Output current Output impedance	0 to 1 V for 0 to 100 % void fraction 50 mA (max.) 50 Ω (max.) with a minus line being grounded
Integration time interval	A: 5.24288 s B: 2.62144 C: 1.31072 D: 0.65536 E: 0.32768 F: 0.16384
Internal clock Oscillator	about 100 KHz about 10 MHz (X'tal)
Accuracy Resolution	±2 % (typical) 0.0244 % of full scale (2.44 % void fraction)

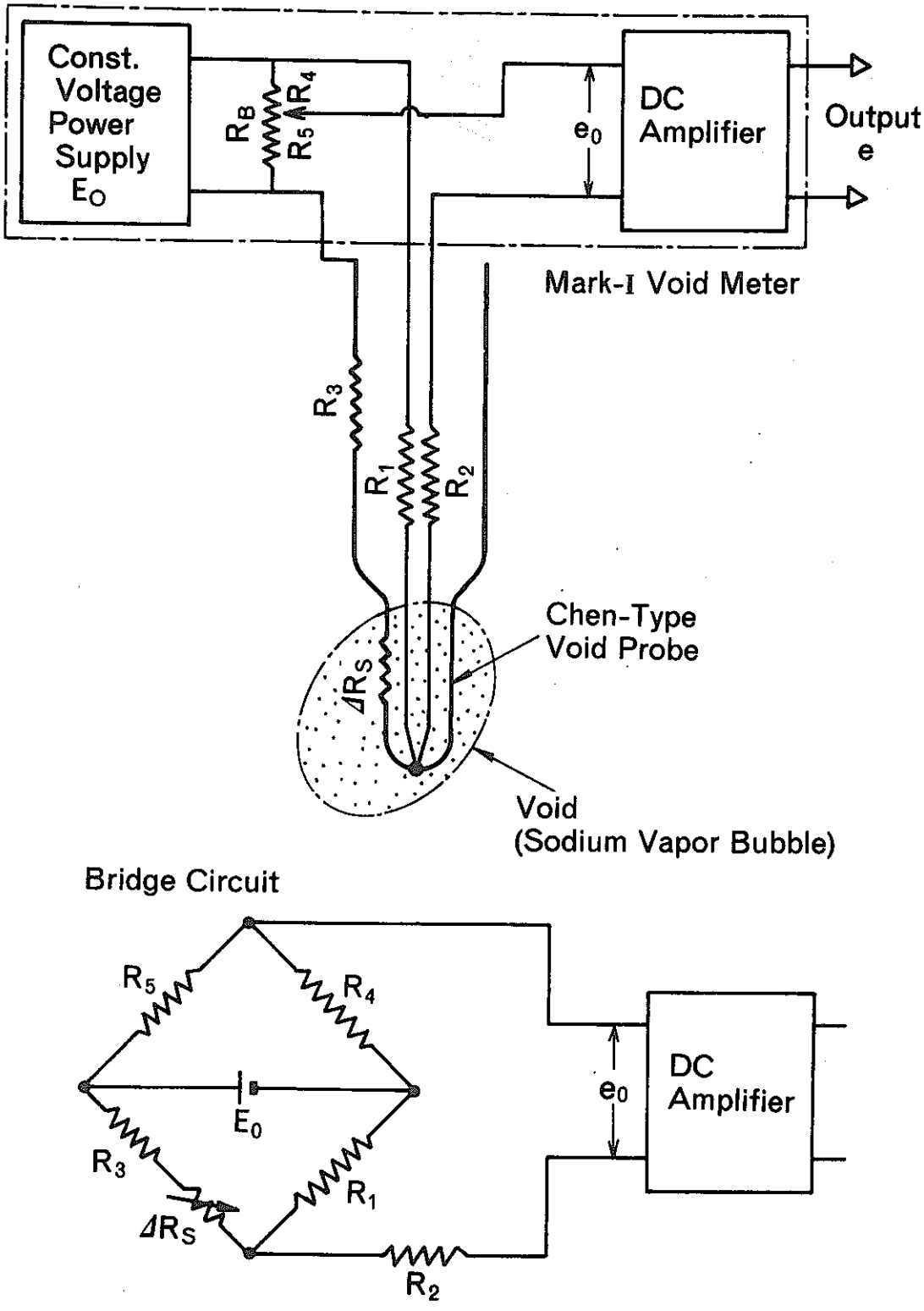

Fig. C.1 Chen-type void probe and its void meter circuit (Mark-I void meter)

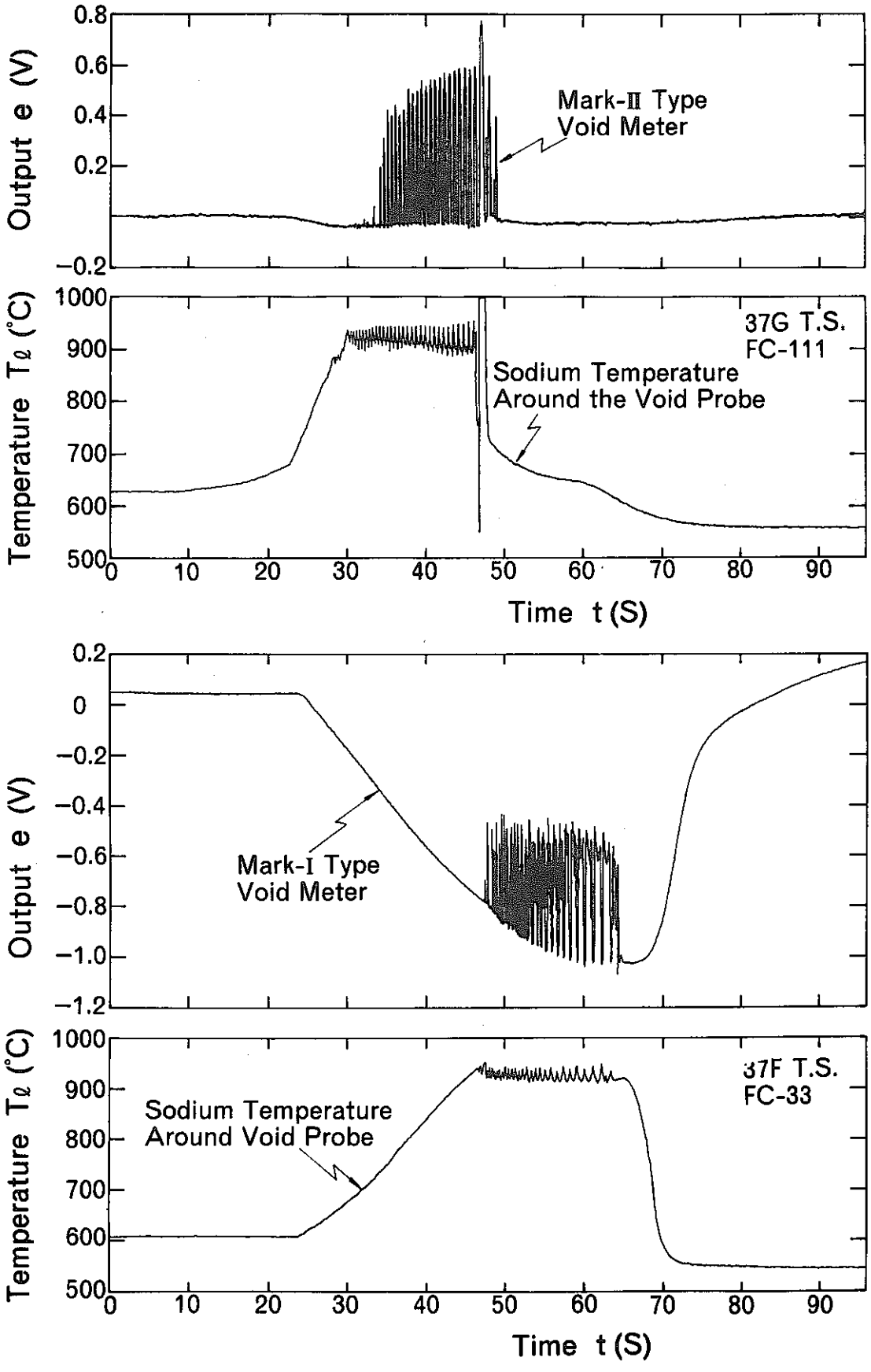

Fig. C.2 Typical signal of the void meter connected to the Chen-type void probe

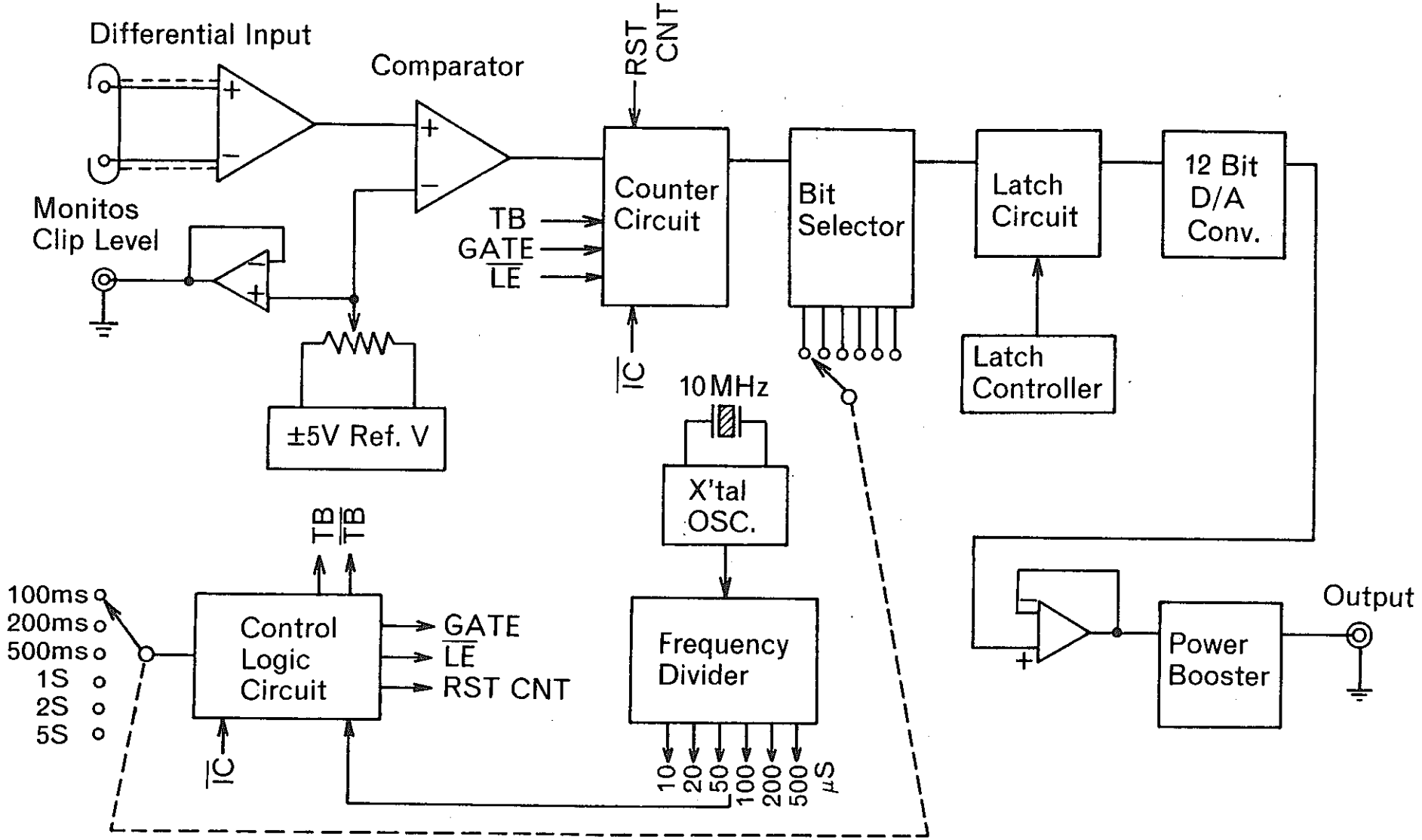

Fig. C.3 Block diagram of the void fraction meter

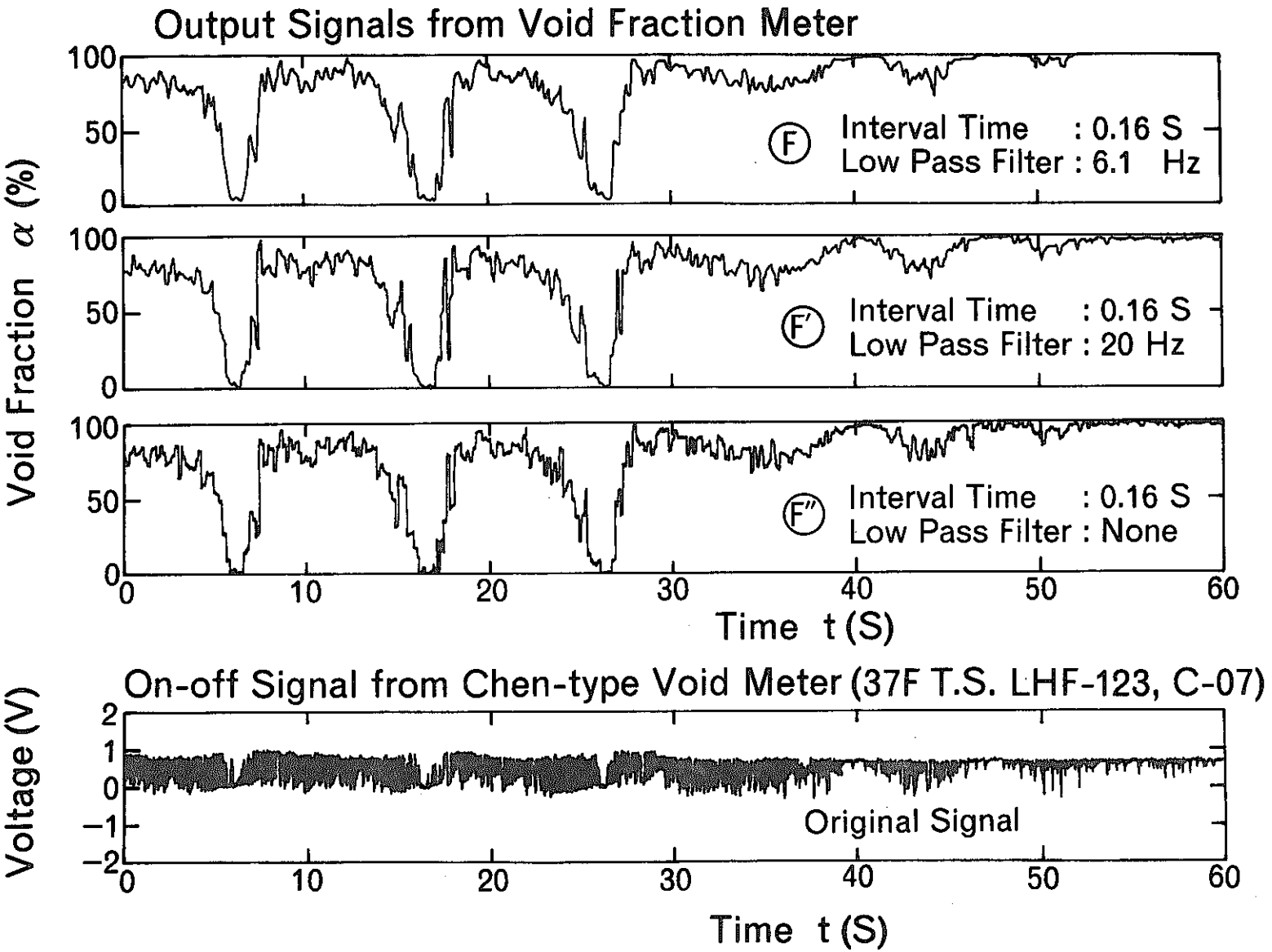

Fig. C.4 Typical signals measured by the Chen-type void meter and the void fraction meter

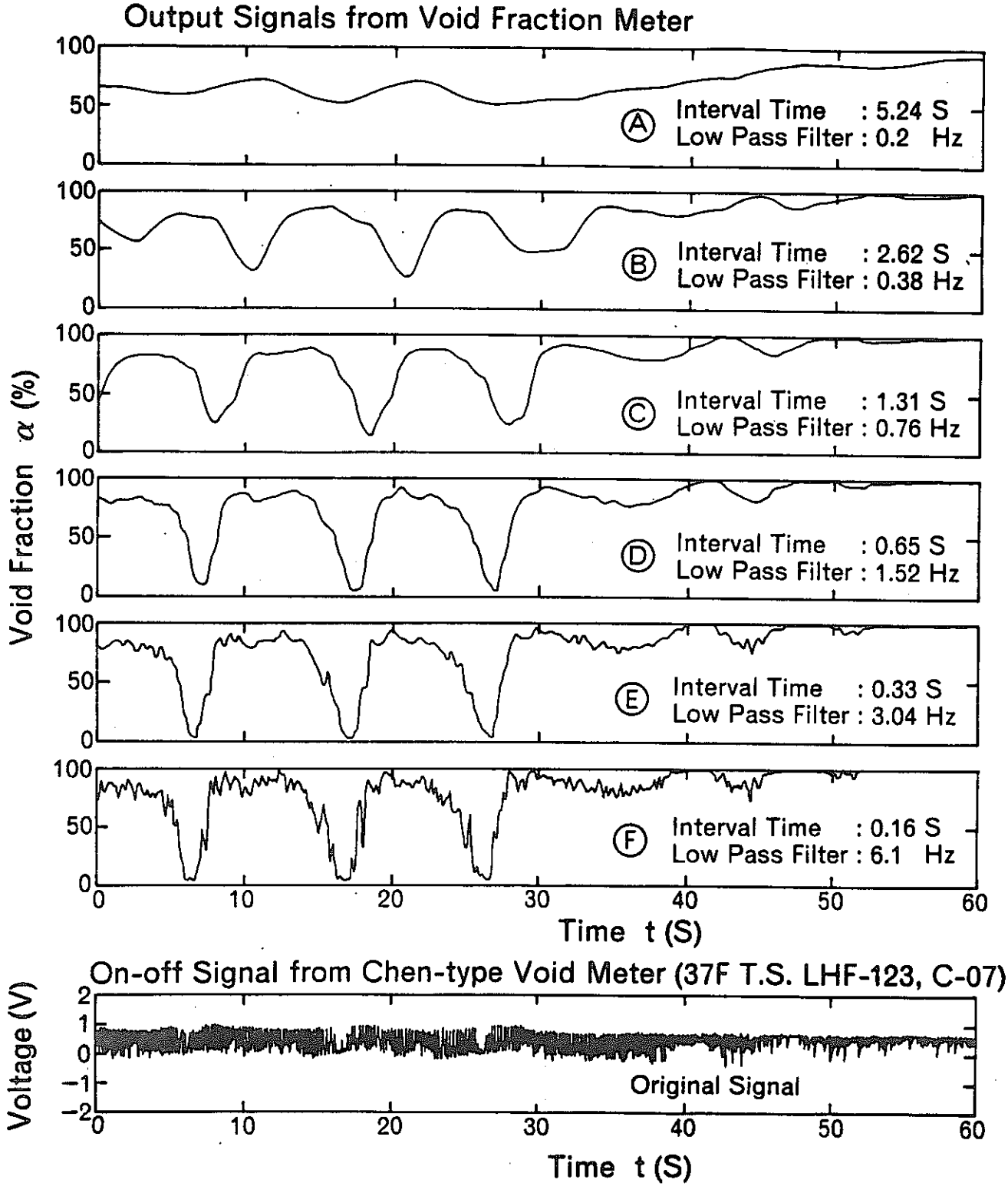

Fig. C.5 Typical signals measured by the Chen-type void meter and the void fraction meter

Appendix D: Evaluation of Heat Flux Profile during Experiment

The heater element is made of tantalum. Its electrical resistance changes widely depending on its temperature. This nature leads to a complex behavior of pin power profile during the experiment. The evaluation of power profile is, however, strongly required for analyzing the experimental results in detail. Therefore, an empirical method for this purpose was made available and checked as follows.

D.1 Resistance of heater pin

From many literatures, it can be confirmed that the electrical resistance of tantalum changes as expressed by a nonlinear function of its temperature. However, it was approximated here by a simple linear function as correlated in Fig. D.1, where the resistances of every heater pins used in the present experiments were correlated with those data measured under uniform temperature conditions and with the property data from literatures. When the power is fed to the heater pin, the temperature of tantalum increases over the environment temperature level by up to a few hundred degree C depending on the power. This power dependent term of resistance change was correlated secondary as shown in Fig. D.2. These results led to a correlation equation as expressed by:

$$R = 9.0E\text{-}4\ T + 1.125E\text{-}4\ Q + 0.27$$

where R means the resistance of each pin in [Ω] unit, T is a sodium temperature around the pin in [°C] unit, and Q is a heat flux of the tested pin in [kW/m^2] unit.

To confirm the accuracy of estimating the resistances by the above equation, the estimated values of resistances were plotted against those measured directly. The result is drawn in Fig. D.3, indicating that there is an uncertainty of 5 to 10 %, the major component of which is ascribed to the difficulty in quality management at the pin manufacturing process. However, the correlation would be concluded as being valid well for all heater pins.

D.2 Estimation of axial power shape

Using the equation thus derived, the axial pin power shape can be estimated as follows:

$$R(z) = 2.0E\text{-}3\ T_{Na}(z) + 2.5E\text{-}4\ q''(z) + 0.6$$

$$q''(z) = 1.0E\text{-}3\ I^2R(z)dz/dS$$

$$\int_{T_{in}}^{T_{Na}(z)} c_p\rho AUdT = \int_0^z q''(z)dS$$

where

U : flow velocity [m/s]
A : equivalent flow area around a pin [m^2]

$q''(z)$: local heat flux [kW/m^2]
ρ : sodium density [kg/m^3]
dS : heating surface area in control volume [m^2]
c_p : specific heat of sodium [1.256 kJ/kg°C]
I : electrical current [A]
$R(z)$: local electrical resistance [Ω/m]
dz : axial distance in control volume [m]
$T_{Na}(z)$: local sodium temperature [°C]

If the electrical current of each pin is given, these equations can be solved for an axial node to yield:

$$q''_n = \frac{(2.0E\text{-}6\ T_{Na,n} + 0.6E\text{-}3)\ I^2}{\Delta S/\Delta z - 2.5E\text{-}7\ I^2}$$

$$c_p \rho A U\ (T_{Na,n+1} - T_{Na,n}) = \Delta S q''_n$$

where

n : node number, = 1, 2, ...
T_1 : inlet temperature (= T_{in})
ΔS : heating surface area in each node
Δz : node height

Figure D.4 shows the estimated results of a typical case, i.e. the initial condition of Run 37(34)LHF-234. The electrical current of 686 A was supplied to 34 heater pins and the averaged heat flux was 41.7 kW/m^2. Upon assuming the uniform radial power shape, a current value of 686/34 (= 20.176) A was used for the heat balance calculation of a hypothetical flow channel having flow area of 924/34 mm^2 (924 mm^2: total flow area of the 37G bundle). The estimated axial power shape becomes a trapezoidal form whose maximum point is located at the top end of the heated section. The maximum-to-average or minimum-to-average power peaking is around ±17 to ±19 % for this case. In this calculation, however, there appeared an estimation error of about -14 % in heat flux on average, which introduced error of about -30 % in local sodium temperatures (including that caused by using the larger equivalent flow area in the calculation).

The major part for these errors might be ascribed to the estimation error of pin resistance or to the measurement error of electrical current. Therefore, the power profile should be checked (by multiplying a certain modification factor) to equalize the calculated averaged heat flux to that measured directly. Figure D.5 shows the results of the modified calculations, where the power and temperature profiles are traced for three cases: one is the best estimated calculation giving precise averaged power and the other two are 10 % over and under power calculation cases. For all cases, the calculations lead to lower values of estimated temperatures. The utilization of a smaller value for the equivalent flow area leads to a better agreement between calculated and measured results. For instance, a 10 to 20 % smaller value of flow area would lead to a reasonable situation.

The above discussion is restricted to the single-phase flow cases. The power profile becomes flat at the boiling region, being connected with the partial trapezoidal zone corresponding to the non-boiling region. Especially at the dryout step of each run, more than three quarters of the heated section is covered with saturated sodium and its vapor. Therefore, the steeply slopened

power increase is considered only at the lower part of the heated section, and the maximum heat flux becomes close to the averaged one measured. The precise power shape can be obtained by stopping the above mentioned marching calculation when the temperature exceeds the saturation point and by drawing the flat line thereafter.

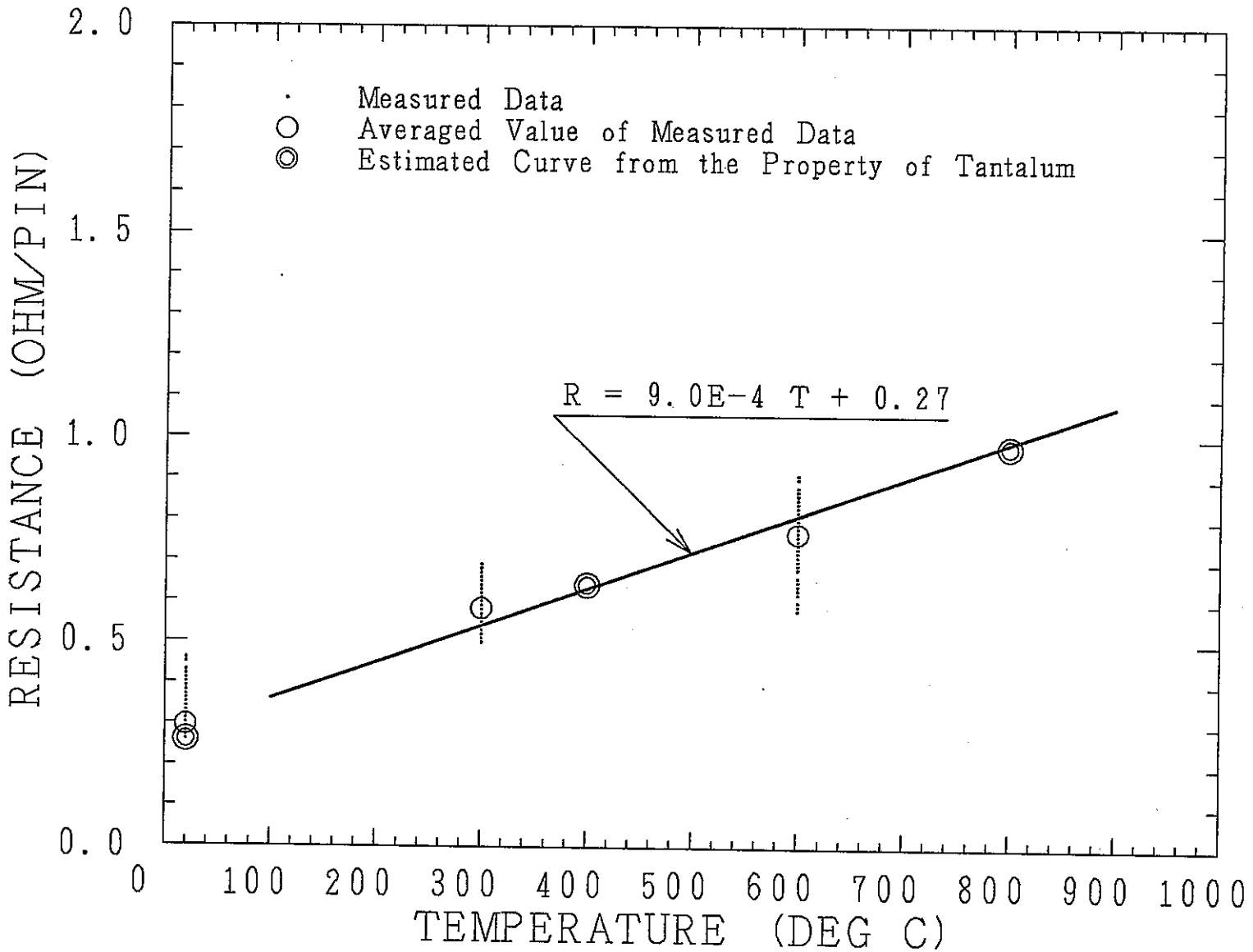

Fig. D.1 Temperature dependency of the electrical resistance of tantalum

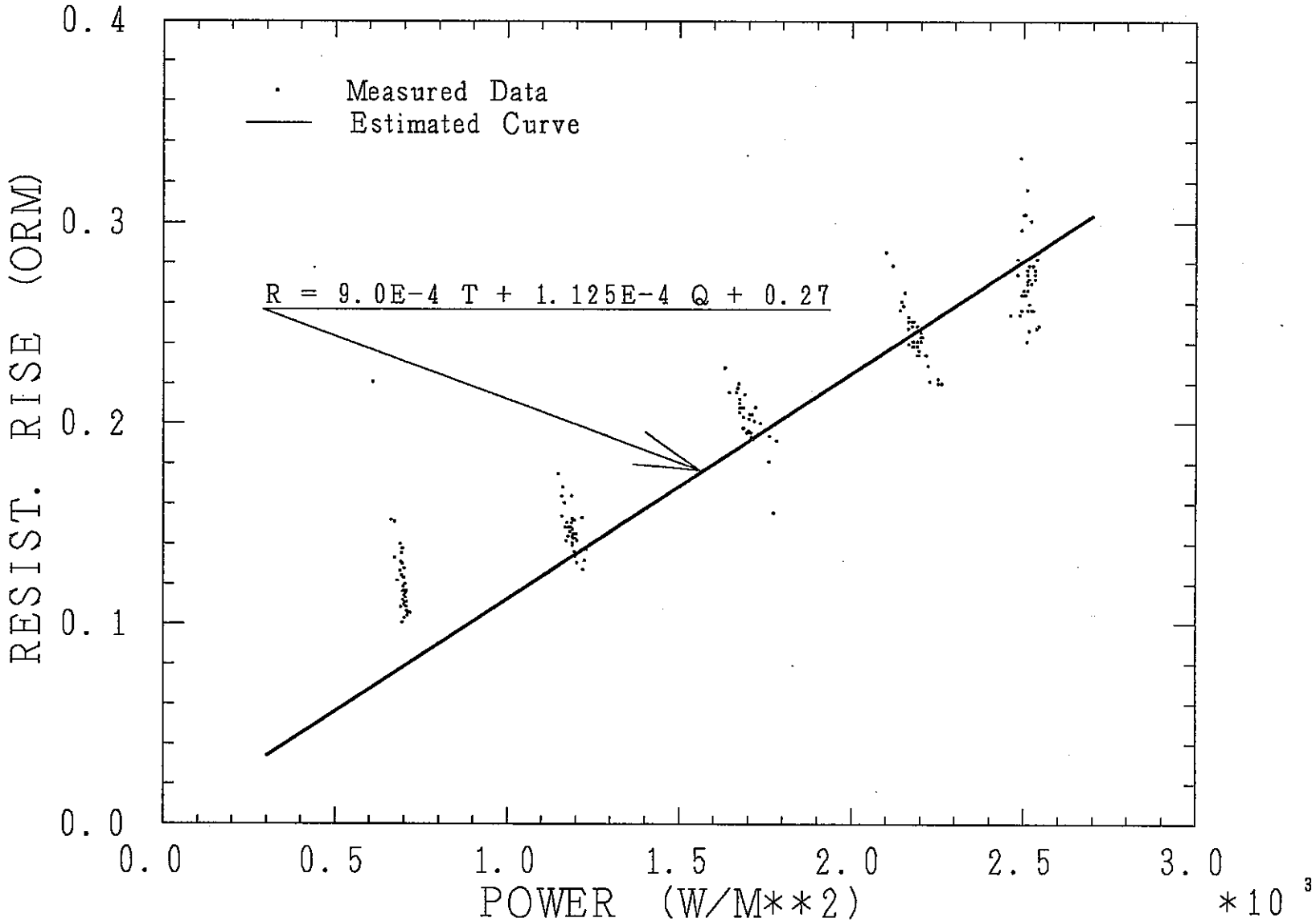

Fig. D.2 Dependencies of the pin resistance on the sodium temperature and the heater power

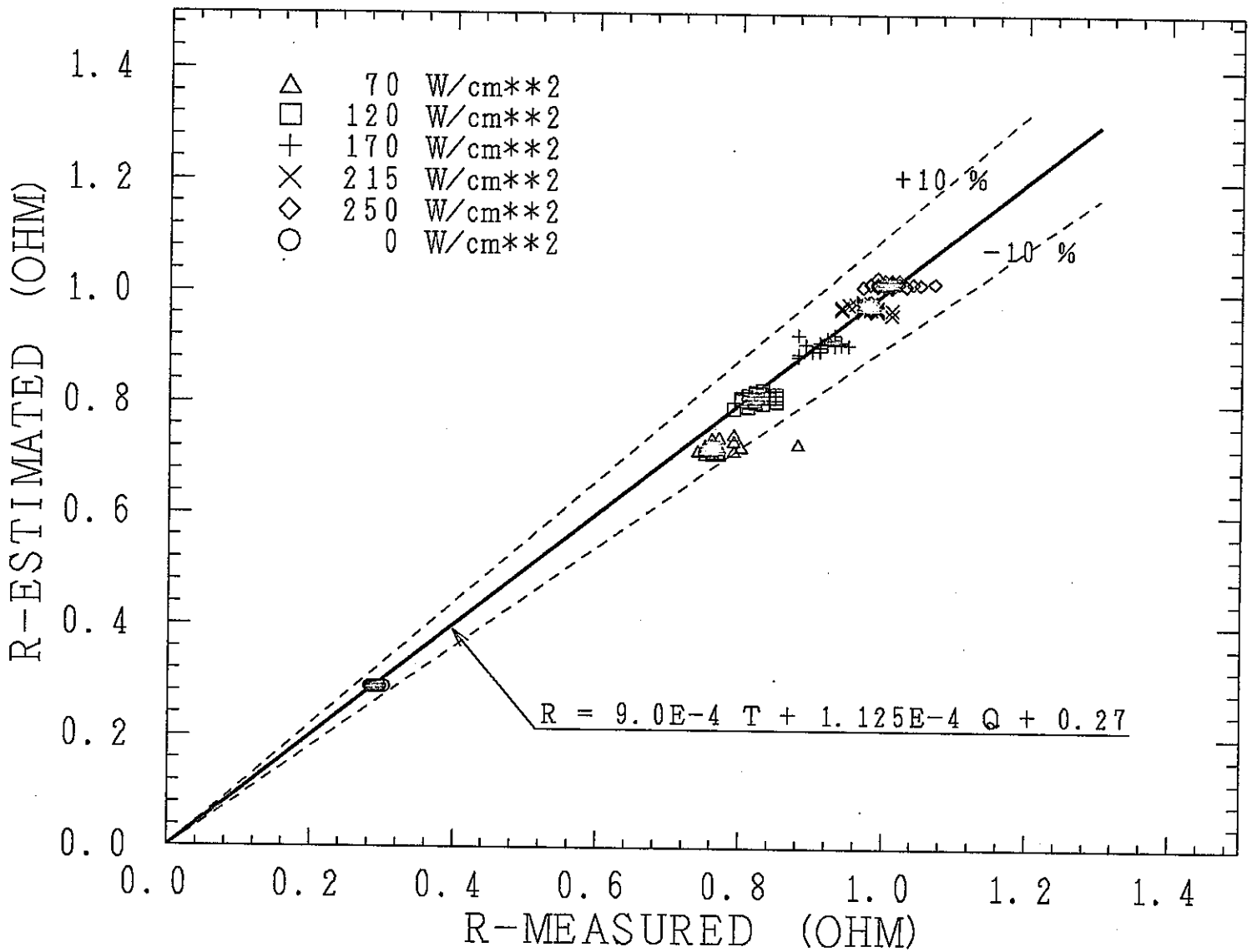

Fig. D.3 Comparison of the estimated pin resistances with the measured data

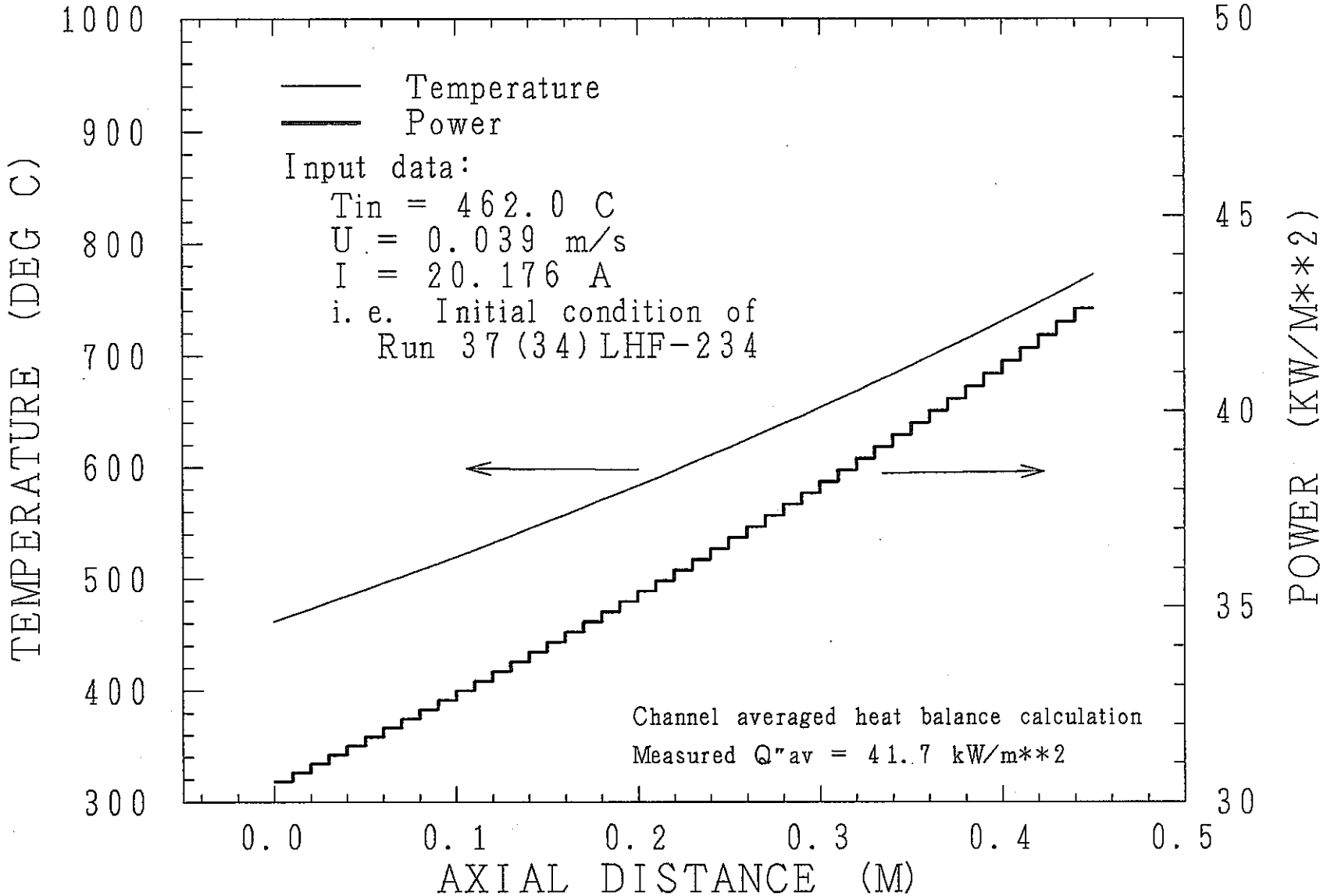

Fig. D.4 Axial shapes of the pin power and the sodium temperature estimated with the heat balance equation

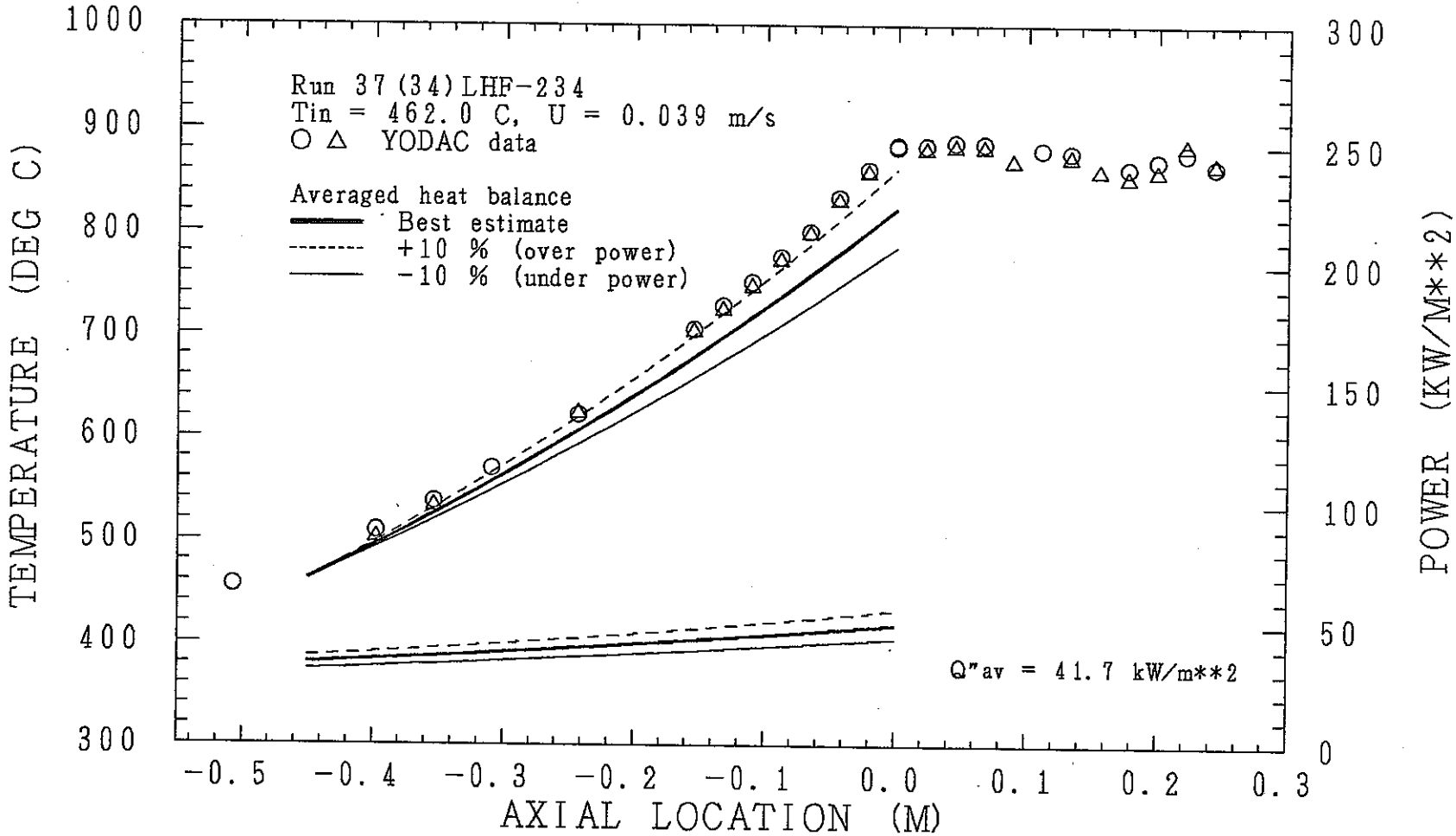

Fig. D.5 Check of the power profile calculation method using the sodium temperature data

Appendix E: Calibration of Flow, Pressure and Temperature Signals

The low-heat-flux boiling experiments deal with so small signals of powers, flows, pressures and temperatures that a careless treatment of these data introduces large errors in the heat and mass balances of the sodium flow which might lead to misleading understandings on the observed phenomena. The instrumentation system of the SIENA facility was so aged that the hardwares of the measurements were not qualified high enough to guarantee the accuracies of measurements by themselves. Therefore, the data accuracies were improved chiefly by the software technique checking the offsets and gains of measurements with many calibration data.

E.1 Calibration of flow signals

Among five flow-meters in the facility, four flow-meters, i.e. F-101, F-103, F-106 and F-107, are located at the main line. It is possible to check the outputs from these flow-meters each other for the relative calibration of these flow-meters. The most reliable flow-meter F-103 having a well fixed unit conversion factor (7.843E+2 (m/s)/(V)) and a high gain accuracy (±0.002 m/s) was used as a standard flow-meter for the relative calibration.

First of all, the offset values of the flow-meter signals were fixed by the zero flow calibration data. The results are illustrated in Fig. E.1. Only six cases of zero-flow data were available for the HP-2116C system. On the contrary, there were many YODAC or HP-9845T data points from which general tendencies of the offset vaules of individual flow-meters were derived. These data were, therefore, used as supplemental back-data to compensate for the scarcity of the HP-2116C data. The scalings of two vertical axes for each flow-meter case are arbitrary shifted so that it can be easily find that the HP-2116C data have the same tendency as the YODAC or HP-9845T data. The sodium temperature data are also shown to examine the possible drift of the offset value by the sodium temperature change, while the drift cannot be identified. There appeared a jump in the traced lines of the offset values of F-106 when the SIENA operation was renewed from 141th to 142th operations. It corresponds to the occurrence of a trouble in the measurement network of F-106.

The relative calibrations of the flow-meters F-101, F-106 and F-107 by the standard flow-meter F-103 were conducted, selecting the YODAC data of the single-phase flow runs of 139th and 140th operations as data bases. The results are shown in Fig. E.2, where the offsets of the flow-meters are subtracted beforehand. Due to the misconnection of signal cables, the sign of F-106 signal was reversed, while it is tentatively reversed again in Fig. E.2 to plot the data in positive domain. For F-107 case, there appeared two groups of data sets each having different sensitivities against standard signal F-103. It is known to be caused by the difference in temperatures of F-107. From the relative calibration shown above, the unit conversion factors of the tested flow-meters can be obtained by dividing the factor of F-103 (i.e. 7.843E+2 (m/s)/(V)) by the linear coefficients of the fitting lines of individual flow-meters noted in Fig. E.2.

Finally, the signal processing accuracy was assessed by comparing the reproduced data of test runs within the low flow range. The results are shown in Fig. E.3, where the data from F-106 are not plotted because of the failure of the flow-meters at the test runs. A glance at the figure impiles that the flow-meter F-107 cannot be used for the data analysis of low-flow runs. The fairly large error of F-101 at especially low flow region of loss than 0.05 m/s would be caused by the noise component of the flow-meter.

E.2 Calibration of pressure signals

It has been known that the pressure transducer is very sensitive to the temperature change. The offset value drifts widely depending on the positive or negative temperature coefficient unique to each pressure transducer. Especially, the drift of P-109 is so large that the surrounding temperature of the pressure sensor must be controlled within the range of ±10 °C to obtain the ±0.005 MPa accuracy of P-109.

Several depressurization boiling runs were conducted in the present experiments. The cover-gas pressure was reduced there stepwise to reach sodium saturation condition under nearly constant sodium temperature condition and to intensify boiling conditions after sodium boiling was initiated. It was concluded that the steady data of the earlier single-phase flow steps of these runs applied most reasonably to the relative calibrations of all pressure sensors to fix the unit conversion factors at first. The standard pressure signal of the calibration was selected as P-201, whose unit conversion factor, offset and accuracy were evaluated as 7.355E+4 Pa/V, 400 counts and ±0.001 MPa (= ±5 counts). Figures E.4(a) through E.4(e) show the results of the calibrations using the data of depressurization runs of 37(35)LHF-220, 37(35)LHF-222 through 37(35)LHF-224. The zero point of the individual pressure amplifiers were left intact at least throughout these four runs. The upper figures mean the first data fitting results obtained by fixing the offsets being zero, and the lower figures mean the second results rearranged by subtracting the offsets by suggested values at the first fitting works. In these calibrations, the tentative criterion was used that the outputs from the tested pressure sensors must be equal to those from standard pressure sensor, neglecting the presence of liquid head (and frictional pressure drop). The calibration results indicate that the unit conversion factors can be properly evaluated by the above method.

The offset values of the pressure singnals were estimated so that the results of the head calculations of individual sensors for every low-heat-flux boiling runs become to agree with the initial pressures derived from the individual sensors. In the head calculation, the sodium free surface was assumed as being at EL-9100 mm level, and the initial outlet temperature T-004 was use for calculating the sodium density. Figure E.5 shows the relation between the offset values thus derived and the environment temperatures of each sensor. The offset of P-108 did not depend on the sensor temperature represented by the temperature T-003. However, the offsets of the other sensors were, more or less, sensitive to the changes of sensor temperatures represented by either T-003 or T-004. The estimated data of the offset values of these sensors also scattered rather widely around the most likelihood fitting lines.

Although the estimation errors of the initial steady data of pressure signals can be minimized within ±0.005 MPa by using the accurated offset values from the head calculations, the transient data include unfixed large errors

depending on the temperature drifts of the offset values. These errors would become small if the time series values of temperature drift component are estimated and subtracted from the raw data using the correlations shown in Fig. E.5. An example of such a special data processing method is shown in Fig. E.6, where the data of P-108, P-109 and P-111 and the artificially processed results of P-109 and P-111 with the above offset subtraction method are traced for comparison. Since the transient history of the sensor temperature is not measured, the moving averaged temperature of T-004 for time intervals of 460 s with a heat transport delay time of 60 s are used instead as the sensor temperature, i.e.

$$T_{sens}(t) = \frac{1}{t_M} \int_{t-t_M-t_D}^{t-t_D} T\text{-}004(t)dt$$

where

T_{sens} : sensor temperature [°C]
t_M : averaging time [460 s]
t_D : delay time [60 s]

Figure E.6 indicates that the supplemental data processing method like this would bring about better results as expected. However, the maximum error included in this data processing method cannot be estimated precisely at present.

E.3 Calibration of temperature signals

Most of the thermocouples are 0.3 mm in sheathed outer diameters. Their source impedances are very high (for instance, the DC resistances are around 1.0 kΩ at room temperature, 1.4 kΩ at 400°C level and 1.7 kΩ at 900°C level). It is therefore very difficult to measure the temperature precisely, avoiding the possible mismatching with the convenient data logging devices. In addition, there were no signal isolation amplifires until the beginning of the 141th SIENA operation by which the active circuit for a burn-out detection of heater pin can be isolated from the thermocouple connected. Therefore, some of the earlier temperature data included errors caused by the foreign EMF (electromotive force) from the active circuits. Further, the temperature measurement circuits of the HP-2116C system had no devices to fix the cold-junctions of the thermocouples to be zero degree C. Therefore, the temperature difference between the truth and a certain cold-junction temperature must be estimated and added to the raw data.

Besides these insufficiencies in constructing the instrumentation system, the quality of the thermocouple fabrication becomes in question, because the thermocouples equipped are of 0.75 % class (maximum error of ±7.5 °C at 1000 °C level) and easily deteriorate under heavy utilization beyond the allowable temperature range of up to 600 °C.

There were many calibration runs conducted under the conditions of zero power, i.e. under the isothermal conditions. These runs were scheduled to be carried out at the beginnings of every SIENA operations. The isothermal data from all thermocouples were measured with the high accuracy data scanner YODAC which had a function of supplementing the cold-junction temperatures. These data were, therefore, used for the calibration, taking the most reliable thermocouple T-003 as the standard thermocouple. There were several unappropriate runs for the calibration. For such runs, the calibration data

were located apart from the linear fitting line, Y = AX + B. These data indicated that there might be great amounts of temperature falls due to heat losses when sodium was driven very slowly from the inlet of the test section to the inside of the test section. Therefore, the data measured under very slow sodium flow were discarded from the data base for the calibration. From the fitting equation, one can estimate both the degree of global mismatching and the over-all offset unique to each thermocouple. The calibration work was conducted with the aid of the interactive SISCO (Sensor Information Service Code). First of all, the grouping information of the instrumentation conditions was examined to fix the data base for the calibration of each thermocouple, while it was sometimes modified based on the calibration results. For every groups of calibration data, the fitting equations were obtained. Therefore, if the instrumentation network is altered once or twice throughout the 37G experiments, plural sets of sensor information are deduced for those thermocouples concerned. Two typical results of the calibrations of those thermocouples having simple data bases are illustrated in Figs. E.7(a) and (b), where the upper figure means the result of the fitting of raw data and the lower figure the fitting of the artificially corrected data in respect to mismatching and offset. It can be found that the gain correction factors (inverse of the mismatching factor) of T-1012 M and T-02S are 1.0342 and 1.0150, respectively. The reason of causing the difference in these values lies in different instrumentation network, i.e. the thermocouple T-1012M was connected to the HP-2116C system while the T-02S was not.

Figure E.7(c) shows the case of T-1011M which was connected to the burn-out detection circuit of the heater pin. The burn-out detection circuit was isolated at the beginning of the 141th operation. Therefore, the data base was divided into two groups (based on whether or not the isolation amplifier was in operation) to yield two fitting lines for two groups of data sets. The gain correction factors for those thermocouples connected to the burn-out detection circuits without isolations were very large, e.g. 1.0646 for T-1011M. In addition, large magnitudes of offsets were added to such thermocouples, e.g. 34.5 °C for T1011M, while they were small for the other thermocouples, e.g. 3.9 and 1.8 °C for T-1012M and T-02S, respectively. The introduction of the isolation amplifier extracted the bad influence of the burn-out detection circuit to lead to the normal values of the gain correction factor and offset like those of the thermocouples which did not connected to the burn-out detection circuit.

The instumentation network was often altered prior to renewing the SIENA operation. At some times, the buffer amplifiers which had been used for the thermocouples whose fluctuation signals were measured simultaneously with high amplifications were disconnected from the instrumentation network. The calibration result of such a case is illustrated in Fig. E.7(d), where the case of the thermocouple T-01F is selected as an example. The gain correction factor and offset of the thermocouples connected to the buffer amplifiers differ quite randomly depending on the random adjustments of the amplifiers.

There are a few thermocouples whose outer diameters are 1.3 mm. The calibration result of the thermocouple T-012M is shown in Fig. E.7(e). The gain correction factor of such a large diameter thermocouple is close to 1.0, i.e. 1.0123 for T-012M, because of its small source impedance. Therefore, it would be reasonable to treat the thermocouples located at the outside of the isothermal sodium boundary as being precisely measured.

After fixing the gain correction factors and offsets of individual

thermocouples, the common offsets of all thermocouple signals measured by the HP-2116C system were evaluated. A common offset to all channels of HP-2116C system to which the thermocouples are connected can be regarded as being composed of two components: One is a negative-signed value of common EMF corresponding to the cold-junction temperature, and the other is an ordinary offset of the front multiplexer of the A/D converter. In the present data processing method, these two were treated not separately by comprehensively by the name "cold-junction temperature".

The addition of the cold-junction temperature to the initial value of the time series data from HP-2116C must lead to the reliable data measured by the YODAC prior to starting the HP-2116C system, if the initial condition of each run is stationary. From this principle, two data sets of HP-2116C and YODAC were compared to see the agreement of temperature values from both measurements. Figure E.8 shows a typical result of this exercise, where the axial temperature profiles are drawn. The upper figure shows the raw plots of HP-2116C data and YODAC data, and the lower figure shows the comparison of the raw data of YODAC and the artificially corrected data of HP-2116C by adding a constant value to all HP-2116C data so that the inlet temperature T-003 becomes equal to that of YODAC data. It can be concluded that the addition of a certain constant value (i.e. the cold-junction temperature) to the HP-2116C data leads to the agreement with the YODAC data. The change of the cold-junction temperature thus obtained during one day of SIENA operation is illustrated in Fig. E.9, taking the absolute time of each run as a horizontal axis. From these data, it would be said that the cold-junction temperature can be estimated reasonably for many cases. However, one should note that this method does not necessarily lead to appropriate results for all cases due to the non-stationarities of the initial conditions.

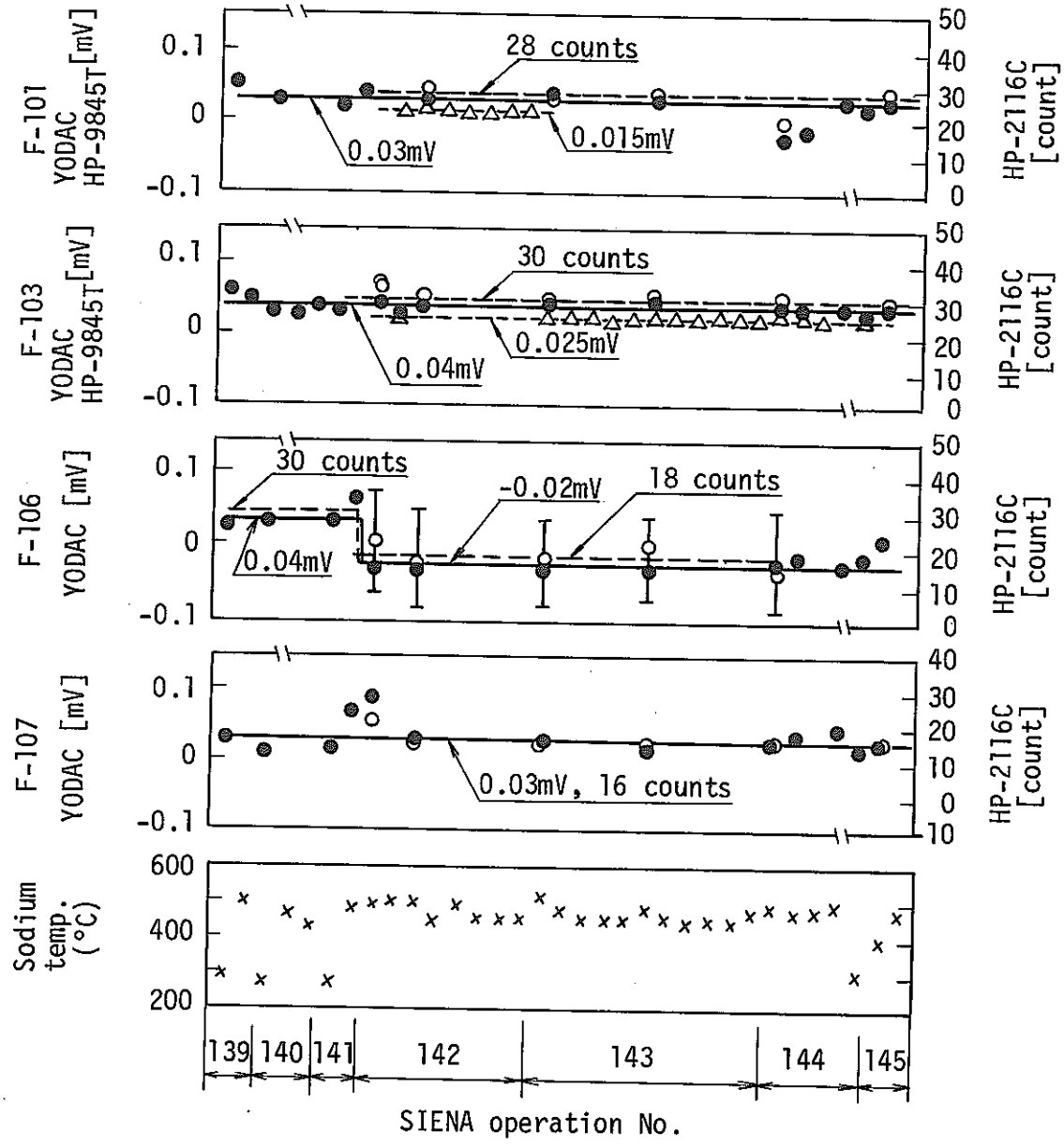

Fig. E.1 Zero-flow calibration data of the flow-meters
(● : YODAC, ○ : HP-2116C, △ : HP-9845T)

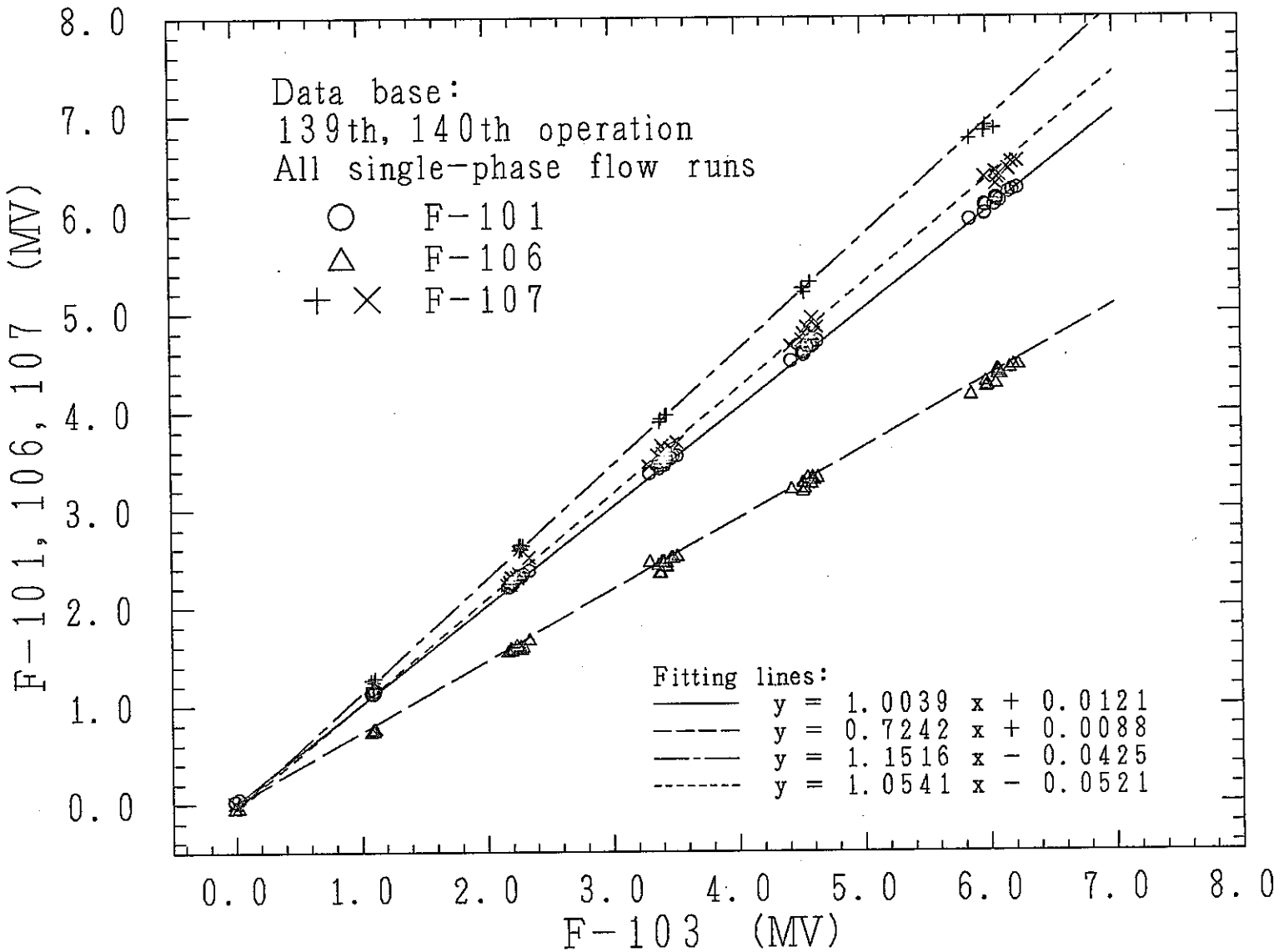

Fig. E.2 Relative calibration of the flow-meters F-101, F-106 and F-107 using the standard flow-meter F-103

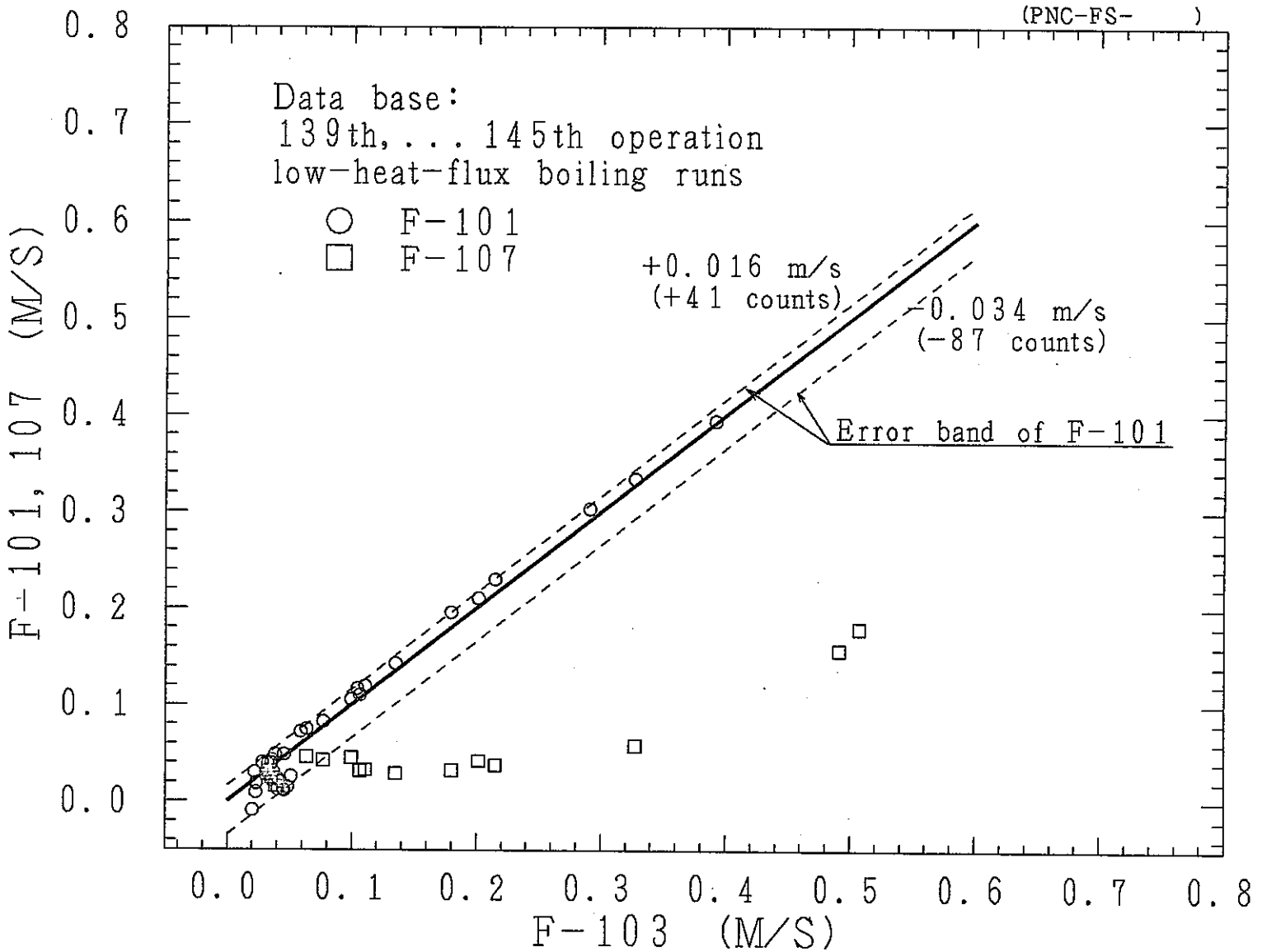

Fig. E.3 Evaluation of the accuracies of flow-meters

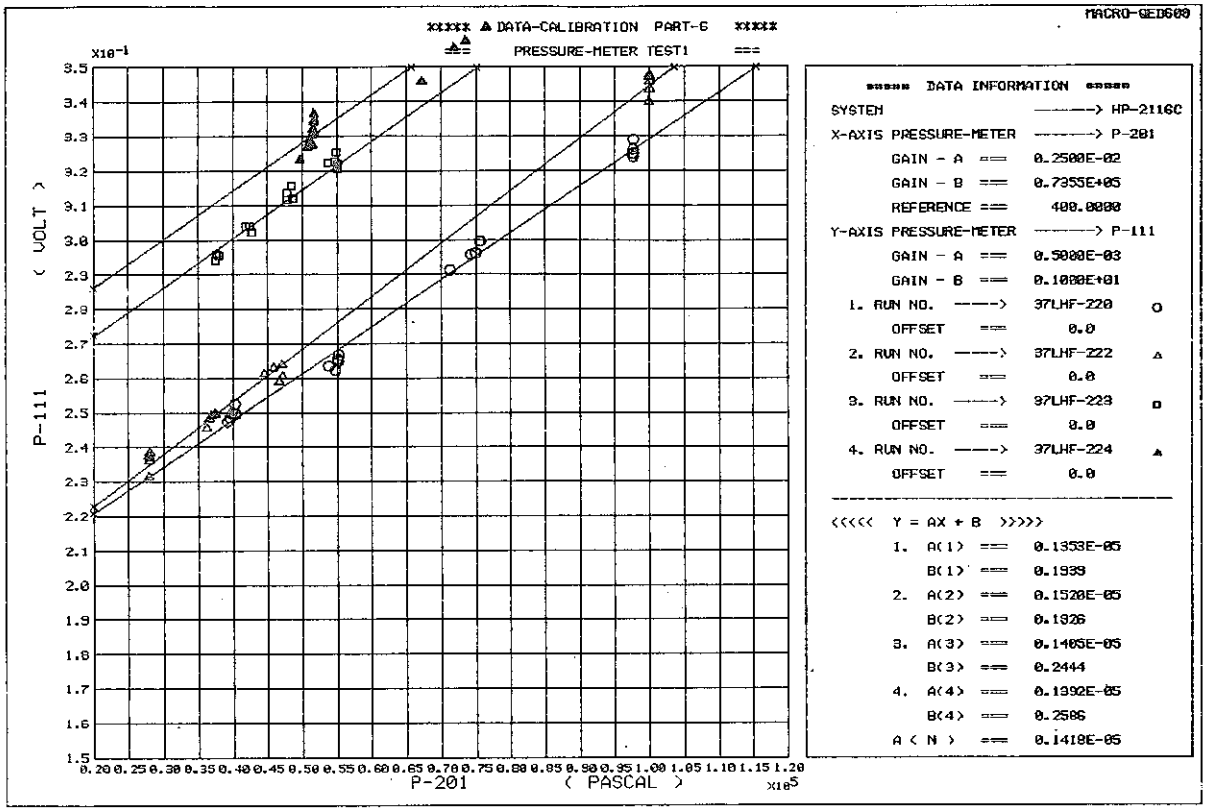

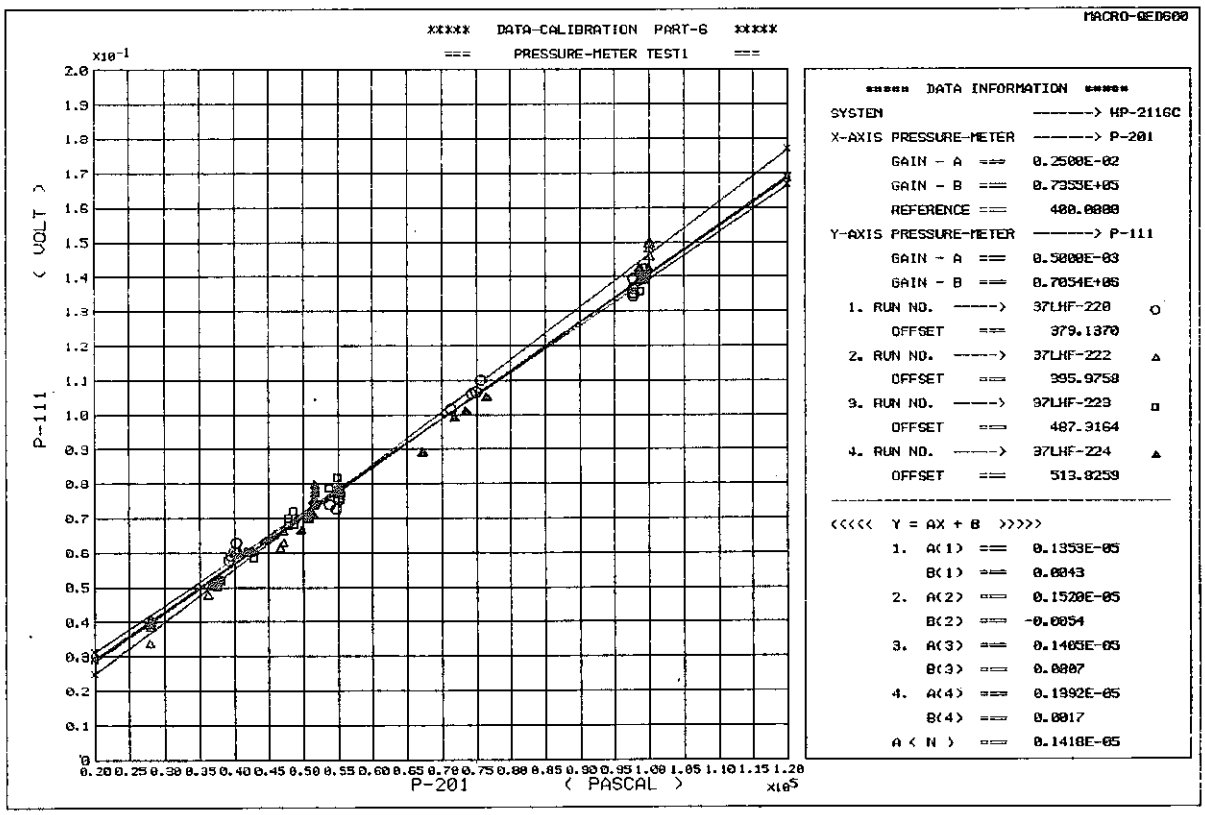

Fig. E.4(a) Calibration of the pressure transducer P-111

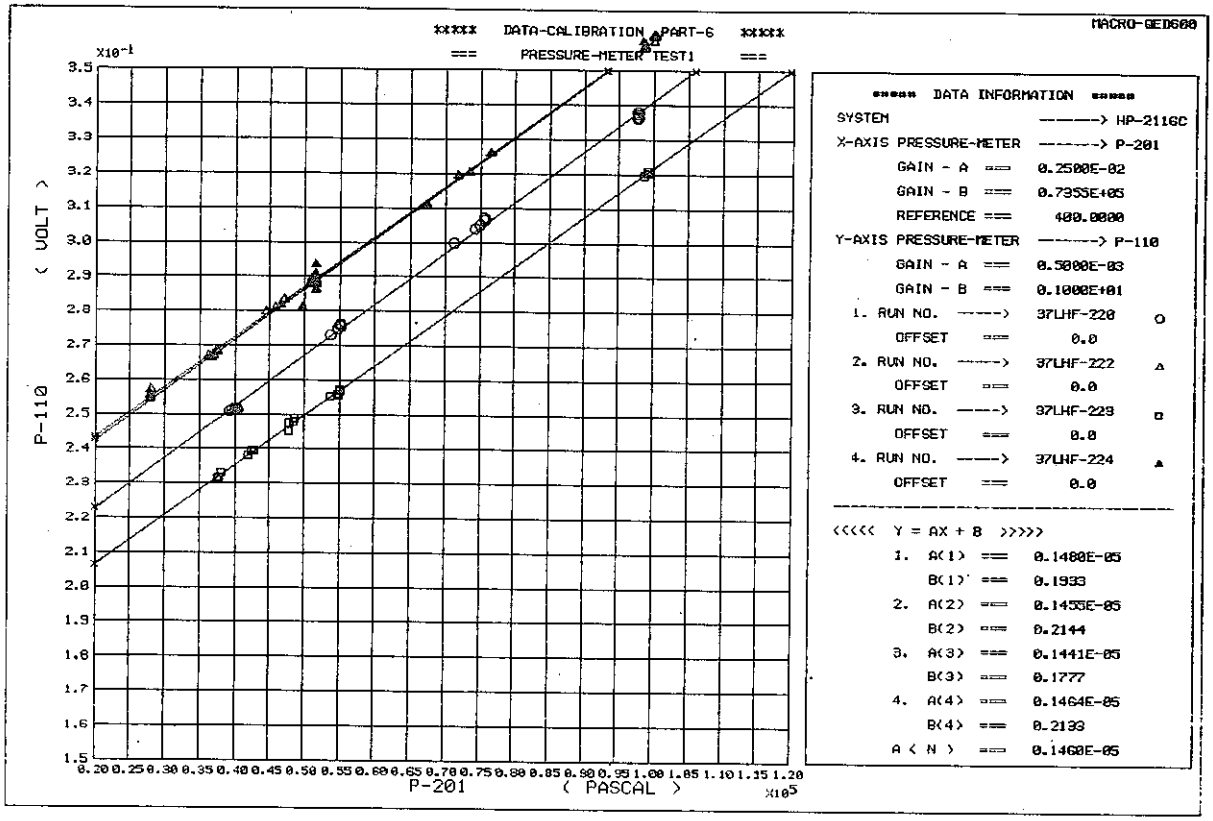

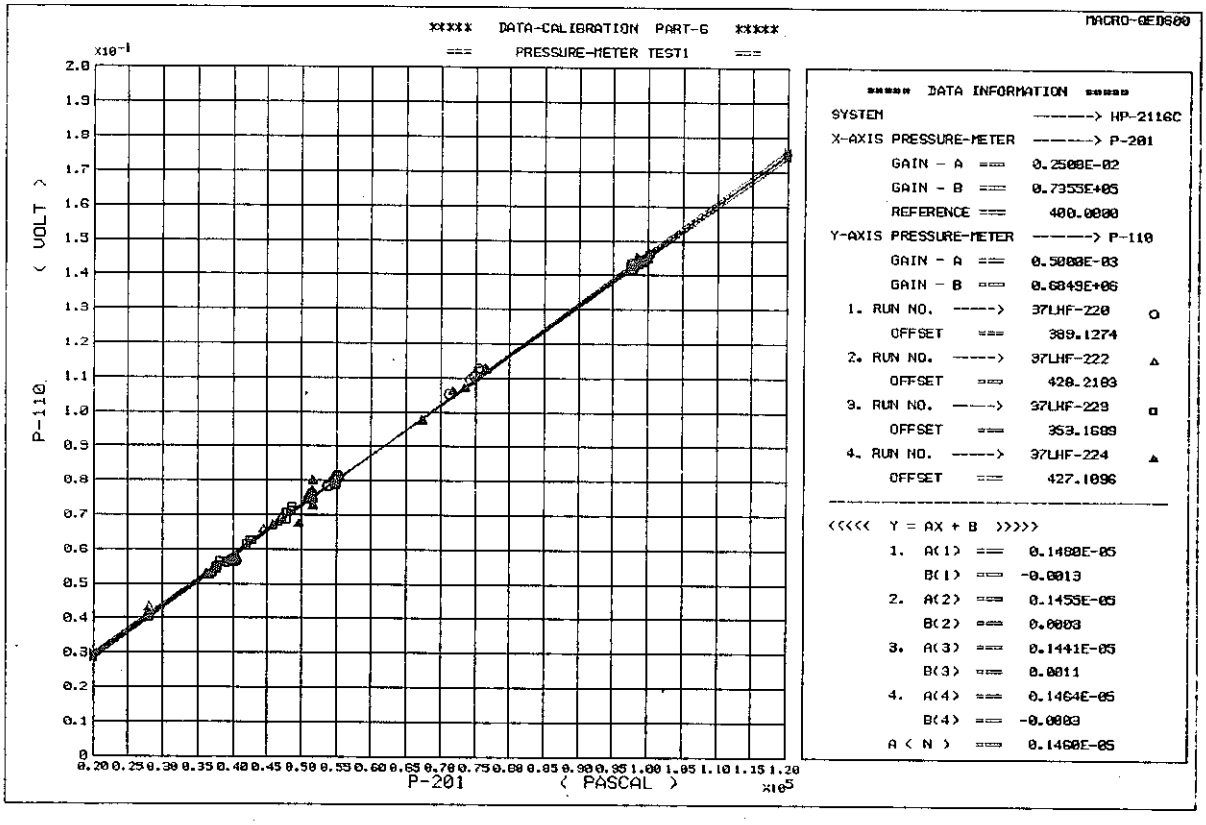

Fig. E.4(b) Calibration of the pressure transducer P-110

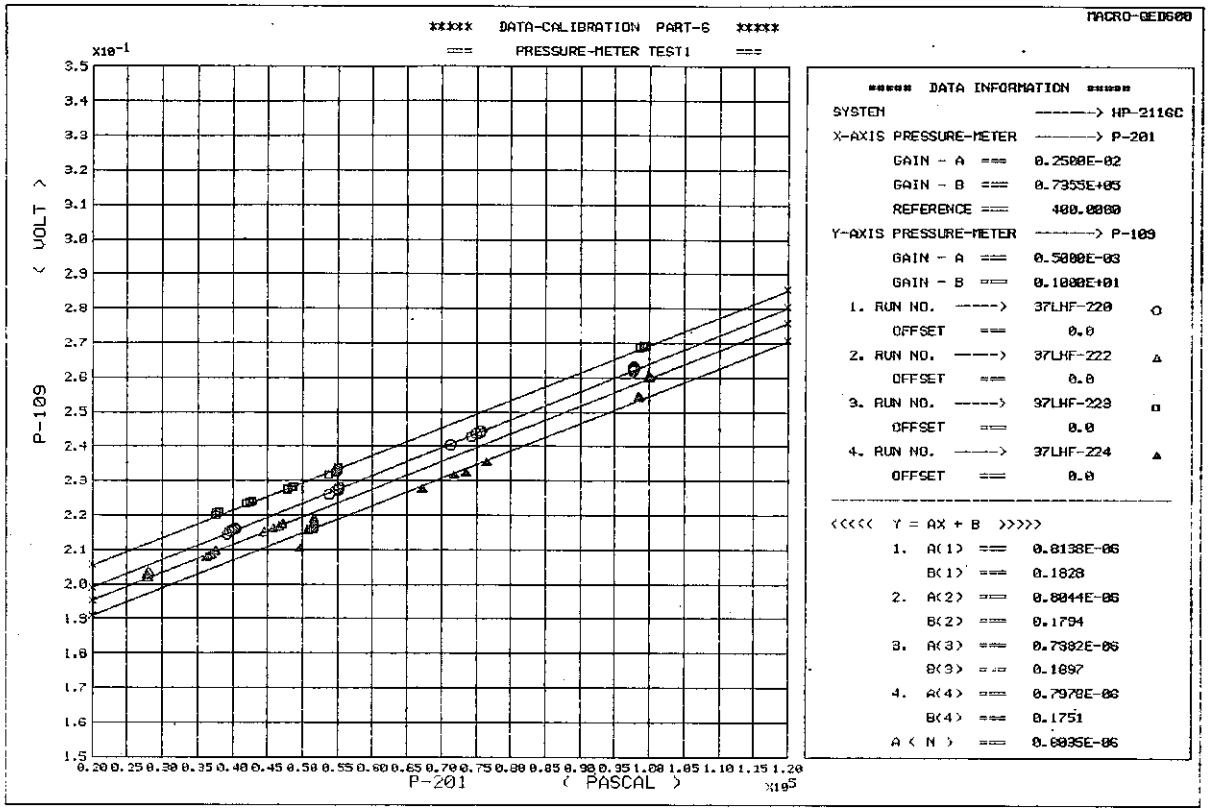

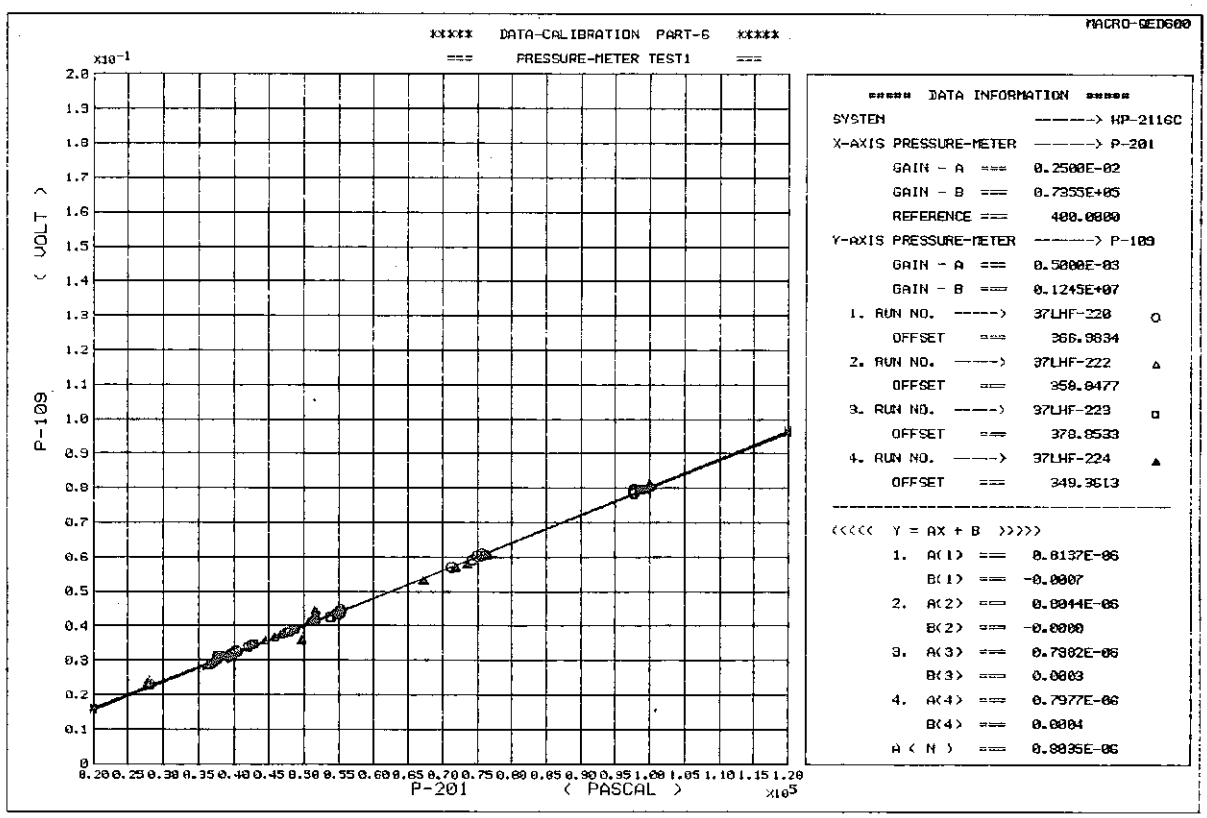

Fig. E.4(c) Calibration of the pressure transducer P-109

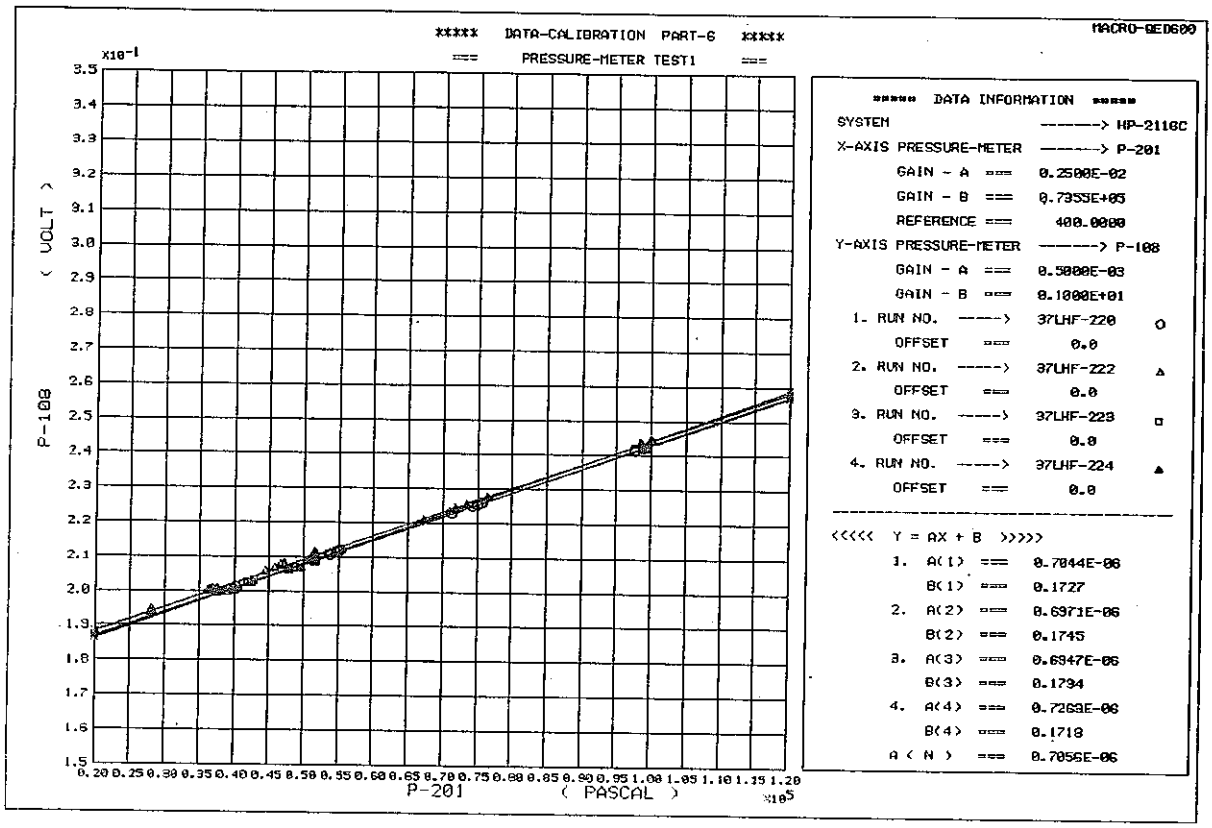

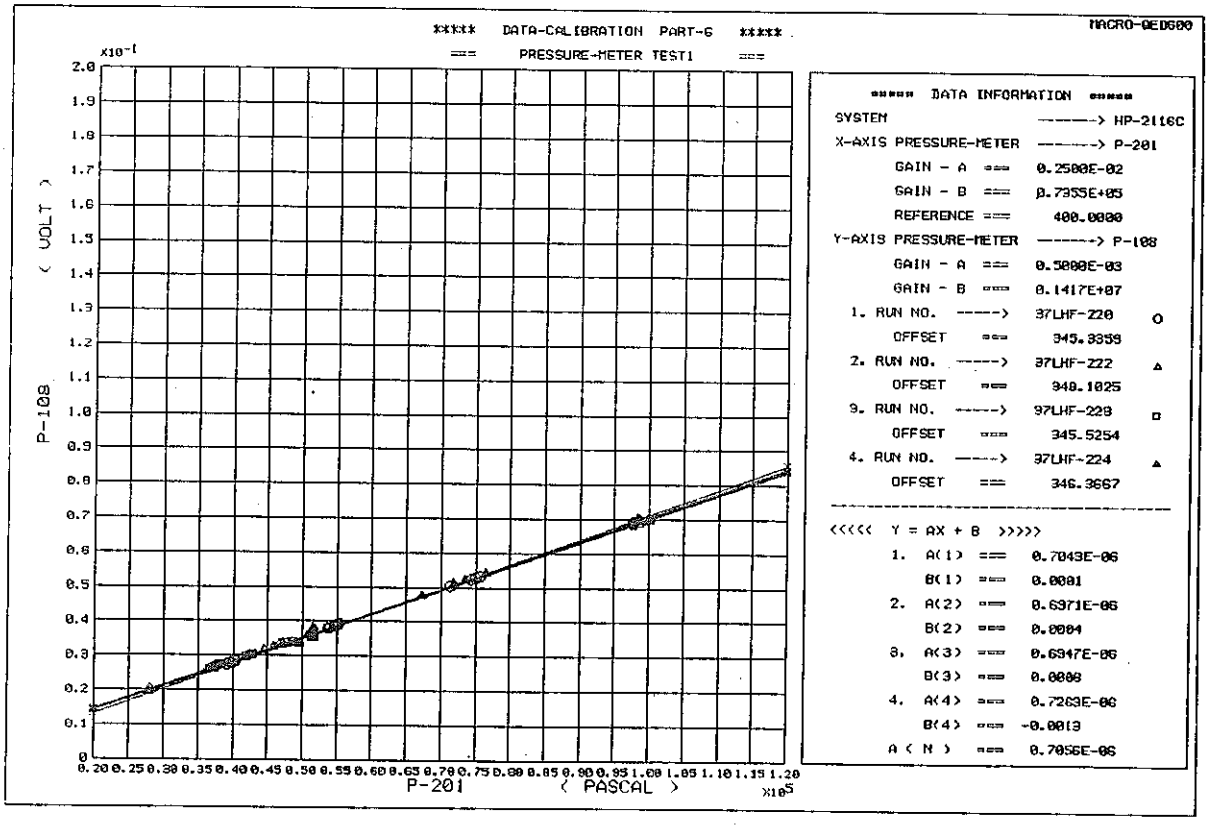

Fig. E.4(d) Calibration of the pressure transducer P-108

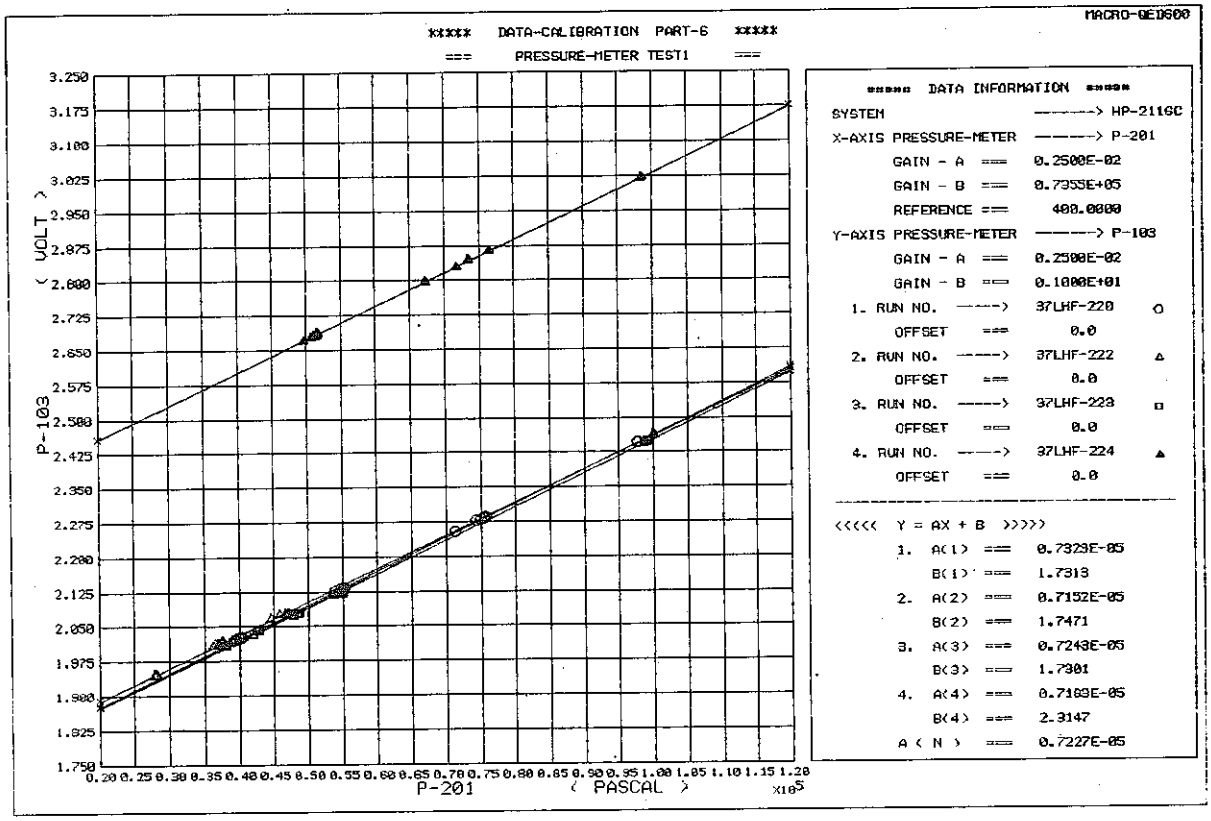

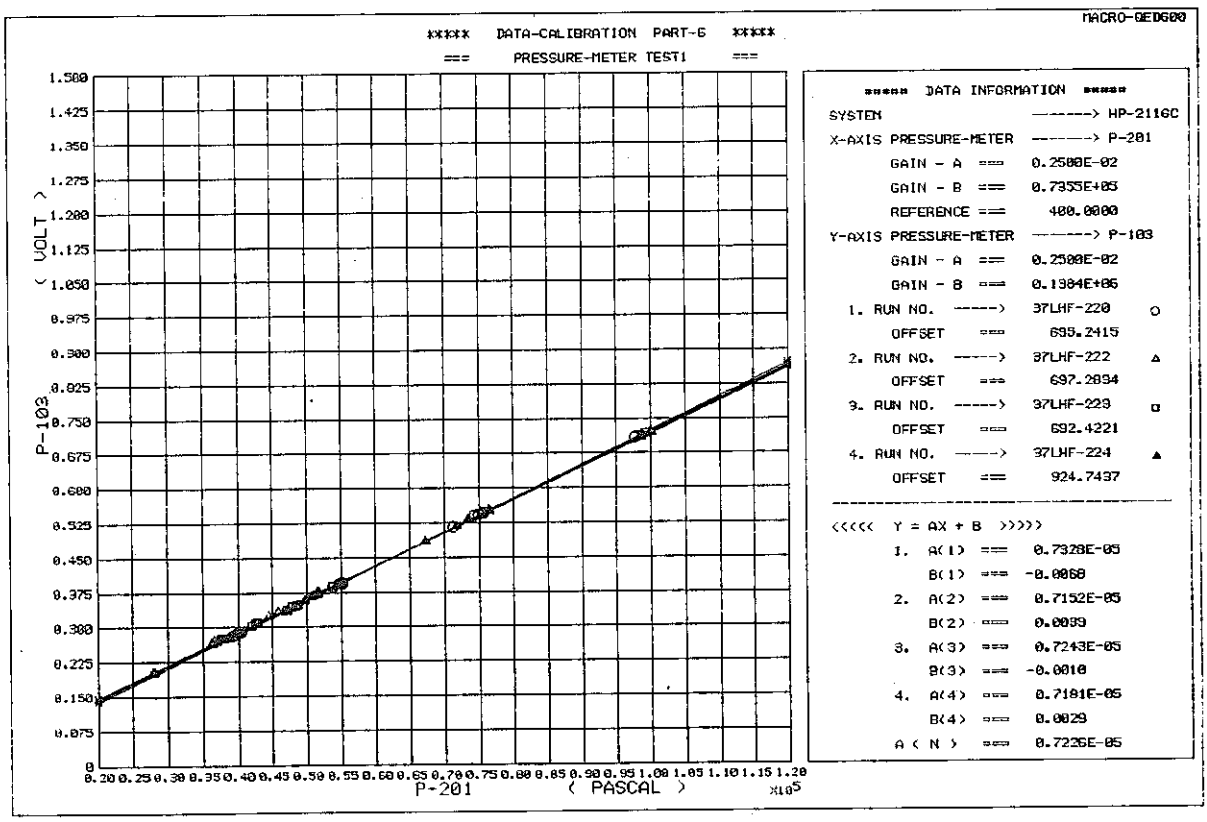

Fig. E.4(e) Calibration of the pressure transducer P-103

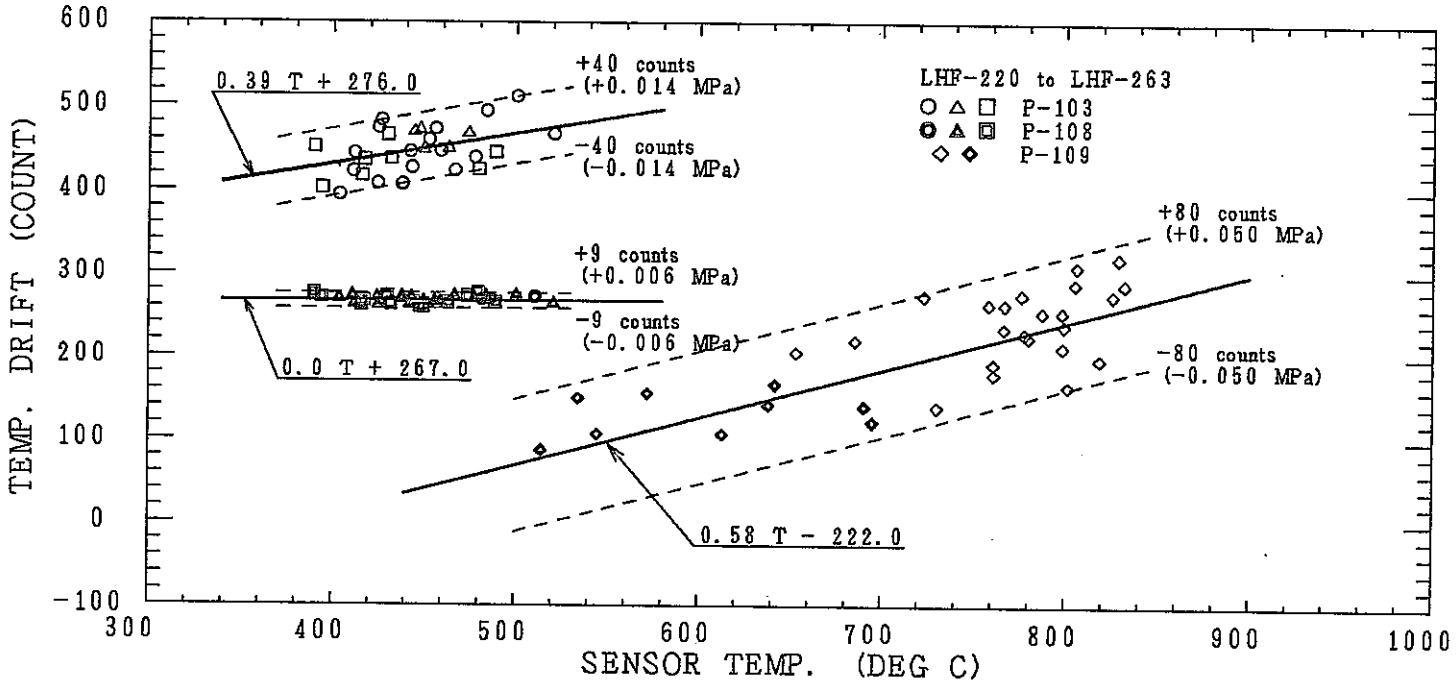

Fig. E.5(a) Temperature drifts of the offsets of pressure transducers P-103, P-108, P-109

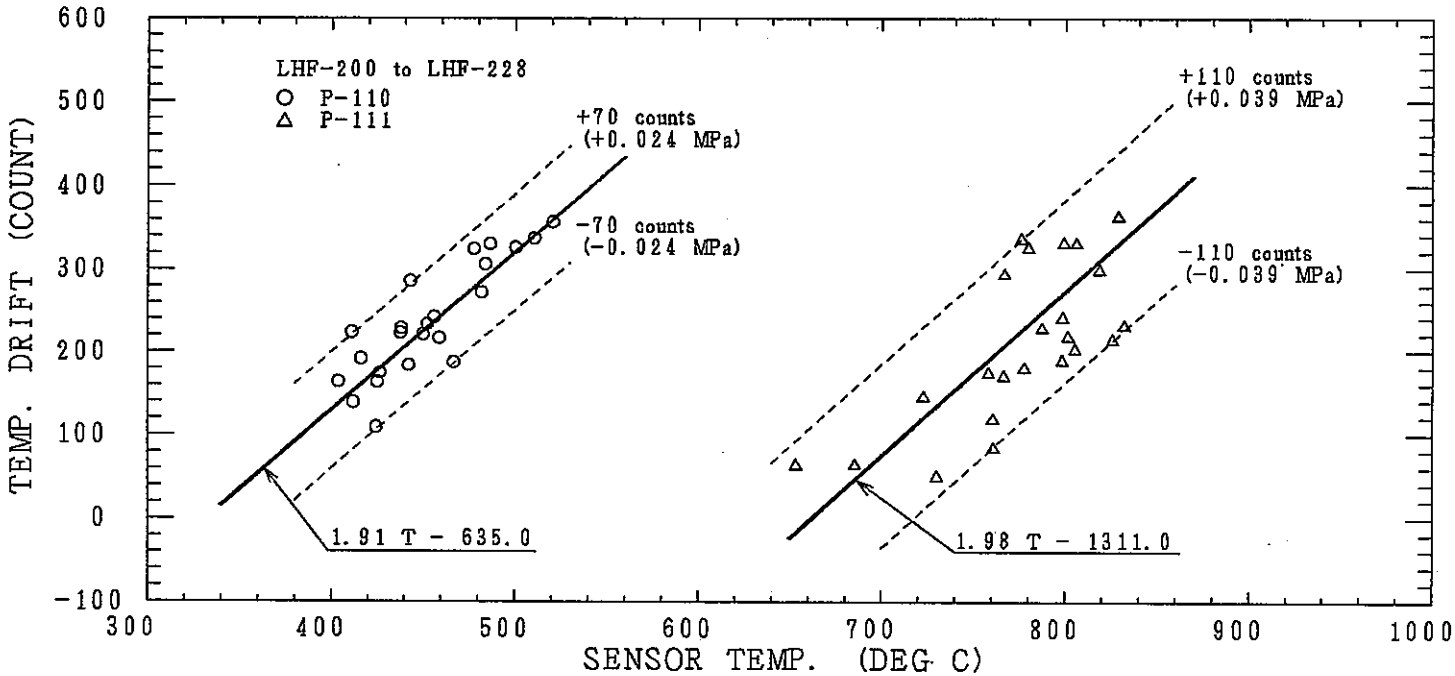

Fig. E.5(b) Temperature drifts of the offsets of pressure transducers P-110, P-111

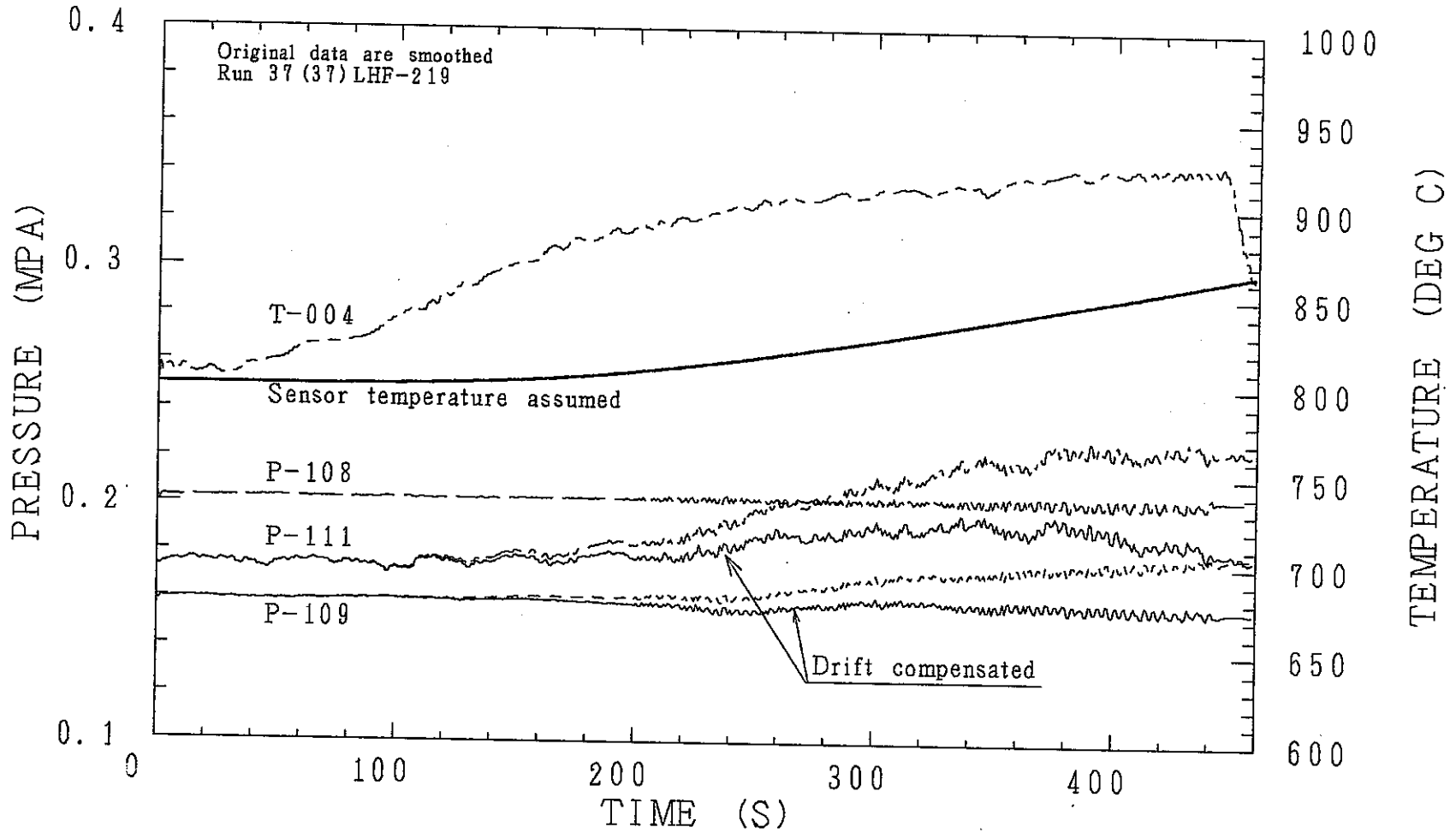

Fig. E.6 Compensation calculations of the temperature drift components of the offsets of pressure transducers

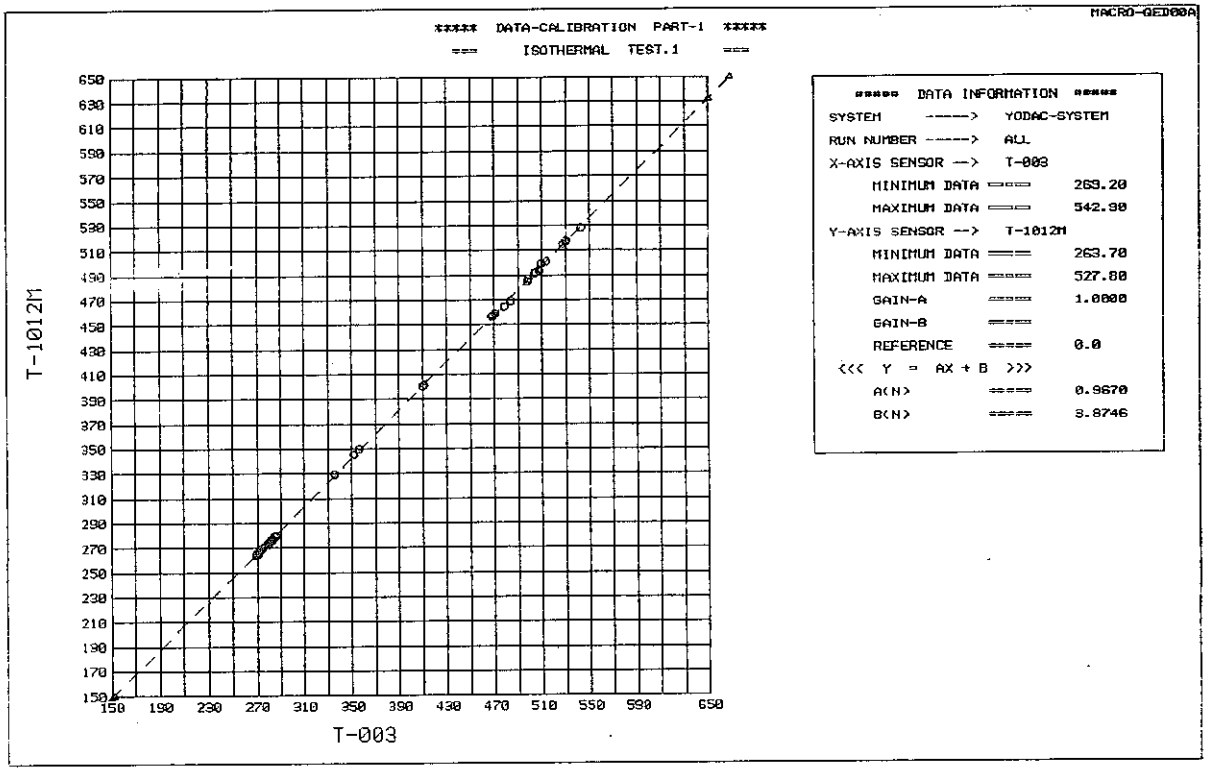

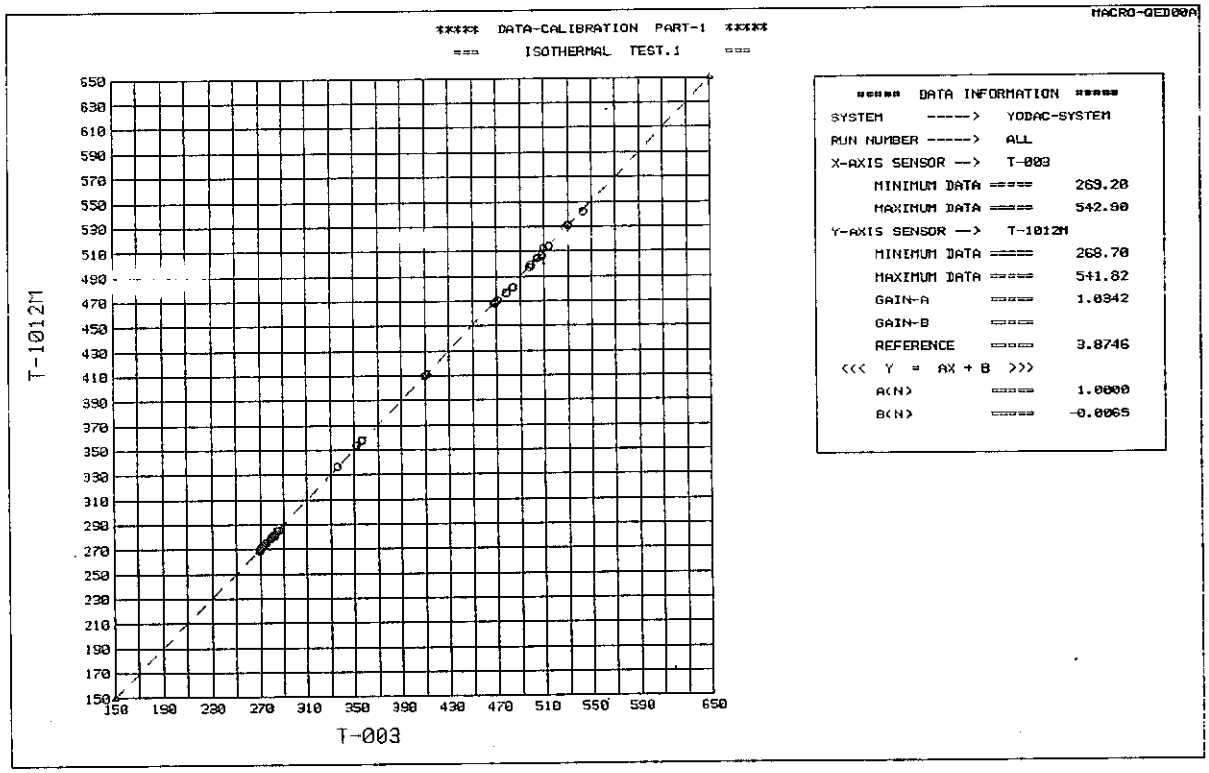

Fig. E.7(a) Calibration of the thermocouples T-1012M
(standard case mismatching with HP-2116C)

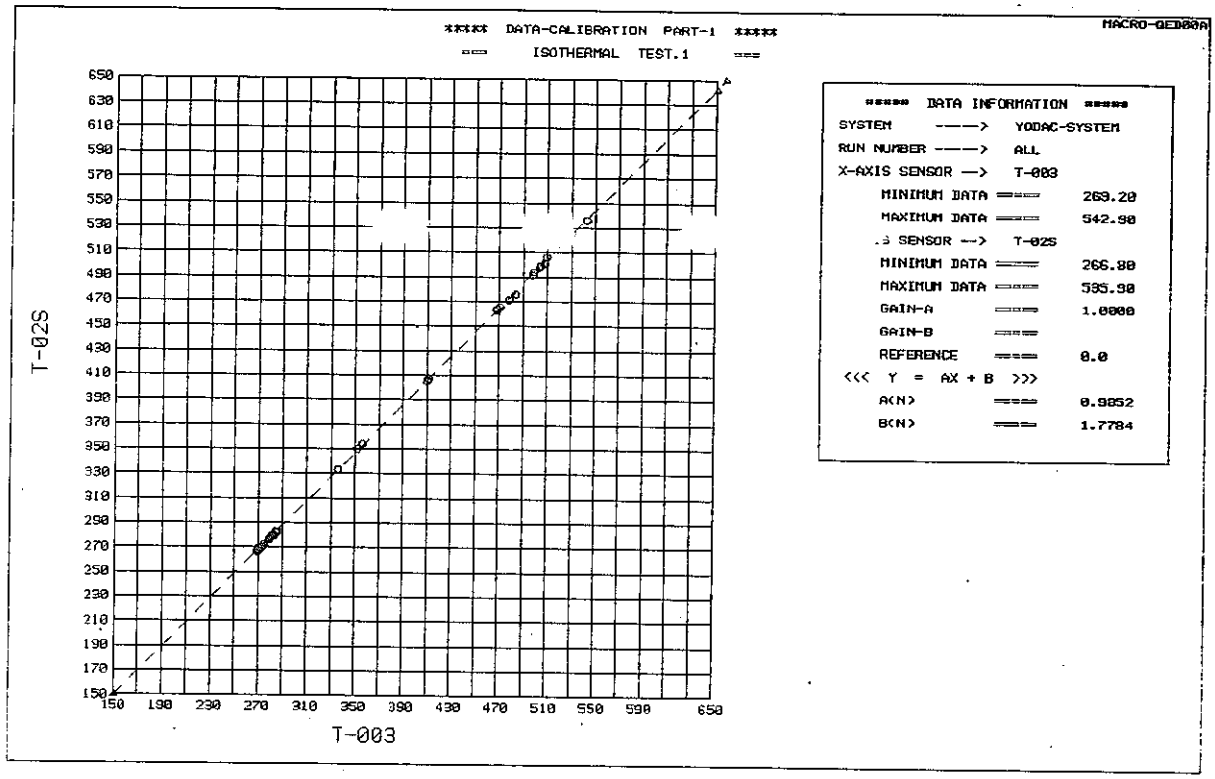

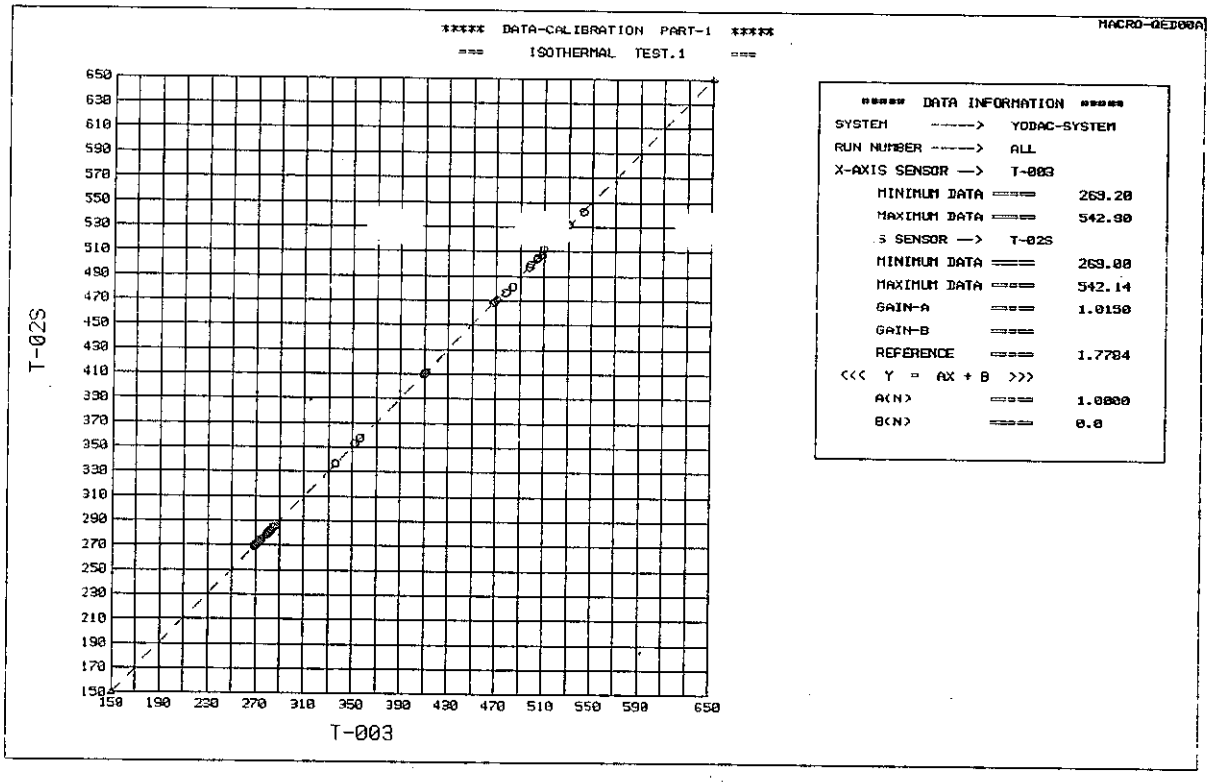

Fig. E.7(b) Calibration of the thermocouples T-02S (smallest mismatching case)

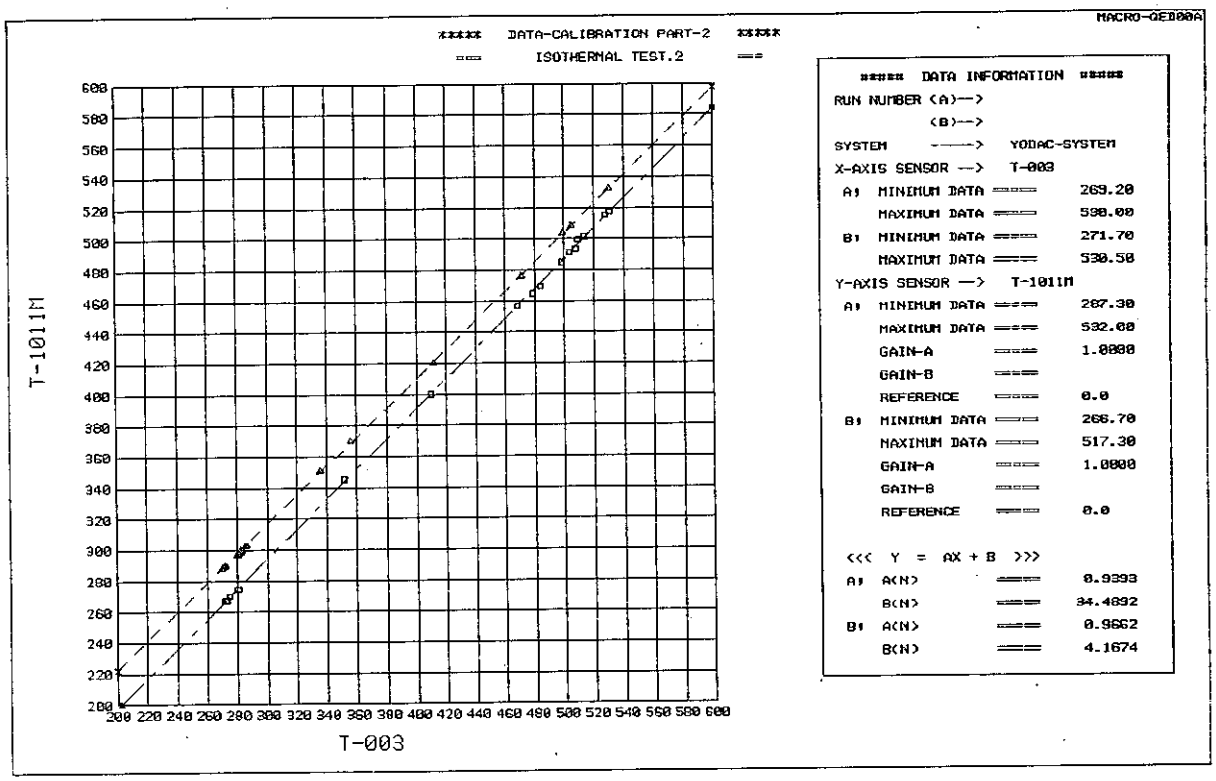

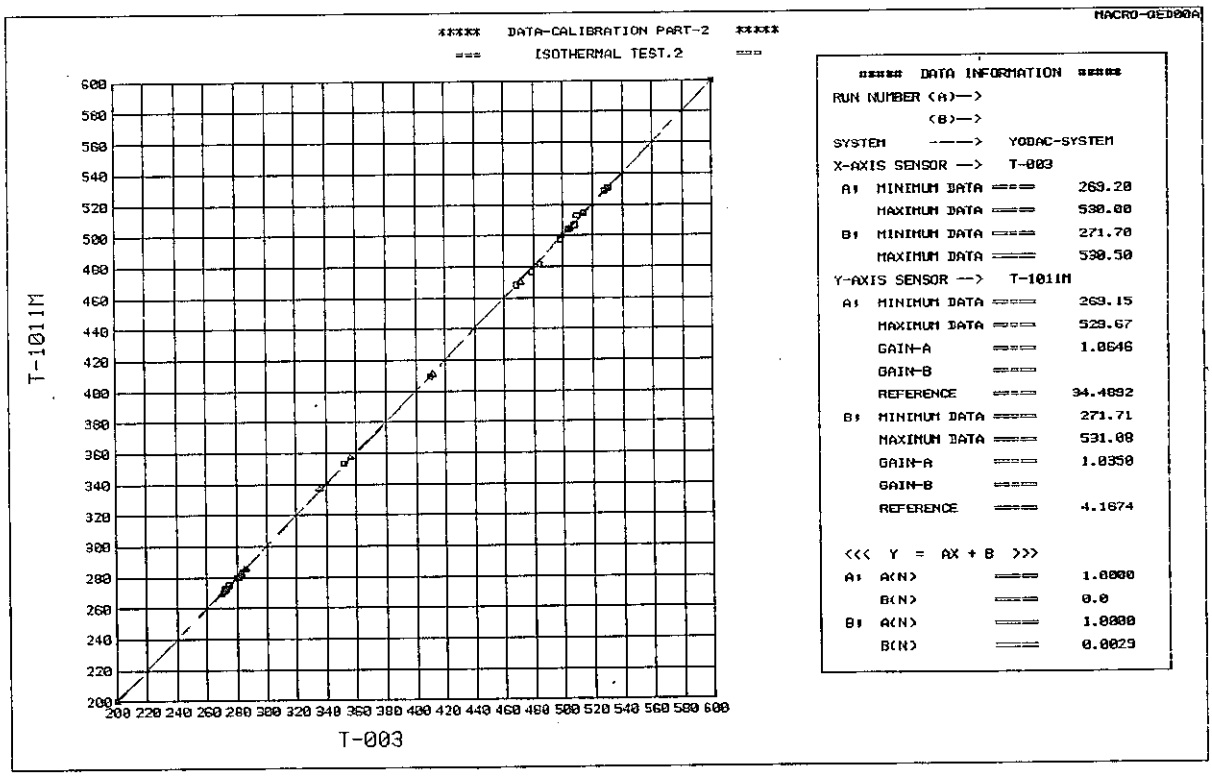

Fig. E.7(c) Calibration of the thermocouples T-1011M
(mismatching with the burn-out detection circuit)

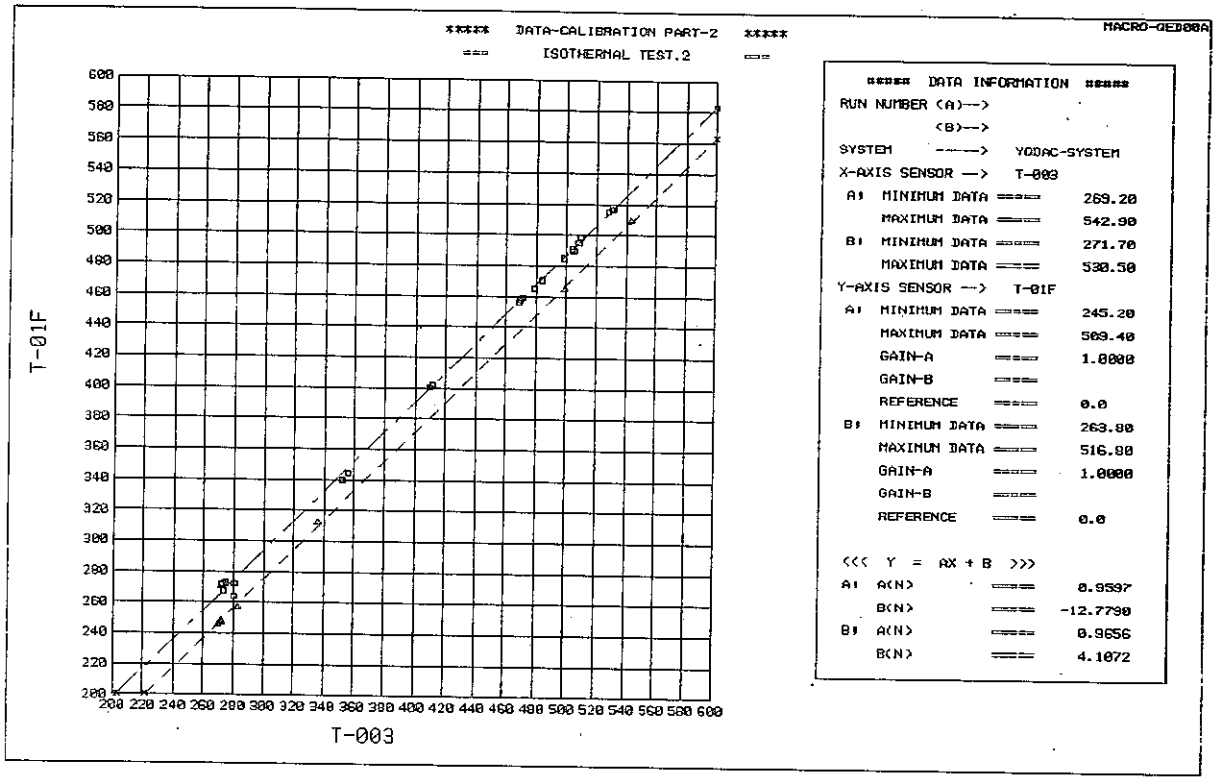

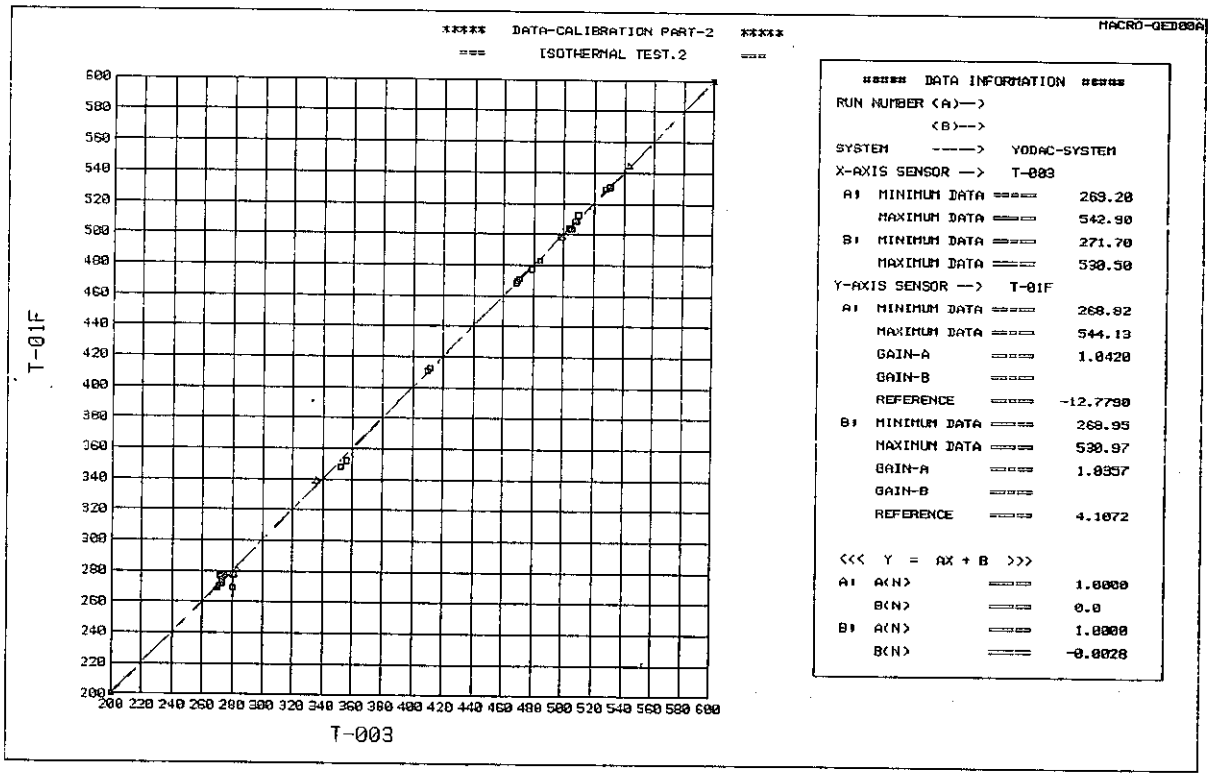

Fig. E.7(d) Calibration of the thermocouples T-01F
(mismatching with the fluctuation measurement amplifier)

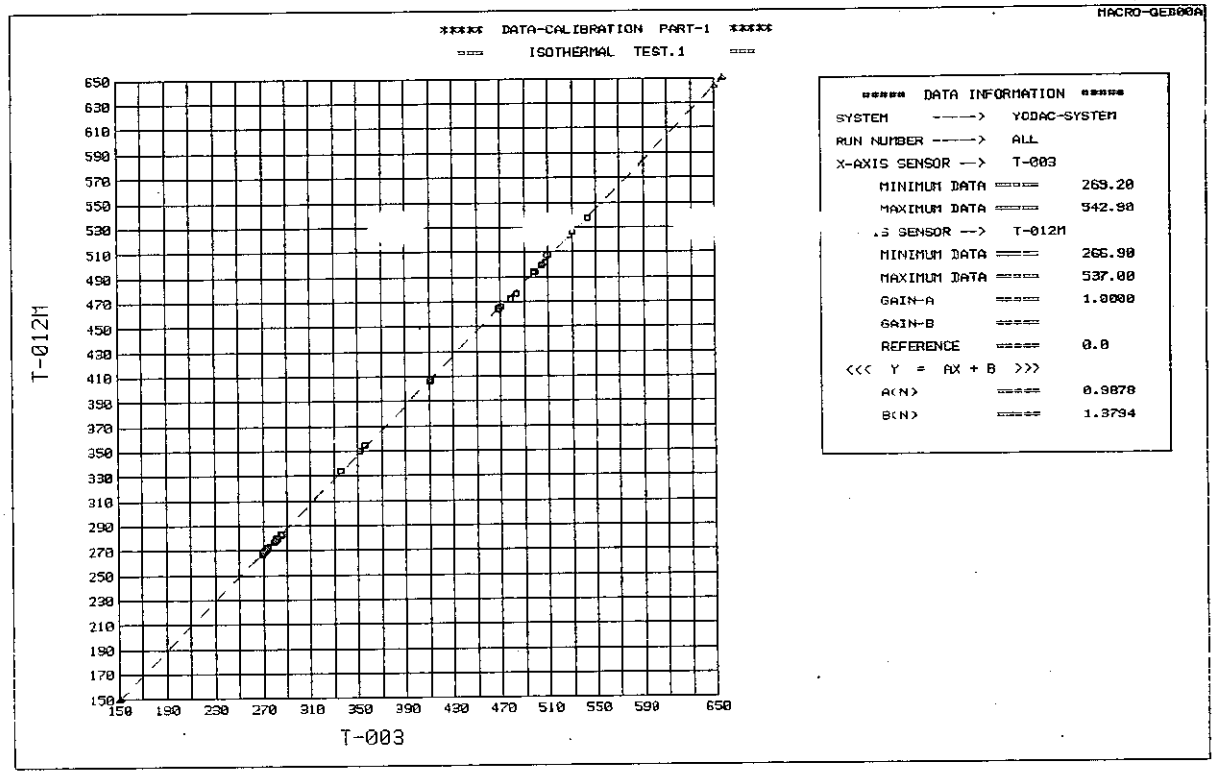

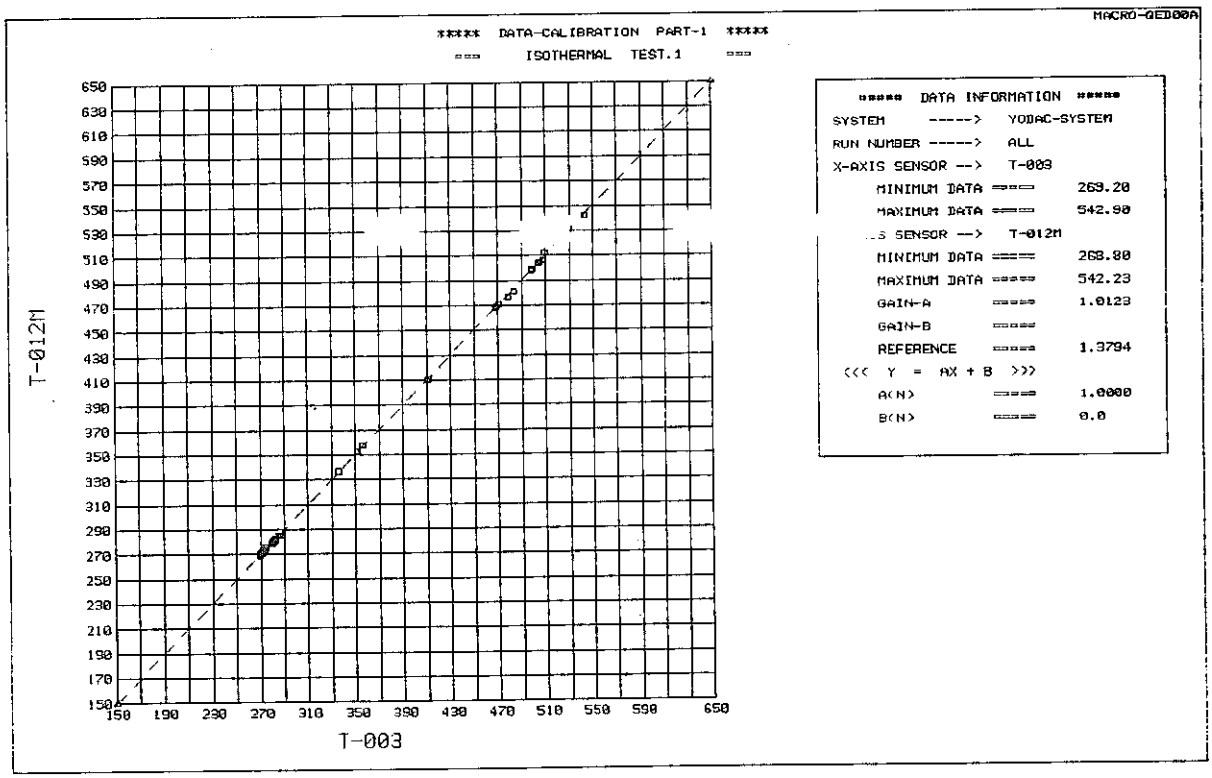

Fig. E.7(e) Calibration of the thermocouples T-012M
(special case of 1.3 mm dia. thermocouple)

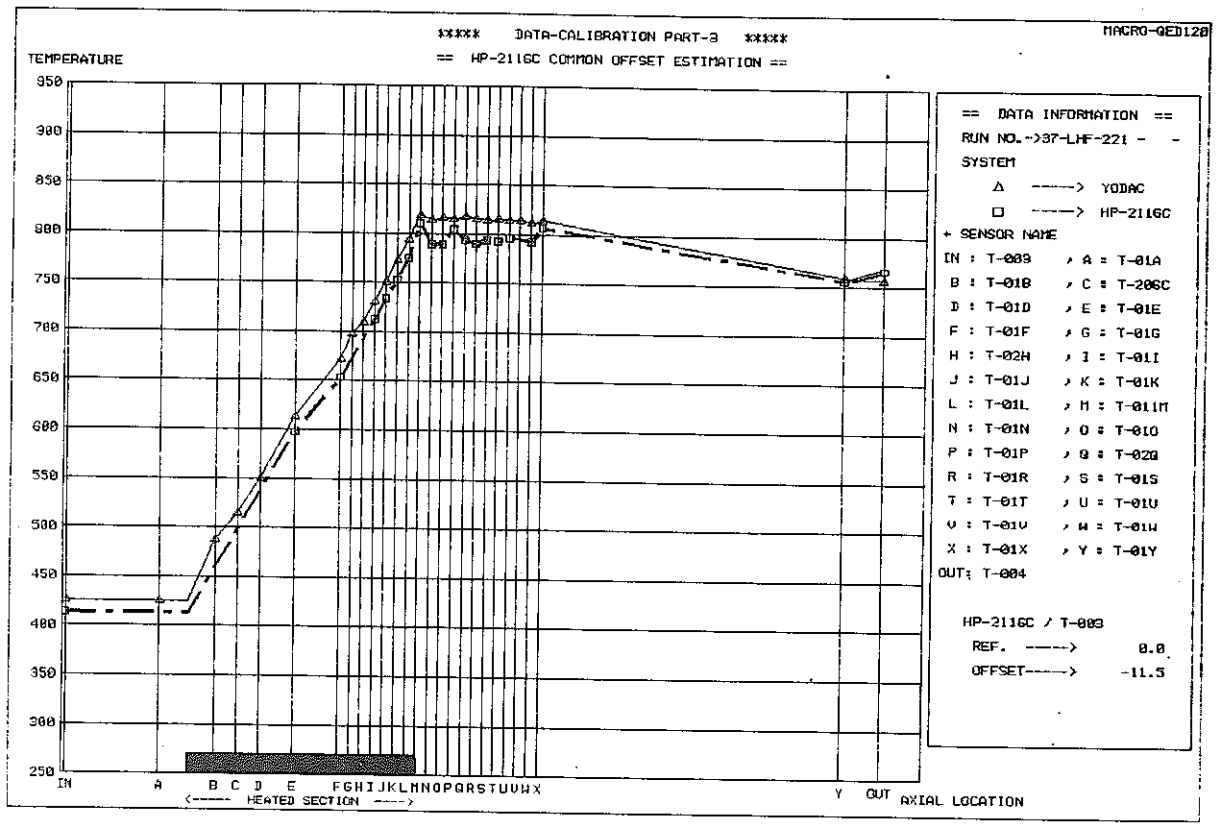

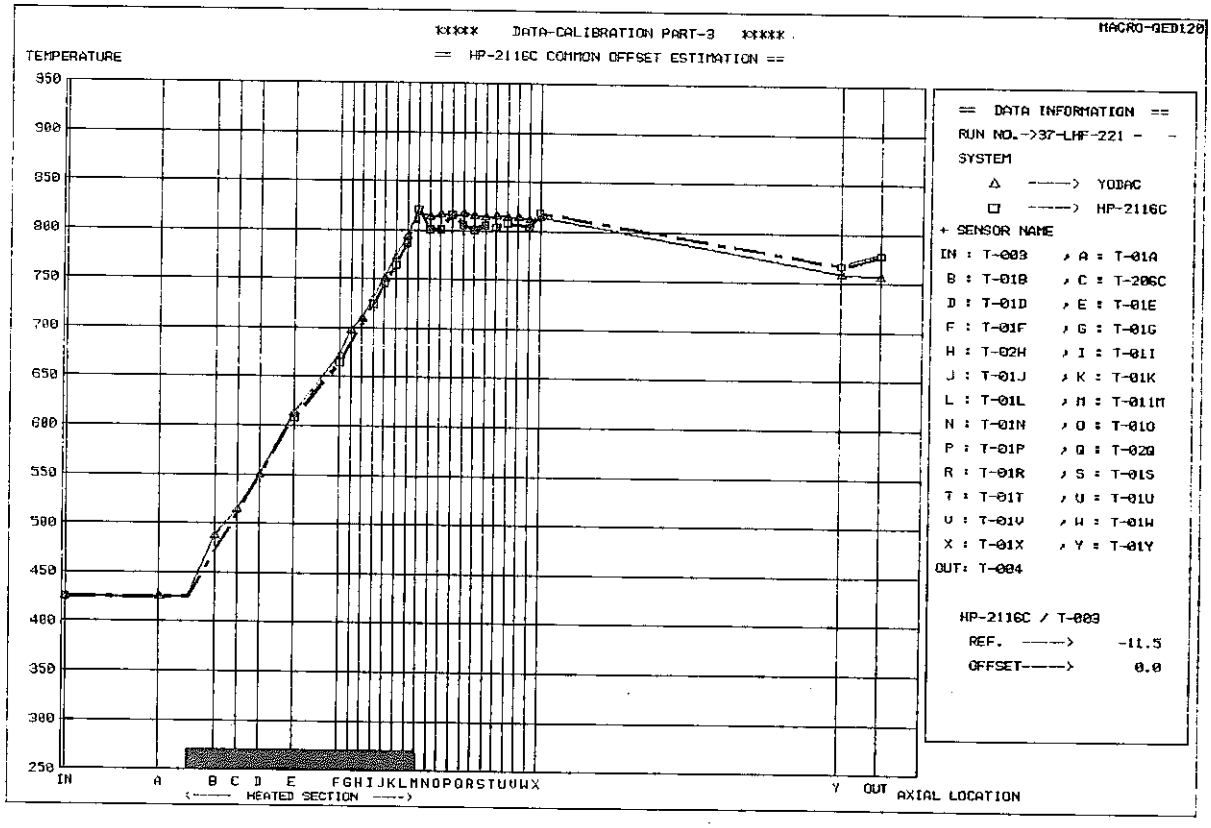

Fig. E.8 Compensation of the cold-junction temperature

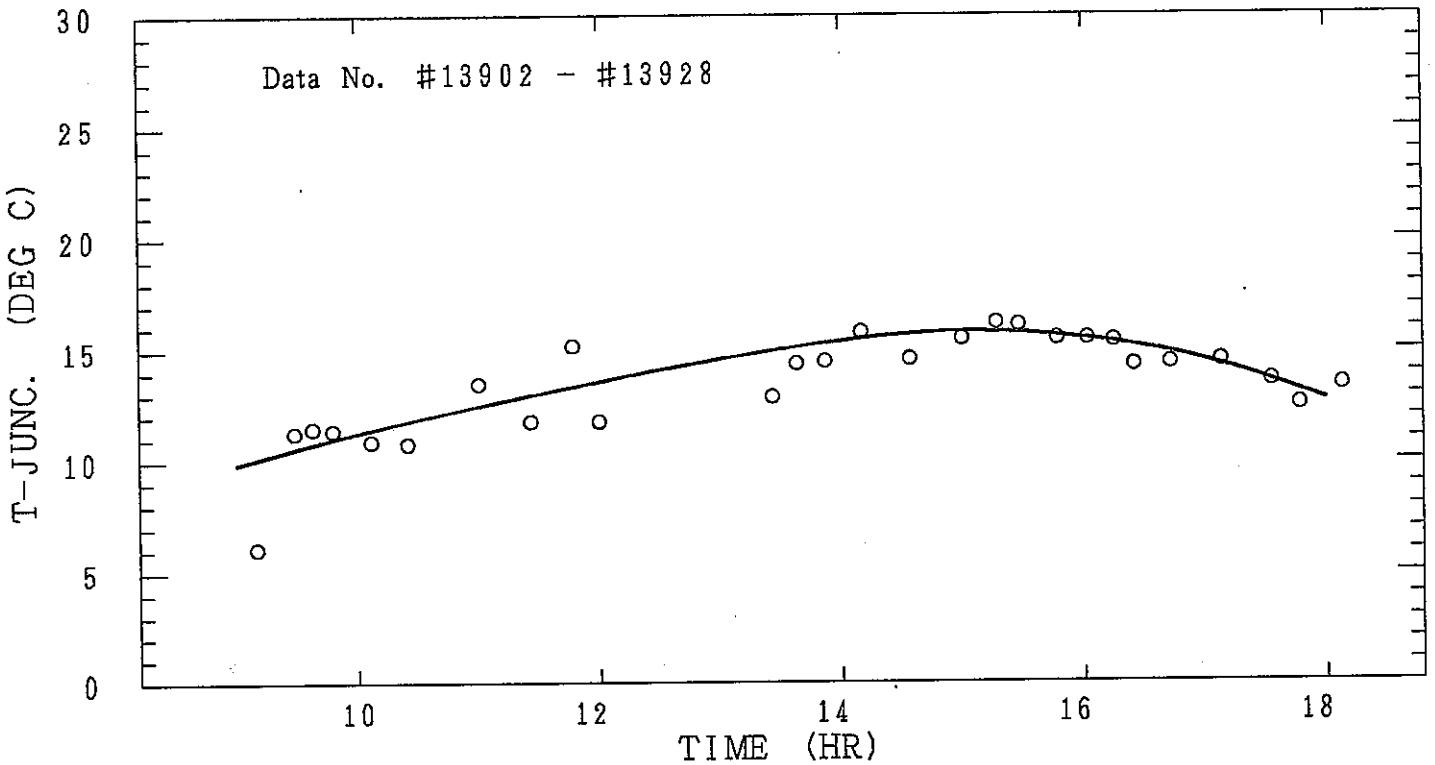

Fig. E.9 Change of the cold-junction temperature during one day

Appendix F: Records of the SIENA Operations for 37G Experiments

In the following lists of the 37G operation records, the experimental procedures are summarized using the data from some monitor recorders and the HP-9845T monitoring system. The numerical data representing instantaneous status may have unfixed errors at present. They will be corrected in the forthcoming examinations.

The SIENA facility was operated seven times for the low-heat-flux boiling experiments. The serial operation numbers are 139, 140, 141, 142, 143, 144, and 145. A total of 50 runs are carried out as follows:

139th operation: (1979, 11.20-22)	Low-heat-flux boiling runs; series (1) (examination of boiling inception conditions under low-flow)	
	Run 37(37)LHF-200 through 203	4 cases
140th operation: (1979, 12.4-6)	Low-heat-flux boiling runs; series (1) (continued)	
	Run 37(37)LHF-210 through 219	10 cases
141th operation: (1980, 1.16-18)	Low-heat-flux boiling runs; series (1) (continued)	
	Run 37(35)LHF-220 through 228	9 cases
142th operation: (1980, 1.30-2.1)	Low-heat-flux boiling runs; series (2) (examination of dryout conditions under low-flow)	
	Run 37(36)LHF-230 through 232	3 cases
	Run 37(34)LHF-233 through 239	7 cases
143th operation: (1980, 2.26-28)	Low-heat-flux boiling runs; series (2) (continued)	
	Run 37(33)LHF-240 through 248	9 cases
144th operation: (1980, 3.17-19)	Low-heat-flux boiling runs; series (2) (continued)	
	Run 37(29)LHF-250 through 253	4 cases
145th operation: (1980, 4.8-10)	Low-heat-flux boiling runs; series (3) (examination of the effect of gas injection)	
	Run 37(26)LHF-260 through 261	2 cases
	Run 37(24)LHF-262	1 case
	Run 37(20)LHF-263	1 case
	total	50 cases

The test parameters examined are: (1) inlet flow velocity, (2) heat flux, (3) system pressure, and (4) effect of gas injection. To attain aiming test conditions, the weak forced convection method was adopted with the inlet valve being throttled close to 0% opening.

The analysis of the low-heat-flux and low-flow runs requires a highly qualified data in their accuracies. The calibration runs of various sensors used were conducted, therefore, frequently through all operation times. They are also

documented in the following lists. The record of the last SIENA operation (i.e. the 146th operation: 1980, 5.7-8) is appended for seeing the procedures of the final calibration runs which are available for the data checking works.

Record of the 139th operation

1979.11.20

8:20 Preheater power on
(aiming temperature level = 250 ±25 °C)

13:46 Sodium charge
(sodium level = EL-9100 mm)

Pump operation sequence check

14:52 Valve setting

VH-101	VA-102	VM-103	VH-104	VH-109	VH-110
100 %	close	0 %	100 %	100 %	100 %

14:56 Pump on and off
14:58 Valve setting

VH-101	VA-102	VM-103	VH-104	VH-109	VH-110
100 %	close	100 %	100 %	0 %	0 %

15:02 Pump on (~50 l/min)
15:06 Pump power up (~100 → ~150 → ~200 → ~250 → ~290 l/min)
15:15 Pump off

Circulation & purification operation

15:16 Valve setting

VH-101	VA-102	VM-103	VH-104	VH-109	VH-110
100 %	open	100 %	100 %	100 %	100 %

15:18 Pump on (~150 l/min)

SBL & FPL power supplyer check

16:53 FPL power on and up
17:00 FPL power down and off
17:07 SBL power on and up
17:12 SBL power down and off

1979.11.21

Thermocouple and flow-meter calibration runs

Run 37(0)CAL-0150-139-A (No. 1, #13901)

8:52 YODAC scanning
T-003 = 286.1 °C, T-1011M = 287.4 °C, F-103 = 0.549 m/s

Run 37(0)CAL-0-139 (No. 2, #13902)

8:58 Pump off
8:59 Valve setting

VH-101	VA-102	VM-103	VH-104	VH-109	VH-110
100 %	close	0 %	100 %	0 %	0 %

9:09 YODAC scanning
T-003 = 294.0 °C, T-1011M = ... °C, F-103 = 0.008 m/s
9:10 HP-2116C start
9:11 HP-2116C stop

Run 37(0)CAL-050-139 (No. 3, #13903)

9:15 Valve setting

VH-101	VA-102	VM-103	VH-104	VH-109	VH-110
100 %	close	100 %	100 %	0 %	0 %

9:18 Pump on (~50 l/min)
9:28 YODAC scanning
T-003 = 279.3 °C, T-1011M = 281.2 °C, F-103 = 0.847 m/s
9:29 HP-2116C start
9:30 HP-2116C stop

Run 37(0)CAL-0100-139 (No. 4, #13904)

9:33 Pump power up (~100 l/min)
9:37 YODAC scanning
T-003 = 281.5 °C, T-1011M = 283.1 °C, F-103 = 1.780 m/s
9:38 HP-2116C start
9:39 HP-2116C stop

Run 37(0)CAL-0150-139-B (No. 5, #13905)

9:43 Pump power up (~150 l/min)
9:47 YODAC scanning
T-003 = 281.4 °C, T-1011M = 283.5 °C, F-103 = 2.659 m/s
9:48 HP-2116C start
9:49 HP-2116C stop

Run 37(0)CAL-0200-139 (No. 6, #13906)

10:01 Pump power up (~200 l/min)
10:06 YODAC scanning
T-003 = 281.9 °C, T-1011M = 284.4 °C, F-103 = 3.600 m/s
10:07 HP-2116C start
10:08 HP-2116C stop

Run 37(0)CAL-0260-139 (No. 7, #13907)

10:10 Pump power up (~260 l/min)
10:24 YODAC scanning
T-003 = 284.8 °C, T-1011M = 287.3 °C, F-103 = 4.596 m/s
10:25 HP-2116C start
10:26 HP-2116C stop

Single-phase flow runs, series (1)
(examination of temperature profiles under uniform heating)

Run 37(37)H-260-10 (No. 8, #13908)

10:34 SBL & FPL power on
(central 13 pins are connected to FPL and peripheral 24 pins are to SBL)

	Step No.	Power (kW) Total	Heat flux (W/cm^2) FPL/SBL	F-103 (m/s)	T-003 (°C)	T-1011M (°C)	Hold time	Note
10:34	1	0.04	0.03/ 0.00					
10:38	2	0.83	0.54/ 0.16					
	3	5.67	2.38/ 1.28					
	4	14.22	2.38/ 5.16					
	5	16.31	4.13/ 5.16					
	6	23.37	7.09/ 6.76					
	7	27.82	7.97/ 8.30					
	8	29.60	9.59/ 9.07					
10:54	9	34.35	10.07/10.12	4.690	295.5	309.1		

11:01 YODAC scanning
T-003 = 295.5 °C, T-1011M = 309.1 °C, F-103 = 4.690 m/s
11:03 HP-2116C start
11:04 HP-2116C stop

Run 37(37)H-260-30 (No. 9, #13909)

SBL & FPL power up

Step No.	Power (kW) Total	Heat flux (W/cm^2) FPL/SBL	F-103 (m/s)	T-003 (°C)	T-1011M (°C)	Hold time	Note
1	40.95	12.42/11.84					
2	47.83	14.36/13.91					
3	55.09	16.29/16.15					
4	61.99	18.12/18.29					
5	77.48	22.24/23.08					
6	86.61	25.21/25.62					
7	91.36	26.46/27.09					
8	98.44	29.00/28.92					
9	100.95	29.94/29.55	4.753	298.8	333.3		

11:25 YODAC scanning
T-003 = 298.8 °C, T-1011M = 333.3 °C, F-103 = 4.753 m/s
11:26 HP-2116C start
11:27 HP-2116C stop

Run 37(37)H-260-20 (No. 10, #13910)

SBL & FPL power down

Step No.	Power (kW) Total	Heat flux (W/cm^2) FPL/SBL	F-103 (m/s)	T-003 (°C)	T-1011M (°C)	Hold time	Note
1	99.58	28.33/29.81					
2	83.64	24.49/24.66					
3	72.65	21.89/21.99					
11:43 4	69.48	20.45/20.42	4.698	280.2	304.7		

11:46 YODAC scanning
T-003 = 280.2 °C, T-1011M = 304.7 °C, F-103 = 4.698 m/s
11:47 HP-2116C start
11:48 HP-2116C stop

Run 37(37)H-150-20 (No. 11, #13911)

Pump power down (~150 l/min)

Step No.	Power (kW) Total	Heat flux (W/cm^2) FPL/SBL	F-103 (m/s)	T-003 (°C)	T-1011M (°C)	Hold time	Note
1	68.13	20.71/20.13	2.651	269.8	311.0		

11:59 YODAC scanning
T-003 = 269.8 °C, T-1011M = 311.0 °C, F-103 = 2.651 m/s
12:00 HP-2116C start
12:01 HP-2116C stop
12:05 SBL & FPL power down and off

Run 37(37)H-200-10 (No. 12, #13912)

13:05 Pump power up (~200 l/min)
13:10 SBL & FPL power on

Step No.	Power (kW) Total	Heat flux (W/cm^2) FPL/SBL	F-103 (m/s)	T-003 (°C)	T-1011M (°C)	Hold time	Note
1	5.34	1.97/ 1.36					
2	10.08	3.08/ 2.90					
3	20.40	5.92/ 6.04					
4	28.04	8.29/ 8.22					
5	34.10	10.09/ 9.99	3.561	282.9	299.9		

13:25 YODAC scanning
T-003 = 282.9 °C, T-1011M = 299.9 °C, F-103 = 3.561 m/s
13:26 HP-2116C start
13:27 HP-2116C stop

Run 37(37)H-150-10 (No. 13, #13913)

13:31 Pump power down (~150 l/min)

Step No.	Power (kW) Total	Heat flux (W/cm^2) FPL/SBL	F-103 (m/s)	T-003 (°C)	T-1011M (°C)	Hold time	Note
1	33.95	10.09/ 9.93	2.698	278.4	299.8		

13:36 YODAC scanning

T-003 = 278.4 °C, T-1011M = 299.8 °C, F-103 = 2.698 m/s
13:38 HP-2116C start
13:39 HP-2116C stop

Run 37(37)H-100-10 (No. 14, #13914)

13:45 Pump power down (~100 l/min)

Step No.	Power (kW) Total	Heat flux (W/cm^2) FPL/SBL	F-103 (m/s)	T-003 (°C)	T-1011M (°C)	Hold time	Note
1	34.59	10.23/10.14	1.796	270.5	301.5		

13:50 YODAC scanning
T-003 = 270.5 °C, T-1011M = 301.5 °C, F-103 = 1.796 m/s
13:52 HP-2116C start
13:53 HP-2116C stop

Run 37(37)H-50-10 (No. 15, #13915)

13:55 Pump power down (~50 l/min)

Step No.	Power (kW) Total	Heat flux (W/cm^2) FPL/SBL	F-103 (m/s)	T-003 (°C)	T-1011M (°C)	Hold time	Note
1	34.50	10.12/10.16	0.871	254.8	314.8		

14:09 YODAC scanning
T-003 = 254.8 °C, T-1011M = 314.8 °C, F-103 = 0.871 m/s
14:10 HP-2116C start
14:11 HP-2116C stop

Run 37(37)H-50-20 (No. 16, #13916)

14:20 SBL & FPL power up

	Step No.	Power (kW) Total	Heat flux (W/cm^2) FPL/SBL	F-103 (m/s)	T-003 (°C)	T-1011M (°C)	Hold time	Note
14:20	1	41.63	12.50/12.11					
	2	50.29	14.55/14.92					
	3	57.05	16.39/16.99					
	4	65.46	18.66/19.57					
	5	69.16	20.17/20.44	0.863	243.6	362.3		

14:32 YODAC scanning
T-003 = 243.6 °C, T-1011M = 362.3 °C, F-103 = 0.863 m/s
14:34 HP-2116C start
14:35 HP-2116C stop

Run 37(37)H-50-30 (No. 17, #13917)

14:45 SBL & FPL power up

Step No.	Power (kW) Total	Heat flux (W/cm^2) FPL/SBL	F-103 (m/s)	T-003 (°C)	T-1011M (°C)	Hold time	Note
1	73.86	21.60/21.79					
2	83.74	24.20/24.86					
3	88.26	26.45/25.70					
4	93.20	27.37/27.43					
5	99.23	29.49/29.02					
6	103.07	30.10/30.43	0.863	252.5	427.7		

14:59 YODAC scanning
T-003 = 252.5 °C, T-1011M = 427.7 °C, F-103 = 0.863 m/s
15:00 HP-2116C start
15:01 HP-2116C stop

Run 37(37)H-100-30 (No. 18, #13918)

15:07 Pump power up (~100 l/min)

Step No.	Power (kW) Total	Heat flux (W/cm^2) FPL/SBL	F-103 (m/s)	T-003 (°C)	T-1011M (°C)	Hold time	Note
1	102.03	29.66/30.20	1.788	272.2	359.4		

15:15 YODAC scanning
T-003 = 272.2 °C, T-1011M = 359.4 °C, F-103 = 1.788 m/s
15:17 HP-2116C start
15:18 HP-2116C stop

Run 37(37)H-150-30 (No. 19, #13919)

15:23 Pump power up (~150 l/min)

Step No.	Power (kW) Total	Heat flux (W/cm^2) FPL/SBL	F-103 (m/s)	T-003 (°C)	T-1011M (°C)	Hold time	Note
1	104.68	30.73/30.82	2.690	264.1	323.5		

15:27 YODAC scanning
T-003 = 264.1 °C, T-1011M = 323.5 °C, F-103 = 2.690 m/s
15:28 HP-2116C start
15:29 HP-2116C stop

Run 37(37)H-200-30 (No. 20, #13920)

15:34 Pump power up (~200 l/min)

Step No.	Power (kW) Total	Heat flux (W/cm^2) FPL/SBL	F-103 (m/s)	T-003 (°C)	T-1011M (°C)	Hold time	Note
1	104.92	31.10/30.73	3.553	252.5	298.4		

15:46 YODAC scanning
T-003 = 252.5 °C, T-1011M = 298.4 °C, F-103 = 3.553 m/s
15:47 HP-2116C start
15:48 HP-2116C stop

Run 37(37)H-200-20 (No. 21, #13921)

SBL & FPL power down

Step No.	Power (kW) Total	Heat flux (W/cm^2) FPL/SBL	F-103 (m/s)	T-003 (°C)	T-1011M (°C)	Hold time	Note
1	92.73	26.49/27.70					
2	82.65	23.43/24.78					
3	73.37	21.08/21.85					
15:54 4	68.77	20.13/20.28	3.545	255.5	286.4		

16:00 YODAC scanning
T-003 = 255.5 °C, T-1011M = 286.4 °C, F-103 = 3.545 m/s
16:02 HP-2116C start
16:03 HP-2116C stop

Run 37(37)H-100-20 (No. 22, #13922)

16:08 Pump power down (~100 l/min)

Step No.	Power (kW) Total	Heat flux (W/cm^2) FPL/SBL	F-103 (m/s)	T-003 (°C)	T-1011M (°C)	Hold time	Note
1	67.93	19.86/20.05	1.773	252.4	309.5		

16:14 YODAC scanning
T-003 = 252.4 °C, T-1011M = 309.5 °C, F-103 = 1.773 m/s
16:15 HP-2116C start
16:16 HP-2116C stop

Single-phase flow runs; series (2)
(examination of temperature profiles undre non-uniform heating)

Run 37(37)HA-100-25-A (No. 23, #13923)

FPL power up (center > periphery)

Step No.	Power (kW) Total	Heat flux (W/cm^2) FPL/SBL	F-103 (m/s)	T-003 (°C)	T-1011M (°C)	Hold time	Note
1	70.25	21.80/20.05					
2	72.69	23.84/20.05					
16:23 3	73.19	24.59/19.87	1.780	259.3	327.3		

16:24 YODAC scanning
T-003 = 259.3 °C, T-1011M = 327.3 °C, F-103 = 1.780 m/s
16:25 HP-2116C start
16:26 HP-2116C stop

Run 37(37)HA-100-25-B (No. 24, #13924)

SBL power up (center = periphery)

Step No.	Power (kW) Total	Heat flux (W/cm^2) FPL/SBL	F-103 (m/s)	T-003 (°C)	T-1011M (°C)	Hold time	Note
1	77.39	24.59/21.77					
2	81.95	24.59/23.84					
16:32 3	82.17	24.05/24.23	1.780	272.4	341.8		

16:42 YODAC scanning
T-003 = 272.4 °C, T-1011M = 341.8 °C, F-103 = 1.780 m/s
16:43 HP-2116C start
16:44 HP-2116C stop

Run 37(37)HA-100-25-C (No. 25, #13925)

SBL power up (center < periphery)

Step No.	Power (kW) Total	Heat flux (W/cm^2) FPL/SBL	F-103 (m/s)	T-003 (°C)	T-1011M (°C)	Hold time	Note
1	87.46	24.05/26.63					
2	91.14	24.18/28.23					
3	93.50	24.22/29.28	1.773	281.0	354.0		

17:04 YODAC scanning
T-003 = 281.0 °C, T-1011M = 354.0 °C, F-103 = 1.773 m/s
17:08 HP-2116C start
17:09 HP-2116C stop

Run 37(37)HA-50-25-C (No. 26, #13926)

17:16 Pump power down (~50 l/min)

Step No.	Power (kW) Total	Heat flux (W/cm^2) FPL/SBL	F-103 (m/s)	T-003 (°C)	T-1101M (°C)	Hold time	Note
1	91.30	23.76/28.53	0.855	275.6	424.5		

17:32 YODAC scanning
T-003 = 275.6 °C, T-1011M = 424.5 °C, F-103 = 0.855 m/s
17:33 HP-2116C start
17:34 HP-2116C stop

Run 37(37)HA-50-25-B (No. 27, #13927)

17:39 SBL power down (center = periphery)

Step No.	Power (kW) Total	Heat flux (W/cm^2) FPL/SBL	F-103 (m/s)	T-003 (°C)	T-1011M (°C)	Hold time	Note
17:39 1	83.69	24.46/24.70	0.863	288.5	434.3		

17:45 YODAC scanning
T-003 = 288.5 °C, T-1011M = 434.3 °C, F-103 = 0.863 m/s
17:47 HP-2116C start
17:48 HP-2116C stop

Run 37(37)HA-50-25-A (No. 28, #13928)

SBL power down (center > periphery)

Step No.	Power (kW) Total	Heat flux (W/cm^2) FPL/SBL	F-103 (m/s)	T-003 (°C)	T-1011M (°C)	Hold time	Note
1	76.91	24.46/21.62					
2	73.92	24.46/20.27	0.855	287.4	427.8		

17:54

18:05 YODAC scanning
T-003 = 287.4 °C, T-1011M = 427.8 °C, F-103 = 0.855 m/s
18:08 HP-2116C start
18:09 HP-2116C stop
18:10 SBL & FPL power down and off

Circulation & purification operation

18:12 Pump off
18:13 Valve setting

VH-101	VA-102	VM-103	VH-104	VH-109	VH-110
100 %	open	100 %	100 %	100 %	100 %

18:21 Pump on (~150 l/min)
: Change of the HP-2116C measurement network

1979.11.22

Circulation & heat-up operation

0:20 Auxiliary heater power on
(temperature level change from 250 °C to 500 °C)

Thermocouple calibration run

Run 37(0)CAL-0150-139-C (No. 29, #13929)

8:50 YODAC scanning
T-003 = 542.9 °C, T-1011M = 544.1 °C, F-103 = 0.596 m/s

Low-flow forced convection operation check

9:18 Auxiliary heater power on
9:18 Pump off
9:18 Valve setting

VH-101	VA-102	VM-103	VH-104	VH-109	VH-110
100 %	close	100 %	100 %	0 %	0 %

9:28 Pump on (~200 l/min)
: :
: :
10:27 Valve setting

VH-101	VA-102	VM-103	VH-104	VH-109	VH-110
100 %	open	5 %	100 %	100 %	0 %

10:28 YODAC scanning
T-003 = 465.6 °C, T-1011M = 469.3 °C, F-103 = 0.039 m/s

Circulation and mixing operation

10:32 Valve setting

VH-101	VA-102	VM-103	VH-104	VH-109	VH-110
100 %	open	100 %	100 %	100 %	0 %

10:35 Auxiliary heater power on
(sodium temperature adjustment from 460 °C to 480 °C)
10:46 Auxiliary heater power off

Low-heat-flux boiling run; series (1)
(examination of boiling conditions under low-flow)

Run 37(37)LHF-200 (flow decrease method; No. 30, #13930)

10:47 Valve setting

VH-101	VA-102	VM-103	VH-104	VH-109	VH-110
100 %	open	100 %	100 %	100 %	0 %

10:50 Pump power adjust (F-103 = ~25 l/min)
10:53 SBL & FPL power on

Step No.	Power (kW) Total	Heat flux (W/cm^2) FPL/SBL	F-103 (m/s)	T-003 (°C)	T-1011M (°C)	Hold time	Note
1	0.04	0.02/ 0.00	.....	.....	.....	.....	
2	3.74	1.12/ 1.19	.....	.....	.....	.....	
3	8.46	2.73/ 2.36	.....	.....	.....	.....	
4	13.00	3.55/ 3.97	.....	.....	.....	.....	
5	20.60	6.11/ 6.03	.....	.....	.....	.....	
6	29.19	9.04/ 8.34	.....	.....	.....	.....	
7	41.32	12.53/11.95	.....	.....	.....	.....	
8	50.14	14.51/14.88	.....	.....	.....	.....	
9	61.08	18.24/17.82	.....	.....	.....	.....	
10	67.38	19.91/19.77	.....	.....	.....	.....	
11	68.21	20.22/19.97	.....	.....	.....	.....	
12	71.76	23.20/19.97	.....	.....	.....	.....	
13	73.54	25.01/19.79	0.502	490.5	823.0	.....	

11:20 YODAC scanning
T-003 = 486.4 °C, T-1011M = 747.0 °C, F-103 = 0.502 m/s
11:41 HP-2116C start
11:42 Valve close (VM-103: 100% + 15%) and pump power down

14	73.54	25.01/19.79	0.199	475.5	913.5	.....	IB
15	"	"	0.137	470.0	906.0	.....	B

P-201 = ... MPa, T_{sat} = (913.5) °C

11:53 Valve open (VM-103: 15% → 100%) and pump power up (~150 l/min)
11:54 HP-2116C stop
11:55 SBL & FPL power down and off

Circulation & mixing operation

11:59 Auxiliary heater power on
(sodium temperature adjustment from 480 °C to 520 °C)
14:10 Auxiliary heater power off

Low-heat-flux boiling runs; series (1) (continued)
(examination of boiling conditions under low-flow)

Run 37(37)LHF-201 (flow decrease method; No. 31, #13931)

14:22 Pump power adjust (F-103 = ~25 l/min)
14:23 SBL & FPL power on

Step No.	Power (kW) Total	Heat flux (W/cm^2) FPL/SBL	F-103 (m/s)	T-003 (°C)	T-1011M (°C)	Hold time	Note
1	0.03	0.02/ 0.00	.....	.....	.....	.....	
2	7.47	2.36/ 2.11	.....	.....	.....	.....	
3	18.79	5.91/ 5.32	.....	.....	.....	.....	
4	31.49	9.36/ 9.21	.....	.....	.....	.....	
5	46.33	14.10/13.37	.....	.....	.....	.....	
6	55.95	16.24/16.57	.....	.....	.....	.....	
7	68.34	20.69/19.78	.....	.....	.....	.....	
8	74.51	22.85/21.41	.....	.....	.....	.....	
9	76.04	24.85/21.02	.....	.....	.....	.....	
10	72.29	21.17/21.31	0.480	516.0	740	.....	

14:48 YODAC scanning
T-003 = 510.5 °C, T-1011M = 743.0 °C, F-103 = 0.486 m/s
14:53 HP-2116C start
14:54 Valve close (VM-103: 100% → 15%) and pump power down

11	72.29	21.17/21.31	0.194	511.0	907.8	.....	IB
12	"	"	0.217	510.0	913.5	.....	B

P-201 = ... MPa, T_{sat} = (907.8) °C

15:00 Valve open (VM-103: 15% → 100%)
15:01 HP-2116C stop
15:02 SBL & FPL power down and off

Run 37(37)LHF-202 (power increase method; No. 32, #13932)

15:16 Pump off
15:18 Valve setting

VH-101	VA-102	VM-103	VH-104	VH-109	VH-110
100 %	close	3 %	100 %	0 %	0 %

15:21 Pump on (F-103 = ~2 l/min)

15:26 SBL & FPL power on

Step No.	Power (kW) Total	Heat flux (W/cm^2) FPL/SBL	F-103 (m/s)	T-003 (°C)	T-1011M (°C)	Hold time	Note
1	0.04	0.03/ 0.00	.....	.....	.....	.....	
2	3.48	1.08/ 0.99	.....	.....	.....	.....	
3	8.33	2.57/ 2.38	.....	.....	.....	.....	
4	11.74	3.51/ 3.42	.....	.....	.....	.....	
5	17.11	4.95/ 5.08	0.070	481.0	.....	.....	

15:37 YODAC scanning
T-003 = 481.7 °C, T-1011M = 879.7 °C, F-103 = 0.063 m/s
15:39 HP-2116C start
15:40 SBL & FPL power up

6	20.34	6.03/ 5.96	0.076	467.0	.....	.....	
7	22.07	6.84/ 6.30	0.086	463.5	908.5	.....	IB

P-201 = ... MPa, T_{sat} = 908.5 °C

15:45 Valve setting

VH-101	VA-102	VM-103	VH-104	VH-109	VH-110
100 %	close	5 %	100 %	0 %	0 %

15:48 HP-2116C stop

Run 37(37)LHF-203 (power increase method; No. 33, #13933)

16:01 YODAC scanning
T-003 = 416.2 °C, T-1011M = 757.5 °C, F-103 = 0.110 m/s
16:03 HP-2116C start
16:04 SBL & FPL power up

Step No.	Power (kW) Total	Heat flux (W/cm^2) FPL/SBL	F-103 (m/s)	T-003 (°C)	T-1011M (°C)	Hold time	Note
1	23.88	7.37/ 6.83	.....	.....	.....	.....	
2	29.58	8.64/ 8.73	0.090	.....	.....	.....	
3	33.20	9.84/ 9.72	.....	416.2	.....	.....	
4	36.31	10.76/10.63	.....	.....	.....	.....	
5	40.95	10.76/12.73	0.110	406.0	910.0	.....	IB
6	42.31	11.91/12.73	0.112	406.0	913.5	.....	B

P-201 = ... MPa, T_{sat} = 910.0 °C

16:11 Valve open (VM-103: 5% → 20%)
16:12 HP-2116C stop
16:13 SBL & FPL power down and off

Circulation & mixing operation

16:15 Pump off
16:16 Valve setting

VH-101	VA-102	VM-103	VH-104	VH-109	VH-110

100 %	open	100 %	100 %	100 %	100 %

16:18 Re-setting of the preheater power controller
(changed from 500 ±25 °C to 250 ±25 °C)

16:20 Pump on (~150 l/min)

Chen-type void-meter & thermocouple calibration run

Run 37(0)CAL-0150-139-D (No. ..., #13934)

17:37 HP-2116C start
17:39 HP-2116C stop

18:30 Pump off
18:50 Sodium drain

20:31 Preheater power off

Record of the 140th operation

1979.12.4

8:30 Preheater power on
(aiming temperature level = 250 ±25 °C)

14:40 Sodium charge
(sodium level = EL-9100 mm)

Circulation & purification operation

15:30 Valve setting

VH-101	VA-102	VM-103	VH-104	VH-109	VH-110
100 %	open	100 %	100 %	100 %	100 %

15:40 Pump on (~150 l/min)

Thermocouple and flow-meter calibration runs

Run 37(0)CAL-0150-140-A (No. 34, #14001)

16:07 YODAC scanning
T-003 = 282.5 °C, T-1011M = 284.8 °C, F-103 = 0.588 m/s

1979.12.5

Run 37(0)CAL-0-140 (No. 35, #14002)

8:40 Pump off
8:42 Valve setting

VH-101	VA-102	VM-103	VH-104	VH-109	VH-110
100 %	close	0 %	100 %	0 %	0 %

8:53 YODAC scanning.
T-003 = 271.5 °C, T-1011M = ... °C, F-103 = -0.008 m/s

Run 37(0)CAL-0100-140 (No. 36, #14003)

8:55 Valve setting

VH-101	VA-102	VM-103	VH-104	VH-109	VH-110
100 %	close	100 %	100 %	0 %	0 %

8:56 Pump on (~100 l/min)
9:00 YODAC scanning
T-003 = 271.6 °C, T-1011M = 273.8 °C, F-103 = 1.835 m/s

Run 37(0)CAL-0150-140-B (No. 37, #14004)

9:04 Pump power up (~150 l/min)

9:07 YODAC scanning
T-003 = 269.2 °C, T-1011M = 271.4 °C, F-103 = 2.667 m/s

Run 37(0)CAL-0200-140 (No. 38, #14005)

9:11 Pump power up (~200 l/min)
9:14 YODAC scanning
T-003 = 269.6 °C, T-1011M = 271.7 °C, F-103 = 3.608 m/s

Run 37(0)CAL-0260-140 (No. 39, #14006)

9:16 Pump power up (~260 l/min)
9:21 YODAC scanning
T-003 = 271.0 °C, T-1011M = 273.5 °C, F-103 = 4.690 m/s

Single-phase flow runs; series (2) (continued)
(examination of temperature profiles under non-uniform heating)

Run 37(37)HA-260-25-A (No. 40, #14007)

9:28 SBL & FPL power on (center > periphery)
(central 13 pins are connected to FPL and peripheral 24 pins are to SBL)

	Step No.	Power (kW) Total	Heat flux (W/cm^2) FPL/SBL	F-103 (m/s)	T-003 (°C)	T-1011M (°C)	Hold time	Note
9:28	1	0.48	0.03/ 0.01					
	2	7.33	5.18/ 0.52					
	3	10.44	5.18/ 1.93					
	4	17.34	5.18/ 5.06					
	5	23.33	6.70/ 6.95					
	6	34.48	9.90/10.27					
	7	44.04	13.22/12.81					
	8	51.47	15.17/15.12					
	9	61.63	18.42/17.97					
	10	68.50	20.63/19.88					
9:48	11	74.69	25.38/20.12	4.863	286.1	315.4		

9:52 YODAC scanning
T-003 = 286.1 °C, T-1011M = 315.4 °C, F-103 = 4.863 m/s
9:53 HP-2116C start
9:54 HP-2116C stop

Run 37(37)HA-260-25-B (No. 41, #14008)

SBL power up (center = periphery)

	Step No.	Power (kW) Total	Heat flux (W/cm^2) FPL/SBL	F-103 (m/s)	T-003 (°C)	T-1011M (°C)	Hold time	Note
	1	79.65	24.80/22.68					
9:58	2	85.04	25.23/24.89	4.894	291.3	321.5		

10:04 YODAC scanning

T-003 = 291.3 °C, T-1011M = 321.5 °C, F-103 = 4.894 m/s

10:05 HP-2116C start
10:06 HP-2116C stop

Run 37(37)HA-260-25-C (No. 42, #148009)

SBL power up (center < periphery)

Step No.	Power (kW) Total	Heat flux (W/cm^2) FPL/SBL	F-103 (m/s)	T-003 (°C)	T-1011M (°C)	Hold time	Note
1	92.14	25.23/28.11					
2	95.25	24.51/29.91	4.761	289.7	320.4		

10:11

10:14 YODAC scanning
T-003 = 289.7 °C, T-1011M = 320.4 °C, F-103 = 4.761 m/s
10:15 HP-2116C start
10:16 HP-2116C stop

Single-phase flow runs; series (1) (continued)
(examination of temperature profiles under uniform heating)

Run 37(37)H-260-40 (No. 43, #14010)

SBL & FPL power up

Step No.	Power (kW) Total	Heat flux (W/cm^2) FPL/SBL	F-103 (m/s)	T-003 (°C)	T-1011M (°C)	Hold time	Note
1	100.82	29.17/29.91					
2	118.01	34.84/34.63					
3	123.79	39.34/34.82					
4	125.56	39.98/35.82	4.769	301.6	347.8		

10:30 YODAC scanning
T-003 = 301.6 °C, T-1011M = 347.8 °C, F-103 = 4.769 m/s
10:31 HP-2116C start
10:32 HP-2116C stop

Run 37(37)H-200-40 (No. 44, #14011)

10:36 Pump power down (~200 l/min)

Step No.	Power (kW) Total	Heat flux (W/cm^2) FPL/SBL	F-103 (m/s)	T-003 (°C)	T-1011M (°C)	Hold time	Note
1	128.92	39.18/37.24	3.545	303.6	365.1		

10:36

10:45 YODAC scanning
T-003 = 303.6 °C, T-1011M = 365.1 °C, F-103 = 3.545 m/s
10:46 HP-2116C start
10:47 HP-2116C stop

Run 37(37)H-150-40 (No. 45, #14012)

10:48 Pump power down (~150 l/min)

Step No.	Power (kW) Total	Heat flux (W/cm^2) FPL/SBL	F-103 (m/s)	T-003 (°C)	T-1011M (°C)	Hold time	Note
1	131.76	39.50/38.35	2.588	297.0	380.5		

10:55 YODAC scanning
T-003 = 297.0 °C, T-1011M = 380.5 °C, F-103 = 2.588 m/s
10:56 HP-2116C start
10:57 HP-2116C stop

Run 37(37)H-100-40 (No. 46, #14013)

10:58 Pump power up (~100 l/min)

Step No.	Power (kW) Total	Heat flux (W/cm^2) FPL/SBL	F-103 (m/s)	T-003 (°C)	T-1011M (°C)	Hold time	Note
1	131.57	39.05/38.50	1.718	288.3	411.0		

11:08 YODAC scanning
T-003 = 288.3 °C, T-1011M = 411.0 °C, F-103 = 1.718 m/s
11:09 HP-2116C start
11:10 HP-2116C stop

Run 37(37)H-100-50 (No. 47, #14014)

11:13 SBL & FPL power up
(SBL power reached full power level)

Step No.	Power (kW) Total	Heat flux (W/cm^2) FPL/SBL	F-103 (m/s)	T-003 (°C)	T-1011M (°C)	Hold time	Note
1	141.08	44.77/39.72					
2	144.75	47.84/39.72					
3	147.28	50.12/39.63	1.718	288.4	437.8		

11:13

11:16 YODAC scanning
T-003 = 288.4 °C, T-1011M = 437.8 °C, F-103 = 1.718 m/s
11:17 HP-2116C start
11:18 HP-2116C stop

Run 37(37)H-150-50 (No. 48, #14015)

11:19 Pump power up (~150 l/min)

Step No.	Power (kW) Total	Heat flux (W/cm^2) FPL/SBL	F-103 (m/s)	T-003 (°C)	T-1011M (°C)	Hold time	Note
1	144.83	49.14/39.05	2.737	315.3	409.1		

11:19

11:28 YODAC scanning
T-003 = 315.3 °C, T-1011M = 409.1 °C, F-103 = 2.737 m/s
11:29 HP-2116C start

11:30 HP-2116C stop

Run 37(37)H-200-50 (No. 49, #14016)

11:31 Pump power up (~200 l/min)

Step No.	Power (kW) Total	Heat flux (W/cm^2) FPL/SBL	F-103 (m/s)	T-003 (°C)	T-1011M (°C)	Hold time	Note
1	147.65	49.78/39.98	3.608	320.0	393.3		

11:39 YODAC scanning
T-003 = 320.0 °C, T-1011M = 393.3 °C, F-103 = 3.608 m/s
11:40 HP-2116C start
11:41 HP-2116C stop

Run 37(37)H-260-50 (No. 50, #14017)

11:43 Pump power up (~260 l/min)

Step No.	Power (kW) Total	Heat flux (W/cm^2) FPL/SBL	F-103 (m/s)	T-003 (°C)	T-1011M (°C)	Hold time	Note
1	147.89	49.85/40.05	4.761	327.0	383.6		

11:47 YODAC scanning
T-003 = 327.0 °C, T-1011M = 383.6 °C, F-103 = 4.761 m/s
11:48 HP-2116C start
11:49 HP-2116C stop
11:53 SBL & FPL power down and off
11:54 Pump power down (~150 l/min)

Single-phase flow runs; series (2) (continued)
(examination of temperature profile under non-uniform heating)

Run 37(37)HA-150-25-A (No. 51, #14018)

13:09 SBL & FPL power on (center > periphery)

	Step No.	Power (kW) Total	Heat flux (W/cm^2) FPL/SBL	F-103 (m/s)	T-003 (°C)	T-1011M (°C)	Hold time	Note
13:09	1	3.21	1.85/ 0.45					
	2	9.76	4.83/ 1.81					
	3	20.61	6.47/ 5.84					
	4	27.35	7.96/ 8.09					
	5	44.24	13.21/12.90					
	6	57.90	17.55/16.75					
	7	71.70	22.53/20.31					
13:19	8	71.97	24.09/19.58	2.682	294.2	342.0		

13:27 YODAC scanning
T-003 = 294.2 °C, T-1011M = 342.0 °C, F-103 = 2.682 m/s
13:28 HP-2116C start
13:29 HP-2116C stop

Run 37(37)HA-200-25-A (No. 52, #14019)

13:31 Pump power up (~200 l/min)

Step No.	Power (kW) Total	Heat flux (W/cm^2) FPL/SBL	F-103 (m/s)	T-003 (°C)	T-1011M (°C)	Hold time	Note
1	71.81	24.09/19.51	3.553	294.4	331.1		

13:39 YODAC scanning
T-003 = 294.4 °C, T-1011M = 331.1 °C, F-103 = 3.553 m/s
13:40 HP-2116C start
13:41 HP-2116C stop

Run 37(37)HA-100-25-AA (No. 53, #14020)

13:42 Pump power down (~100 l/min)

Step No.	Power (kW) Total	Heat flux (W/cm^2) FPL/SBL	F-103 (m/s)	T-003 (°C)	T-1011M (°C)	Hold time	Note
1	69.68	23.35/18.94	1.725	294.1	365.3		

13:53 YODAC scanning
T-003 = 294.1 °C, T-1011M = 365.3 °C, F-103 = 1.725 m/s
13:54 HP-2116C start
13:55 HP-2116C stop

Run 37(37)HA-100-25-BA (No. 54, #14021)

13:56 SBL power up (center = periphery)

Step No.	Power (kW) Total	Heat flux (W/cm^2) FPL/SBL	F-103 (m/s)	T-003 (°C)	T-1011M (°C)	Hold time	Note
1	87.19	25.27/25.80	1.733	292.4	372.6		

14:01 YODAC scanning
T-003 = 292.4 °C, T-1011M = 372.6 °C, F-103 = 1.733 m/s
14:02 HP-2116C start
14:03 HP-2116C stop

Run 37(37)HA-150-25-B (No. 55, #14022)

14:04 Pump power up (~150 l/min)

Step No.	Power (kW) Total	Heat flux (W/cm^2) FPL/SBL	F-103 (m/s)	T-003 (°C)	T-1011M (°C)	Hold time	Note
1	87.58	25.46/25.92	2.674	307.9	360.2		

14:07 YODAC scanning
T-003 = 307.9 °C, T-1011M = 360.2 °C, F-103 = 2.674 m/s
14:08 HP-2116C start
14:09 HP-2116C stop

Run 37(37)HA-200-25-B (No. 56, #14023)

14:10 Pump power up (~200 l/min)

Step No.	Power (kW) Total	Heat flux (W/cm^2) FPL/SBL	F-103 (m/s)	T-003 (°C)	T-1011M (°C)	Hold time	Note
1	89.10	25.85/26.39	3.576	297.9	338.2		

14:20 YODAC scanning
T-003 = 297.9 °C, T-1011M = 338.2 °C, F-103 = 3.576 m/s
14:21 HP-2116C start
14:22 HP-2116C stop

Run 37(37)HA-200-25-C (No. 57, #14024)

14:25 SBL power up (center < periphery)

Step No.	Power (kW) Total	Heat flux (W/cm^2) FPL/SBL	F-103 (m/s)	T-003 (°C)	T-1011M (°C)	Hold time	Note
1	92.46	25.85/27.92					
2	96.71	25.90/29.82	3.616	295.0	336.2		

14:27 YODAC scanning
T-003 = 295.0 °C, T-1011M = 336.2 °C, F-103 = 3.616 m/s
14:28 HP-2116C start
14:29 HP-2116C stop

Run 37(37)HA-150-25-C (No. 58, #14025)

14:30 Pump power down (~150 l/min)

Step No.	Power (kW) Total	Heat flux (W/cm^2) FPL/SBL	F-103 (m/s)	T-003 (°C)	T-1011M (°C)	Hold time	Note
1	96.34	25.40/29.92	2.643	301.0	355.6		

14:43 YODAC scanning
T-003 = 301.0 °C, T-1011M = 355.6 °C, F-103 = 2.643 m/s
14:44 HP-2116C start
14:45 HP-2116C stop

Run 37(37)HA-100-25-CA (No. 59, #14026)

14:46 Pump power down (~100 l/min)

Step No.	Power (kW) Total	Heat flux (W/cm^2) FPL/SBL	F-103 (m/s)	T-003 (°C)	T-1011M (°C)	Hold time	Note
1	96.83	25.33/30.18	1.773	296.5	377.9		

14:54 YODAC scanning
T-003 = 296.5 °C, T-1011M = 377.9 °C, F-103 = 1.773 m/s
14:55 HP-2116C start
14:56 HP-2116C stop

Run 37(37)HA-100-35-A (No. 60, #14027)

14:57 FPL power up (center > periphery)

Step No.	Power (kW) Total	Heat flux (W/cm^2) FPL/SBL	F-103 (m/s)	T-003 (°C)	T-1011M (°C)	Hold time	Note
1	102.94	30.45/30.18					
2	107.40	34.56/29.98	1.757	295.0	397.2		

14:57
14:58

15:02 YODAC scanning
T-003 = 295.0 °C, T-1011M = 397.2 °C, F-103 = 1.757 m/s
15:03 HP-2116C start
15:04 HP-2116C stop

Run 37(37)HA-150-35-A (No. 61, #14028)

15:06 Pump power up (~150 l/min)

Step No.	Power (kW) Total	Heat flux (W/cm^2) FPL/SBL	F-103 (m/s)	T-003 (°C)	T-1011M (°C)	Hold time	Note
1	105.29	34.15/29.25	2.698	309.8	375.9		

15:12 YODAC scanning
T-003 = 309.8 °C, T-1011M = 375.9 °C, F-103 = 2.698 m/s
15:13 HP-2116C start
15:14 HP-2116C stop

Run 37(37)HA-200-35-A (No. 62, #14029)

15:16 Pump power up (~200 l/min)

Step No.	Power (kW) Total	Heat flux (W/cm^2) FPL/SBL	F-103 (m/s)	T-003 (°C)	T-1011M (°C)	Hold time	Note
1	108.69	34.91/30.37	3.600	308.8	360.9		

15:23 YODAC scanning
T-003 = 308.8 °C, T-1011M = 360.9 °C, F-103 = 3.600 m/s
15:24 HP-2116C start
15:25 HP-2116C stop

Run 37(37)HA-260-35-A (No. 63, #14030)

15:26 Pump power up (~260 l/min)

Step No.	Power (kW) Total	Heat flux (W/cm^2) FPL/SBL	F-103 (m/s)	T-003 (°C)	T-1011M (°C)	Hold time	Note
1	108.29	34.77/30.26	4.784	306.5	346.5		

15:35 YODAC scanning

T-003 = 306.5 °C, T-1011M = 346.5 °C, F-103 = 4.784 m/s

15:36 HP-2116C start
15:37 HP-2116C stop

Run 37(37)HA-260-35-B (No. 64, #14031)

15:39 SBL power up (center = periphery)

Step No.	Power (kW) Total	Heat flux (W/cm^2) FPL/SBL	F-103 (m/s)	T-003 (°C)	T-1011M (°C)	Hold time	Note
1	119.76	35.46/35.09	4.839	307.1	348.2		

15:46 YODAC scanning
T-003 = 307.1 °C, T-1011M = 348.2 °C, F-103 = 4.839 m/s
15:47 HP-2116C start
15:48 HP-2116C stop

Run 37(37)HA-200-35-B (No. 65, #14032)

15:49 Pump power down (~200 l/min)

Step No.	Power (kW) Total	Heat flux (W/cm^2) FPL/SBL	F-103 (m/s)	T-003 (°C)	T-1011M (°C)	Hold time	Note
1	119.22	35.20/34.99	3.474	299.1	354.2		

15:54 YODAC scanning
T-003 = 299.1 °C, T-1011M = 354.2 °C, F-103 = 3.474 m/s

15:55 HP-2116C start
15:56 HP-2116C stop

Run 37(37)HA-150-35-B (No. 66, #14033)

15:57 Pump power down (~150 l/min)

Step No.	Power (kW) Total	Heat flux (W/cm^2) FPL/SBL	F-103 (m/s)	T-003 (°C)	T-1011M (°C)	Hold time	Note
1	118.36	34.77/34.83	2.761	302.6	370.8		

16:10 YODAC scanning
T-003 = 302.6 °C, T-1011M = 370.8 °C, F-103 = 2.761 m/s
16:11 HP-2116C start
16:12 HP-2116C stop

Run 37(37)HA-100-35-B (No. 67, #14034)

16:13 Pump power down (~100 l/min)

Step No.	Power (kW) Total	Heat flux (W/cm^2) FPL/SBL	F-103 (m/s)	T-003 (°C)	T-1011M (°C)	Hold time	Note
1	118.83	34.91/34.97	1.718	285.4	394.0		

16:24 YODAC scanning
T-003 = 285.4 °C, T-1011M = 394.0 °C, F-103 = 1.718 m/s
16:25 HP-2116C start
16:26 HP-2116C stop

Run 37(37)HA-100-35-C (No. 68, #14035)

16:27 SBL power up (center < periphery)

Step No.	Power (kW) Total	Heat flux (W/cm^2) FPL/SBL	F-103 (m/s)	T-003 (°C)	T-1011M (°C)	Hold time	Note
1	124.09	34.91/37.36					
2	128.61	34.60/39.57	1.702	282.6	395.0		

16:36 YODAC scanning
T-003 = 282.6 °C, T-1011M = 395.0 °C, F-103 = 1.702 m/s
16:37 HP-2116C start
16:38 HP-2116C stop

Run 37(37)HA-150-35-C (No. 69, #14036)

16:39 Pump power up (~150 l/min)

Step No.	Power (kW) Total	Heat flux (W/cm^2) FPL/SBL	F-103 (m/s)	T-003 (°C)	T-1011M (°C)	Hold time	Note
1	130.45	35.08/40.15	1.937	300.3	372.1		

16:46 YODAC scanning
T-003 = 300.3 °C, T-1011M = 372.1 °C, F-103 = 1.937 m/s
16:47 HP-2116C start
16:48 HP-2116C stop

Run 37(37)HA-200-35-C (No. 70, #14037)

16:49 Pump power up (~200 l/min)

Step No.	Power (kW) Total	Heat flux (W/cm^2) FPL/SBL	F-103 (m/s)	T-003 (°C)	T-1011M (°C)	Hold time	Note
1	132.45	35.52/40.81	3.639	303.3	358.1		

16:56 YODAC scanning
T-003 = 303.3 °C, T-1011M = 358.1 °C, F-103 = 3.639 m/s
16:57 HP-2116C start
16:58 HP-2116C stop

Run 37(37)HA-260-35-C (No. 71, #14038)

16:59 Pump power up (~260 l/min)

Step No.	Power (kW) Total	Heat flux (W/cm^2) FPL/SBL	F-103 (m/s)	T-003 (°C)	T-1011M (°C)	Hold time	Note

1	131.07	35.00/40.47	4.769	307.0	348.8		

17:05 YODAC scanning
T-003 = 307.0 °C, T-1011M = 348.8 °C, F-103 = 4.769 m/s
17:06 HP-2116C start
17:07 HP-2116C stop
17:08 SBL & FPL power off

Circulation & purification operation

17:10 Pump off
17:12 Valve setting

VH-101	VA-102	VM-103	VH-104	VH-109	VH-110
100 %	open	100 %	100 %	100 %	100 %

17:18 Pump on (~150 l/min)
: Change of the HP-2116C measurement network

Circulation & heat-up operation

23:35 Auxiliary heater power on
(temperature level change from 250 °C to 500 °C)

1979.12.6

7:05 Re-setting of the preheater power controller
(changed from 250 ±25 °C to 500 ±25 °C)

Thermocouple and flow-meter calibration runs

Run 37(0)CAL-0150-140-C (No. 72, #14039)

8:50 YODAC scanning
T-003 = 498.8 °C, T-1011M = 501.6 °C, F-103 = 0.580 m/s
9:03 Auxiliary heater power off

Run 37(0)CAL-05-140 (No. 73, #14040)

9:03 Pump off
9:04 Valve setting

VH-101	VA-102	VM-103	VH-104	VH-109	VH-110
100 %	close	100 %	100 %	0 %	0 %

9:07 Pump on (~5 l/min)
9:13 YODAC scanning
T-003 = 476.9 °C, T-1011M = 488.0 °C, F-103 = 0.173 m/s

Low-heat-flux boiling runs; series (1) (continued)
(examination of boiling condition under low-flow)

Run 37(37)LHF-210 (power increase method; No. 74, #14041)

9:15 Pump off
9:17 Confirmation of flow-meter offset
9:18 Valve setting

VH-101	VA-102	VM-103	VH-104	VH-109	VH-110
100 %	close	2.5 %	100 %	0 %	0 %

9:25 Pump on (~1 l/min)
9:28 SBL & FPL power on

Step No.	Power (kW) Total	Heat flux (W/cm^2) FPL/SBL	F-103 (m/s)	T-003 (°C)	T-1011M (°C)	Hold time	Note
1	0.04	0.03/ 0.01	.....	.....	.....	.....	
2	3.32	1.02/ 0.95	0.031	.....	.....	.....	
3	6.37	1.99/ 1.81	"	.....	.....	.....	
4	9.79	2.91/ 2.86	"	.....	.....	.....	
9:39 5	11.49	3.34/ 3.40	0.030	438.1	870.0	17'30"	

9:51 Valve re-setting

VH-101	VA-102	VM-103	VH-104	VH-109	VH-110
100 %	close	2.5 %	0 %	0 %	100 %

9:54 YODAC scanning
T-003 = 438.1 °C, T-1011M = 888.0 °C, F-103 = 0.031 m/s
9:56 HP-2116C start
9:57 SBL & FPL power up

6	13.80	4.10/ 4.03	0.033	438.1	.....	.....	
7	15.19	4.49/ 4.45	0.033	"	914.0	2'11"	IB
8	16.68	4.93/ 4.89	0.038	"	913.5	1'41"	B

P-201 = 0.1059 MPa, T_{sat} = 914.0 °C

10:02 Valve setting

VH-101	VA-102	VM-103	VH-104	VH-109	VH-110
100 %	close	4.5 %	0 %	0 %	100 %

10:03 HP-2116C stop

Run 37(37)LHF-212 (power increase method; No. 75, #14042)

10:11 SBL & FPL power up

Step No.	Power (kW) Total	Heat flux (W/cm^2) FPL/SBL	F-103 (m/s)	T-003 (°C)	T-1011M (°C)	Hold time	Note
1	22.56	6.81/ 6.54	0.067	.....	.....	10'00"	

10:19 YODAC scanning
T-003 = 403.8 °C, T-1011M = 838.4 °C, F-103 = 0.071 m/s
10:20 HP-2116C start
10:21 SBL & FPL power up

	2	27.08	8.08/ 7.90	0.067	403.8	.....	.....	
	3	28.51	8.49/ 8.33	0.066	"	912.8	1'57"	IB
	4	30.44	8.96/ 8.95	0.070	"	910.6	2'08"	B

$P\text{-}201 = 0.1059$ MPa, $T_{sat} = 912.8$ °C

10:29 Valve setting

VH-101	VA-102	VM-103	VH-104	VH-109	VH-110
100 %	close	6 %	0 %	0 %	100 %

10:31 HP-2116C stop

Run 37(37)LHF-214 (power increase method, No. 76, #14043)

Step No.	Power (kW) Total	Heat flux (W/cm^2) FPL/SBL	F-103 (m/s)	T-003 (°C)	T-1011M (°C)	Hold time	Note
1	31.69	9.35/ 9.31	0.102	424.5	840	12'30"	

10:44 YODAC scanning
T-003 = 424.5 °C, T-1011M = 837.7 °C, F-103 = 0.102 m/s
10:45 HP-2116C start
10:46 SBL & FPL power up

	2	35.03	10.35/10.27	.....	424.5	.....	.....	
10:49	3	35.57	10.43/10.48	.....	"	.....	.....	
10:51	4	38.80	11.43/11.40	0.118	"	909.0	1'58"	IB

$P\text{-}201 =$ ..... MPa, $T_{sat} = 909.0$ °C

10:53 Valve setting

VH-101	VA-102	VM-103	VH-104	VH-109	VH-110
100 %	close	8 %	0 %	0 %	100 %

10:54 HP-2116C stop

Run 37(37)LHF-215 (power increase method, No. 77, #14044)

Step No.	Power (kW) Total	Heat flux (W/cm^2) FPL/SBL	F-103 (m/s)	T-003 (°C)	T-1011M (°C)	Hold time	Note
1	39.06	11.51/11.47	0.127	437.8	834.3	14'00"	

11:05 YODAC scanning
T-003 = 437.8 °C, T-1011M = 850.6 °C, F-103 = 0.133 m/s
11:06 HP-2116C start
11:07 SBL & FPL power up

	2	43.35	12.71/12.77	0.127	437.8	855.0	.....	
11:10	3	45.62	13.43/13.41	0.127	"	901.5	1'50"	IB
11:12	4	48.88	14.43/14.35	0.131	"	905.5	1'53"	B

$P\text{-}201 =$ ..... MPa, $T_{sat} = 901.5$ °C

11:14 Valve setting

VH-101	VA-102	VM-103	VH-104	VH-109	VH-110
100 %	close	10 %	0 %	0 %	100 %

11:15 HP-2116C stop

Run 37(37)LHF-216 (power increase method; No. 78, #14045)

Step No.	Power (kW) Total	Heat flux (W/cm^2) FPL/SBL	F-103 (m/s)	T-003 (°C)	T-1011M (°C)	Hold time	Note
1	49.65	14.66/14.57	0.168	466.6	848.5	13'45"	

11:28 YODAC scanning
T-003 = 466.6 °C, T-1011M = 863.6 °C, F-103 = 0.165 m/s
11:29 HP-2116C start
11:30 SBL & FPL power up

	2	52.37	15.44/15.38	.....	466.6	.....	.....	
	3	55.60	16.31/16.37	.....	"	.....	.....	
11:32	4	58.75	17.20/17.32	0.173	"	905.0	2'45"	IB
11:35	5	62.42	18.36/18.36	0.180	"	912.5	1'48"	B

$P\text{-}201 =$ ..... MPa, $T_{sat} = 905.0$ °C

11:38 Valve setting

VH-101	VA-102	VM-103	VH-104	VH-109	VH-110
100 %	close	13 %	0 %	0 %	100 %

11:39 HP-2116C stop

Circulation & mixing operation

11:44 SBL & FPL power emergency scram
(warning of a smoke detector)

11:47 Valve setting

VH-101	VA-102	VM-103	VH-104	VH-109	VH-110
100 %	close	100 %	0 %	0 %	100 %

11:48 Pump on (~100 l/min)
11:54 Pump off
11:54 Valve setting

VH-101	VA-102	AM-103	VH-104	VH-109	VH-110
100 %	open	100 %	100 %	100 %	100 %

11:58 Pump on (~150 l/min)
12:58 Auxiliary heater power on
13:23 Auxiliary heater power off

Run 37(37)LHF-211 (power increase method; No. 79, #14046)

13:23 Pump off

13:24 Valve setting

VH-101	VA-102	VM-103	VH-104	VH-109	VH-110
100 %	close	3 %	100 %	0 %	100 %

13:25 Pump on (~1 l/min)
13:29 SBL & FPL power on

Step No.	Power (kW) Total	Heat flux (W/cm^2) FPL/SBL	F-103 (m/s)	T-003 (°C)	T-1011M (°C)	Hold time	Note
1	0.05	0.03/ 0.01	0.024	.....	.....	.....	
2	4.73	1.55/ 1.30	.....	.....	.....	.....	
3	7.96	2.37/ 2.32	.....	.....	.....	.....	
4	9.49	2.76/ 2.81	.....	.....	.....	.....	
5	11.27	3.30/ 3.32	.....	.....	.....	.....	IB
6	9.76	2.86/ 2.88	.....	.....	.....	.....	B
7	7.04	2.06/ 2.07	.....	.....	.....	.....	B
8	5.21	1.52/ 1.54	.....	.....	.....	.....	B
9	0	0 / 0	.....	.....	.....	.....	

SBL & FPL power manual-scram
13:40 Pump off
13:42 Confirmation of flow-meter offset & valve throttling
13:47 Pump on (~1 l/min)
13:48 SBL & FPL power on

	10	4.20	1.30/ 1.20	.....	.....	.....	.....	
	11	6.46	1.92/ 1.89	.....	.....	.....	.....	
14:08	12	11.44	3.40/ 3.35	0.031	411.2	792.2	13'15"	

14:12 YODAC scanning
T-003 = 411.2 °C, T-1011M = 812.4 °C, F-103 = 0.031 m/s
14:13 HP-2116C start
14:14 SBL & FPL power up

	13	13.45	3.98/ 3.94	.....	.....	.....	.....	
14:17	14	16.60	4.90/ 4.87	0.027	.....	910.0	1'25"	IB
	15	19.40	5.66/ 5.73	.....	.....	.....	.....	NB
	16	19.98	5.84/ 5.90	.....	.....	.....	.....	NB
14:21	17	21.86	6.40/ 6.44	0.041	.....	908.8	1'42"	B

P-201 = 0.1030 MPa, T_{sat} = 910.0 °C

14:23 Valve setting

VH-101	VA-102	VM-103	VH-104	VH-109	VH-110
100 %	close	5.5 %	0 %	0 %	100 %

14:24 HP-2116C stop

Run 37(37)LHF-213 (power increase method; No. 80, #14047)

14:30 Pump power up (~5 l/min)
14:38 Valve re-setting

VH-101	VA-102	VM-103	VH-104	VH-109	VH-110
100 %	close	5 %	0 %	0 %	100 %

Step No.	Power (kW) Total	Heat flux (W/cm^2) FPL/SBL	F-103 (m/s)	T-003 (°C)	T-1011M (°C)	Hold time	Note
1	23.11	6.84/ 6.78	0.090	443.1	775.2	10'00"	

14:46 YODAC scanning
T-003 = 443.1 °C, T-1011M = 795.6 °C, F-103 = 0.094 m/s
14:47 HP-2116C start
14:48 SBL & FPL power up

	2	27.46	8.16/ 8.03	.....	.....	.....	.....	
	3	30.37	8.92/ 8.94	.....	.....	.....	.....	
	4	33.44	9.85/ 9.83	.....	.....	.....	.....	
	5	36.76	10.83/10.80	0.097	.....	903.6	1'19"	IB
14:57	6	41.95	12.29/12.36	0.101	.....	910.0	1'44"	B

P-201 = ... MPa, T_{sat} = 903.6 °C

14:59 Valve setting

VH-101	VA-102	VM-103	VH-104	VH-109	VH-110
100 %	close	5.5 %	0 %	0 %	100 %

15:00 HP-2116C stop
15:01 Pump power up (~... l/min)

Run 37(37)LHF-217 (power increase method; No. 81, #14048)

15:05 Pump power down (~10 l/min)

Step No.	Power (kW) Totel	Heat flux (W/cm^2) FPL/SBL	F-103 (m/s)	T-003 (°C)	T-1011M (°C)	Hold time	Note
1	42.93	12.63/12.62	0.185	477.6	780.0	10'15"	

15:14 YODAC scanning
T-003 = 477.6 °C, T-1011M = 802.3 °C, F-103 = 0.188 m/s
15:15 HP-2116C start
15:16 SBL & FPL power up

	2	47.21	13.85/13.91	.....	.....	.....	.....	
	3	52.05	15.29/15.32	.....	.....	.....	.....	
	4	57.09	16.83/16.77	.....	.....	.....	.....	
15:21	5	63.49	18.63/18.70	0.195	.....	910.5	1'58"	IB
15:23	6	69.91	20.65/20.51	0.197	.....	909.3	1'41"	B

P-201 = ... MPa, T_{sat} = 910.5 °C

15:25 SBL & FPL power down & off

Circulation & mixing operation

15:30 Valve setting

VH-101	VA-102	VM-103	VH-104	VH-109	VH-110
100 %	close	100 %	0 %	0 %	100 %

15:31 Pump power adjust (~50 l/min)

Run 37(37)LHF-218 (power increase method; No. 82, #14049)

15:43 Pump off
15:43 Valve setting

VH-101	VA-102	VM-103	VH-104	VH-109	VH-110
100 %	close	3.5 %	0 %	0 %	100 %

15:44 Pump on (~12 l/min)
15:45 SBL & FPL power on

Step No.	Power (kW) Total	Heat flux (W/cm^2) FPL/SBL	F-103 (m/s)	T-003 (°C)	T-1011M (°C)	Hold time	Note
1	0.27	0.13/ 0.05	0.211	.....	.....	.....	
2	8.24	2.52/ 2.37	.....	.....	.....	.....	
3	16.78	4.95/ 4.93	.....	.....	.....	.....	
4	26.11	7.46/ 7.80	.....	.....	.....	.....	
5	40.39	12.43/11.58	.....	.....	.....	.....	
6	49.83	14.60/14.69	0.200	500.3	817.8	10'45"	

15:55 YODAC scanning
T-003 = 500.3 °C, T-1011M = 842.7 °C, F-103 = 0.204 m/s
15:56 HP-2116C start
15:57 SBL & FPL power up

	7	57.48	16.93/16.89	.....	.....	.....	.....	
	8	63.44	18.56/18.71	.....	.....	.....	.....	
16:00	9	67.76	18.56/20.67	0.203	.....	913.5	1'58"	
16:02	10	70.37	20.75/20.67	0.210	.....	912.0	1'59"	

P-201 = ... MPa, T_{sat} = 913.5 °C

16:04 Pump power up (~19 l/min)
16:05 HP-2116C stop

Run 37(37)LHF-219 (power increase method; No. 83, #14050)

16:10 Pump power adjust (~17 l/min)

Step No.	Power (kW) Total	Heat flux (W/cm^2) FPL/SBL	F-103 (m/s)	T-003 (°C)	T-1011M (°C)	Hold time	Note
1	73.28	21.71/21.47	0.300	483.8	811.5	12'45"	

16:15 YODAC scanning
T-003 = 483.8 °C, T-1011M = 845.1 °C, F-103 = 0.306 m/s
16:16 HP-2116C start
16:17 SBL & FPL power up

	2	80.71	23.85/23.68	.....	.....	.....	.....	
	3	90.18	26.60/26.48	.....	.....	.....	.....	
	4	94.14	27.76/27.65	.....	.....	.....	.....	
16:20	5	97.68	28.73/28.73	0.298	.....	910.5	1'52"	IB
16:22	6	101.15	29.70/29.77	0.310	.....	910.0	1'45"	B

P-201 = ... MPa, T_{sat} = 910.5 °C

16:24 Valve setting

VH-101	VA-102	VM-103	VH-104	VH-109	VH-110
100 %	close	5 %	0 %	0 %	100 %

16:25 HP-2116C stop
16:25 SBL & FPL power down and off

Circulation & mixing operation

16:33 Valve setting

VH-101	VA-102	VM-103	VH-104	VH-109	VH-110
100 %	close	100 %	0 %	0 %	100 %

16:34 Pump power adjust (~50 l/min)
16:48 Pump power up (~150 l/min)
17:29 Pump off
17:30 Valve setting

VH-101	VA-102	VM-103	VH-104	VH-109	VH-110
100 %	open	100 %	100 %	100 %	100 %

17:38 Pump on (~50 l/min)
17:43 Pump power up (~150 l/min)

Thermocouple calibration run

Run 37(0)CAL-0150-140-D (No. 84, #14051)

18:14 YODAC scanning
T-003 = 335.4 °C, T-1011M = 339.1 °C, F-103 = 0.533 m/s

18:48 Pump off
18:54 Sodium drain

20:05 Preheater power off

Record of the 141th operation

1980.1.16

8:50 Preheater power on
(aiming temperature level = 250 ±25 °C)

16:20 Sodium charge
(sodium level = EL-9100 mm)

Circulation & purification operation

16:50 Valve setting

VH-101	VA-102	VM-103	VH-104	VH-109	VH-110
100 %	open	100 %	100 %	100 %	100 %

17:10 Pump on (~150 l/min)

Thermocouple calibration runs
(check of the signal isolation buffer amplifiers introduced)

Run 37(0)CAL-0150-141-A (without isolation; No. 85, #14101)

20:05 YODAC scanning
T-003 = 269.9 °C, T-1011M = 272.9 °C, F-103 = ... m/s

Run 37(0)CAL-0150-141-B (with isolation; No. 86, #14102)

20:08 YODAC scanning
T-003 = 271.8 °C, T-1011M = 272.0 °C, F-103 = ... m/s

1980.1.17

Run 37(0)CAL-0-141-A (No. 87, #14103)

8:41 Pump off
8:43 Valve setting

VH-101	VA-102	VM-103	VH-104	VH-109	VH-110
100 %	close	0 %	0 %	0 %	100 %

9:10 YODAC scanning
T-003 = 272.5 °C, T-1011M = ... °C, F-101 = -0.008 m/s
: Occurrence of a trouble in flow measurement by F-103
(F-101 was used for a backup operation)

Run 37(0)CAL-050-141 (with isolation; No. 88, #14104)

9:13 Valve setting

VH-101	VA-102	VM-103	VH-104	VH-109	VH-110
100 %	close	100 %	0 %	0 %	100 %

9:14 Pump on (~50 l/min)
9:17 YODAC scanning
T-003 = 272.5 °C, T-1011M = 272.7 °C, F-101 = 1.090 m/s

Run 37(0)CAL-0100-141 (with isolation; No. 89, #14105)

9:18 Pump power up (~100 l/min)
9:32 YODAC scanning
T-003 = 271.7 °C, T-1011M = 271.9 °C, F-101 = 1.796 m/s

Run 37(0)CAL-0150-141-C (with isolation; No. 90, #14106)

9:34 Pump power up (~150 l/min)
9:39 YODAC scanning
T-003 = 271.9 °C, T-1011M = 272.2 °C, F-101 = 2.729 m/s

Run 37(0)CAL-0200-141 (with isolation; No. 91, #14107)

9:41 Pump power up (~200 l/min)
9:46 YODAC scanning
T-003 = 272.8 °C, T-1011M = 273.1 °C, F-101 = 3.647 m/s

Run 37(0)CAL-0260-141 (with isolation; No. 92, #14108)

9:48 Pump power up (~260 l/min)
9:53 YODAC scanning
T-003 = 274.6 °C, T-1011M = 275.0 °C, F-101 = 4.659 m/s

Single-phase flow runs; series (3)
(examination of temperature profiles under non-uniform heating)

Run 37(37)HB-260-20 (No. 93, #14109)

9:58 SBL & FPL power on

Step No.	Power (kW) Total	Heat flux (W/cm^2) FPL/SBL	F-101 (m/s)	T-003 (°C)	T-1011M (°C)	Hold time	Note
1	0.04	0.01/ 0.02					
2	6.97	2.08/ 2.00					
3	17.13	5.14/ 4.83					
4	28.09	8.10/ 8.60					
5	37.91	11.23/10.99					
6	50.06	14.66/14.85					
7	61.18	17.96/18.06		286.0			
8	67.85	20.10/19.66	4.742	296.5	317.4		

10:29 YODAC scanning
T-003 = 296.5 °C, T-1011M = 317.4 °C, F-101 = 4.742 m/s
10:30 HP-2116C start
10:31 HP-2116C stop

Run 37(37)HB-260-25 (No. 94, #14110)

10:33 SBL & FPL power up

Step No.	Power (kW) Total	Heat flux (W/cm^2) FPL/SBL	F-101 (m/s)	T-003 (°C)	T-1011M (°C)	Hold time	Note
1	81.59	23.95/24.10					
2	86.25	25.39/25.33	4.703	288.7	317.9		

10:39 YODAC scanning
T-003 = 288.7 °C, T-1011M = 317.9 °C, F-101 = 4.703 m/s
10:40 HP-2116C start
10:41 HP-2116C stop

Run 37(37)HB-200-25 (No. 95, #14111)

10:42 Pump power down (~200 l/min)

Step No.	Power (kW) Total	Heat flux (W/cm^2) FPL/SBL	F-101 (m/s)	T-003 (°C)	T-1011M (°C)	Hold time	Note
1	85.70	25.24/25.13	3.562	283.7	321.5		

10:49 YODAC scanning
T-003 = 283.7 °C, T-1011M = 321.5 °C, F-101 = 3.562 m/s
10:50 HP-2116C start
10:51 HP-2116C stop

Run 37(37)HB-150-25 (No. 96, #14112)

10:53 Pump power down (~150 l/min)

Step No.	Power (kW) Total	Heat flux (W/cm^2) FPL/SBL	F-101 (m/s)	T-003 (°C)	T-1011M (°C)	Hold time	Note
1	85.13	25.11/24.89	2.672	288.5	338.2		

11:06 YODAC scanning
T-003 = 288.5 °C, T-1011M = 338.2 °C, F-101 = 2.672 m/s
11:07 HP-2116C start
11:08 HP-2116C stop

Run 37(37)HB-100-25 (No. 97, #14113)

11:09 Pump power down (~100 l/min)

Step No.	Power (kW) Total	Heat flux (W/cm^2) FPL/SBL	F-101 (m/s)	T-003 (°C)	T-1011M (°C)	Hold time	Note
1	84.44	24.89/24.71	1.860	288.7	359.7		

11:17 YODAC scanning
T-003 = 288.7 °C, T-1011M = 359.7 °C, F-101 = 1.860 m/s
11:19 HP-2116C start
11:20 HP-2116C stop

Run 37(37)HB-100-35 (No. 98, #14114)

11:21 SBL & FPL power up

Step No.	Power (kW) Total	Heat flux (W/cm^2) FPL/SBL	F-101 (m/s)	T-003 (°C)	T-1011M (°C)	Hold time	Note
1	101.86	30.21/29.42					
2	121.22	35.76/35.44	1.852	289.1	391.7		

11:36 YODAC scanning
T-003 = 289.1 °C, T-1011M = 391.7 °C, F-101 = 1.852 m/s
11:37 HP-2116C start
11:38 HP-2116C stop

Run 37(37)HB-150-35 (No. 99, #14115)

11:41 Pump power up (~150 l/min)

Step No.	Power (kW) Total	Heat flux (W/cm^2) FPL/SBL	F-101 (m/s)	T-003 (°C)	T-1011M (°C)	Hold time	Note
1	120.29	35.49/35.15	2.664	285.3	356.1		

11:53 YODAC scanning
T-003 = 285.3 °C, T-1011M = 356.1 °C, F-101 = 2.664 m/s
11:54 HP-2116C start
11:55 HP-2116C stop
11:57 SBL & FPL power down and off

Run 37(37)HB-100-10 (No. 100, #14116)

13:05 Pump power down (~100 l/min)
13:05 SBL & FPL power on

	Step No.	Power (kW) Total	Heat flux (W/cm^2) FPL/SBL	F-101 (m/s)	T-003 (°C)	T-1011M (°C)	Hold time	Note
13:05	1	18.19	5.46/ 5.11					
	2	27.78	8.25/ 8.00		280			
13:09	3	35.40	10.44/10.36	1.907	285.2	314.5		

13:16 YODAC scanning
T-003 = 285.2 °C, T-1011M = 314.5 °C, F-101 = 1.907 m/s
13:17 HP-2116C start
13:18 HP-2116C stop

Run 37(37)HB-100-20 (No. 101, #14117)

13:20 SBL & FPL power up

	Step No.	Power (kW) Total	Heat flux (W/cm^2) FPL/SBL	F-101 (m/s)	T-003 (°C)	T-1011M (°C)	Hold time	Note
13:20	1	51.48	15.40/14.61					
	2	62.70	18.59/18.14					
13:23	3	67.05	19.91/19.33	1.899	289.8	346.7		

13:38 YODAC scanning
T-003 = 289.8 °C, T-1011M = 346.7 °C, F-101 = 1.899 m/s
13:39 HP-2116C start
13:40 HP-2116C stop

Run 37(37)HB-100-30 (No. 102, #14118)

13:41 SBL & FPL power up

	Step No.	Power (kW) Total	Heat flux (W/cm^2) FPL/SBL	F-101 (m/s)	T-003 (°C)	T-1011M (°C)	Hold time	Note
13:41	1	84.42	24.89/24.70					
	2	95.87	28.21/28.17					
13:45	3	102.92	30.37/30.07	1.836	267.6	358.7		

13:51 YODAC scanning
T-003 = 267.6 °C, T-1011M = 358.7 °C, F-101 = 1.836 m/s
13:52 HP-2116C start
13:53 HP-2116C stop

Run 37(37)HB-100-40 (No. 103, #14119)

13:55 SBL & FPL power up

	Step No.	Power (kW) Total	Heat flux (W/cm^2) FPL/SBL	F-101 (m/s)	T-003 (°C)	T-1011M (°C)	Hold time	Note
13:55	1	119.59	35.00/35.53					
	2	134.64	38.95/40.95					
13:57	3	136.17	39.86/40.45	1.828	268.3	386.6		

14:07 YODAC scanning
T-003 = 268.3 °C, T-1011M = 386.6 °C, F-101 = 1.828 m/s
14:08 HP-2116C start
14:09 HP-2116C stop

Run 37(37)HB-100-50 (No. 104, #14120)

14:11 SBL & FPL power up

	Step No.	Power (kW) Total	Heat flux (W/cm^2) FPL/SBL	F-101 (m/s)	T-003 (°C)	T-1011M (°C)	Hold time	Note
14:11	1	152.51	44.80/44.97					
	2	164.70	48.53/48.26					
14:13	3	168.42	49.65/49.29	1.852	280.6	425.5		

14:26 YODAC scanning
T-003 = 280.6 °C, T-1011M = 425.5 °C, F-101 = 1.852 m/s
14:27 HP-2116C start
14:28 HP-2116C stop

Run 37(37)HB-100-60 (No. 105, #14121)

14:30 SBL & FPL power up

	Step No.	Power (kW) Total	Heat flux (W/cm^2) FPL/SBL	F-101 (m/s)	T-003 (°C)	T-1011M (°C)	Hold time	Note
14:30	1	184.48	53.85/55.11					
	2	195.54	57.28/58.01					
14:33	3	200.67	59.02/59.01	1.899	300.5	468.7		

14:48 YODAC scanning
T-003 = 300.5 °C, T-1011M = 468.7 °C, F-101 = 1.899 m/s
14:49 HP-2116C start
14:50 HP-2116C stop

Run 37(37)HB-150-60 (No. 106, #14122)

14:53 Pump power up (~150 l/min)

Step No.	Power (kW) Total	Heat flux (W/cm^2) FPL/SBL	F-101 (m/s)	T-003 (°C)	T-1011M (°C)	Hold time	Note
1	206.03	60.50/60.81	2.789	329.2	449.0		

14:59 YODAC scanning
T-003 = 329.2 °C, T-1011M = 449.0 °C, F-101 = 2.789 m/s
15:00 HP-2116C start
15:01 HP-2116C stop

Run 37(37)HB-200-60 (No. 107, #14123)

15:02 Pump power up (~200 l/min)

Step No.	Power (kW) Total	Heat flux (W/cm^2) FPL/SBL	F-101 (m/s)	T-003 (°C)	T-1011M (°C)	Hold time	Note
1	193.37	56.51/57.63	3.633	341.9	427.3		

15:10 YODAC scanning
T-003 = 341.9 °C, T-1011M = 427.3 °C, F-101 = 3.633 m/s
15:11 HP-2116C start
15:12 HP-2116C stop

Run 37(37)HB-260-60 (No. 108, #14124)

15:13 Pump power up (~260 l/min)
15:13 SBL & FPL power up

	Step No.	Power (kW) Total	Heat flux (W/cm^2) FPL/SBL	F-101 (m/s)	T-003 (°C)	T-1011M (°C)	Hold time	Note
15:13	1	205.35	59.87/61.50	4.757	352.5	422.9		

15:21 YODAC scanning
T-003 = 352.5 °C, T-1011M = 422.9 °C, F-101 = 4.757 m/s
15:22 HP-2116C start

15:23 HP-2116C stop

Run 37(37)HB-260-70 (No. 109, #14125)

15:25 SBL & FPL power up

	Step No.	Power (kW) Total	Heat flux (W/cm^2) FPL/SBL	F-101 (m/s)	T-003 (°C)	T-1011M (°C)	Hold time	Note
15:25	1	222.47	65.41/65.48					
	2	240.68	70.79/70.78					
15:29	3	246.12	72.06/73.08	4.688	398.7	484.4		

15:51 YODAC scanning
T-003 = 398.7 °C, T-1011M = 484.4 °C, F-101 = 4.688 m/s
15:52 HP-2116C start
15:53 HP-2116C stop

Run 37(37)HB-260-80 (No. 110, #14126)

16:54 SBL & FPL power up (reached upper limit)

	Step No.	Power (kW) Total	Heat flux (W/cm^2) FPL/SBL	F-101 (m/s)	T-003 (°C)	T-1011M (°C)	Hold time	Note
16:54	1	264.52	77.95/77.50					
15:56	2	272.85	79.90/80.97	4.719	432.2	526.7		

16:19 YODAC scanning
T-003 = 432.2 °C, T-1011M = 526.7 °C, F-101 = 4.719 m/s
16:20 HP-2116C start
16:21 HP-2116C stop

Run 37(37)HB-260-50 (No. 111, #14127)

16:23 SBL & FPL power down

	Step No.	Power (kW) Total	Heat flux (W/cm^2) FPL/SBL	F-101 (m/s)	T-003 (°C)	T-1011M (°C)	Hold time	Note
16:23	1	209.08	61.71/61.05		430			
	2	173.73	51.04/51.23					
	3	168.54	49.73/49.24					
	4				300			
	5	155.62	49.13/38.77					
16:51	6	169.82	49.92/50.00	4.602	309.9	365.7		

16:53 YODAC scanning
T-003 = 309.9 °C, T-1011M = 365.7 °C, F-101 = 4.602 m/s
16:54 HP-2116C start
16:55 HP-2116C stop

Run 37(37)HB-260-40 (No. 112, #14128)

16:57 SBL & FPL power down

	Step No.	Power (kW) Total	Heat flux (W/cm^2) FPL/SBL	F-101 (m/s)	T-003 (°C)	T-1011M (°C)	Hold time	Note
16:57	1	154.56	45.36/45.66					
16:58	2	137.82	40.43/40.76	4.539	284.5	329.7		

17:20 YODAC scanning
T-003 = 284.5 °C, T-1011M = 329.7 °C, F-101 = 4.539 m/s
17:21 HP-2116C start
17:22 HP-2116C stop

Run 37(37)HB-260-35 (No. 113, #14129)

SBL & FPL power down

	Step No.	Power (kW) Total	Heat flux (W/cm^2) FPL/SBL	F-101 (m/s)	T-003 (°C)	T-1011M (°C)	Hold time	Note
	1	122.64	36.05/36.13	4.734	271.8	309.9		

17:39 YODAC scanning
T-003 = 271.8 °C, T-1011M = 309.9 °C, F-101 = 4.734 m/s
17:40 HP-2116C start
17:41 HP-2116C stop

Run 37(37)HB-260-30 (No. 114, #14130)

17:43 SBL & FPL power down

	Step No.	Power (kW) Total	Heat flux (W/cm^2) FPL/SBL	F-101 (m/s)	T-003 (°C)	T-1011M (°C)	Hold time	Note
17:43	1	103.24	30.33/30.45	4.656	269.9	302.1		

17:48 YODAC scanning
T-003 = 269.9 °C, T-1011M = 302.1 °C, F-101 = 4.656 m/s
17:49 HP-2116C start
17:50 HP-2116C stop

Run 37(37)HB-200-35 (No. 115, #14131)

17:52 Pump power down (~200 l/min)
17:53 SBL & FPL power up

	Step No.	Power (kW) Total	Heat flux (W/cm^2) FPL/SBL	F-101 (m/s)	T-003 (°C)	T-1011M (°C)	Hold time	Note
	1	118.79	35.04/34.73	3.523	264.8	314.1		

18:00 YODAC scanning
T-003 = 264.8 °C, T-1011M = 314.1 °C, F-101 = 3.523 m/s
18:01 HP-2116C start
18:02 HP-2116C stop

Run 37(37)HB-260-10 (No. 116, #14132)

18:04 Pump power up (~260 l/min)
18:07 SBL & FPL power down

Step No.	Power (kW) Total	Heat flux (W/cm^2) FPL/SBL	F-101 (m/s)	T-003 (°C)	T-1011M (°C)	Hold time	Note
1	35.64	10.28/10.90	4.719	275.8	286.7		

18:13 YODAC scanning
T-003 = 275.8 °C, T-1011M = 286.7 °C, F-101 = 4.719 m/s
18:14 HP-2116C start
18:15 HP-2116C stop
18:16 SBL & FPL power down and off

Circulation & purification operation

18:20 Pump off
18:20 Valve setting

VH-101	VA-102	VM-103	VH-104	VH-109	VH-110
100 %	open	100 %	100 %	100 %	100 %

18:28 Pump on (~150 l/min)
: Change of the HP-2116C measurement network

1980.1.18

Circulation & heat-up operation

0:10 Auxiliary heater power on
(temperature level change from 250 °C to 500 °C)
7:00 Re-setting of the preheater power controller
(changed from 250 ±25 °C to 450 ±25 °C)

Thermocouple calibration runs
(check of the signal isolation buffer amplifiers)

Run 37(0)CAL-0150-141-D (without isolation; No. 117, #14133)

8:32 YODAC scanning
T-003 = 530.0 °C, T-1011M = 531.9 °C, F-101 = ... m/s

Run 37(0)CAL-0150-141-E (with isolation; No. 118, #14134)

8:34 YODAC scanning
T-003 = 530.5 °C, T-1011M = 531.2 °C, F-101 = ... m/s

Preparation for the tests

8:48 Occurrence of pin trouble (#206 & #311)
(insulating resistance = 0)
9:38 Separation of #206 and #311 pins
9:53 Exhaust of argon gas from SBL gas volume
10:10 Auxiliary heater power off

Flow-meter calibration run

Run 37(0)CAL-0-141-B (No. 119, #14135)

10:12 Pump off
10:12 Valve setting

VH-101	VA-102	VM-103	VH-104	VH-109	VH-110
100 %	close	0 %	100 %	0 %	0 %

10:35 YODAC scanning
T-003 = 483.2 °C, T-1011M = 489.8 °C, F-101 = 0.008 m/s

Low-heat-flux boiling runs; series (1) (continued)
(examination of boiling condition under low-flow)

Run 37(35)LHF-220 (pressure decrease method; No. 120, #14136)

10:39 Valve setting

VH-101	VA-102	VM-103	VH-104	VH-109	VH-110
100 %	close	2.5 %	100 %	0 %	0 %

10:40 Pump on (~2 l/min)
SBL & FPL power on

Step No.	Power (kW) Total	Heat flux (W/cm^2) FPL/SBL	F-101 (m/s)	T-003 (°C)	T-1011M (°C)	Hold time	Note
1	0.03	0.01/ 0.02	.....	.....	.....	.....	
2	2.93	1.11/ 0.42	.....	.....	.....	.....	
3	6.49	2.02/ 2.01	.....	.....	.....	.....	
4	9.36	2.86/ 3.02	.....	.....	.....	.....	
5	10.74	3.40/ 3.19	.....	.....	.....	.....	
6	12.12	3.76/ 3.79	.....	.....	.....	.....	
7	10.26	3.19/ 3.19	.....	.....	.....	.....	
8	8.61	2.61/ 2.86	.....	.....	.....	.....	
9	3.94	1.30/ 1.05	.....	.....	.....	.....	
10	7.06	2.21/ 2.16	.....	.....	.....	.....	
11	9.72	2.99/ 3.11	.....	.....	.....	.....	
12	11.20	3.50/ 3.44	.....	.....	.....	.....	
13	12.03	3.72/ 3.78	.....	.....	.....	.....	
14	13.43	4.16/ 4.21	.....	.....	.....	.....	
15	15.46	4.76/ 4.92	0.066	440.8	810.0	6'50"	

11:10 YODAC scanning
T-001 = 442.2 °C, T-1011M = 802.8 °C, F-101 = 0.063 m/s
11:12 HP-2116C start
11:13 Start of pressure reduction

16	15.46	4.76/ 4.92	0.068	440.8	810.3	.....	
17	"	"	0.064	"	810.0	.....	

18	"	"	0.067	"	810.3	.....	
19	12.80	3.98/ 3.98	0.012	439.9	810.8	1'35"	IB
20	11.29	3.51/ 3.51	0.002	434.7	807.7	1'41"	B(D)

P-201 = 0.0190 MPa, T_{sat} = 810.0 °C

11:18 SBL & FPL power down and off
(observation of an unexpected dryout)
11:19 HP-2116C stop
11:23 Valve operation to fill the FPL with argon gas

Run 37(35)LHF-221 (power increase method; No. 121, #14137)

11:33 SBL & FPL power on

Step No.	Power (kW) Total	Heat flux (W/cm^2) FPL/SBL	F-101 (m/s)	T-003 (°C)	T-1011M (°C)	Hold time	Note
1	7.84	2.44/ 2.43	.....	.....	.....	.....	
2	14.47	4.48/ 4.54	.....	.....	.....	.....	
3	21.37	6.60/ 6.77	.....	.....	.....	.....	
4	25.33	7.85/ 7.95	0.086	425.0	800.7	5'45"	

11:41 YODAC scanning
T-003 = 425.0 °C, T-1011M = 813.1 °C, F-101 = 0.086 m/s
11:42 HP-2116C start
11:43 SBL & FPL power up

5	29.34	9.15/ 9.05	.....	.....	.....	.....	
6	31.76	9.87/ 9.87	.....	.....	.....	.....	
7	34.97	10.88/10.87	0.086	414.5	906.0	2'00"	IB
8	38.60	12.00/12.01	0.102	411.0	905.0	1'47"	B

P-201 = 0.0991 MPa, T_{sat} = 906.0 °C

11:47 Valve setting

VH-101	VA-102	VM-103	VH-104	VH-109	VH-110
100 %	close	100 %	100 %	0 %	0 %

11:48 HP-2116C stop
11:50 SBL & FPL power down and off

Circulation and mixing operation

11:53 Pump off
11:54 Valve setting

VH-101	VA-102	VM-103	VH-104	VH-109	VH-110
100 %	open	100 %	100 %	100 %	100 %

11:55 Pump on (~150 l/min)
11:55 Auxiliary heater power on
11:56 Exhaust of argon gas from SBL gas volume
13:01 Auxiliary heater power off

Run 37(35)LHF-222 (pressure decrease method; No. 122, #14138)

13:02 Pump off
13:03 Valve setting

VH-101	VA-102	VM-103	VH-104	VH-109	VH-110
100 %	close	4.5 %	100 %	0 %	0 %

13:07 Pump on (~6 l/min)
13:08 SBL & FPL power on

Step No.	Power (kW) Total	Heat flux (W/cm^2) FPL/SBL	F-101 (m/s)	T-003 (°C)	T-1011M (°C)	Hold time	Note
1	6.84	2.02/ 2.39	.....	.....	.....	.....	
2	12.43	3.86/ 3.88	.....	.....	.....	.....	
3	18.95	5.94/ 5.77	.....	.....	.....	.....	
4	24.93	7.80/ 7.62	.....	.....	.....	.....	
13:17 5	29.40	9.12/ 9.20	0.110	458.8	798.1	8'25"	

13:20 YODAC scanning
T-003 = 458.8 °C, T-1011M = 811.1 °C, F-101 = 0.110 m/s
13:21 HP-2116C start
13:22 start of pressure reduction

6	29.40	9.12/ 9.20	.....	.....	.....	.....	
7	"	"	.....	.....	.....	.....	
8	29.69	9.22/ 9.26	0.110	455.0	810.0	1'38"	IB
9	29.20	9.06/ 9.13	0.106	452.0	801.5	1'39"	B

P-201 = 0.0284 MPa, T_{sat} = 810.0 °C

13:27 SBL & FPL power down and off
13:28 HP-2116C stop

Run 37(35)LHF-223 (pressure decrease method; No. 123, #14139)

13:31 Valve operation to fill the FPL with argon gas
13:35 Pump power adjust (~5 l/min)
13:42 Exhaust of argon gas from SBL gas volume
13:42 SBL & FPL power on

Step No.	Power (kW) Total	Heat flux (W/cm^2) FPL/SBL	F-101 (m/s)	T-003 (°C)	T-1011M (°C)	Hold time	Note
1	7.15	2.16/ 2.39	.....	.....	.....	.....	
2	12.63	3.85/ 4.11	.....	.....	.....	.....	
3	18.92	5.94/ 5.74	.....	.....	.....	.....	
13:45 4	21.60	6.72/ 6.71	0.071	412.0	788.3	11'50"	

13:52 YODAC scanning
T-003 = 412.0 °C, T-1011M = 803.1 °C, F-101 = 0.071 m/s
13:53 HP-2116C start
13:54 Start of pressure reduction

5	21.60	6.72/ 6.71	0.071	.....	.....	.....	
6	"	"	.....	.....	.....	.....	
7	"	"	.....	.....	.....	.....	

8	21.48	6.67/ 6.70	0.083	404.0	832.0	1'38"	IB
9	"	"	0.102	.....	.....	.....	

P-201 = 0.0382 MPa, T_{sat} = 832.0 °C

13:57 SBL & FPL power down and off
13:57 HP-2116C stop

Run 37(35)LHF-224 (pressure decrease method; No. 124, #14140)

14:02 Pump off
14:03 Valve setting

VH-101	VA-102	VM-103	VH-104	VH-109	VH-110
100 %	close	3 %	100 %	0 %	0 %

14:17 Pump on (~7 l/min)
14:28 Valve operation to fill the FPL with argon gas
14:29 Exhaust of argon gas from SBL gas volume
14:30 SBL & FPL power on

Step No.	Power (kW) Total	Heat flux (W/cm^2) FPL/SBL	F-101 (m/s)	T-003 (°C)	F-1011M (°C)	Hold time	Note
1	10.85	3.26/ 3.65	.....	.....	.....	.....	
2	18.40	5.71/ 5.75	.....	.....	.....	.....	
3	28.30	8.73/ 8.97	.....	.....	.....	.....	
4	36.99	11.33/11.93	0.133	450.0	800.9	9'10"	

14:40 YODAC scanning
T-003 = 450.0 °C, T-1011M = 814.8 °C, F-101 = 0.132 m/s
14:41 HP-2116C start
14:42 Start of pressure reduction

5	36.99	11.33/11.93	0.133	.....	.....	.....	
6	36.54	11.17/11.84	0.122	453.0	851.5	1'43"	IB
7	36.17	11.07/11.68	0.114	452.0	850.5	1'47"	B

P-201 = 0.0510 MPa, T_{sat} = 851.5 °C

14:45 SBL & FPL power down and off
14:46 HP-2116C stop
14:51 Valve operation to fill the FPL & SBL with argon gas

Run 37(35)LHF-225 (power increase method; No. 125, #14141)

14:55 Valve setting

VH-101	VA-102	VM-103	VH-104	VH-109	VH-110
100 %	close	4 %	100 %	0 %	0 %

14:56 Pump power adjust (~9 l/min)
14:57 SBL & FPL power on

Step No.	Power (kW) Total	Heat flux (W/cm^2) FPL/SBL	F-101 (m/s)	T-003 (°C)	T-1011M (°C)	Hold time	Note
1	11.18	3.29/ 3.93	.....	.....	.....	.....	
2	19.50	6.03/ 6.13	.....	.....	.....	.....	
3	28.58	8.84/ 8.99	.....	.....	.....	.....	
4	37.87	11.82/11.65	.....	.....	.....	.....	
5	43.80	13.61/13.65	0.157	456.1	794.0	5'10"	

15:08 YODAC scanning
T-003 = 456.1 °C, T-1011M = 809.0 °C, F-101 = 0.157 m/s
15:09 HP-2116C start
15:10 SBL & FPL power up

	6	48.08	14.92/15.02	.....	.....	.....	.....	
	7	54.40	16.88/17.01	.....	.....	.....	.....	
	8	58.08	18.07/18.04	.....	.....	.....	.....	
15:14	9	60.78	18.81/18.93	.....	.....	.....	.....	
15:16	10	66.80	20.71/20.79	.....	.....	.....	2'05"	IB
							1'34"	B

P-201 = ... MPa, T_{sat} = ... °C

15:18 Valve setting

VH-101	VA-102	VM-103	VH-104	VH-109	VH-110
100 %	close	5 %	100 %	0 %	0 %

15:19 HP-2116C stop
15:20 SBL & FPL power 10 % down

Run 37(35)LHF-226 (power increase method; No. 126, #14142)

15:23 Pump power adjust (~11 l/min)
15:26 SBL & FPL power up

Step No.	Power (kW) Total	Heat flux (W/cm^2) FPL/SBL	F-101 (m/s)	T-003 (°C)	T-1011M (°C)	Hold time	Note
1	57.66	18.80/15.74	.....	.....	.....	.....	
2	59.62	18.80/17.87	.....	.....	.....	.....	
3	60.84	18.87/19.02	0.212	426.5	785.0	9'40"	

15:30 YODAC scanning
T-003 = 426.5 °C, T-1011M = 798.9 °C, F-101 = 0.211 m/s
15:31 HP-2116C start
15:32 SBL & FPL power up

	4	66.83	20.70/20.97	.....	.....	.....	.....	
	5	71.01	22.07/22.11	.....	.....	.....	.....	
	6	76.45	23.79/23.71	.....	.....	.....	.....	
15:35	7	79.56	24.91/24.58	.....	.....	.....	.....	
15:37	8	85.00	26.43/26.42	.....	.....	.....	2'12"	IB
							1'40"	B

P-201 = ... MPa, T_{sat} = ... °C

15:39 Pump power adjust (~15 l/min)
15:39 HP-2116C stop

Run-37(35)LHF-227 (power increase method; No. 127, #14143)

15:43 SBL & FPL power up

Step No.	Power (kW) Total	Heat flux (W/cm^2) FPL/SBL	F-101 (m/s)	T-003 (°C)	T-1011M (°C)	Hold time	Note
1	88.10	27.41/27.35	0.290	452.4	837.2	14'00"	

15:50 YODAC scanning
T-003 = 452.4 °C, T-1011M = 852.7 °C, F-101 = 0.289 m/s
15:51 HP-2116C start
15:52 SBL & FPL power up

15:52	2	92.71	28.82/28.84	.....	.....	.....	.....	
15:53	3	98.69	30.62/30.84	0.290	460.0	898.5	1'35"	IB
15:55	4	105.59	32.84/32.81	0.294	461.0	901.5	2'02"	B

P-201 = ... MPa, T_{sat} = 898.5 °C
15:57 Pump power up (~25 l/min)
15:58 HP-2116C stop

Run 37(35)LHF-228 (power increase method; No. 128, #14144)

Pump power adjust (~20 l/min)

Step No.	Power (kW) Total	Heat flux (W/cm^2) FPL/SBL	F-101 (m/s)	T-003 (°C)	T-1011M (°C)	Hold time	Note
1	105.95	32.88/33.10	0.376	520.6	883.5	21'45"	

16:19 YODAC scanning
T-003 = 520.6 °C, T-1011M = 896.3 °C, F-101 = 0.375 m/s
16:20 HP-2116C start
16:21 SBL & FPL power up

16:21	2	109.50	34.08/33.96	.....	.....	.....	1'29"	IB
16:23	3	119.00	37.05/36.87	.....	.....	.....	1'26"	B

P-201 = ... MPa, T_{sat} = ... °C
16:24 Pump power up (~30 l/min)
16:25 HP-2116C stop
16:27 SBL & FPL power down and off

Circulation & mixing operation

16:40 Pump off
16:41 Valve setting

VH-101	VA-102	VM-103	VH-104	VH-109	VH-110
100 %	open	100 %	100 %	100 %	100 %

16:45 Re-setting of the preheater power controller
(changed from 450 ±25 °C to 250 ±25 °C)
16:45 Pump on (~150 l/min)

Thermocouple calibration runs

(check of the signal isolation buffer amplifiers)

Run 37(0)CAL-0150-141-F (without isolation; No. 129, #14145)

17:18 YODAC scanning
T-003 = 356.0 °C, T-1011M = 359.3 °C, F-101 = ... m/s

Run 37(0)CAL-0150-141-G (with isolation; No. 130, #14146)

17:20 YODAC scanning
T-003 = 351.7 °C, T-1011M = 353.1 °C, F-101 = ... m/s

17:55 Pump off
18:00 Sodium drain

19:30 Preheater power off

Record of the 142th operation

1980.1.30

8:30 Preheater power on
(aiming temperature level = 250 ±25 °C)

14:43 Sodium charge
(sodium level = EL-9100 mm)

Circulation & purification operation

15:26 Valve setting

VH-101	VA-102	VM-103	VH-104	VH-109	VH-110
100 %	open	100 %	100 %	100 %	100 %

15:43 Pump on (~150 l/min)

Thermocouple calibration runs
(check of the signal isolation buffer amplifiers)

Run 37(0)CAL-0150-142-A (without isolation; No. 131, #14201)

15:52 YODAC scanning
T-003 = 280.2 °C, T-1011M = 281.4 °C, F-103 = ... m/s

Run 37(0)CAL-0150-142-B (with isolation; No. 132, #14202)

15:54 YODAC scanning
T-003 = 280.4 °C, T-1011M = 279.9 °C, F-103 = ... m/s

Circulation & heat-up operation

23:00 Auxiliary heater power on
(temperature level change from 250 °C to 500 °C)
23:10 Re-setting of the preheater power controller
(changed from 250 ±25 °C to 450 ±25 °C)

1980.1.31

Thermocouple calibration runs
(check of the signal isolation buffer amplifiers)

Run 37(0)CAL-0150-142-C (with isolation; No. 133, #14203)

4:02 YODAC scanning
T-003 = 410.0 °C, T-1011M = 409.8 °C, F-103 = ... m/s

Run 37(0)CAL-0150-142-D (without isolation; No. 134, #14204)

4:03 YODAC scanning
T-003 = 411.3 °C, T-1011M = 412.7 °C, F-103 = ... m/s

Run 37(0)CAL-0150-142-E (with isolation; No. 135, #14205)

5:06 YODAC scanning
T-003 = 468.2 °C, T-1011M = 468.4 °C, F-103 = ... m/s

Run 37(0)CAL-0150-142-F (with isolation; No. 136, #14206)
(burn-out detection circuits was switched off)

5:07 YODAC scanning
T-003 = 469.0 °C, T-1011M = 468.8 °C, F-103 = ... m/s

Run 37(0)CAL-0150-142-G (without isolation; No. 137, #14207)

5:09 YODAC scanning
T-003 = 470.7 °C, T-1011M = 471.4 °C, F-103 = ... m/s

Run 37(0)CAL-0150-142-H (without isolation; No. 138, #14208)
(burn-out detection circuits was switched off)

5:10 YODAC scanning
T-003 = 471.3 °C, T-1011M = (449.0) °C, F-103 = ... m/s

Run 37(0)CAL-0150-142-I (with isolation; No. 139, #14209)

6:04 YODAC scanning
T-003 = 503.9 °C, T-1011M = 504.2 °C, F-103 = ... m/s

Run 37(0)CAL-0150-142-J (without isolation; No. 140, #14210)

6:06 YODAC scanning
T-003 = 504.7 °C, T-1011M = 506.4 °C, F-103 = ... m/s

Flow-meter and thermocouple calibration runs

Run 37(0)CAL-0-142-A (No. 141, #14211)

9:10 Auxiliary heater power off
9:10 Pump off
9:11 Valve setting

VH-101	VA-102	VM-103	VH-104	VH-109	VH-110
25 %	close	0 %	25 %	0 %	0 %

9:15 HP-9845T start
9:16 HP-9845T stop
9:16 YODAC scanning
T-003 = 503.9 °C, T-1011M = 531.3 °C, F-103 = 0.000 m/s
9:16 HP-2116C start
9:17 HP-2116C stop

Run 37(0)CAL-05-142-A (No. 142, #14212)

9:17 Valve setting

VH-101	VA-102	VM-103	VH-104	VH-109	VH-110

25 %	close	3 %	25 %	0 %	0 %

9:20 Pump on (~15 l/min)
9:23 HP-9845T start
9:25 HP-9845T stop
9:26 YODAC scanning
T-003 = 507.9 °C, T-1011M = 506.6 °C, F-103 = 0.259 m/s
: Occurrence of a trouble in flow measurements by F-101 and F-103
9:51 HP-9845T start
9:52 HP-9845T stop
9:52 HP-2116C start
9:53 HP-2116C stop

Low heat-flux boiling runs; series (2)
(examination of dryout condition under low-flow)

Run 37(36)LHF-230 (power increase method; No. 143, #14213)

9:55 Pump power adjust (~1 l/min)
10:00 FPL power on

Step No.	Power (kW)	Heat flux (W/cm^2)	F-103 (m/s)	T-003 (°C)	T-1011M (°C)	Hold time	Note
1	0.02	0.01	.....	.....	.....	.....	
2	3.50	1.06	.....	.....	.....	.....	
3	6.04	1.83	.....	.....	.....	.....	
4	9.10	2.75	.....	.....	.....	.....	
5	10.36	3.13	.....	.....	.....	.....	
6	7.20	2.18	0.024	410.5	824.2	17'00"	

10:22 YODAC scanning
T-003 = 410.5 °C, T-1011M = 805.4 °C, F-103 = 0.016 m/s
10:23 HP-2116C start
10:24 HP-9845T start
10:24 FPL power up

7	9.65	2.92	0.022	405	912	30"	IB
8	13.10	3.96	0.018	"	913	36"	B
9	16.38	4.95	0.017	403	"	43"	B
10	19.63	5.93	0.015	402	"	54"	B
11	23.19	7.01	0.011	401	"	34"	B
12	26.39	7.98	0.012	"	"	52"	B
13	29.57	8.94	0.012	400	"	36"	B(D)
14	33.06	9.99	0.014	"	914	57"	B(D)
15	34.92	10.56	0.012	"	"	39"	B(D)
16	36.40	11.00	0.011	"	"	49"	B(D)
17	39.77	12.02	0.010	"	915	29"	B(D)
18	41.12	12.43	0.014	"	914	43"	B(D)
19	44.70	13.50	0.010	"	915	8"	B(D)

P-201 = 0.1059 MPa, T_{sat} = 912.0 °C

10:32 FPL power auto-scram ..... high temperature
(trigger signal = T-307M)
10:33 HP-9845T stop
10:34 HP-2116C stop

Run 37(36)LHF-231 (power increase method; No. 144, #14214)

: Recurrence of a trouble in flow measurement by F-103
(F-101 was used for a backup operation)
11:08 Pump power adjust (~2 l/min)
11:09 FPL power on

Step No.	Power (kW)	Heat flux (W/cm^2)	F-101 (m/s)	T-003 (°C)	T-1011M (°C)	Hold time	Note
1	0.02	0.01	.....	.....	.....	.....	
2	3.59	1.08	.....	.....	.....	.....	
3	6.33	1.91	.....	.....	.....	.....	
4	9.48	2.86	.....	.....	.....	.....	
5	7.79	2.36	0.013	411.5	730.8	12'45"	

11:20 YODAC scanning
T-003 = 411.5 °C, T-1011M = 700.4 °C, F-101 = 0.000 m/s
11:21 HP-2116C start
11:22 HP-9845T start
11:22 FPL power up

6	10.06	3.04	0.012	405	808	32"	
7	12.99	3.93	"	403	859	30"	IB
8	19.20	5.80	0.013	402	906	36"	B
9	22.65	6.85	0.014	"	"	46"	B
10	29.06	8.78	0.015	"	907	44"	B
11	32.88	9.94	0.014	401	"	42"	B
12	36.11	10.92	0.016	"	"	54"	B(D)
13	39.31	11.88	0.013	400	908	1'06"	B(D)
14	43.33	13.10	0.011	399	910	1'16"	B(D)
15	45.87	13.87	"	"	914	55"	B(D)
16	49.71	15.03	"	398	"	44"	B(D)
17	52.63	15.91	0.010	397	915	40"	B(D)
18	57.71	17.45	0.009	"	918	35"	B(D)
19	63.18	19.10	0.010	"	922	41"	B(D)
20	69.20	20.92	0.012	"	927	5"	B(D)

P-201 = 0.0981 MPa, T_{sat} = 906.0 °C

11:30 FPL power auto-scram ..... high temperature
(trigger signals = T-101L & T-306M)
11:32 HP-2116C stop
11:32 HP-9845T stop

Circulation & heat-up operation

11:43 Pump off
11:43 Valve setting

VH-101	VA-102	VH-103	VH-104	VH-109	VH-110
100 %	open	100 %	100 %	100 %	100 %

11:46 Pump on (~150 l/min)
11:47 Auxiliary heater power on
(temperature level change from 400 °C to 500 °C)
13:02 Auxiliary heater power off

Run 37(36)LHF-232 (power increase method; No. 145, #14215)

13:03 Pump off
13:04 Valve setting

VH-101	VA-102	VM-103	VH-104	VH-109	VH-110
25 %	close	3 %	0 %	0 %	6.25 %

13:06 Pump on (~1 l/min)
13:07 FPL power on

Step No.	Power (kW)	Heat flux (W/cm^2)	F-103 (m/s)	T-003 (°C)	T-1011M (°C)	Hold time	Note
1	0.02	0.01	.....	.....	.....	.....	
2	3.43	1.04	.....	.....	.....	.....	
3	7.15	2.16	.....	.....	.....	.....	
4	10.75	3.25	.....	.....	.....	.....	
5	9.18	2.78	0.016	456.7	809.6	14'35"	(IB)

13:18 YODAC scanning
T-003 = 456.7 °C, T-1011M = 798.6 °C, F-103 = 0.031 m/s
13:19 Boiling was initiated before starting data loggers
13:19 HP-2116C start
13:19 HP-9845T start
13:20 FPL power up

6	12.76	3.86	0.015	449	905	37"	B
7	17.69	5.35	0.011	447	907	35"	B
8	22.73	6.87	0.010	444	"	42"	B
9	29.16	8.82	0.007	442	"	39"	B
10	35.92	10.86	0.008	439	"	1'02"	B(D)
11	43.08	13.02	"	437	909	1'01"	B(D)
12	45.16	13.65	0.009	"	913	48"	B(D)
13	49.64	15.01	0.007	435	915	38"	B(D)
14	53.93	16.30	0.005	"	916	40"	B(D)
15	62.08	18.77	0.008	"	925	45"	B(D)
16	66.10	19.99	0.011	434	927	1"	B(D)

P-201 = 0.0991 MPa, T_{sat} = 905.0 °C

13:30 FPL power auto-scram ..... high temperature
(trigger signals = T-101L, T-306M & T-307M)
13:31 HP-2116C stop
13:31 HP-9845T stop

: Alternation of heater pin connection
(The electrical insulation of #413 & #414 pair was broken)

Circulation & purification operation

15:04 Pump off
15:05 Valve setting

VH-101	VA-102	VM-103	VH-104	VH-109	VH-110
100 %	open	100 %	100 %	100 %	100 %

15:07 Pump on (~150 l/min)

1980.2.1

Circulation and heat-up operation

0:25 Auxiliary heater power on
(sodium temperature change from 250 °C to 500 °C)
8:50 Auxiliary heater power off

Flow-meter & thermocouple calibration runs

Run 37(0)CAL-0-142-B (No. 146, #14216)

8:50 Pump off
8:50 Valve setting

VH-101	VA-102	VM-103	VH-104	VH-109	VH-110
25 %	close	0 %	0 %	0 %	6.25 %

8:58 YODAC scanning
T-003 = 503.8 °C, T-1011M = 520.7 °C, F-103 = -0.008 m/s
8:59 HP-9845T start
9:00 HP-2116C start
9:01 HP-9845T stop
9:01 HP-2116C stop

Run 37(0)CAL-05-142-B (No. 147, #14217)

9:02 Valve setting

VH-101	VA-102	VM-103	VH-104	VH-109	VH-110
25 %	close	3 %	0 %	0 %	6.25 %

9:02 Pump on (~2 l/min)
9:06 YODAC scanning
T-003 = 505.4 °C, T-1011M = 500.8 °C, F-103 = 0.039 m/s
9:07 HP-9845T start
9:08 HP-2116C start
9:09 HP-9845T stop
9:09 HP-2116C stop

Low-heat-flux boiling runs; series (2) (continued)
(examination of dryout condition under low-flow)

Run 37(34)LHF-233 (power increase method; No. 148, #14218)

FPL power on

Step No.	Power (kW)	Heat flux (W/cm^2)	F-103 (m/s)	T-003 (°C)	T-1011M (°C)	Hold time	Note
1	0.06	0.02	.....	.....	.....	.....	
2	3.55	1.14	.....	.....	.....	.....	
3	6.18	1.98	.....	.....	.....	.....	

4	9.16	2.93	.....	.....	.....	.....	
5	12.23	3.92	.....	.....	.....	.....	
6	15.43	4.94	.....	.....	.....	.....	
7	13.61	4.36	.....	.....	.....	.....	
8	12.46	3.99	.....	.....	.....	.....	
9	14.36	4.60	0.047	462.5	861.2	15'50"	

9:29 YODAC scanning
T-003 = 462.5 °C, T-1011M = 867.3 °C, F-103 = 0.031 m/s
9:29 HP-9845T start
9:30 HP-9845T stop
9:33 HP-2116C start
9:34 HP-9845T re-start
9:34 FPL power up

10	18.71	5.99	0.050	447	885	37"	
11	24.67	7.90	0.048	445	912	43"	IB
12	27.59	8.83	0.046	444	910	48"	B
13	30.77	9.85	0.048	441	908	46"	B
14	37.13	11.88	0.056	440	907	1'02"	B
15	46.18	14.78	0.055	438	"	41"	B
16	54.73	17.52	0.050	436	"	52"	B
17	61.70	19.75	0.055	435	"	46"	B
18	69.08	22.11	0.059	434	906	37"	B
19	77.58	24.83	"	432	907	1'33"	B
20	83.88	26.85	0.055	430	909	1'33"	B(D)
21	92.57	29.63	0.050	429	911	2'10"	B(D)
22	102.30	32.75	0.048	428	"	0"	B(D)

P-201 = 0.0991 MPa, T_{sat} = 912.0 °C

9:46 FPL power auto-scram ..... high temperature
(trigger signal = T-312M, x_D = 0.50)
9:47 HP-9845T stop
9:48 HP-2116C stop

Run 37(34)LHF-234 (power increase method; No. 149, #14219)

10:05 Guard heater of the test section was cut-off
10:11 Pump power adjust (~2 l/min)
10:12 FPL power on

Step No.	Power (kW)	Heat flux (W/cm^2)	F-103 (m/s)	T-003 (°C)	T-1011M (°C)	Hold time	Note
1	0.06	0.02	0.036	470	.....	.....	
2	6.65	2.13	.....	.....	.....	.....	
3	9.46	3.03	.....	.....	.....	.....	
4	12.12	3.88	.....	.....	.....	.....	
5	15.04	4.81	0.034	464	.....	.....	
6	13.03	4.17	0.038	462.0	878.0	12'10"	

10:31 YODAC scanning
T-003 = 462.0 °C, T-1011M = 884.5 °C, F-103 = 0.039 m/s
10:31 HP-9845T start
10:31 HP-9845T stop
10:33 HP-2116C start
10:34 FPL power up

7	17.96	5.75	0.038	458	901	44"	
8	24.99	8.00	"	"	911	49"	IB
9	30.38	9.73	0.043	"	909	31"	B
10	36.72	11.75	"	"	"	32"	B
11	43.62	13.96	0.046	"	907	48"	B
12	48.83	15.63	"	457	909	35"	B
13	55.43	17.74	"	455	911	32"	B
14	61.34	19.63	0.030	436	909	5'18"	B(D)

P-201 = 0.0991 MPa, T_{sat} = 911.0 °C

10:45 FPL power auto-scram ..... high temperature
(trigger signal = T-311M, x_D = 0.56)
10:49 HP-2116C stop

Run 37(34)LHF-235 (power increase & flow decrease method; No. 150, #14220)

11:01 Pump power adjust (~2 l/min)
11:03 FPL power on

Step No.	Power (kW)	Heat flux (W/cm^2)	F-103 (m/s)	T-003 (°C)	T-1011M (°C)	Hold time	Note
1	0.06	0.02	0.035	464	.....	.....	
2	1.08	0.35	.....	.....	.....	.....	
3	6.20	1.98	.....	.....	.....	.....	
4	10.67	3.42	.....	.....	.....	.....	
5	12.58	4.03	0.034	456.6	813.7	10'07"	(IB)

11:19 YODAC scanning
T-003 = 456.6 °C, T-1011M = 815.8 °C, F-103 = 0.031 m/s
11:19 HP-9845T start
11:20 HP-9845T stop
11:22 Boiling was initiated before starting data loggers
11:23 HP-2116C start
11:24 HP-9845T re-start
11:24 FPL power up

6	19.27	6.17	0.032	453	909	30"	B
7	24.26	7.77	0.028	"	911	34"	B
8	29.82	9.55	0.029	452	910	39"	B
9	36.75	11.76	0.031	"	908	20"	B
10	37.46	11.99	0.033	451	907	1'20"	B

11:28 Pump power down

11	36.79	11.77	0.025	450	908	2'00"	B
12	36.65	11.73	0.027	446	906	4'20"	B(D)

11:34 Valve close (VM-103: 3 % + ~0 %)

13	36.65	11.73	0.007	443	905	18"	B(D)

P-201 = 0.1000 MPa, T_{sat} = 909.0 °C

11:34 FPL power emergency down and off

(observation of an unexpected temperature excursion of T-01H)

11:35 Valve open (VM-103: ~0 % → 10 %)
11:36 HP-9845T stop
11:37 HP-2116C stop

Circulation and heat-up operation

11:37 Pump off
11:37 Valve setting

VH-101	VA-102	VM-103	VH-104	VH-109	VH-110
100 %	open	100 %	100 %	100 %	100 %

11:39 Pump on (~150 l/min)
11:39 Auxiliary heater power on
(sodium temperature level change from 450 °C to 500 °C)

Flow-meter calibration run

Run 37(0)CAL-0-142-C (No. ..., #.....)

11:45 Valve setting

VH-101	VA-102	VM-103	VH-104	VH-109	VH-110
100 %	open	0 %	100 %	100 %	100 %

11:49 HP-9845T start
11:50 HP-9845T stop

Circulation & heat-up operation (continued)

11:51 Valve setting

VH-101	VA-102	VM-103	VH-104	VH-109	VH-110
100 %	open	100 %	100 %	100 %	100 %

13:02 Auxiliary heater power off

Flow-meter calibration run

Run 37(0)CAL-0-142-D (No. ..., #.....)

13:02 Pump off
13:04 Valve setting

VH-101	VA-102	VM-103	VH-104	VH-109	VH-110
25 %	close	0 %	0 %	0 %	6.25 %

13:05 HP-9845T start
13:08 HP-9845T stop

Low-heat-flux boiling run; series (2) (continued)

Run 37(34)LHF-236 (power increase and flow decrease method;
No. 151, #14221)

13:09 Valve setting

VH-101	VA-102	VM-103	VH-104	VH-109	VH-110
25 %	close	3 %	0 %	0 %	6.25 %

13:10 Pump on (~2 l/min)
13:11 FPL power on

Step No.	Power (kW)	Heat flux (W/cm^2)	F-103 (m/s)	T-003 (°C)	T-1011M (°C)	Hold time	Note
1	0.06	0.02	0.039	508	.....	.....	
2	6.05	1.94	.....	504	.....	.....	
3	8.68	2.78	0.023	499.7	679.1	8'00"	

13:19 YODAC scanning
T-003 = 499.7 °C, T-1011M = 650.7 °C, F-103 = 0.047 m/s
13:20 HP-9845T start
13:21 HP-9845T stop
13:23 HP-2116C start
13:23 HP-9845T re-start
13:24 FPL power up

4	15.02	4.81	.....	.....	.....	40"	
5	15.60	5.00	.....	.....	.....	42"	
6	18.25	5.84	.....	.....	.....	43"	IB
7	21.51	6.88	0.015	488	909	57"	B
8	24.06	7.70	0.010	484	"	43"	B
9	25.08	8.03	0.008	478	908	2'30"	B

13:30 Pump power down

10	24.56	7.86	0.007	470	908	1'40"	B(D)
11	24.15	7.73	0.004	465	"	1'40"	B(D)
12	24.40	7.81	0.001	459	"	2'00"	B(D)
13	24.31	7.78	0.000	455	907	1'40"	B(D)

13:37 FPL power up

14	28.01	8.97	0.000	451	908	2'17"	B(D)

P-201 = 0.1000 MPa, T_{sat} = 908.0 °C

13:40 FPL power manual down & off
(time over for the data logging)
13:40 HP-2116C stop
13:41 Valve open (VM-103: 3 % → ~10 %)
13:41 HP-9845T stop

Flow-meter calibration run

Run 37(0)CAL-0-142-E (No. ..., #.....)

13:55 Pump off
13:56 Valve setting

VH-101	VA-102	VM-103	VH-104	VH-109	VH-110

25 %	close	0 %	0 %	0 %	6.25 %

13:57 HP-9845T start
14:00 HP-9845T stop

Low-heat-flux boiling run; series (2) (continued)

Run 37(34)LHF-237 (power increase and flow decrease method; No. 152, #14222)

14:01 Valve setting

VH-101	VA-102	VM-103	VH-104	VH-109	VH-110
25 %	close	3 %	0 %	0 %	6.25 %

14:02 Pump on (~2 l/min)
14:02 FPL power on

Step No.	Power (kW)	Heat flux (W/cm^2)	F-103 (m/s)	T-003 (°C)	T-1011M (°C)	Hold time	Note
1	0.06	0.02	.....	.....	.....	.....	
2	6.69	2.14	.....	.....	.....	.....	
3	11.51	3.69	.....	.....	.....	.....	
4	14.00	4.48	0.021	459.9	820.4	10'15"	

14:14 YODAC scanning
T-003 = 459.9 °C, T-1011M = 777.2 °C, F-103 = 0.031 m/s
14:15 HP-9845T start
14:16 HP-9845T stop
14:17 HP-2116C start
14:17 HP-9845T start
14:18 FPL power up

5	18.45	5.90	.....	.....	.....	46"	IB
6	22.39	7.17	.....	.....	.....	34"	B
7	25.44	8.14	.....	.....	.....	38"	B
8	30.53	9.77	.....	.....	.....	44"	B
9	36.16	11.57	.....	.....	.....	46"	B(D)
10	37.33	11.95	0.021	448	909	1'30"	B(D)

14:23 Pump power down

11	37.20	11.91	0.020	444	909	1'20"	B(D)
12	37.06	11.86	0.016	441	"	1'40"	B(D)
13	37.10	11.87	0.012	435	"	1'20"	B(D)
14	36.82	11.79	"	431	"	2'00"	B(D)
15	36.65	11.73	0.010	427	"	1'25"	B(D)

14:31 Pump off

16	36.65	11.73	.....	.....	.....	.....	B(D)

14:32 FPL power up

17	40.65	13.01	0.011	422	911	1'08"	B(D)
18	43.82	14.02	0.010	419	914	2'00"	B(D)

P-201 = 0.1000 MPa, T_{sat} = 909.0 °C

14:35 FPL power manual down and off
(time over for the data logging)
14:36 Valve open (VM-103: 3 % → ~10 %)
14:36 HP-9845T stop
14:37 HP-2116C stop

Flow-meter calibration run

Run 37(0)CAL-0-142-F (No. ..., #.....)

14:55 Valve setting

VH-101	VA-102	VM-103	VH-104	VH-109	VH-110
25 %	close	0 %	0 %	0 %	6.25 %

14:56 HP-9845T start
14:59 HP-9845T stop

Low-heat-flux boiling run; series (2) (continued)

Run 37(34)LHF-238 (power increase method; No. 153, #14223)

15:00 Valve setting

VH-101	VA-102	VM-103	VH-104	VH-109	VH-110
25 %	close	3 %	0 %	0 %	6.25 %

15:01 Pump on (~2 l/min)
15:01 FPL power on

Step No.	Power (kW)	Heat flux (W/cm^2)	F-103 (m/s)	T-003 (°C)	T-1011M (°C)	Hold time	Note
1	0.06	0.02	0.040	463.6	.....	.....	
2	6.61	2.12	.....	.....	.....	.....	
3	11.85	3.79	.....	.....	.....	.....	
4	16.37	5.24	0.024	457.0	881.0	8'20"	(IB)

15:13 Boiling was initiated before starting data loggers
15:13 HP-2116C start
15:13 HP-9845T start
15:14 FPL power up

5	19.60	6.27	0.024	457.0	910	30"	B
6	27.69	8.86	0.025	"	"	34"	B
7	33.77	10.81	0.029	"	909	42"	B
8	39.04	12.50	0.033	"	910	2'06"	B
9	44.79	14.34	0.024	456	"	1'16"	B(D)
10	52.66	16.85	0.037	455	908	1'54"	B(D)
11	58.53	18.73	0.046	456	907	1'44"	B(D)
12	61.72	19.75	0.031	454	908	3'42"	B(D)
13	65.40	20.93	0.025	453	"	0"	B(D)

P-201 = 0.1000 MPa, T_{sat} = 910.0 °C

15:28 FPL power auto-scram ..... high temperature
(trigger signals = T-312M & T-3091M, x_D = 0.56)
15:28 HP-2116C stop
15:28 Valve open (VM-103: 3 % + ~10 %)
15:29 HP-9845T stop

Flow-meter calibration run

Run 37(0)CAL-0-142-G (No. ..., #.....)

15:43 Pump off
15:43 Valve setting

VH-101	VA-102	VM-103	VH-104	VH-109	VH-110
25 %	close	0 %	0 %	0 %	6.25 %

15:44 HP-9845T start
15:46 HP-9845T stop

Low-heat-flux boiling run; series (2) (continued)

Run 37(34)LHF-239 (power increase method; No. 154, #14224)

15:50 Valve setting

VH-101	VA-102	VM-103	VH-104	VH-109	VH-110
25 %	close	3 %	0 %	0 %	6.25 %

15:51 Pump on (~1 l/min)
15:54 FPL power on

Step No.	Power (kW)	Heat flux (W/cm^2)	F-103 (m/s)	T-003 (°C)	T-1011M (°C)	Hold time	Note
1	0.06	0.02	0.028	470.0	.....	.....	
2	6.19	1.98	.....	.....	.....	.....	
3	10.68	3.42	0.014	455.0	716.4	.....	

16:00 HP-9845T start
16:01 YODAC scanning
T-003 = 455.0 °C, T-1011M = 642.5 °C, F-103 = 0.047 m/s
16:02 HP-9845T stop
16:04 HP-2116C start
16:05 HP-9845T re-start
16:05 FPL power up

4	15.10	4.83	0.006	448	846	52"	
5	20.25	6.48	0.005	445	909	1'30"	IB
6	24.62	7.88	0.004	439	912	1'08"	B
7	30.78	9.85	0.002	437	911	1'12"	B(D)
8	34.70	11.10	0.003	435	"	1'28"	B(D)
9	37.84	12.11	"	433	912	1'56"	B(D)
10	40.66	13.01	0.002	431	915	1'44"	B(D)
11	46.72	14.95	"	430	921	1'32"	B(D)
12	52.90	16.93	0.003	"	927	1'42"	B(D)
13	59.10	18.93	0.004	"	"	2"	B(D)

P-201 = 0.1000 MPa, T_{sat} = 909.0 °C

16:18 FPL power auto-scram ..... high temperature
(trigger signal = T-3031M)
16:19 HP-2116C stop
16:20 Valve open (VM-103: 3 % + ~10 %)
16:21 HP-9845T stop

Circulation & mixing operation

16:23 Pump off
16:26 Valve setting

VH-101	VA-102	VM-103	VH-104	VH-109	VH-110
100 %	open	100 %	100 %	100 %	100 %

16:30 Re-setting of the preheater power controller
(changed from 450 ±25 °C to 250 ±25 °C)
16:30 Pump on (~150 l/min)

Flow-meter calibration run

Run 37(0)CAL-0-142-H (No. ..., #.....)

16:37 Pump off
16:37 Valve setting

VH-101	VA-102	VM-103	VH-104	VH-109	VH-110
100 %	open	0 %	100 %	100 %	100 %

16:38 HP-9845T start
16:42 HP-9845T stop

Circulation & mixing operation

16:43 Valve setting

VH-101	VA-102	VM-103	VH-104	VH-109	VH-110
100 %	open	100 %	100 %	100 %	100 %

16:44 Pump on (~150 l/min)

18:05 Pump off
18:14 Sodium drain

20:13 Preheater power off

Record of the 143th operation

1980.2.26

8:30 Preheater power on
(aiming temperature level = 250 ±25 °C)

15:05 Sodium charge
(sodium level = EL-9100 mm)

Circulation & purification operation

16:04 Valve setting

VH-101	VA-102	VM-103	VH-104	VH-109	VH-110
100 %	open	100 %	100 %	100 %	100 %

16:05 Pump on (~150 l/min)

1980.2.27

Circulation & heat-up operation

0:03 Auxiliary heater power on
(temperature level change from 250 ±25 °C to 450 ±25 °C)
: Occurrence of pin trouble (#310 & #415)
(insulating resistance = 0)
5:55 Separation of #310 and #415 pins
8:54 Auxiliary heater power off

Flow-meter & thermocouple calibration runs

Run 37(0)CAL-0-143-A (No. 155, #14301)

9:00 Pump off
9:02 Valve setting

VH-101	VA-102	VM-103	VH-104	VH-109	VH-110
100 %	close	0 %	100 %	0 %	0 %

9:06 YODAC scanning
T-003 = 520.8 °C, T-1011M = 530.5 °C, F-103 = 0.000 m/s
9:07 HP-2116C start
9:08 HP-2116C stop

Run 37(0)CAL-05-143-A (No. 156, #14302)

9:10 Valve setting

VH-101	VA-102	VM-103	VH-104	VH-109	VH-110
100 %	close	100 %	100 %	0 %	0 %

9:12 Pump on (~7 l/min)

9:22 YODAC scanning
T-003 = 509.5 °C, T-1011M = 512.9 °C, F-103 = 0.125 m/s
9:23 HP-2116C start
9:24 HP-2116C stop

Periodical inspection of the SBL & FPL power supplies

9:24 Pump power up (~200 l/min)
9:25 FPL power on
: :
: :
10:20 FPL power off

Single-phase flow natural circulation runs

Run 37(33)NCT-1 (power increase method; No. ..., #14303)

10:45 Pump off
10:45 Valve setting

VH-101	VA-102	VM-103	VH-104	VH-109	VH-110
100 %	close	100 %	0 %	0 %	100 %

10:48 HP-9845T start
10:48 HP-2116C start
10:50 FPL power on

Step No.	Power (kW)	Heat flux (W/cm^2)	F-103 (m/s)	T-003 (°C)	T-1011M (°C)	Hold time	Note
1	0.09	0.03	0	473	...	5"	
2	5.25	1.73	.....	...	...	15"	
3	15.31	5.05	0.123	...	...	5'40"	

10:56 FPL power auto-scram ..... over-current (= 1100 A)
10:57 Change of trigger current level
10:57 HP-9845T stop
10:58 HP-2116C stop

Run 37(33)NCT-2 (power increase & decrease method; No. ..., #14304)

11:06 HP-9845T start
11:06 HP-2116C start
11:08 Pump on (~150 l/min)
11:11 Pump off
11:12 Valve close and open (VM-103: 100 % → 0 % → 100 %)
11:13 FPL power on

Step No.	Power (kW)	Heat flux (W/cm^2)	F-103 (m/s)	T-003 (°C)	T-1011M (°C)	Hold time	Note
1	15.73	5.19	0.117	...	...	5'35"	
2	30.07	9.92	0.150	424	...	5'23"	
3	44.34	14.62	0.179	...	...	4'48"	
4	30.91	10.19	0.155	420	...	5'12"	
5	15.67	5.17	0.110	"	...	5'58"	

P-201 = 0.1000 MPa, T_{sat} = 910.0 °C

15:28 FPL power auto-scram ..... high temperature
(trigger signals = T-312M & T-3091M, x_D = 0.56)
15:28 HP-2116C stop
15:28 Valve open (VM-103: 3 % → ~10 %)
15:29 HP-9845T stop

Flow-meter calibration run

Run 37(0)CAL-0-142-G (No. ..., #.....)

15:43 Pump off
15:43 Valve setting

VH-101	VA-102	VM-103	VH-104	VH-109	VH-110
25 %	close	0 %	0 %	0 %	6.25 %

15:44 HP-9845T start
15:46 HP-9845T stop

Low-heat-flux boiling run; series (2) (continued)

Run 37(34)LHF-239 (power increase method; No. 154, #14224)

15:50 Valve setting

VH-101	VA-102	VM-103	VH-104	VH-109	VH-110
25 %	close	3 %	0 %	0 %	6.25 %

15:51 Pump on (~1 l/min)
15:54 FPL power on

Step No.	Power (kW)	Heat flux (W/cm^2)	F-103 (m/s)	T-003 (°C)	T-1011M (°C)	Hold time	Note
1	0.06	0.02	0.028	470.0	.....	.....	
2	6.19	1.98	.....	.....	.....	.....	
3	10.68	3.42	0.014	455.0	716.4	.....	

16:00 HP-9845T start
16:01 YODAC scanning
T-003 = 455.0 °C, T-1011M = 642.5 °C, F-103 = 0.047 m/s
16:02 HP-9845T stop
16:04 HP-2116C start
16:05 HP-9845T re-start
16:05 FPL power up

4	15.10	4.83	0.006	448	846	52"	
5	20.25	6.48	0.005	445	909	1'30"	IB
6	24.62	7.88	0.004	439	912	1'08"	B
7	30.78	9.85	0.002	437	911	1'12"	B(D)
8	34.70	11.10	0.003	435	"	1'28"	B(D)
9	37.84	12.11	"	433	912	1'56"	B(D)
10	40.66	13.01	0.002	431	915	1'44"	B(D)
11	46.72	14.95	"	430	921	1'32"	B(D)
12	52.90	16.93	0.003	"	927	1'42"	B(D)
13	59.10	18.93	0.004	"	"	2"	B(D)

P-201 = 0.1000 MPa, T_{sat} = 909.0 °C

16:18 FPL power auto-scram ..... high temperature
(trigger signal = T-3031M)
16:19 HP-2116C stop
16:20 Valve open (VM-103: 3 % → ~10 %)
16:21 HP-9845T stop

Circulation & mixing operation

16:23 Pump off
16:26 Valve setting

VH-101	VA-102	VM-103	VH-104	VH-109	VH-110
100 %	open	100 %	100 %	100 %	100 %

16:30 Re-setting of the preheater power controller
(changed from 450 ±25 °C to 250 ±25 °C)
16:30 Pump on (~150 l/min)

Flow-meter calibration run

Run 37(0)CAL-0-142-H (No. ..., #.....)

16:37 Pump off
16:37 Valve setting

VH-101	VA-102	VM-103	VH-104	VH-109	VH-110
100 %	open	0 %	100 %	100 %	100 %

16:38 HP-9845T start
16:42 HP-9845T stop

Circulation & mixing operation

16:43 Valve setting

VH-101	VA-102	VM-103	VH-104	VH-109	VH-110
100 %	open	100 %	100 %	100 %	100 %

16:44 Pump on (~150 l/min)

18:05 Pump off
18:14 Sodium drain

20:13 Preheater power off

Record of the 143th operation

1980.2.26

8:30 Preheater power on
(aiming temperature level = 250 ±25 °C)

15:05 Sodium charge
(sodium level = EL-9100 mm)

Circulation & purification operation

16:04 Valve setting

VH-101	VA-102	VM-103	VH-104	VH-109	VH-110
100 %	open	100 %	100 %	100 %	100 %

16:05 Pump on (~150 l/min)

1980.2.27

Circulation & heat-up operation

0:03 Auxiliary heater power on
(temperature level change from 250 ±25 °C to 450 ±25 °C)
: Occurrence of pin trouble (#310 & #415)
(insulating resistance = 0)
5:55 Separation of #310 and #415 pins
8:54 Auxiliary heater power off

Flow-meter & thermocouple calibration runs

Run 37(0)CAL-0-143-A (No. 155, #14301)

9:00 Pump off
9:02 Valve setting

VH-101	VA-102	VM-103	VH-104	VH-109	VH-110
100 %	close	0 %	100 %	0 %	0 %

9:06 YODAC scanning
T-003 = 520.8 °C, T-1011M = 530.5 °C, F-103 = 0.000 m/s
9:07 HP-2116C start
9:08 HP-2116C stop

Run 37(0)CAL-05-143-A (No. 156, #14302)

9:10 Valve setting

VH-101	VA-102	VM-103	VH-104	VH-109	VH-110
100 %	close	100 %	100 %	0 %	0 %

9:12 Pump on (~7 l/min)

9:22 YODAC scanning
T-003 = 509.5 °C, T-1011M = 512.9 °C, F-103 = 0.125 m/s
9:23 HP-2116C start
9:24 HP-2116C stop

Periodical inspection of the SBL & FPL power supplies

9:24 Pump power up (~200 l/min)
9:25 FPL power on
: :
: :
10:20 FPL power off

Single-phase flow natural circulation runs

Run 37(33)NCT-1 (power increase method; No. ..., #14303)

10:45 Pump off
10:45 Valve setting

VH-101	VA-102	VM-103	VH-104	VH-109	VH-110
100 %	close	100 %	0 %	0 %	100 %

10:48 HP-9845T start
10:48 HP-2116C start
10:50 FPL power on

Step No.	Power (kW)	Heat flux (W/cm^2)	F-103 (m/s)	T-003 (°C)	T-1011M (°C)	Hold time	Note
1	0.09	0.03	0	473	...	5"	
2	5.25	1.73	.....	...	...	15"	
3	15.31	5.05	0.123	...	...	5'40"	

10:56 FPL power auto-scram ..... over-current (= 1100 A)
10:57 Change of trigger current level
10:57 HP-9845T stop
10:58 HP-2116C stop

Run 37(33)NCT-2 (power increase & decrease method; No. ..., #14304)

11:06 HP-9845T start
11:06 HP-2116C start
11:08 Pump on (~150 l/min)
11:11 Pump off
11:12 Valve close and open (VM-103: 100 % → 0 % → 100 %)
11:13 FPL power on

Step No.	Power (kW)	Heat flux (W/cm^2)	F-103 (m/s)	T-003 (°C)	T-1011M (°C)	Hold time	Note
1	15.73	5.19	0.117	...	...	5'35"	
2	30.07	9.92	0.150	424	...	5'23"	
3	44.34	14.62	0.179	...	...	4'48"	
4	30.91	10.19	0.155	420	...	5'12"	
5	15.67	5.17	0.110	"	...	5'58"	

11:40 FPL power down and off
11:46 HP-2116C stop
11:46 HP-9845T stop

Circulation & mixing operation

11:49 Valve setting

VH-101	VA-102	VM-103	VH-104	VH-109	VH-110
100 %	open	100 %	100 %	100 %	100 %

11:53 Pump on (~150 l/min)
11:54 Auxiliary heater power on
13:05 Auxiliary heater power off

Flow-meter calibration run

Run 37(0)CAL-0-143-B (No. ..., #.....)

13:06 Pump off
13:07 Valve setting

VH-101	VA-102	VM-103	VH-104	VH-109	VH-110
100 %	close	0 %	0 %	0 %	6.25 %

13:16 HP-9845T start
13:20 HP-9845T stop

Low-heat-flux boiling run; series (2) (continued)

Run 37(33)LHF-240 (power increase and flow decrease method; No. 157, #14305)

13:28 Valve setting

VH-101	VA-102	VM-103	VH-104	VH-109	VH-110
100 %	close	3 %	0 %	0 %	6.25 %

13:28 Pump on (~3 l/min)
13:30 HP-9845T start
13:30 FPL power on

Step No.	Power (kW)	Heat flux (W/cm^2)	F-103 (m/s)	T-003 (°C)	T-1011M (°C)	Hold time	Note
1	0.09	0.03	.....	490	.....	.....	
2	1.16	0.38	.....	.....	.....	.....	
3	11.77	3.88	.....	.....	.....	.....	
4	13.35	4.40	0.046	481.4	882.7	13'40"	(IB)

13:36 Boiling was initiated before starting data loggers
13:37 YODAC scanning
T-003 = 481.4 °C, T-1011M = 878.0 °C, F-103 = 0.039 m/s
13:42 HP-2116C start
13:44 FPL power up

5	20.19	6.66	0.030	472	908	1'26"	B
6	27.38	9.03	0.025	"	907	1'46"	B
7	29.90	9.86	0.023	"	"	1'50"	B

13:49 Pump power down

8	29.75	9.81	0.016	.....	.....	1'43"	B
9	29.60	9.76	0.012	.....	.....	1'37"	B(D)
10	29.00	9.56	0.009	.....	.....	3'49"	B(D)

P-201 = 0.0991 MPa, T_{sat} = 908 °C

13:56 FPL power manual down & off
13:58 HP-2116C stop
13:59 Pump power up (~10 l/min)
14:03 HP-9845T stop
14:04 Exhaust of argon gas from SBL & FPL gas volume

Flow-meter calibration run

Run 37(0)CAL-0-143-C (No. ..., #.....)

14:43 Pump off
14:43 HP-9845T start
14:44 Valve setting

VH-101	VA-102	VM-103	VH-104	VH-109	VH-110
100 %	close	0 %	0 %	0 %	6.25 %

14:47 HP-9845T stop

Low-heat-flux boiling run; series (2) (continued)

Run 37(33)LHF-241 (power increase and flow decrease method; No. 158, #14306)

14:48 Valve setting

VH-101	VA-102	VM-103	VH-104	VH-109	VH-110
100 %	close	3 %	0 %	0 %	6.25 %

14:48 Pump on (~2 l/min)
14:49 FPL power on

Step No.	Power (kW)	Heat flux (W/cm^2)	F-103 (m/s)	T-003 (°C)	T-1011M (°C)	Hold time	Note
1	0.10	0.03	.....	.....	.....	.....	
2	9.16	3.02	0.033	456.1	761.5	15'00"	

14:59 HP-9845T start
15:01 YODAC scanning
T-003 = 456.1 °C, T-1011M = 761.5 °C, F-103 = 0.031 m/s
15:04 HP-2116C start
15:05 FPL power up

3	17.73	5.85	0.032	451	803	1'24"	IB
4	25.66	8.46	0.028	"	"	1'52"	B
5	35.17	11.60	0.026	449	"	2'13"	B
6	44.75	14.76	0.031	450	"	2'04"	B(D)

15:13 Pump power down

7	44.00	14.51	0.021	449	803	.....	B(D)

P-201 = 0.0294 MPa, T_{sat} = 803.0 °C

15:13 FPL power auto-scram ..... high temperature
(trigger signal = T-201M, x_D = 0.57)
15:15 Pump power up (~2 l/min)
15:16 HP-9845T stop
15:20 HP-2116C stop
15:22 Pump power up (~10 l/min)

Flow-meter calibration run

Run 37(0)CAL-0-143-D (No. ..., #.....)

15:44 HP-9845T start
15:44 Pump off
15:44 Valve setting

VH-101	VA-102	VM-103	VH-104	VH-109	VH-110
100 %	close	0 %	0 %	0 %	6.25 %

15:46 HP-9845T stop

Low-heat-flux boiling run; series (2) (continued)

Run 37(33)LHF-242 (power increase method; No. 159, #14307)

15:51 Valve setting

VH-101	VA-102	VM-103	VH-104	VH-109	VH-110
100 %	close	3 %	0 %	0 %	6.25 %

15:51 Pump on (~2 l/min)
15:52 FPL power on

Step No.	Power (kW)	Heat flux (W/cm^2)	F-103 (m/s)	T-003 (°C)	T-1011M (°C)	Hold time	Note
1	0.10	0.03	0.036	.....	.....	.....	
2	4.80	1.58	.....	.....	.....	.....	
3	8.16	2.69	0.036	453.9	690	12'00"	

16:02 YODAC scanning
T-003 = 453.9 °C, T-1011M = 696.4 °C, F-103 = 0.039 m/s
16:04 HP-9845T start
16:04 HP-2116C start
16:05 FPL power up

4	17.53	5.78	0.033	.....	.....	1'18"	IB
5	25.82	8.52	0.008	430	803	1'33"	B(D)

P-201 = 0.0294 MPa, T_{sat} = 803.0 °C

16:08 FPL power auto-scram ..... high temperature
(trigger signal = T-101L, x_D = 0.98)
16:09 HP-2116C stop
16:10 HP-9845T stop
16:12 Pump power up (~2 + ~10 l/min)

Flow-meter calibration run

Run 37(0)CAL-0-143-E (No. ..., #.....)

16:27 Pump off
16:27 HP-9845T start
16:27 Valve setting

VH-101	VA-102	VM-103	VH-104	VH-109	VH-110
100 %	close	0 %	0 %	0 %	6.25 %

16:30 HP-9845T stop

Low-heat-flux boiling run; series (2) (continued)

Run 37(33)LHF-243 (power increase method; No. 160, #14308)

16:31 Valve setting

VH-101	VA-102	VM-103	VH-104	VH-109	VH-110
100 %	close	3 %	0 %	0 %	6.25 %

16:31 Pump on (~2 l/min)
16:32 FPL power on

Step No.	Power (kW)	Heat flux (W/cm^2)	F-103 (m/s)	T-003 (°C)	T-1011M (°C)	Hold time	Note
1	0.09	0.03	.....	.....	.....	.....	
2	9.16	3.02	0.043	447.6	.....	13'00"	

16:40 YODAC scanning
T-003 = 447.6 °C, T-1011M = 654.5 °C, F-103 = 0.039 m/s
16:43 HP-9845T start
16:44 HP-2116C start
16:45 FPL power up

3	14.52	4.79	0.018	435.7	805	1'22"	IB
4	24.49	8.08	0.014	429.2	807	1'17"	B(D)

P-201 = 0.0304 MPa, T_{sat} = 805.0 °C

16:48 FPL power auto-scram ..... high temperature
(trigger signal = T-306M, x_D = 0.51)
16:49 HP-2116C stop
16:51 HP-9845T stop

16:53 Pump power up (~2 → ~10 l/min)

Circulation & purification operation

16:58 Valve operation to fill the SBL & FPL with argon gas
17:03 Pump off
17:04 Valve setting

VH-101	VA-102	VM-103	VH-104	VH-109	VH-110
100 %	open	100 %	100 %	100 %	100 %

17:06 Pump on (~150 l/min)

Circulation & heat-up operation

23:53 Auxiliary heater power on

1980.2.28

7:00 Re-setting of the preheater power controller
(changed from 250 ±25 °C to 450 ±25 °C)
8:50 Auxiliary heater power off

Flow-meter and thermocouple calibration runs

Run 37(0)CAL-0-143-F (No. 161, #14309)

8:53 Pump off
8:53 HP-8945T start
8:55 Valve setting

VH-101	VA-102	VM-103	VH-104	VH-109	VH-110
100 %	close	0 %	0 %	0 %	6.25 %

8:58 YODAC scanning
T-003 = 482.5 °C, T-1011M = 499.0 °C, F-103 = 0.008 m/s
9:00 HP-2116C start
9:01 HP-9845T stop
9:01 HP-2116C stop

Run 37(0)CAL-05-143-B (No. 162, #14310)

9:02 Valve setting

VH-101	VA-102	VM-103	VH-104	VH-109	VH-110
100 %	close	100 %	0 %	0 %	6.25 %

9:02 Pump on (~15 l/min)
9:08 YODAC scanning
T-003 = 478.4 °C, T-1011M = 476.7 °C, F-103 = 0.290 m/s
9:08 HP-2116C start
9:09 HP-2116C stop

Low-heat-flux boiling run; series (2) (continued)

Run 37(33)LHF-244 (power increase and flow decrease method;
No. 163, #14311)

9:10 Pump off
9:10 Valve setting

VH-101	VA-102	VM-103	VH-104	VH-109	VH-110
100 %	close	2 %	0 %	0 %	6.25 %

9:10 Pump on (~2 l/min)
9:12 FPL power on

Step No.	Power (kW)	Heat flux (W/cm^2)	F-103 (m/s)	T-003 (°C)	T-1011M (°C)	Hold time	Note
1	0.09	0.03	.....	.....	.....	.....	
2	4.95	1.63	.....	.....	.....	.....	
3	10.09	3.33	.....	.....	.....	.....	
4	13.00	4.29	0.038	463.2	.....	9'00"	

9:29 YODAC scanning
T-003 = 463.2 °C, T-1011M = 846.8 °C, F-103 = 0.039 m/s
9:31 HP-9845T start
9:31 HP-2116C start
9:32 FPL power up

5	20.85	6.88	0.037	.....	.....	1'00"	IB
6	26.09	8.60	0.033	.....	.....	1'28"	B
7	34.50	11.38	0.034	.....	.....	2'10"	B
8	37.28	12.29	0.031	.....	.....	2'20"	B

9:38 Pump power down

9	35.56	11.72	0.024	.....	.....	1'30"	B(D)
10	35.23	11.61	0.022	.....	.....	2'00"	B(D)
11	35.16	11.59	0.020	426	.....	40"	B(D)

P-201 = 0.0991 MPa, T_{sat} = ... °C
9:43 FPL power auto-scram ..... high temperature
(trigger signal = T-201M, x_D = 0.49)
9:44 Pump power up (~3 l/min)
9:46 HP-9845T stop
9:48 HP-2116C stop

Circulation & mixing operation

9:50 Pump off
9:50 Valve setting

VH-101	VA-102	VM-103	VH-104	VH-109	VH-110
100 %	open	100 %	100 %	100 %	100 %

9:54 Pump on (~150 l/min)
9:55 Auxiliary heater power on
(sodium temperature level change from °C to °C)
10:35 Auxiliary heater power off

Flow-meter calibration run

Run 37(0)CAL-0-143-G (No. ..., #.....)

10:37 Pump off
10:37 HP-9845T start
10:38 Valve setting

VH-101	VA-102	VM-103	VH-104	VH-109	VH-110
100 %	close	0 %	0 %	0 %	6.25 %

10:40 HP-9845T stop

Low-heat-flux boiling run; series (2) (continued)

Run 37(33)LHF-245 (power increase and flow decrease method; No. 164, #14312)

10:40 Valve setting

VH-101	VA-102	VM-103	VH-104	VH-109	VH-110
100 %	close	2 %	0 %	0 %	6.25 %

10:40 Pump on (~2 l/min)
10:41 FPL power on

Step No.	Power (kW)	Heat flux (W/cm^2)	F-103 (m/s)	T-003 (°C)	T-1011M (°C)	Hold time	Note
1	0.09	0.03	.....	.....	.....	.....	
2	10.81	3.56	.....	.....	.....	.....	
3	11.69	3.86	0.040	447.2	.....	6'30"	(IB)

10:53 YODAC scanning
T-003 = 447.7 °C, T-1011M = 793.0 °C, F-103 = 0.039 m/s
10:57 HP-9845T start
10:57 HP-2116C start
10:57 Boiling was initiated
10:58 FPL power up

4	19.21	6.34	0.033	.....	.....	1'37"	B
5	30.16	9.95	0.032	.....	.....	1'25"	B
6	38.54	12.71	0.032	.....	.....	1'50"	B
7	48.70	16.06	0.038	.....	.....	1'47"	B(D)

11:05 Pump power down

8	49.13	16.20	0.028	.....	.....	2'03"	B(D)
9	48.01	15.83	0.016	.....	.....	1'55"	B(D)
10	48.01	15.83	0.010	.....	.....	2'20"	B(D)
11	47.52	15.70	0.007	.....	.....	2'02"	B(D)
12	47.93	15.80	0.005	.....	.....	1'50"	B(D)

11:15 FPL power up

13	57.86	19.08	0.003	404	.....	1'23"	B(D)

P-201 = 0.0991 MPa, T_{sat} = ... °C
11:16 HP-2116C error stop
(over-flow of mass strage)
11:16 FPL power auto-scram ..... high temperature
(trigger signal = T-101L)
11:17 Pump power up (~4 l/min)
11:18 HP-9845T stop

11:19 Pump power up (~10 l/min)

Flow-meter calibration run

Run 37(0)CAL-0-143-H (No. ..., #.....)

11:34 Pump off
11:34 Valve setting

VH-101	VA-102	VM-103	VH-104	VH-109	VH-110
100 %	close	0 %	0 %	0 %	6.25 %

11:35 HP-9845T start
11:37 HP-9845T stop

Low-heat-flux boiling run; series (2) (continued)

Run 37(33)LHF-246 (power increase method; No. 165, #14313)

11:38 Valve setting

VH-101	VA-102	VM-103	VH-104	VH-109	VH-110
100 %	close	2 %	0 %	0 %	6.25 %

11:38 Pump on (~2 l/min)
11:38 FPL power on

Step No.	Power (kW)	Heat flux (W/cm^2)	F-103 (m/s)	T-003 (°C)	T-1011M (°C)	Hold time	Note
1	0.09	0.03	.....	.....	.....	.....	
2	8.83	2.91	0.043	449.8	.....	13'00"	

11:48 YODAC scanning
T-003 = 449.8 °C, T-1011M = 712.2 °C, F-103 = 0.039 m/s
11:50 HP-2116C start
11:50 HP-9845T start
11:51 FPL power up

3	20.24	6.67	0.047	.....	.....	1'44"	
4	21.86	7.20	"	.....	.....	0"	

FPL power auto-scram ..... high temperature
(trigger signal = ...: super heat)
11:54 HP-2116C stop
11:54 HP-9845T stop

Circulation & heat-up operation

11:57 Pump off
11:57 Valve setting

VH-101	VA-102	VM-103	VH-104	VH-109	VH-110
100 %	open	100 %	100 %	100 %	100 %

11:59 Pump on (~150 l/min)
12:00 Auxiliary heater power on
(sodium temperature level change from °C to °C)

13:00 Auxiliary heater power off

Flow-meter calibration run

Run 37(0)CAL-0-143-I (No. ..., #.....)

13:01 Pump off
13:03 Valve setting

VH-101	VA-102	VM-103	VH-104	VH-109	VH-110
100 %	close	0 %	0 %	0 %	6.25 %

13:10 HP-9845T start
13:11 HP-9845T stop

Low-heat-flux boiling run; series (2) (continued)

Run 37(33)LHF-247 (power increase and flow decrease method;
No. 166, #14314)

13:12 Valve setting

VH-101	VA-102	VM-103	VH-104	VH-109	VH-110
100 %	close	2 %	0 %	0 %	6.25 %

13:12 Pump on (~1 l/min)
13:13 FPL power on

Step No.	Power (kW)	Heat flux (W/cm^2)	F-103 (m/s)	T-003 (°C)	T-1011M (°C)	Hold time	Note
1	0.09	0.03	.....	.....	.....	.....	
2	10.04	3.31	.....	.....	.....	.....	
3	11.02	3.63	0.020	444.4	.....	13'30"	

13:24 YODAC scanning
T-003 = 444.4 °C, T-1011M = 712.3 °C, F-103 = 0.016 m/s
13:26 HP-9845T start
13:26 HP-2116C start
13:27 FPL power up

4	16.48	5.44	0.023	.....	.....	1'25"	
5	20.22	6.67	0.020	.....	.....	1'50"	IB
6	27.65	9.12	0.018	.....	.....	1'50"	B
7	30.09	9.92	"	.....	.....	1'43"	B(D)

13:34 Pump power down

8	29.80	9.82	0.008	.....	.....	1'37"	B(D)
9	29.32	9.67	0.004	.....	.....	1'37"	B(D)
10	27.42	9.04	0.000	.....	.....	1'35"	B(D)
11	27.69	9.13	-0.001	.....	.....	1'42"	B(D)
12	27.26	8.99	-0.002	.....	.....	2'35"	B(D)

P-201 = 0.0991 MPa, T_{sat} = ... °C
13:42 HP-2116C error stop
(over-flow of mass strage)
13:43 FPL power manual-scram ..... time up
13:44 Pump power up (~4 l/min)
13:44 HP-9845T stop

Flow-meter calibration run

Run 37(0)CAL-0-143-J (No. ..., #.....)

13:56 Pump off
13:56 HP-9845T start
13:56 Valve setting

VH-101	VA-102	VM-103	VH-104	VH-109	VH-110
100 %	close	0 %	0 %	0 %	6.25 %

13:59 HP-9845T stop

Low-heat-flux boiling run; series (2) (continued)

Run 37(33)LHF-248 (power increase and flow decrease method;
No. 167, #14315)

14:01 Valve setting

VH-101	VA-102	VM-103	VH-104	VH-109	VH-110
100 %	close	2 %	0 %	0 %	6.25 %

14:01 Pump on (~2 l/min)
14:02 FPL power on

Step No.	Power (kW)	Heat flux (W/cm^2)	F-103 (m/s)	T-003 (°C)	T-1011M (°C)	Hold time	Note
1	0.09	0.03	.....	.....	.....	.....	
2	10.15	3.35	.....	.....	.....	.....	
3	11.89	3.92	0.036	474.0	.....	16'00"	

14:16 YODAC scanning
T-003 = 474.0 °C, T-1011M = 833.3 °C, F-103 = 0.039 m/s
14:18 HP-9845T start
14:18 HP-2116C start
14:19 FPL power up

4	23.61	7.79	0.036	.....	.....	1'52"	IB
5	33.62	11.09	0.035	.....	.....	55"	B

6	43.87	14.47	0.034	.....	.....	1'33"	B
7	53.32	17.59	"	.....	.....	2'06"	B
8	62.73	20.69	"	.....	.....	1'56"	B
9	72.11	23.78	0.037	.....	.....	2'02"	B

14:29 Pump power down

10	71.50	23.58	0.029	420	.....	1'27"	B(D)

P-201 = 0.1000 MPa, T_{sat} = ... °C

14:31 FPL power auto-scram ..... high temperature
(trigger signal = T-307M, x_D = 0.75)
14:31 Pump power up (~4 l/min)
14:32 HP-9845T stop
14:33 Pump power up (~15 l/min)
14:34 HP-2116C stop
14:40 Pin failures are found
(#204 & #307, #404 & #405, #401 & #402)

Circulation & mixing operation

14:55 Pump off
14:58 Valve setting

VH-101	VA-102	VM-103	VH-104	VH-109	VH-110
100 %	open	100 %	100 %	100 %	100 %

15:03 Pump on (~150 l/min)
15:04 Re-setting of the preheater power controller
(changed from 450 ±25 °C to 250 ±25 °C)

18:21 Pump off
18:26 Sodium drain

19:45 Preheater power off

Records of the 144th operation

1980.3.17

8:40 Preheater power on
(aiming temperature level = 250 ±25 °C)

15:17 Sodium charge
(sodium level = EL-9100 mm)

Circulation & purification operation

16:35 Valve setting

VH-101	VA-102	VM-103	VH-104	VH-109	VH-110
100 %	open	100 %	100 %	100 %	100 %

16:40 Pump on (~150 l/min)

Circulation & heat-up operation

23:30 Auxiliary heater power on
(temperature level change from 250 ±25 °C to 450 ±25 °C)
23:32 Re-setting of the preheater power controller
(changed from 250 ±25 °C to 450 ±25 °C)

1980.3.18

Flow-meter and thermocouple calibration runs

Run 37(0)CAL-0150-144-A (No. 168, #14401)

8:48 YODAC scanning
T-003 = 513.9 °C, T-1011M = 514.6 °C, F-103 = 0.565 m/s

Run 37(0)CAL-0-144-A (No. 169, #14402)

9:20 Auxiliary heater power off
9:20 Pump off
9:22 Valve setting

VH-101	VA-102	VM-103	VH-104	VH-109	VH-110
25 %	open	0 %	0 %	0 %	6.25 %

9:23 HP-9845T start
9:26 YODAC scanning
T-003 = 492.5 °C, T-1011M = 521.9 °C, F-103 = 0.000 m/s

Run 37(0)CAL-0-144-B (No. 170, #14403)

9:31 YODAC scanning
T-003 = 477.6 °C, T-1011M = 522.8 °C, F-103 = 0.000 m/s
9:31 HP-2116C start
9:32 HP-2116C stop
9:32 HP-9845T stop

Run 37(0)CAL-05-144-A (No. 171, #14404)

9:34 Valve setting

VH-101	VA-102	VM-103	VH-104	VH-109	VH-110
25 %	open	100 %	0 %	0 %	6.25 %

9:35 Pump on (~5 l/min)
9:38 HP-9845T start
9:40 YODAC scanning
T-003 = 483.9 °C, T-1011M = 481.5 °C, F-103 = 0.047 m/s
9:41 HP-2116C start
9:42 HP-2116C stop
9:43 HP-9845T stop

Low-heat-flux boiling runs; series (2) (continued)
(examination of dryout condition under low-flow)

Run 37(29)LHF-250 (power increase and flow decrease method; No. 172, #14405)

9:55 Valve setting

VH-101	VA-102	VM-103	VH-104	VH-109	VH-110
25 %	open	100 %	0 %	50 %	6.25 %

9:58 Pump power adjust (F-103: ~2 l/min)
10:03 FPL power on

Step No.	Power (kW)	Heat flux (W/cm^2)	F-103 (m/s)	T-003 (°C)	T-1011M (°C)	Hold time	Note
1	0.07	0.02	.....	.....	.....	.....	
2	2.57	0.96	.....	.....	.....	.....	
3	5.18	1.95	.....	.....	.....	.....	
4	8.01	3.01	.....	.....	.....	.....	

10:24 FPL power down & off
(F-103 becomes too large due to the reversal flow of T-2 line)
10:25 Valve re-setting

VH-101	VA-102	VM-103	VH-104	VH-109	VH-110
25 %	open	3 %	0 %	0 %	6.25 %

10:25 Pump on (F-103: ~2 l/min)
10:26 FPL power on
10:26 HP-9845T start

	5	0.08	0.03	.....	.....	.....	.....	
	6	2.93	1.10	.....	.....	.....	.....	
10:27	7	5.13	1.92	.....	.....	.....	1'38"	
10:29	8	7.56	2.84	.....	.....	.....	1'27"	
10:31	9	8.97	3.37	.....	.....	.....	3'16"	

10:34	10	9.71	3.64	0.031	431.9	.....	.....	

10:39 YODAC scanning
T-003 = 431.9 °C, T-1011M = 766.8 °C, F-103 = 0.031 m/s
10:41 HP-9845T stop
10:43 HP-2116C start
10:44 HP-9845T start
10:44 FPL power up

11	15.53	5.83	0.024	.....	.....	1'00"	IB
12	20.53	7.70	"	.....	.....	1'51"	B
13	25.28	9.49	0.018	.....	.....	1'57"	B
14	31.41	11.79	0.039	.....	.....	2'51"	B
15	33.57	12.60	0.034	.....	.....	2'41"	B

10:54 Pump power down

16	33.01	12.39	0.035	.....	.....	1'41"	B
17	"	"	0.037	.....	.....	1'47"	B
18	"	"	0.038	.....	.....	1'45"	B

10:59 Pump off (natural circulation)

19	33.30	12.50	0.040	.....	.....	1'48"	B

P-201 = 0.0991 MPa, T_{sat} = ... °C

11:00 HP-2116C error stop
(over-flow of mass strage)
11:01 FPL power down & off
11:02 Pump on (~10 l/min)
11:03 HP-9845T stop

Run 37(29)LHF-251 (power increase and flow decrease method; No. 173, #14406)

11:23 Valve setting

VH-101	VA-102	VM-103	VH-104	VH-109	VH-110
25 %	open	2 %	0 %	0 %	6.25 %

11:23 Pump power adjust (F-103: ~1 l/min)
11:25 HP-9845T start
11:26 FPL power on

Step No.	Power (kW)	Heat flux (W/cm^2)	F-103 (m/s)	T-003 (°C)	T-1011M (°C)	Hold time	Note
1	0.08	0.03	0.028	.....	.....	28"	
2	4.21	1.58	0.028	.....	.....	1'31"	
11:28 3	11.99	4.50	0.031	417.4	.....	.....	

11:37 YODAC scanning
T-003 = 417.4 °C, T-1011M = 806.5 °C, F-103 = 0.031 m/s
11:38 HP-9845T stop
11:39 HP-2116C start
11:40 FPL power up

4	17.00	6.38	.....	.....	.....	1'47"	
5	20.32	7.62	.....	.....	.....	1'31"	IB
6	25.91	9.72	0.043	.....	.....	2'04"	B

11:43 HP-9845T start

7	31.15	11.69	0.047	.....	.....	2'16"	B
8	33.49	12.57	0.044	.....	.....	1'53"	B

11:49 Pump power down

9	33.15	12.44	0.042	.....	.....	1'52"	B
10	33.00	12.39	0.041	.....	.....	1'46"	B
11	32.35	12.14	0.035	.....	.....	1'38"	B
12	31.81	11.94	0.032	.....	.....	1'43"	B

Pump off (natural circulation)

13	32.57	12.22	0.035	.....	.....	3'00"	B

P-201 = 0.0991 MPa, T_{sat} = ... °C

11:59 HP-2116C error stop
(over-flow of mass strage)
11:59 FPL power down & off
12:00 Pump on (~2 l/min)
12:00 HP-9845T stop

Circulation & mixing operation

12:10 Pump off
12:10 Valve setting

VH-101	VA-102	VM-103	VH-104	VH-109	VH-110
100 %	open	100 %	100 %	100 %	100 %

12:12 Pump on (~150 l/min)
12:12 Auxiliary heater power on
13:05 Auxiliary heater power off

Flow-meter calibration run

Run 37(0)CAL-0-144-C (No. ..., #.....)

13:06 HP-9845T start
13:06 Pump off
13:06 Valve setting

VH-101	VA-102	VM-103	VH-104	VH-109	VH-110
100 %	open	0 %	0 %	0 %	100 %

13:08 HP-9845T stop

Low-heat-flux boiling runs; series (2) (continued)

Run 37(29)LHF-252 (power increase and flow decrease method;
No. 174, #14407)

13:10 Valve setting

VH-101	VA-102	VM-103	VH-104	VH-109	VH-110
100 %	open	2 %	0 %	0 %	100 %

13:10 Pump on (~1 l/min)
13:11 FPL power on

Step No.	Power (kW)	Heat flux (W/cm^2)	F-103 (m/s)	T-003 (°C)	T-1011M (°C)	Hold time	Note
1	0.07	0.03	0.009	.....	.....	13'00"	

: Check of the heater pin resistance
(total pin resistance is unexpectedly high)
13:24 HP-9845T start
13:24 FPL power up

2	5.38	2.02	0.026	.....	.....	3'10"	
3	7.26	2.72	0.037	.....	.....	3'00"	
4	7.51	2.82	0.050	488.9	.....	7'00"	

13:29 YODAC scanning
T-003 = 488.9 °C, T-1011M = 733.1 °C, F-103 = 0.047 m/s
13:30 HP-9845T stop
13:32 HP-2116C start
13:32 FPL power up

5	12.84	4.82	0.052	.....	.....	58"	IB

13:33 HP-9845T start

6	19.14	7.18	0.050	.....	.....	1'03"	B
7	24.74	9.29	0.054	.....	.....	1'03"	B
8	30.18	11.32	0.042	.....	.....	1'28"	B
9	33.10	12.42	0.049	.....	.....	1'58"	B(D)

13:39 Pump power down

10	33.10	12.42	0.052	.....	.....	1'06"	B(D)
11	33.00	12.38	0.055	.....	.....	2'04"	B(D)
12	33.20	12.46	0.055	.....	.....	1'43"	B(D)
13	33.10	12.42	0.057	.....	.....	1'52"	B(D)

13:46 Pump off (natural circulation)

14	33.10	12.42	0.059	.....	.....	2'42"	B(D)

P-201 = 0.0991 MPa, T_{sat} = ... °C

13:48 FPL power down & off
13:50 HP-9845T stop
13:50 HP-2116C stop

Run 37(29)LHF-253 (power increase and flow decrease method;
No. 175, #14408)

14:16 Valve setting

VH-101	VA-102	VM-103	VH-104	VH-109	VH-110
12.5 %	open	1.8 %	0 %	0 %	6.25 %

14:20 Pump on (~1 l/min)
14:20 FPL power on

Step No.	Power (kW)	Heat flux (W/cm^2)	F-103 (m/s)	T-003 (°C)	T-1011M (°C)	Hold time	Note
1	0.09	0.03	.....	.....	.....	.....	
2	5.38	2.02	.....	.....	.....	.....	

14:24 HP-9845T start
14:27 Pump power adjust (~1 l/min)

14:28	3	7.99	3.00	0.010	.....	.....	.....

14:34 YODAC scanning
T-003 = 416.0 °C, T-1011M = 722.6 °C, F-103 = 0.008 m/s
14:35 HP-9845T stop
14:36 HP-2116C start
14:37 FPL power up
14:38 HP-9845T start

4	14.52	5.45	0.010	.....	.....	1'04"	IB
5	19.78	7.42	0.009	.....	.....	1'05"	B
6	24.94	9.36	"	.....	.....	1'04"	B
7	31.66	11.88	0.005	.....	.....	2'15"	B(D)
8	32.95	12.37	0.006	.....	.....	1'51"	B(D)

14:45 Pump power down

9	33.00	12.39	0.006	.....	.....	1'37"	B(D)
10	33.10	12.43	"	.....	.....	1'36"	B(D)
11	"	"	"	.....	.....	1'28"	B(D)
12	"	"	"	.....	.....	1'37"	B(D)

14:51 Pump off (natural circulation)

13	33.10	12.43	0.006	.....	.....	1'48"	B(D)

P-201 = 0.0991 MPa, T_{sat} = ... °C

14:53 Valve open (VM-103: 1.8 % → 2.0 % → 2.2 %)
14:56 FPL power down & off
14:56 HP-2116C stop
14:57 HP-9845T stop
15:00 Pin failures are found
(#409 & #306, #410 & #411 ..... insulation is broken)
: Separation of the failed pins

Circulation & purification operation

15:10 Valve setting

VH-101	VA-102	VM-103	VH-104	VH-109	VH-110
100 %	open	100 %	100 %	100 %	100 %

15:15 Pump on (~150 l/min)
23:00 Auxiliary heater power on

1980.3.19

8:00 Auxiliary heater power off

Flow-meter & thermocouple calibration runs

Run 37(0)CAL-0-144-D (No. 176, #14409)

8:55 Pump off
8:55 Valve setting

VH-101	VA-102	VM-103	VH-104	VH-109	VH-110
100 %	close	0 %	0 %	0 %	100 %

8:56 HP-9845T start
9:01 HP-9845T stop
9:02 YODAC scanning
T-003 = 498.9 °C, T-1011M = 547.7 °C, F-103 = 0.000 m/s

Run 37(0)CAL-05-144-B (No. 177, #14410)

9:06 Valve setting

VH-101	VA-102	VM-103	VH-104	VH-109	VH-110
100 %	close	3 %	0 %	0 %	100 %

9:06 Pump on (~3 l/min)
9:07 HP-9845T start
9:18 HP-9845T stop
9:20 YODAC scanning
T-003 = 494.1 °C, T-1011M = 507.5 °C, F-103 = 0.047 m/s

Heat balance check runs

Run 37(25)H-001 (No. 178, #14411)

9:29 HP-9845T start
9:30 FPL power on

Step No.	Power (kW)	Heat flux (W/cm^2)	F-103 (m/s)	T-003 (°C)	T-1011M (°C)	Hold time	Note
1	0.07	0.03	0.029	.....	.....	5"	
2	3.97	1.73	0.036	438.3	.....	16'00"	

9:41 YODAC scanning
T-003 = 438.3 °C, T-1011M = 567.6 °C, F-103 = 0.031 m/s

9:42 HP-9845T stop

Run 37(25)H-002 (No. 179, #14412)

9:45 Pump power adjust (~4 l/min)
9:46 FPL power up

1	4.17	1.82	0.070	423.7	.....	10'00"	

9:47 HP-9845T start
9:53 HP-9845T stop
9:53 YODAC scanning
T-003 = 423.7 °C, T-1011M = 496.2 °C, F-103 = 0.071 m/s

Run 37(25)H-003 (No. 180, #14413)

9:56 FPL power up

1	6.72	2.92	0.068	430.8	.....	13'00"	

9:57 HP-9845T start
10:08 HP-9845T stop
10:08 YODAC scanning
T-003 = 430.8 °C, T-1011M = 546.5 °C, F-103 = 0.063 m/s
10:09 FPL power down & off

Run 37(25)H-004 (No. 181, #14414)

10:40 Pump power adjust (~3 l/min)
10:40 FPL power on

Step No.	Power (kW)	Heat flux (W/cm^2)	F-103 (m/s)	T-003 (°C)	T-1011M (°C)	Hold time	Note
1	0.07	0.03	.....	.....	.....	5"	
2	4.88	2.12	0.060	416.4	.....	12'00"	

10:47 HP-9845T start
10:49 HP-9845T stop
10:49 YODAC scanning
T-003 = 416.4 °C, T-1011M = 507.4 °C, F-103 = 0.055 m/s

Run 37(25)H-005 (No. 182, #14415)

10:53 FPL power up

Step No.	Power (kW)	Heat flux (W/cm^2)	F-103 (m/s)	T-003 (°C)	T-1011M (°C)	Hold time	Note
1	7.74	3.37	0.060	414.9	.....	4'00"	

10:54 HP-9845T start
10:56 HP-9845T stop
10:56 YODAC scanning
T-003 = 414.9 °C, T-1011M = 555.6 °C, F-103 = 0.055 m/s

Run 37(25)H-006 (No. 183, #14416)

10:57 FPL power up

Step No.	Power (kW)	Heat flux (W/cm^2)	F-103 (m/s)	T-003 (°C)	T-1011M (°C)	Hold time	Note
1	9.04	3.93	0.061	413.7	.....	7'00"	

10:59 HP-9845T start
11:01 HP-9845T stop
11:01 YODAC scanning
T-003 = 413.7 °C, T-1011M = 574.8 °C, F-103 = 0.063 m/s

Run 37(25)H-007 (No. 184, #14417)

11:03 HP-9845T start
11:04 Pump power down (~2 l/min)

Step No.	Power (kW)	Heat flux (W/cm^2)	F-103 (m/s)	T-003 (°C)	T-1011M (°C)	Hold time	Note
1	8.72	3.80	0.037	410.4	.....	8'00"	

11:10 HP-9845T stop
11:10 YODAC scanning
T-003 = 410.4 °C, T-1011M = 654.7 °C, F-103 = 0.031 m/s

Run 37(25)H-008 (No. 185, #14418)

11:12 FPL power down

Step No.	Power (kW)	Heat flux (W/cm^2)	F-103 (m/s)	T-003 (°C)	T-1011M (°C)	Hold time	Note
1	6.70	2.91	0.028	409.1	.....	8'00"	

11:14 HP-9845T start
11:17 YODAC scanning
T-003 = 409.1 °C, T-1011M = 602.5 °C, F-103 = 0.031 m/s
11:18 HP-9845T stop

Run 37(25)H-009 (No. 186, #14419)

11:20 Pump power down (~1 l/min)

Step No.	Power (kW)	Heat flux (W/cm^2)	F-103 (m/s)	T-003 (°C)	T-1011M (°C)	Hold time	Note
1	6.42	2.80	0.022	394.0	.....	12'00"	

11:21 HP-9845T start
11:35 YODAC scanning
T-003 = 394.0 °C, T-1011M = 692.6 °C, F-103 = 0.016 m/s
11:36 HP-9845T stop

Run 37(25)H-010 (No. 187, #14420)

11:38 Pump power down (~0.8 l/min)

Step	Power	Heat flux	F-103	T-003	T-1011M	Hold	Note

No.	(kW)	(W/cm^2)	(m/s)	(°C)	(°C)	time	
1	6.38	2.78	0.017	.....	.....	.....	

11:40 HP-9845T start
12:04 YODAC scanning
T-003 = 373.7 °C, T-1011M = 725.9 °C, F-103 = 0.016 m/s
12:05 HP-9845T stop
12:06 FPL power down & off

Circulation & cooling opration

12:08 Pump off
12:08 Valve setting

VH-101	VA-102	VM-103	VH-104	VH-109	VH-110
100 %	open	100 %	100 %	100 %	100 %

12:10 Pump on (~150 l/min)
12:11 Re-setting of the preheater power controller
(changed from 450 ±25 °C to 250 ±25 °C)
13:00 Pump off
13:01 Valve setting

VH-101	VA-102	VM-103	VH-104	VH-109	VH-110
100 %	open	100 %	100 %	100 %	0 %

13:02 Pump on (~150 l/min)
13:02 FPL main air cooler on
13:38 FPL main air cooler off

Flow-meter & thermocouple calibration runs

Run 37(0)CAL-0-144-E (No. 188, #14421)

13:38 Pump off
13:40 Valve setting

VH-101	VA-102	VM-103	VH-104	VH-109	VH-110
100 %	close	0 %	0 %	0 %	100 %

13:42 HP-9845T start
13:45 HP-9845T stop
13:45 YODAC scanning
T-003 = 295.2 °C, T-1011M = 315.8 °C, F-103 = -0.008 m/s

Run 37(0)CAL-05-144-C (No. 189, #14422)

13:46 Valve setting

VH-101	VA-102	VM-103	VH-104	VH-109	VH-110
100 %	close	3 %	0 %	0 %	100 %

13:47 Pump on (~5 l/min)
13:47 HP-9845T start
13:55 HP-9845T start

13:55 YODAC scanning
T-003 = 295.0 °C, T-1011M = 313.0 °C, F-103 = 0.071 m/s

Heat balance check runs (continued)

Run 37(25)H-101 (No. 190, #14423)

13:58 FPL power on

Step No.	Power (kW)	Heat flux (W/cm^2)	F-103 (m/s)	T-003 (°C)	T-1011M (°C)	Hold time	Note
1	0.08	0.04	.....	.....	.....	5"	
2	6.89	3.00	0.079	293.4	.....	8'00"	

14:00 HP-9845T start
14:03 YODAC scanning
T-003 = 293.4 °C, T-1011M = 383.3 °C, F-103 = 0.078 m/s
14:04 HP-9845T stop

Run 37(25)H-102 (No. 191, #14424)

14:06 Pump power down (~3 l/min)

Step No.	Power (kW)	Heat flux (W/cm^2)	F-103 (m/s)	T-003 (°C)	T-1011M (°C)	Hold time	Note
1	6.54	2.85	0.048	290.7	.....	9'00"	

14:07 HP-9845T start
14:13 HP-9845T stop
14:13 YODAC scanning
T-003 = 290.7 °C, T-1011M = 414.1 °C, F-103 = 0.047 m/s

Run 37(25)H-103 (No. 192, #14425)

14:15 Pump power down (~1 l/min)

Step No.	Power (kW)	Heat flux (W/cm^2)	F-103 (m/s)	T-003 (°C)	T-1011M (°C)	Hold time	Note
1	6.30	2.74	0.022	289.8	.....	.....	

14:16 HP-9845T start
14:21 HP-9845T stop
14:21 YODAC scanning
T-003 = 289.8 °C, T-1011M = 484.5 °C, F-103 = 0.016 m/s
14:23 FPL power down & off

LOF controller test runs

14:28 Pump off
14:28 Valve setting

VH-101	VA-102	VM-103	VH-104	VH-109	VH-110
100 %	open	100 %	0 %	100 %	100 %

14:29 Pump on (~40 l/min)

: :
: :

15:25 Pump off

Circulation & mixing operation

15:30 Valve setting

VH-101	VA-102	VM-103	VH-104	VH-109	VH-110
100 %	open	100 %	100 %	100 %	100 %

15:40 Pump on (~150 l/min)

16:21 Pump off
16:26 Sodium drain

19:10 Preheater power off

Record of the 145th operation

1980.4.8

8:30 Preheater power on
(aiming temperature level = 250 ±25 °C)

14:37 Sodium charge
(sodium level = EL-9100 mm)

Circulation & purification operation

15:20 Valve setting

VH-101	VA-102	VM-103	VH-104	VH-109	VH-110
100 %	open	100 %	100 %	100 %	100 %

15:23 Pump on (~150 l/min)

Circulation & heat-up operation

22:40 Auxiliary heater power on
(temperature level change from 250 ±25 °C to 450 ±25 °C)

1980.4.9

8:00 Re-setting of the preheater power controller
(changed from 250 ±25 °C to 450 ±25 °C)
9:00 Operation check of the gas injection system
9:45 Auxiliary heater power off

Gas release test operation

9:45 Pump off
9:46 Valve setting

VH-101	VA-102	VM-103	VH-104	VH-109	VH-110
100 %	close	3 %	0 %	0 %	6.25 %

9:48 VA-150 open
(gas injection from inlet piping)
Gas plenum pressure = ... MPa, F-103 = ... m/s
Gas release rate = ... g/s (steady)
10:20 VA-150 close
(stop gas injection)
10:22 ETK gas purge from VA-207 & VA-208 valves

Flow-meter & thermocouple calibration runs

Run 37(0)CAL-05-145-A (No. 193, #14501)

10:54 Pump on (~3 l/min)
10:59 YODAC scanning
T-003 = 430.9 °C, T-1011M = 410.8 °C, F-103 = 0.063 m/s
11:00 HP-2116C start
11:01 HP-2116C stop

Run 37(0)CAL-0-145-A (No. 194, #14502)

11:02 HP-9845T start
11:07 Pump off
11:07 Valve setting

VH-101	VA-102	VM-103	VH-104	VH-109	VH-110
100 %	close	0 %	0 %	0 %	6.25 %

11:08 YODAC scanning
T-003 = 397.4 °C, T-1011M = 410.9 °C, F-103 = 0.000 m/s
11:09 HP-2116C start
11:10 HP-9845T stop
11:10 HP-2116C stop

Low-heat-flux boiling runs; series (3)
(examination of the effect of gas release on the coolability)

Run 37(26)LHF-260 (power increase and flow decrease method; No. 195, #14503)

11:21 Valve setting

VH-101	VA-102	VM-103	VH-104	VH-109	VH-110
100 %	close	2.5 %	0 %	0 %	6.25 %

11:22 Pump on (~2 l/min)
11:24 SBL & FPL power on

Step No.	Power (kW) Total	Heat flux (W/cm^2) FPL/SBL	F-103 (m/s)	T-003 (°C)	T-1011M (°C)	Hold time	Note
1	0.10	0.05/ 0.03	.....	.....	.....	30"	
2	4.88	2.10/ 1.71	0.024	.....	.....	2'30"	

11:26 HP-9845T start
11:27 SBL & FPL power up

3	10.60	4.51/ 4.02	0.023	394.2	.....	23'00"	

11:38 HP-9845T stop
11:38 YODAC scanning
T-003 = 394.2 °C, T-1011M = 730.7 °C, F-103 = 0.024 m/s
11:49 HP-2116C start
11:49 HP-9845T start
11:50 SBL & FPL power up

4	19.02	7.97/ 7.90	0.023	.....	.....	1'27"	
5	26.79	11.20/11.29	0.025	.....	.....	1'40"	IB
6	33.19	13.92/13.75	0.032	.....	.....	2'00"	B
7	39.45	16.53/16.41	0.035	.....	.....	1'40"	B

11:57 VA-150 open
(start of gas injection from inlet piping)
Gas plenum pressure = ... MPa
Gas release rate = ... g/s

8	39.70	16.63/16.51	0.035	.....	.....	3'00"	B

12:00 Increase gas pressure
Gas plenum pressure = ... MPa
Gas release rate = ... g/s

9	38.83	16.27/16.15	0.031	.....	.....	3'00"	B

12:03 Increase gas pressure
Gas plenum pressure = ... MPa
Gas release rate = ... g/s

10	39.37	16.50/16.38	0.031	.....	.....	3'00"	B

P-201 = 0.0991 MPa, T_{sat} = ... °C

12:06 SBL & FPL power down & off
12:07 HP-2116C stop
12:07 HP-9845T stop
12:08 VA-150 close
(stop gas injection)

Circulation & mixing operation

12:10 Pump off
12:10 Valve setting

VH-101	VA-102	VM-103	VH-104	VH-109	VH-110
100 %	open	100 %	100 %	100 %	100 %

12:15 Pump on (~150 l/min)
12:15 Auxiliary heater power on
13:00 Auxiliary heater power off

Flow-meter calibration run

Run 37(0)CAL-0-145-B (No. ..., #.....)

13:11 HP-9845T start
13:13 Pump off
13:13 Valve setting

VH-101	VA-102	VM-103	VH-104	VH-109	VH-110
100 %	close	0 %	0 %	0 %	6.25 %

13:15 HP-9845T stop

Low-heat-flux boiling runs; series (3) (continued)

Run 37(26)LHF-261 (power increase method; No. 196, #14504)

13:16 Valve setting

VH-101	VA-102	VM-103	VH-104	VH-109	VH-110
100 %	close	1.5 %	0 %	0 %	6.25 %

13:17 Pump on (~3 l/min)
13:19 HP-9845T start
13:19 Pump off
(confirmation of zero-flow offset of F-103)
13:23 Pump on (~1 l/min)
13:30 SBL & FPL power on

Step No.	Power (kW) Total	Heat flux (W/cm^2) FPL/SBL	F-103 (m/s)	T-003 (°C)	T-1011M (°C)	Hold time	Note
1	0.08	0.03/ 0.02	0.010	.....	.....	0"	
2	9.14	3.81/ 3.89	0.009	.....	.....	14'00"	

13:40 HP-9845T stop
13:42 YODAC scanning
T-003 = 479.6 °C, T-1011M = 812.0 °C, F-103 = 0.039 m/s
13:43 HP-9845T start
13:43 HP-2116C start
13:44 SBL & FPL power up

3	18.24	7.63/ 7.64	0.010	.....	.....	1'12"	IB
4	28.53	12.00/11.62	0.014	.....	.....	1'44"	B
5	37.45	15.74/15.33	0.015	.....	.....	1'42"	B(D)
6	38.37	15.74/17.83	"	.....	.....	6"	B(D)

P-201 = 0.0991 MPa, T_{sat} = ... °C

13:49 High temperature alarm with no auto-scram
(trigger signal = T-311M)
13:49 SBL & FPL power manual-scram
13:51 HP-2116C stop
13:53 HP-9845T stop
: Pin failures are found (#416 & #417 pins)
: Separation of failed pins from power supplies

Run 37(24)LHF-262 (power increase and flow reduction method; No. 197, #14505)

14:26 Pump off
14:27 Valve setting

VH-101	VA-102	VM-103	VH-104	VH-109	VH-110
100 %	close	2 %	0 %	0 %	6.25 %

14:27 Pump on (~1 l/min)
14:28 HP-9845T start
14:31 SBL & FPL power on

Step No.	Power (kW) Total	Heat flux (W/cm^2) FPL/SBL	F-103 (m/s)	T-003 (°C)	T-1011M (°C)	Hold time	Note

1	0.08	0.04/ 0.03	0.027	.....	.....	1'02"	
2	4.57	2.12/ 1.55	0.018	.....	.....	2'08"	
3	7.69	3.49/ 3.41	0.014	.....	.....	15'30"	

14:47 HP-9845T stop
14:49 YODAC scanning
T-003 = 429.9 °C, T-1011M = 761.6 °C, F-103 = 0.024 m/s
14:49 HP-2116C start
14:49 SBL & FPL power up

4	12.99	5.92/ 5.59	0.014	.....	.....	2'04"	IB

14:50 HP-9845T start
14:51 SBL & FPL power up

5	18.95	8.59/ 8.68	0.014	.....	.....	1'34"	B
6	25.06	11.38/11.23	0.015	.....	.....	2'07"	B
7	29.79	13.52/13.44	0.014	.....	.....	1'33"	B

14:57 VA-150 open
(start of gas injection from inlet piping)
Gas plenum pressure = ... MPa
Gas release rate = ... g/s

8	29.79	13.52/13.44	0.012	.....	.....	3'10"	B

15:00 Pump power down

9	28.80	13.07/12.99	0.009	.....	.....	2'07"	B(D)
10	28.36	12.90/12.45	0.004	.....	.....	2'04"	B(D)
11	27.91	12.70/12.25	0.001	.....	.....	25"	B(D)

P-201 = 0.0991 MPa, T_{sat} = ... °C

15:04 SBL & FPL power auto-scram ..... high temperature
(trigger signal = T-305M)
15:05 Pump power up (~4 l/min)
15:05 VA-150 close
(stop gas injection)
15:05 HP-9845T stop
15:07 HP-2116C stop
: Pin failures are found (#203 & #305, #407 & #408)
: Separation of failed pins from power suppliers

Run 37(20)LHF-263 (power increase and flow reduction method; No. 198, #14506)

16:05 Pump power adjust (~1 l/min)
16:05 HP-9845T start
16:07 FPL power on (no pin is connected to the SBL power supply)

Step No.	Power (kW)	Heat flux (W/cm^2)	F-103 (m/s)	T-003 (°C)	T-1011M (°C)	Hold time	Note
1	0.07	0.04	0.018	.....	.....	.....	
2	7.53	4.09	0.012	.....	.....	9'27"	
16:16:45 3	9.18	5.00	0.012	.....	.....	25'52"	

16:29 HP-9845T stop
16:30 YODAC scanning
T-003 = 390.2 °C, T-1011M = 826.0 °C, F-103 = 0.016 m/s
16:40 HP-9845T start
16:41 HP-2116C start
16:42 FPL power up

4	16.34	8.89	0.025	.....	.....	46"	
5	20.88	11.36	0.019	.....	.....	1'56"	
6	24.95	13.57	0.016	.....	.....	1'37"	IB
7	30.55	16.62	0.028	.....	.....	2'18"	B

16:49 VA-150 open
(start of gas injection from inlet piping)
Gas plenum pressure = ... MPa
Gas release rate = ... g/s

8	30.73	16.72	0.035	.....	.....	1'35"	B

16:50 Pump power down

9	29.91	16.28	0.016	.....	.....	1'55"	B
10	29.34	15.96	0.010	.....	.....	1'32"	B
11	28.97	15.76	0.008	.....	.....	1'34"	B
12	28.52	15.52	0.005	.....	.....	1'14"	B(D)

P-201 = 0.0991 MPa, T_{sat} = ... °C

16:57 FPL power auto-scram ..... high temperature
(trigger signal = T-2022M)
16:58 HP-9845T stop
16:59 Pump power up (~4 l/min)
17:00 Pump power up (~10 l/min)
17:01 HP-2116C stop
17:02 VA-150 close
(stop gas injection)

Circulation & purification operation

17:09 Pump off
17:10 Valve setting

VH-101	VA-102	VM-103	VH-104	VH-109	VH-110
100 %	open	100 %	100 %	100 %	100 %

17:13 Pump on (~150 l/min)
17:14 Re-setting of the preheater power controller
(changed from 450 ±25 °C to 250 ±25 °C)

LOF controller check runs

19:15 Pump off
: :
: :
20:38 Pump on (~150 l/min)

1980.4.10

Circulation & heat-up operation

0:00 Auxiliary heater power on
6:05 Re-setting of the preheater power controller
(changed from 250 ±25 °C to 450 ±25 °C)
8:50 Auxiliary heater power off

Thermocouple calibration run

Run 37(0)CAL-0260-145 (No. 199, #14507)

9:16 Pump off
9:17 Valve setting

VH-101	VA-102	VM-103	VH-104	VH-109	VH-110
100 %	close	100 %	100 %	0 %	0 %

9:19 Pump on (~260 l/min)
9:21 YODAC scanning
T-003 = 498.0 °C, T-1011M = 497.6 °C, F-103 = 4.476 m/s
9:22 HP-2116C start
9:23 HP-2116C stop

LOF controller check runs

Run 37(0)FC-100 (No. ..., #.....)

9:23 Presetting of the pump controller (~280 l/min)
9:24 Test of pump power decay ($V = V_0 e^{-t/7}$, IVR = 4 s)
9:26 Pump power adjust (~260 l/min)

Run 37(0)FC-101 (No. ..., #.....)

9:30 Presetting of the pump controller (~280 l/min)
9:31 Test of pump power decay ($V = V_0 e^{-t/7}$, IVR = 10 s)
9:32 Pump power adjust (~260 l/min)

LOF boiling runs

Run 37(20)FC-102 (No. 200, #14508)

9:35 FPL power on

Step No.	Power (kW)	Heat flux (W/cm^2)	F-103 (m/s)	T-003 (°C)	T-1011M (°C)	Hold time	Note
1	0.06	0.03					
2	9.76	5.31					
3	18.44	10.03					
4	0	0					
5	18.30	9.96					
6	33.95	18.47					
7	45.48	24.75					
8	71.57	38.94					
9	92.22	50.18					
10	127.32	69.27					
11	154.26	83.93					
12	176.00	95.76					
13	185.75	101.07					
14	191.75	104.33		464	520		
15	198.99	108.27					

9:42 FPL power auto-scram ..... over current
9:43 Change of the trigger current level
9:48 FPL power on

Presetting of the pump power controller (~260 l/min)
10:23 YODAC scanning
T-003 = 458.7 °C, T-1011M = 506.5 °C, F-103 = 4.761 m/s
10:24 HP-2116C start
10:25 Start of pump power decay ($V = V_0 e^{-t/7}$, IVR = 4 s)

16							IB

P-201 = 0.1059 MPa, T_{sat} = °C, ΔT_{SH} = °C
10:26 FPL power down and off
10:27 HP-2116C stop

Run 37(20)FC-103 (No. 201, #14509)

10:30 Pump power on (~260 l/min)
10:39 FPL power on

Step No.	Power (kW)	Heat flux (W/cm^2)	F-103 (m/s)	T-003 (°C)	T-1011M (°C)	Hold time	Note
1	0.07	0.04					
2	38.86	21.15					
3	74.01	40.27					
4	110.26	59.99					
5	143.50	78.08					
6	178.19	96.95					
7	191.44	104.16					

Presetting of the pump power controller (~280 l/min)
11:02 YODAC scanning
T-003 = 473.0 °C, T-1011M = 527.9 °C, F-103 = 4.980 m/s
11:02 HP-9845T start
11:02 HP-2116C start
11:02 Start of pump power decay ($V = V_0 e^{-t/3}$, IVR = 4 s)

8							IB

P-201 = MPa, T_{sat} = °C, ΔT_{SH} = °C
11:04 FPL power down and off
11:04 HP-9845T stop
11:05 HP-2116C stop

Run 37(20)FC-104 (No. 202, #14510)

11:07 Pump power on (~260 l/min)
11:10 FPL power on

Step No.	Power (kW)	Heat flux (W/cm^2)	F-103 (m/s)	T-003 (°C)	T-1011M (°C)	Hold time	Note
1	0.06	0.04					
2	37.86	20.60					
3	74.04	40.29					
4	109.04	59.33					
5	145.99	79.43					
6	176.06	95.80					
7	192.76	104.88					

Presetting of the pump power controller (~280 l/min)
11:25 YODAC scanning
T-003 = 486.2 °C, T-1011M = 543.3 °C, F-103 = 5.027 m/s
11:25 HP-9845T start
11:25 HP-2116C start
11:25 Start of pump power decay ($V = V_0 e^{-t/10}$, IVR = 4 s)

8						IB

P-201 = MPa, T_{sat} = °C, ΔT_{SH} = °C
11:28 FPL power down and off
11:28 HP-9845T stop
11:29 HP-2116C stop

Run 37(20)FC-105 (No. 203, #14511)

11:30 Pump power on (~260 l/min)
11:31 FPL power on

Step No.	Power (kW)	Heat flux (W/cm^2)	F-103 (m/s)	T-003 (°C)	T-1011M (°C)	Hold time	Note
1	0.06	0.03					
2	36.99	20.13					
3	66.35	36.10					
4	107.36	58.41					
5	139.81	76.07					
6	173.69	94.50					
7	198.65	108.09					

Presetting of the pump power controller (~280 l/min)
11:47 YODAC scanning
T-003 = 474.6 °C, T-1011M = 516.1 °C, F-103 = 4.902 m/s
11:48 HP-9845T start
11:48 HP-2116C start
11:49 Start of pump power decay ($V = V_0 e^{-t/5}$, IVR = 4 s)

8						IB

P-201 = MPa, T_{sat} = °C, ΔT_{SH} = °C
11:51 FPL power down and off
11:52 HP-9845T stop
11:52 HP-2116C stop

Circulation & mixing operation

11:54 Pump off
11:55 Valve setting

VH-101	VA-102	VM-103	VH-104	VH-109	VH-110
100 %	open	100 %	100 %	100 %	100 %

11:56 Pump on (~150 l/min)
11:56 Auxiliary heater power on
13:03 Auxiliary heater power off

LOF boiling runs (continued)

Run 37(20)FC-106 (No. 204, #14512)

13:04 Pump power up (~260 l/min)
13:05 FPL power on

Step No.	Power (kW)	Heat flux (W/cm^2)	F-103 (m/s)	T-003 (°C)	T-1011M (°C)	Hold time	Note
1	0.06	0.03					
2	33.24	18.09					
3	63.51	34.55					
4	102.42	55.73					
5	144.29	78.51					
6	179.40	97.61					
7	190.39	103.59					

Presetting of the pump power controller (~280 l/min)
13:24 YODAC scanning
T-003 = 495.5 °C, T-1011M = 552.7 °C, F-103 = 4.855 m/s
13:26 HP-9845T start
13:26 HP-2116C start
13:26 Start of pump power decay ($V = V_0 e^{-t/20}$, IVR = 4 s)

8						IB

P-201 = MPa, T_{sat} = °C, ΔT_{SH} = °C
13:28 FPL power down and off
13:29 HP-9845T stop
13:30 HP-2116C stop

Run 37(20)FC-107 (No. 205, #14513)

13:32 Pump power up (~260 l/min)
13:42 FPL power on

Step No.	Power (kW)	Heat flux (W/cm^2)	F-103 (m/s)	T-003 (°C)	T-1011M (°C)	Hold time	Note
1	0.06	0.03					
2	35.74	19.44					
3	65.81	35.81					
4	106.00	57.68					
5	149.67	81.43					

6	179.73	97.79					
7	214.00	116.44					
8	249.47	135.74					
9	275.38	149.84					
10	288.93	157.21					

Presetting of the pump power controller (~280 l/min)
13:59 YODAC scanning
T-003 = 475.0 °C, T-1011M = 559.0 °C, F-103 = 4.980 m/s
14:00 HP-9845T start
14:00 HP-2116C start
14:00 Start of pump power decay ($V = V_0 e^{-t/7}$, IVR = 4 s)

11							IB

P-201 = MPa, T_{sat} = °C, ΔT_{SH} = °C
14:01 FPL power auto-scram ..... high temperature
(trigger signals = T-2022M & T-201M)
14:02 HP-9845T stop
14:02 HP-2116C stop
: Pin failures are found (#202 & #303, #302 & #403 pins)
: Separation of failed pins from power supply

Run 37(16)FC-108 (No. 206, #14514)

14:05 Pump power up (~260 l/min)
14:42 FPL power on

Step No.	Power (kW)	Heat flux (W/cm^2)	F-103 (m/s)	T-003 (°C)	T-1011M (°C)	Hold time	Note
1	0.05	0.04					
2	33.57	22.83					
3	60.52	41.16					
4	89.74	61.03					
5	123.67	84.11					
6	149.59	101.73					
7	178.03	121.08					
8	205.73	139.92					
9	229.70	156.22					

Presetting of the pump power controller (~280 l/min)
15:01 YODAC scanning
T-003 = 478.6 °C, T-1011M = 566.5 °C, F-103 = 4.957 m/s
15:03 HP-9845T start
15:03 HP-2116C start
15:03 Start of pump power decay ($V = V_0 e^{-t/3}$, IVR = 4 s)

10							

P-201 = MPa, T_{sat} = °C, ΔT_{SH} = °C
15:05 FPL power down and off
15:06 HP-9845T stop
15:06 HP-2116C stop

Run 37(16)FC-109 (No. 207, #14515)

15:10 Pump power up (~260 l/min)
15:14 FPL power on

Step No.	Power (kW)	Heat flux (W/cm^2)	F-103 (m/s)	T-003 (°C)	T-1011M (°C)	Hold time	Note
1	0.05	0.03					
2	32.66	22.21					
3	55.90	38.02					
4	82.70	56.24					
5	109.26	74.31					
6	135.14	91.91					
7	174.08	118.39					
8	204.33	138.97					
9	230.37	156.67					

Presetting of the pump power controller (~280 l/min)
15:27 YODAC scanning
T-003 = 485.1 °C, T-1011M = 561.0 °C, F-103 = 4.871 m/s
15:28 HP-9845T start
15:28 HP-2116C start
15:29 Start of pump power decay ($V = V_0 e^{-t/20}$)

10							

P-201 = MPa, T_{sat} = °C, ΔT_{SH} = °C
15:32 FPL power down and off
15:33 HP-9845T stop
15:33 HP-2116C stop
15:34 Pump off

Circulation & mixing operation

15:36 Pump on (~150 l/min)
17:05 Pump off
17:07 Valve setting

VH-101	VA-102	VM-103	VH-104	VH-109	VH-110
100 %	open	100 %	100 %	100 %	100 %

17:11 Pump on (~150 l/min)

17:43 Pump off
17:49 Sodium drain

19:10 Preheater power off

Record of the 146th operation

1980.5.7

8:25 Preheater power on
(aiming temperature level = 250 ±25 °C)

14:30 Sodium charge
(sodium level = EL-9100 mm)

Circulation & purification operation

15:29 Valve setting

VH-101	VA-102	VM-103	VH-104	VH-109	VH-110
100 %	open	100 %	100 %	100 %	100 %

15:35 Pump on (~150 l/min)

Circulation & heat-up operation

22:39 Auxiliary heater power on
22:45 Re-setting of the preheater power controller
(changed from 250 ±25 °C to 450 ±25 °C)

1980.5.8

Flow-meter & thermocouple calibration runs

Run 37(0)CAL-0150-146-A (No. 208, #14601)

8:21 YODAC scanning
T-003 = 527.9 °C, T-1011M = 529.1 °C, F-103 = 0.573 m/s
: Occurrence of a trouble in MT device of HP-2116C system
10:00 Tentative recovery of the trouble

Run 37(0)CAL-0-146 (No. ..., #.....)

10:24 Pump off
10:24 Valve setting

VH-101	VA-102	VM-103	VH-104	VH-109	VH-110
100 %	close	0 %	100 %	0 %	0 %

10:25 HP-9845T start
10:28 HP-9845T stop

Run 37(0)CAL-0260-146 (No. 209, #14602)

10:29 Valve setting

VH-101	VA-102	VM-103	VH-104	VH-109	VH-110
100 %	close	100 %	100 %	0 %	0 %

10:30 Pump on (~260 l/min)
10:45 YODAC scanning
T-003 = ... °C, T-1011M = 500.4 °C, F-103 = 4.635 m/s
(T-003 is failed)

LOF boiling run, (continued)

Run 37(19)FC-110 (No. 210, #.....)

10:50 FPL power on

Step No.	Power (kW)	Heat flux (W/cm^2)	F-103 (m/s)	T-003 (°C)	T-1011M (°C)	Hold time	Note
1	0.05	0.03					
2	7.81	4.47					
3	16.14	9.24					
4	53.71	30.76					
5	88.88	50.91					
6	134.57	77.08					
7	180.23	103.23					
8	213.88	122.50					
9	256.86	147.12					
10	265.47	152.05					

Presetting of the pump power controller (~280 l/min)
11:28 YODAC scanning
T-003 = ... °C, T-1011M = 574.7 °C, F-103 = 4.619 m/s
11:29 FPL power auto-scram ..... high temperature, over current
(occurrence of a pin trouble)
: Pin failures are found (#101, #201 & #301, #205 & #309, #203, #311 & #418)
: Separation of failed pins from power supply

Circulation & mixing operation

11:45 Pump off
11:45 Valve setting

VH-101	VA-102	VM-103	VH-104	VH-109	VH-110
100 %	open	100 %	0 %	100 %	100 %

11:46 Pump on (~150 l/min)
11:46 Auxiliary heater power on
13:39 Auxiliary heater power off
13:39 Pump off
13:40 Valve setting

VH-101	VA-102	VM-103	VH-104	VH-109	VH-110
100 %	open	100 %	100 %	100 %	0 %

13:40 Pump on (~150 l/min)
13:40 Auxiliary heater power on
14:35 Auxiliary heater power off

LOF boiling run (continued)

Run 37(11)FC-111 (No. 211, #14603)

14:36 Pump off
14:38 Valve setting

VH-101	VA-102	VM-103	VH-104	VH-109	VH-110
100 %	close	100 %	100 %	0 %	0 %

14:40 Pump on (~260 l/min)
14:41 FPL power on

Step No.	Power (kW)	Heat flux (W/cm^2)	F-103 (m/s)	T-003 (°C)	T-1011M (°C)	Hold time	Note
1	0.03	0.02					
2	26.12	25.84					
3	49.39	48.86					
4	81.13	80.26					
5	98.46	97.40					
6	123.31	121.99					
7	147.32	145.74					
8	155.97	154.31					

Presetting of the pump power controller (~280 l/min)
14:59 YODAC scanning
T-003 = ... °C, T-1011M = 519.6 °C, F-103 = 4.737 m/s
15:01 HP-9845T start
15:01 HP-2116C start
15:02 Start of the pump power controller ($V = V_0 e^{-t/7}$, IVR = 4 s)

9							

15:02 Pump power off
15:02 Valve close (VM-103: 100 % → 0 %)

10							IB(D)

P-201 = MPa, T_{sat} = °C, ΔT_{SH} = °C
15:03 FPL power auto-scram ..... high temperature, over current
(trigger signals = T-2022M, T-3022M, T-308M, T-3031M & T-3091M)
15:04 HP-9845T stop
15:04 HP-2116C stop
: Pin failure are found (#303 & #403, #308 & #412)

Thermocouple calibration run

Run 37(0)CAL-0150-146-B (No. ..., #14604)

15:09 Valve open

VH-101	VA-102	VM-103	VH-104	VH-109	VH-110
100 %	close	100 %	100 %	0 %	0 %

15:10 Pump on (~150 l/min)
15:14 HP-2116C start
15:16 HP-2116C stop

Circulation & mixing operation

15:18 Pump off
15:18 Valve setting

VH-101	VA-102	VM-103	VH-104	VH-109	VH-110
100 %	open	100 %	100 %	100 %	100 %

15:20 Pump on (~150 l/min)

17:05 Pump off
17:15 Sodium drain

18:40 Preheater power off

Appendix G: Data of Individual Runs

In the following, the typical signals were plotted to see the differences of all low-heat-flux boiling runs.

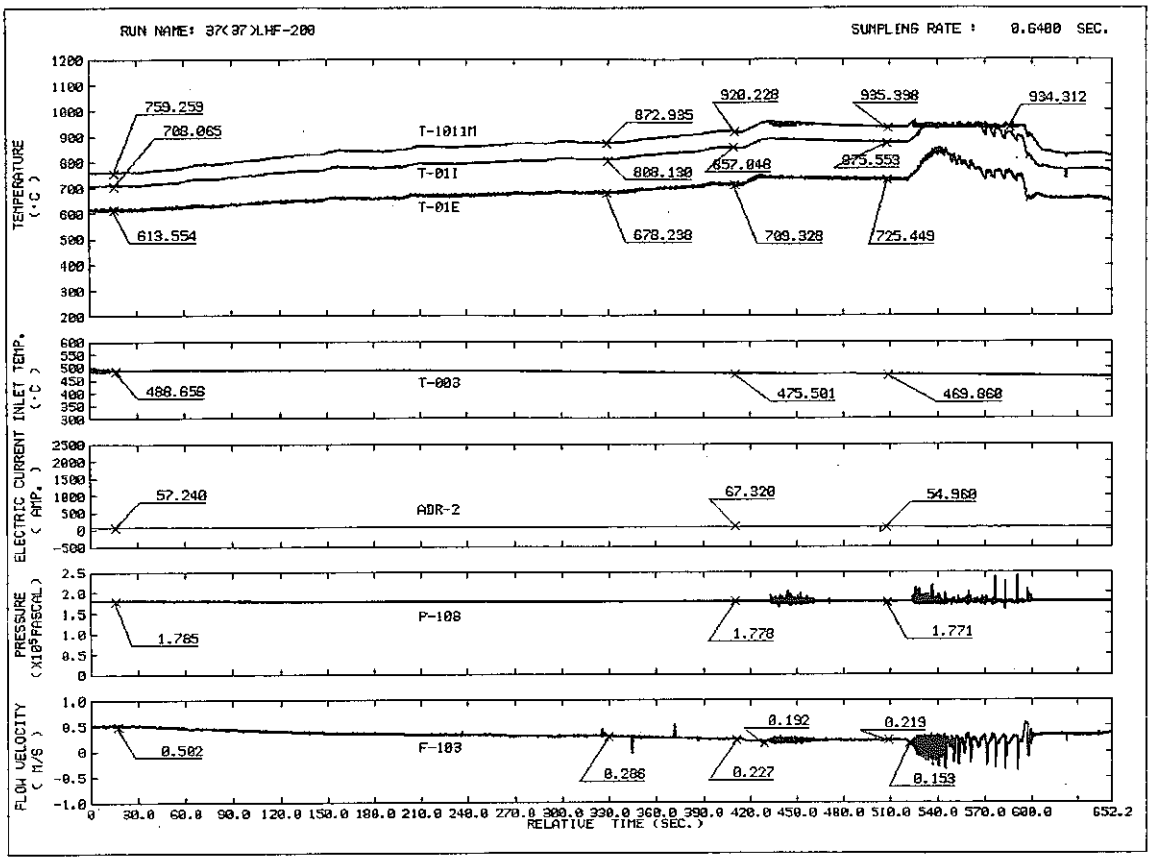
RUN NAME: 37(37)LHF-200
SAMPLING RATE : 0.6400 SEC.
TEMPERATURE (°C)
759.259
708.065
T-1011M
872.935
920.228
935.398
934.312
T-01I
808.130
857.048
875.559
T-01E
613.554
678.238
709.328
725.449
INLET TEMP. (°C)
488.658
T-003
475.501
469.868
ELECTRIC CURRENT (AMP.)
57.240
ADR-2
67.320
54.968
PRESSURE (X10⁵PASCAL)
1.765
P-108
1.778
1.771
FLOW VELOCITY (M/S)
0.502
F-103
0.192
0.219
0.286
0.227
0.153
RELATIVE TIME (SEC.)

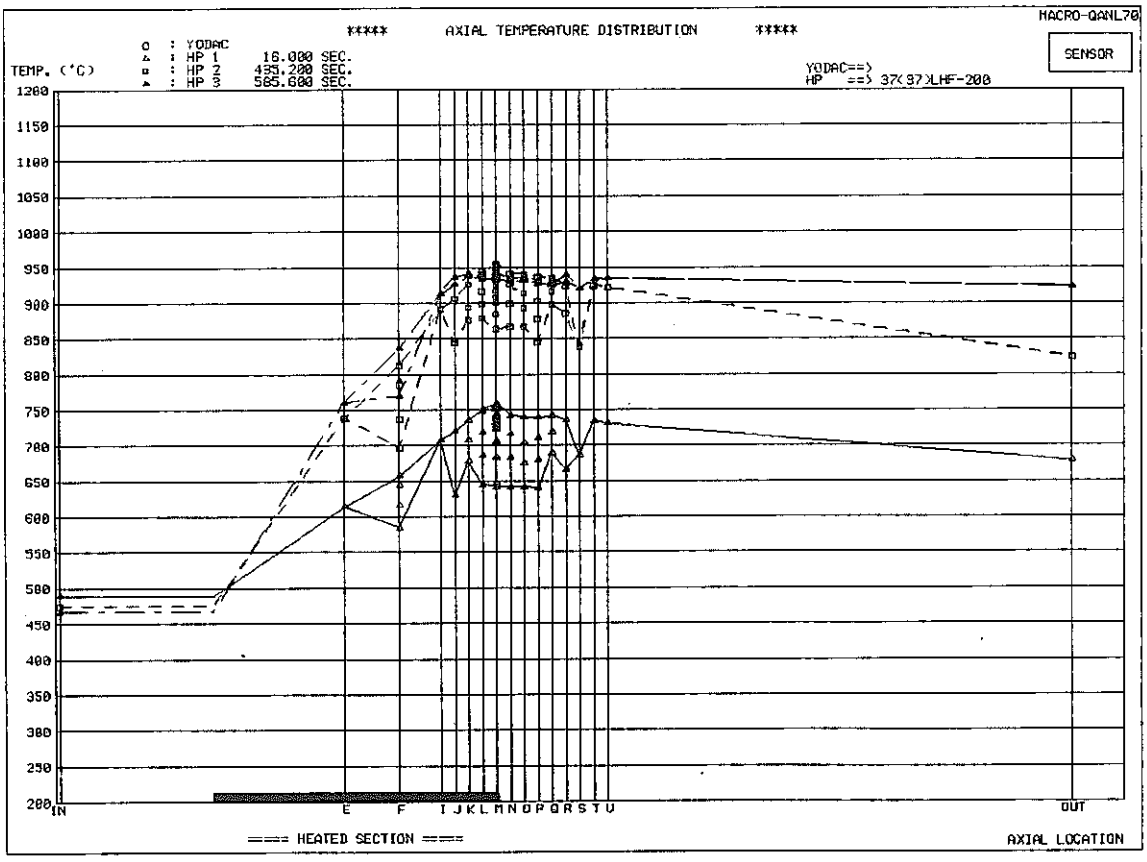
MACRO-QANL70
***** AXIAL TEMPERATURE DISTRIBUTION *****
SENSOR
○ : YODAC
△ : HP 1 16.000 SEC.
□ : HP 2 435.200 SEC.
▲ : HP 3 585.600 SEC.
TEMP. (°C)
YODAC==)
HP ==) 37(37)LHF-200
IN
E F I J K L M N O P Q R S T U
OUT
==== HEATED SECTION ====
AXIAL LOCATION

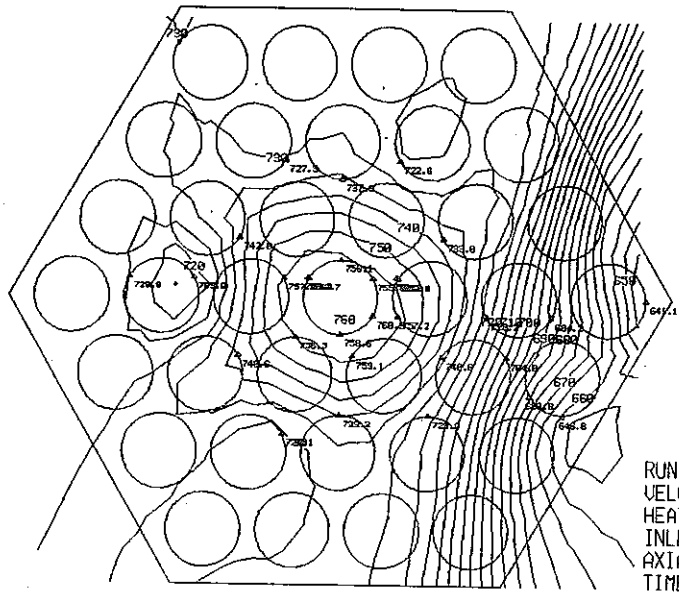

RUN NAME 37(37)LHF-200
VELOCITY 0.506 M/S
HEAT FLUX 21.63 W/CM2
INLET TEMP. 488.7 C
AXIAL 0.0 MM
TIME 16.000 SEC.

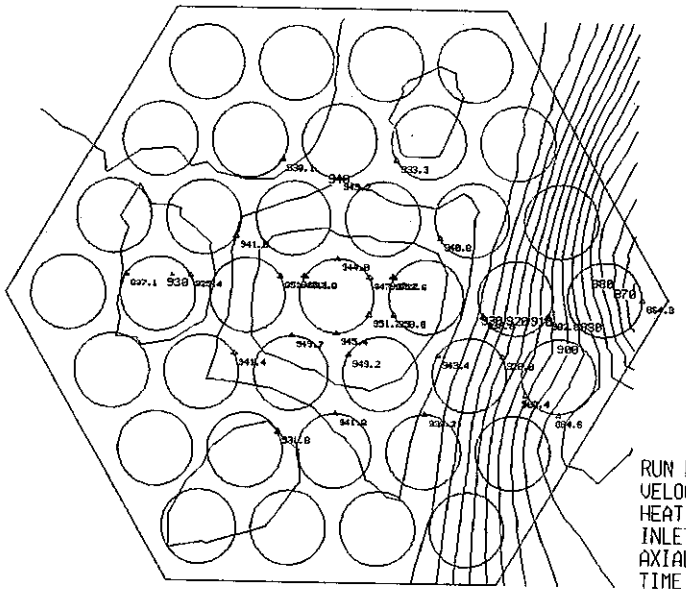

RUN NAME 37(37)LHF-200
VELOCITY 0.196 M/S
HEAT FLUX 21.63 W/CM2
INLET TEMP. 475.5 C
AXIAL 0.0 MM
TIME 435.200 SEC.

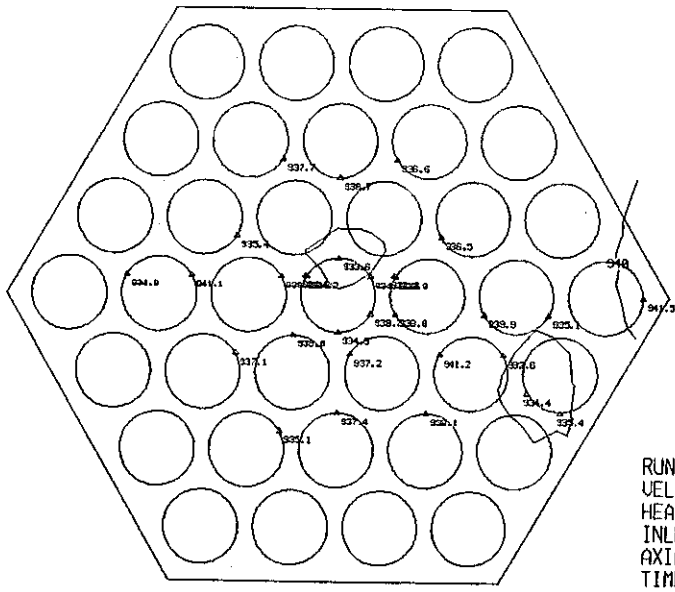

RUN NAME 37(37)LHF-200
VELOCITY 0.149 M/S
HEAT FLUX 21.63 W/CM2
INLET TEMP. 467.0 C
AXIAL 0.0 MM
TIME 585.600 SEC.

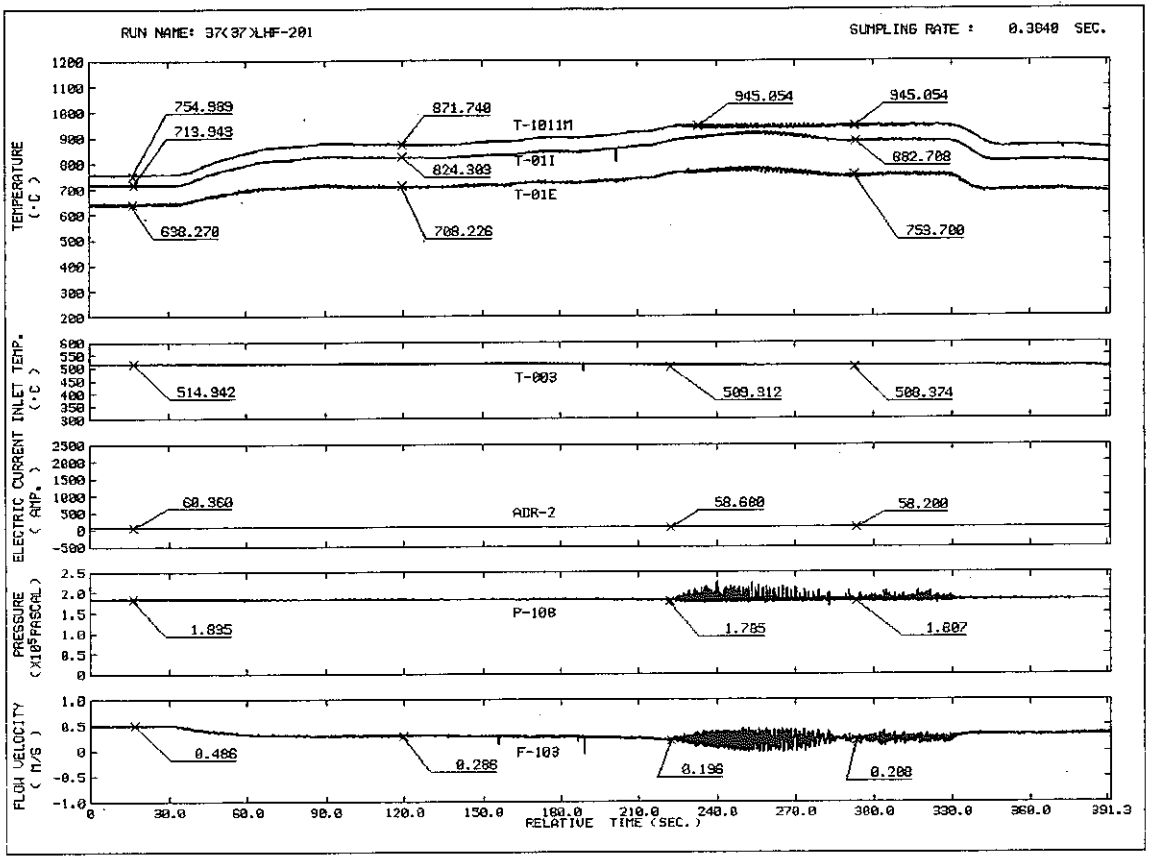
RUN NAME: 37(37)LHF-201
SUMPLING RATE : 0.3040 SEC.
TEMPERATURE ('C)
754.989
713.943
698.270
871.748
824.309
708.226
945.054
945.054
882.708
759.700
T-1011M
T-01I
T-01E
ELECTRIC CURRENT INLET TEMP. ('C) (AMP.)
514.942
509.912
508.374
T-003
PRESSURE (X10⁵PASCAL)
60.360
58.680
58.200
ADR-2
1.835
1.785
1.807
P-108
FLOW VELOCITY (M/S)
0.486
0.288
0.198
0.208
F-103
RELATIVE TIME (SEC.)

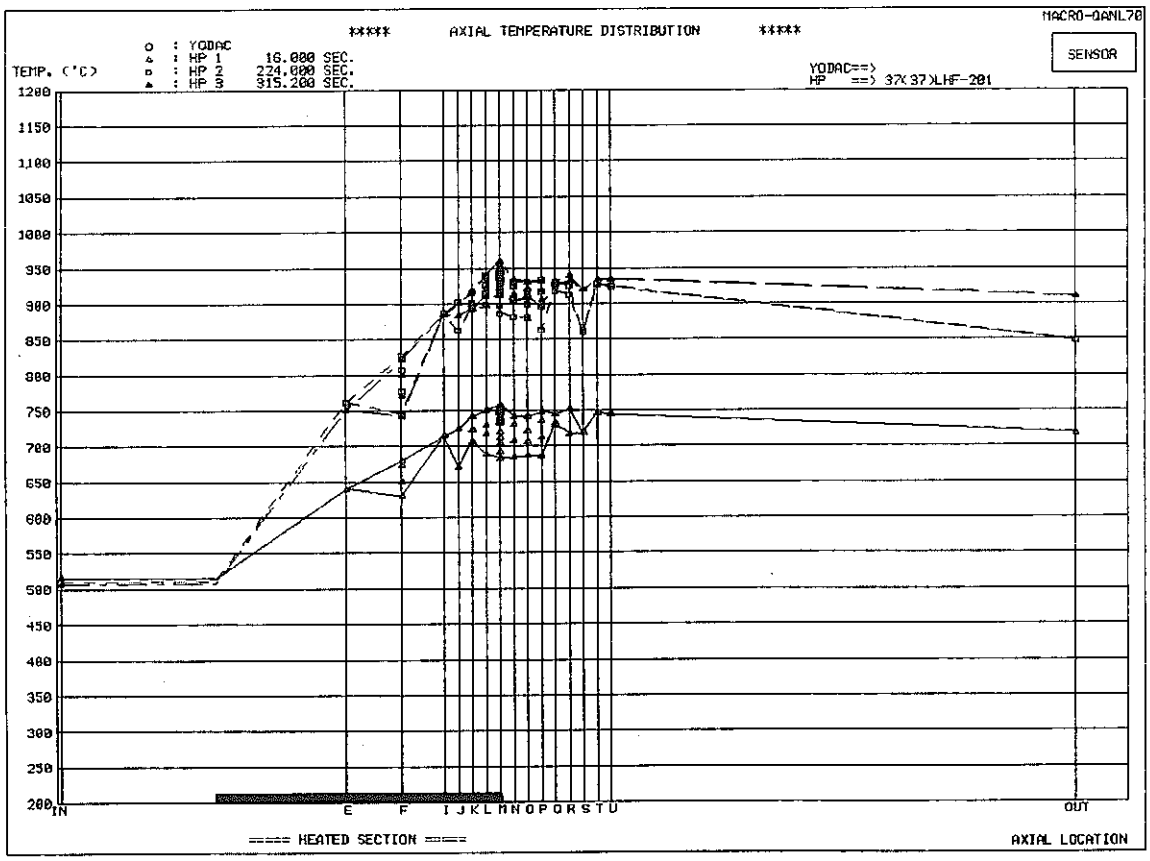
MACRO-QANL70
***** AXIAL TEMPERATURE DISTRIBUTION *****
SENSOR
o : YODAC
Δ : HP 1 16.000 SEC.
□ : HP 2 224.000 SEC.
▲ : HP 3 315.200 SEC.
TEMP. ('C)
YODAC==>
HP ==> 37(37)LHF-201
IN
E F I J K L M N O P Q R S T U
OUT
==== HEATED SECTION ====
AXIAL LOCATION

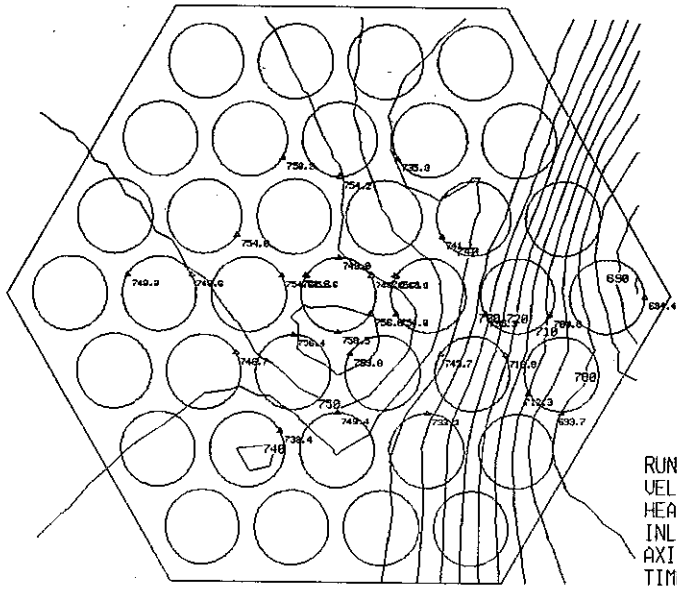

RUN NAME 37(37)LHF-201
VELOCITY 0.482 M/S
HEAT FLUX 21.26 W/CM2
INLET TEMP. 514.9 C
AXIAL 0.0 MM
TIME 16.000 SEC.

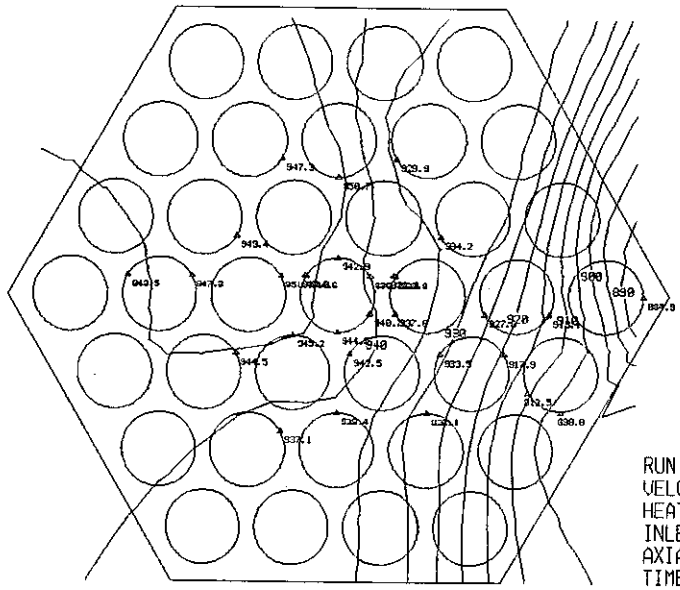

RUN NAME 37(37)LHF-201
VELOCITY 0.208 M/S
HEAT FLUX 21.26 W/CM2
INLET TEMP. 511.2 C
AXIAL 0.0 MM
TIME 224.000 SEC.

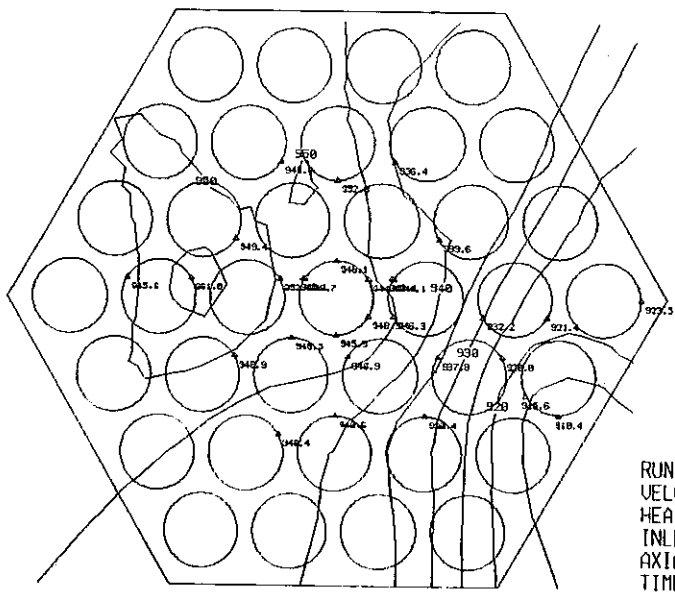

RUN NAME 37(37)LHF-201
VELOCITY 0.274 M/S
HEAT FLUX 21.26 W/CM2
INLET TEMP. 509.3 C
AXIAL 0.0 MM
TIME 315.200 SEC.

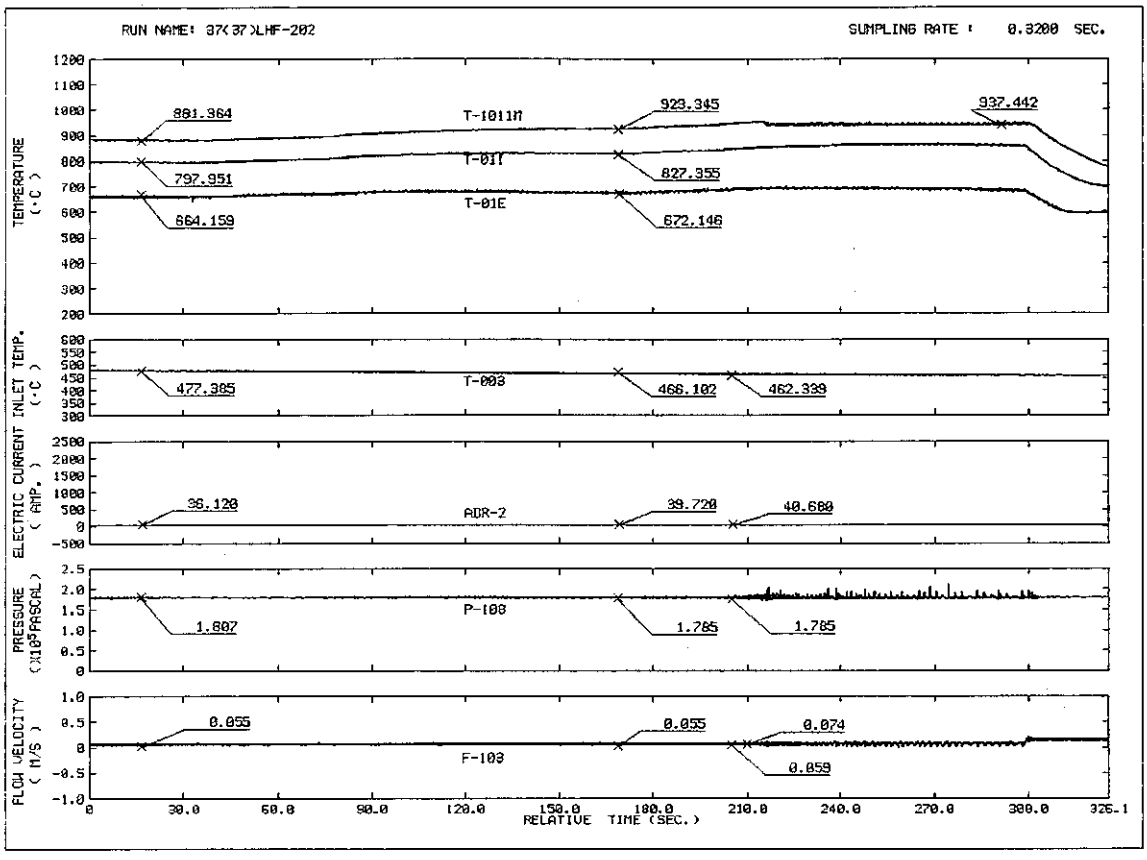
RUN NAME: 37<37>LHF-202
SUMPLING RATE : 0.3200 SEC.
TEMPERATURE (°C)
881.364
T-1011T
923.345
937.442
797.951
T-011T
827.355
664.159
T-01IE
672.146
ELECTRIC CURRENT INLET TEMP. (°C)
477.385
T-003
466.102
462.339
(AMP.)
38.120
ADR-2
39.720
40.680
PRESSURE (x10⁵PASCAL)
1.807
P-108
1.785
1.785
FLOW VELOCITY (M/S)
0.055
F-103
0.055
0.074
0.059
RELATIVE TIME (SEC.)

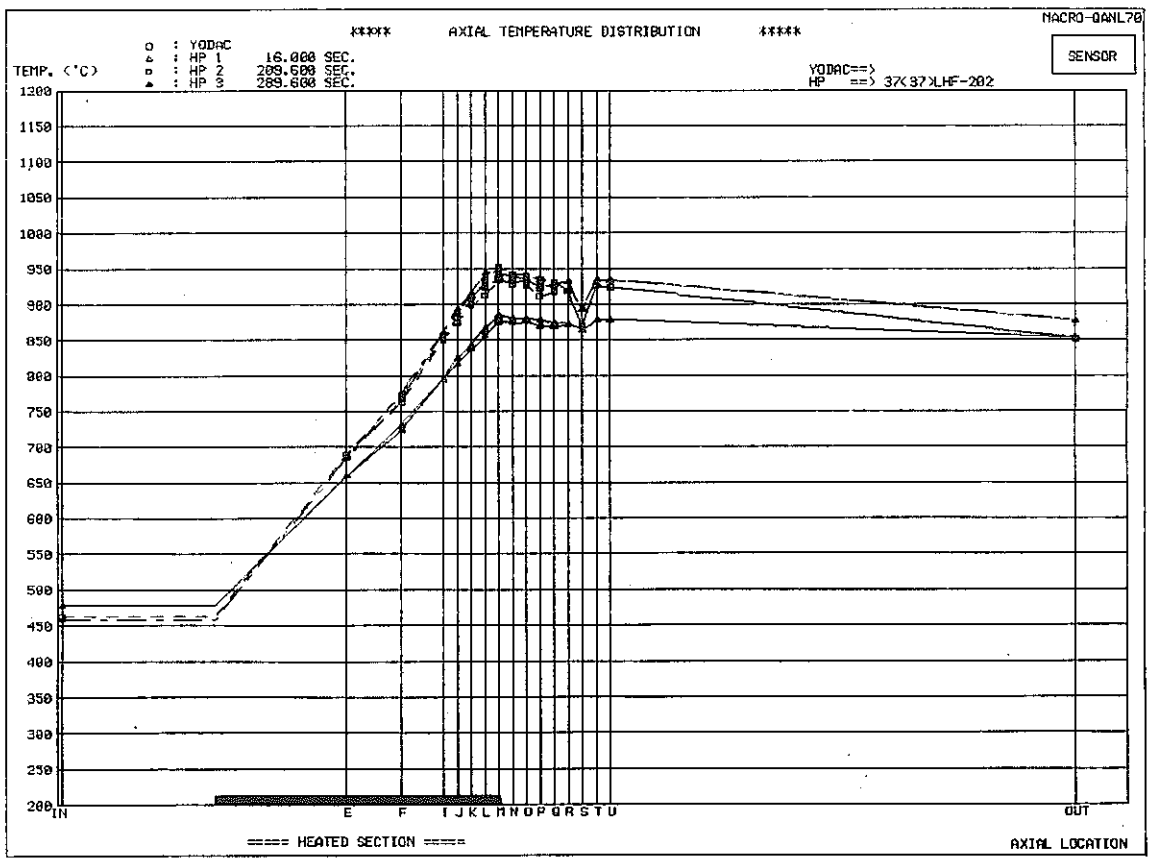
MACRO-QANL70
SENSOR
***** AXIAL TEMPERATURE DISTRIBUTION *****
○ : YODAC 16.000 SEC.
△ : HP 1 289.600 SEC.
□ : HP 2 289.600 SEC.
▲ : HP 3
TEMP. (°C)
YODAC==>
HP ==> 37<37>LHF-202
IN
E F I J K L M N O P Q R S T U
OUT
==== HEATED SECTION ====
AXIAL LOCATION

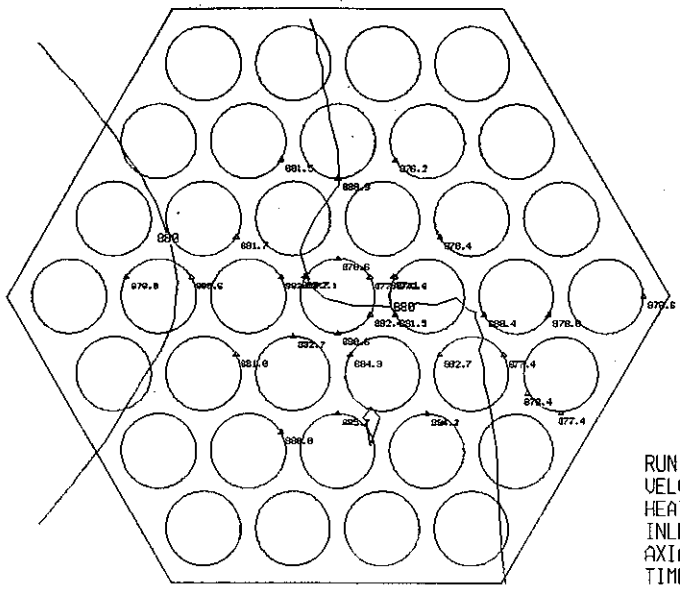

RUN NAME 37(37)LHF-202
VELOCITY 0.070 M/S
HEAT FLUX 5.03 W/CM2
INLET TEMP. 477.4 C
AXIAL 0.0 MM
TIME 16.000 SEC.

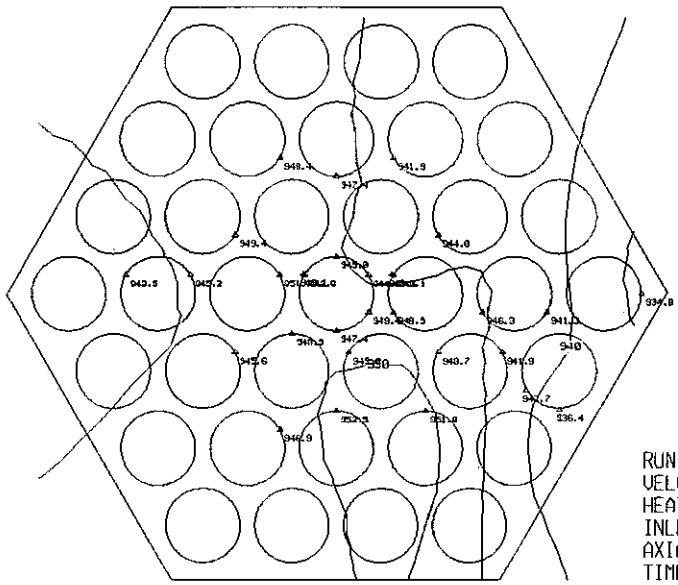

RUN NAME 37(37)LHF-202
VELOCITY 0.074 M/S
HEAT FLUX 6.49 W/CM2
INLET TEMP. 462.3 C
AXIAL 0.0 MM
TIME 209.600 SEC.

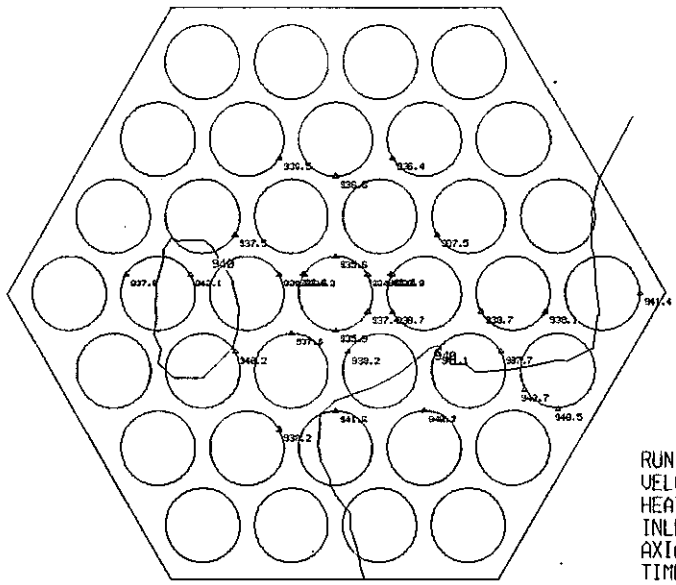

RUN NAME 37(37)LHF-202
VELOCITY 0.082 M/S
HEAT FLUX 6.49 W/CM2
INLET TEMP. 458.6 C
AXIAL 0.0 MM
TIME 209.600 SEC.

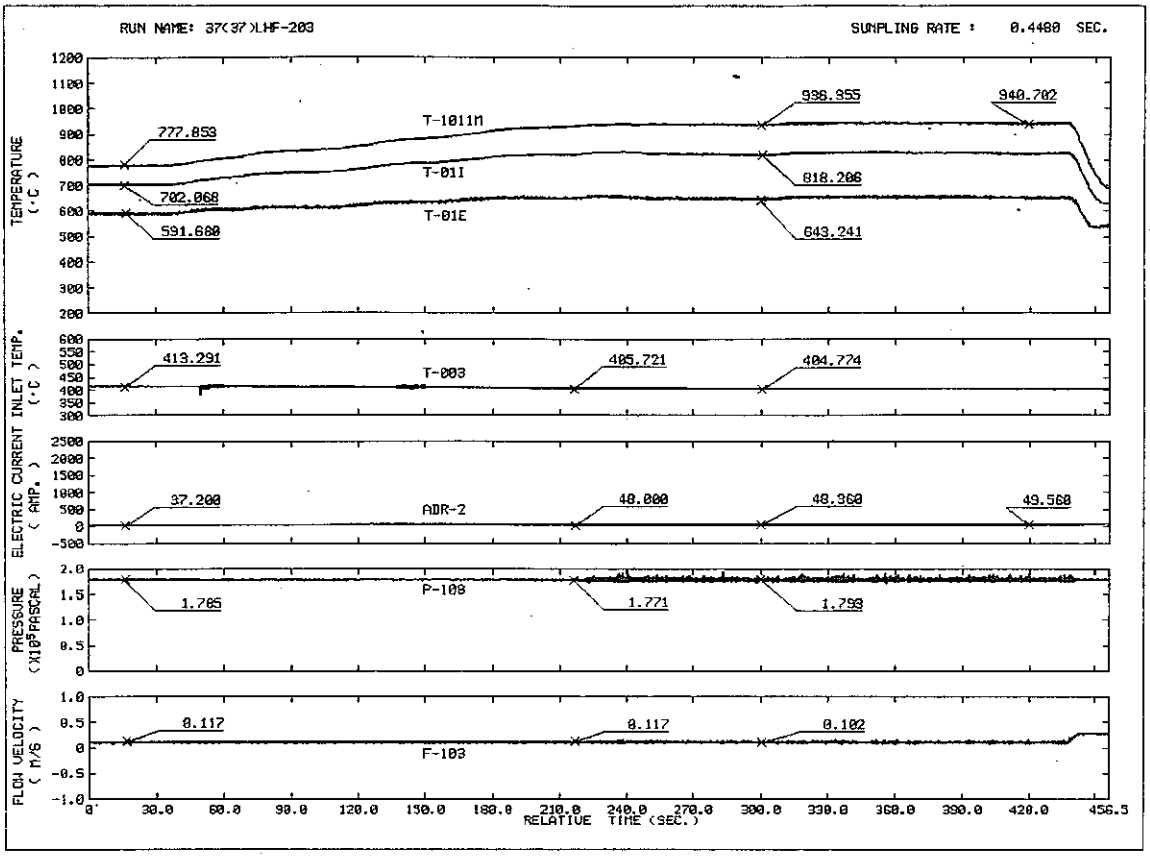
RUN NAME: 37(37)LHF-203
SAMPLING RATE : 0.4480 SEC.
TEMPERATURE (°C)
777.859
T-1011M
938.855
940.702
702.068
T-01I
818.208
591.680
T-01E
643.241
ELECTRIC CURRENT INLET TEMP. (°C)
413.291
T-003
405.721
404.774
(AMP.)
37.200
ADR-2
48.000
48.360
49.568
PRESSURE (X10⁵PASCAL)
1.765
P-108
1.771
1.793
FLOW VELOCITY (M/S)
0.117
0.117
0.102
F-103
RELATIVE TIME (SEC.)

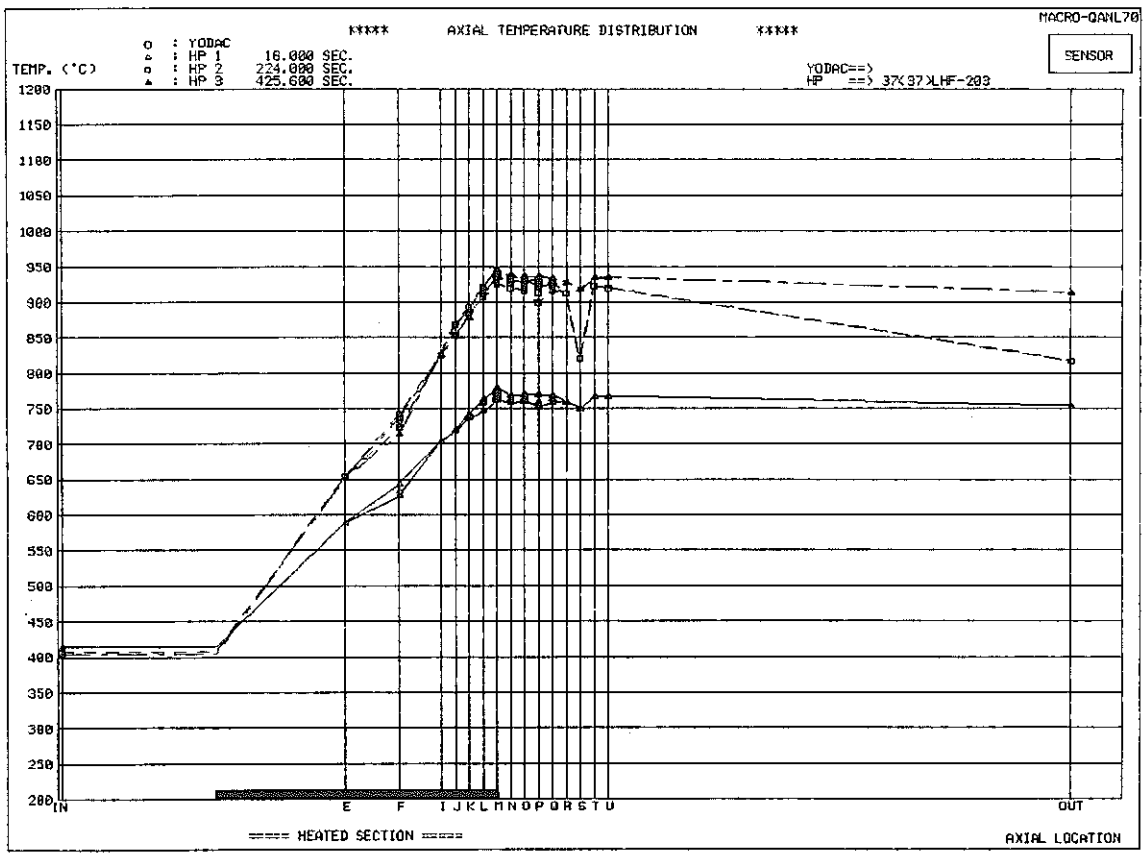
MACRO-QANL70
***** AXIAL TEMPERATURE DISTRIBUTION *****
SENSOR
o : YODAC
Δ : HP 1 16.000 SEC.
□ : HP 2 224.000 SEC.
▲ : HP 3 425.600 SEC.
TEMP. (°C)
YODAC==>
HP ==> 37(37)LHF-203
IN
E F I J K L M N O P Q R S T U
OUT
==== HEATED SECTION ====
AXIAL LOCATION

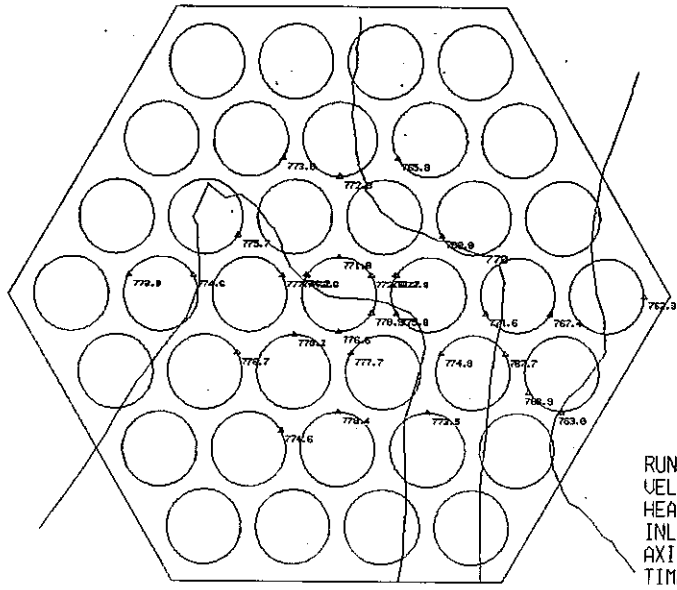

RUN NAME 37(37)LHF-203
VELOCITY 0.098 M/S
HEAT FLUX 7.02 W/CM2
INLET TEMP. 415.2 C
AXIAL 0.0 MM
TIME 16.000 SEC.

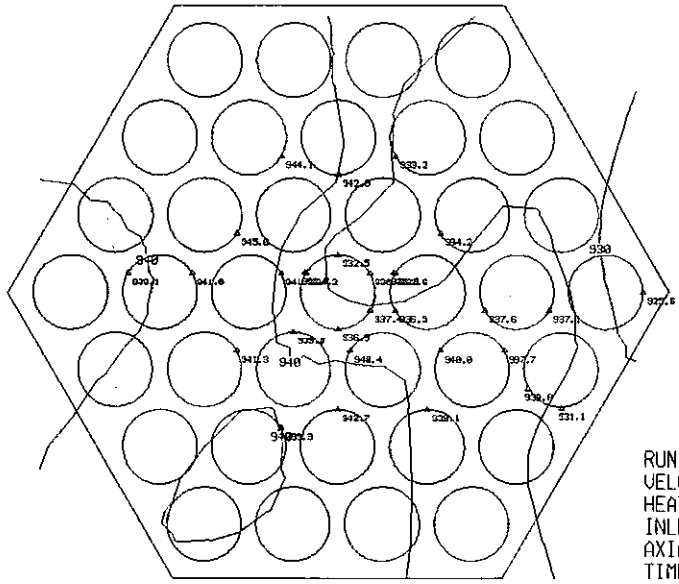

RUN NAME 37(37)LHF-203
VELOCITY 0.098 M/S
HEAT FLUX 12.04 W/CM2
INLET TEMP. 406.7 C
AXIAL 0.0 MM
TIME 224.000 SEC.

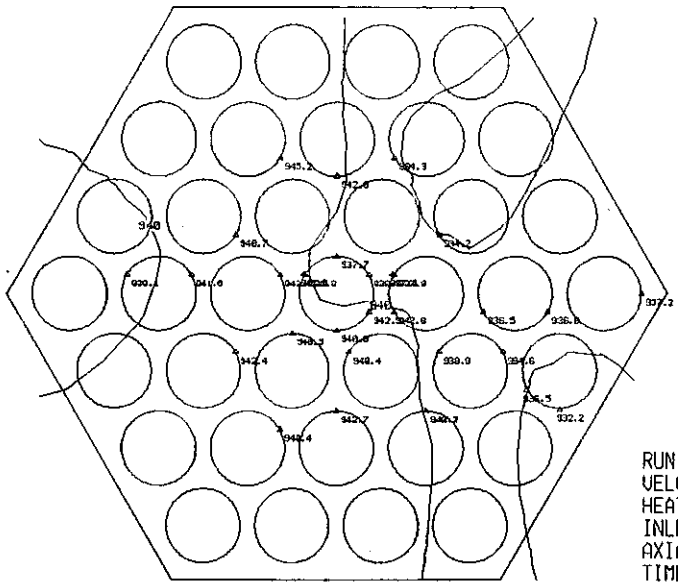

RUN NAME 37(37)LHF-203
VELOCITY 0.121 M/S
HEAT FLUX 12.44 W/CM2
INLET TEMP. 404.8 C
AXIAL 0.0 MM
TIME 425.600 SEC.

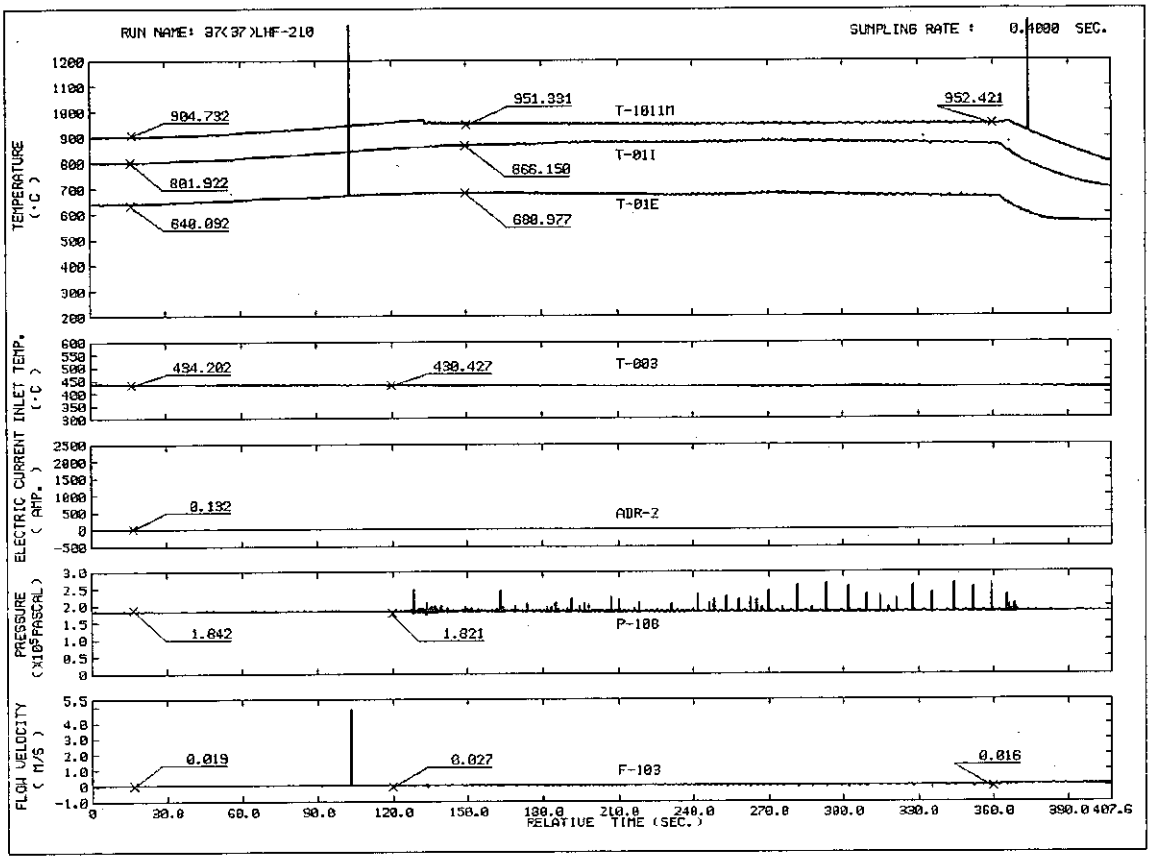
RUN NAME: 37(37)LHF-210
SUMPLING RATE : 0.4000 SEC.
TEMPERATURE ('C)
904.732
951.331
952.421
T-1011M
T-011
866.150
801.922
T-01E
848.092
688.977
ELECTRIC CURRENT INLET TEMP. ('C)
484.202
480.427
T-003
ELECTRIC CURRENT (AMP.)
0.132
ADR-Z
PRESSURE (X10⁵PASCAL)
1.842
1.821
P-108
FLOW VELOCITY (M/S)
0.019
0.027
0.016
F-103
RELATIVE TIME (SEC.)

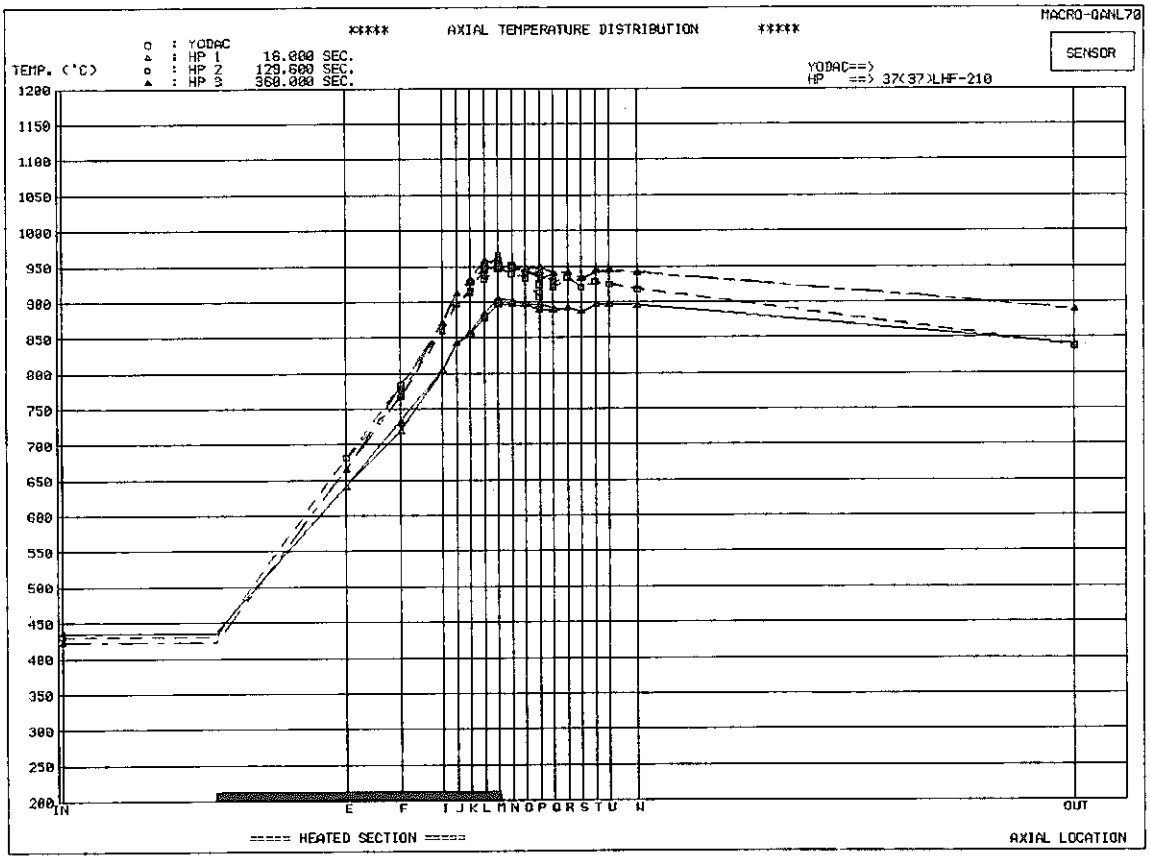
MACRO-GANL70
***** AXIAL TEMPERATURE DISTRIBUTION *****
SENSOR
TEMP. ('C)
: YODAC
: HP 1 18.000 SEC.
: HP 2 129.600 SEC.
: HP 3 360.000 SEC.
YODAC==>
HP ==> 37(37)LHF-210
IN
E F I J K L M N O P Q R S T U W
OUT
===== HEATED SECTION =====
AXIAL LOCATION

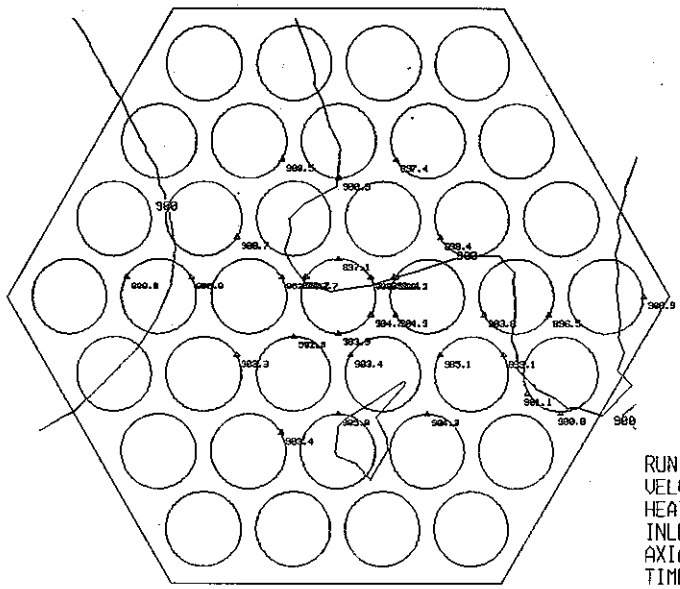

RUN NAME 37(37)LHF-210
VELOCITY 0.035 M/S
HEAT FLUX 3.38 W/CM2
INLET TEMP. 436.1 C
AXIAL 0.0 MM
TIME 16.000 SEC.

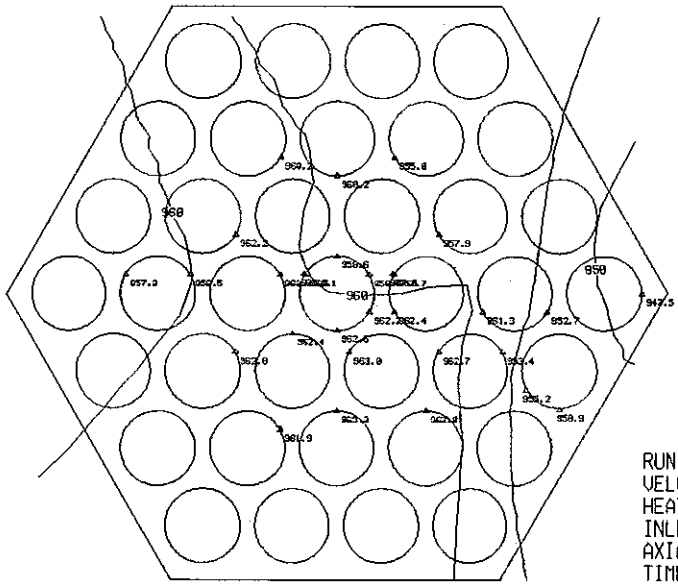

RUN NAME 37(37)LHF-210
VELOCITY 0.051 M/S
HEAT FLUX 4.47 W/CM2
INLET TEMP. 431.4 C
AXIAL 0.0 MM
TIME 129.600 SEC.

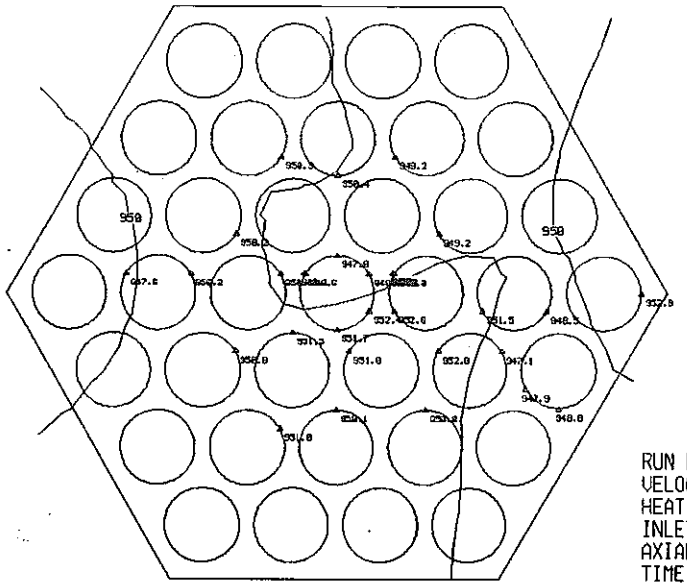

RUN NAME 37(37)LHF-210
VELOCITY 0.016 M/S
HEAT FLUX 4.91 W/CM2
INLET TEMP. 422.9 C
AXIAL 0.0 MM
TIME 360.000 SEC.

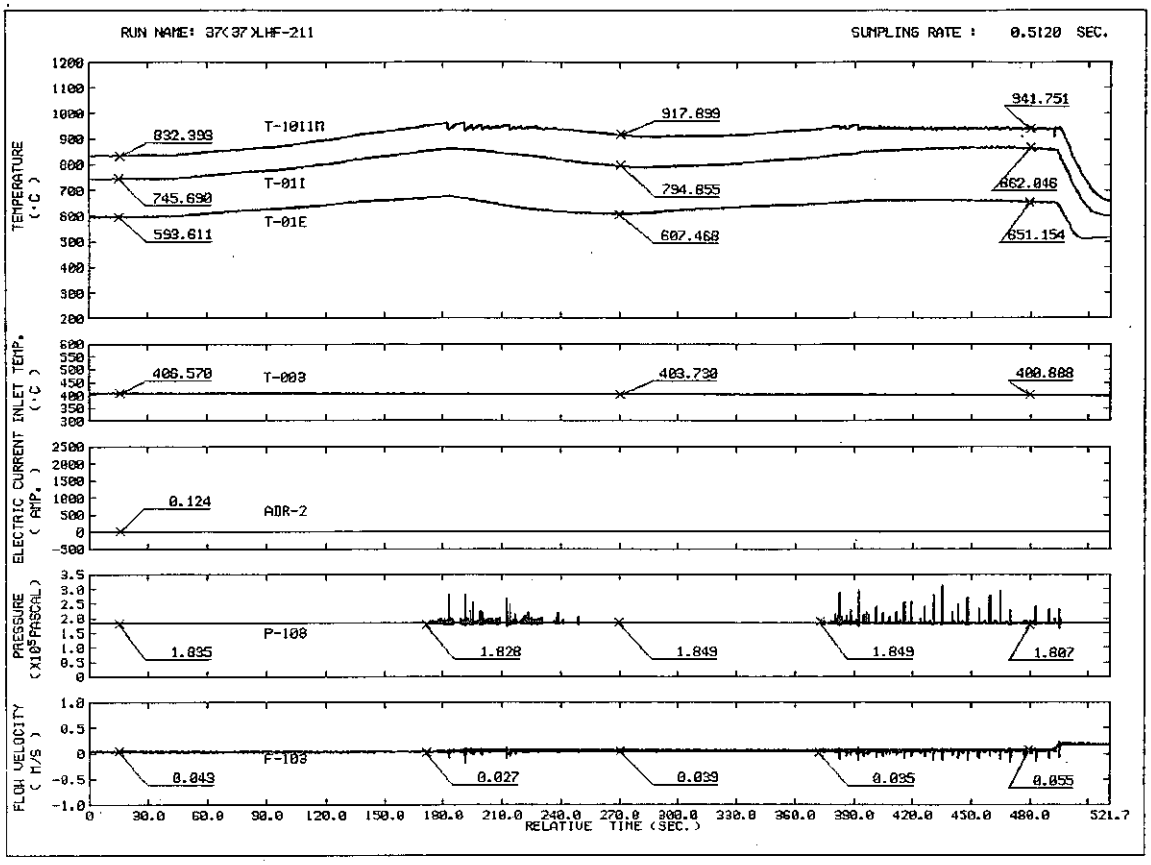
RUN NAME: 37(37)LHF-211
SUMPLING RATE : 0.5120 SEC.
TEMPERATURE (°C)
T-1011R
T-011
T-01E
832.399
745.690
593.611
917.899
794.855
607.468
941.751
862.046
851.154
INLET TEMP. (°C)
T-003
406.570
403.730
400.888
ELECTRIC CURRENT (AMP.)
AOR-2
0.124
PRESSURE (X10⁵PASCAL)
P-108
1.835
1.828
1.849
1.849
1.807
FLOW VELOCITY (M/S)
F-103
0.049
0.027
0.039
0.035
0.055
RELATIVE TIME (SEC.)

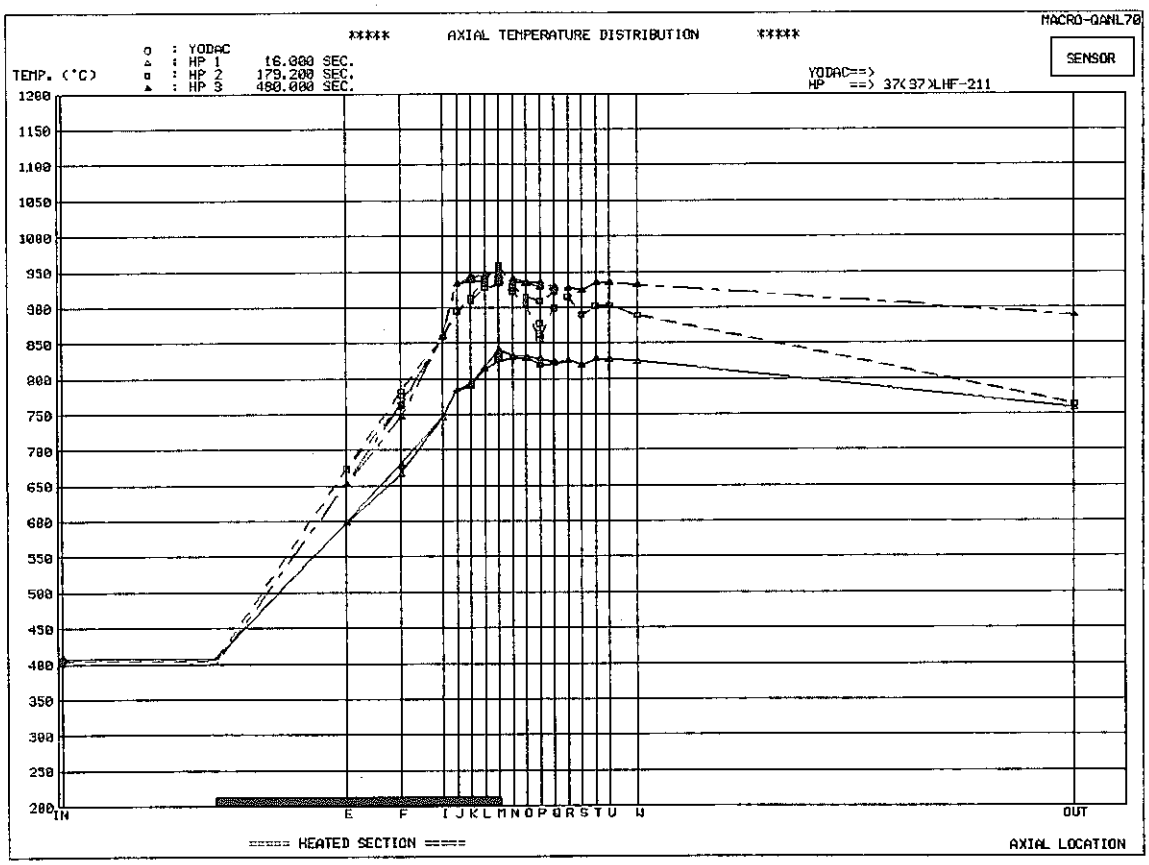
MACRO-QANL70
SENSOR
***** AXIAL TEMPERATURE DISTRIBUTION *****
○ : YODAC
△ : HP 1 16.000 SEC.
□ : HP 2 179.200 SEC.
▲ : HP 3 480.000 SEC.
TEMP. (°C)
YODAC==>
HP ==> 37(37)LHF-211
IN
E F I J K L M N O P Q R S T U W
OUT
===== HEATED SECTION =====
AXIAL LOCATION

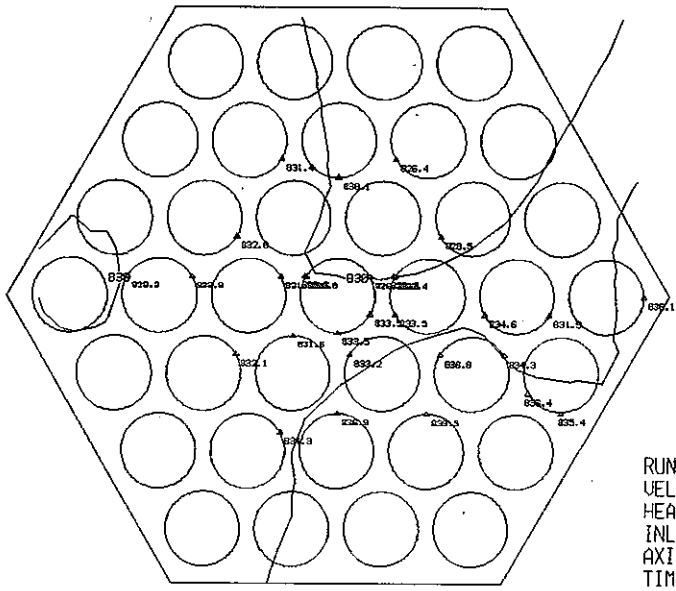

RUN NAME 37(37)LHF-211
VELOCITY 0.051 M/S
HEAT FLUX 3.36 W/CM2
INLET TEMP. 407.5 C
AXIAL 0.0 MM
TIME 16.000 SEC.

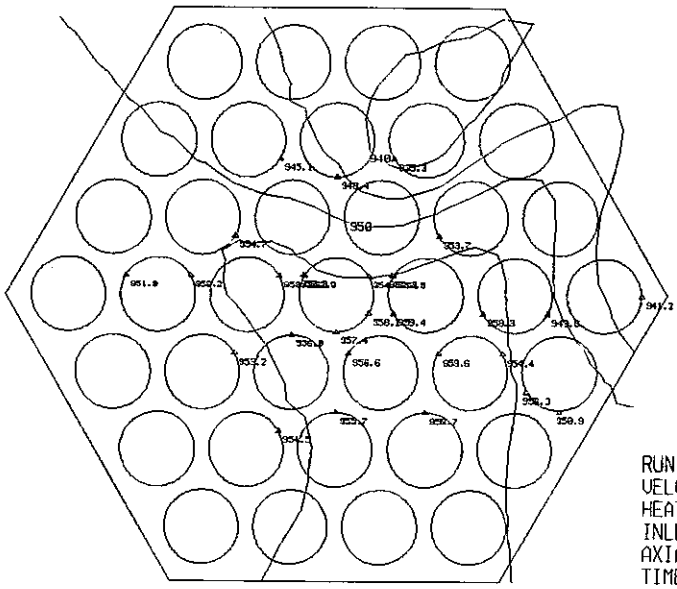

RUN NAME 37(37)LHF-211
VELOCITY 0.027 M/S
HEAT FLUX 4.88 W/CM2
INLET TEMP. 404.7 C
AXIAL 0.0 MM
TIME 179.200 SEC.

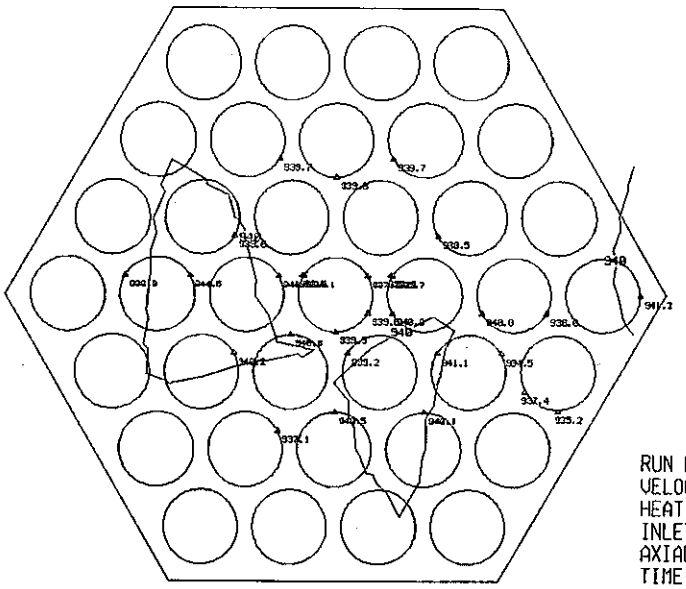

RUN NAME 37(37)LHF-211
VELOCITY 0.059 M/S
HEAT FLUX 6.43 W/CM2
INLET TEMP. 399.9 C
AXIAL 0.0 MM
TIME 480.000 SEC.

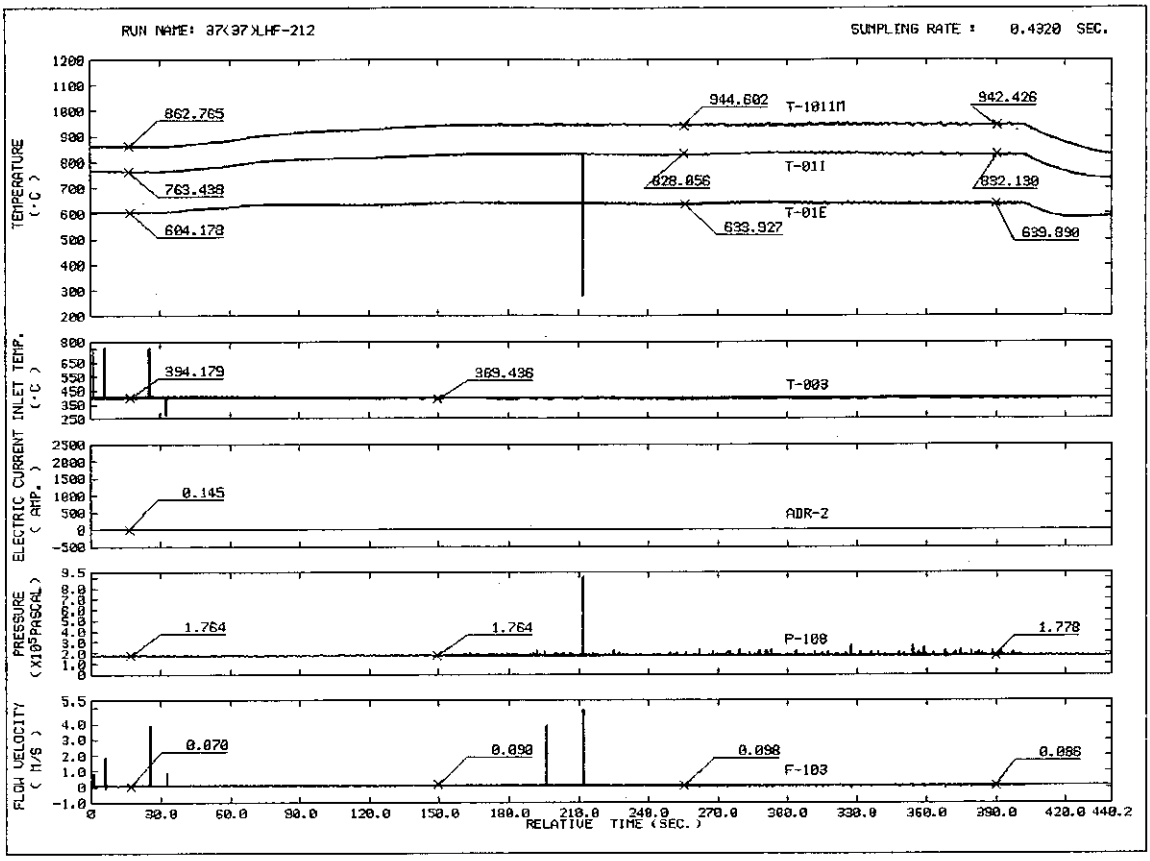
RUN NAME: 37(37)LHF-212
SUMPLING RATE : 0.4320 SEC.
TEMPERATURE (°C)
862.765
944.602
T-1011M
942.426
763.438
828.056
T-011I
892.130
604.178
633.927
T-01IE
699.890
ELECTRIC CURRENT INLET TEMP. (°C)
394.179
389.436
T-003
(AMP.)
0.145
ADR-2
PRESSURE (X10⁵PASCAL)
1.764
1.764
P-108
1.778
FLOW VELOCITY (M/S)
0.070
0.090
0.098
F-103
0.086
RELATIVE TIME (SEC.)

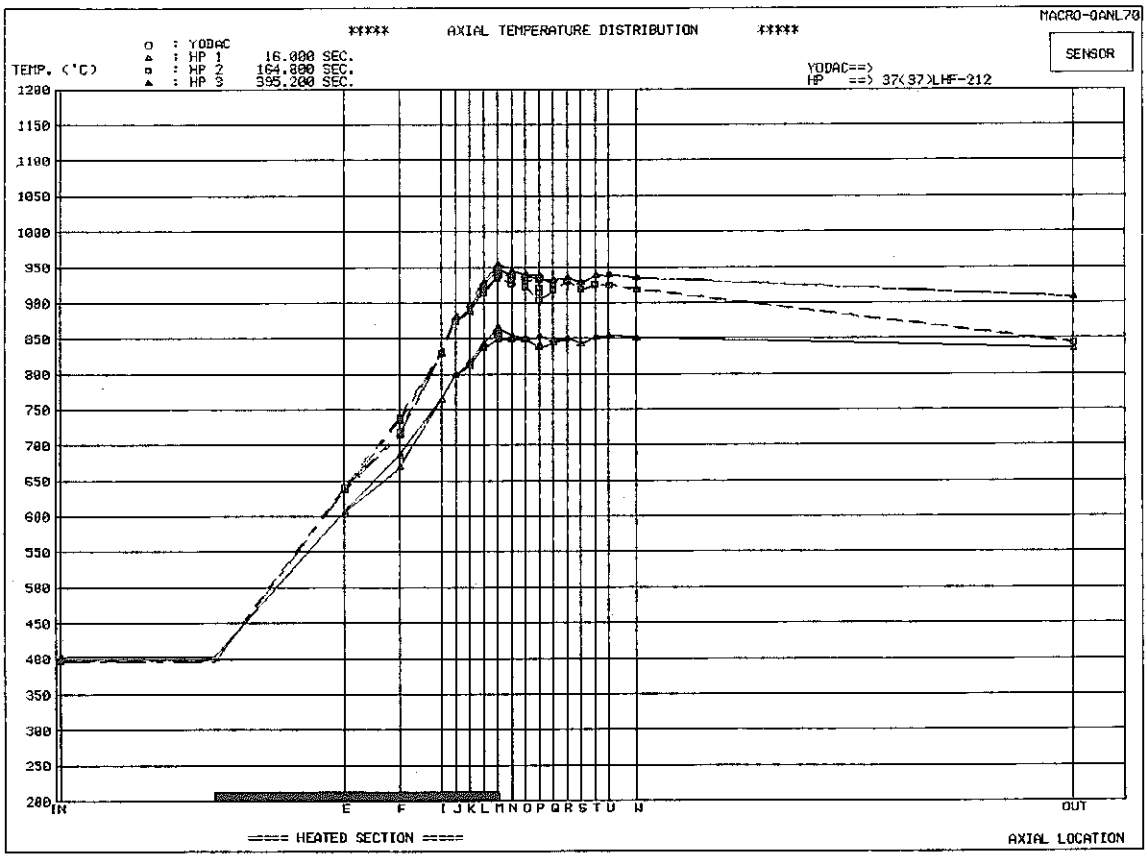
MACRO-GANL70
***** AXIAL TEMPERATURE DISTRIBUTION *****
SENSOR
○ : YODAC
△ : HP 1 16.000 SEC.
□ : HP 2 164.800 SEC.
▲ : HP 3 395.200 SEC.
TEMP. (°C)
YODAC==)
HP ==) 37(37)LHF-212
IN
E F I J K L M N O P Q R S T U W
OUT
==== HEATED SECTION ====
AXIAL LOCATION

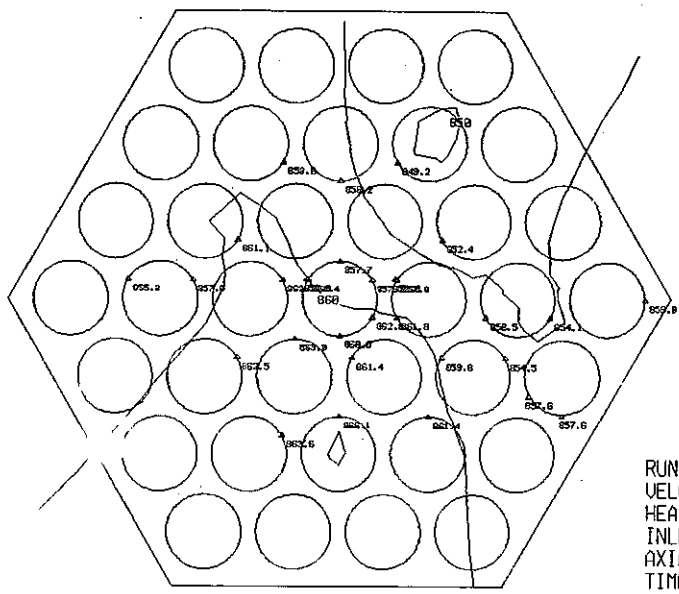

RUN NAME 37(37)LHF-212
VELOCITY 0.070 M/S
HEAT FLUX 6.64 W/CM2
INLET TEMP. 404.6 C
AXIAL 0.0 MM
TIME 16.000 SEC.

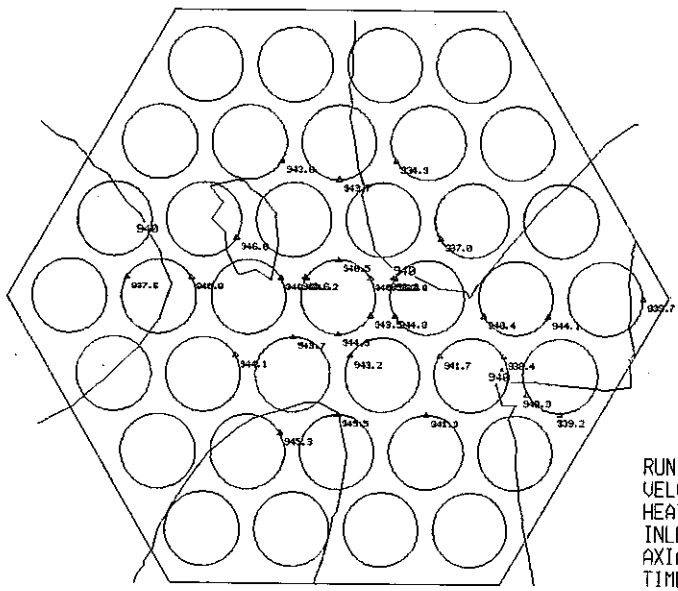

RUN NAME 37(37)LHF-212
VELOCITY 0.070 M/S
HEAT FLUX 8.39 W/CM2
INLET TEMP. 403.7 C
AXIAL 0.0 MM
TIME 164.800 SEC.

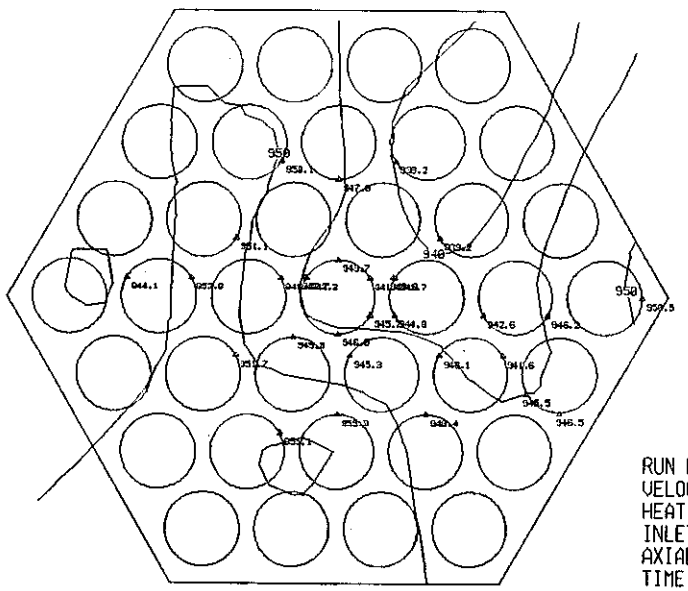

RUN NAME 37(37)LHF-212
VELOCITY 0.090 M/S
HEAT FLUX 8.95 W/CM2
INLET TEMP. 391.3 C
AXIAL 0.0 MM
TIME 395.200 SEC.

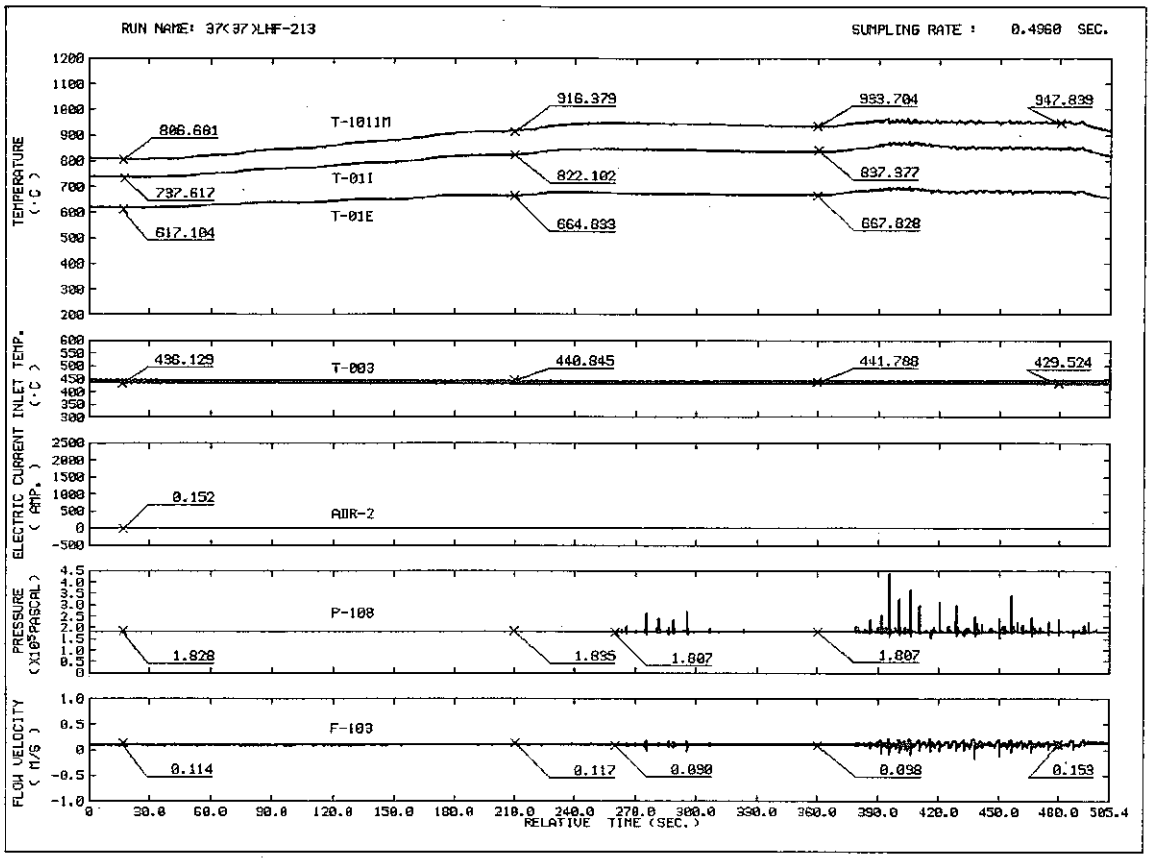
RUN NAME: 37(37)LHF-213
SAMPLING RATE : 0.4960 SEC.
TEMPERATURE (°C)
T-1011M
T-01I
T-01E
806.681
737.617
617.104
916.379
822.102
664.833
983.704
837.377
667.828
947.839
INLET TEMP. (°C)
T-003
486.129
440.845
441.788
429.524
ELECTRIC CURRENT (AMP.)
AUR-2
0.152
PRESSURE (X10⁵PASCAL)
P-108
1.828
1.835
1.807
1.807
FLOW VELOCITY (M/S)
F-103
0.114
0.117
0.090
0.098
0.153
RELATIVE TIME (SEC.)

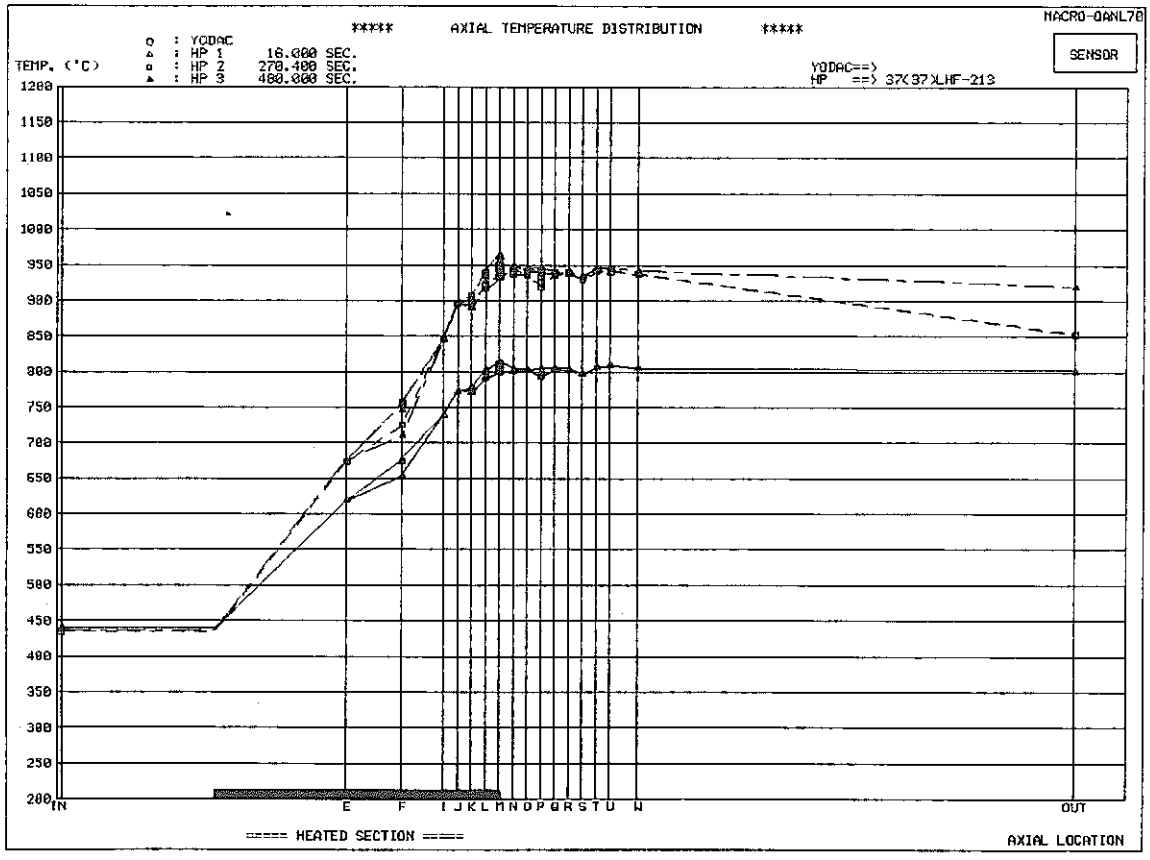
***** AXIAL TEMPERATURE DISTRIBUTION *****
MACRO-GANL70
SENSOR
○ : YODAC
△ : HP 1 16.000 SEC.
□ : HP 2 270.400 SEC.
▲ : HP 3 480.000 SEC.
TEMP. (°C)
YODAC==>
HP ==> 37(37)LHF-213
IN
E F I J K L M N O P Q R S T U W
OUT
===== HEATED SECTION =====
AXIAL LOCATION

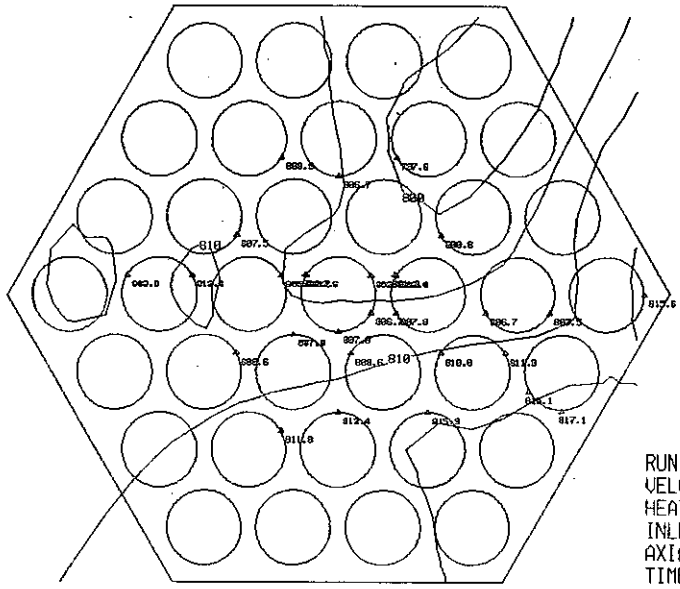

RUN NAME 37(37)LHF-213
VELOCITY 0.106 M/S
HEAT FLUX 6.80 W/CM2
INLET TEMP. 445.6 C
AXIAL 0.0 MM
TIME 16.000 SEC.

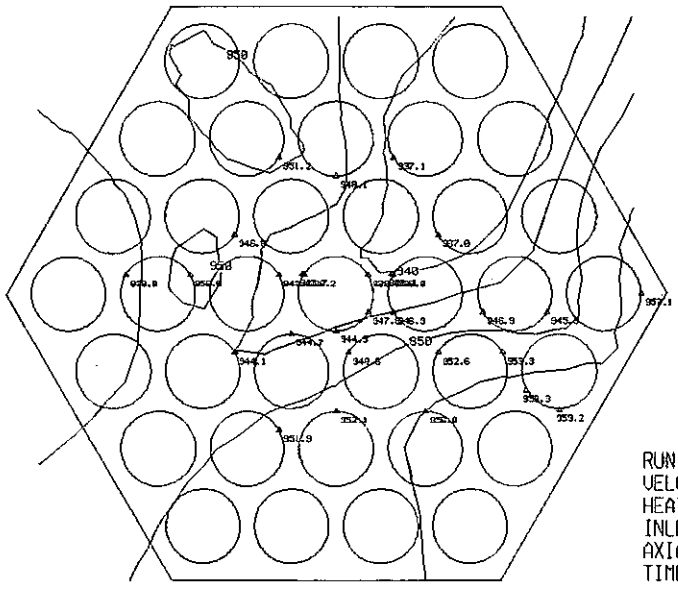

RUN NAME 37(37)LHF-213
VELOCITY 0.098 M/S
HEAT FLUX 10.81 W/CM2
INLET TEMP. 436.1 C
AXIAL 0.0 MM
TIME 270.400 SEC.

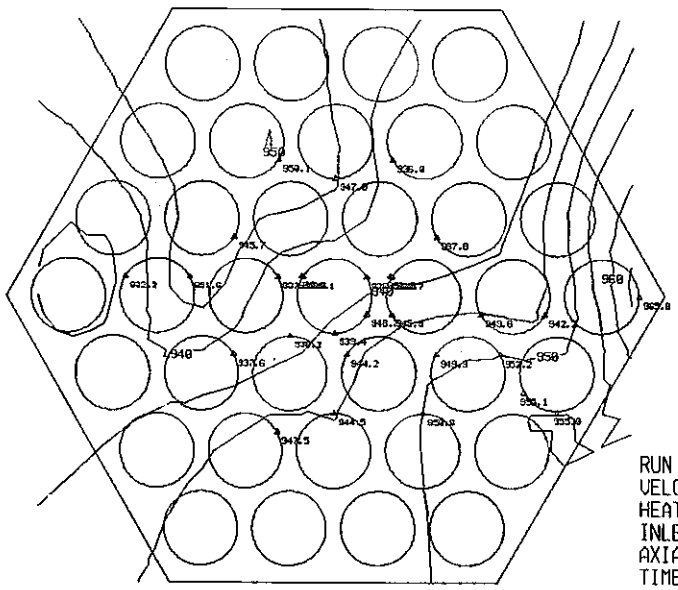

RUN NAME 37(37)LHF-213
VELOCITY 0.161 M/S
HEAT FLUX 12.34 W/CM2
INLET TEMP. 440.8 C
AXIAL 0.0 MM
TIME 480.000 SEC.

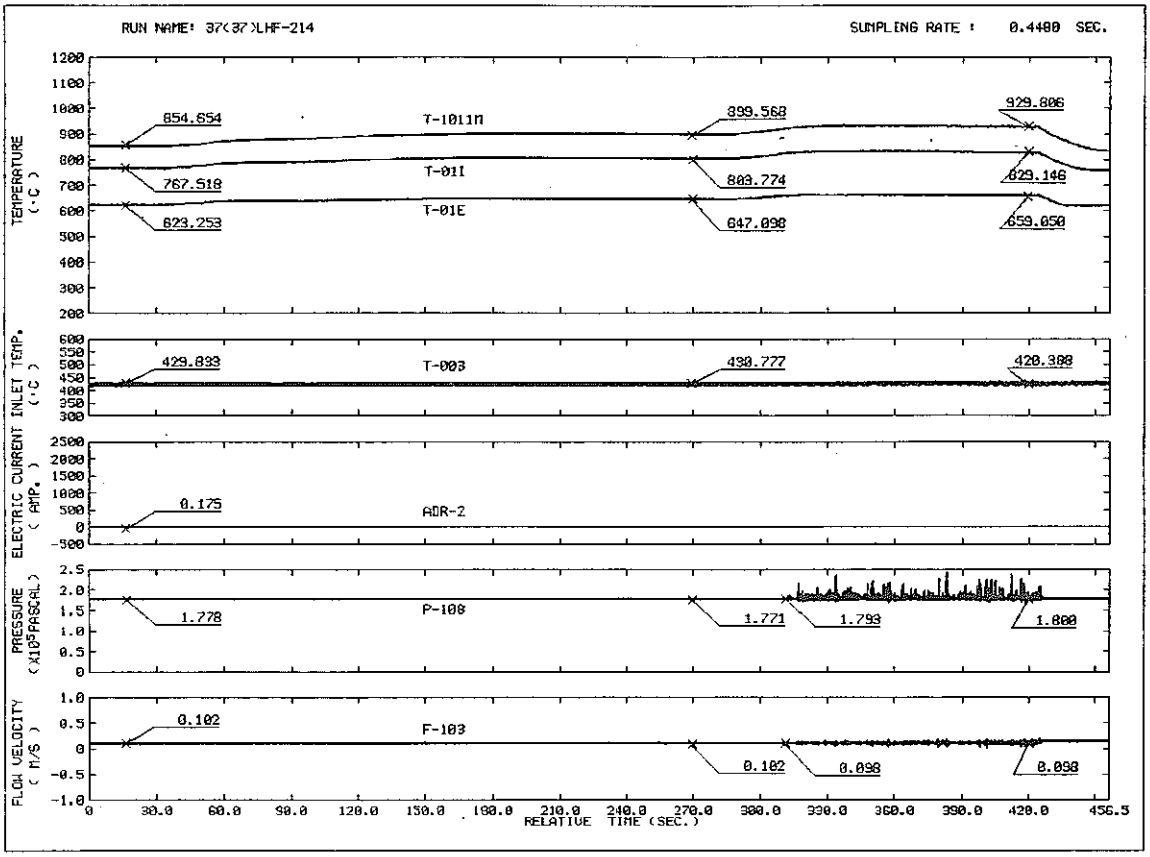
RUN NAME: 37(37)LHF-214
SAMPLING RATE : 0.4480 SEC.
TEMPERATURE (°C)
854.654
T-1011M
399.568
929.806
767.518
T-01I
803.774
829.146
623.253
T-01E
647.098
659.050
INLET TEMP. (°C)
429.893
T-003
430.777
420.388
ELECTRIC CURRENT (AMP.)
0.175
ADR-2
PRESSURE (X10⁵PASCAL)
1.778
P-108
1.771
1.793
1.800
FLOW VELOCITY (M/S)
0.102
F-103
0.102
0.098
0.098
RELATIVE TIME (SEC.)

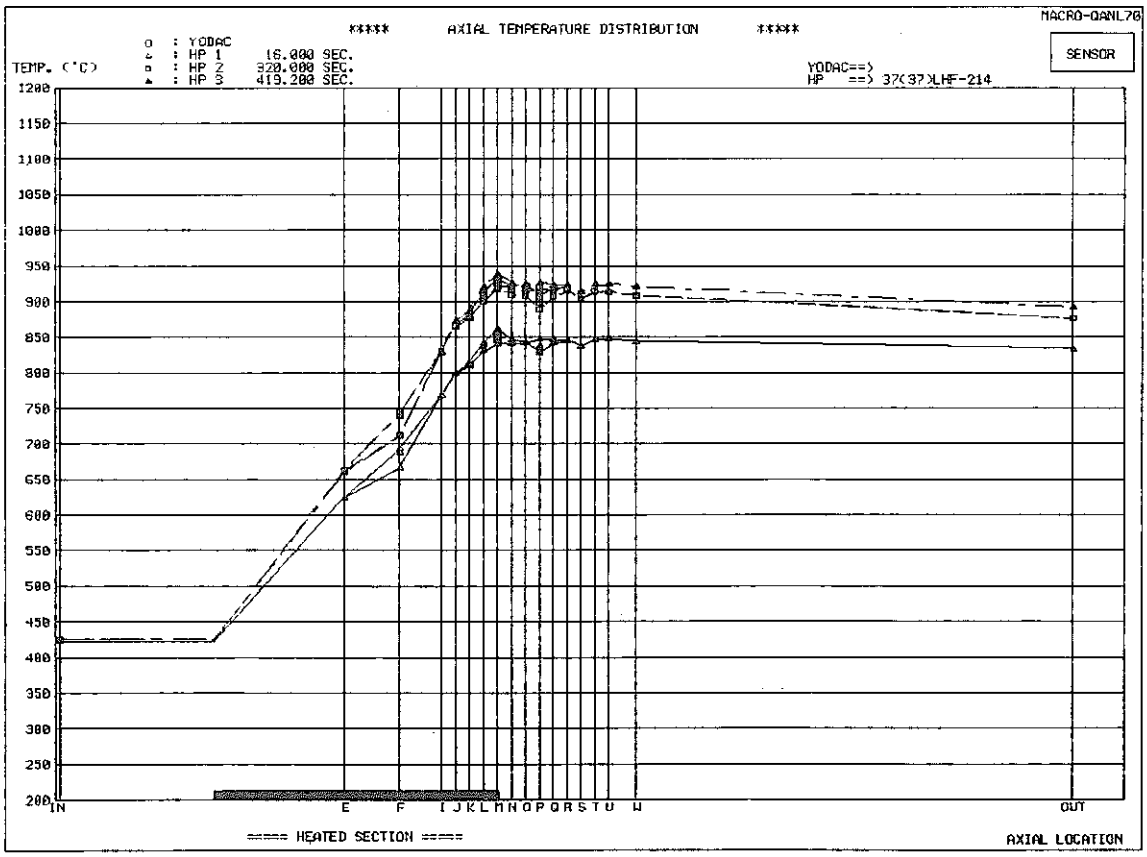
MACRO-QANL76
SENSOR
***** AXIAL TEMPERATURE DISTRIBUTION *****
o : YODAC
: HP 1 16.000 SEC.
: HP 2 320.000 SEC.
▲ : HP 3 419.200 SEC.
TEMP. (°C)
YODAC==>
HP ==> 37(37)LHF-214
IN
E F I J K L M N O P Q R S T U W
OUT
==== HEATED SECTION ====
AXIAL LOCATION

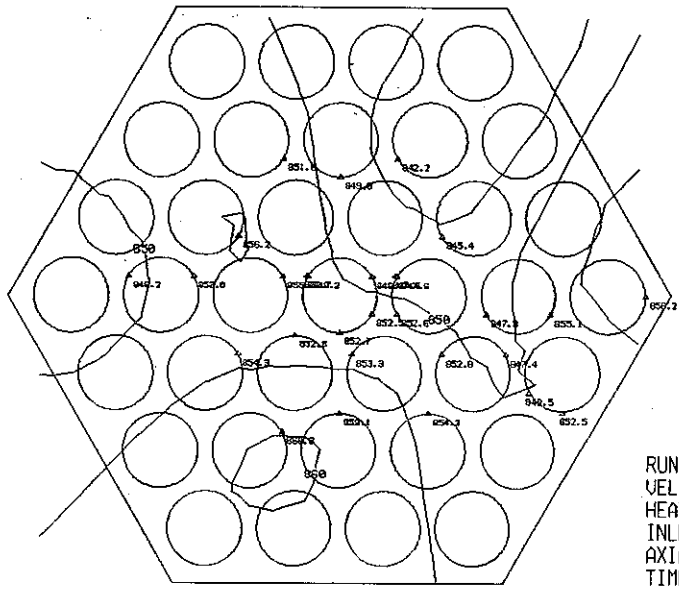

RUN NAME 37(37)LHF-214
VELOCITY 0.117 M/S
HEAT FLUX 9.32 W/CM2
INLET TEMP. 424.2 C
AXIAL 0.0 MM
TIME 16.000 SEC.

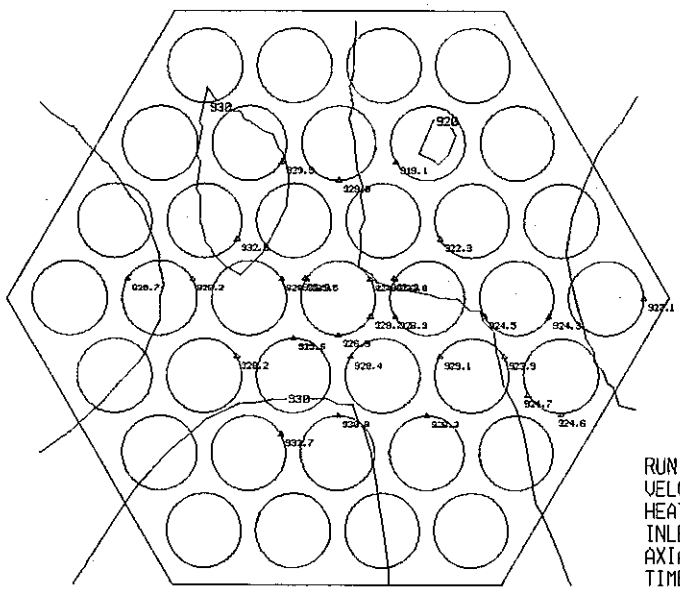

RUN NAME 37(37)LHF-214
VELOCITY 0.114 M/S
HEAT FLUX 11.41 W/CM2
INLET TEMP. 423.2 C
AXIAL 0.0 MM
TIME 320.000 SEC.

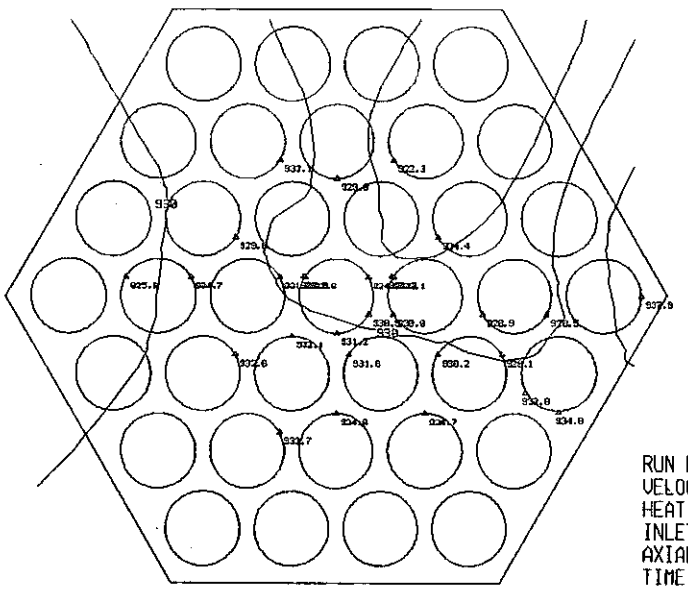

RUN NAME 37(37)LHF-214
VELOCITY 0.114 M/S
HEAT FLUX 11.41 W/CM2
INLET TEMP. 425.1 C
AXIAL 0.0 MM
TIME 419.200 SEC.

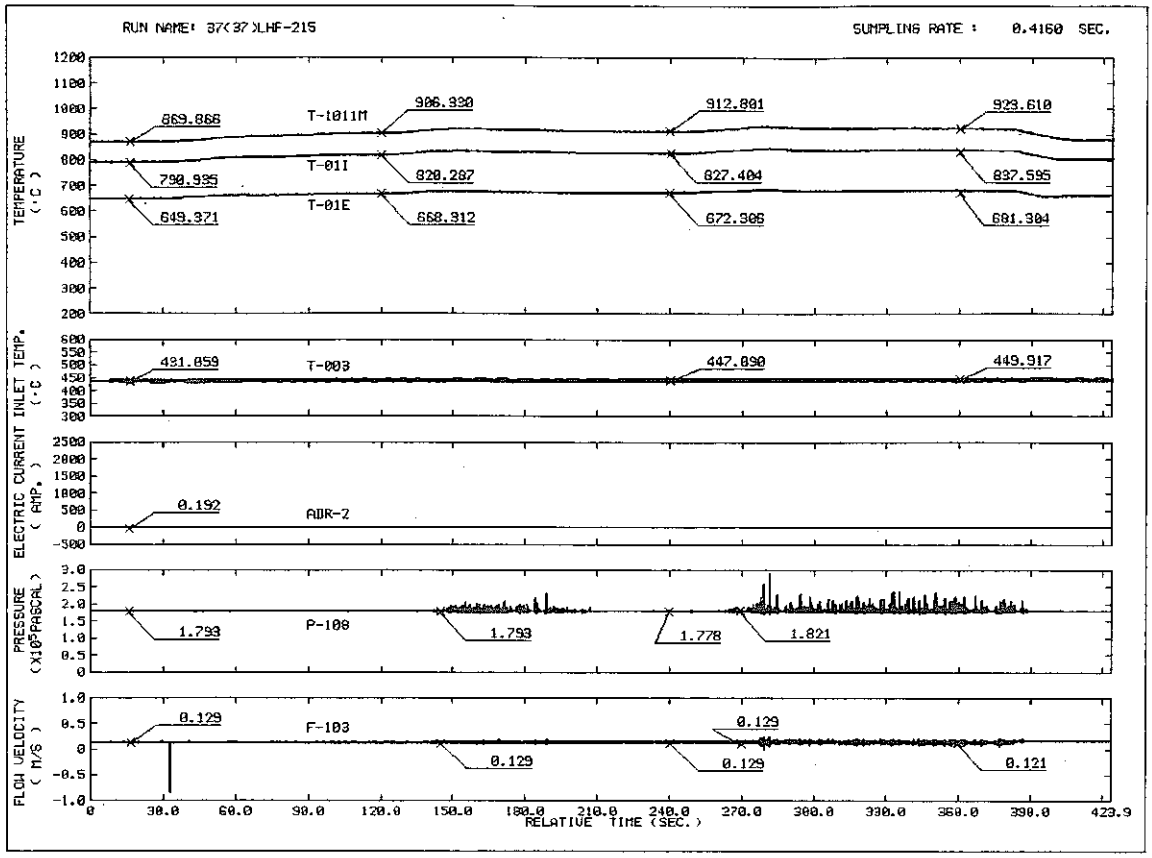
RUN NAME: 37(37)LHF-215
SUMPLING RATE : 0.4160 SEC.
TEMPERATURE (°C)
869.866
T-1011M
906.930
912.801
923.610
790.935
T-01I
820.287
827.404
897.595
649.371
T-01E
668.912
672.906
681.304
INLET TEMP. (°C)
481.059
T-003
447.890
449.917
ELECTRIC CURRENT (AMP.)
0.192
ADR-2
PRESSURE (X10⁵PASCAL)
1.793
P-108
1.793
1.778
1.821
FLOW VELOCITY (M/S)
0.129
F-103
0.129
0.129
0.129
0.121
RELATIVE TIME (SEC.)

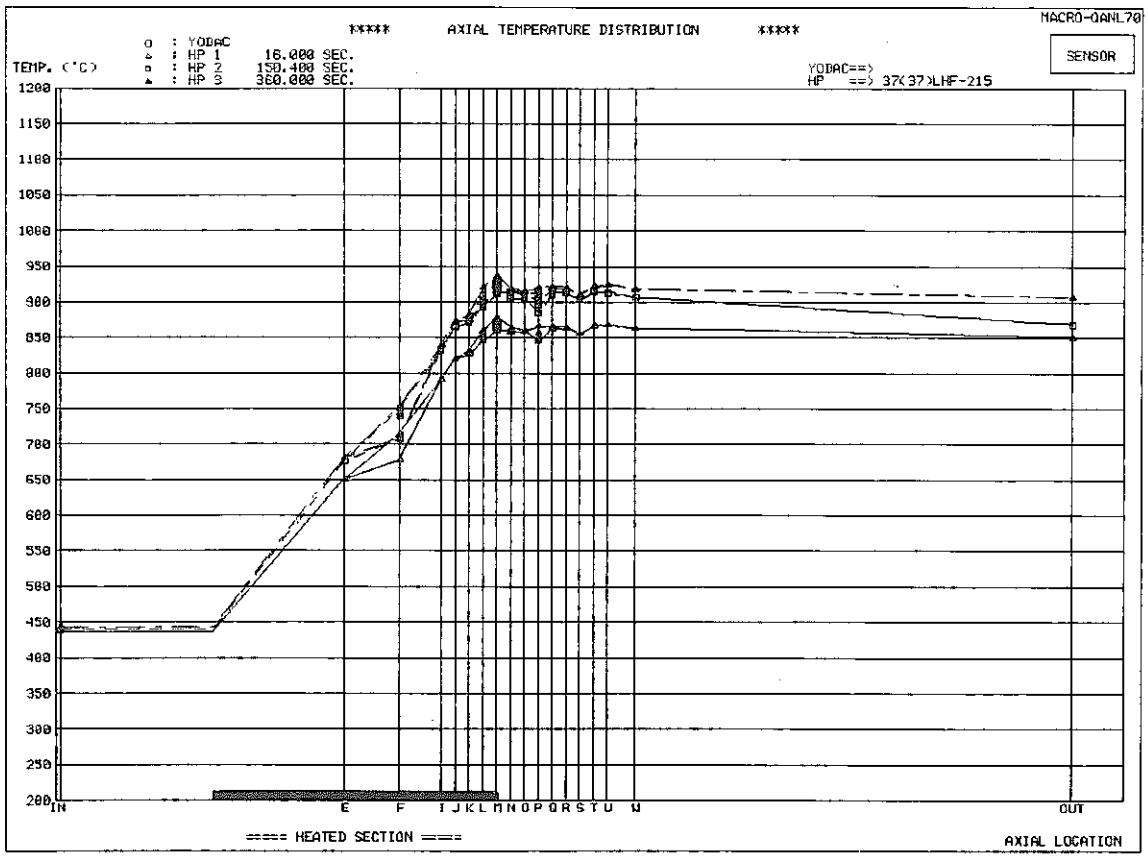
***** AXIAL TEMPERATURE DISTRIBUTION *****
MACRO-QANL70
SENSOR
o : YODAC
▵ : HP 1 16.000 SEC.
□ : HP 2 150.400 SEC.
▲ : HP 3 360.000 SEC.
TEMP. (°C)
YODAC==>
HP ==> 37(37)LHF-215
IN
E F I J K L M N O P Q R S T U W
OUT
==== HEATED SECTION ====
AXIAL LOCATION

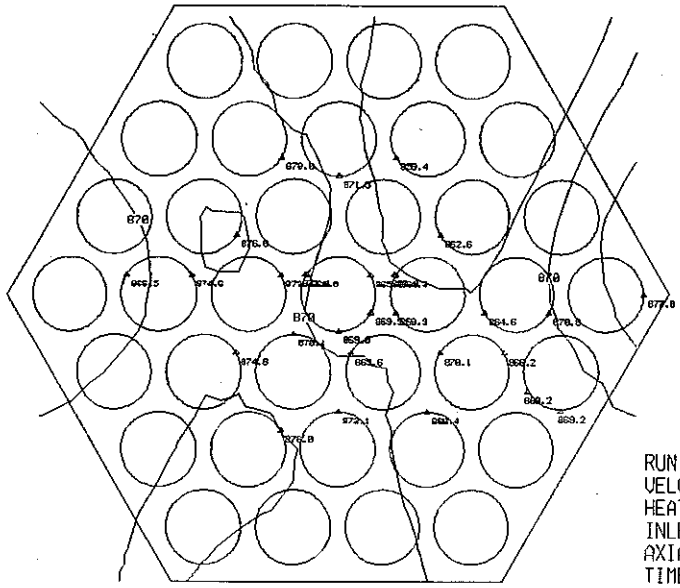

RUN NAME 37(37)LHF-215
VELOCITY 0.129 M/S
HEAT FLUX 11.49 W/CM2
INLET TEMP. 442.4 C
AXIAL 0.0 MM
TIME 16.000 SEC.

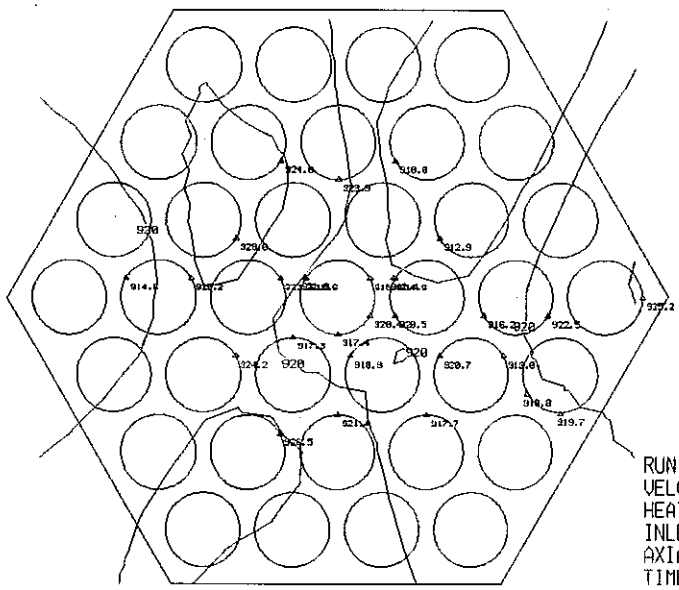

RUN NAME 37(37)LHF-215
VELOCITY 0.137 M/S
HEAT FLUX 13.42 W/CM2
INLET TEMP. 446.1 C
AXIAL 0.0 MM
TIME 150.400 SEC.

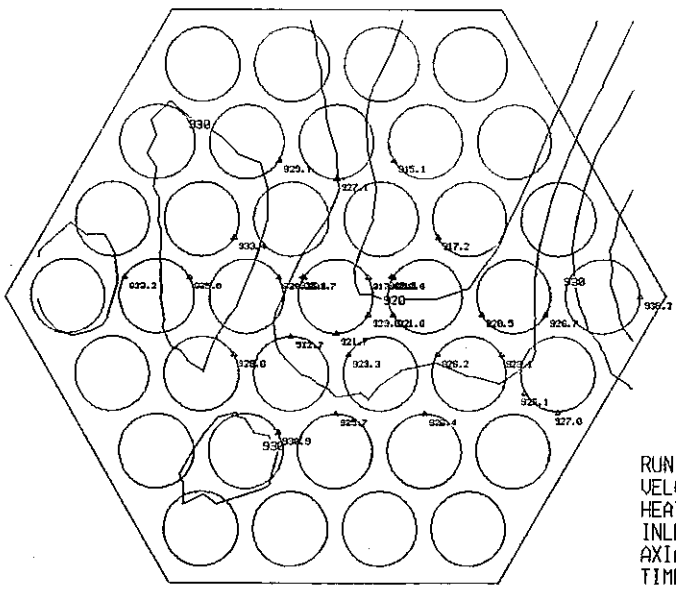

RUN NAME 37(37)LHF-215
VELOCITY 0.161 M/S
HEAT FLUX 14.38 W/CM2
INLET TEMP. 436.7 C
AXIAL 0.0 MM
TIME 360.000 SEC.

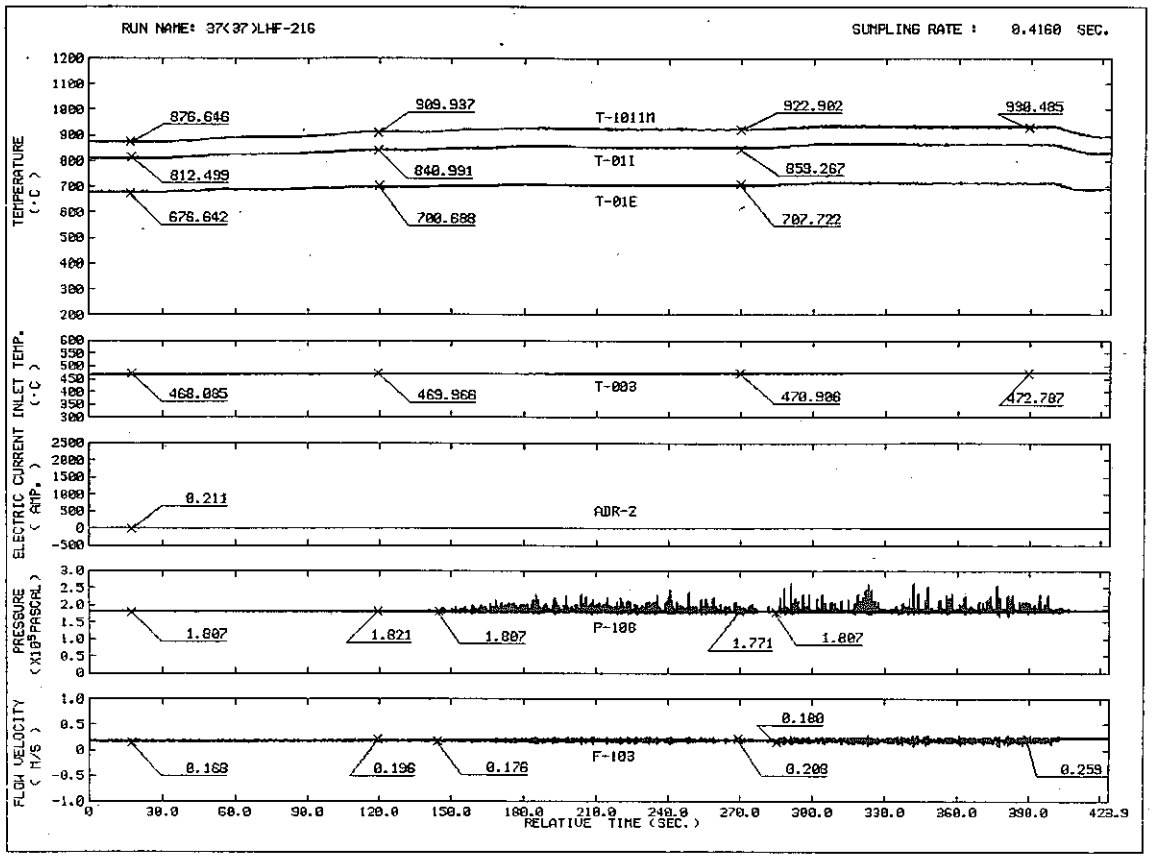
RUN NAME: 37(37)LHF-216
SAMPLING RATE : 0.4160 SEC.
TEMPERATURE (°C)
876.646
909.937
T-1011M
922.902
930.485
812.499
840.991
T-011I
853.267
678.642
700.688
T-01IE
707.722
TEMP. (°C)
468.085
469.968
T-003
470.908
472.787
ELECTRIC CURRENT (AMP.)
0.211
ADR-2
PRESSURE (X10³PASCAL)
1.807
1.821
1.807
P-108
1.771
1.807
FLOW VELOCITY (M/S)
0.168
0.196
0.176
F-103
0.180
0.209
0.259
RELATIVE TIME (SEC.)

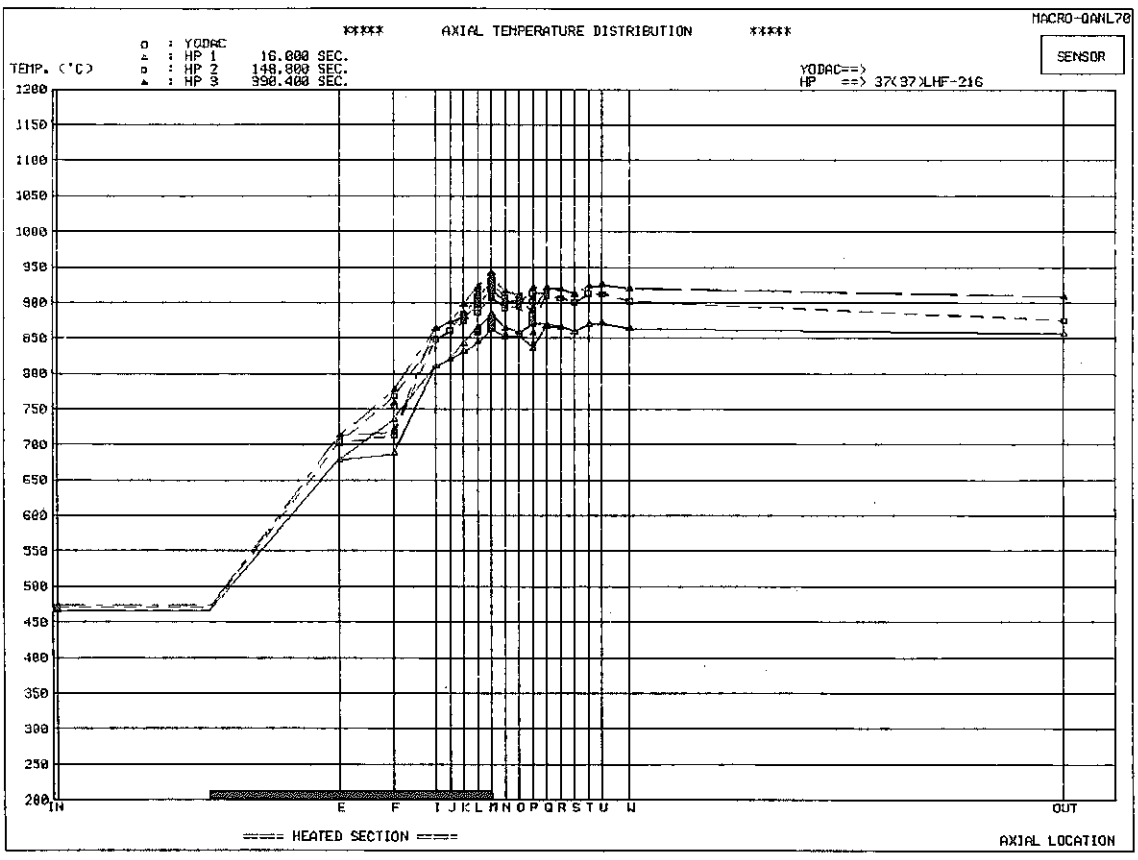
***** AXIAL TEMPERATURE DISTRIBUTION *****
MACRO-QANL70
SENSOR
o : YODAC
Δ : HP 1 16.000 SEC.
□ : HP 2 148.000 SEC.
▲ : HP 3 398.400 SEC.
TEMP. (°C)
YODAC==>
HP ==> 37(37)LHF-216
IN
E F I J K L M N O P Q R S T U W
OUT
==== HEATED SECTION ====
AXIAL LOCATION

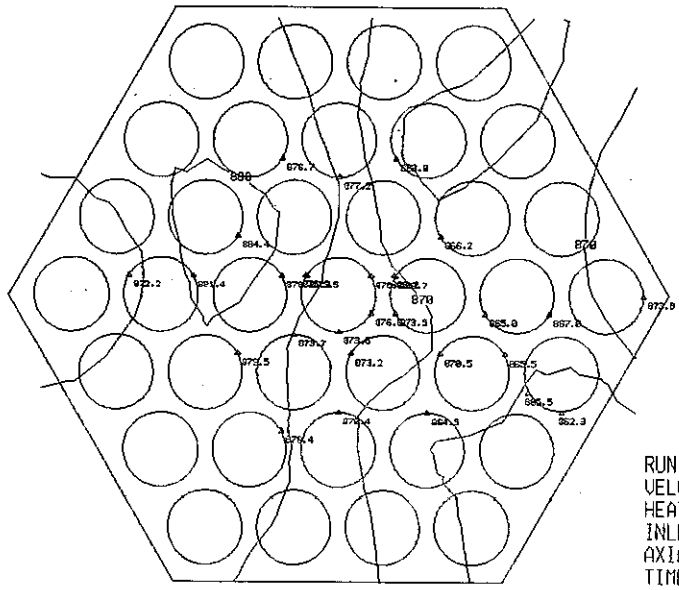

RUN NAME 37(37)LHF-216
VELOCITY 0.180 M/S
HEAT FLUX 14.60 W/CM2
INLET TEMP. 466.2 C
AXIAL 0.0 MM
TIME 16.000 SEC.

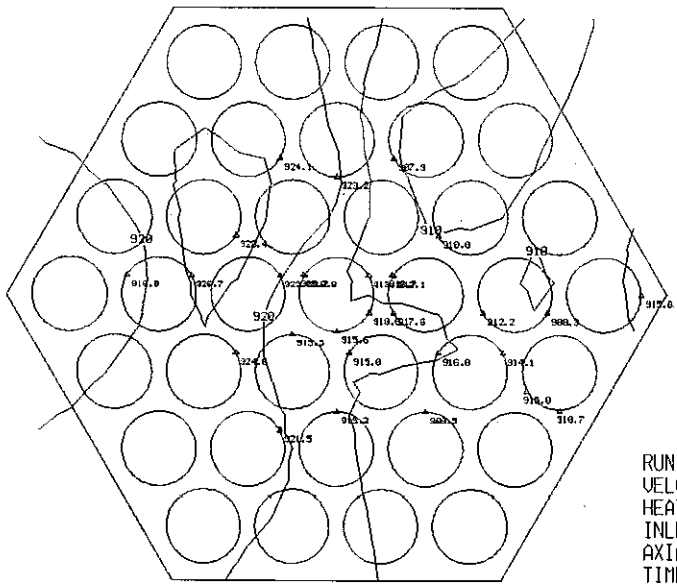

RUN NAME 37(37)LHF-216
VELOCITY 0.184 M/S
HEAT FLUX 17.28 W/CM2
INLET TEMP. 470.0 C
AXIAL 0.0 MM
TIME 148.800 SEC.

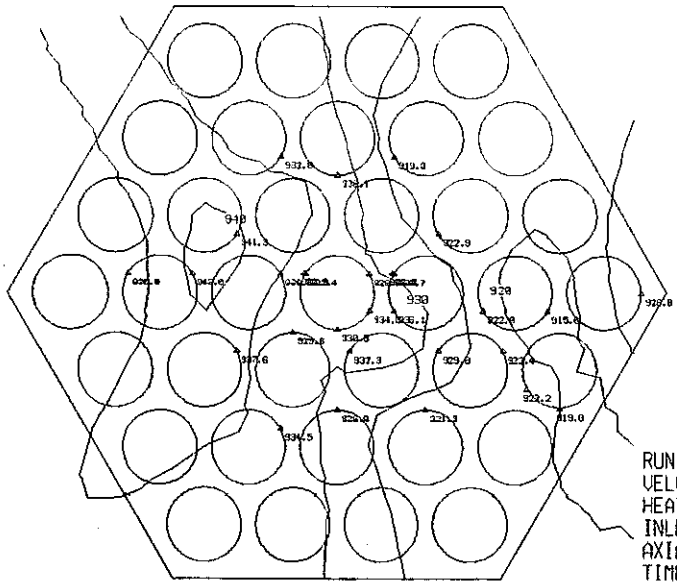

RUN NAME 37(37)LHF-216
VELOCITY 0.219 M/S
HEAT FLUX 18.36 W/CM2
INLET TEMP. 473.7 C
AXIAL 0.0 MM
TIME 390.400 SEC.

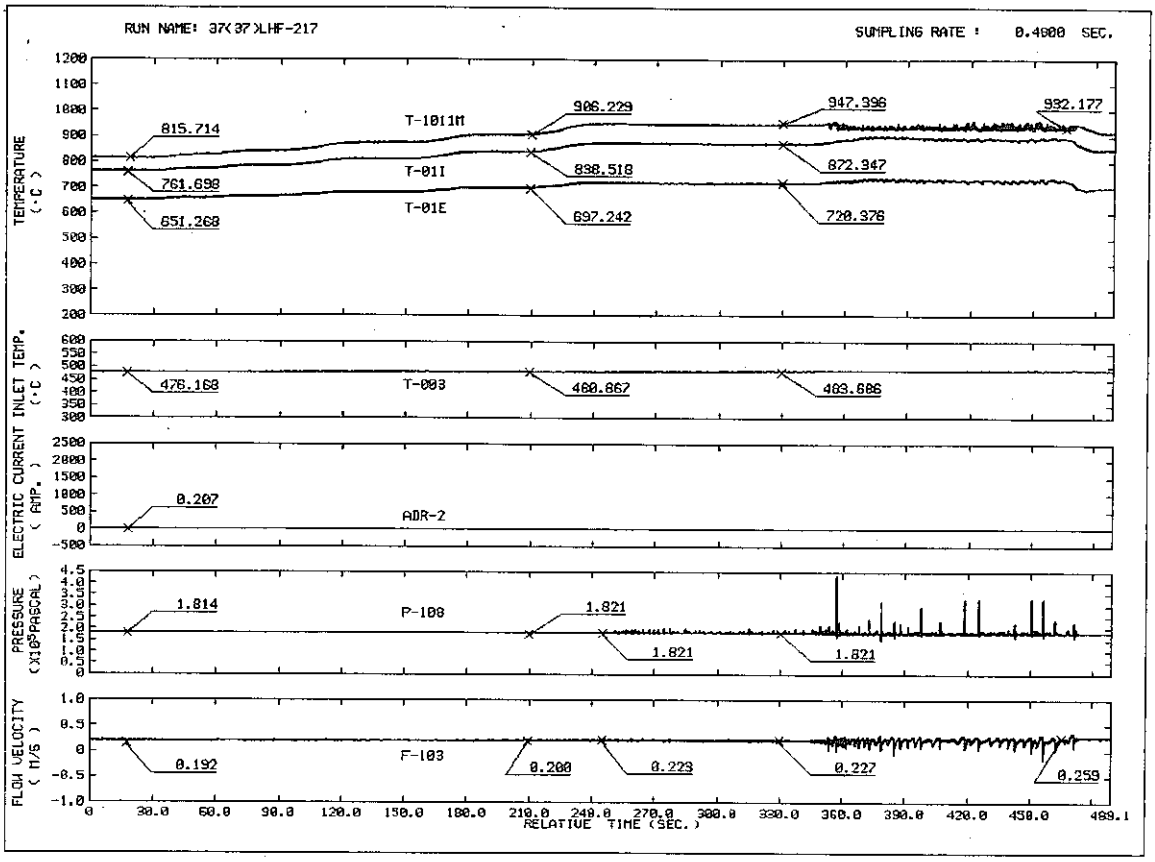
RUN NAME: 37(37)LHF-217
SUMPLING RATE : 0.4000 SEC.
TEMPERATURE (°C)
815.714
761.698
651.268
T-1011
T-01I
T-01E
906.229
838.518
697.242
947.396
872.347
720.378
932.177
ELECTRIC CURRENT INLET TEMP. (°C)
476.168
T-003
460.867
483.686
(AMP.)
0.207
ADR-2
PRESSURE (X10⁶PASCAL)
1.814
P-108
1.821
1.821
1.821
FLOW VELOCITY (M/S)
0.192
F-103
0.200
0.229
0.227
0.259
RELATIVE TIME (SEC.)

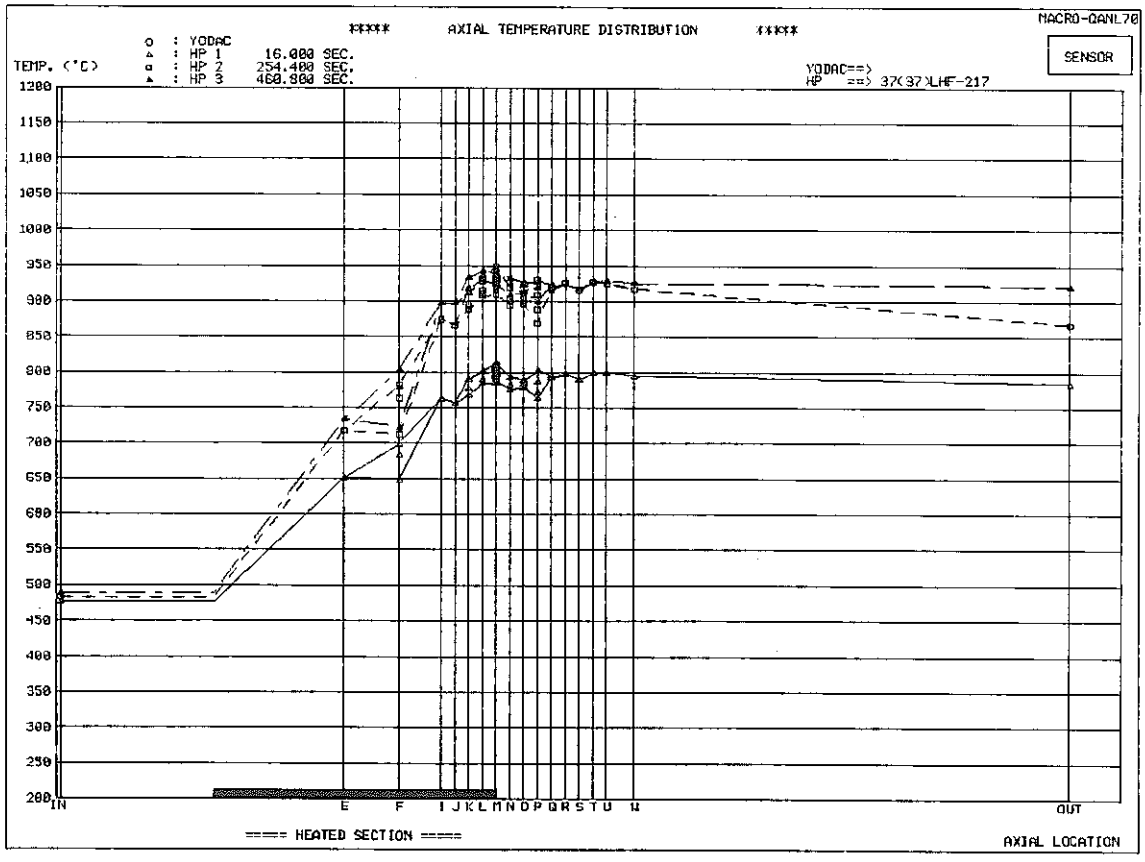
***** AXIAL TEMPERATURE DISTRIBUTION *****
MACRO-QANL70
SENSOR
o : YODAC
Δ : HP 1 16.000 SEC.
□ : HP 2 254.400 SEC.
▲ : HP 3 460.800 SEC.
TEMP. (°C)
YODAC==)
HP ==) 37(37)LHF-217
IN
E F I J K L M N O P Q R S T U W
OUT
==== HEATED SECTION ====
AXIAL LOCATION

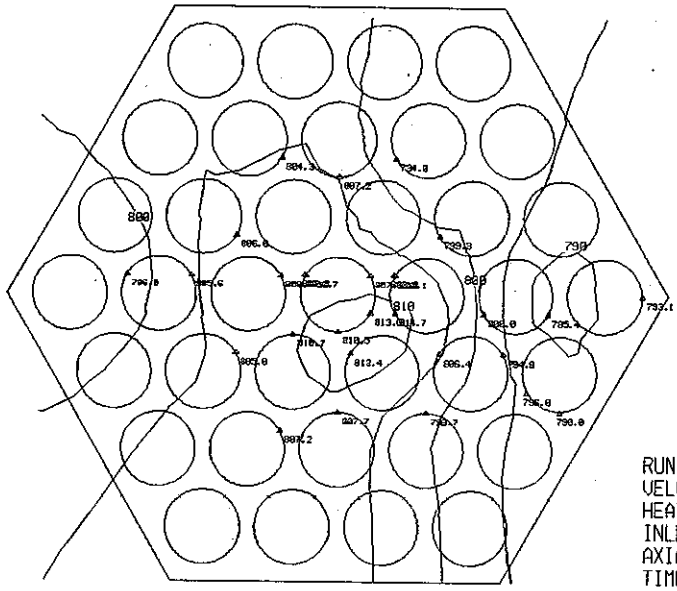

RUN NAME 37(37)LHF-217
VELOCITY 0.200 M/S
HEAT FLUX 12.63 W/CM2
INLET TEMP. 477.1 C
AXIAL 0.0 MM
TIME 16.000 SEC.

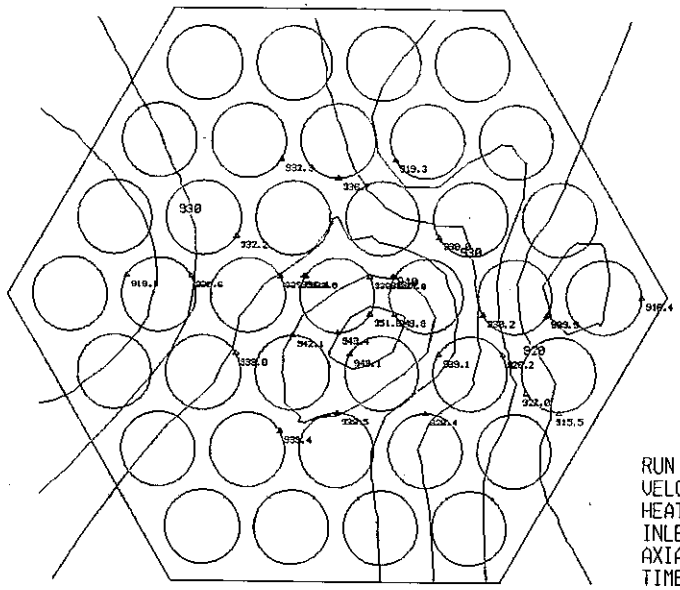

RUN NAME 37(37)LHF-217
VELOCITY 0.196 M/S
HEAT FLUX 18.67 W/CM2
INLET TEMP. 483.7 C
AXIAL 0.0 MM
TIME 254.400 SEC.

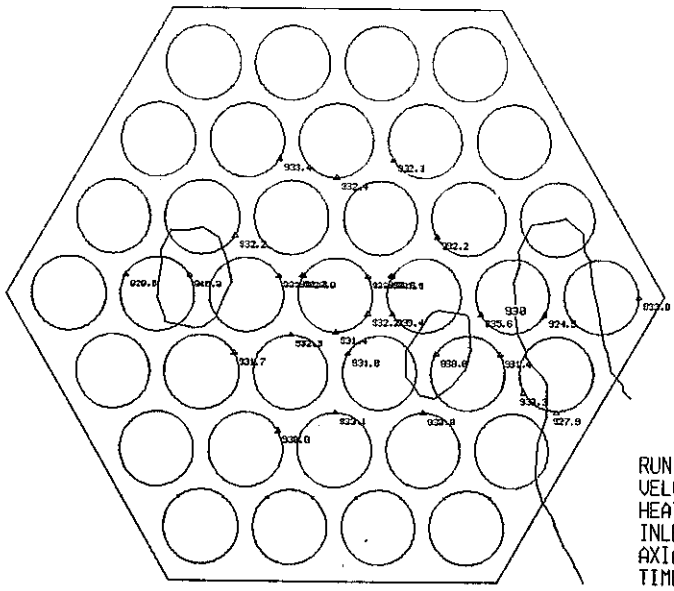

RUN NAME 37(37)LHF-217
VELOCITY 0.251 M/S
HEAT FLUX 20.56 W/CM2
INLET TEMP. 488.4 C
AXIAL 0.0 MM
TIME 460.800 SEC.

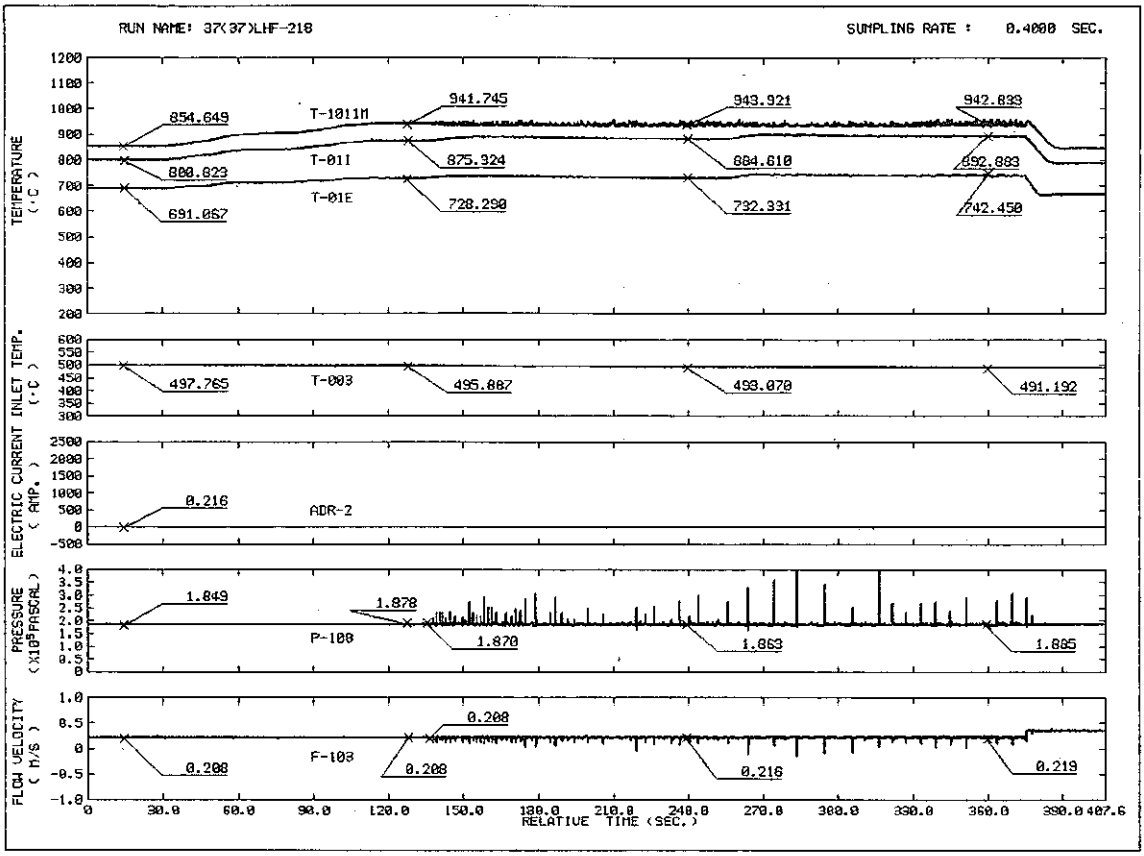
RUN NAME: 37(37)LHF-218
SUMPLING RATE : 0.4000 SEC.
TEMPERATURE (°C)
T-1011M
T-011
T-01E
854.649
941.745
943.921
942.833
800.823
875.324
884.810
892.883
691.067
728.290
732.331
742.450
INLET TEMP. (°C)
T-003
497.765
495.887
493.070
491.192
ELECTRIC CURRENT (AMP.)
ADR-2
0.216
PRESSURE (X10⁴PASCAL)
P-100
1.849
1.878
1.870
1.863
1.885
FLOW VELOCITY (M/S)
F-103
0.208
0.208
0.208
0.216
0.219
RELATIVE TIME (SEC.)

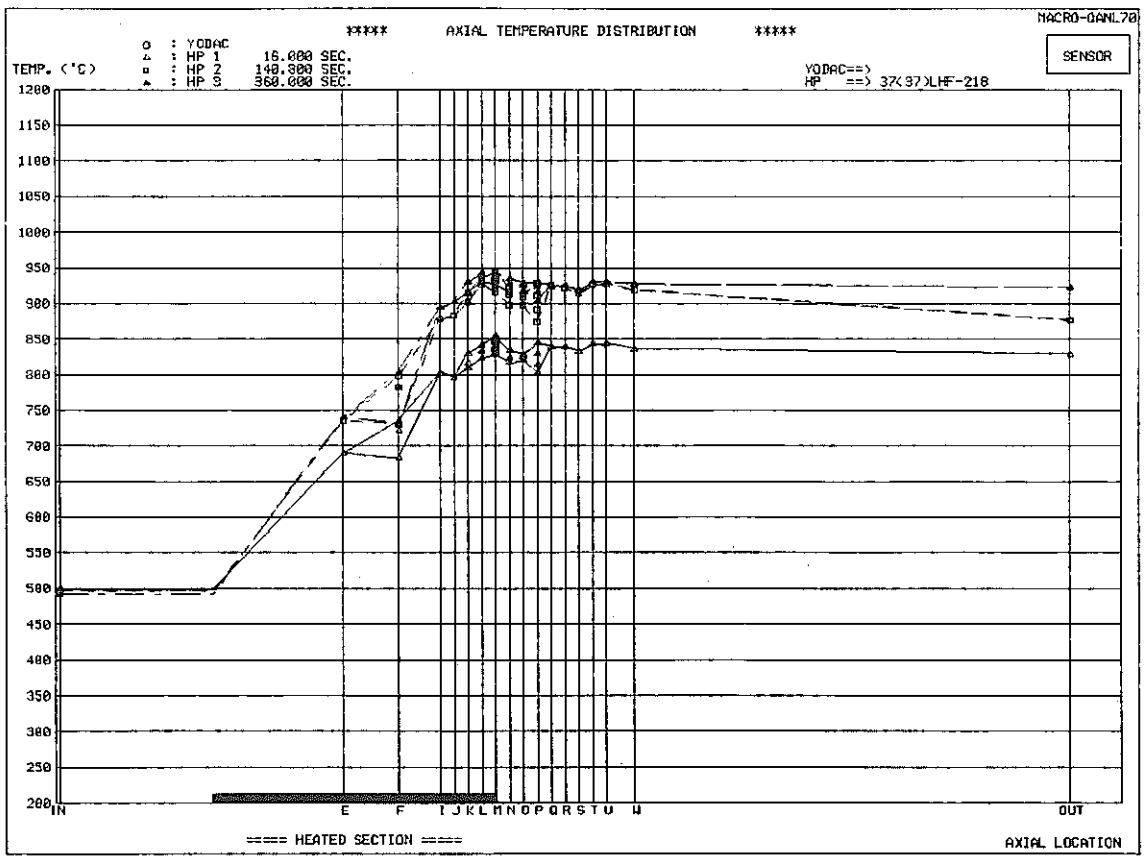
MACRO-GANL70
***** AXIAL TEMPERATURE DISTRIBUTION *****
SENSOR
○ : YODAC
△ : HP 1 16.000 SEC.
□ : HP 2 140.000 SEC.
▲ : HP 3 360.000 SEC.
TEMP. (°C)
YODAC==)
HP ==) 37(37)LHF-218
IN
E F I J K L M N O P Q R S T U W
OUT
==== HEATED SECTION ====
AXIAL LOCATION

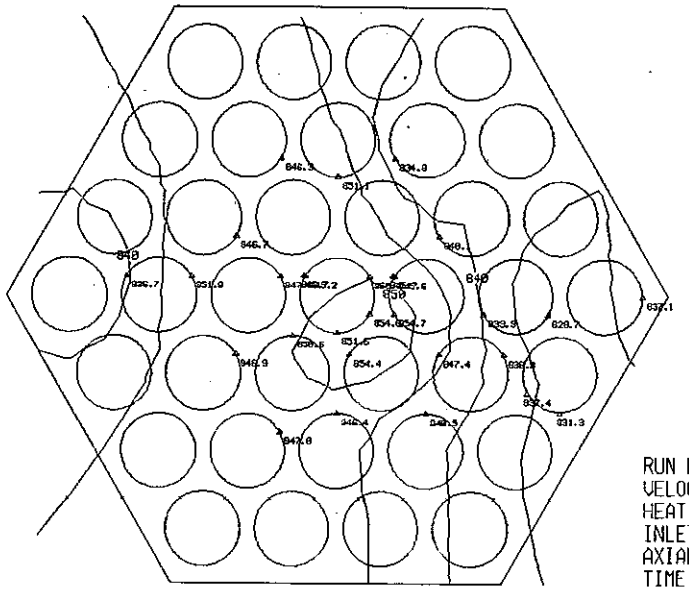

RUN NAME 37(37)LHF-218
VELOCITY 0.223 M/S
HEAT FLUX 14.66 W/CM2
INLET TEMP. 498.7 C
AXIAL 0.0 MM
TIME 16.000 SEC.

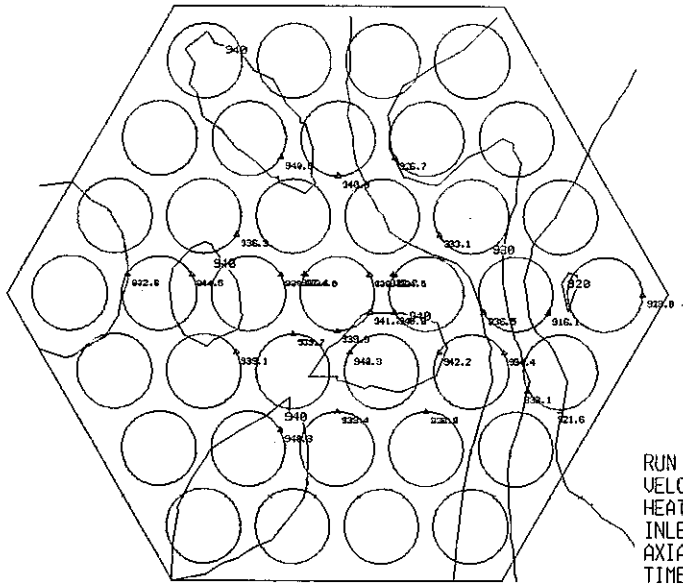

RUN NAME 37(37)LHF-218
VELOCITY 0.223 M/S
HEAT FLUX 19.93 W/CM2
INLET TEMP. 495.9 C
AXIAL 0.0 MM
TIME 140.800 SEC.

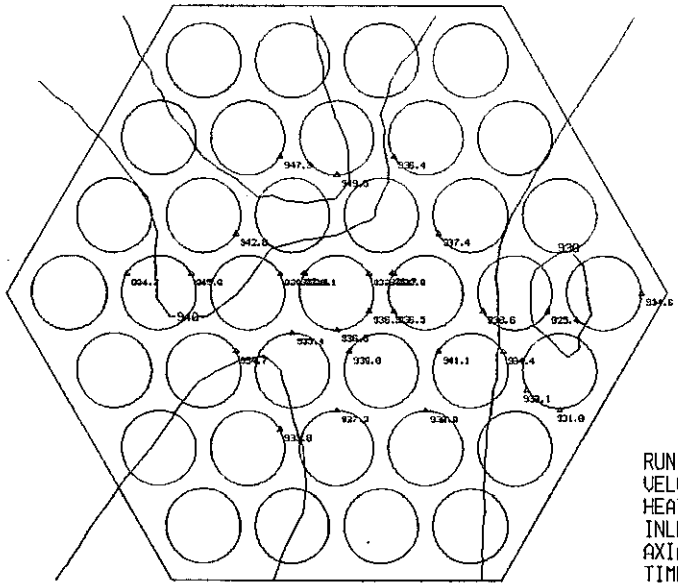

RUN NAME 37(37)LHF-218
VELOCITY 0.231 M/S
HEAT FLUX 20.70 W/CM2
INLET TEMP. 493.1 C
AXIAL 0.0 MM
TIME 360.000 SEC.

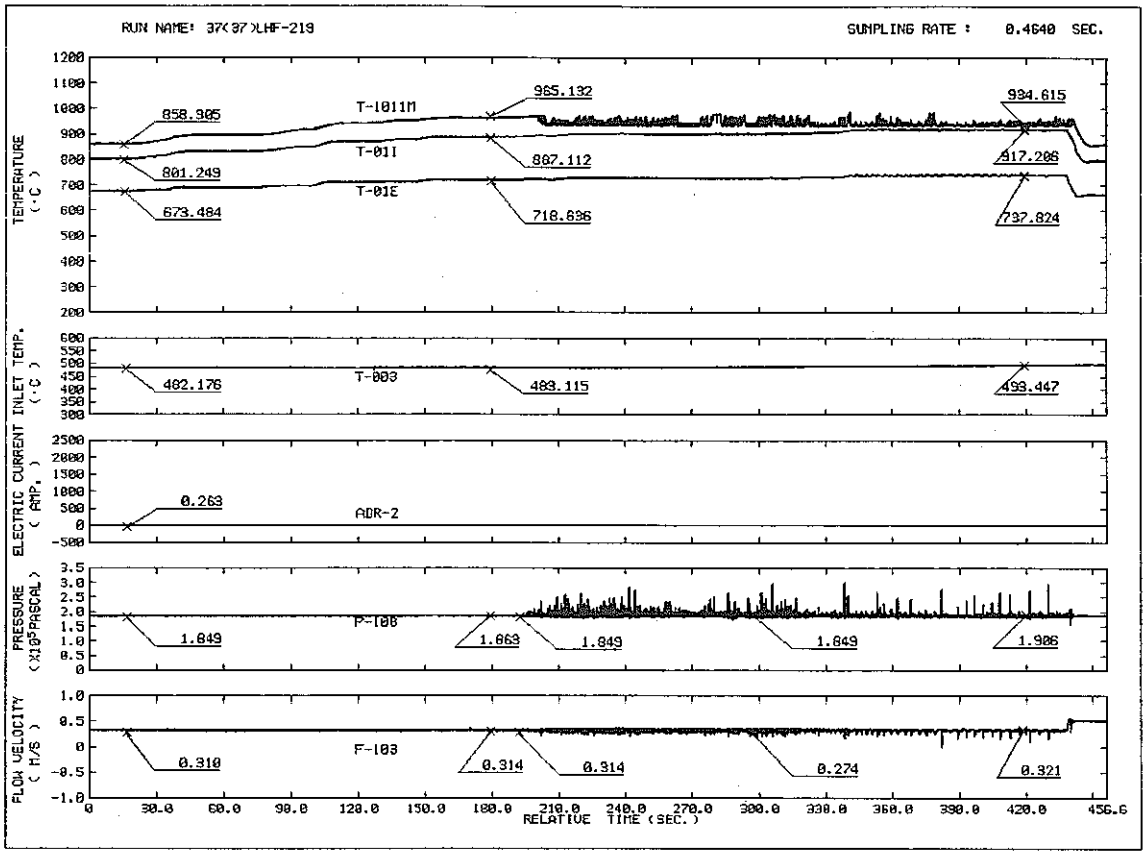
RUN NAME: 37(37)LHF-219
SAMPLING RATE : 0.4640 SEC.
TEMPERATURE (°C)
T-1011M
T-011I
T-01IE
858.305
985.132
934.615
801.249
887.112
917.206
673.484
718.696
737.824
INLET TEMP. (°C)
T-003
482.176
483.115
498.447
ELECTRIC CURRENT (AMP.)
ADR-2
0.263
PRESSURE (X10⁵PASCAL)
P-108
1.849
1.663
1.849
1.849
1.986
FLOW VELOCITY (M/S)
F-103
0.310
0.314
0.314
0.274
0.321
RELATIVE TIME (SEC.)

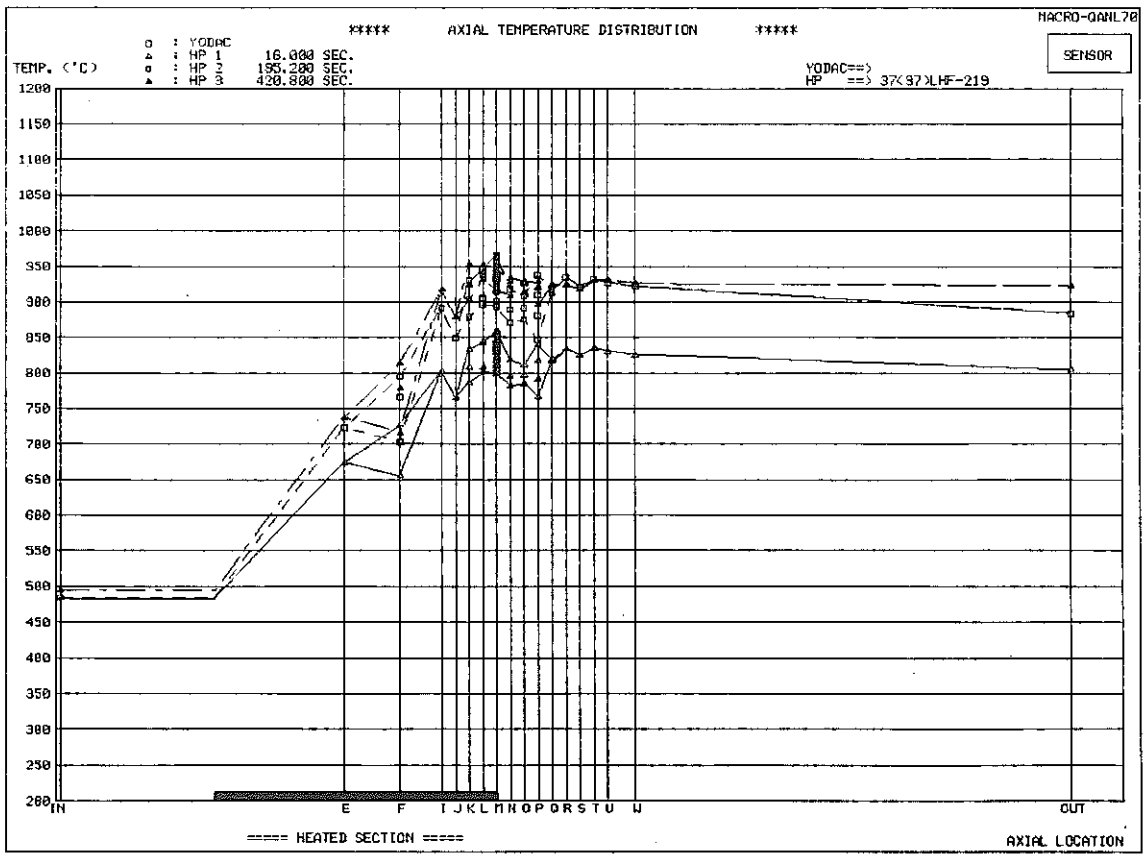
MACRO-QANL70
SENSOR
***** AXIAL TEMPERATURE DISTRIBUTION *****
○ : YODAC
△ : HP 1 16.000 SEC.
□ : HP 2 195.200 SEC.
▲ : HP 3 420.800 SEC.
TEMP. (°C)
YODAC==)
HP ==) 37(37)LHF-219
IN
E F I J K L M N O P Q R S T U W
OUT
===== HEATED SECTION =====
AXIAL LOCATION

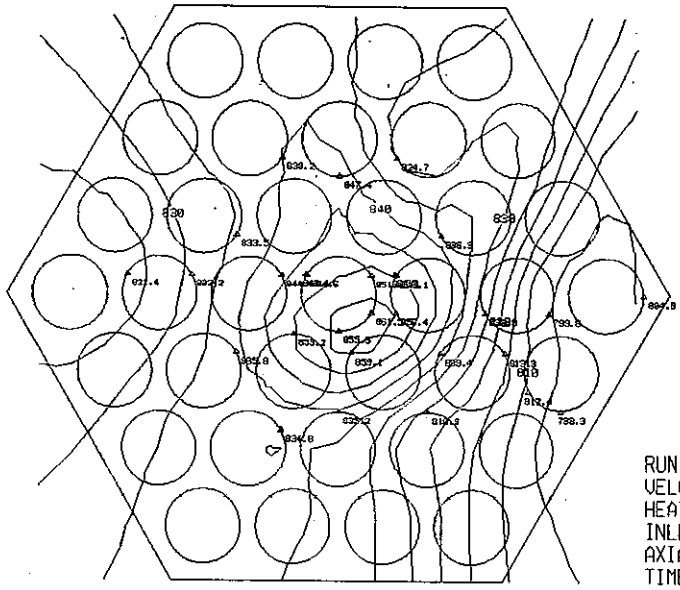

RUN NAME 37(37)LHF-219
VELOCITY 0.321 M/S
HEAT FLUX 21.55 W/CM2
INLET TEMP. 483.1 C
AXIAL 0.0 MM
TIME 16.000 SEC.

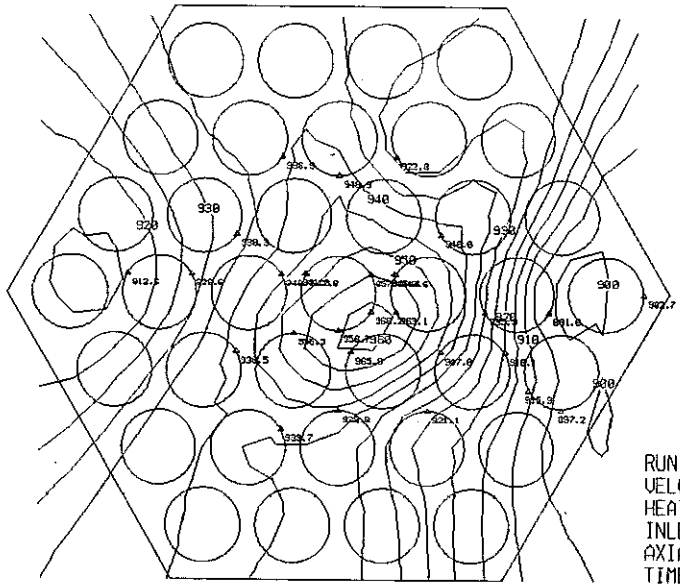

RUN NAME 37(37)LHF-219
VELOCITY 0.321 M/S
HEAT FLUX 28.73 W/CM2
INLET TEMP. 484.1 C
AXIAL 0.0 MM
TIME 195.200 SEC.

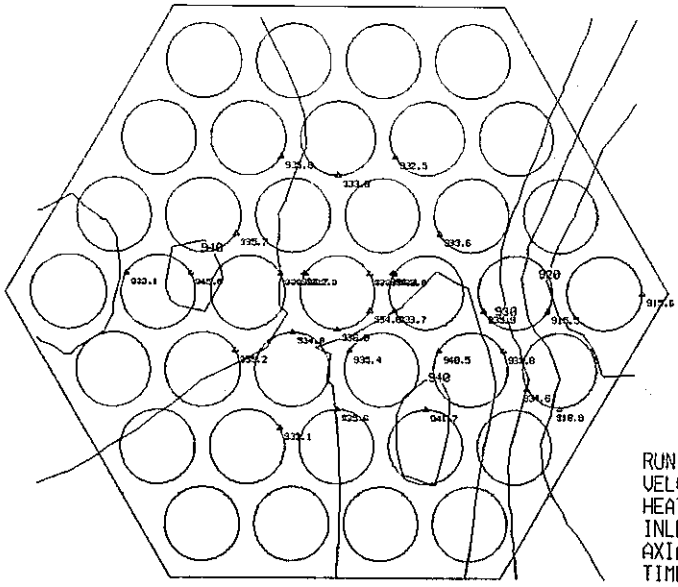

RUN NAME 37(37)LHF-219
VELOCITY 0.337 M/S
HEAT FLUX 29.75 W/CM2
INLET TEMP. 495.3 C
AXIAL 0.0 MM
TIME 420.800 SEC.

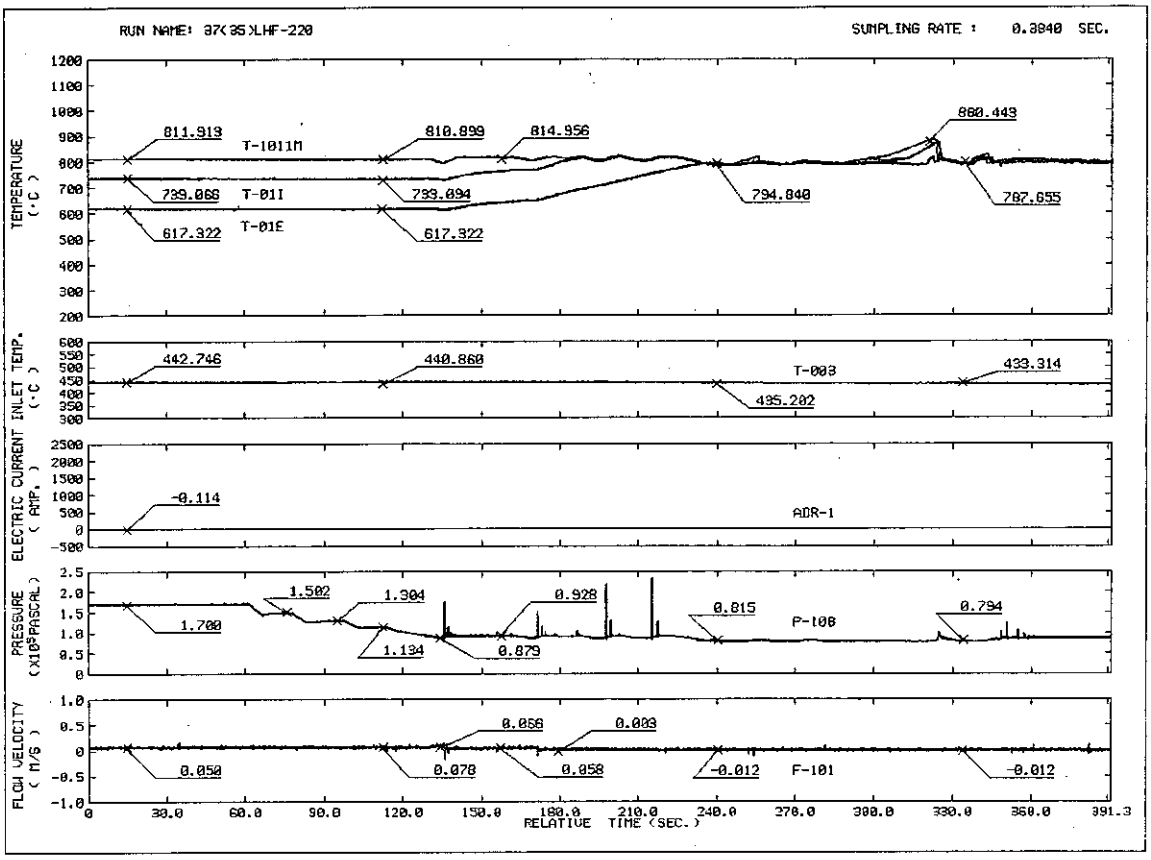
RUN NAME: 37(35)LHF-220
SUMPLING RATE : 0.3840 SEC.
TEMPERATURE (°C)
811.913
T-1011M
810.899
814.956
860.443
739.068
T-01I
733.094
794.840
787.655
617.322
T-01E
617.322
INLET TEMP. (°C)
442.746
440.868
T-003
433.314
435.202
ELECTRIC CURRENT (AMP.)
-0.114
ADR-1
PRESSURE (X10⁵PASCAL)
1.700
1.502
1.304
0.928
0.815
P-108
0.794
1.134
0.879
FLOW VELOCITY (M/S)
0.050
0.078
0.058
0.058
0.009
-0.012
F-101
-0.012
RELATIVE TIME (SEC.)

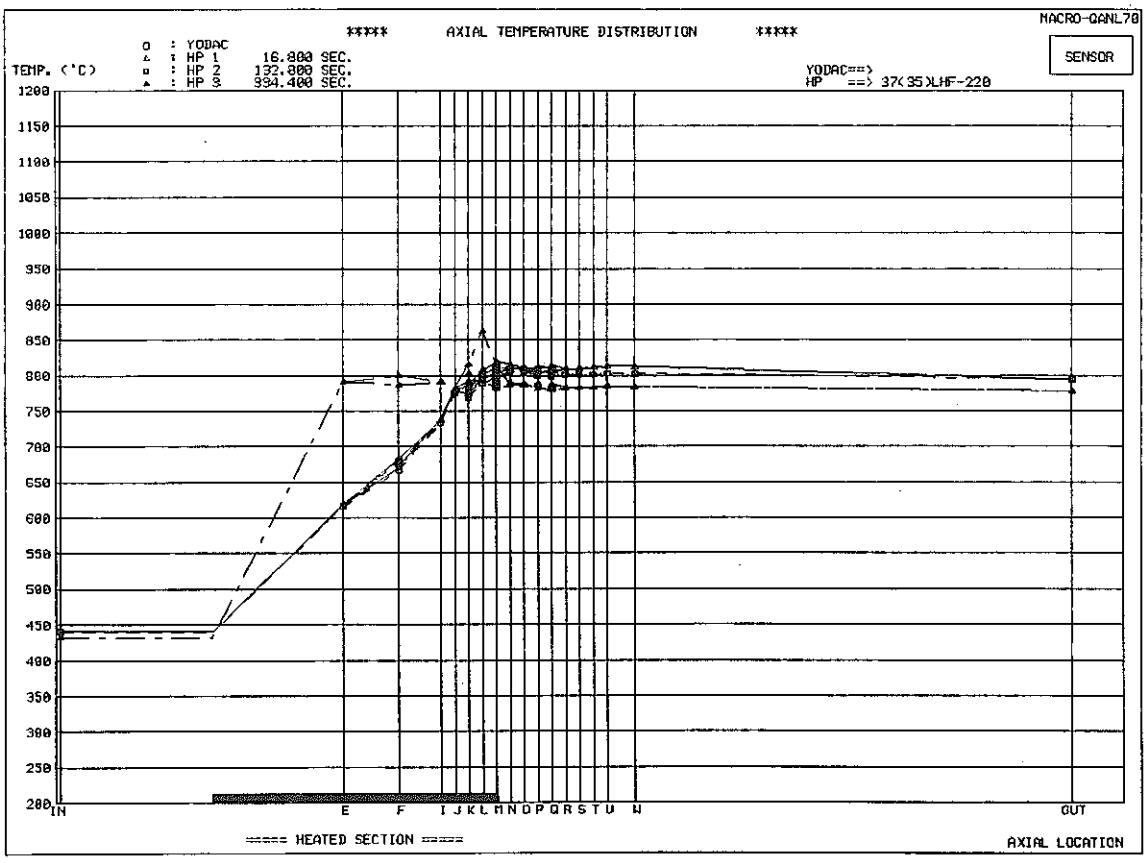
MACRO-QANL70
SENSOR
***** AXIAL TEMPERATURE DISTRIBUTION *****
O : YODAC
Δ : HP 1 16.800 SEC.
□ : HP 2 132.800 SEC.
▲ : HP 3 994.400 SEC.
TEMP. (°C)
YODAC==>
HP ==> 37(35)LHF-220
IN
E F I J K L M N O P Q R S T U W
OUT
===== HEATED SECTION =====
AXIAL LOCATION

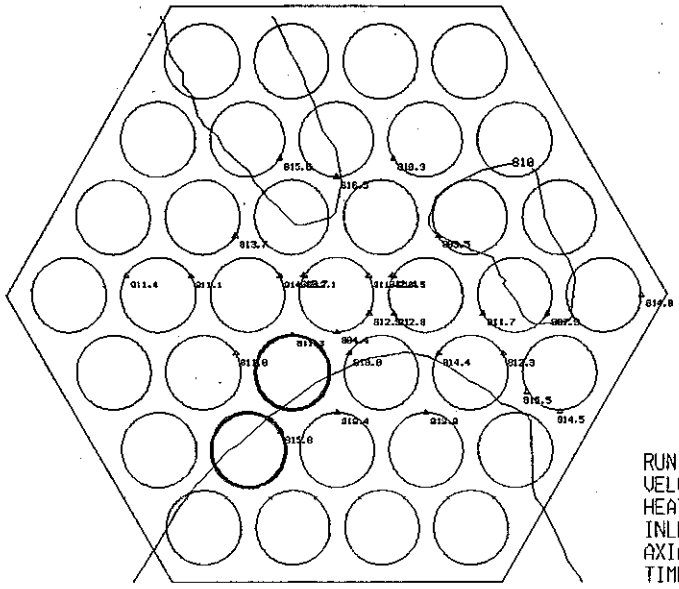

RUN NAME 37(35)LHF-220
VELOCITY 0.0 M/S
HEAT FLUX 4.81 W/CM2
INLET TEMP. 441.8 C
AXIAL 0.0 MM
TIME 16.000 SEC.

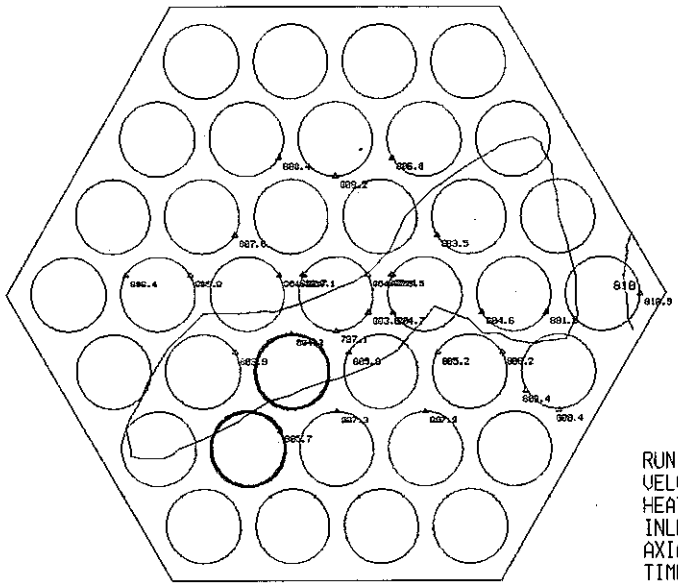

RUN NAME 37(35)LHF-220
VELOCITY 0.0 M/S
HEAT FLUX 4.81 W/CM2
INLET TEMP. 440.9 C
AXIAL 0.0 MM
TIME 132.800 SEC.

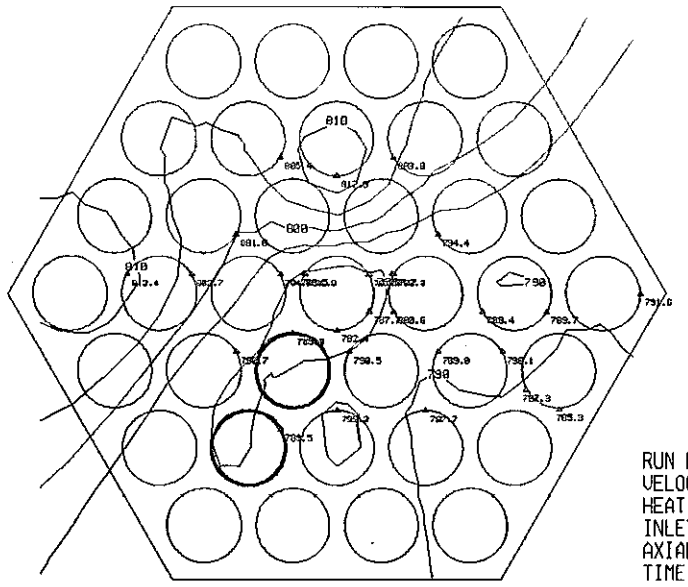

RUN NAME 37(35)LHF-220
VELOCITY 0.0 M/S
HEAT FLUX 4.81 W/CM2
INLET TEMP. 432.4 C
AXIAL 0.0 MM
TIME 334.400 SEC.

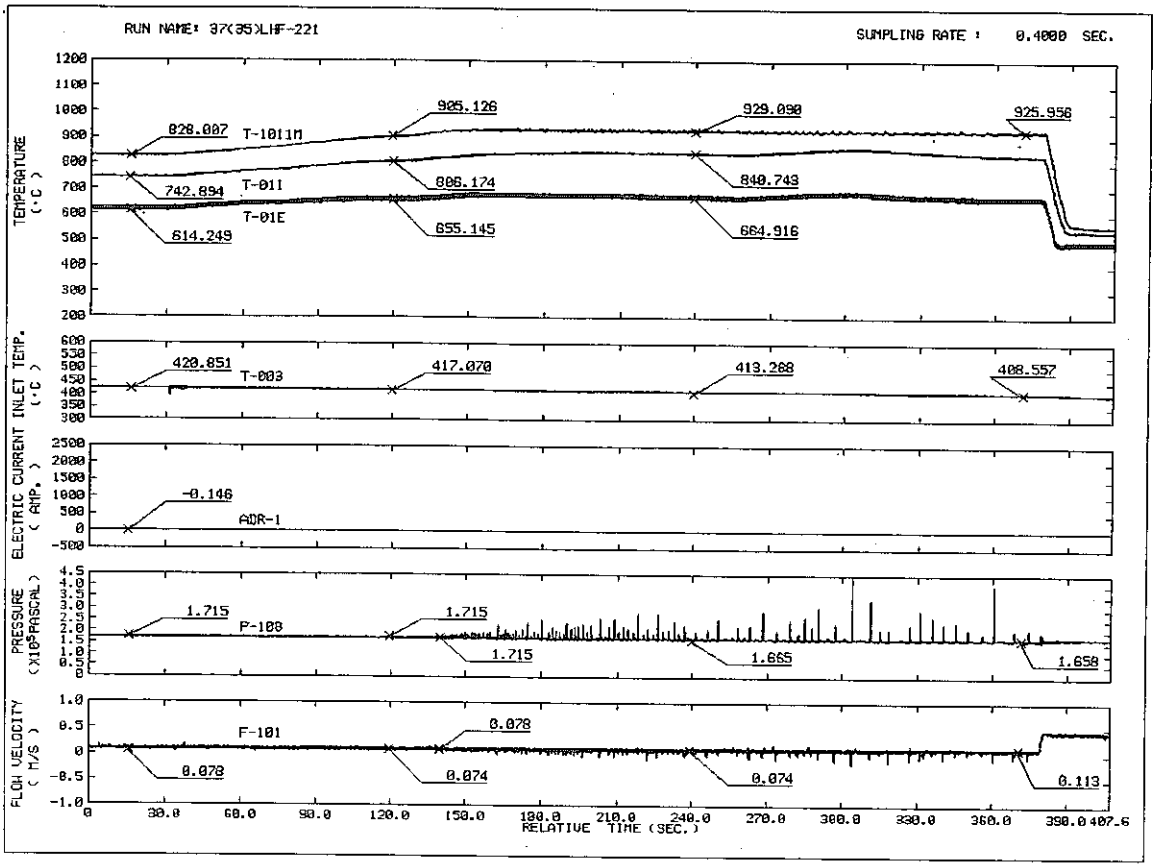
RUN NAME: 37(35)LHF-221
SUMPLING RATE : 0.4000 SEC.
TEMPERATURE ('C)
828.007
T-1011M
905.126
929.090
925.956
742.894
T-011
T-01E
806.174
840.743
814.249
655.145
684.916
ELECTRIC CURRENT INLET TEMP. ('C)
420.851
T-003
417.070
413.268
408.557
-0.146
ADR-1
PRESSURE (X10⁵PASCAL)
1.715
P-108
1.715
1.715
1.665
1.658
FLOW VELOCITY (M/S)
F-101
0.078
0.078
0.074
0.074
0.113
RELATIVE TIME (SEC.)

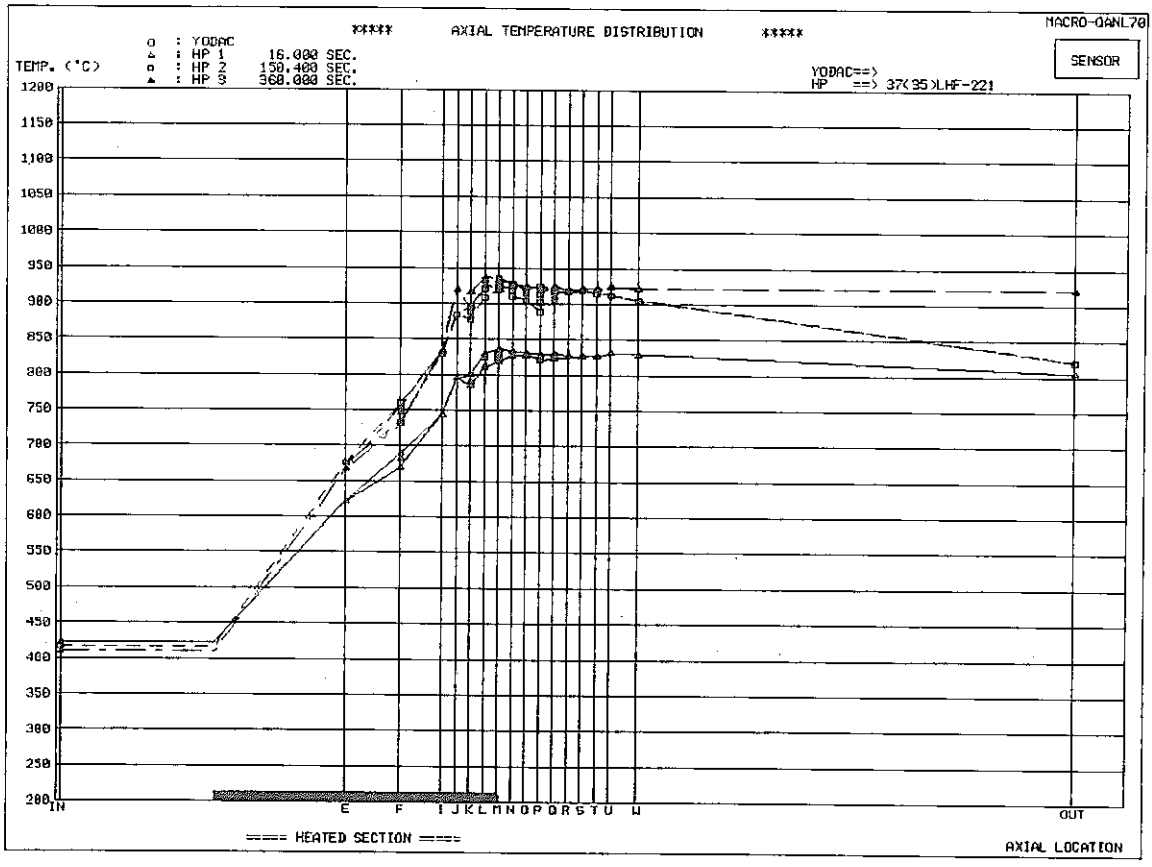
MACRO-QANL70
SENSOR
***** AXIAL TEMPERATURE DISTRIBUTION *****
o : YODAC
Δ : HP 1 16.000 SEC.
□ : HP 2 150.400 SEC.
▲ : HP 3 360.000 SEC.
TEMP. ('C)
YODAC==>
HP ==> 37(35)LHF-221
IN
E F I J K L M N O P Q R S T U W
OUT
==== HEATED SECTION ====
AXIAL LOCATION

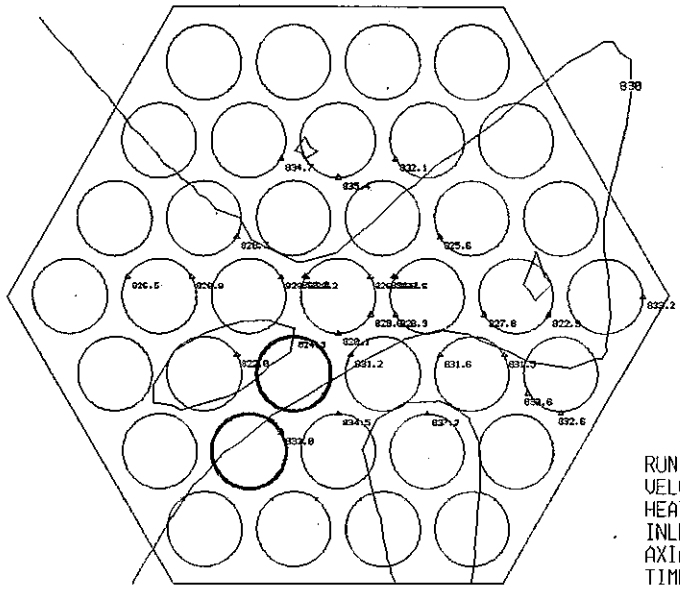

RUN NAME 37(35)LHF-221
VELOCITY 0.0 M/S
HEAT FLUX 7.88 W/CM2
INLET TEMP. 422.7 C
AXIAL 0.0 MM
TIME 16.000 SEC.

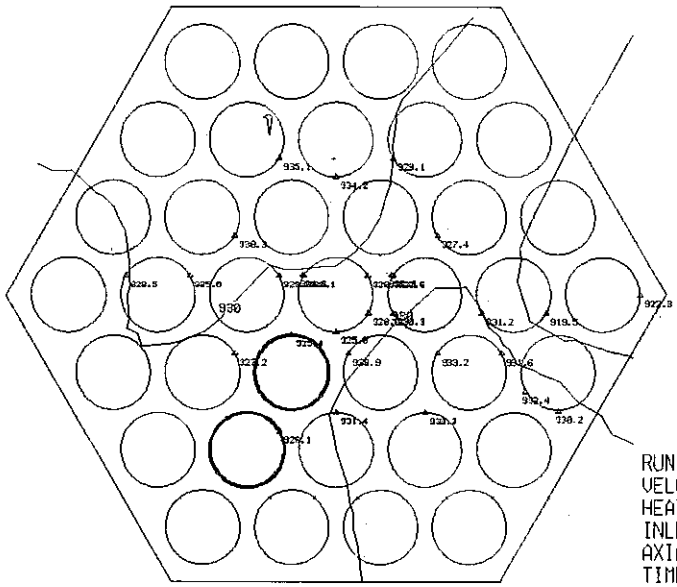

RUN NAME 37(35)LHF-221
VELOCITY 0.0 M/S
HEAT FLUX 10.87 W/CM2
INLET TEMP. 417.1 C
AXIAL 0.0 MM
TIME 150.400 SEC.

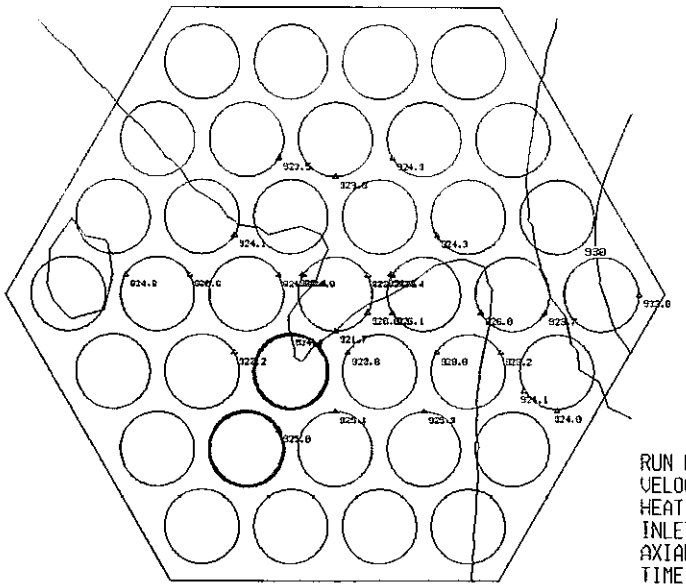

RUN NAME 37(35)LHF-221
VELOCITY 0.0 M/S
HEAT FLUX 12.00 W/CM2
INLET TEMP. 409.5 C
AXIAL 0.0 MM
TIME 360.000 SEC.

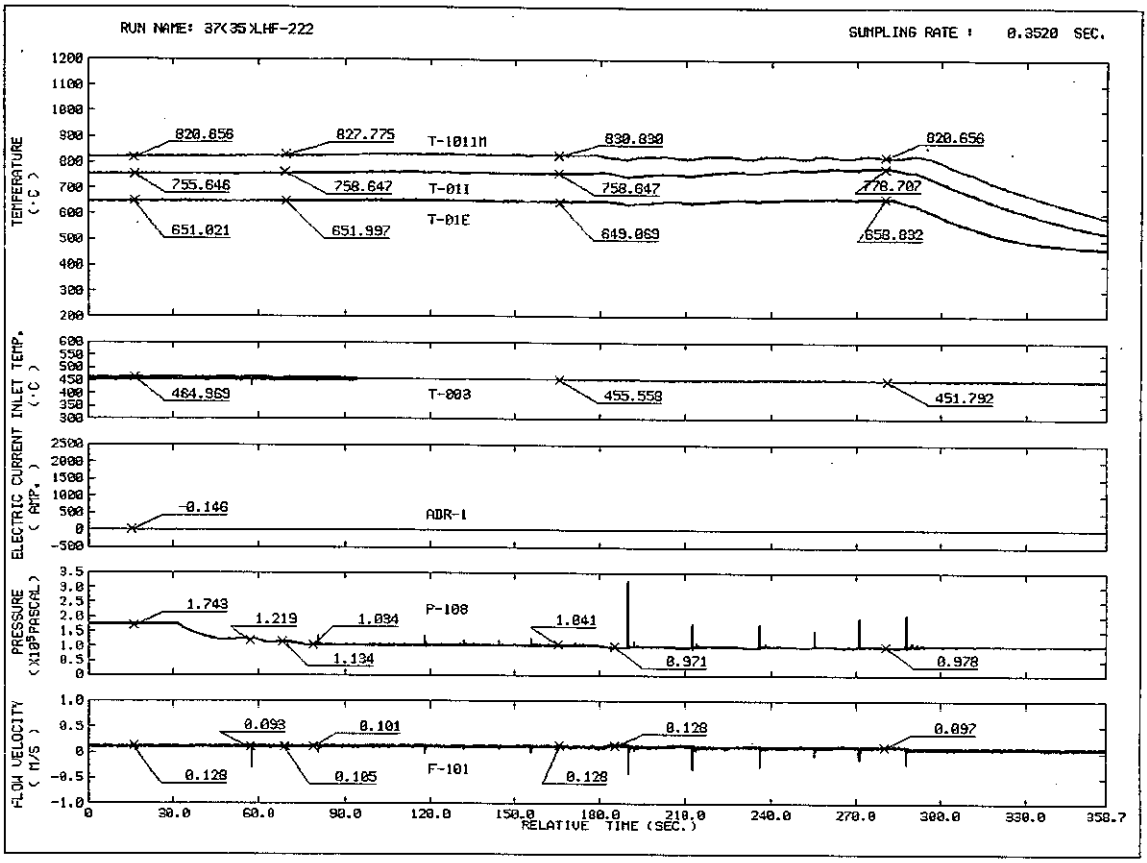
RUN NAME: 37(35)LHF-222
SAMPLING RATE : 0.3520 SEC.
TEMPERATURE (°C)
820.856
827.775
T-1011M
830.830
820.656
755.646
758.647
T-011I
758.647
778.707
651.021
651.997
T-01IE
649.069
658.832
ELECTRIC CURRENT INLET TEMP. (°C)
484.969
T-003
455.559
451.792
(AMP.)
-0.146
ADR-1
PRESSURE (X10⁵PASCAL)
1.743
1.219
1.094
P-108
1.841
1.134
0.971
0.978
FLOW VELOCITY (M/S)
0.093
0.101
0.128
0.097
0.128
0.105
F-101
0.128
RELATIVE TIME (SEC.)

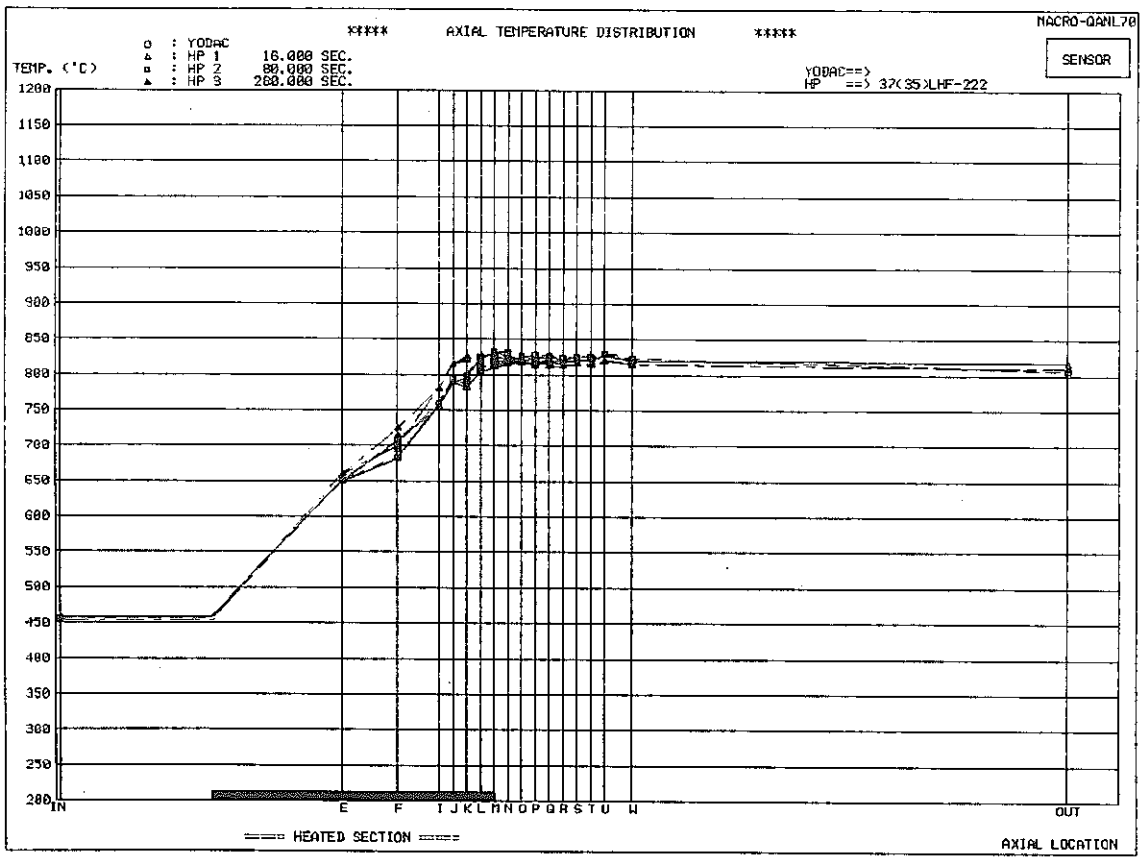
***** AXIAL TEMPERATURE DISTRIBUTION *****
MACRO-QANL70
SENSOR
o : YODAC
Δ : HP 1 16.000 SEC.
□ : HP 2 80.000 SEC.
▲ : HP 3 280.000 SEC.
TEMP. (°C)
YODAC==>
HP ==> 37(35)LHF-222
IN
E F I J K L M N O P Q R S T U W
OUT
==== HEATED SECTION ====
AXIAL LOCATION

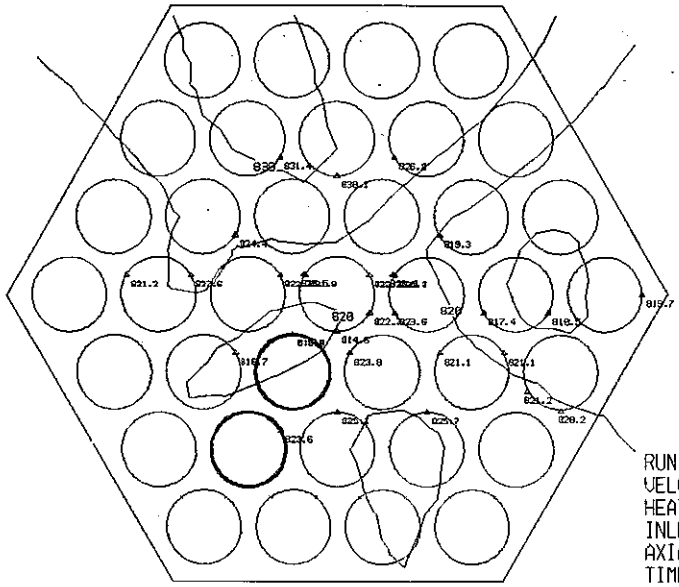

RUN NAME 37(35)LHF-222
VELOCITY 0.0 M/S
HEAT FLUX 9.14 W/CM2
INLET TEMP. 465.0 C
AXIAL 0.0 MM
TIME 16.000 SEC.

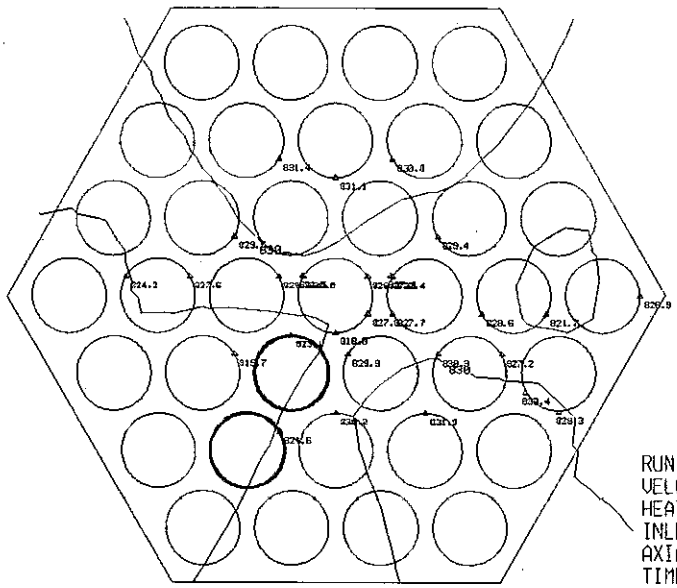

RUN NAME 37(35)LHF-222
VELOCITY 0.0 M/S
HEAT FLUX 9.23 W/CM2
INLET TEMP. 458.4 C
AXIAL 0.0 MM
TIME 80.000 SEC.

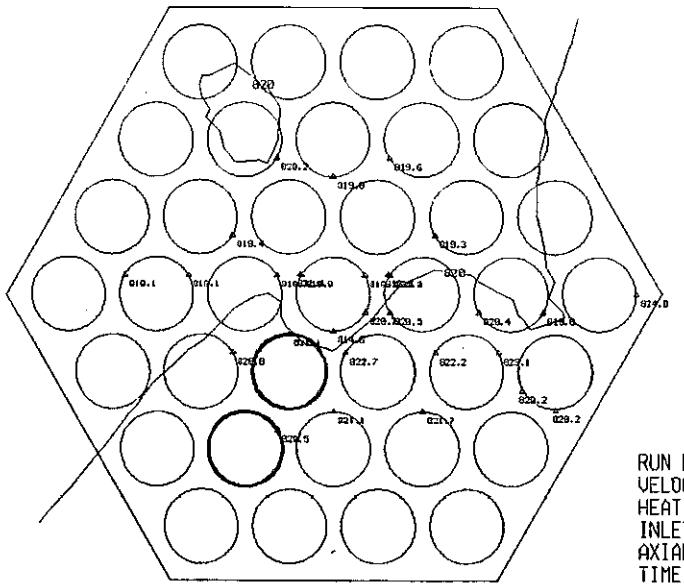

RUN NAME 37(35)LHF-222
VELOCITY 0.0 M/S
HEAT FLUX 9.08 W/CM2
INLET TEMP. 453.7 C
AXIAL 0.0 MM
TIME 280.000 SEC.

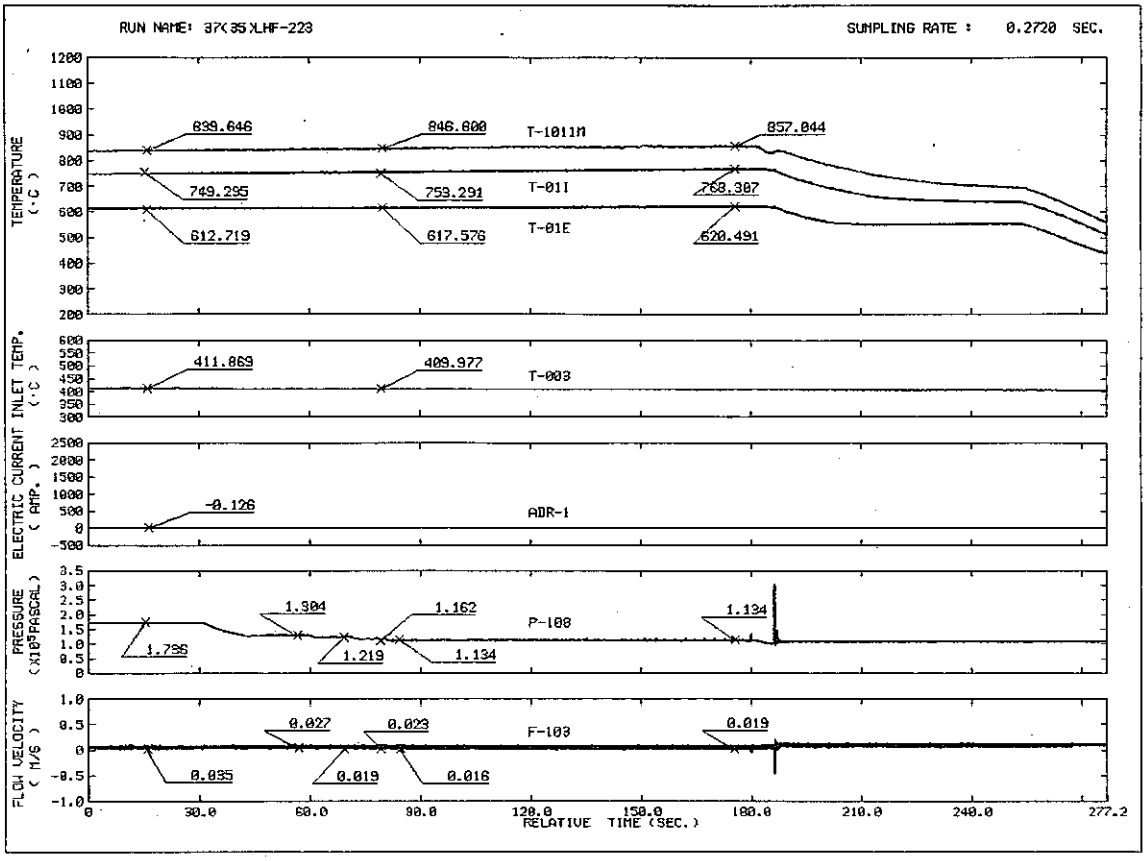
RUN NAME: 37(35)LHF-223
SAMPLING RATE : 0.2720 SEC.
TEMPERATURE (°C)
899.646
846.600
T-1011M
857.044
749.295
759.291
T-011
768.387
612.719
617.576
T-01E
620.491
INLET TEMP. (°C)
411.869
409.977
T-003
ELECTRIC CURRENT (AMP.)
-0.126
ADR-1
PRESSURE (X10⁵PASCAL)
1.736
1.384
1.219
1.162
1.134
P-108
1.134
FLOW VELOCITY (M/S)
0.035
0.027
0.019
0.023
0.016
F-103
0.019
RELATIVE TIME (SEC.)

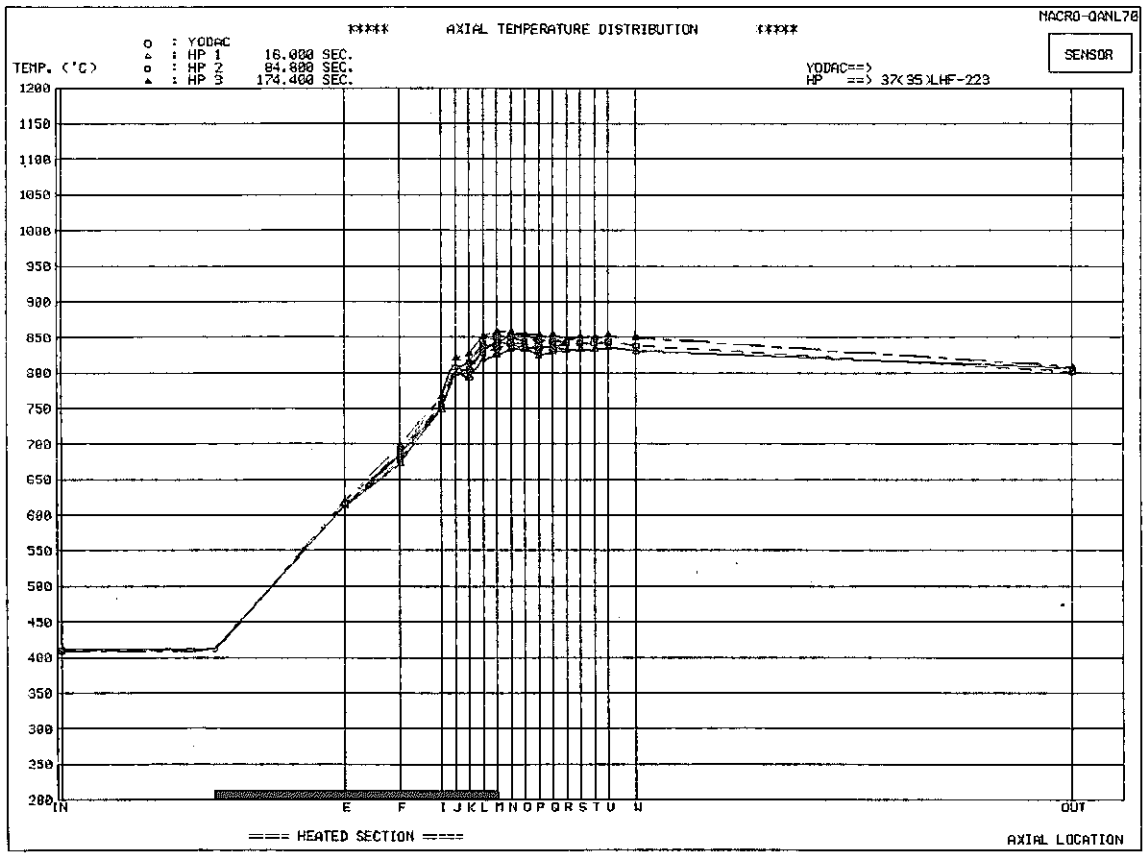
MACRO-QANL78
***** AXIAL TEMPERATURE DISTRIBUTION *****
SENSOR
○ : YODAC
△ : HP 1 16.000 SEC.
□ : HP 2 84.800 SEC.
▲ : HP 3 174.400 SEC.
TEMP. (°C)
YODAC==>
HP ==> 37(35)LHF-223
IN
E F I J K L M N O P Q R S T U V
OUT
==== HEATED SECTION ====
AXIAL LOCATION

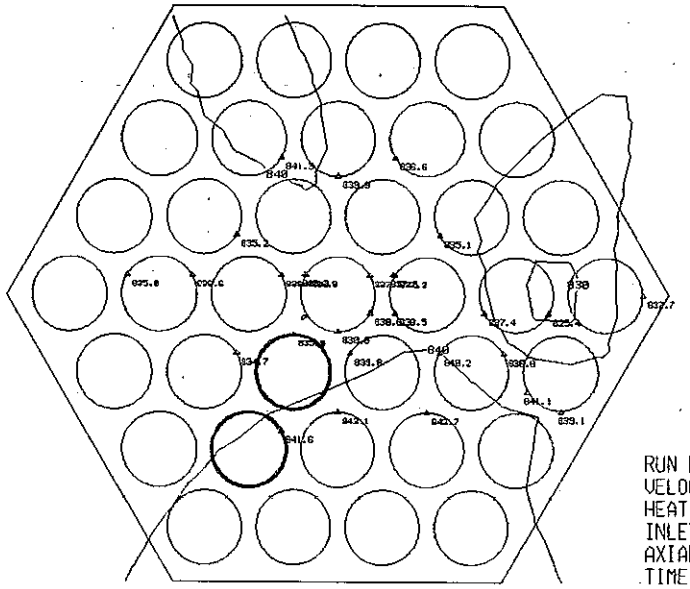

RUN NAME 37(35)LHF-223
VELOCITY 0.059 M/S
HEAT FLUX 6.72 W/CM2
INLET TEMP. 410.9 C
AXIAL 0.0 MM
TIME 16.000 SEC.

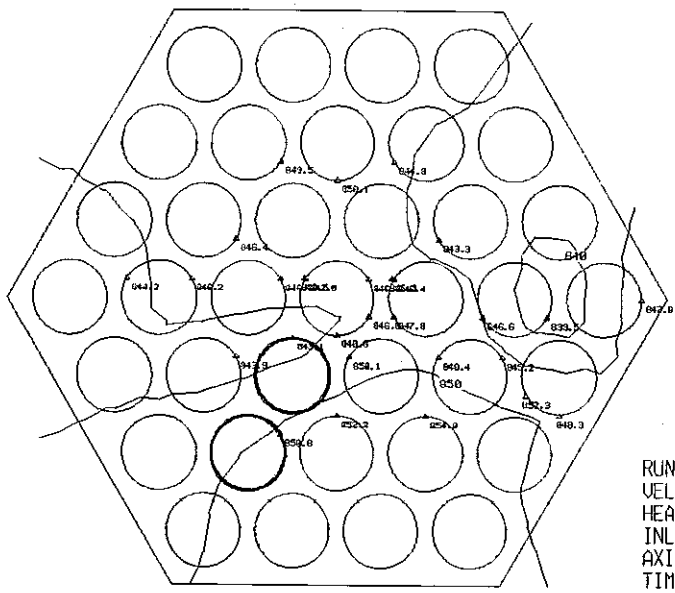

RUN NAME 37(35)LHF-223
VELOCITY 0.051 M/S
HEAT FLUX 6.68 W/CM2
INLET TEMP. 410.0 C
AXIAL 0.0 MM
TIME 84.800 SEC.

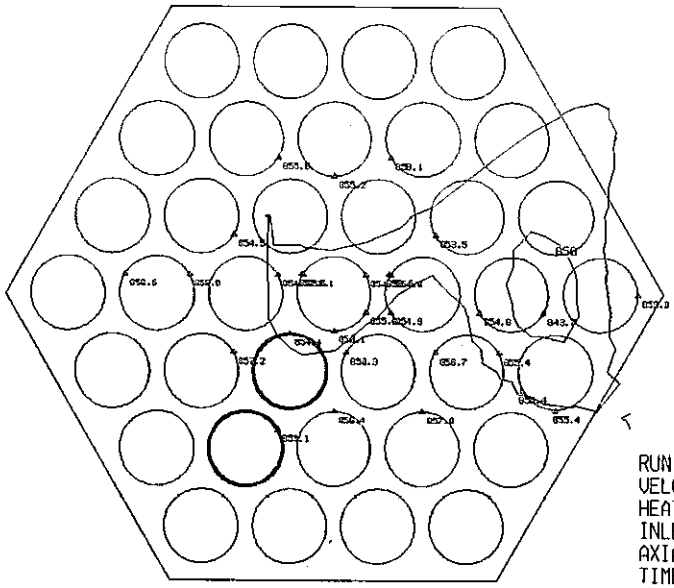

RUN NAME 37(35)LHF-223
VELOCITY 0.070 M/S
HEAT FLUX 6.68 W/CM2
INLET TEMP. 407.1 C
AXIAL 0.0 MM
TIME 174.400 SEC.

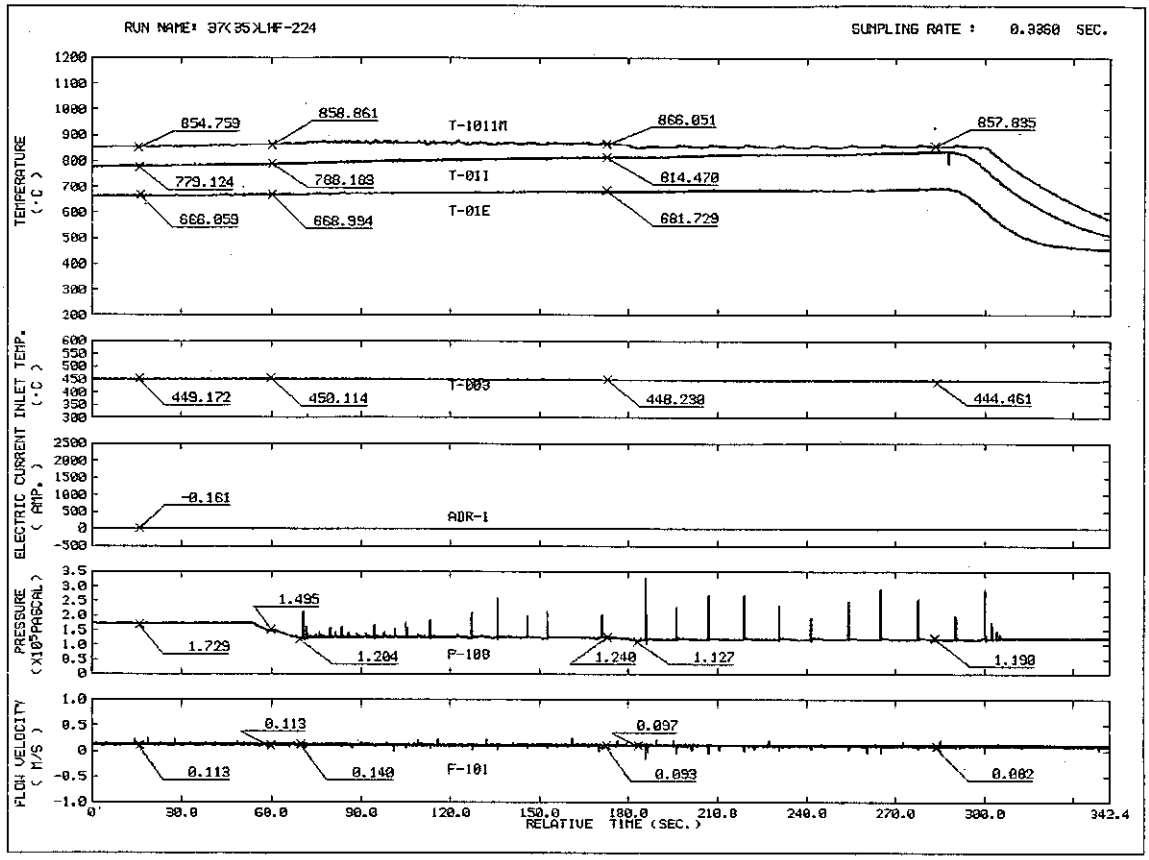
RUN NAME: 37X35XLHF-224
SUMPLING RATE : 0.3360 SEC.
TEMPERATURE (°C)
854.759
858.861
T-1011M
866.051
857.835
779.124
788.168
T-011
814.470
668.059
668.994
T-01E
681.729
ELECTRIC CURRENT INLET TEMP. (°C)
449.172
450.114
T-003
448.238
444.461
(AMP.)
-0.161
ADR-1
PRESSURE (X10⁵PASCAL)
1.495
1.729
1.204
P-100
1.240
1.127
1.190
FLOW VELOCITY (M/S)
0.113
0.097
0.113
0.140
F-101
0.093
0.082
RELATIVE TIME (SEC.)

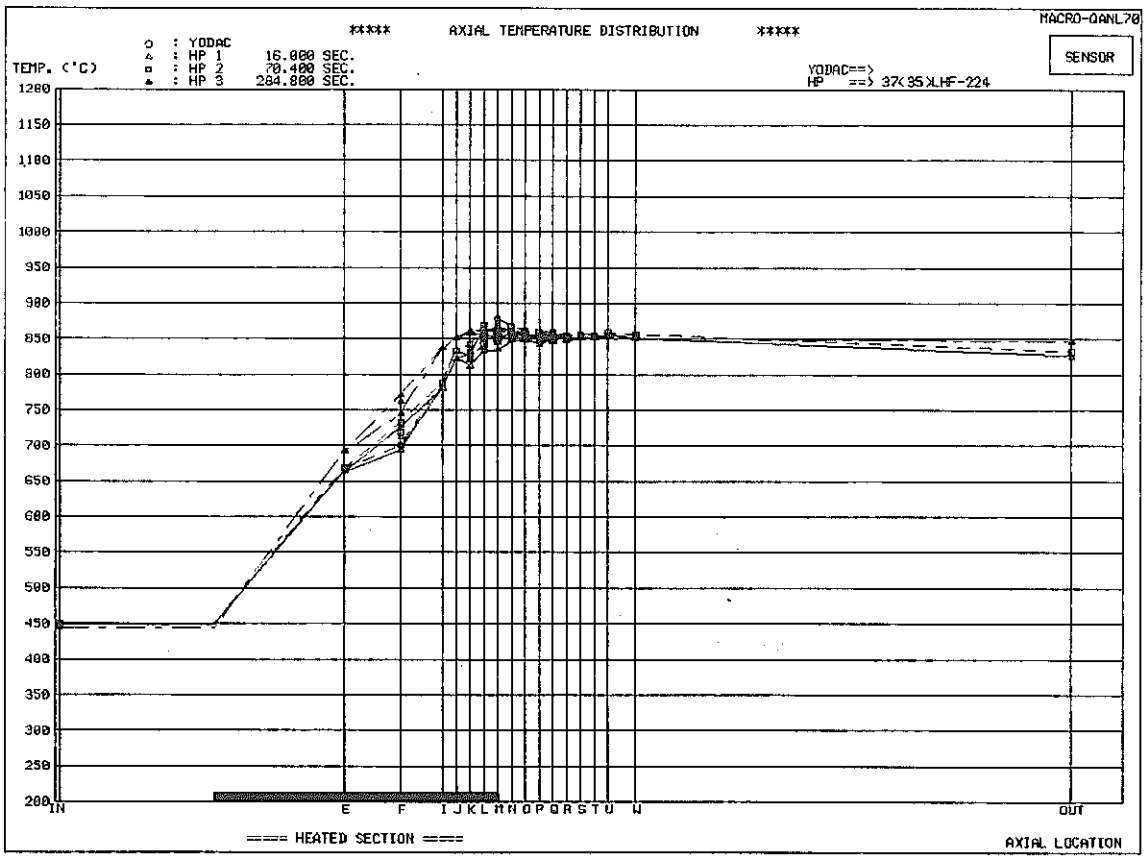
***** AXIAL TEMPERATURE DISTRIBUTION *****
MACRO-QANL70
SENSOR
○ : YODAC
△ : HP 1 16.000 SEC.
□ : HP 2 70.400 SEC.
◇ : HP 3 284.800 SEC.
TEMP. ('C)
YODAC==>
HP ==> 37X35XLHF-224
IN
E F I J K L M N O P Q R S T U W
OUT
==== HEATED SECTION ====
AXIAL LOCATION

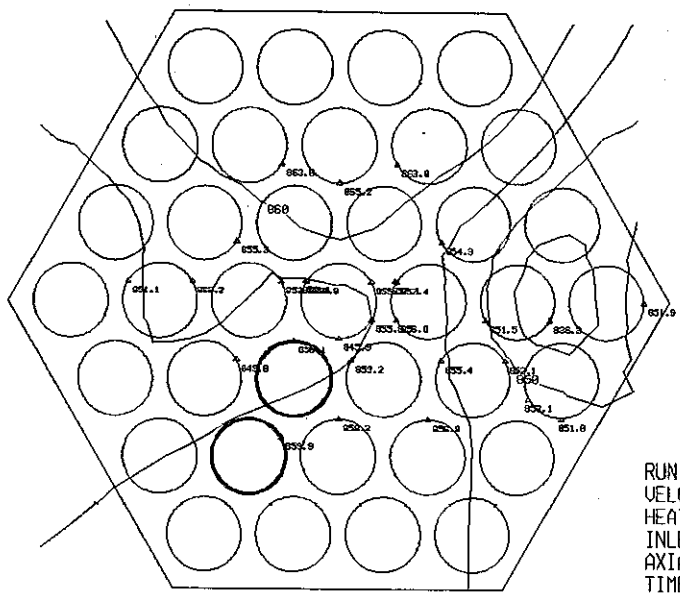

RUN NAME 37(35)LHF-224
VELOCITY 0.0 M/S
HEAT FLUX 11.50 W/CM2
INLET TEMP. 449.2 C
AXIAL 0.0 MM
TIME 16.000 SEC.

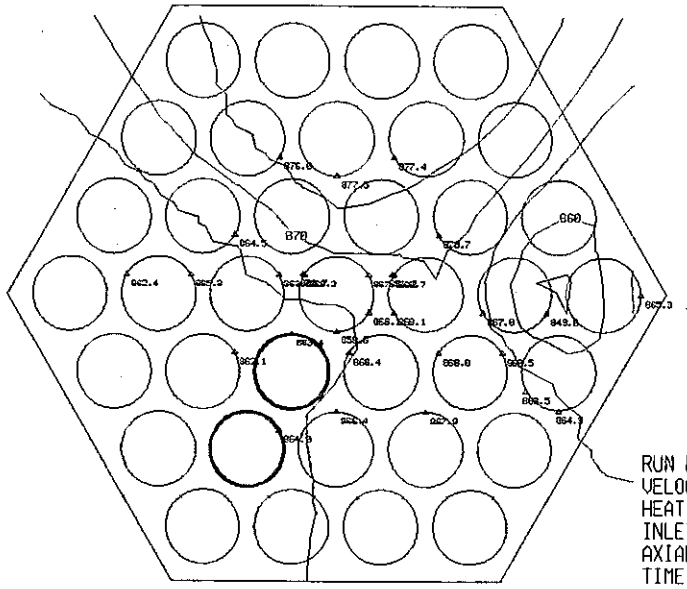

RUN NAME 37(35)LHF-224
VELOCITY 0.0 M/S
HEAT FLUX 11.36 W/CM2
INLET TEMP. 450.1 C
AXIAL 0.0 MM
TIME 70.400 SEC.

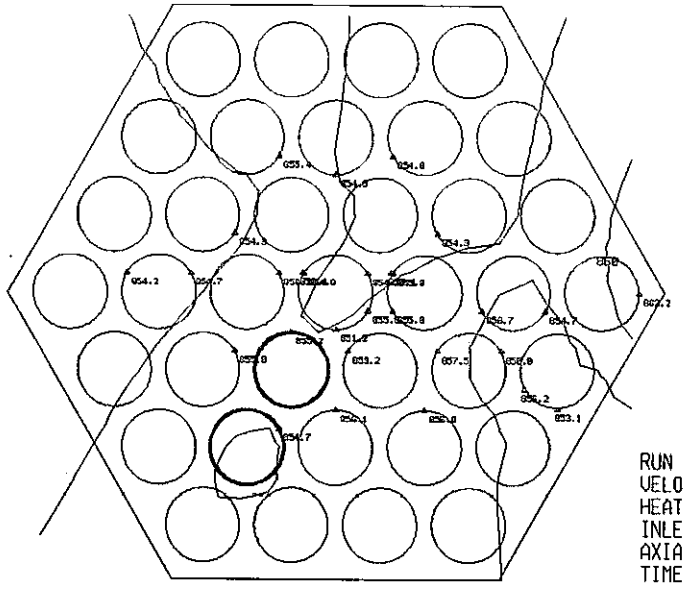

RUN NAME 37(35)LHF-224
VELOCITY 0.0 M/S
HEAT FLUX 11.25 W/CM2
INLET TEMP. 445.4 C
AXIAL 0.0 MM
TIME 284.800 SEC.

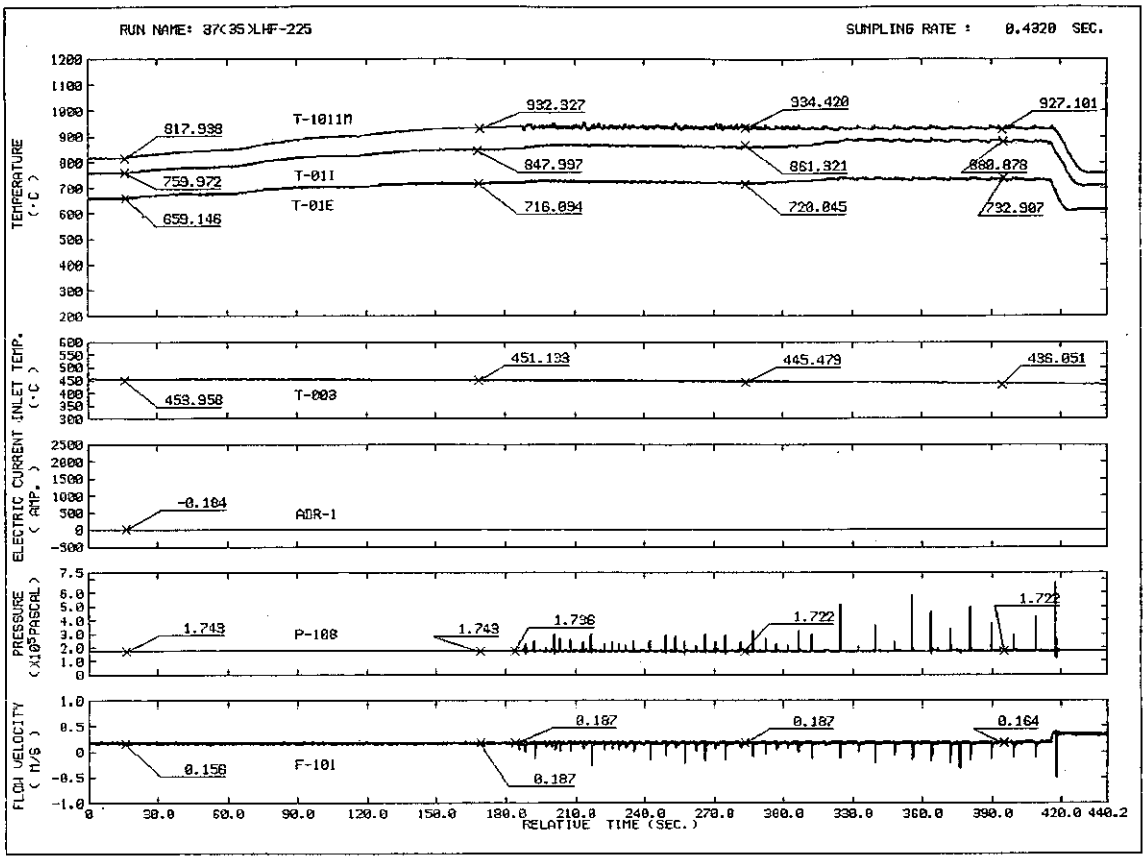
RUN NAME: 37(35)LHF-225
SAMPLING RATE : 0.4320 SEC.
TEMPERATURE (°C)
817.938
T-1011M
932.327
934.420
927.101
759.972
T-011
847.997
861.321
880.878
659.146
T-01E
716.094
720.845
732.907
INLET TEMP. (°C)
453.958
T-003
451.133
445.479
436.051
ELECTRIC CURRENT (AMP.)
-0.184
ADR-1
PRESSURE (X10⁵PASCAL)
1.743
P-108
1.743
1.736
1.722
1.722
FLOW VELOCITY (M/S)
0.156
F-101
0.187
0.187
0.187
0.164
RELATIVE TIME (SEC.)

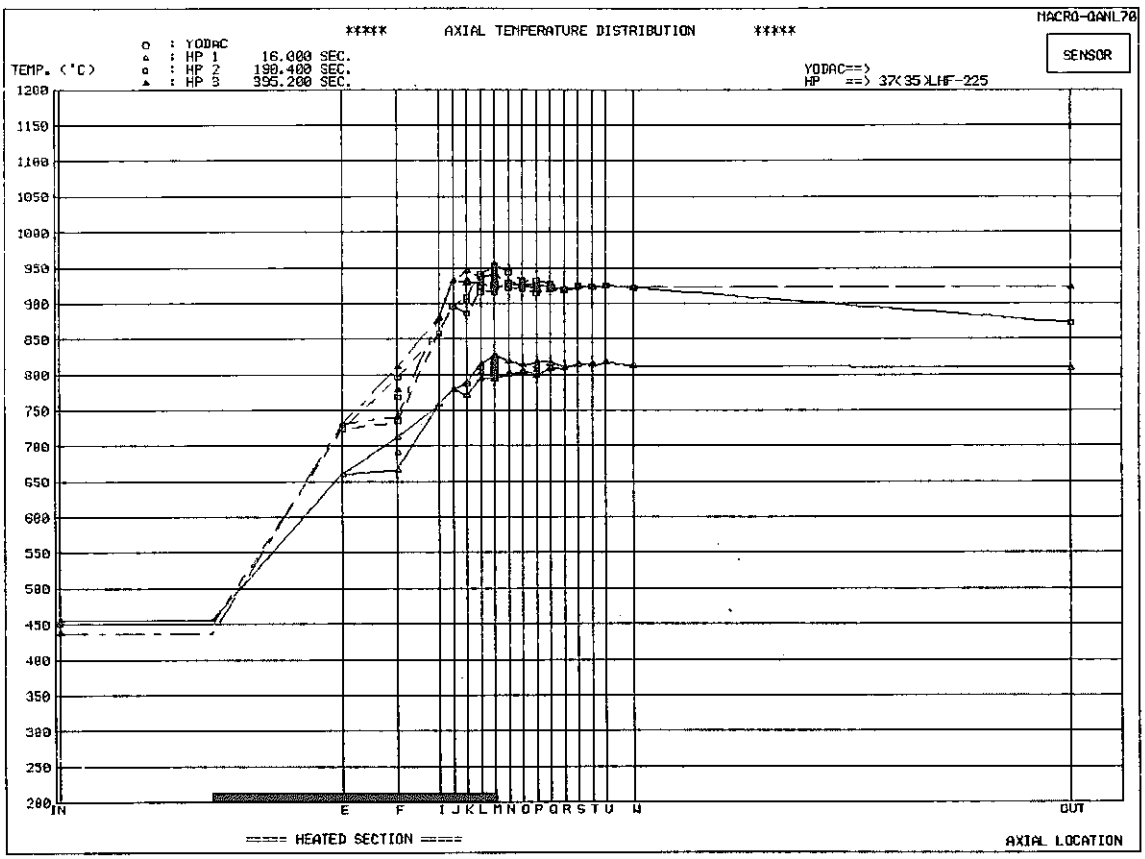
MACRO-QANL70
***** AXIAL TEMPERATURE DISTRIBUTION *****
SENSOR
o : YODAC
Δ : HP 1 16.000 SEC.
□ : HP 2 198.400 SEC.
▲ : HP 3 395.200 SEC.
TEMP. (°C)
YODAC==>
HP ==> 37(35)LHF-225
IN
E F I J K L M N O P Q R S T U W
OUT
==== HEATED SECTION ====
AXIAL LOCATION

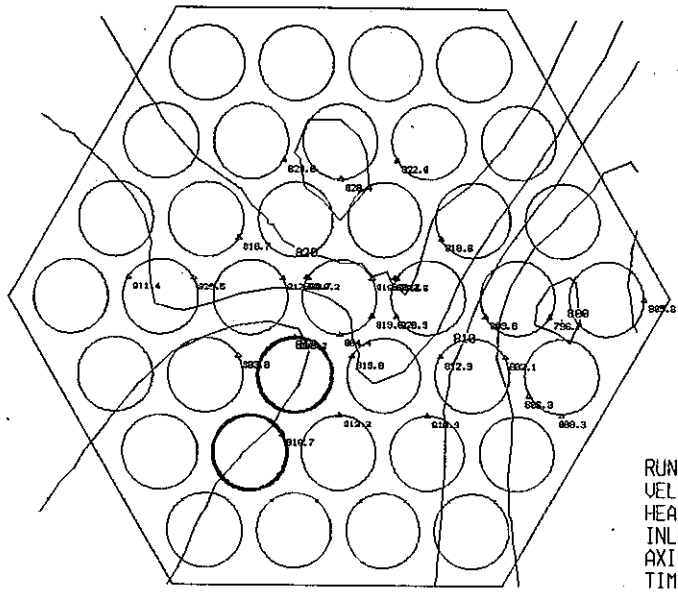

RUN NAME 37(35)LHF-225
VELOCITY 0.0 M/S
HEAT FLUX 13.62 W/CM2
INLET TEMP. 454.9 C
AXIAL 0.0 MM
TIME 16.000 SEC.

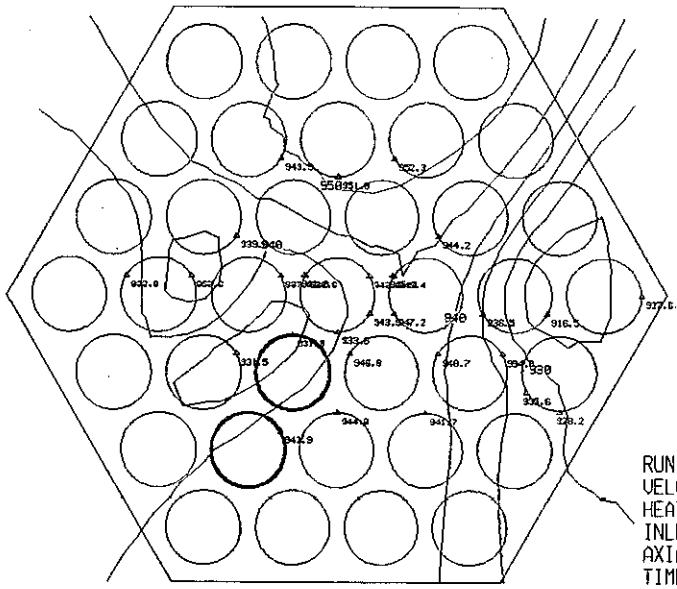

RUN NAME 37(35)LHF-225
VELOCITY 0.0 M/S
HEAT FLUX 18.90 W/CM2
INLET TEMP. 450.2 C
AXIAL 0.0 MM
TIME 190.400 SEC.

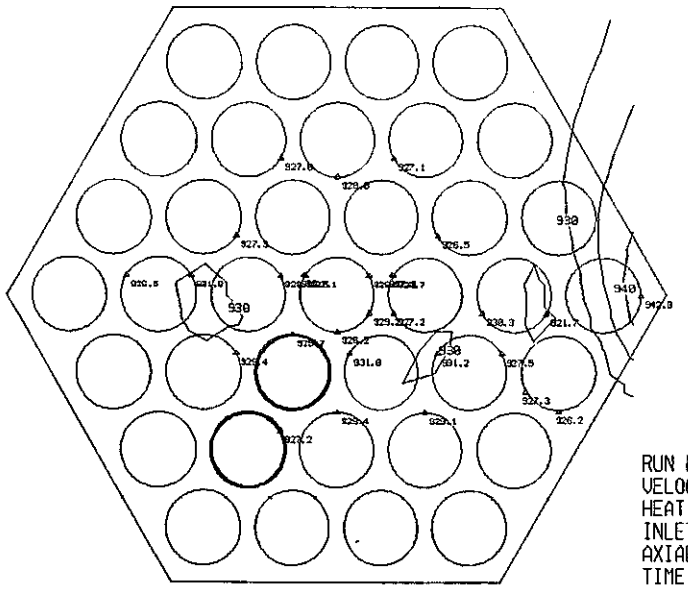

RUN NAME 37(35)LHF-225
VELOCITY 0.0 M/S
HEAT FLUX 20.77 W/CM2
INLET TEMP. 437.9 C
AXIAL 0.0 MM
TIME 395.200 SEC.

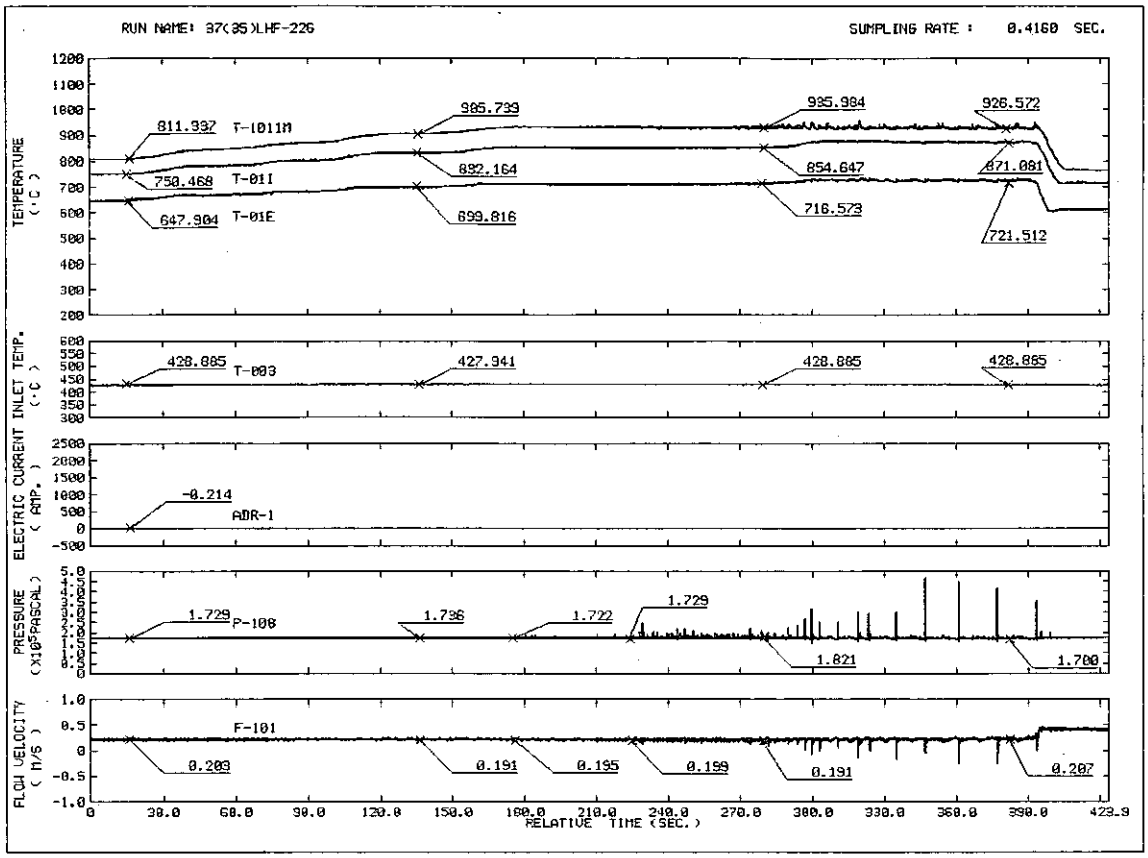
RUN NAME: 37(35)LHF-226
SUMPLING RATE : 0.4160 SEC.
TEMPERATURE (°C)
811.937 T-1011M
750.468 T-01I
647.904 T-01E
985.739
892.164
699.816
935.984
854.647
716.573
926.572
871.081
721.512
ELECTRIC CURRENT INLET TEMP. (°C)
428.885 T-003
427.941
428.885
428.885
(AMP.)
-0.214 ADR-1
PRESSURE (X10⁵PASCAL)
1.729 P-108
1.736
1.722
1.729
1.821
1.700
FLOW VELOCITY (M/S)
F-101
0.209
0.191
0.195
0.199
0.191
0.207
RELATIVE TIME (SEC.)

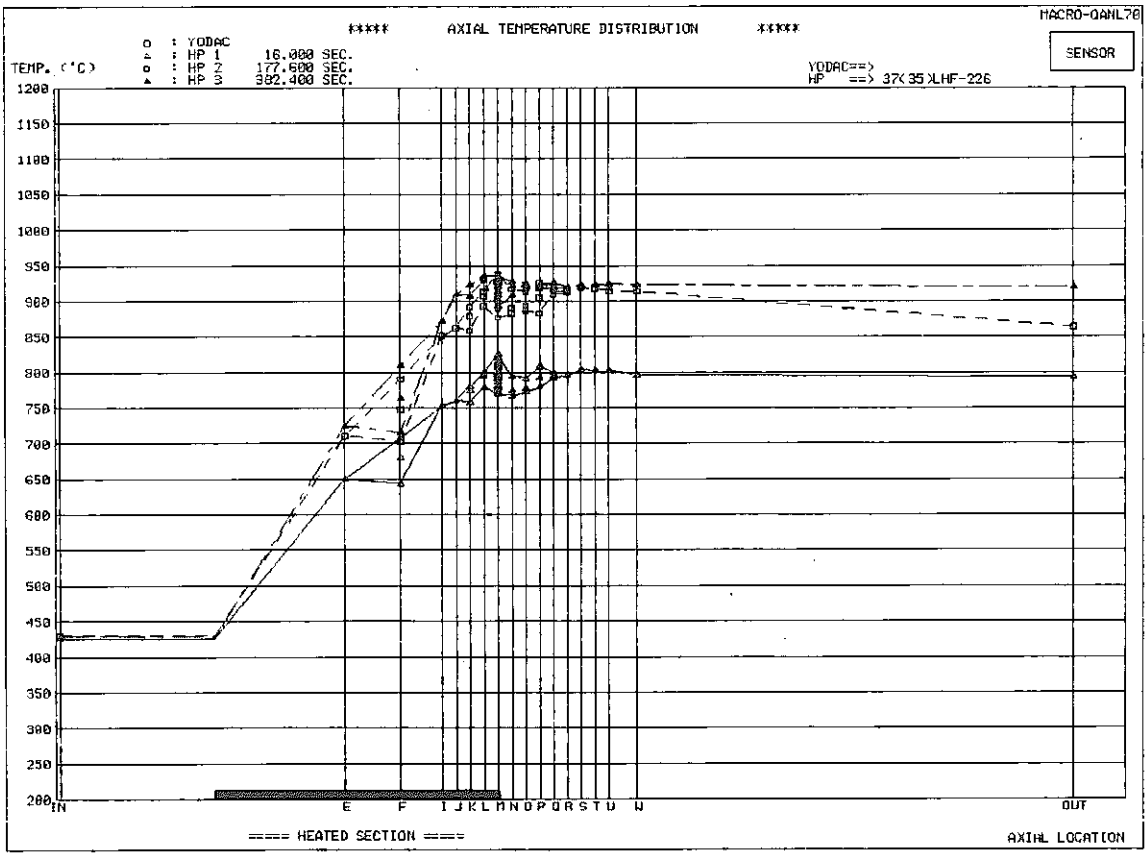
MACRO-QANL78
***** AXIAL TEMPERATURE DISTRIBUTION *****
SENSOR
o : YODAC
Δ : HP 1 16.000 SEC.
o : HP 2 177.600 SEC.
▲ : HP 3 382.400 SEC.
TEMP. (°C)
YODAC==>
HP ==> 37(35)LHF-226
IN
E F I J K L M N O P Q R S T U W
OUT
==== HEATED SECTION ====
AXIAL LOCATION

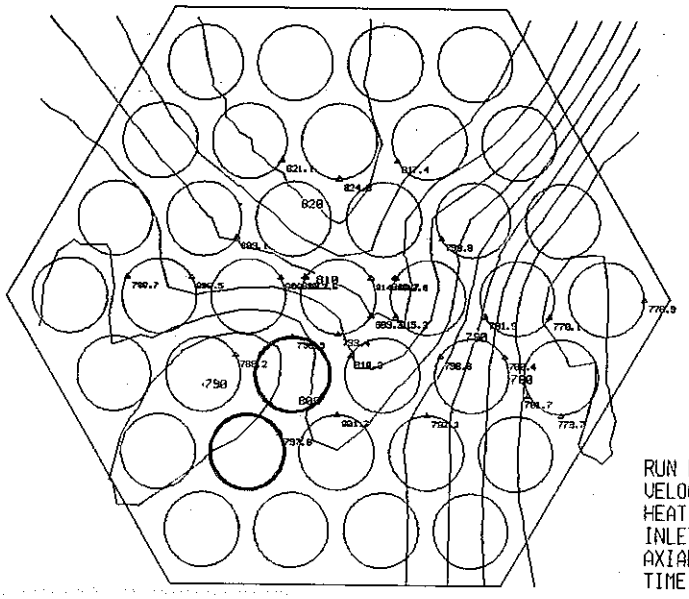

RUN NAME 37(35)LHF-226
VELOCITY 0.0 M/S
HEAT FLUX 18.92 W/CM2
INLET TEMP. 427.0 C
AXIAL 0.0 MM
TIME 16.000 SEC.

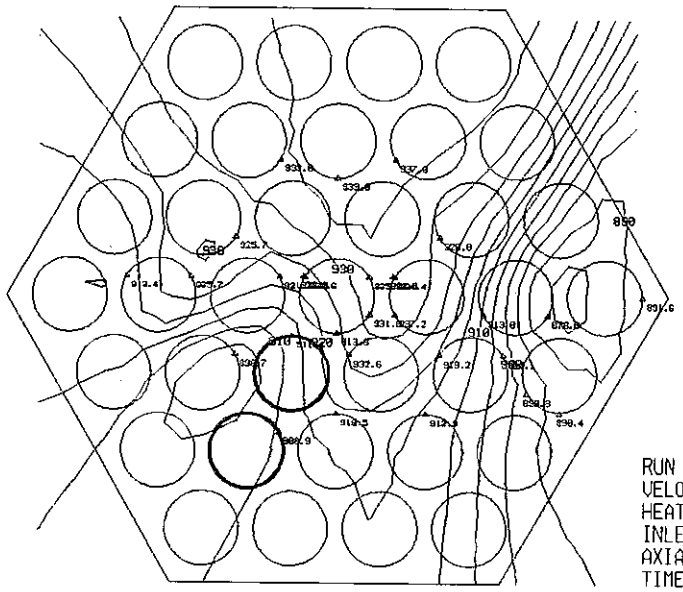

RUN NAME 37(35)LHF-226
VELOCITY 0.0 M/S
HEAT FLUX 24.74 W/CM2
INLET TEMP. 430.8 C
AXIAL 0.0 MM
TIME 177.600 SEC.

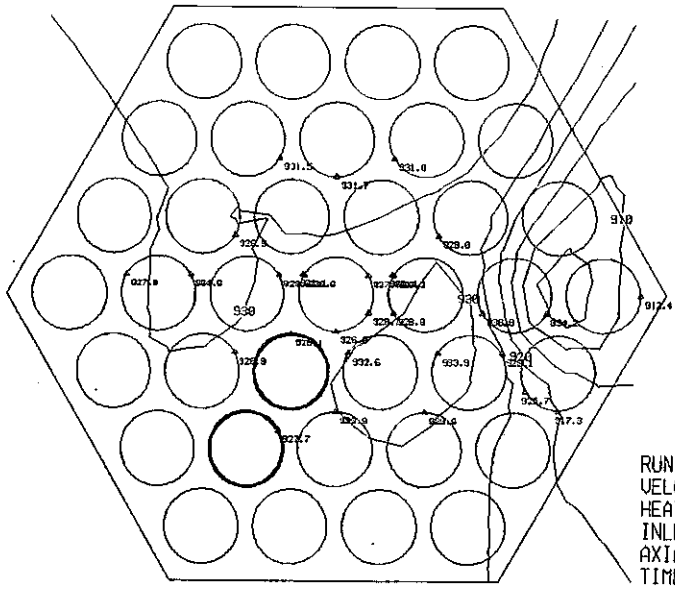

RUN NAME 37(35)LHF-226
VELOCITY 0.0 M/S
HEAT FLUX 26.43 W/CM2
INLET TEMP. 428.9 C
AXIAL 0.0 MM
TIME 382.400 SEC.

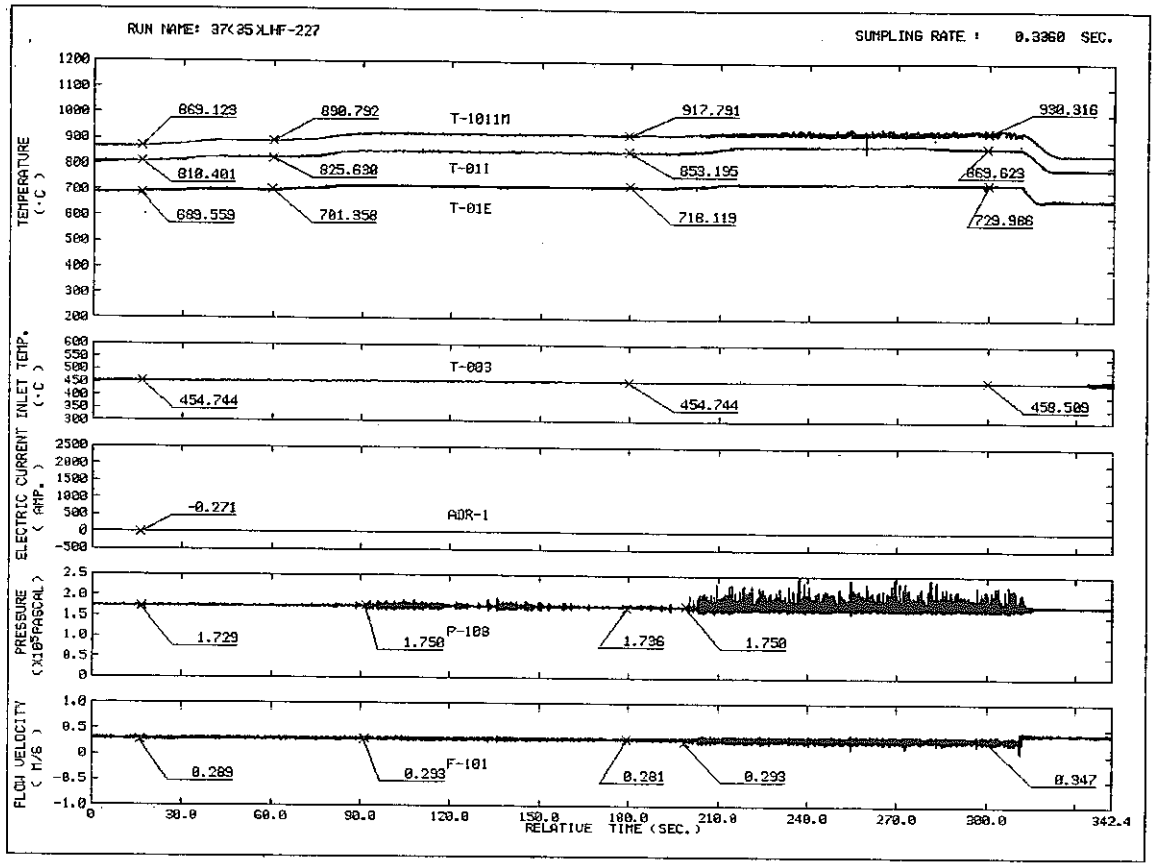
RUN NAME: 37(35)LHF-227
SUMPLING RATE : 0.3360 SEC.
TEMPERATURE (°C)
869.123
890.792
T-1011M
917.791
930.316
810.401
825.630
T-011
853.195
869.623
689.559
701.358
T-01E
718.119
729.988
INLET TEMP. (°C)
T-003
454.744
454.744
458.589
ELECTRIC CURRENT (AMP.)
-0.271
ADR-1
PRESSURE (X10⁵PASCAL)
1.729
1.750
P-108
1.736
1.750
FLOW VELOCITY (M/S)
0.289
0.293
F-101
0.281
0.293
0.347
RELATIVE TIME (SEC.)

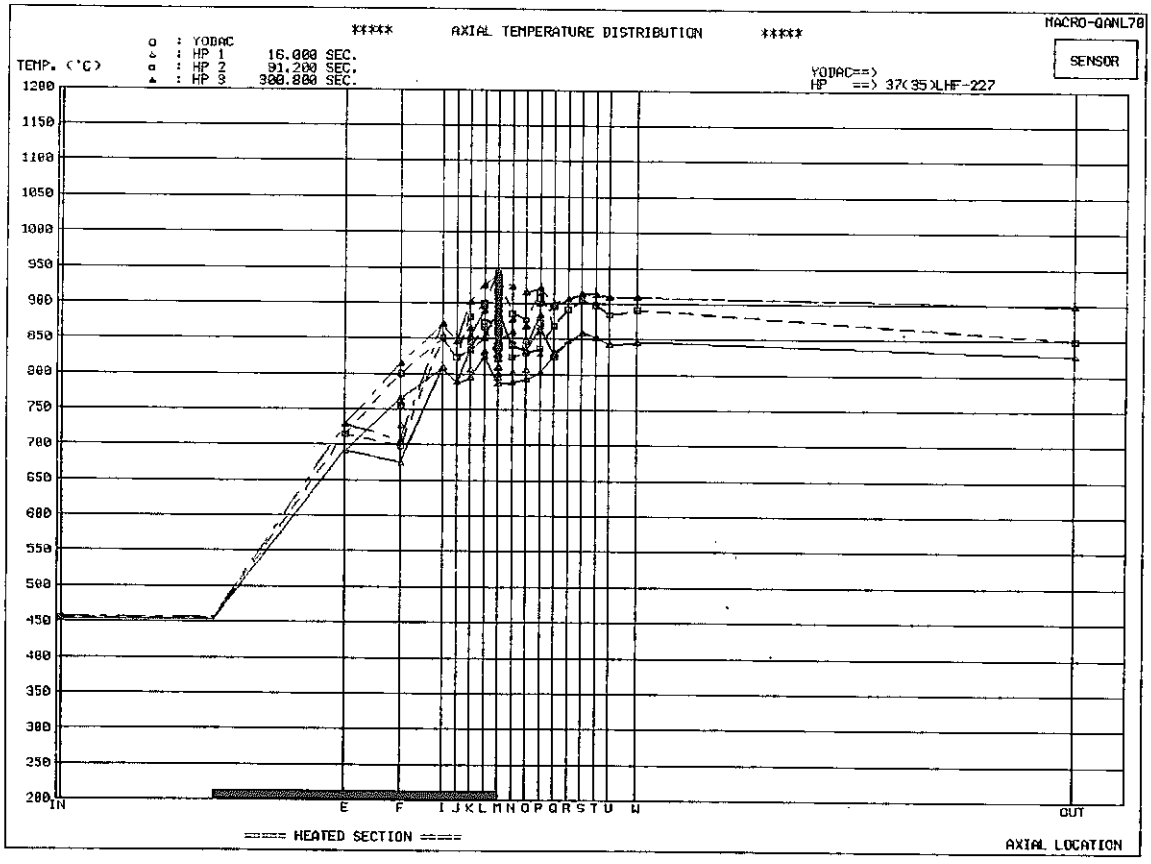
***** AXIAL TEMPERATURE DISTRIBUTION *****
MACRO-QANL70
SENSOR
TEMP. (°C)
: YODAC
: HP 1 16.000 SEC.
: HP 2 91.200 SEC.
: HP 3 300.800 SEC.
YODAC==>
HP ==> 37(35)LHF-227
IN
E F I J K L M N O P Q R S T U W
OUT
===== HEATED SECTION =====
AXIAL LOCATION

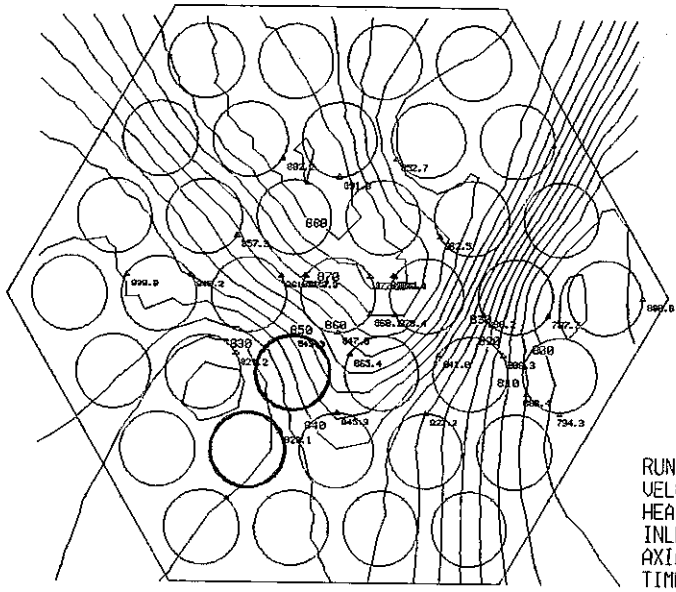

RUN NAME 37(35)LHF-227
VELOCITY 0.0 M/S
HEAT FLUX 27.39 W/CM2
INLET TEMP. 453.8 C
AXIAL 0.0 MM
TIME 16.000 SEC.

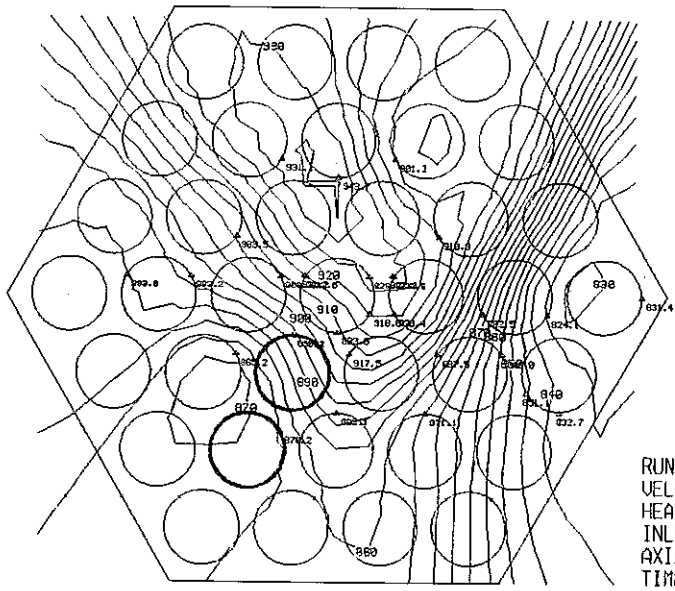

RUN NAME 37(35)LHF-227
VELOCITY 0.0 M/S
HEAT FLUX 30.69 W/CM2
INLET TEMP. 454.7 C
AXIAL 0.0 MM
TIME 91.200 SEC.

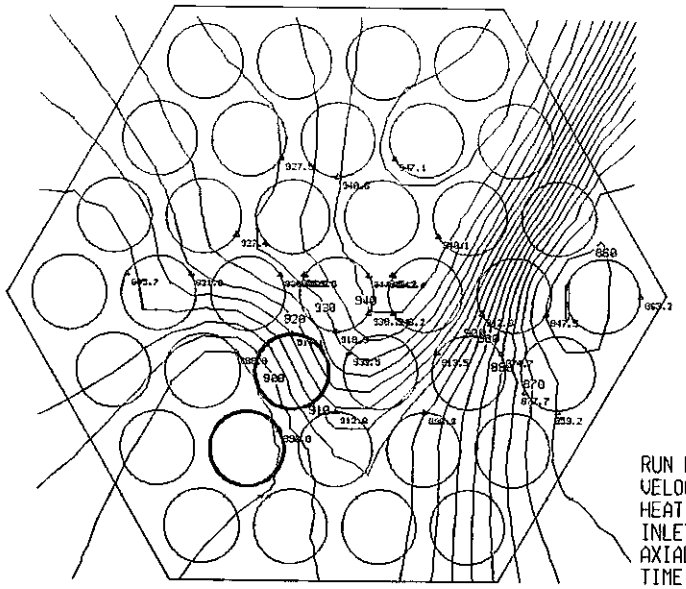

RUN NAME 37(35)LHF-227
VELOCITY 0.0 M/S
HEAT FLUX 32.83 W/CM2
INLET TEMP. 457.6 C
AXIAL 0.0 MM
TIME 300.800 SEC.

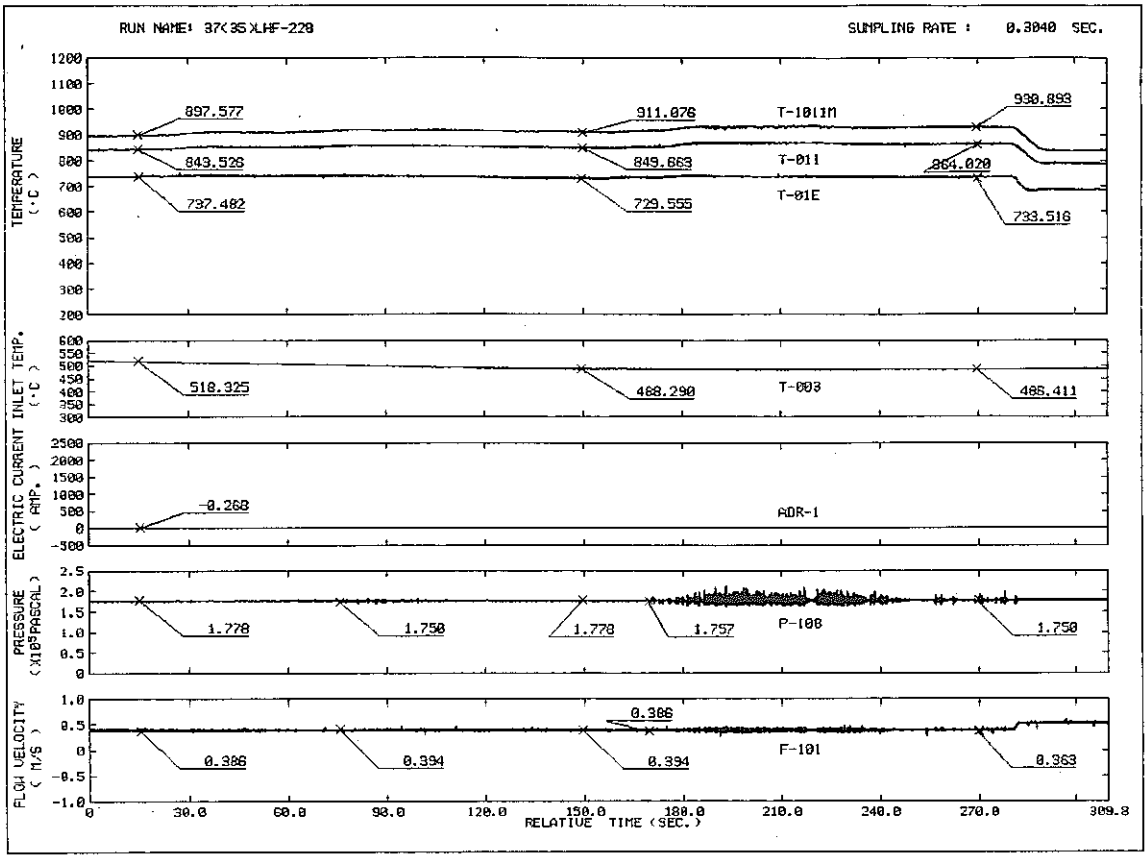
RUN NAME: 37(35)LHF-228
SAMPLING RATE : 0.3040 SEC.
TEMPERATURE ('C)
897.577
911.076
930.893
T-101M
843.526
849.663
864.020
T-011
797.482
729.555
733.516
T-01E
ELECTRIC CURRENT INLET TEMP. ('C)
518.325
488.290
486.411
T-003
PRESSURE (X10⁵PASCAL)
-0.268
ADR-1
1.778
1.750
1.778
1.757
P-108
1.750
FLOW VELOCITY (M/S)
0.386
0.394
0.394
0.363
F-101
RELATIVE TIME (SEC.)

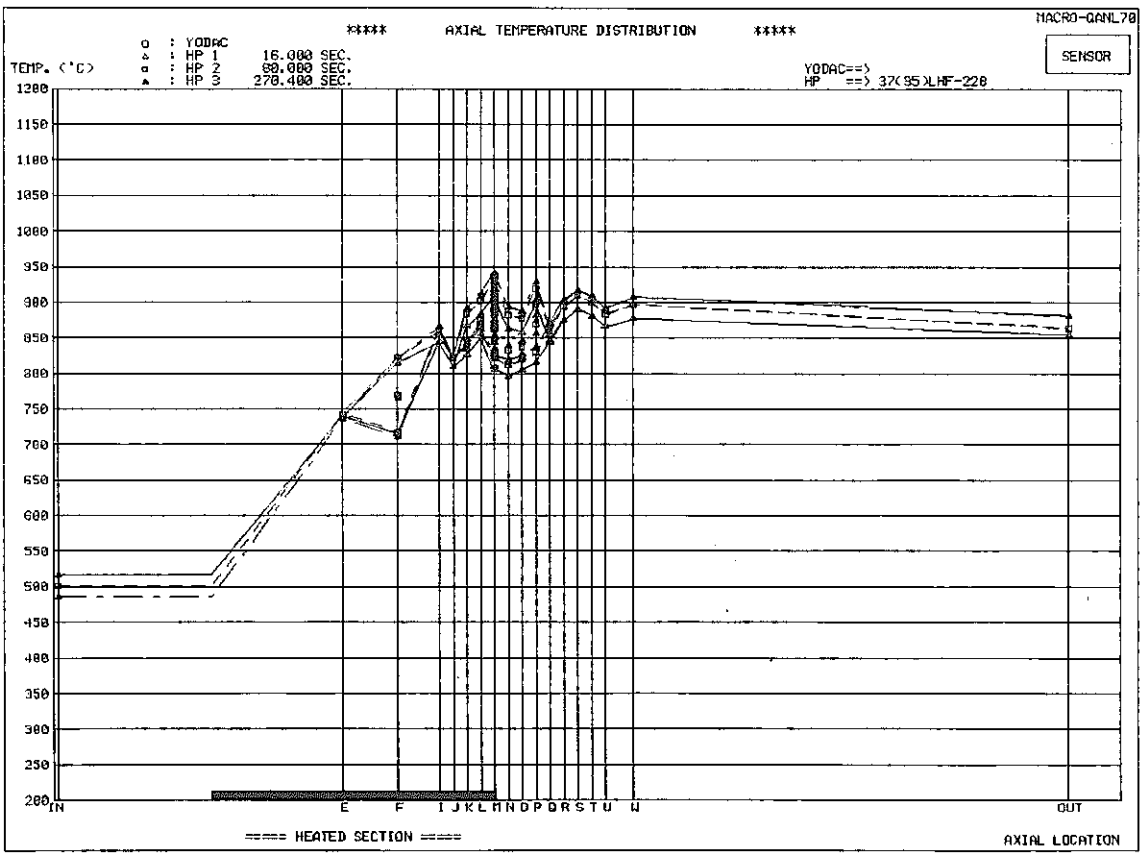
MACRO-QANL70
***** AXIAL TEMPERATURE DISTRIBUTION *****
SENSOR
o : YODAC
▵ : HP 1 16.000 SEC.
▫ : HP 2 80.000 SEC.
▲ : HP 3 270.400 SEC.
TEMP. ('C)
YODAC==>
HP ==> 37(35)LHF-228
IN
E F I J K L M N O P Q R S T U W
OUT
==== HEATED SECTION ====
AXIAL LOCATION

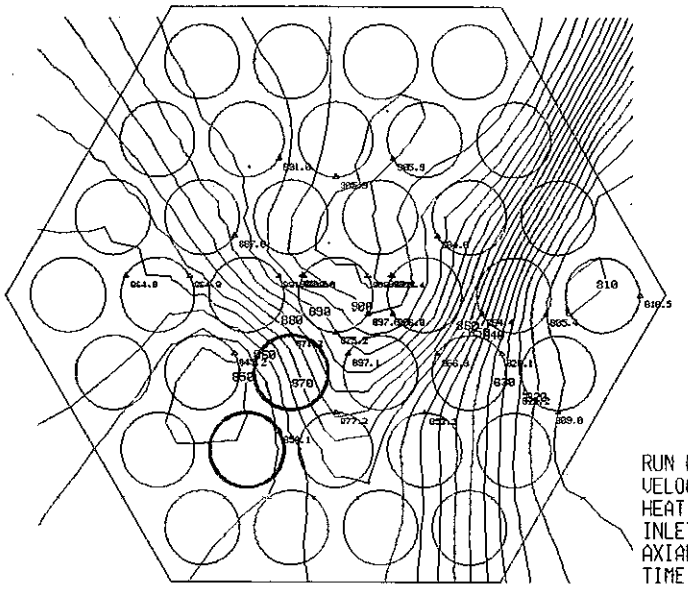

RUN NAME 37(35)LHF-228
VELOCITY 0.384 M/S
HEAT FLUX 32.94 W/CM2
INLET TEMP. 516.4 C
AXIAL 0.0 MM
TIME 16.000 SEC.

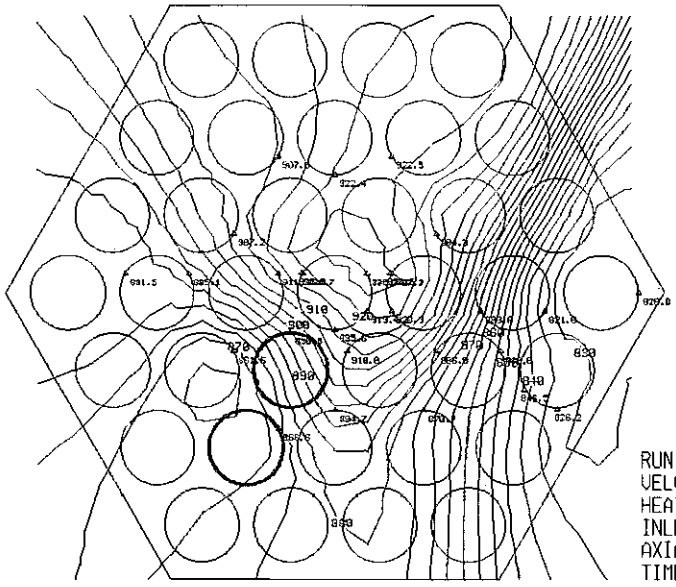

RUN NAME 37(35)LHF-228
VELOCITY 0.372 M/S
HEAT FLUX 34.05 W/CM2
INLET TEMP. 501.4 C
AXIAL 0.0 MM
TIME 80.000 SEC.

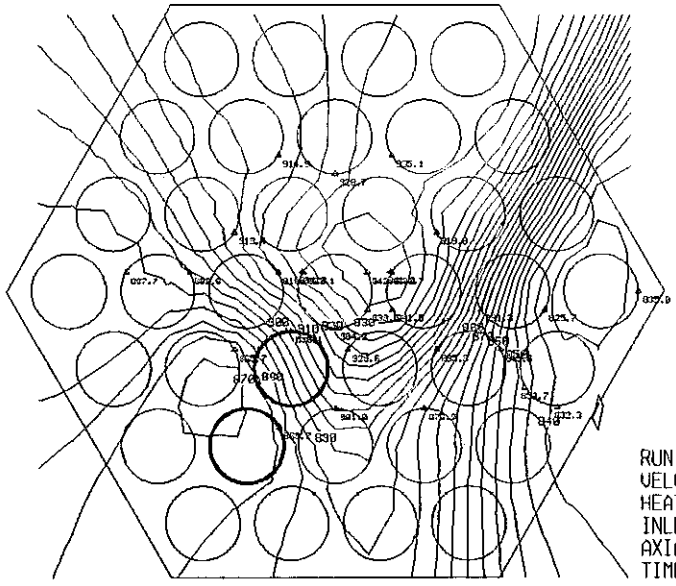

RUN NAME 37(35)LHF-228
VELOCITY 0.372 M/S
HEAT FLUX 37.00 W/CM2
INLET TEMP. 486.4 C
AXIAL 0.0 MM
TIME 270.400 SEC.

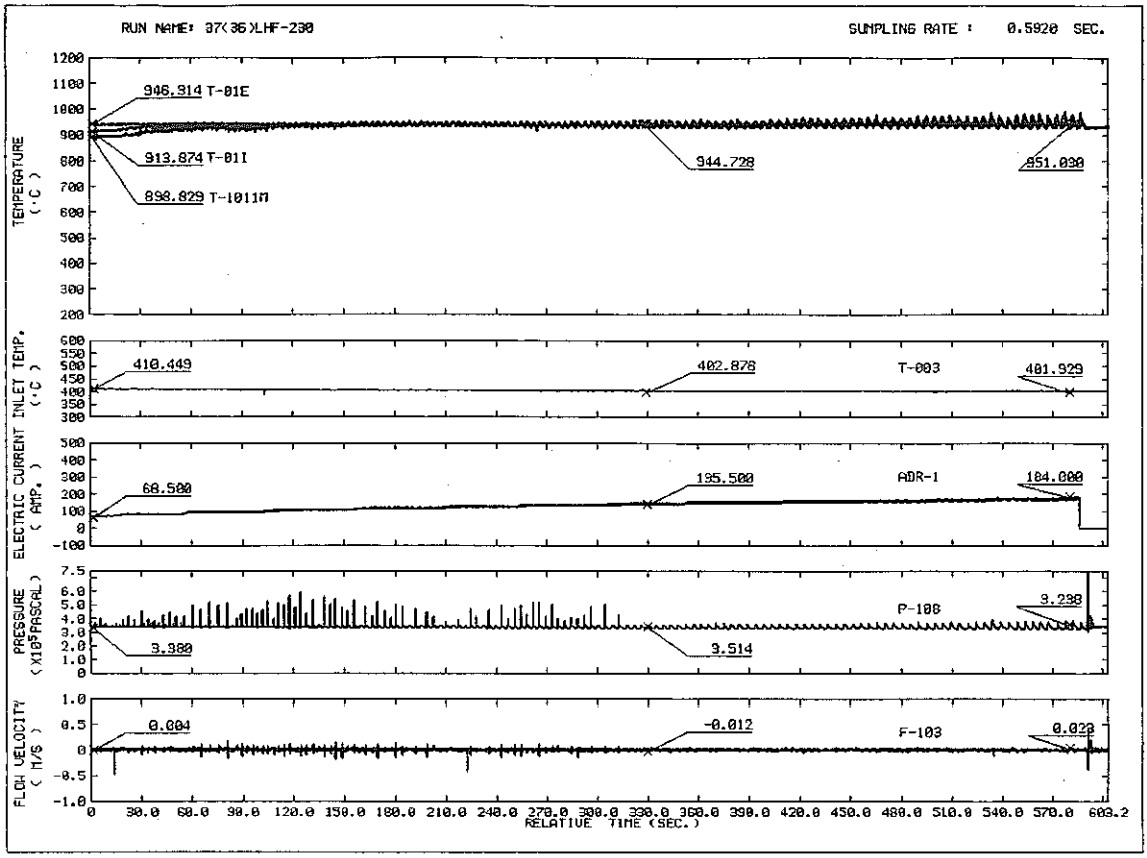
RUN NAME: 37(36)LHF-230
SAMPLING RATE : 0.5920 SEC.
TEMPERATURE (°C)
946.914 T-01E
913.874 T-01I
898.829 T-1011M
944.728
851.090
INLET TEMP. (°C)
410.449
402.876
T-003
401.929
ELECTRIC CURRENT (AMP.)
68.500
195.500
ADR-1
184.000
PRESSURE (X10⁵PASCAL)
3.380
3.514
P-106
3.238
FLOW VELOCITY (M/S)
0.004
-0.012
F-103
0.022
RELATIVE TIME (SEC.)

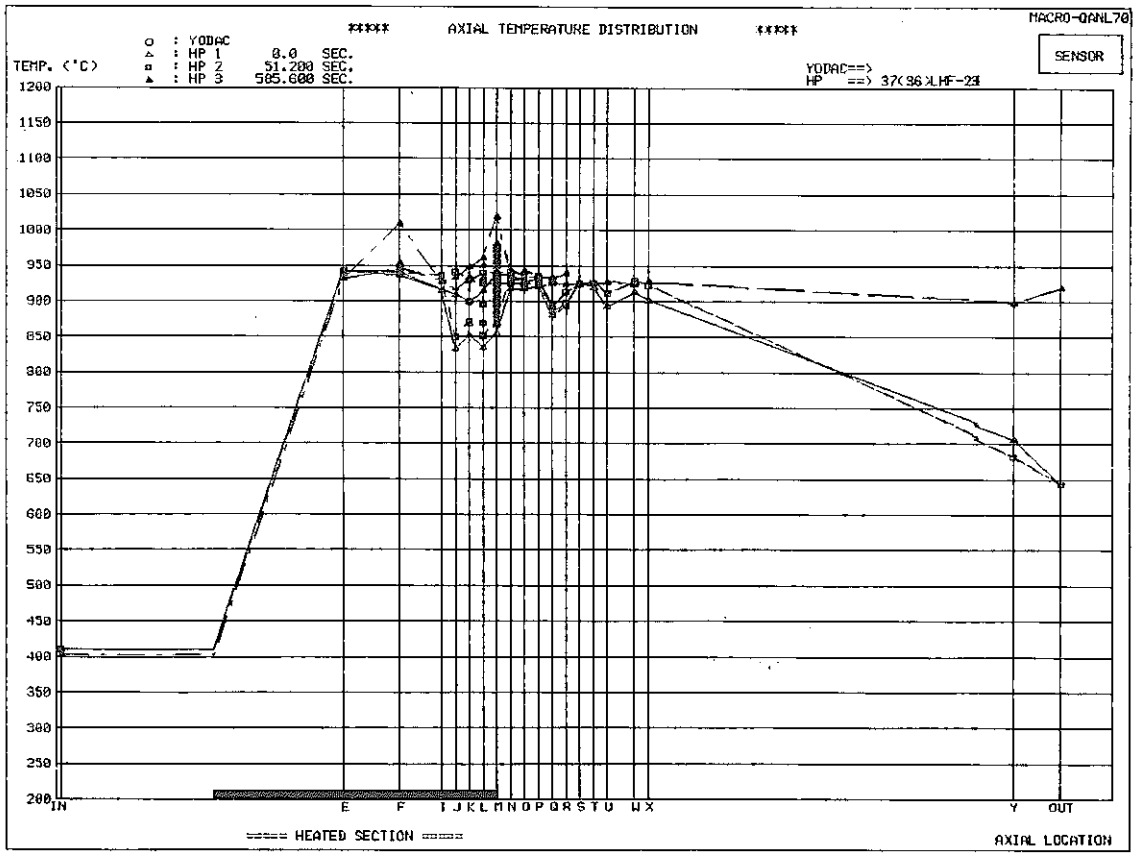
***** AXIAL TEMPERATURE DISTRIBUTION *****
MACRO-QANL70
SENSOR
TEMP. (°C)
○ : YODAC
△ : HP 1 0.0 SEC.
□ : HP 2 51.200 SEC.
▲ : HP 3 585.600 SEC.
YODAC==>
HP ==> 37(36)LHF-23
IN E F I J K L M N O P Q R S T U W X Y OUT
===== HEATED SECTION =====
AXIAL LOCATION

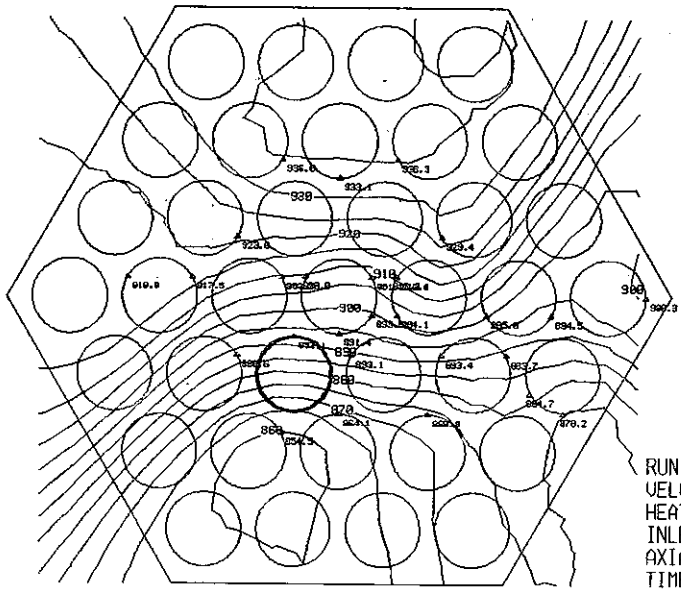

RUN NAME 37(36)LHF-230
VELOCITY 0.027 M/S
HEAT FLUX 2.18 W/CM2
INLET TEMP. 410.4 C
AXIAL 0.0 MM
TIME 0.0 SEC.

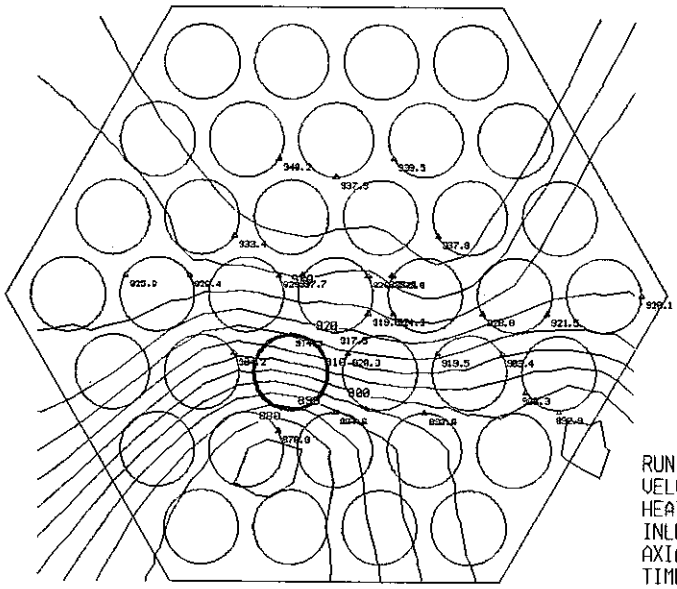

RUN NAME 37(36)LHF-230
VELOCITY 0.012 M/S
HEAT FLUX 2.92 W/CM2
INLET TEMP. 409.5 C
AXIAL 0.0 MM
TIME 51.200 SEC.

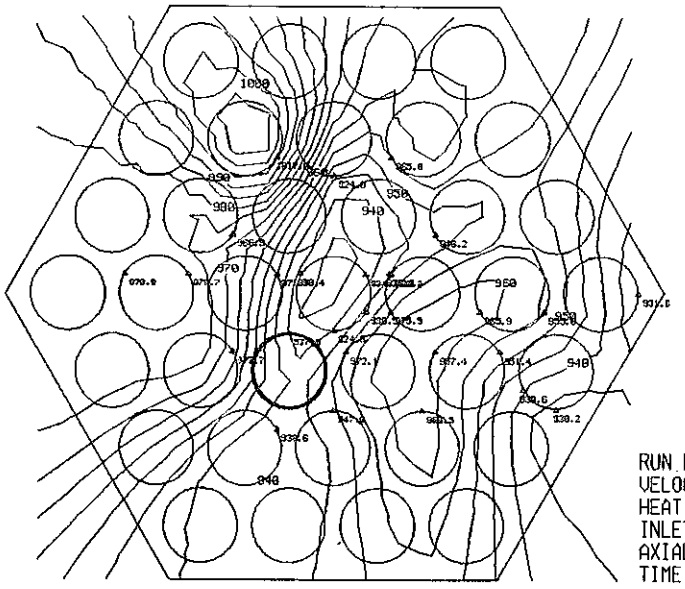

RUN NAME 37(36)LHF-230
VELOCITY 0.012 M/S
HEAT FLUX 13.51 W/CM2
INLET TEMP. 402.9 C
AXIAL 0.0 MM
TIME 585.600 SEC.

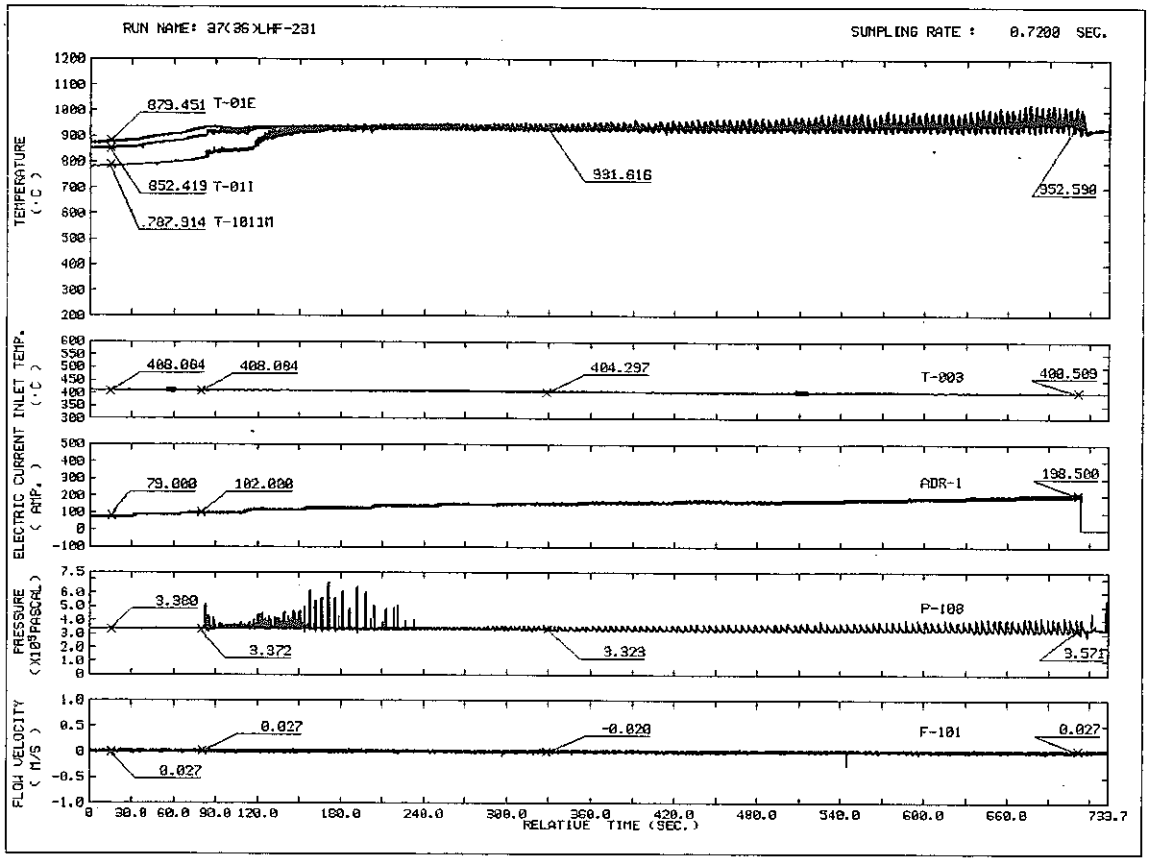
RUN NAME: 37(36)LHF-231
SUMPLING RATE : 0.7200 SEC.
TEMPERATURE ('C)
879.451 T-01E
852.419 T-01I
787.914 T-1011M
991.616
952.590
ELECTRIC CURRENT INLET TEMP. ('C)
408.084
408.084
404.297
T-003
408.589
PRESSURE (X10⁵PASCAL)
79.000
102.000
ADR-1
198.500
3.380
3.372
3.323
P-108
3.571
FLOW VELOCITY ('M/S)
0.027
0.027
-0.020
F-101
0.027
RELATIVE TIME (SEC.)

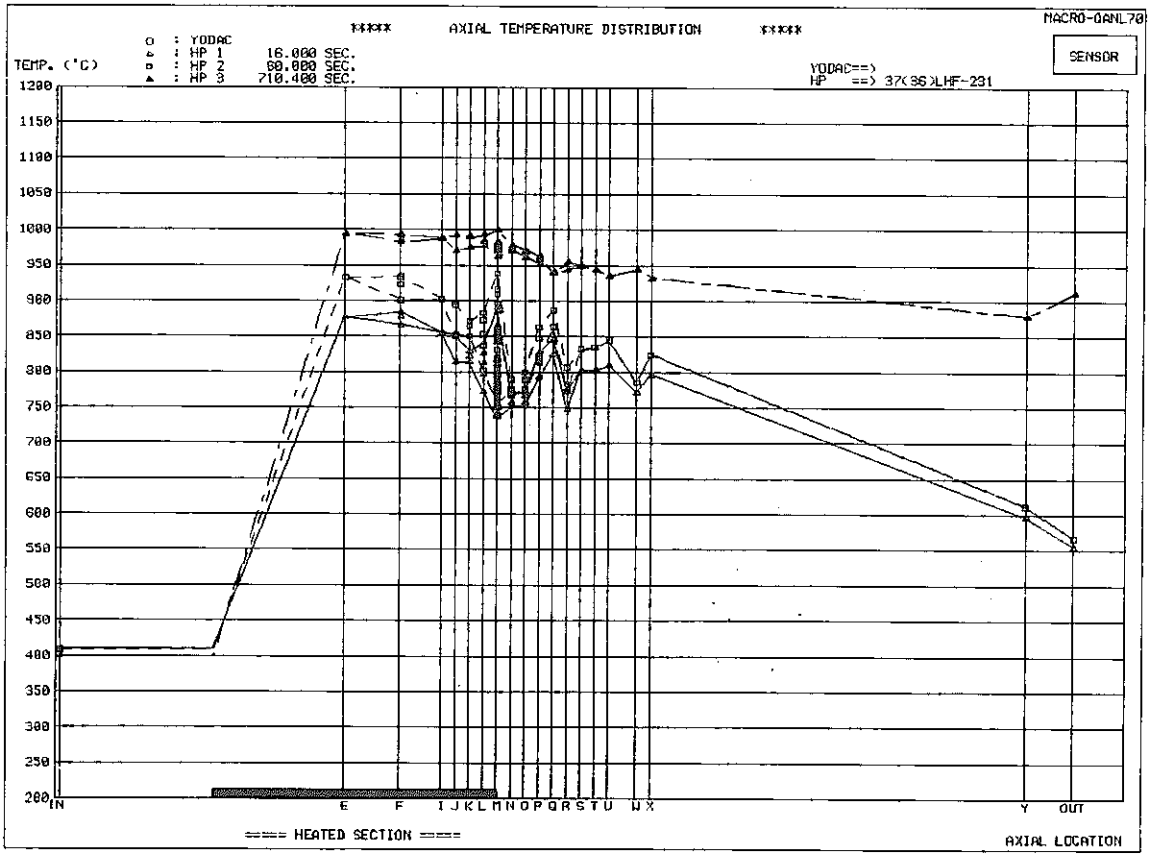
***** AXIAL TEMPERATURE DISTRIBUTION *****
MACRO-GANL70
SENSOR
TEMP. ('C)
YODAC
HP 1 16.000 SEC.
HP 2 80.000 SEC.
HP 3 710.400 SEC.
YODAC==>
HP ==> 37(36)LHF-231
IN
E F I J K L M N O P Q R S T U W X
Y OUT
==== HEATED SECTION ====
AXIAL LOCATION

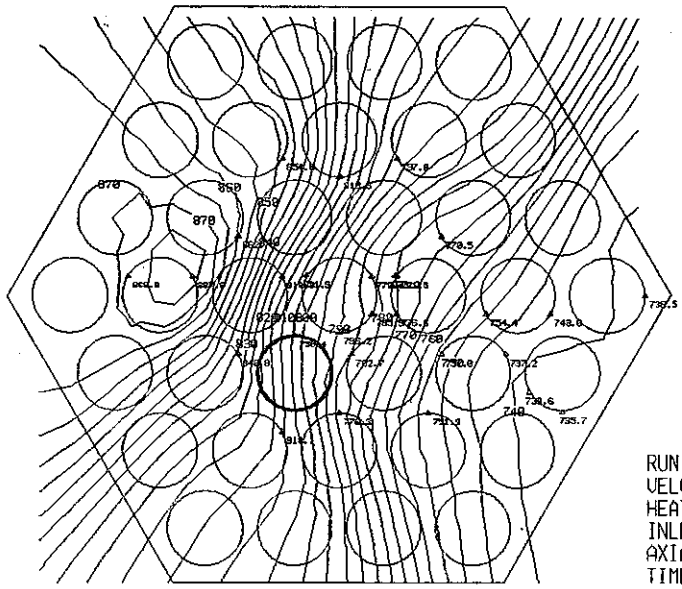

RUN NAME	37(36)LHF-231	
VELOCITY	0.0	M/S
HEAT FLUX	2.36	W/CM2
INLET TEMP.	410.0	C
AXIAL	0.0	MM
TIME	16.000	SEC.

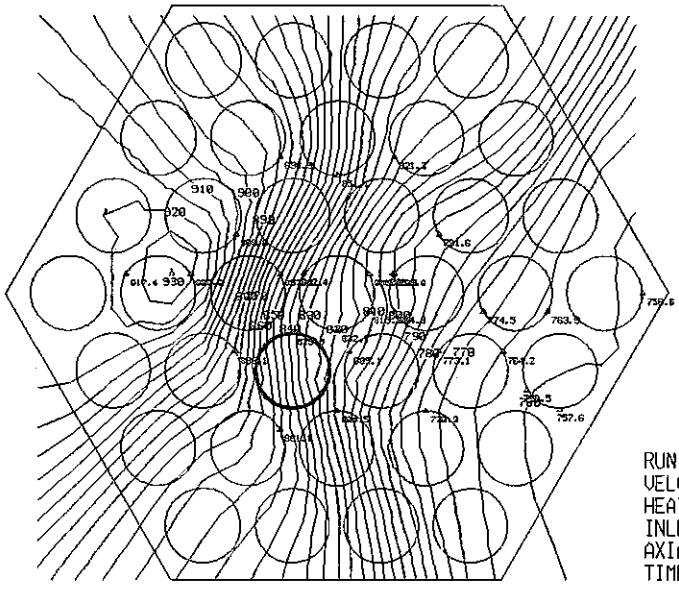

RUN NAME	37(36)LHF-231	
VELOCITY	0.0	M/S
HEAT FLUX	3.93	W/CM2
INLET TEMP.	409.0	C
AXIAL	0.0	MM
TIME	80.000	SEC.

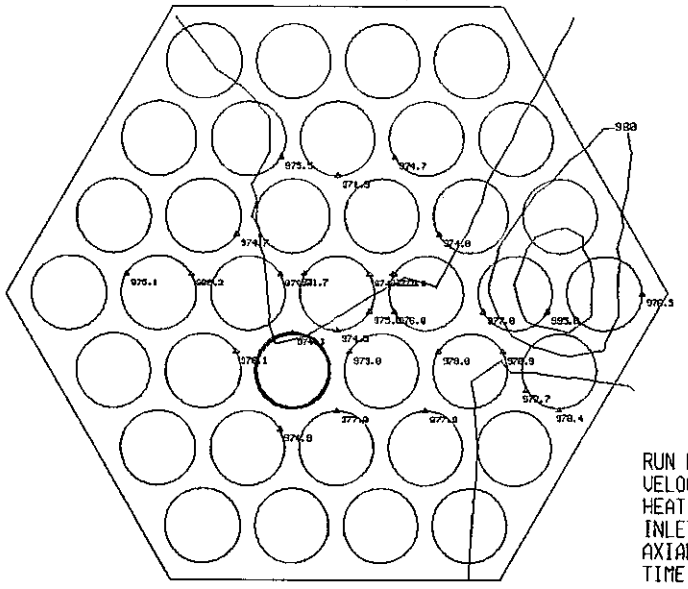

RUN NAME	37(36)LHF-231	
VELOCITY	0.0	M/S
HEAT FLUX	20.92	W/CM2
INLET TEMP.	400.5	C
AXIAL	0.0	MM
TIME	710.400	SEC.

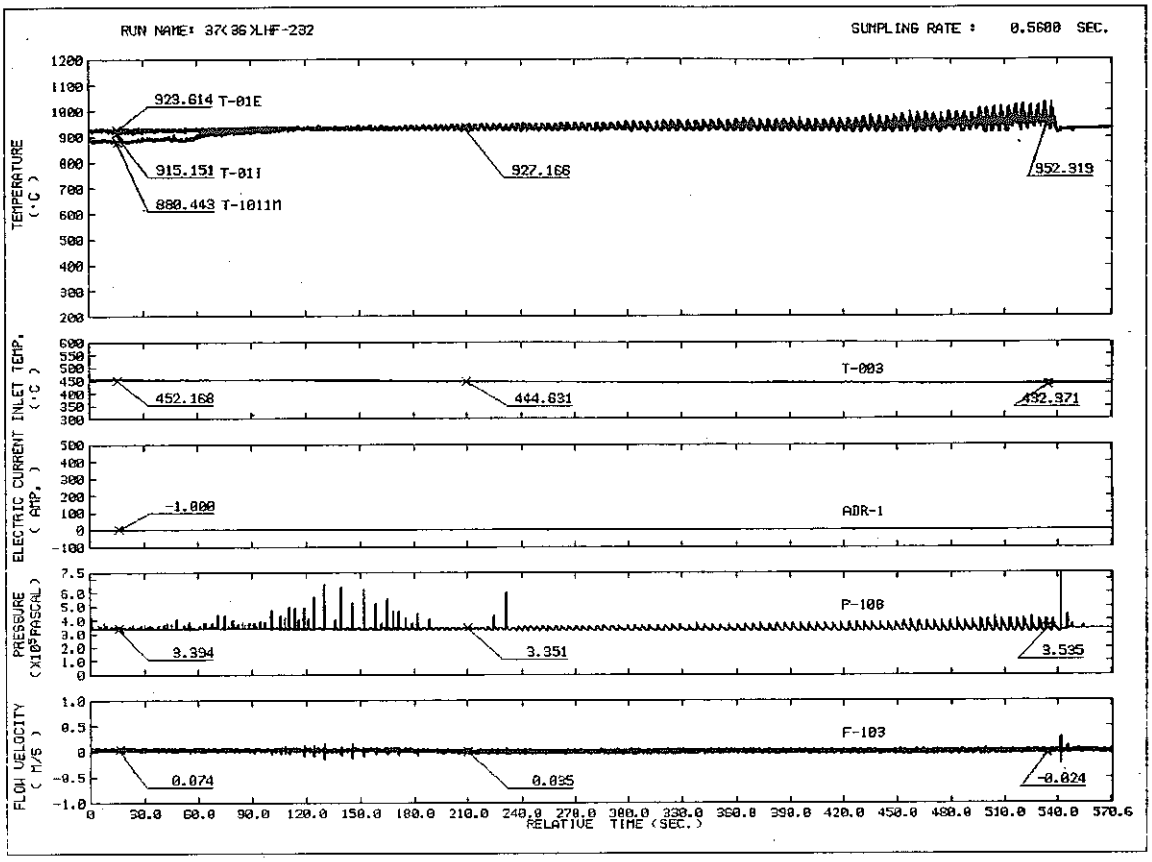
RUN NAME: 37(36)LHF-232
SAMPLING RATE : 0.5600 SEC.
TEMPERATURE (°C)
923.614 T-01E
915.151 T-011
880.443 T-1011M
927.166
952.319
INLET TEMP. (°C)
452.168
444.631
T-003
432.871
ELECTRIC CURRENT (AMP.)
-1.000
ADR-1
PRESSURE (X10⁵PASCAL)
3.394
3.351
P-106
3.535
FLOW VELOCITY (M/S)
0.074
0.085
F-103
-0.024
RELATIVE TIME (SEC.)

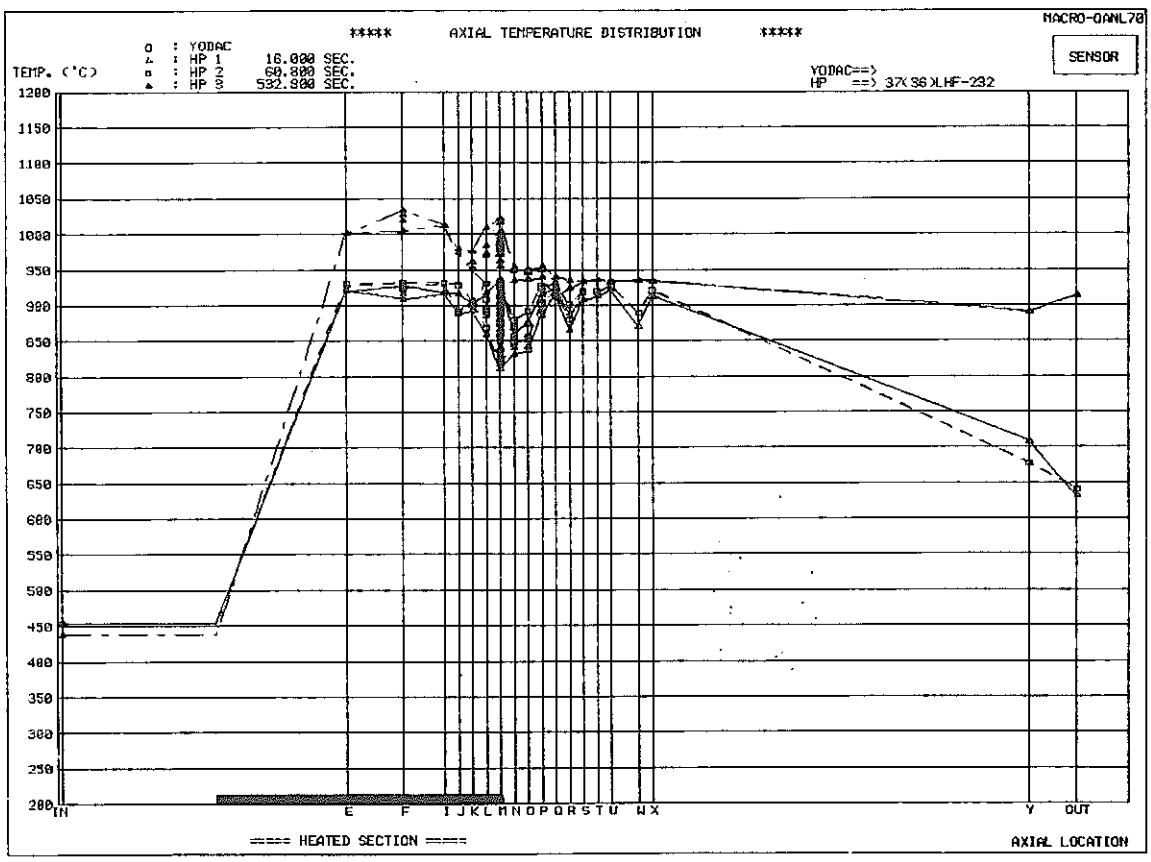
MACRO-QANL70
***** AXIAL TEMPERATURE DISTRIBUTION *****
SENSOR
TEMP. (°C)
○ : YODAC
△ : HP 1 16.000 SEC.
□ : HP 2 60.800 SEC.
▲ : HP 3 532.800 SEC.
YODAC==>
HP ==> 37(36)LHF-232
IN E F I J K L M N O P Q R S T U W X Y OUT
==== HEATED SECTION ====
AXIAL LOCATION

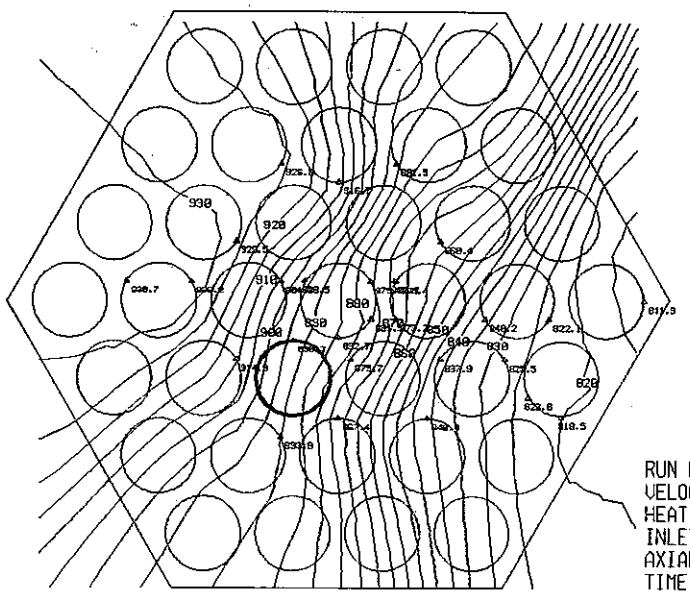

RUN NAME 37(36)LHF-232
VELOCITY 0.035 M/S
HEAT FLUX 2.78 W/CM2
INLET TEMP. 455.0 C
AXIAL 0.0 MM
TIME 16.000 SEC.

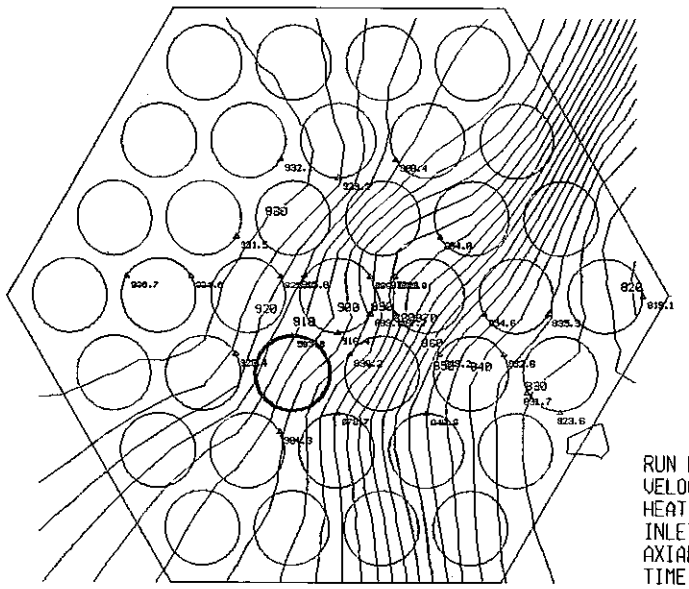

RUN NAME 37(36)LHF-232
VELOCITY 0.023 M/S
HEAT FLUX 3.86 W/CM2
INLET TEMP. 453.1 C
AXIAL 0.0 MM
TIME 60.800 SEC.

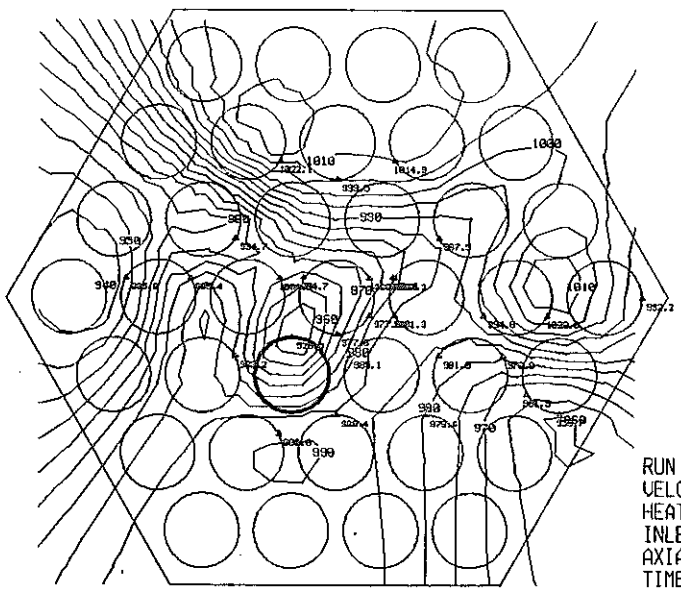

RUN NAME 37(36)LHF-232
VELOCITY -0.004 M/S
HEAT FLUX 18.77 W/CM2
INLET TEMP. 437.1 C
AXIAL 0.0 MM
TIME 532.800 SEC.

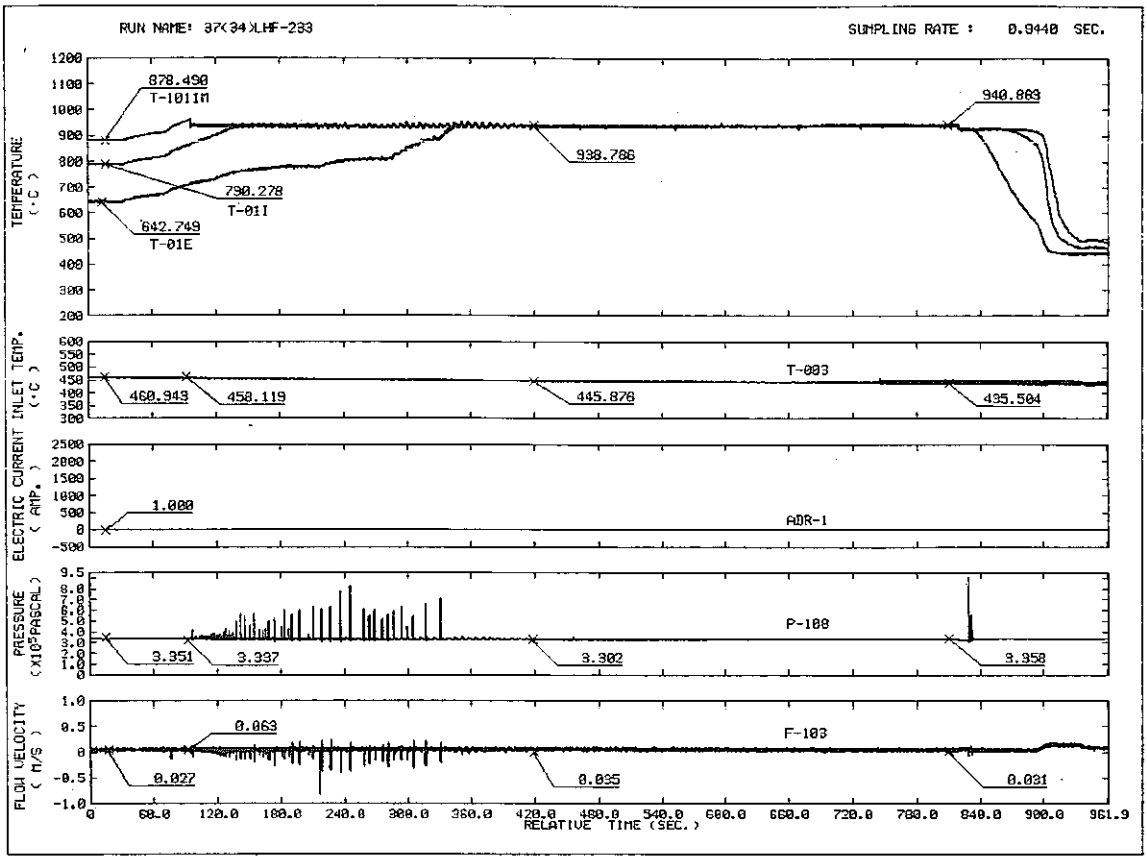
RUN NAME: 37(34)LHF-233
SAMPLING RATE : 0.9440 SEC.
TEMPERATURE (°C)
878.490
T-101M
940.883
938.786
790.278
T-01I
642.749
T-01E
INLET TEMP. (°C)
460.943
458.119
T-003
445.878
435.504
ELECTRIC CURRENT (AMP.)
1.000
ADR-1
PRESSURE (X10⁵PASCAL)
3.351
3.337
P-108
3.302
3.358
FLOW VELOCITY (M/S)
0.063
F-103
0.027
0.035
0.031
RELATIVE TIME (SEC.)

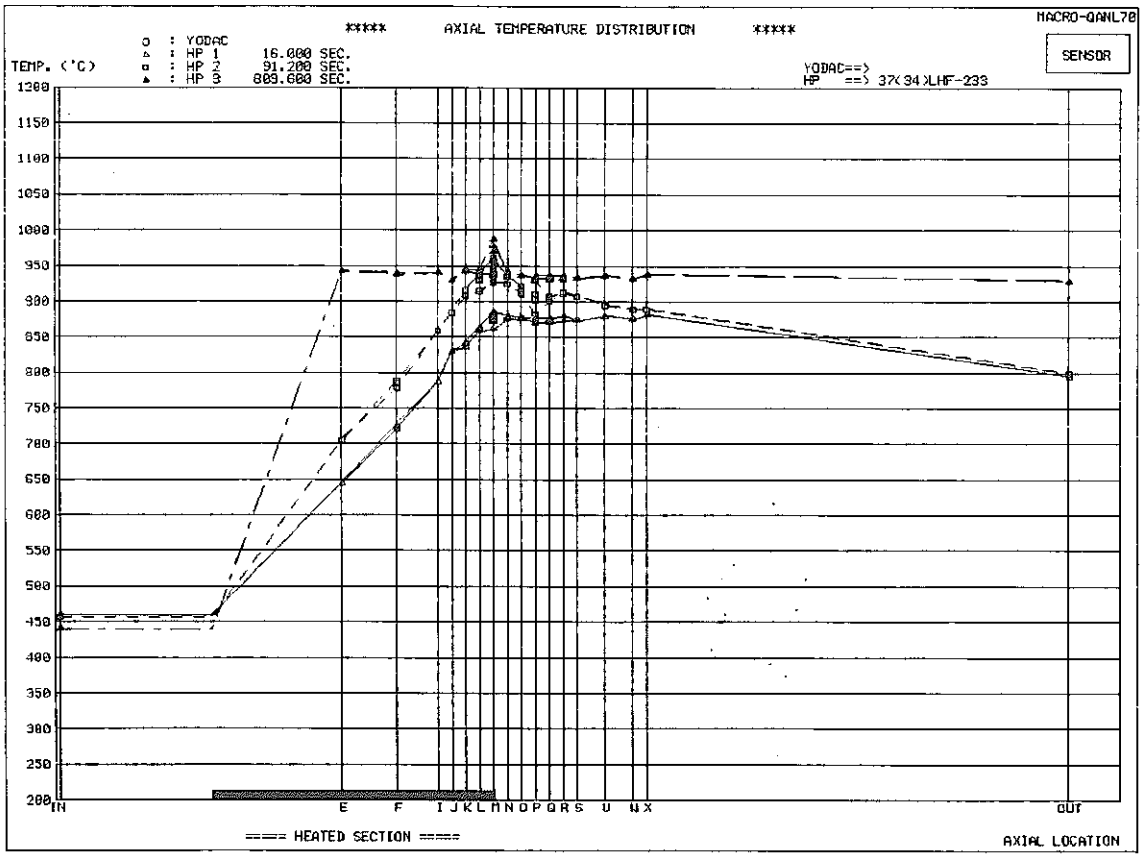
***** AXIAL TEMPERATURE DISTRIBUTION *****
MACRO-QANL70
SENSOR
TEMP. (°C)
○ : YODAC
△ : HP 1 16.000 SEC.
□ : HP 2 91.200 SEC.
▲ : HP 3 809.600 SEC.
YODAC==>
HP ==> 37(34)LHF-233
IN
E F I J K L M N O P Q R S U W X
OUT
==== HEATED SECTION ====
AXIAL LOCATION

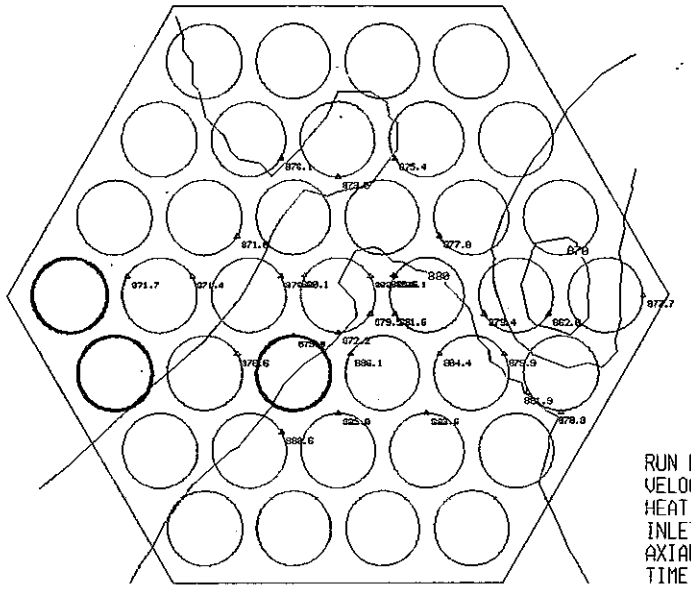

RUN NAME 37(34)LHF-233
VELOCITY 0.043 M/S
HEAT FLUX 14.36 W/CM2
INLET TEMP. 460.9 C
AXIAL 0.0 MM
TIME 16.000 SEC.

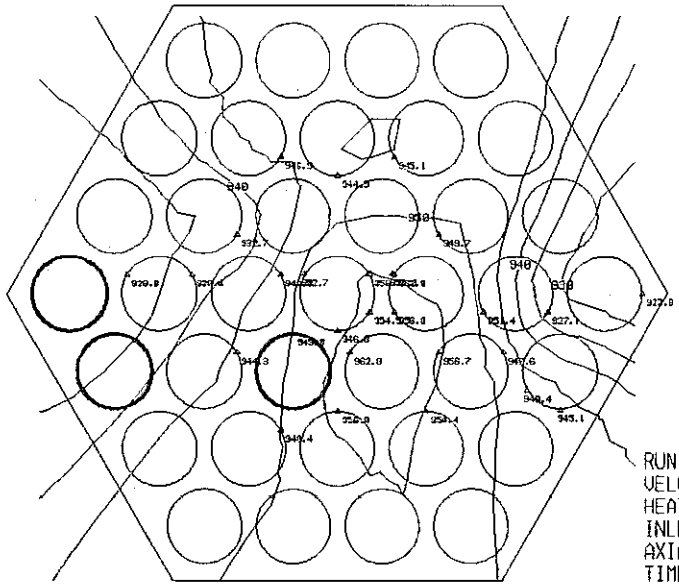

RUN NAME 37(34)LHF-233
VELOCITY 0.043 M/S
HEAT FLUX 24.67 W/CM2
INLET TEMP. 456.2 C
AXIAL 0.0 MM
TIME 91.200 SEC.

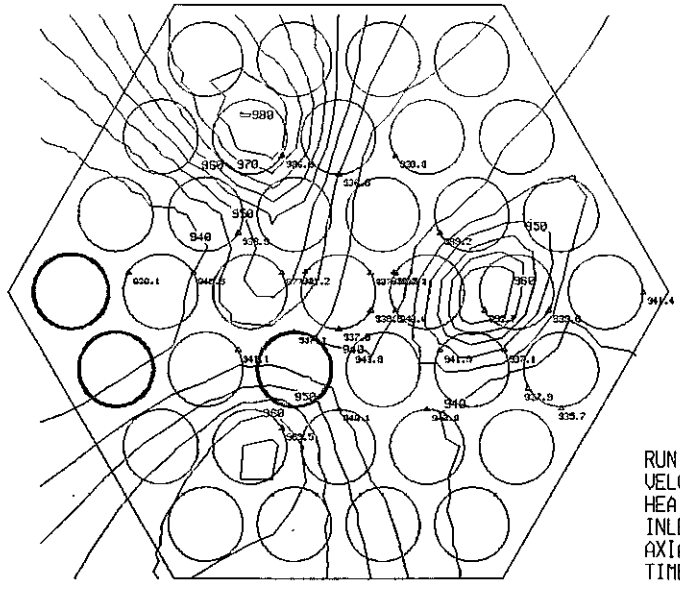

RUN NAME 37(34)LHF-233
VELOCITY 0.043 M/S
HEAT FLUX 92.57 W/CM2
INLET TEMP. 442.1 C
AXIAL 0.0 MM
TIME 809.600 SEC.

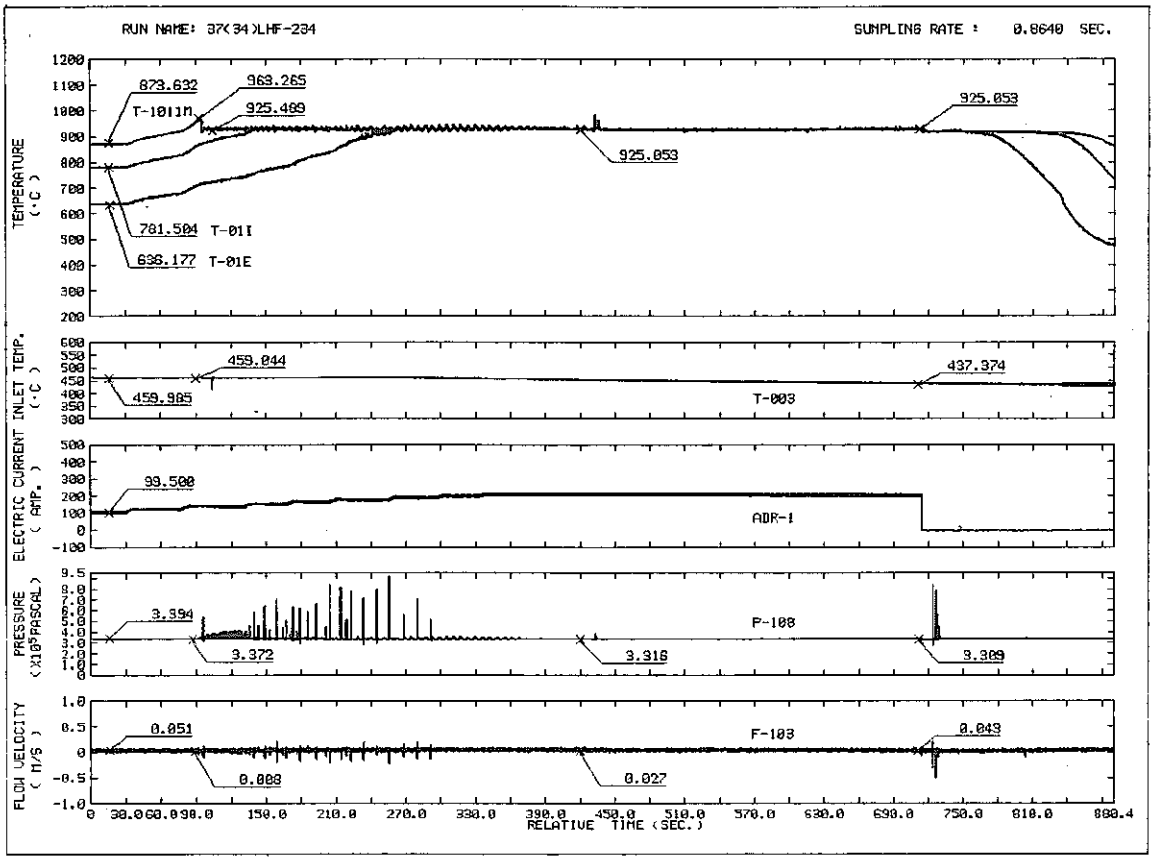
RUN NAME: 37(34)LHF-234
SUMPLING RATE : 0.8640 SEC.
TEMPERATURE (°C)
873.632
T-101M
963.265
925.489
925.053
925.053
781.504 T-01I
638.177 T-01E
459.044
459.985
T-003
437.374
ELECTRIC CURRENT INLET TEMP. (°C)
99.500
ADR-1
PRESSURE (X10⁵PASCAL)
3.394
3.372
P-108
3.318
3.309
FLOW VELOCITY (M/S)
0.051
0.008
F-103
0.027
0.043
RELATIVE TIME (SEC.)

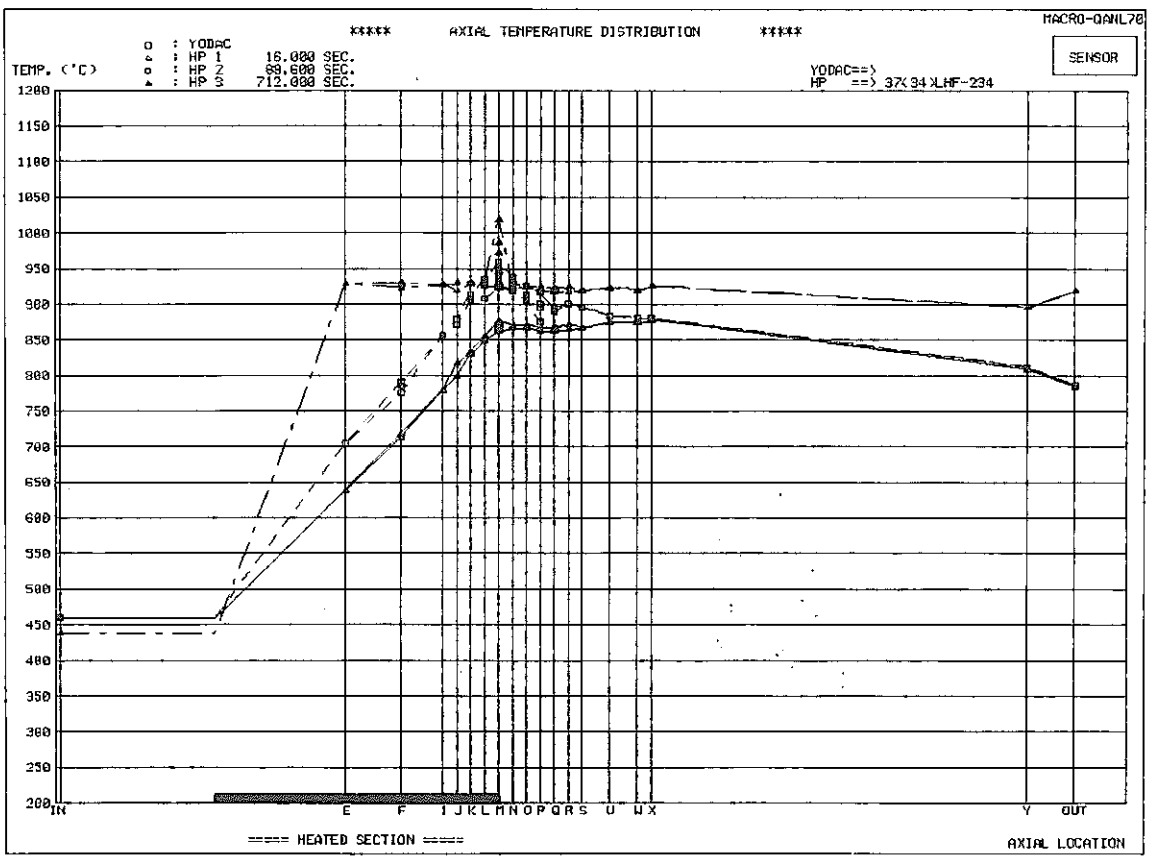
MACRO-QANL70
***** AXIAL TEMPERATURE DISTRIBUTION *****
SENSOR
o : YODAC
▵ : HP 1 16.000 SEC.
o : HP 2 89.600 SEC.
▲ : HP 3 712.000 SEC.
TEMP. (°C)
YODAC==>
HP ==> 37(34)LHF-234
IN E F I J K L M N O P Q R S U W X Y OUT
==== HEATED SECTION ====
AXIAL LOCATION

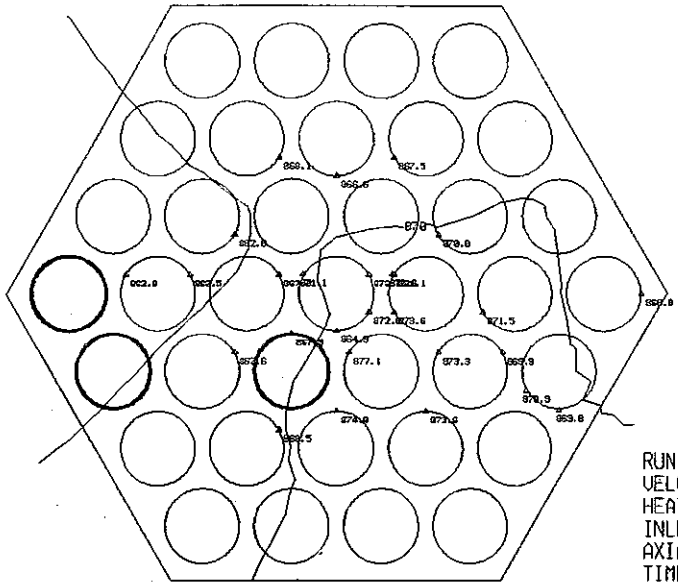

RUN NAME 37(34)LHF-234
VELOCITY 0.035 M/S
HEAT FLUX 4.17 W/CM2
INLET TEMP. 460.0 C
AXIAL 0.0 MM
TIME 16.000 SEC.

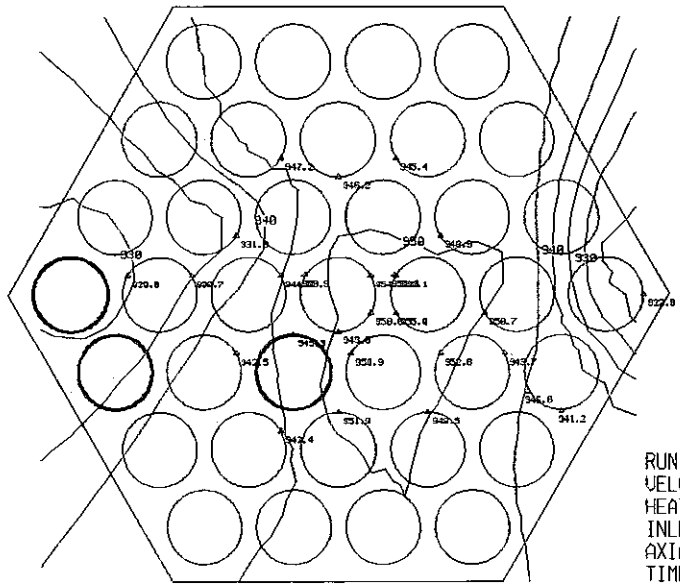

RUN NAME 37(34)LHF-234
VELOCITY 0.035 M/S
HEAT FLUX 8.00 W/CM2
INLET TEMP. 460.0 C
AXIAL 0.0 MM
TIME 89.600 SEC.

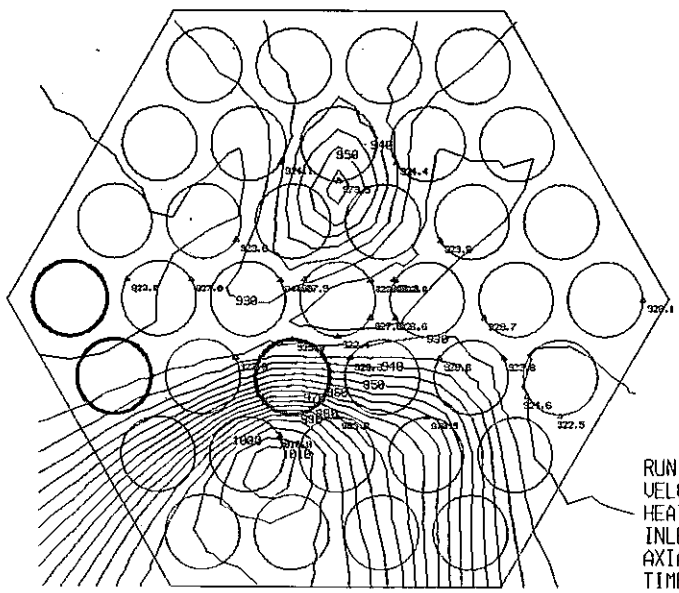

RUN NAME 37(34)LHF-234
VELOCITY 0.027 M/S
HEAT FLUX 19.63 W/CM2
INLET TEMP. 439.3 C
AXIAL 0.0 MM
TIME 712.000 SEC.

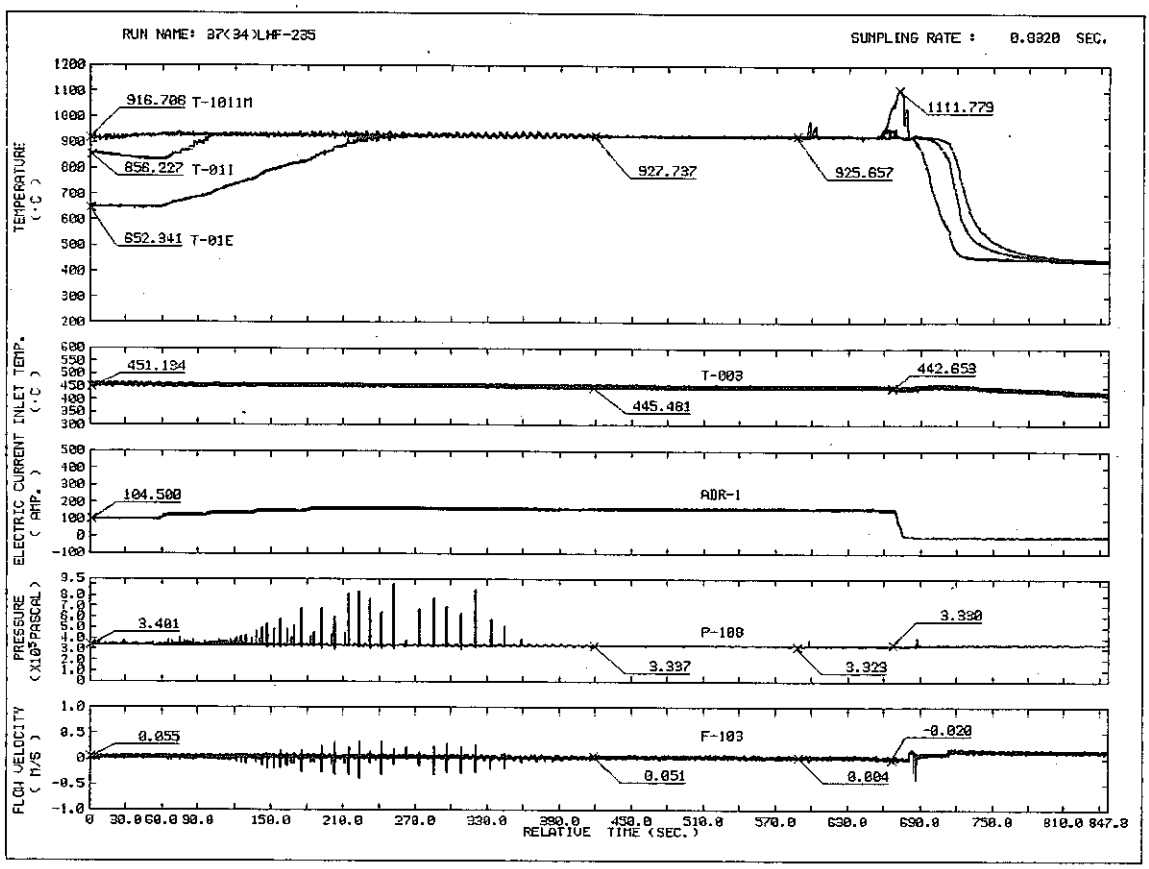
RUN NAME: 37<34>LHF-235
SUMPLING RATE : 0.0020 SEC.
TEMPERATURE (°C)
916.708 T-1011M
856.227 T-011
852.341 T-01E
927.737
925.657
1111.779
ELECTRIC CURRENT INLET TEMP. (°C)
451.134
T-003
445.481
442.653
(AMP.)
104.500
ADR-1
PRESSURE (X10⁵PASCAL)
3.401
P-100
3.397
3.323
3.330
FLOW VELOCITY (M/S)
0.055
F-103
0.051
0.004
-0.020
RELATIVE TIME (SEC.)

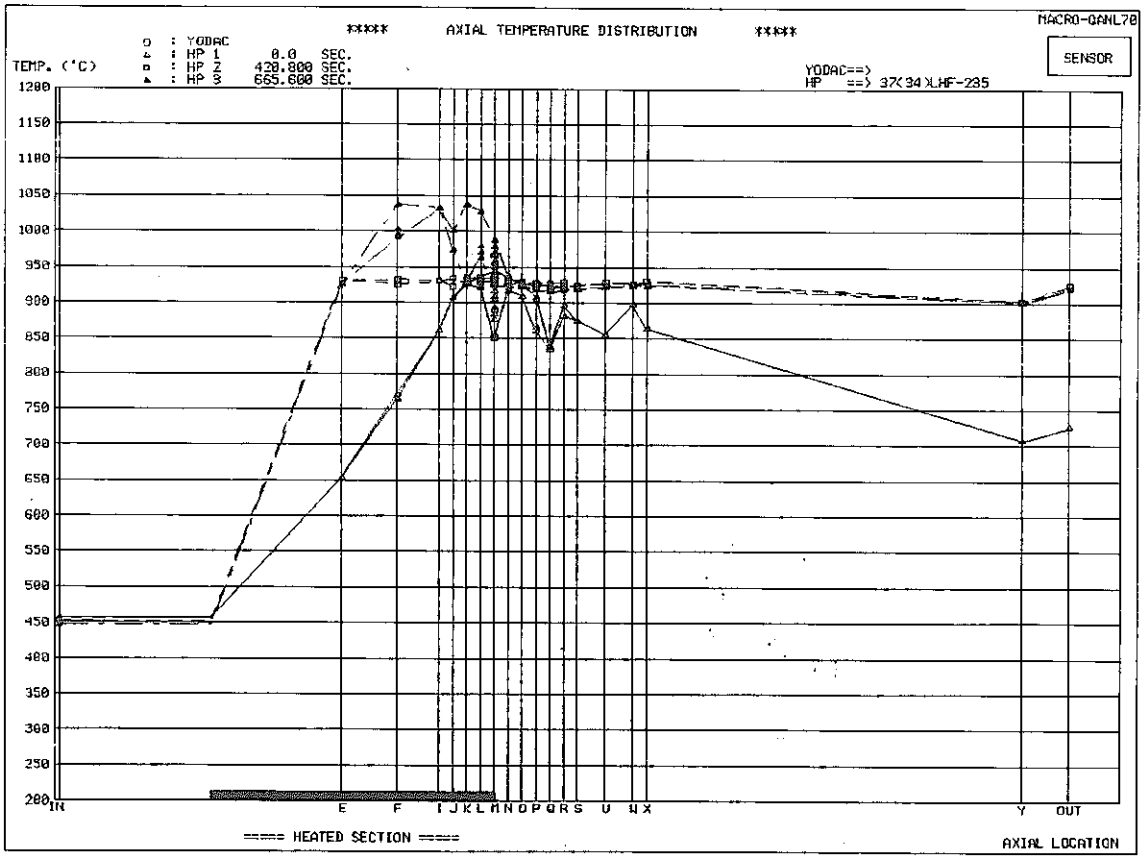
***** AXIAL TEMPERATURE DISTRIBUTION *****
MACRO-GANL70
SENSOR
○ : YODAC
△ : HP 1 0.0 SEC.
□ : HP 2 420.800 SEC.
▲ : HP 3 665.600 SEC.
TEMP. ('C)
YODAC==>
HP ==> 37<34>LHF-235
IN
E F I J K L M N O P Q R S U W X
Y OUT
==== HEATED SECTION ====
AXIAL LOCATION

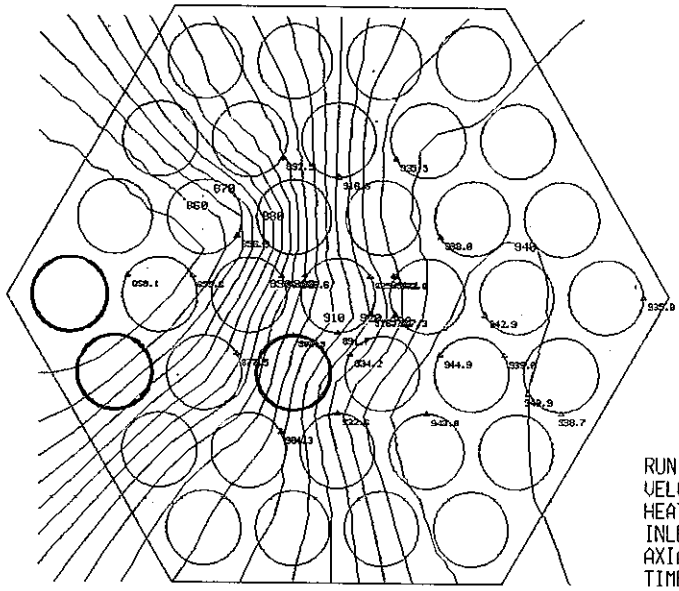

RUN NAME 37(34)LHF-235
VELOCITY 0.035 M/S
HEAT FLUX 4.03 W/CM2
INLET TEMP. 454.0 C
AXIAL 0.0 MM
TIME 0.0 SEC.

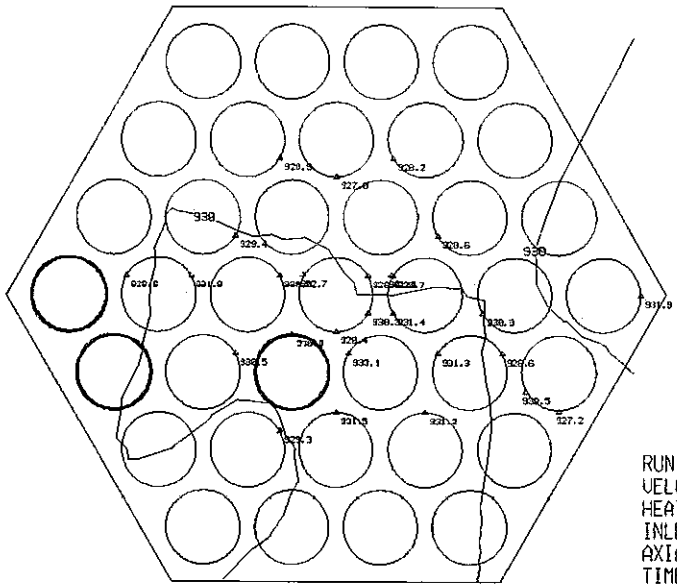

RUN NAME 37(34)LHF-235
VELOCITY 0.012 M/S
HEAT FLUX 11.73 W/CM2
INLET TEMP. 455.8 C
AXIAL 0.0 MM
TIME 420.800 SEC.

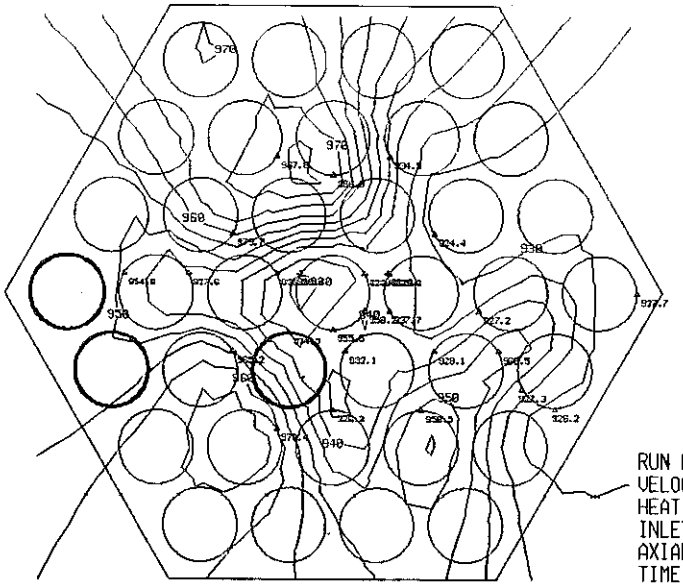

RUN NAME 37(34)LHF-235
VELOCITY 0.012 M/S
HEAT FLUX 11.73 W/CM2
INLET TEMP. 444.5 C
AXIAL 0.0 MM
TIME 665.600 SEC.

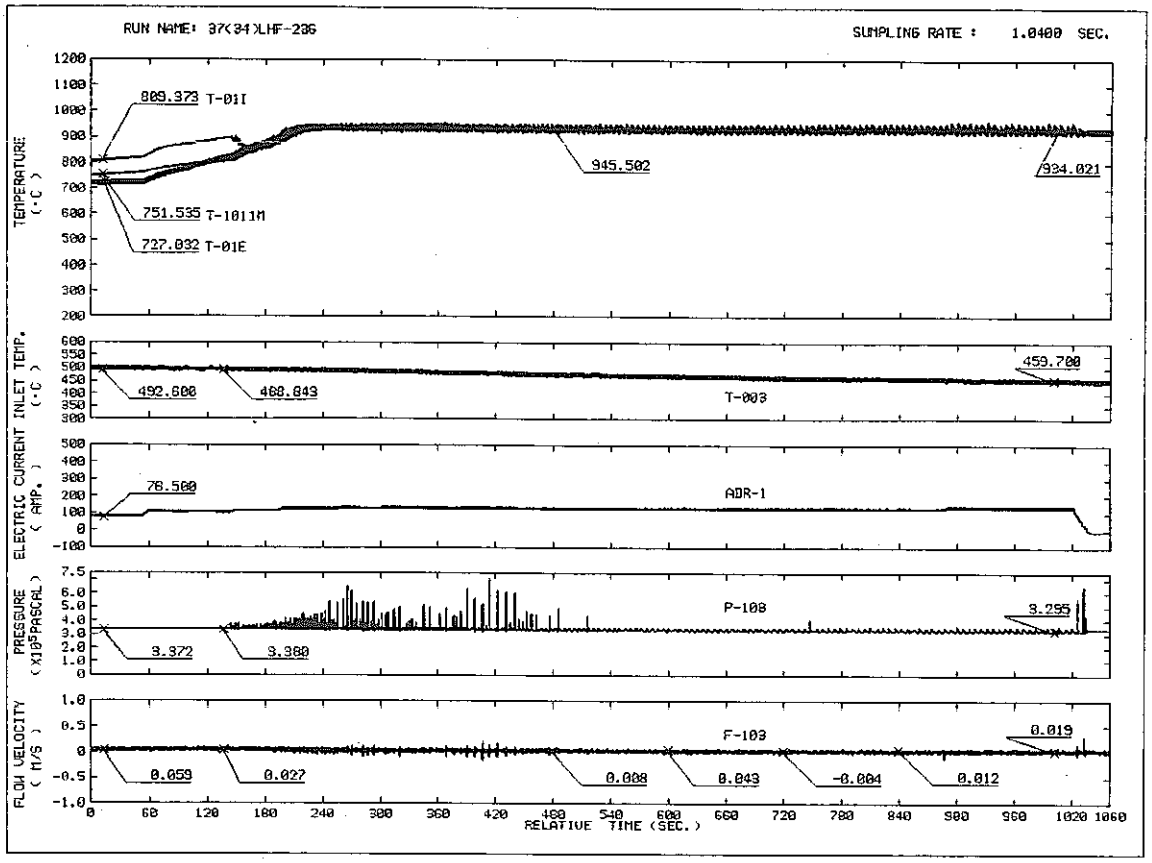
RUN NAME: 37(34)LHF-236
SUMPLING RATE : 1.0400 SEC.
TEMPERATURE (°C)
889.373 T-01I
945.502
934.021
751.535 T-1011M
727.032 T-01E
ELECTRIC CURRENT INLET TEMP. (°C)
492.800
468.843
T-003
459.700
(AMP.)
78.500
ADR-1
PRESSURE (X10⁵PASCAL)
P-108
3.372
3.380
3.295
FLOW VELOCITY (M/S)
F-103
0.059
0.027
0.008
0.043
-0.004
0.012
0.019
RELATIVE TIME (SEC.)

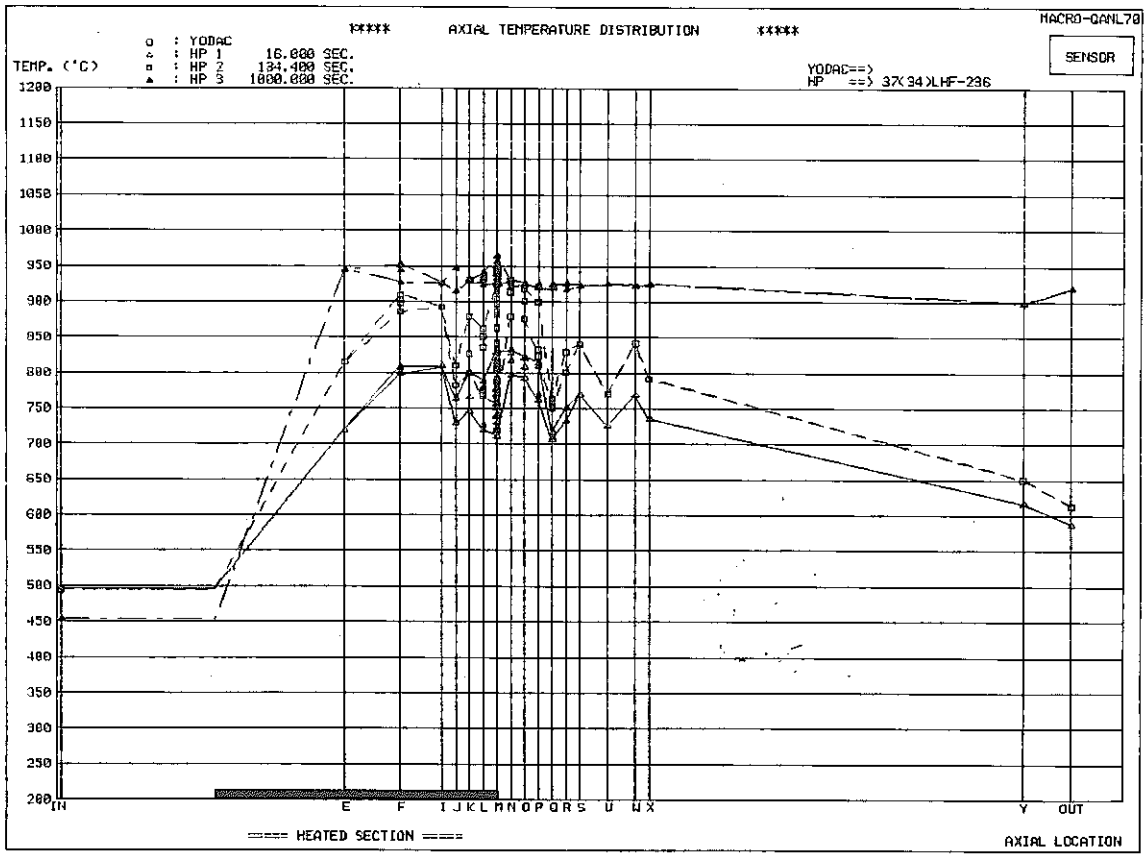
***** AXIAL TEMPERATURE DISTRIBUTION *****
MACRO-QANL70
SENSOR
o : YODAC
△ : HP 1 16.000 SEC.
□ : HP 2 134.400 SEC.
▲ : HP 3 1000.000 SEC.
TEMP. (°C)
YODAC==)
HP ==) 37(34)LHF-236
IN E F I J K L M N O P Q R S U W X Y OUT
==== HEATED SECTION ====
AXIAL LOCATION

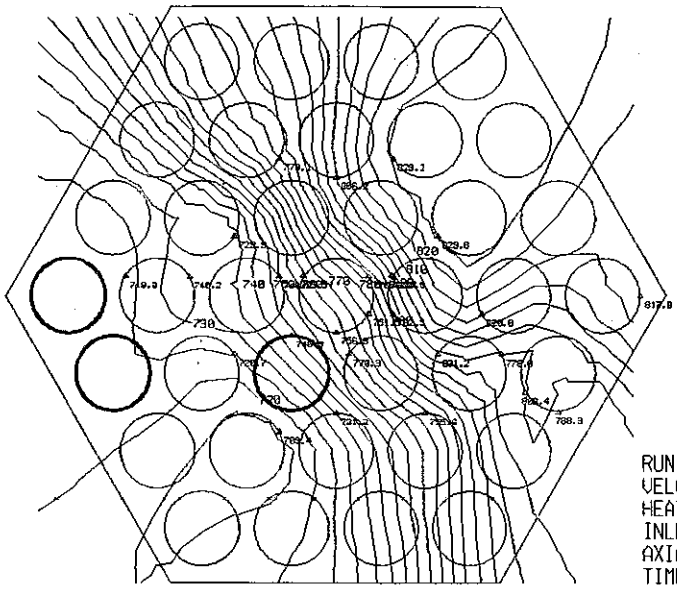

RUN NAME 37(34)LHF-236
VELOCITY 0.043 M/S
HEAT FLUX 2.78 W/CM2
INLET TEMP. 495.4 C
AXIAL 0.0 MM
TIME 16.000 SEC.

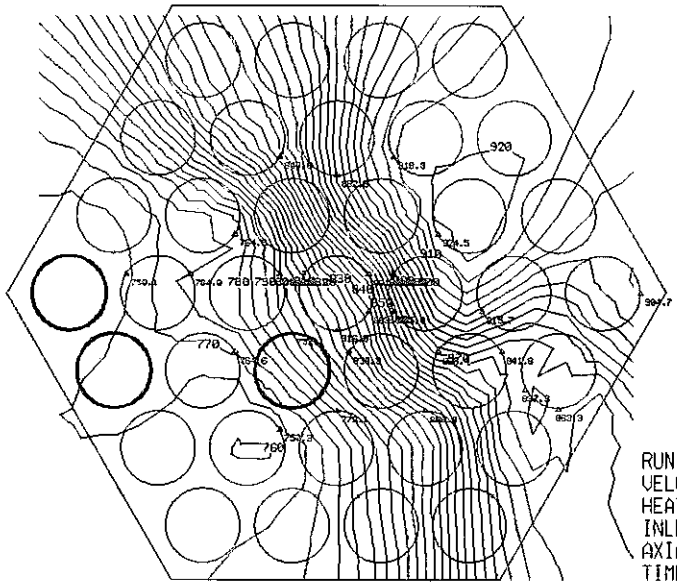

RUN NAME 37(34)LHF-236
VELOCITY 0.059 M/S
HEAT FLUX 5.00 W/CM2
INLET TEMP. 497.3 C
AXIAL 0.0 MM
TIME 134.400 SEC.

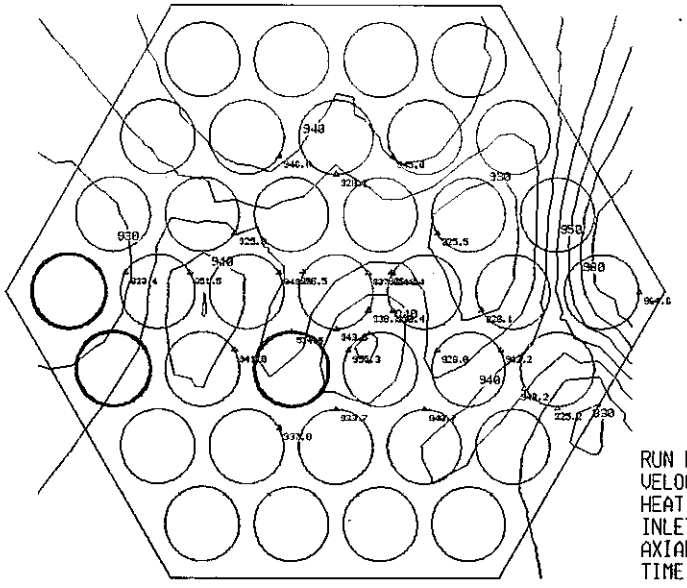

RUN NAME 37(34)LHF-236
VELOCITY 0.035 M/S
HEAT FLUX 8.97 W/CM2
INLET TEMP. 452.2 C
AXIAL 0.0 MM
TIME 1000.000 SEC.

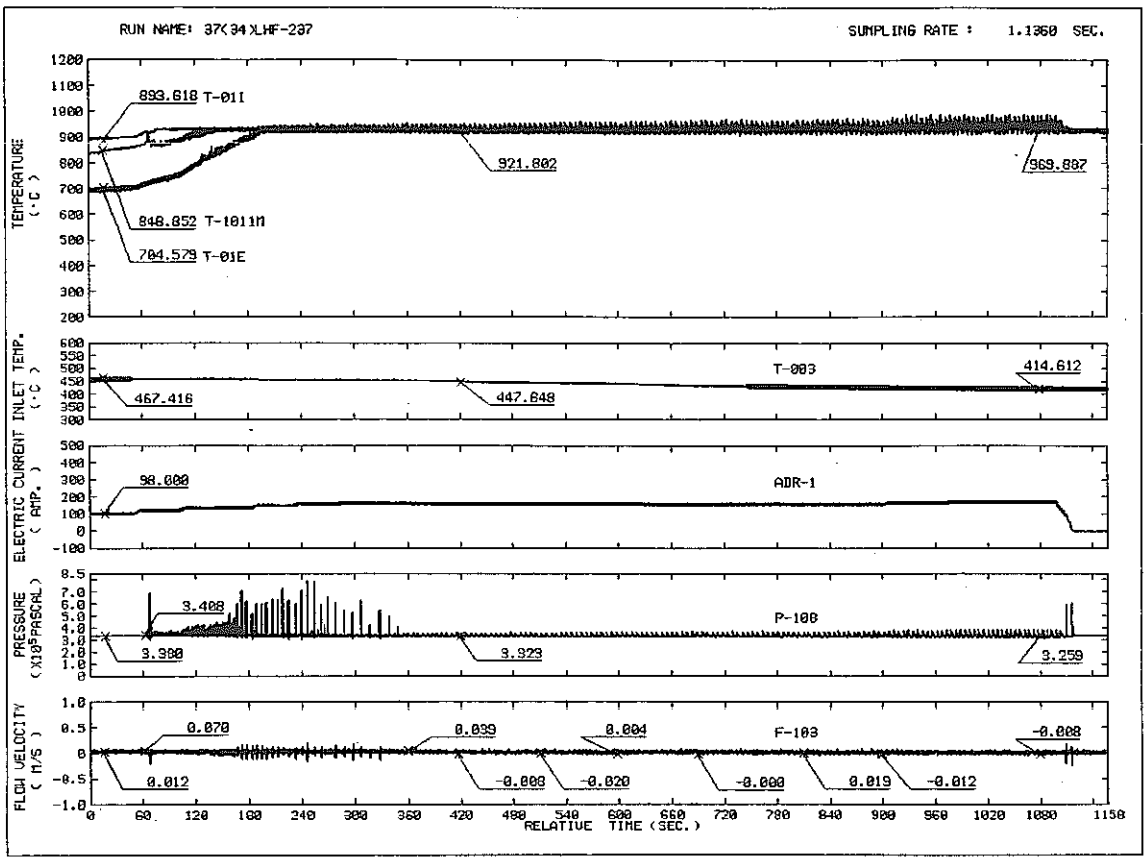
RUN NAME: 37(34)LHF-237
SUMPLING RATE : 1.1360 SEC.
TEMPERATURE (°C)
893.618 T-01I
921.802
969.897
848.852 T-1011M
704.579 T-01E
ELECTRIC CURRENT INLET TEMP. (°C)
T-003
414.612
467.416
447.848
(AMP.)
98.000
ADR-1
PRESSURE (X10⁵PASCAL)
3.408
P-108
3.380
3.323
3.259
FLOW VELOCITY (M/S)
0.070
0.039
0.004
F-103
-0.008
0.012
-0.008
-0.020
-0.000
0.019
-0.012
RELATIVE TIME (SEC.)

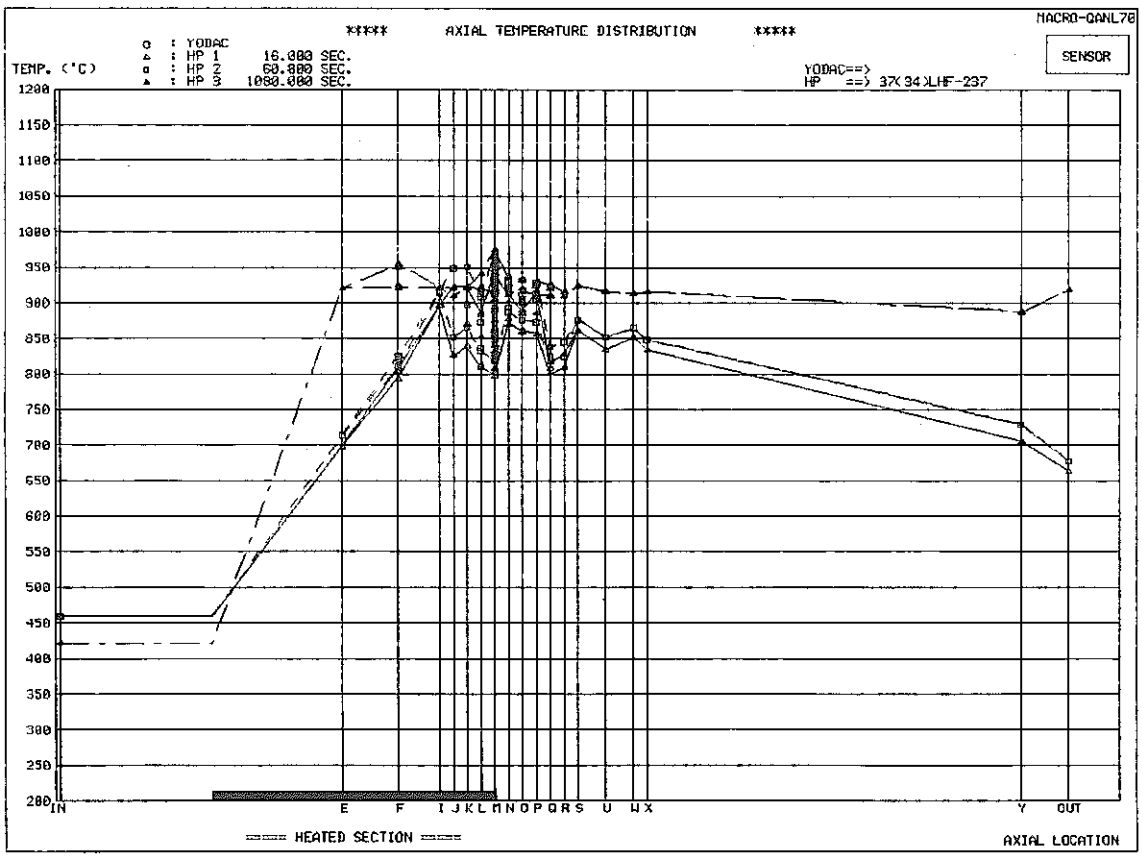
***** AXIAL TEMPERATURE DISTRIBUTION *****
MACRO-QANL70
SENSOR
o : YODAC
Δ : HP 1 16.000 SEC.
□ : HP 2 60.000 SEC.
▲ : HP 3 1080.000 SEC.
TEMP. (°C)
YODAC==>
HP ==> 37(34)LHF-237
IN E F I J K L M N O P Q R S U W X Y OUT
===== HEATED SECTION =====
AXIAL LOCATION

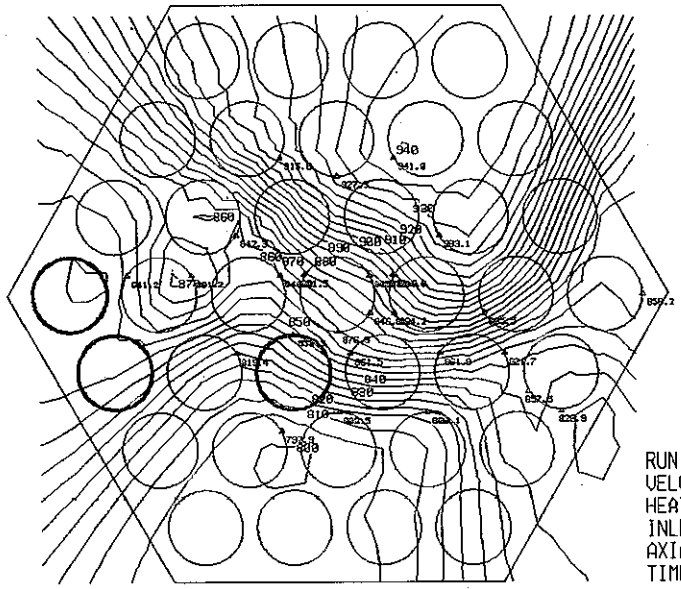

RUN NAME 37(34)LHF-237
VELOCITY 0.035 M/S
HEAT FLUX 4.48 W/CM2
INLET TEMP. 456.1 C
AXIAL 0.0 MM
TIME 16.000 SEC.

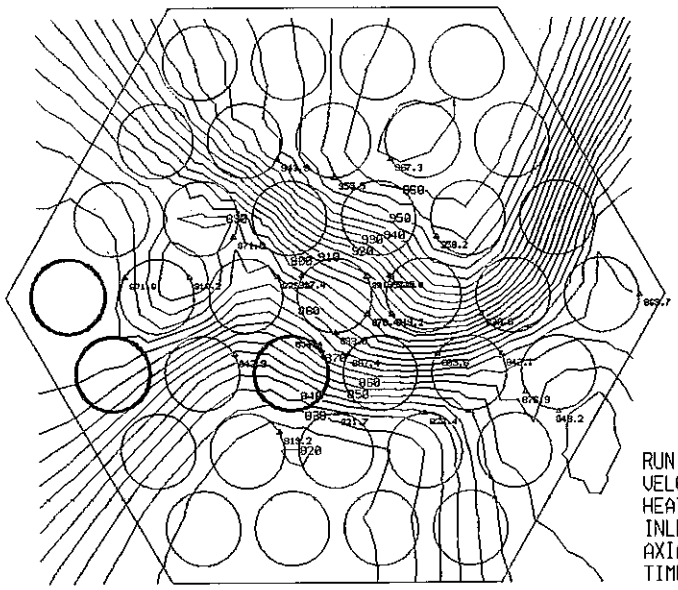

RUN NAME 37(34)LHF-237
VELOCITY 0.039 M/S
HEAT FLUX 5.90 W/CM2
INLET TEMP. 458.9 C
AXIAL 0.0 MM
TIME 60.800 SEC.

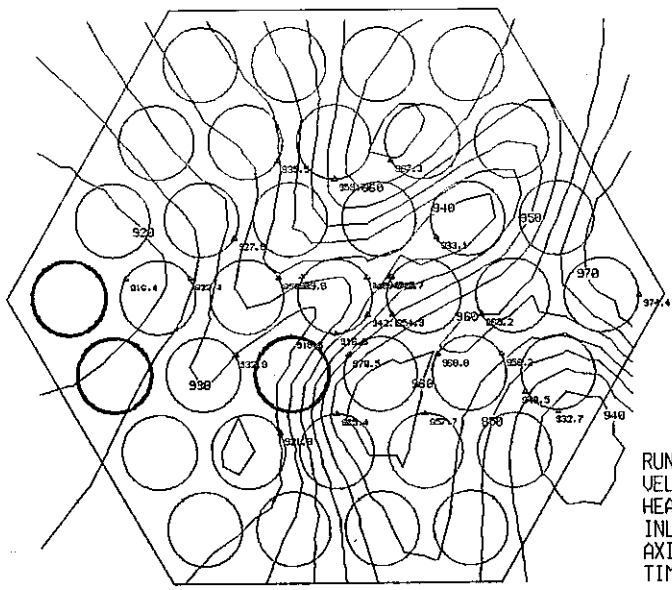

RUN NAME 37(34)LHF-237
VELOCITY 0.004 M/S
HEAT FLUX 14.02 W/CM2
INLET TEMP. 424.1 C
AXIAL 0.0 MM
TIME 1080.000 SEC.

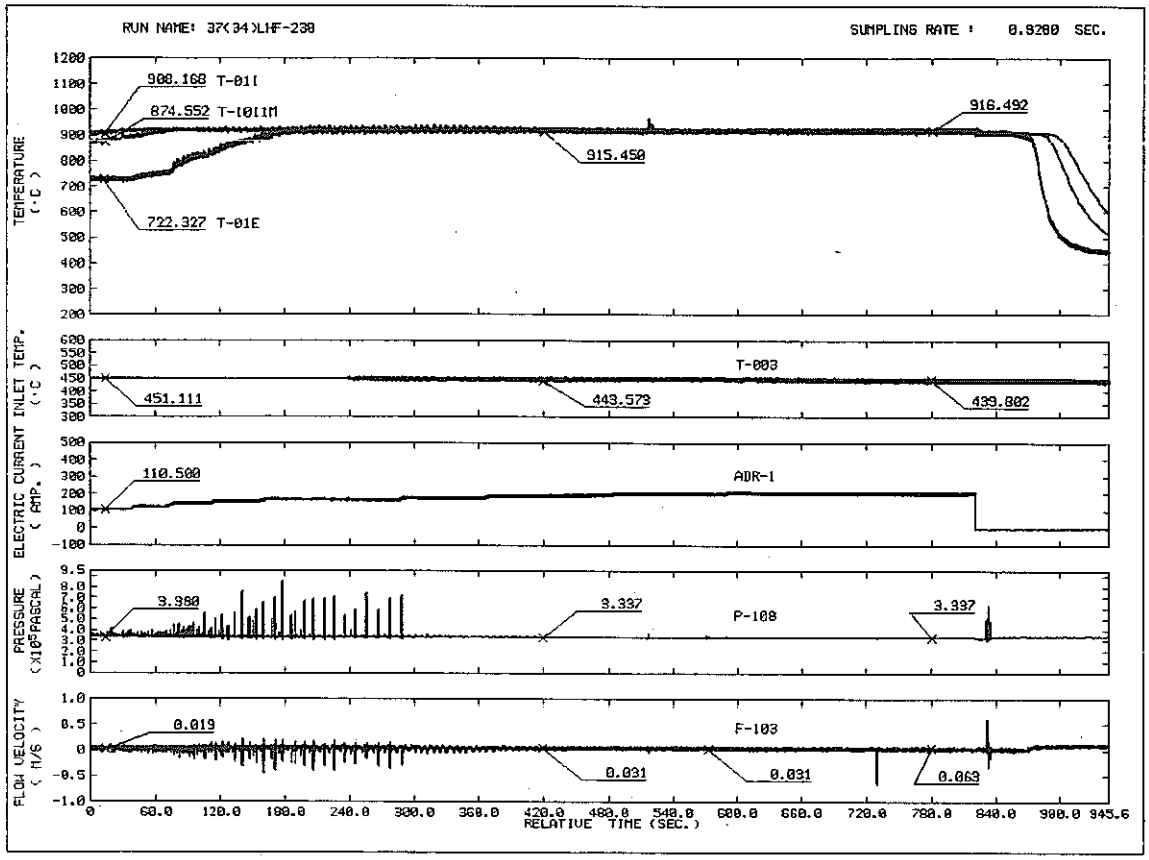
RUN NAME: 37(34)LHF-238
SUMPLING RATE : 0.9200 SEC.
TEMPERATURE ('C)
908.168 T-01I
874.552 T-1011M
916.492
915.450
722.327 T-01E
ELECTRIC CURRENT INLET TEMP. ('C)
T-003
451.111
443.573
439.802
('AMP.)
110.500
ADR-1
PRESSURE (X10⁵PASCAL)
3.980
3.337
P-108
3.337
FLOW VELOCITY ('M/S)
0.019
F-103
0.031
0.031
0.063
RELATIVE TIME (SEC.)

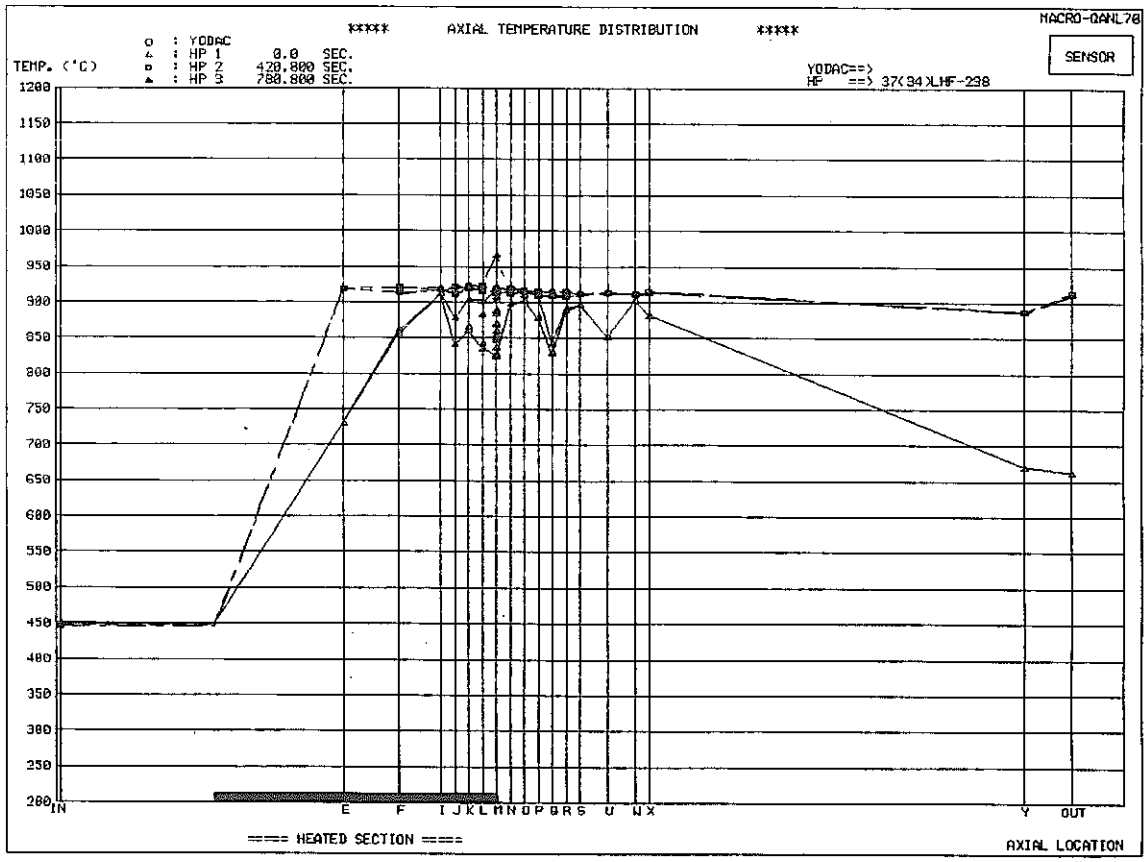
***** AXIAL TEMPERATURE DISTRIBUTION *****
MACRO-QANL70
SENSOR
o : YODAC
Δ : HP 1 0.0 SEC.
□ : HP 2 420.800 SEC.
▲ : HP 3 780.800 SEC.
TEMP. ('C)
YODAC==>
HP ==> 37(34)LHF-238
IN
E F I J K L M N O P Q R S U W X
Y OUT
==== HEATED SECTION ====
AXIAL LOCATION

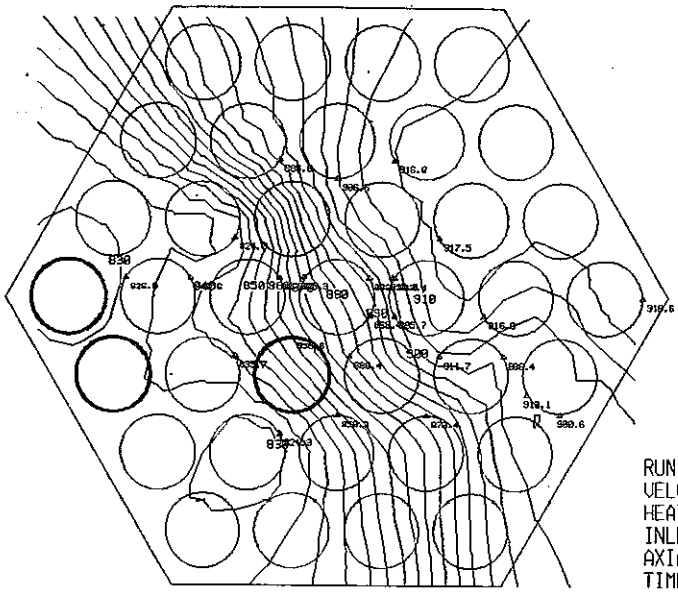

RUN NAME 37(34)LHF-238
VELOCITY 0.031 M/S
HEAT FLUX 16.37 W/CM2
INLET TEMP. 449.2 C
AXIAL 0.0 MM
TIME 0.0 SEC.

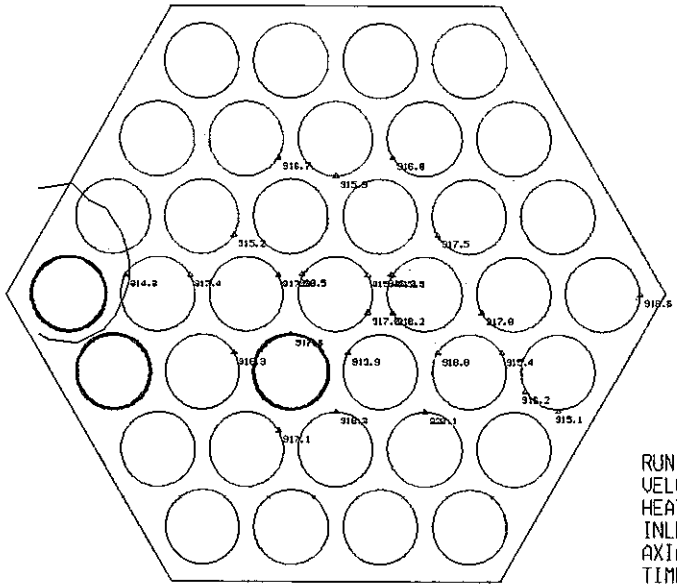

RUN NAME 37(34)LHF-238
VELOCITY 0.043 M/S
HEAT FLUX 16.85 W/CM2
INLET TEMP. 448.3 C
AXIAL 0.0 MM
TIME 420.800 SEC.

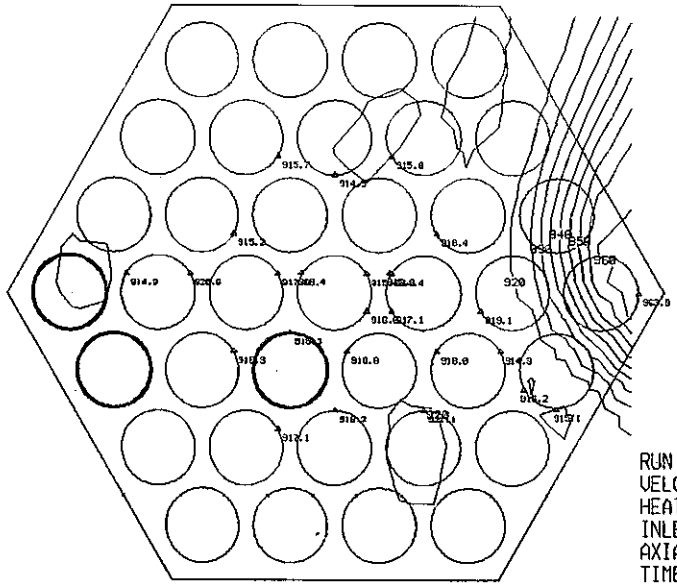

RUN NAME 37(34)LHF-238
VELOCITY 0.039 M/S
HEAT FLUX 19.75 W/CM2
INLET TEMP. 445.5 C
AXIAL 0.0 MM
TIME 780.800 SEC.

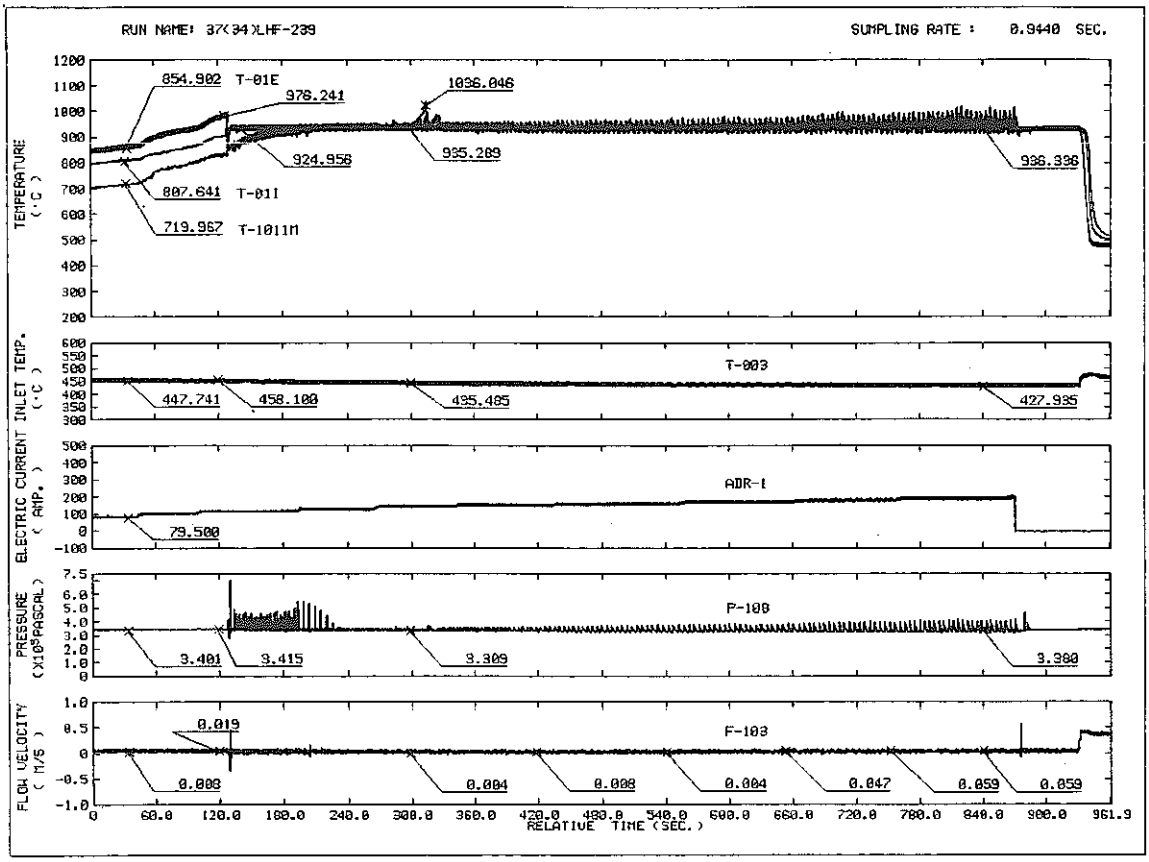
RUN NAME: 37(34)LHF-239
SAMPLING RATE : 0.9440 SEC.
TEMPERATURE ('C)
854.902 T-01E
978.241
1036.046
924.956
935.289
936.336
807.641 T-011
719.967 T-1011M
ELECTRIC CURRENT INLET TEMP. ('C)
T-003
447.741
458.100
495.485
427.935
PRESSURE (X10⁶PASCAL)
ADR-1
79.500
P-108
3.401
3.415
3.309
3.980
FLOW VELOCITY (M/S)
F-103
0.019
0.000
0.004
0.008
0.004
0.047
0.059
0.059
RELATIVE TIME (SEC.)

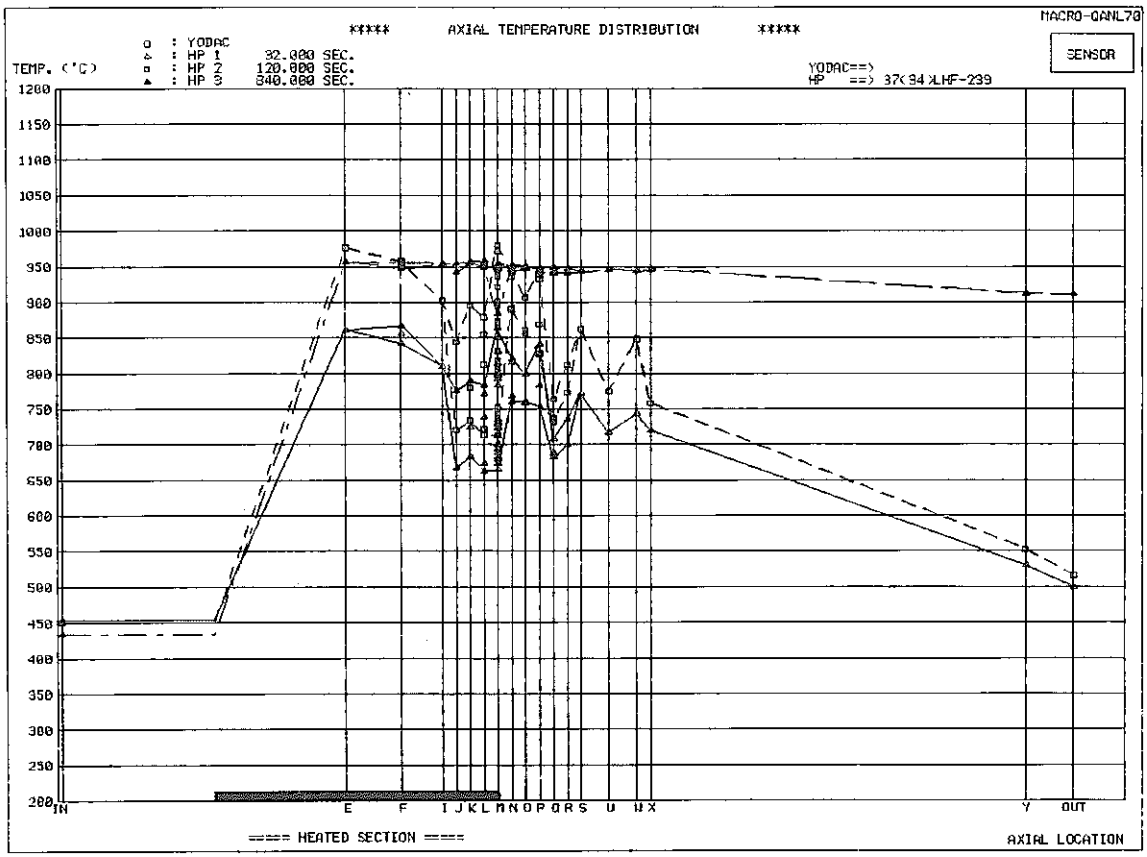
MACRO-QANL70
***** AXIAL TEMPERATURE DISTRIBUTION *****
SENSOR
o : YODAC
Δ : HP 1 32.000 SEC.
□ : HP 2 120.000 SEC.
▲ : HP 3 340.000 SEC.
TEMP. ('C)
YODAC==)
HP ==) 37(34)LHF-239
IN
E F I J K L M N O P Q R S U W X
Y OUT
==== HEATED SECTION ====
AXIAL LOCATION

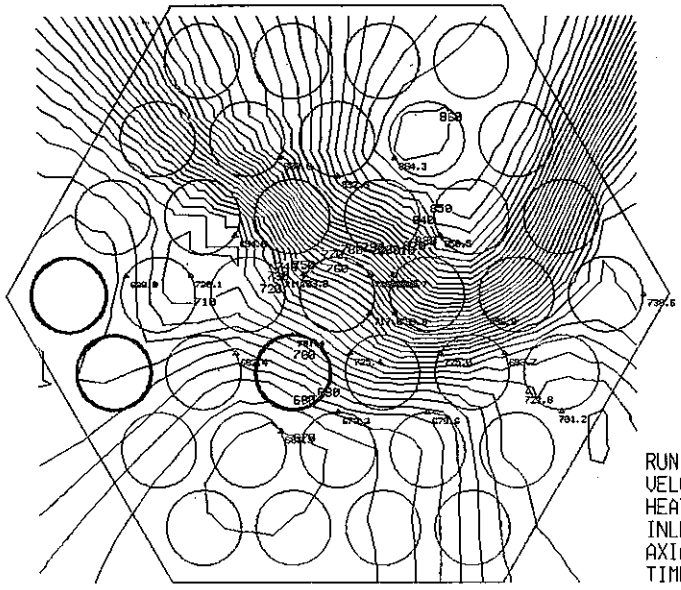

RUN NAME 37(34)LHF-239
VELOCITY 0.035 M/S
HEAT FLUX 3.42 W/CM2
INLET TEMP. 460.0 C
AXIAL 0.0 MM
TIME 32.000 SEC.

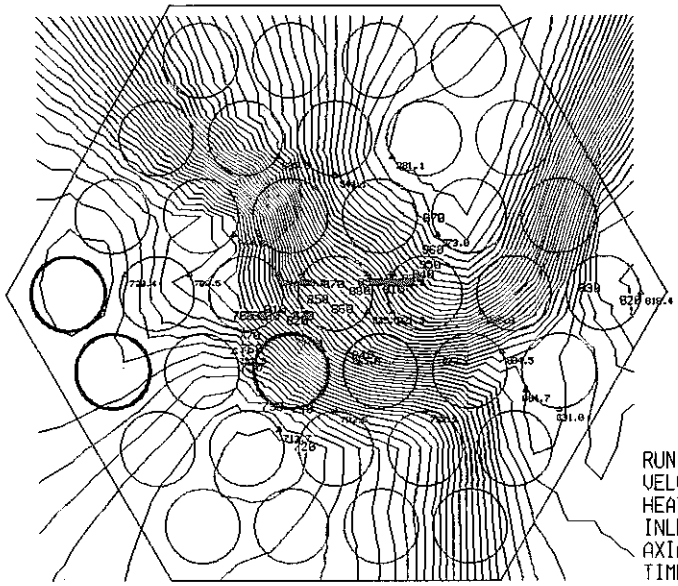

RUN NAME 37(34)LHF-239
VELOCITY 0.074 M/S
HEAT FLUX 6.48 W/CM2
INLET TEMP. 451.5 C
AXIAL 0.0 MM
TIME 120.000 SEC.

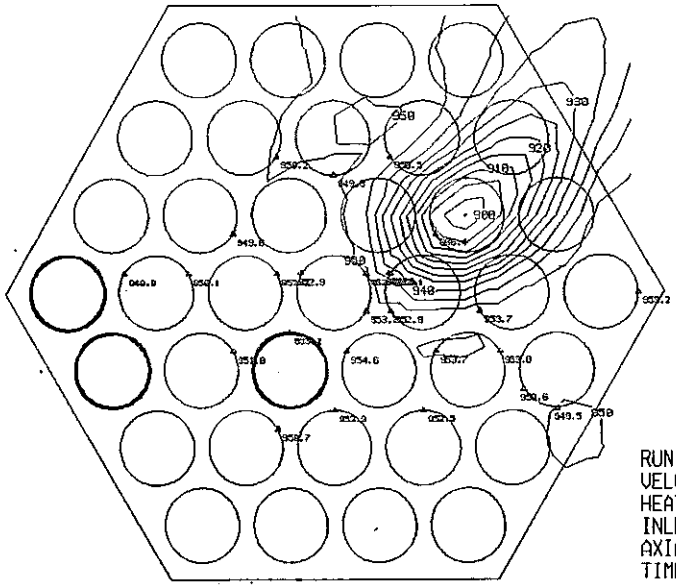

RUN NAME 37(34)LHF-239
VELOCITY 0.023 M/S
HEAT FLUX 16.93 W/CM2
INLET TEMP. 439.3 C
AXIAL 0.0 MM
TIME 840.000 SEC.

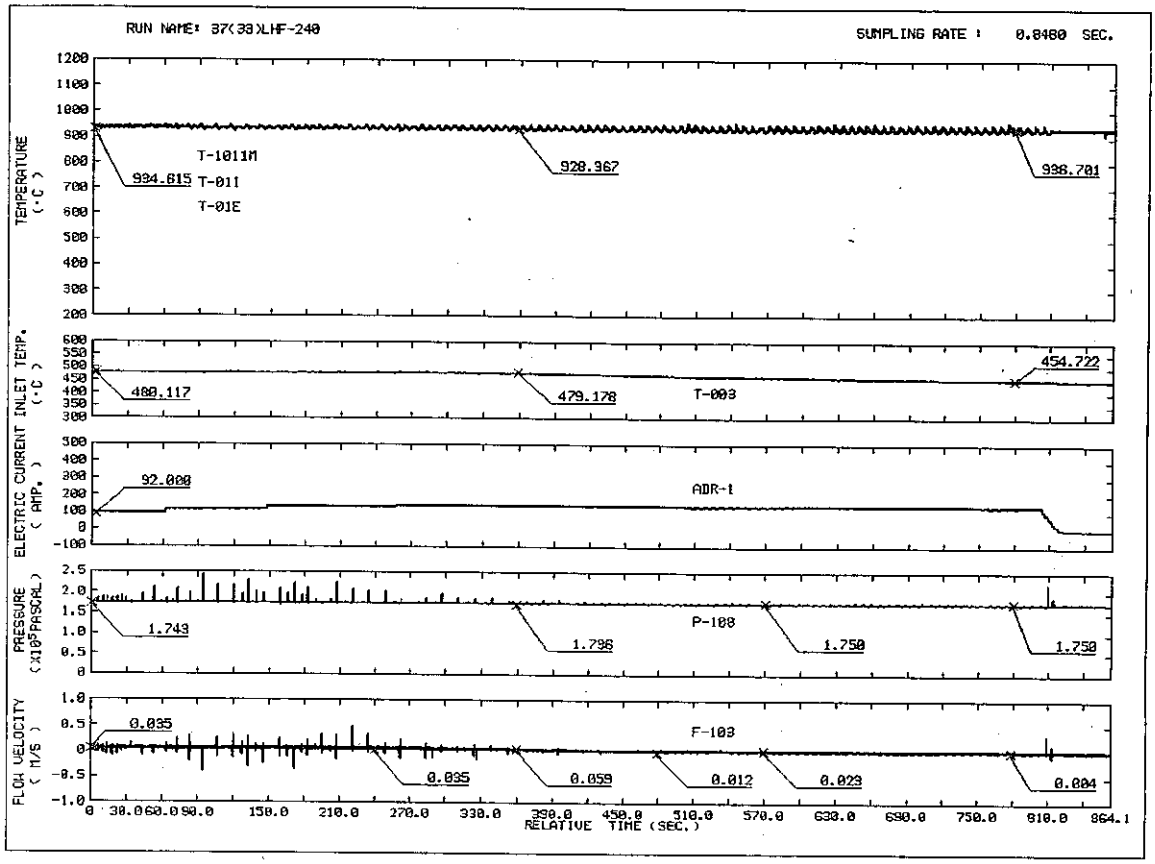
RUN NAME: 37(33)LHF-240
SUMPLING RATE : 0.8480 SEC.
TEMPERATURE (°C)
T-1011M
934.615 T-011
T-01E
928.367
938.701
ELECTRIC CURRENT INLET TEMP. (°C)
480.117
479.178
T-003
454.722
(AMP.)
92.000
ADR-1
PRESSURE (X10⁵PASCAL)
1.743
1.736
P-108
1.750
1.750
FLOW VELOCITY (M/S)
0.035
F-103
0.035
0.059
0.012
0.023
0.004
RELATIVE TIME (SEC.)

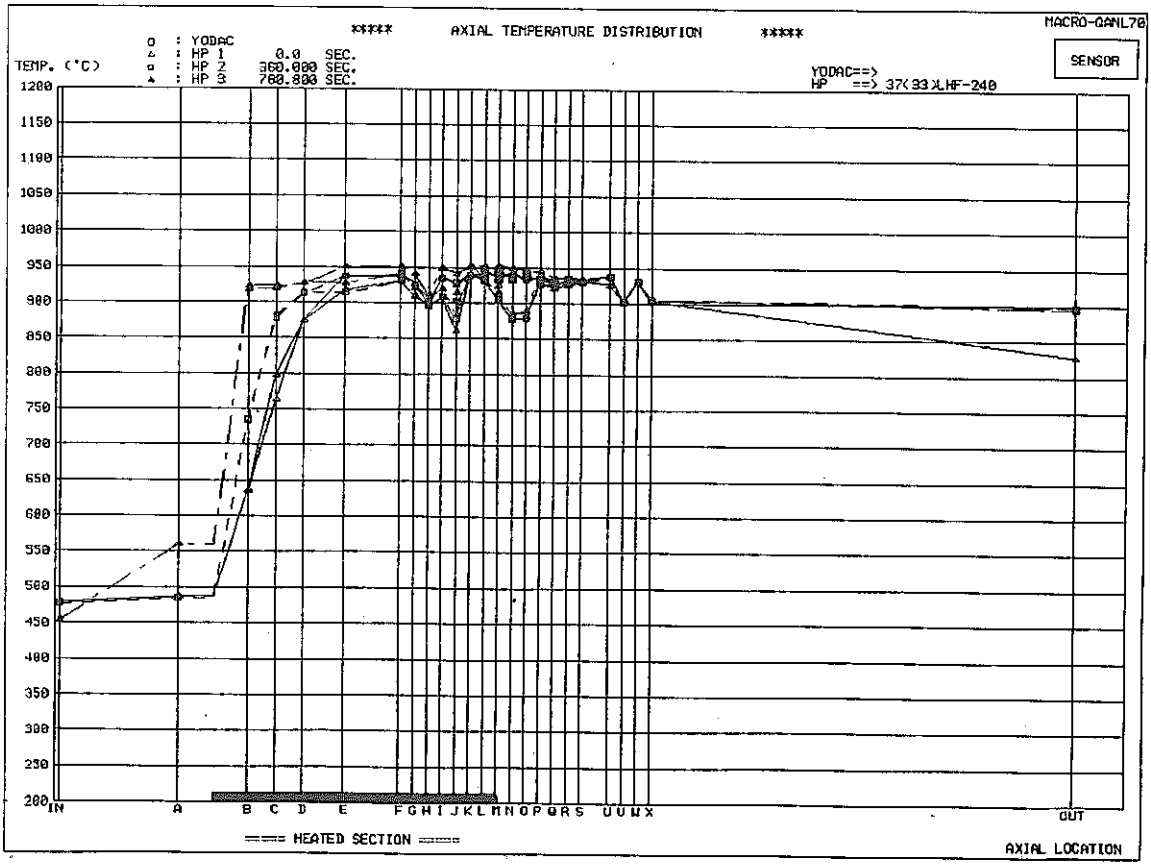
***** AXIAL TEMPERATURE DISTRIBUTION *****
MACRO-GANL70
SENSOR
o : YODAC
Δ : HP 1 0.0 SEC.
□ : HP 2 360.000 SEC.
▲ : HP 3 780.800 SEC.
TEMP. (°C)
YODAC==>
HP ==> 37(33)LHF-240
IN A B C D E F G H I J K L M N O P Q R S U U W X OUT
==== HEATED SECTION =====
AXIAL LOCATION

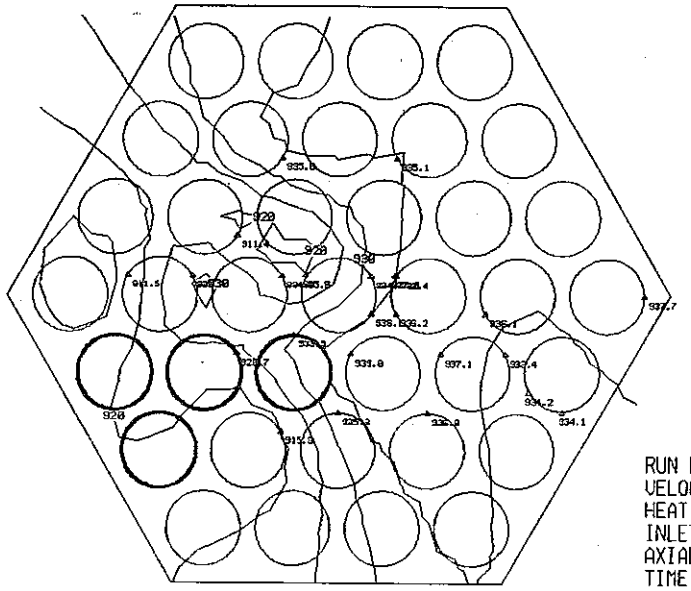

RUN NAME 37(33)LHF-240
VELOCITY 0.043 M/S
HEAT FLUX 4.40 W/CM2
INLET TEMP. 479.2 C
AXIAL 0.0 MM
TIME 0.0 SEC.

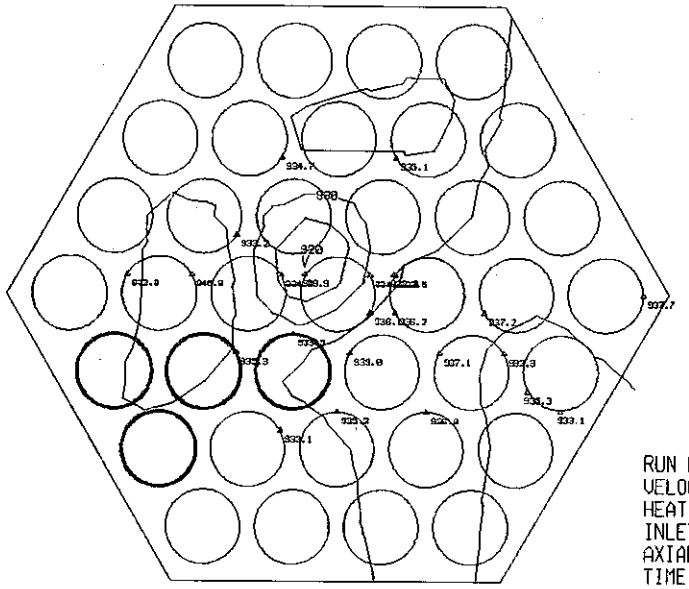

RUN NAME 37(33)LHF-240
VELOCITY 0.039 M/S
HEAT FLUX 9.86 W/CM2
INLET TEMP. 477.3 C
AXIAL 0.0 MM
TIME 360.000 SEC.

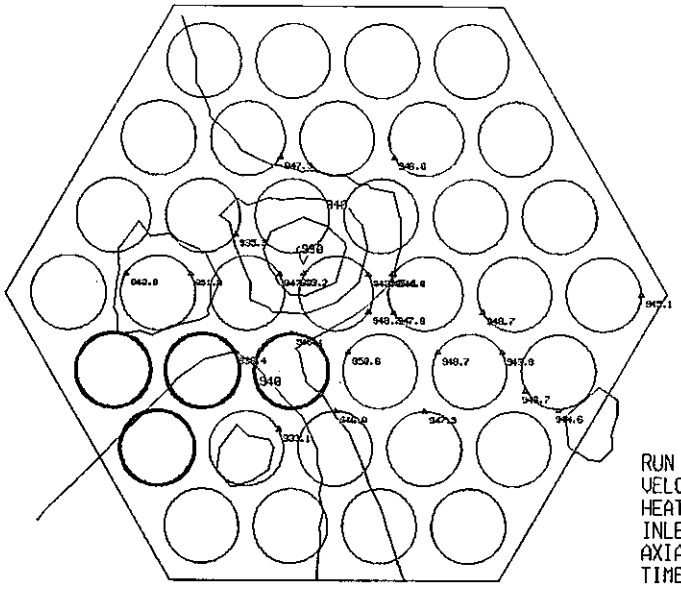

RUN NAME 37(33)LHF-240
VELOCITY 0.004 M/S
HEAT FLUX 9.56 W/CM2
INLET TEMP. 455.7 C
AXIAL 0.0 MM
TIME 780.800 SEC.

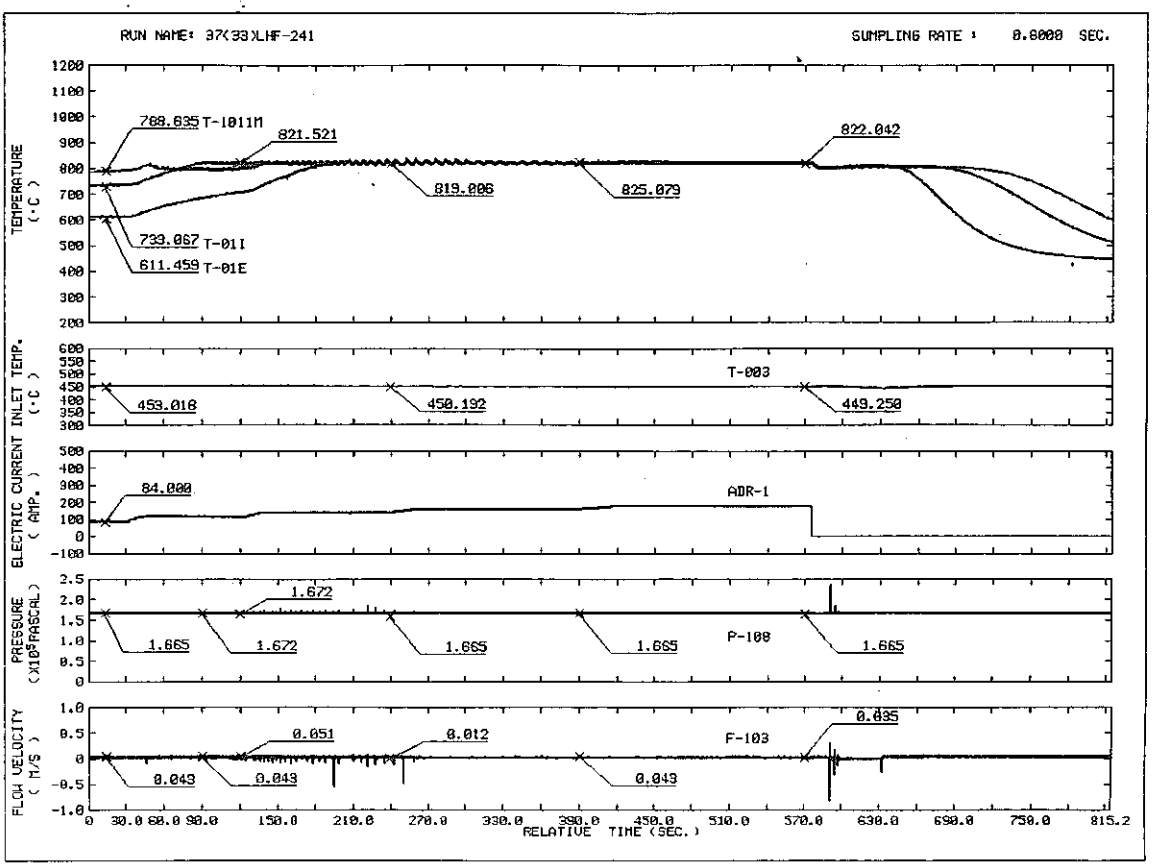
RUN NAME: 37(33)LHF-241
SUMPLING RATE : 0.8000 SEC.
TEMPERATURE (°C)
768.635 T-1011M
821.521
822.042
819.006
825.079
733.067 T-011
611.459 T-01E
ELECTRIC CURRENT INLET TEMP. (°C)
T-003
459.018
450.192
449.250
(AMP.)
84.000
ADR-1
PRESSURE (X10⁵PASCAL)
1.672
1.665
1.672
1.665
1.665
P-108
1.665
FLOW VELOCITY (M/S)
0.051
0.012
F-103
0.035
0.043
0.043
0.043
RELATIVE TIME (SEC.)

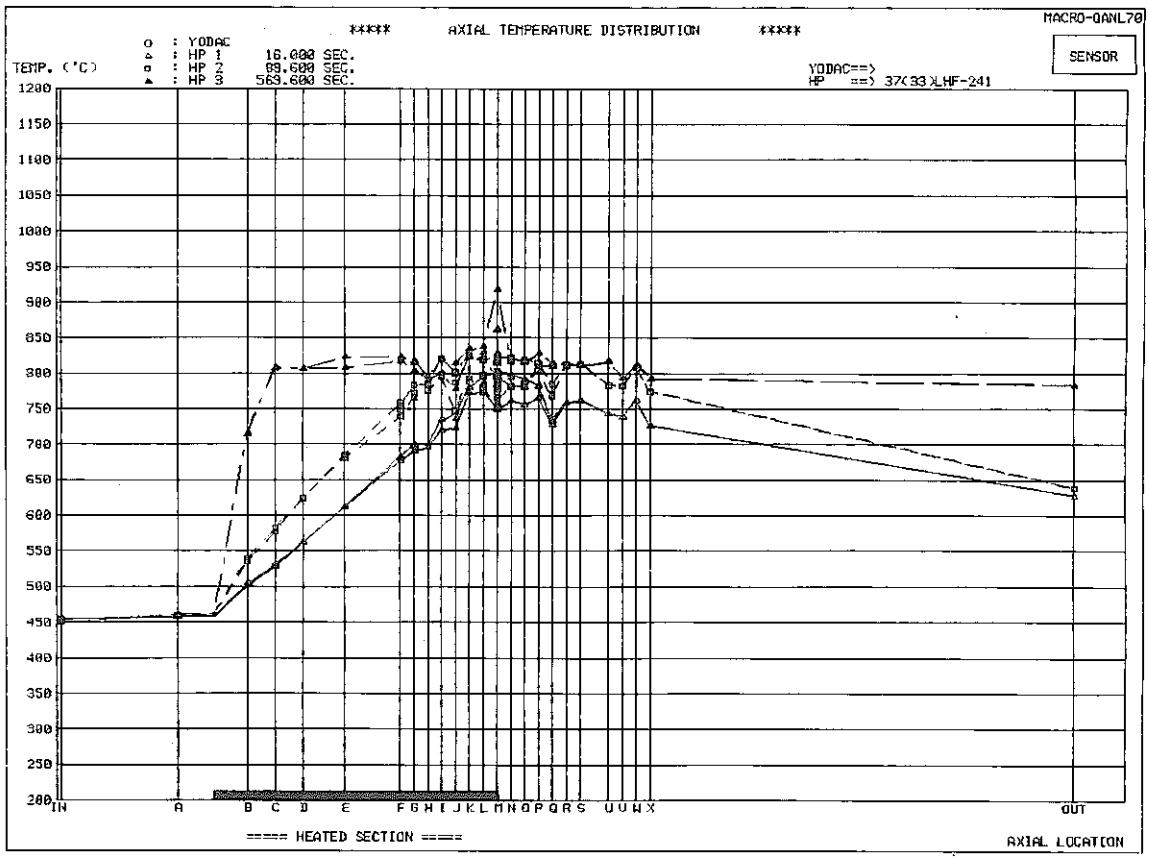
***** AXIAL TEMPERATURE DISTRIBUTION *****
MACRO-QANL70
SENSOR
o : YODAC
Δ : HP 1 16.000 SEC.
□ : HP 2 89.600 SEC.
▲ : HP 3 569.600 SEC.
TEMP. (°C)
YODAC==>
HP ==> 37(33)LHF-241
IN
A
B C D E F G H I J K L M N O P Q R S U V W X
OUT
===== HEATED SECTION =====
AXIAL LOCATION

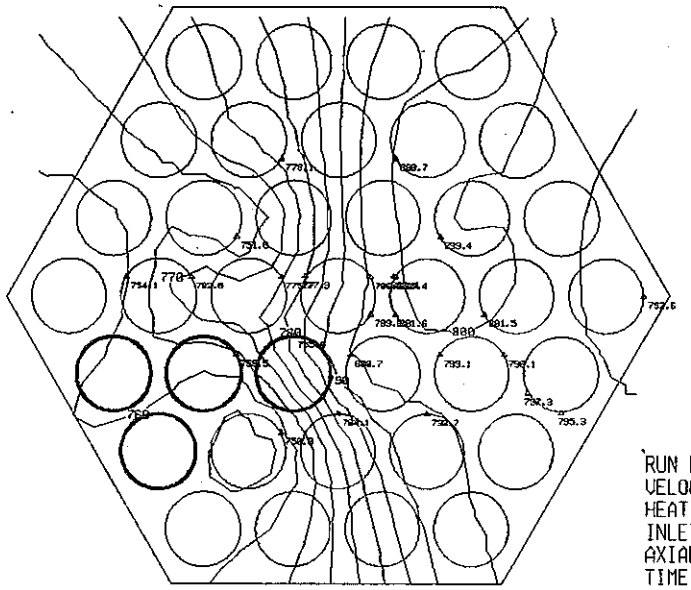

RUN NAME 37(33)LHF-241
VELOCITY 0.027 M/S
HEAT FLUX 3.02 W/CM2
INLET TEMP. 454.9 C
AXIAL 0.0 MM
TIME 16.000 SEC.

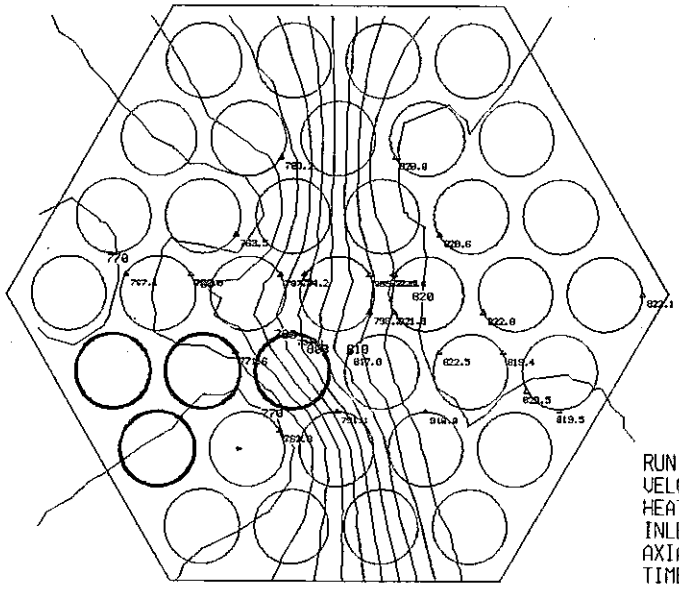

RUN NAME 37(33)LHF-241
VELOCITY 0.031 M/S
HEAT FLUX 5.85 W/CM2
INLET TEMP. 454.0 C
AXIAL 0.0 MM
TIME 89.600 SEC.

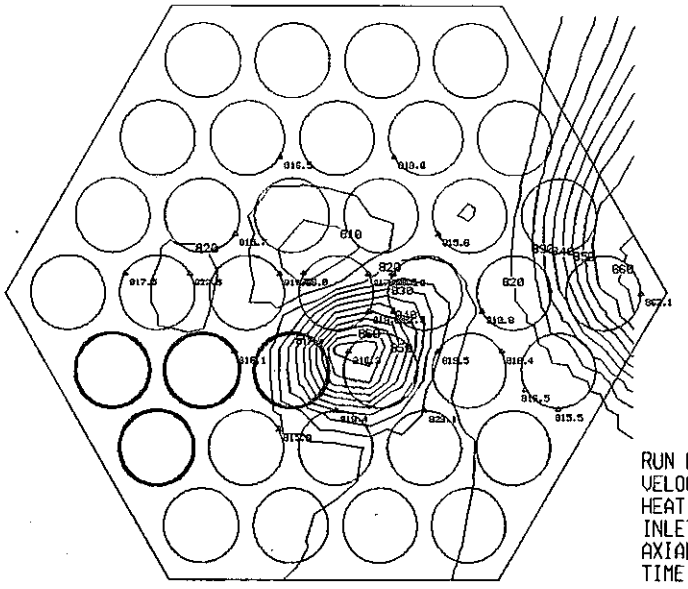

RUN NAME 37(33)LHF-241
VELOCITY 0.023 M/S
HEAT FLUX 14.76 W/CM2
INLET TEMP. 450.2 C
AXIAL 0.0 MM
TIME 569.600 SEC.

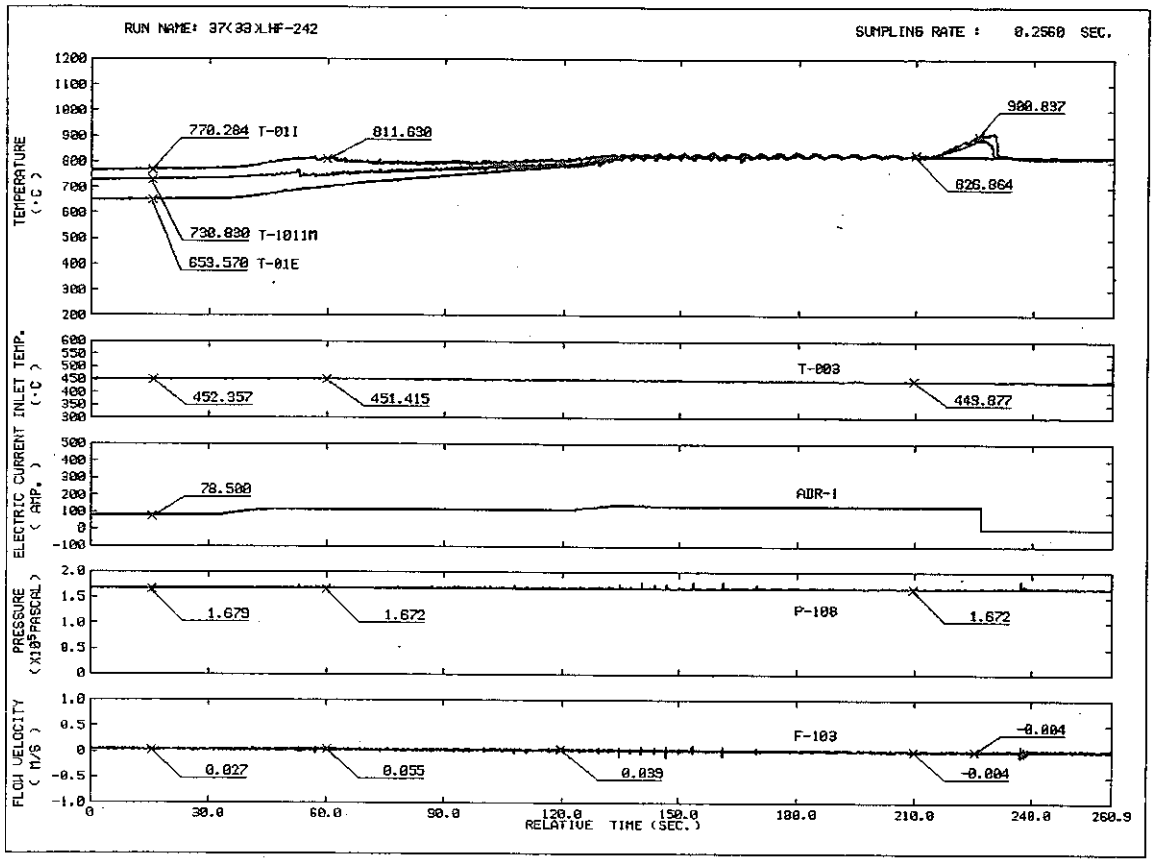
RUN NAME: 37(33)LHF-242
SUMPLING RATE : 0.2560 SEC.
TEMPERATURE (°C)
770.284 T-01I
811.630
900.837
826.864
738.830 T-1011n
653.570 T-01E
INLET TEMP. (°C)
452.357
451.415
T-003
449.877
ELECTRIC CURRENT (AMP.)
78.500
AUR-1
PRESSURE (X10⁵PASCAL)
1.679
1.672
P-108
1.672
FLOW VELOCITY (M/S)
0.027
0.055
0.039
F-103
-0.004
-0.004
RELATIVE TIME (SEC.)

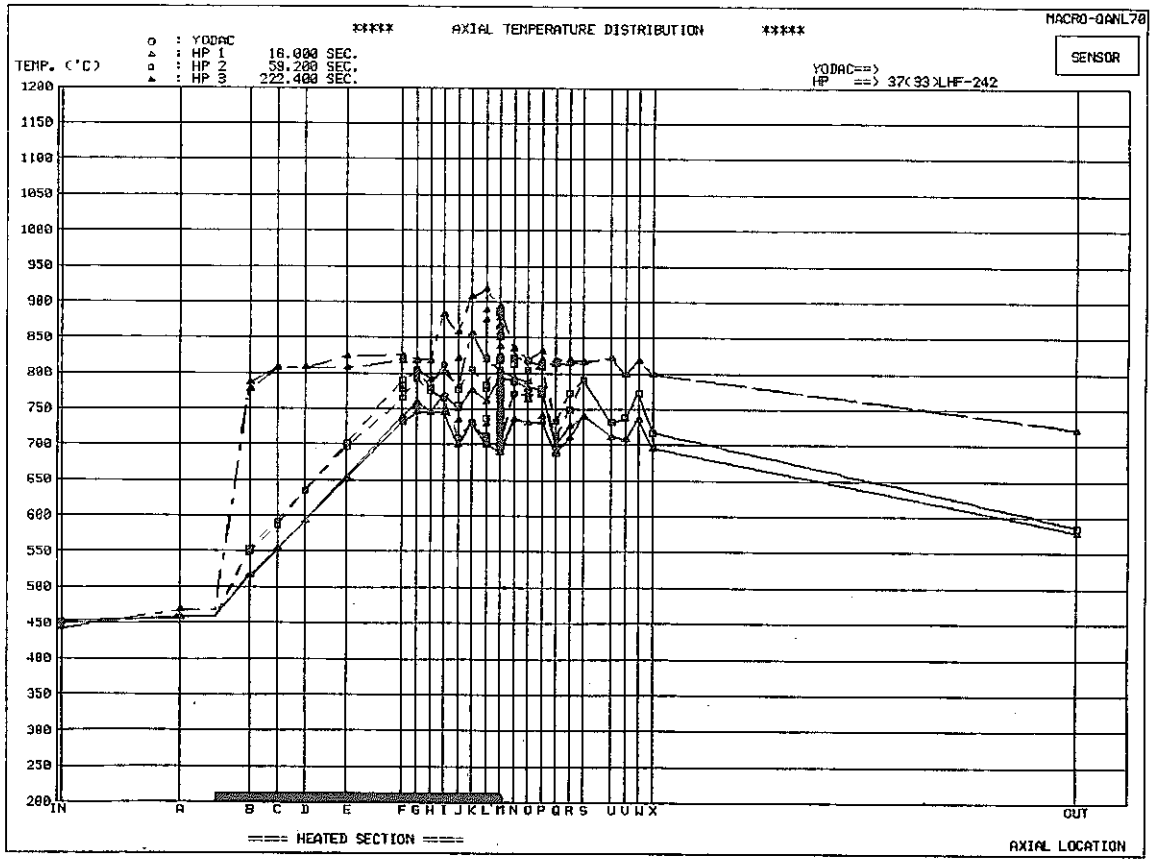
MACRO-QANL70
***** AXIAL TEMPERATURE DISTRIBUTION *****
SENSOR
○ : YODAC
△ : HP 1 16.000 SEC.
□ : HP 2 59.200 SEC.
▲ : HP 3 222.400 SEC.
TEMP. (°C)
YODAC==>
HP ==> 37(33)LHF-242
IN
OUT
==== HEATED SECTION ====
AXIAL LOCATION

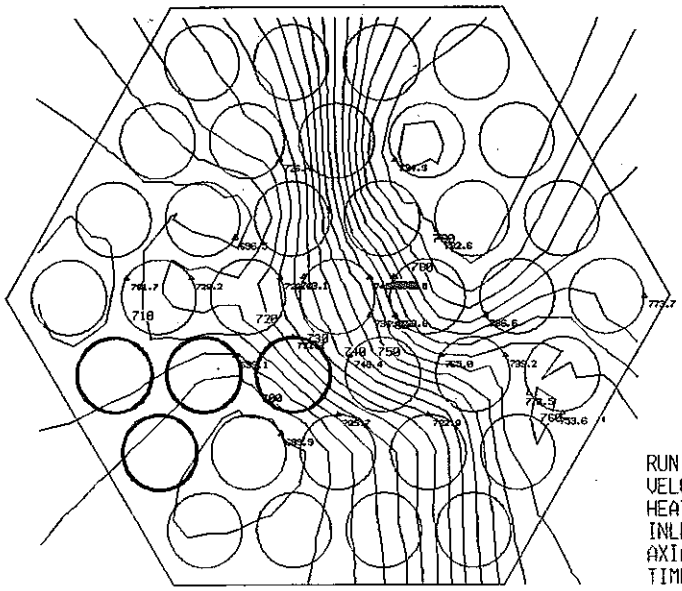

RUN NAME 37(33)LHF-242
VELOCITY 0.031 M/S
HEAT FLUX 2.69 W/CM2
INLET TEMP. 453.3 C
AXIAL 0.0 MM
TIME 16.000 SEC.

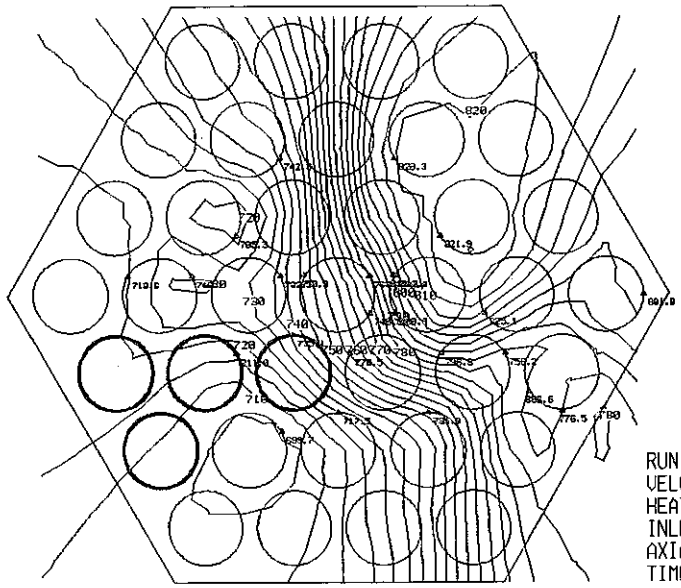

RUN NAME 37(33)LHF-242
VELOCITY 0.027 M/S
HEAT FLUX 5.78 W/CM2
INLET TEMP. 451.4 C
AXIAL 0.0 MM
TIME 59.200 SEC.

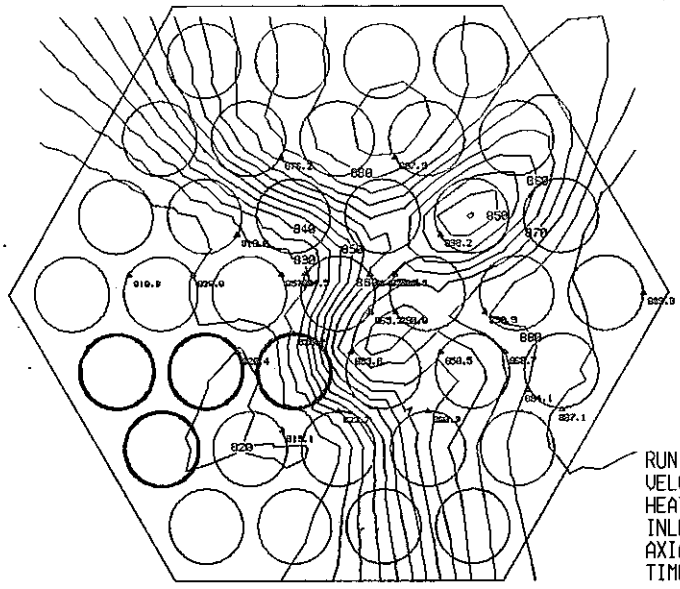

RUN NAME 37(33)LHF-242
VELOCITY 0.004 M/S
HEAT FLUX 8.52 W/CM2
INLET TEMP. 442.9 C
AXIAL 0.0 MM
TIME 222.400 SEC.

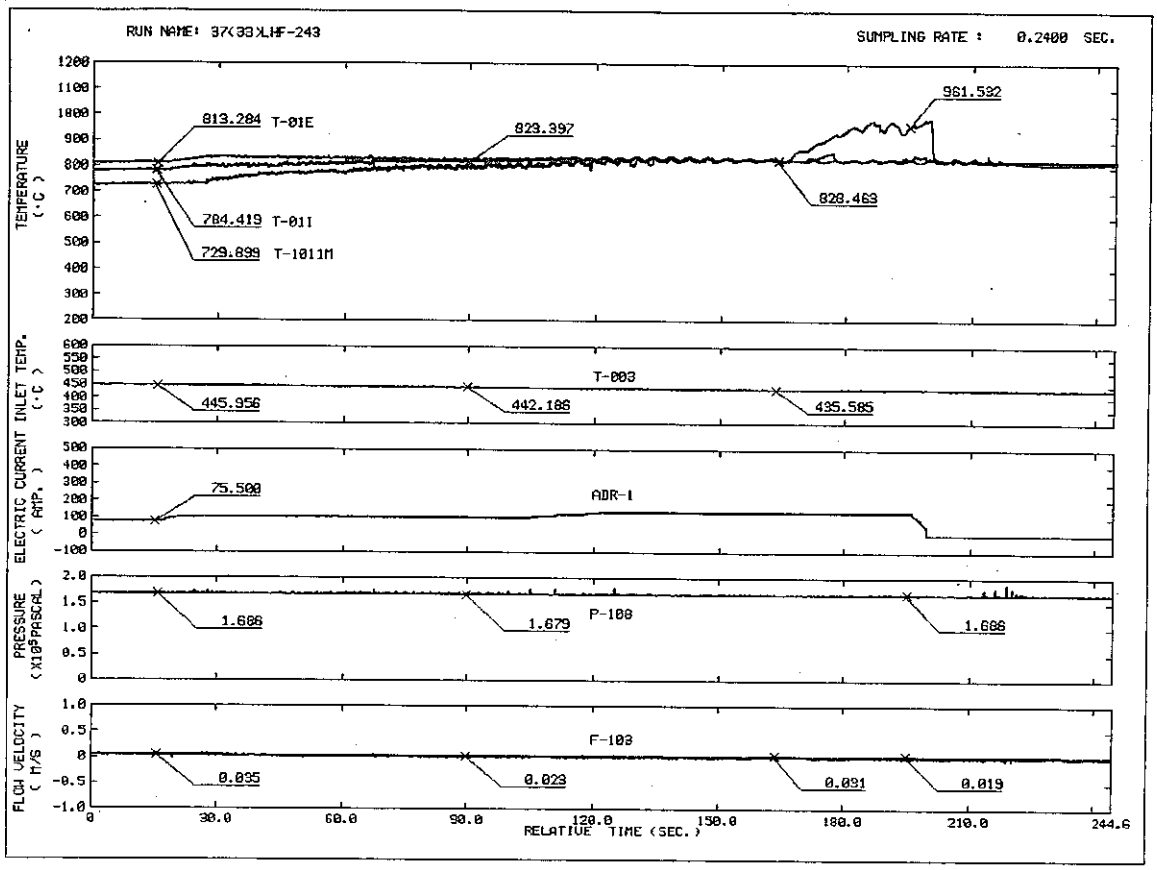
RUN NAME: 37(33)LHF-243
SUMPLING RATE : 0.2400 SEC.
TEMPERATURE (°C)
813.284 T-01E
823.397
961.592
828.463
784.419 T-011
729.899 T-1011M
ELECTRIC CURRENT INLET TEMP. (°C)
T-003
445.956
442.186
435.585
PRESSURE (X10⁵PASCAL)
75.500
ADR-1
1.686
1.679
P-108
1.686
FLOW VELOCITY (M/S)
F-103
0.035
0.023
0.031
0.019
RELATIVE TIME (SEC.)

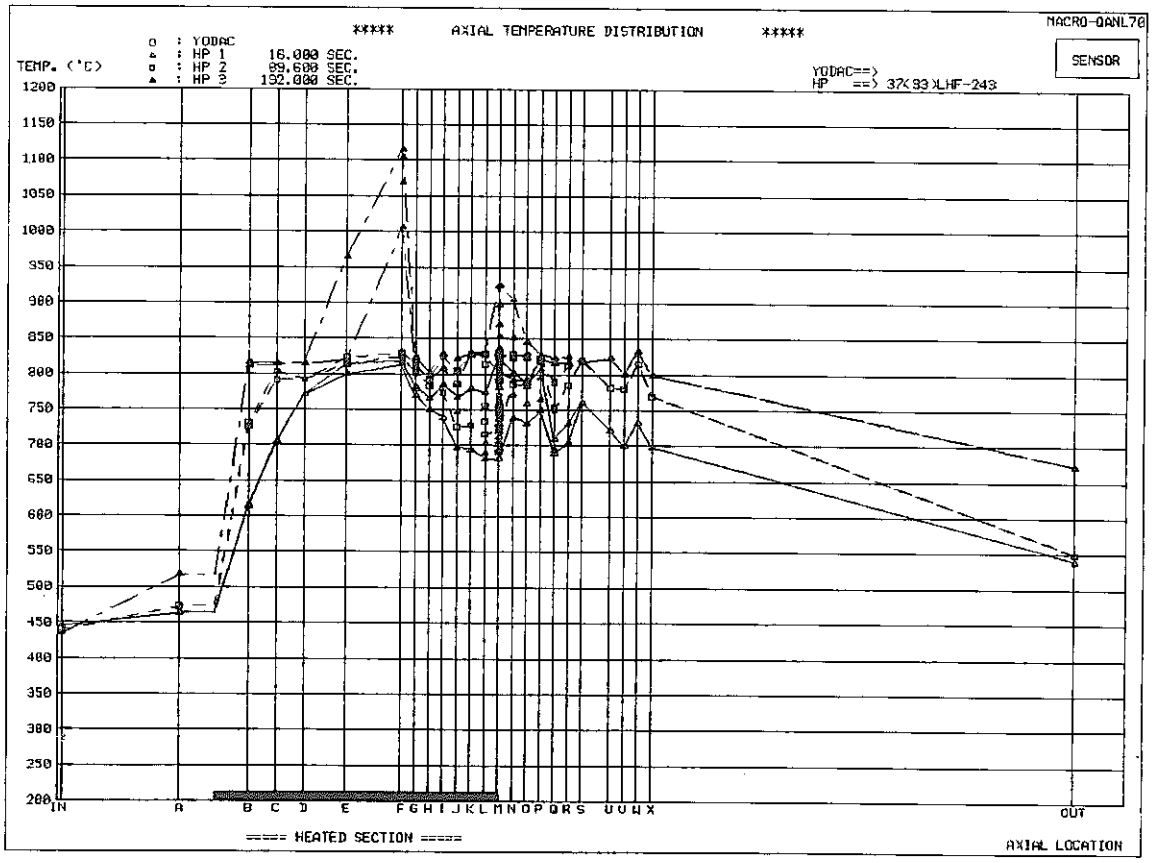
MACRO-QANL70
***** AXIAL TEMPERATURE DISTRIBUTION *****
SENSOR
TEMP. (°C)
□ : YODAC
△ : HP 1 16.000 SEC.
▫ : HP 2 89.600 SEC.
▲ : HP 3 192.000 SEC.
YODAC==>
HP ==> 37(33)LHF-243
IN A B C D E F G H I J K L M N O P Q R S U U W X OUT
==== HEATED SECTION ====
AXIAL LOCATION

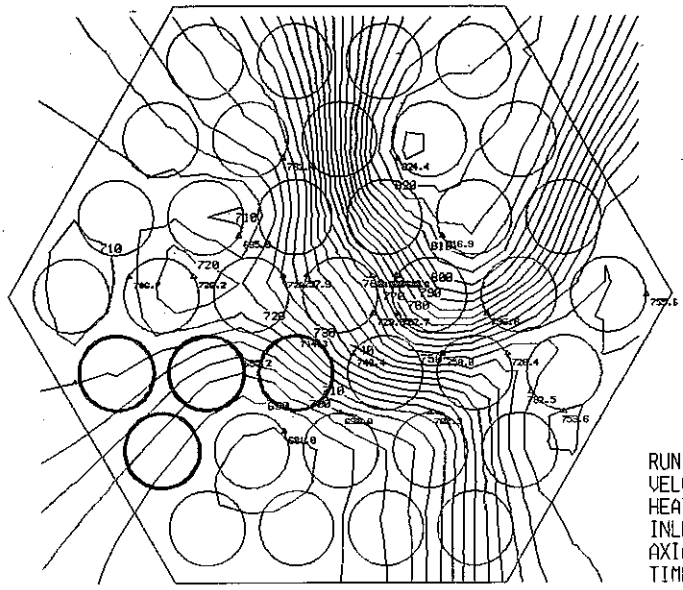

RUN NAME 37(33)LHF-243
VELOCITY 0.047 M/S
HEAT FLUX 3.02 W/CM2
INLET TEMP. 446.0 C
AXIAL 0.0 MM
TIME 16.000 SEC.

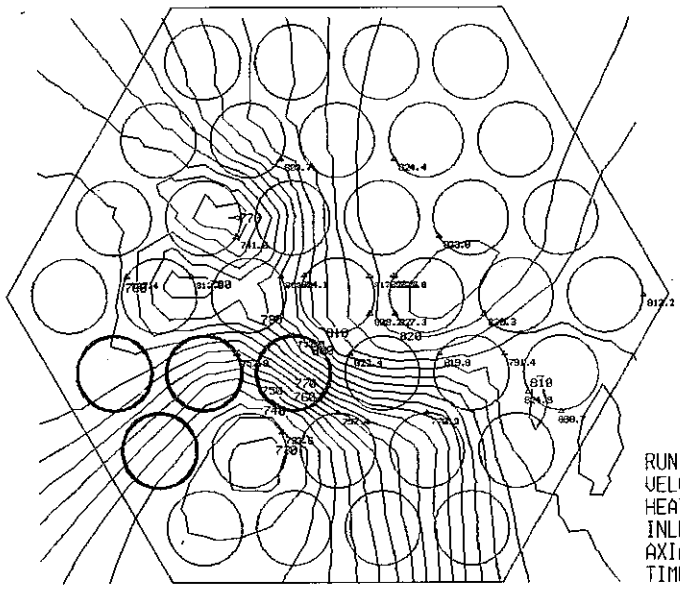

RUN NAME 37(33)LHF-243
VELOCITY 0.004 M/S
HEAT FLUX 4.79 W/CM2
INLET TEMP. 441.2 C
AXIAL 0.0 MM
TIME 89.600 SEC.

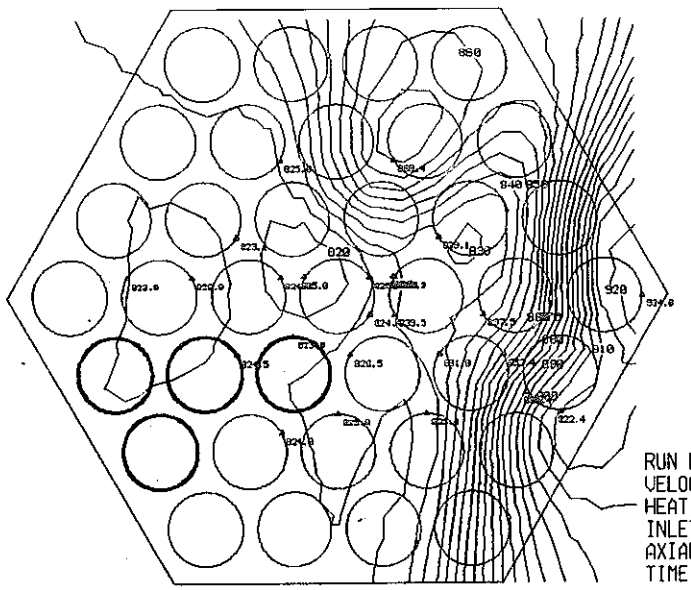

RUN NAME 37(33)LHF-243
VELOCITY 0.012 M/S
HEAT FLUX 8.08 W/CM2
INLET TEMP. 435.6 C
AXIAL 0.0 MM
TIME 192.000 SEC.

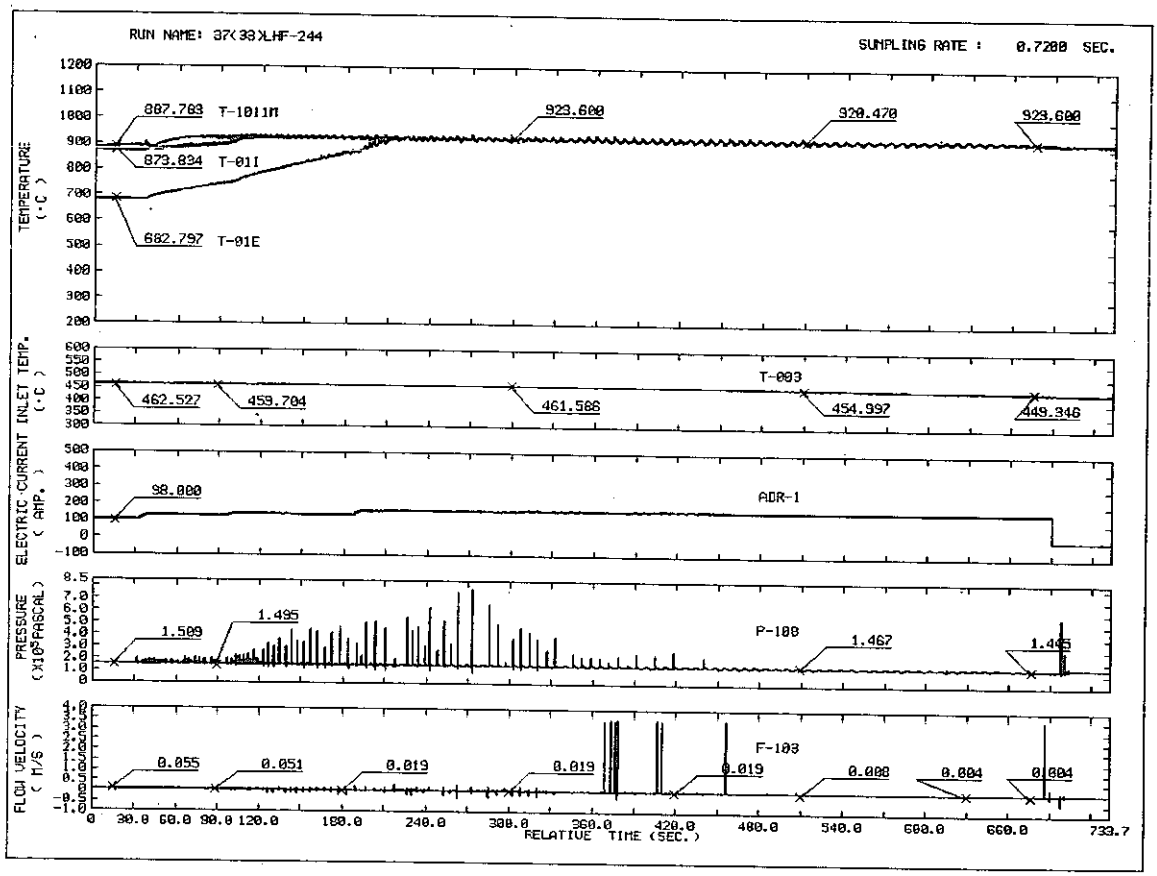
RUN NAME: 37(33)LHF-244
SUNPLING RATE : 0.7200 SEC.
TEMPERATURE (°C)
887.763 T-101M
879.834 T-01I
682.797 T-01E
923.600
920.470
923.600
ELECTRIC CURRENT INLET TEMP. (°C) (AMP.)
462.527
459.704
461.568
T-003
454.992
449.346
98.000
ADR-1
PRESSURE (X10⁵PASCAL)
1.509
1.495
P-108
1.467
1.445
FLOW VELOCITY (M/S)
0.055
0.051
0.019
0.019
F-103
0.019
0.008
0.004
0.004
RELATIVE TIME (SEC.)

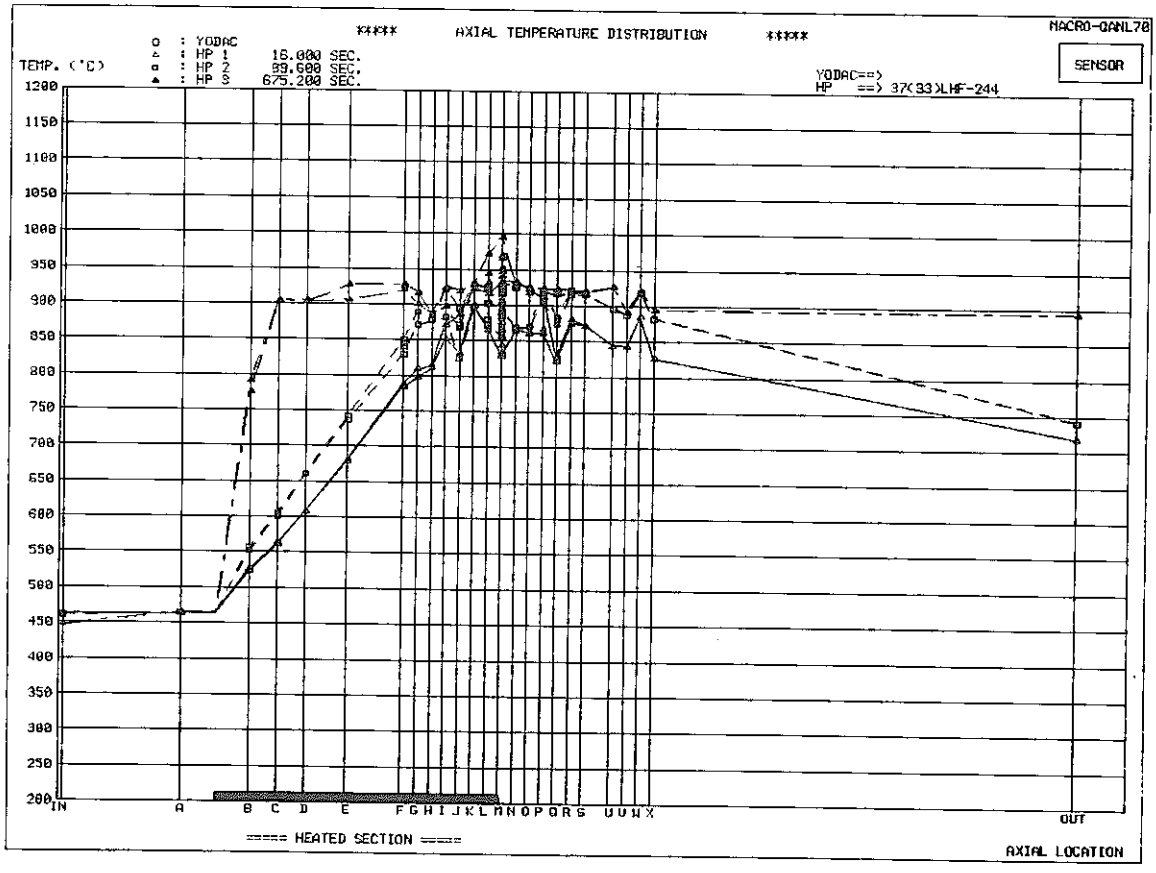
***** AXIAL TEMPERATURE DISTRIBUTION *****
MACRO-QANL70
SENSOR
○ : YODAC
△ : HP 1 16.000 SEC.
□ : HP 2 99.600 SEC.
▲ : HP 3 675.200 SEC.
TEMP. (°C)
YODAC==>
HP ==> 37(33)LHF-244
IN A B C D E F G H I J K L M N O P Q R S U U W X OUT
==== HEATED SECTION ====
AXIAL LOCATION

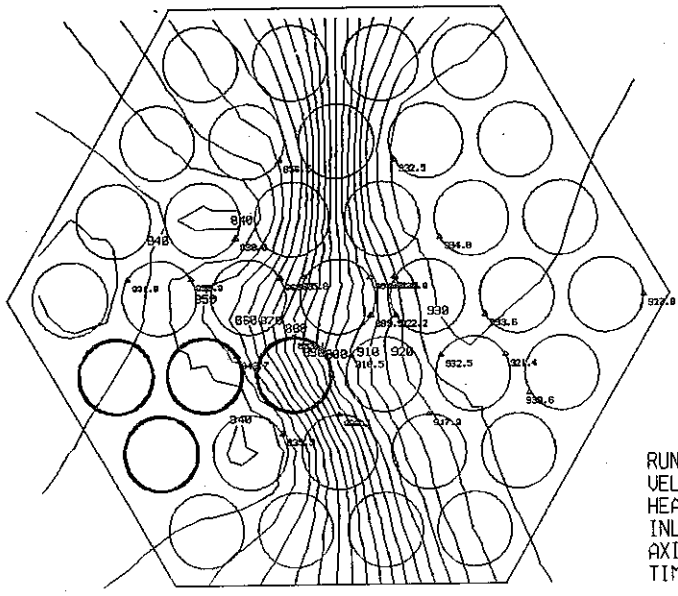

RUN NAME 37(33)LHF-244
VELOCITY 0.043 M/S
HEAT FLUX 4.29 W/CM2
INLET TEMP. 463.5 C
AXIAL 0.0 MM
TIME 16.000 SEC.

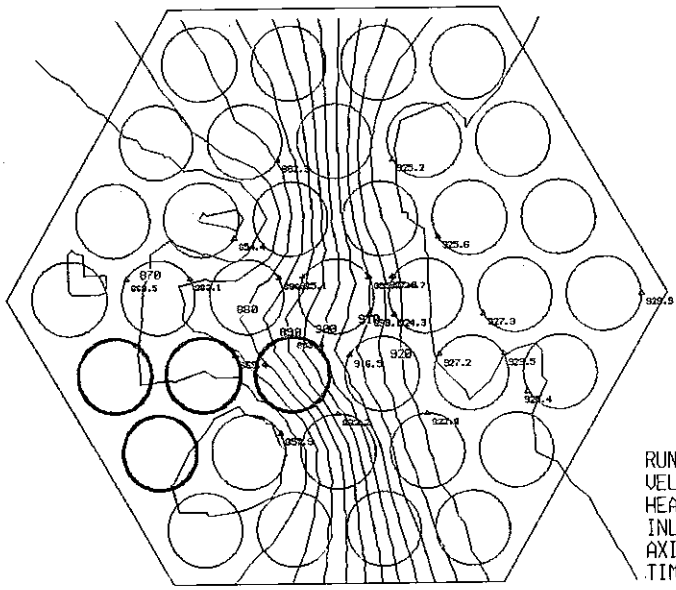

RUN NAME 37(33)LHF-244
VELOCITY 0.039 M/S
HEAT FLUX 6.88 W/CM2
INLET TEMP. 460.6 C
AXIAL 0.0 MM
TIME 89.600 SEC.

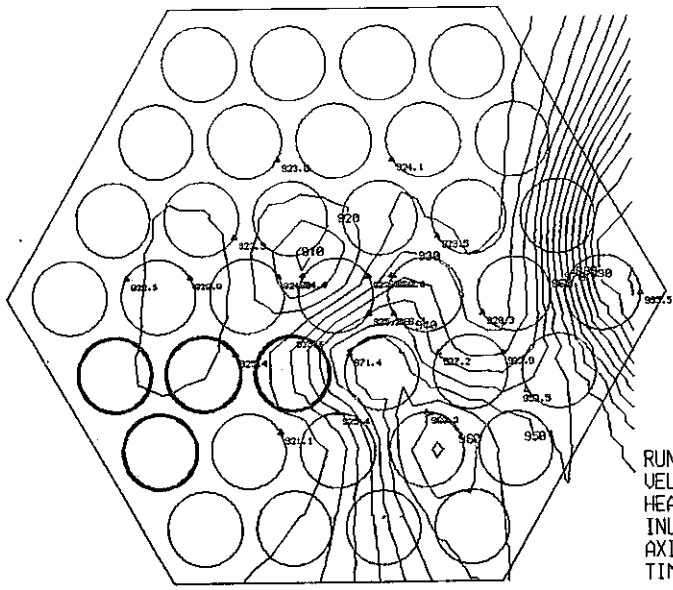

RUN NAME 37(33)LHF-244
VELOCITY 0.023 M/S
HEAT FLUX 11.59 W/CM2
INLET TEMP. 448.4 C
AXIAL 0.0 MM
TIME 675.200 SEC.

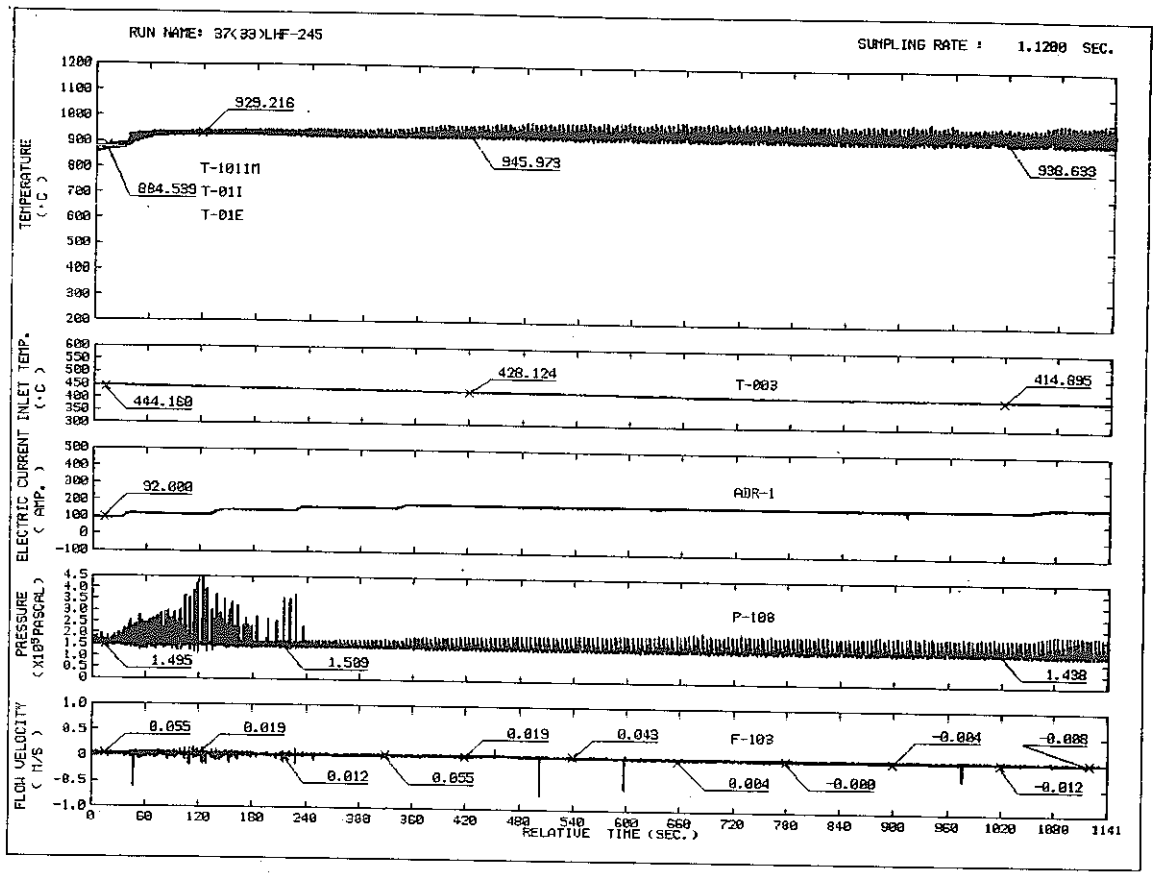
RUN NAME: 37(33)LHF-245
SAMPLING RATE : 1.1200 SEC.
TEMPERATURE (°C)
929.216
945.979
938.693
884.589
T-101M
T-01I
T-01E
ELECTRIC CURRENT INLET TEMP. (°C)
428.124
444.160
T-003
414.895
92.000
ADR-1
PRESSURE (X10⁵PASCAL)
P-108
1.495
1.509
1.488
FLOW VELOCITY (M/S)
0.055
0.019
0.019
0.043
F-103
-0.004
-0.008
0.012
0.055
0.004
-0.000
-0.012
RELATIVE TIME (SEC.)

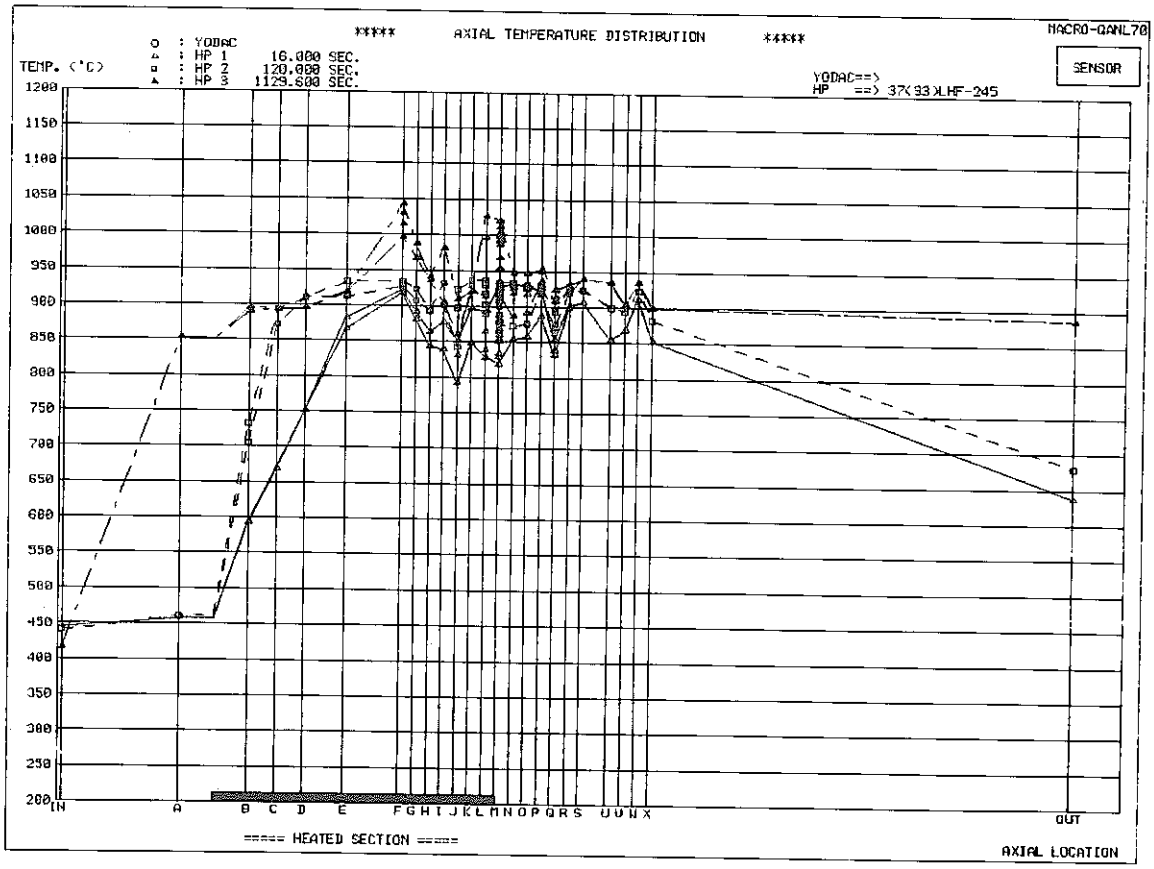
MACRO-QANL70
SENSOR
***** AXIAL TEMPERATURE DISTRIBUTION *****
○ : YODAC
△ : HP 1 16.000 SEC.
□ : HP 2 120.000 SEC.
▲ : HP 3 1129.600 SEC.
TEMP. (°C)
YODAC==>
HP ==> 37(33)LHF-245
IN
A B C D E F G H I J K L M N O P Q R S U U W X
OUT
===== HEATED SECTION =====
AXIAL LOCATION

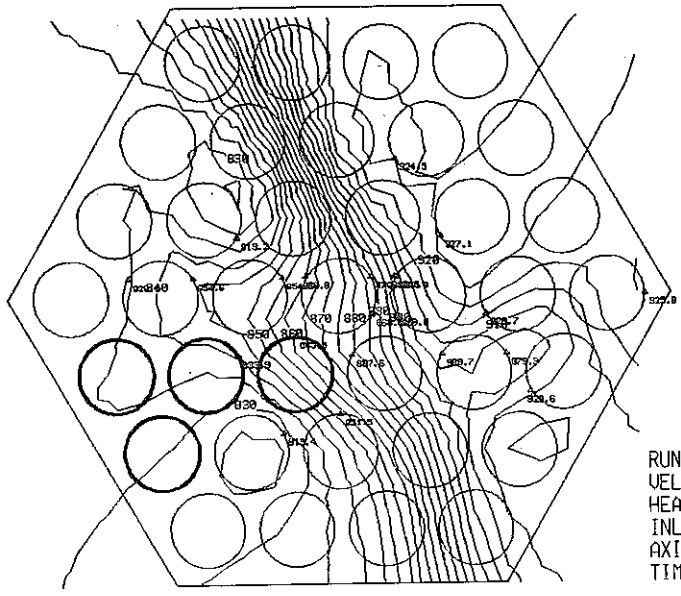

RUN NAME 37(33)LHF-245
VELOCITY 0.035 M/S
HEAT FLUX 3.86 W/CM2
INLET TEMP. 447.0 C
AXIAL 0.0 MM
TIME 16.000 SEC.

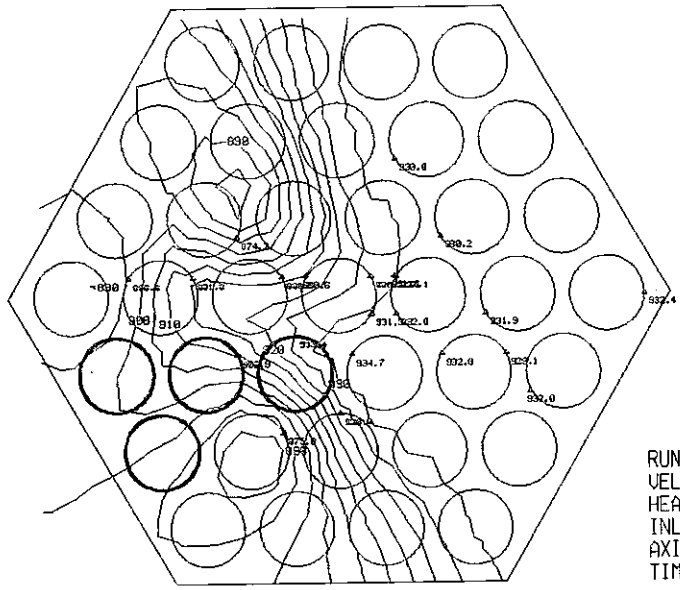

RUN NAME 37(33)LHF-245
VELOCITY 0.039 M/S
HEAT FLUX 6.34 W/CM2
INLET TEMP. 440.4 C
AXIAL 0.0 MM
TIME 120.000 SEC.

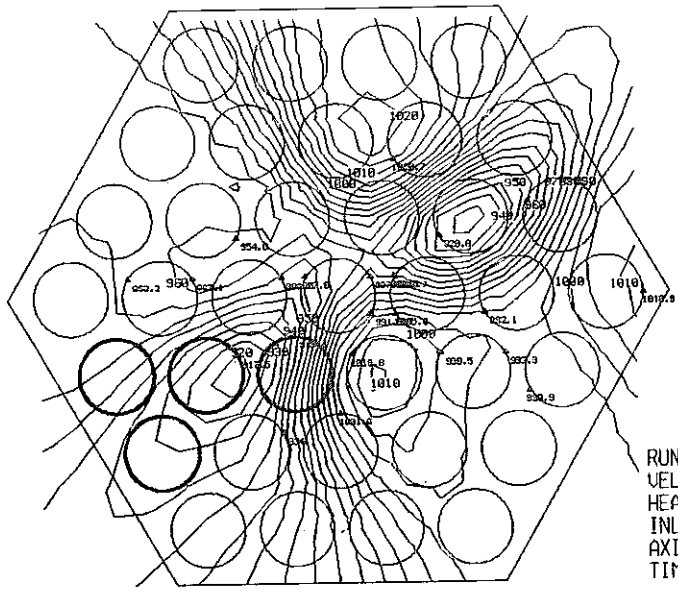

RUN NAME 37(33)LHF-245
VELOCITY -0.004 M/S
HEAT FLUX 19.08 W/CM2
INLET TEMP. 416.8 C
AXIAL 0.0 MM
TIME 1129.600 SEC.

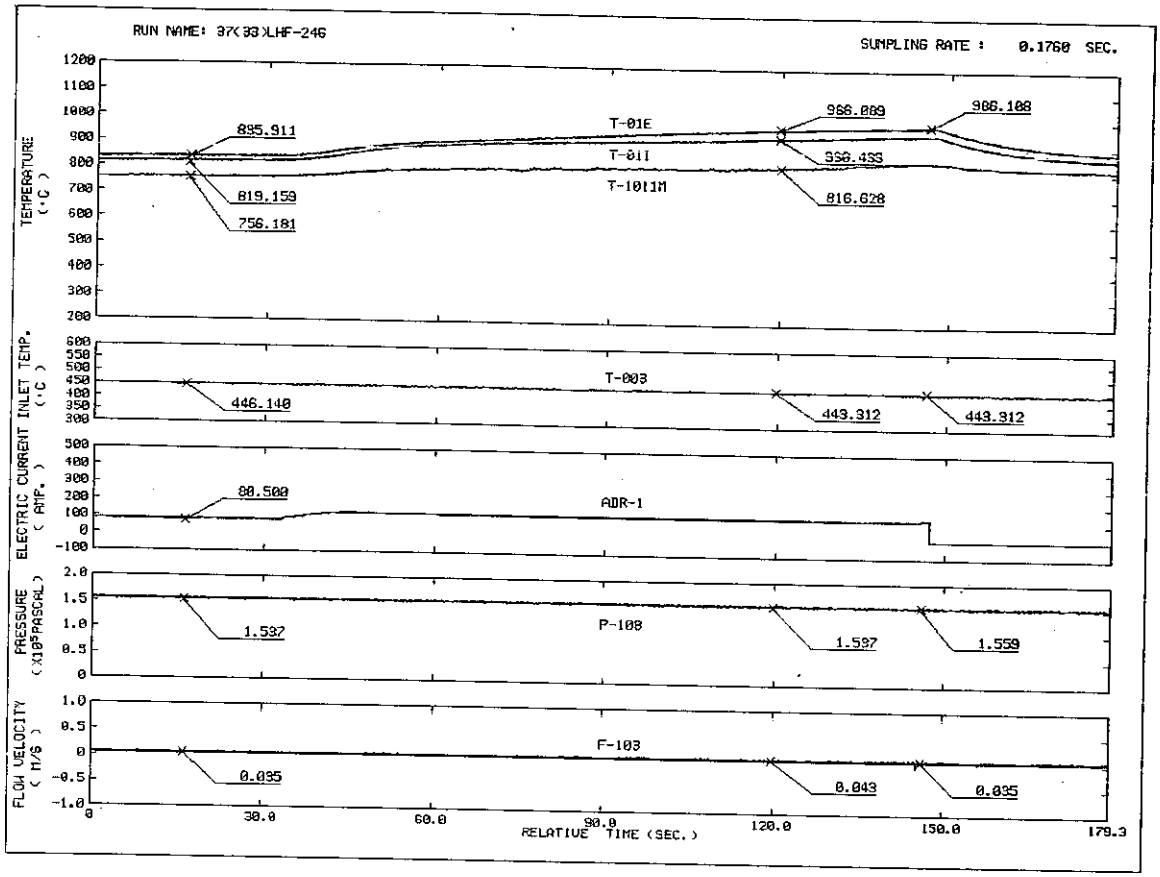
RUN NAME: 37(33)LHF-246
SAMPLING RATE : 0.1760 SEC.
TEMPERATURE ('C)
895.911
819.159
756.181
T-01E
T-01I
T-101M
986.089
988.188
958.455
816.628
ELECTRIC CURRENT INLET TEMP. ('C) (AMP.)
T-003
446.148
443.312
443.312
80.500
ADR-1
PRESSURE (X10⁵PASCAL)
1.537
P-108
1.597
1.559
FLOW VELOCITY (M/S)
F-103
0.035
0.043
0.035
RELATIVE TIME (SEC.)

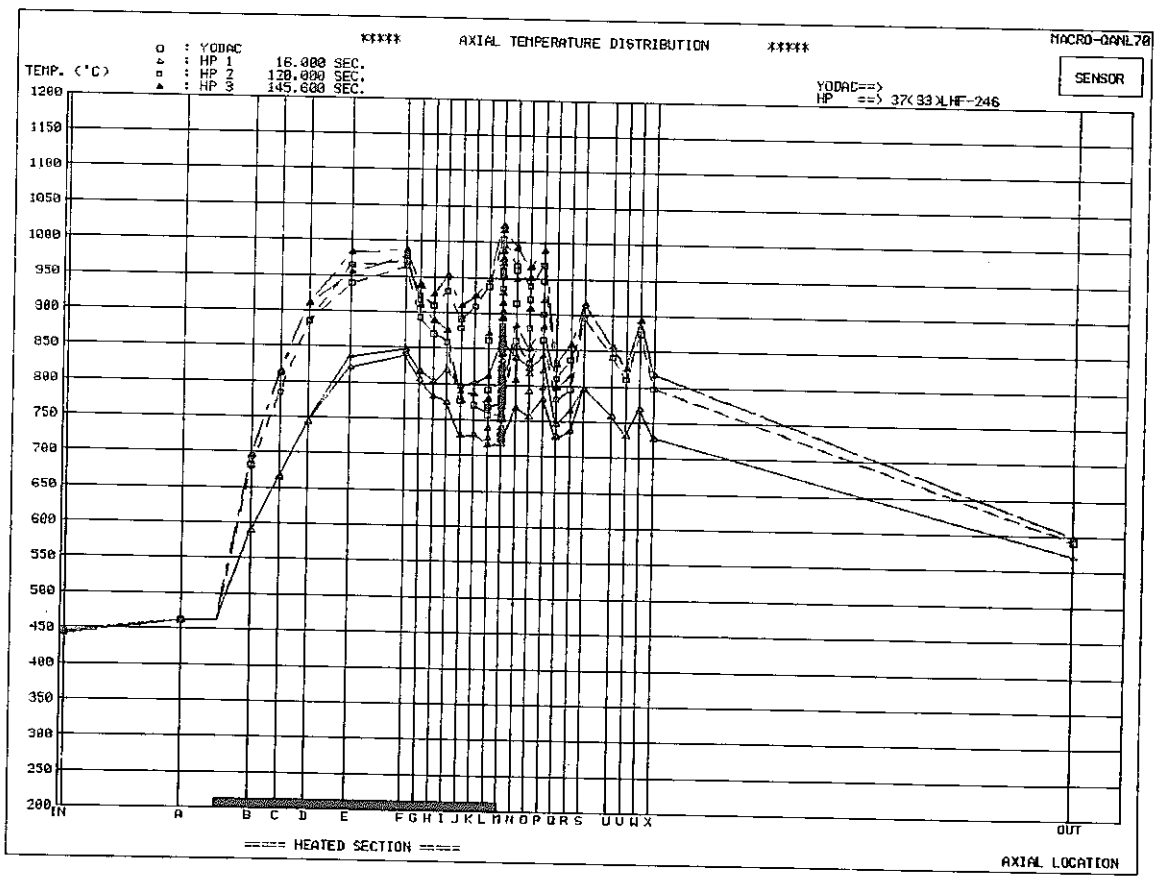
MACRO-QANL70
***** AXIAL TEMPERATURE DISTRIBUTION *****
o : YODAC
Δ : HP 1 16.000 SEC.
□ : HP 2 120.000 SEC.
▲ : HP 3 145.600 SEC.
SENSOR
YODAC==>
HP ==> 37(33)LHF-246
TEMP. ('C)
IN
OUT
==== HEATED SECTION ====
AXIAL LOCATION

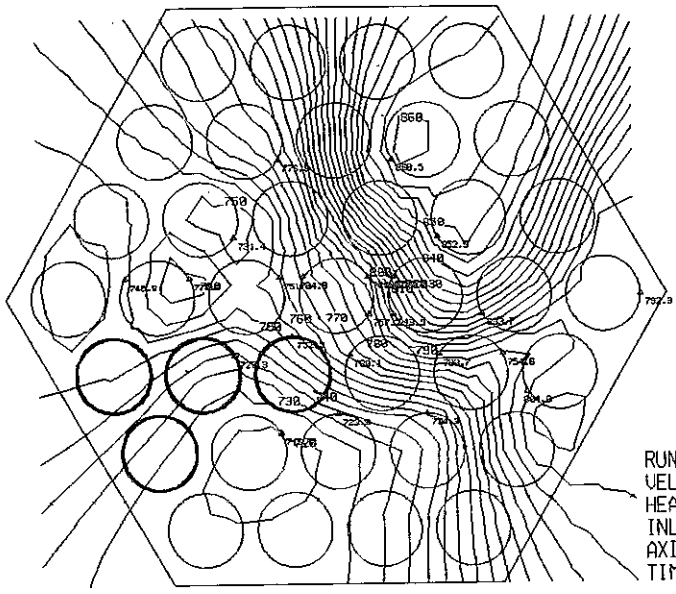

RUN NAME 37(33)LHF-246
VELOCITY 0.039 M/S
HEAT FLUX 2.91 W/CM2
INLET TEMP. 447.1 C
AXIAL 0.0 MM
TIME 16.000 SEC.

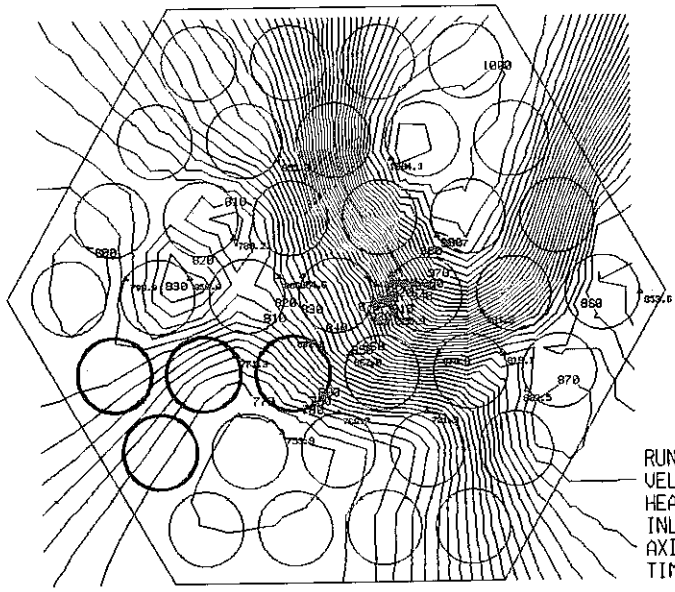

RUN NAME 37(33)LHF-246
VELOCITY 0.051 M/S
HEAT FLUX 6.67 W/CM2
INLET TEMP. 443.3 C
AXIAL 0.0 MM
TIME 120.000 SEC.

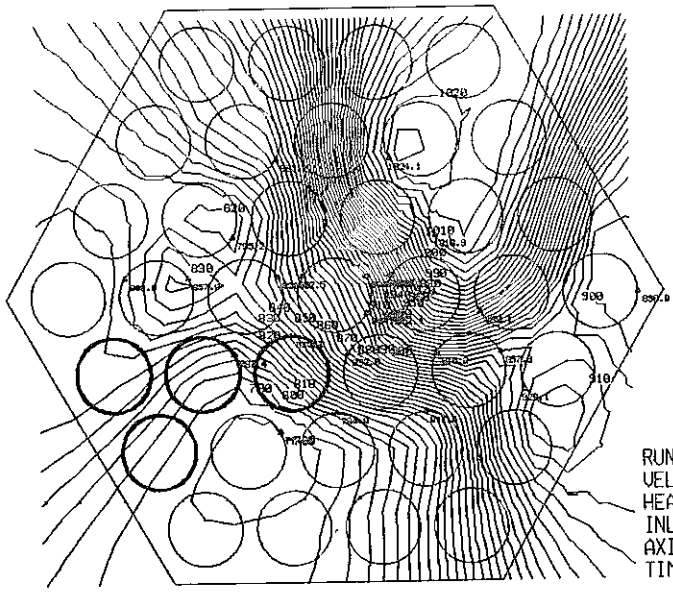

RUN NAME 37(33)LHF-246
VELOCITY 0.043 M/S
HEAT FLUX 6.67 W/CM2
INLET TEMP. 442.4 C
AXIAL 0.0 MM
TIME 145.600 SEC.

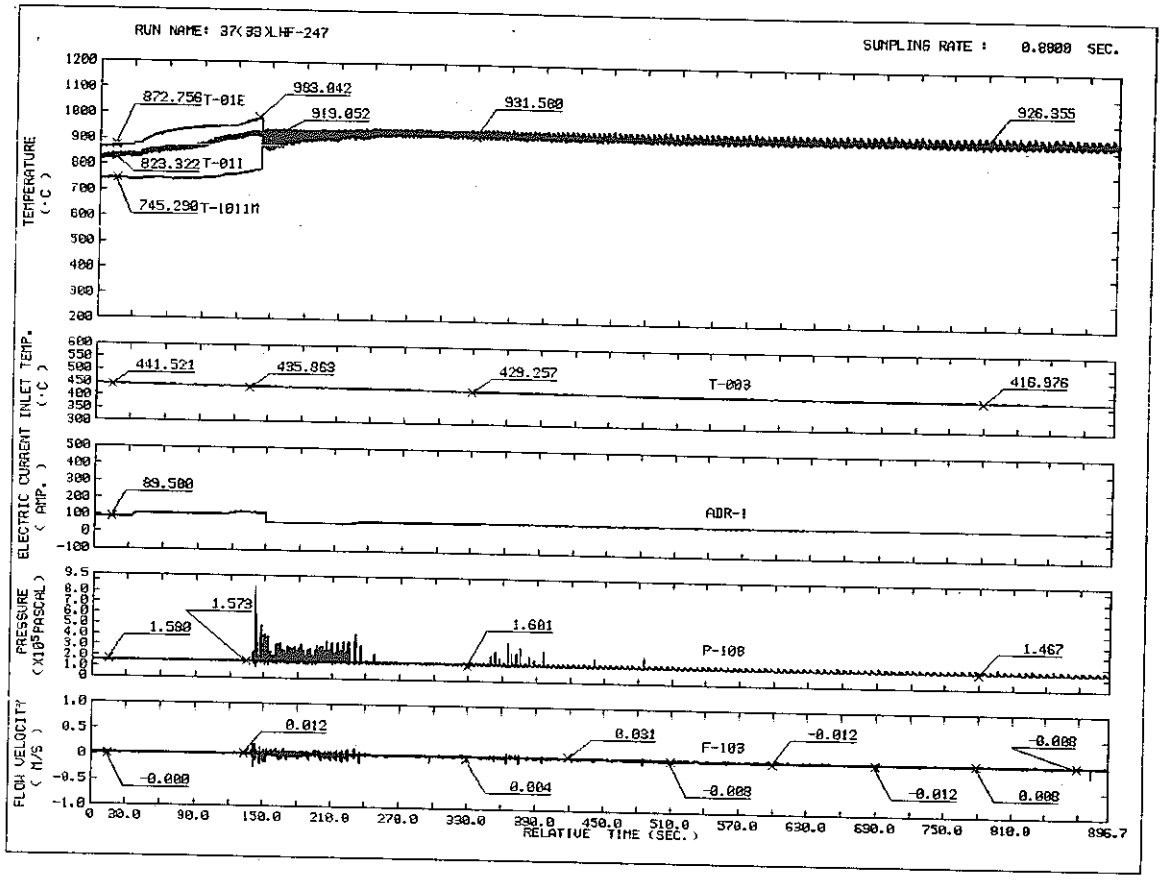
RUN NAME: 37(33)LHF-247
SUMPLING RATE : 0.0000 SEC.
TEMPERATURE (°C)
872.758T-01E
963.042
919.052
931.580
926.355
823.322T-011
745.290T-1011M
ELECTRIC CURRENT INLET TEMP. (°C)
441.521
435.863
429.257
T-003
416.976
(AMP.)
89.580
ADR-1
PRESSURE (X10⁵PASCAL)
1.573
1.580
1.601
P-108
1.467
FLOW VELOCITY (M/S)
0.012
0.031
F-103
-0.012
-0.008
-0.000
0.004
-0.008
-0.012
0.008
RELATIVE TIME (SEC.)

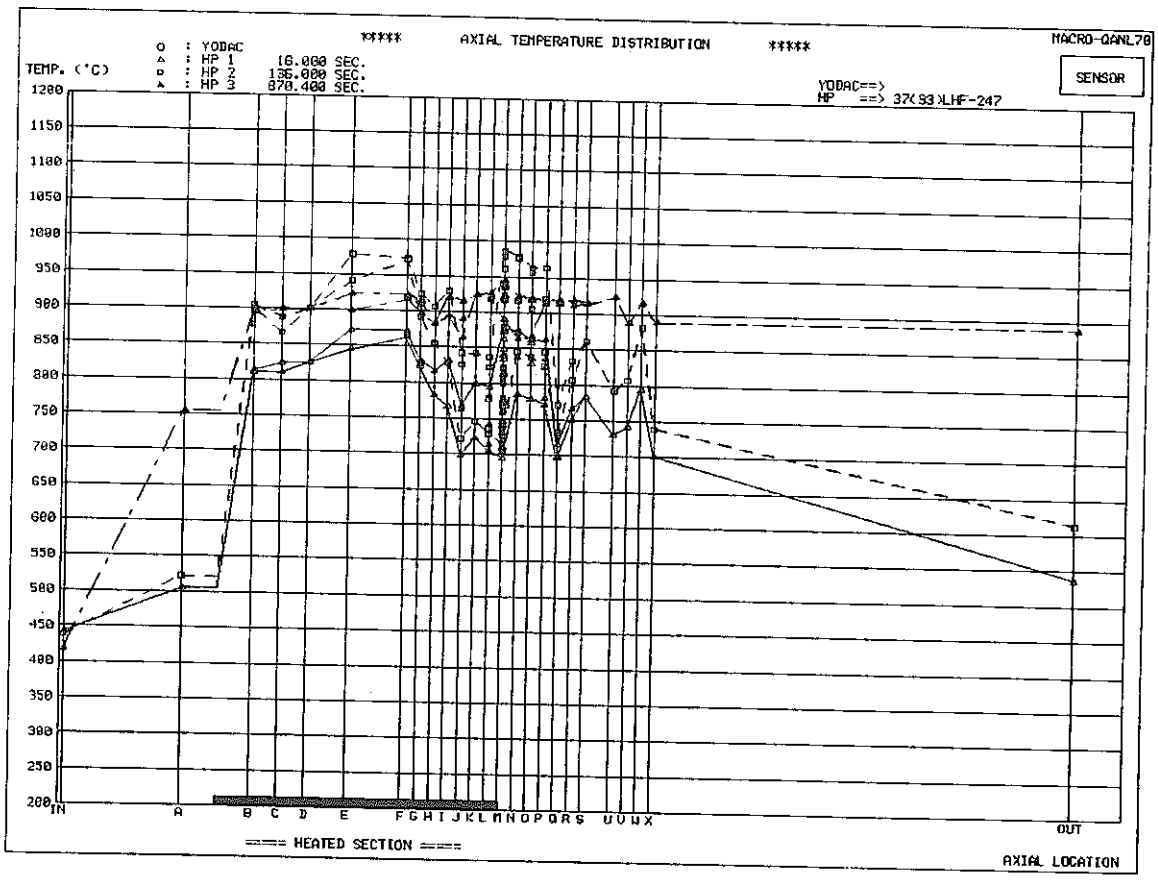
***** AXIAL TEMPERATURE DISTRIBUTION *****
MACRO-QANL78
SENSOR
O : YODAC
Δ : HP 1 16.000 SEC.
□ : HP 2 135.000 SEC.
▲ : HP 3 870.400 SEC.
TEMP. (°C)
YODAC==>
HP ==> 37(33)LHF-247
IN
A B C D E F G H I J K L M N O P Q R S U V W X
OUT
==== HEATED SECTION ====
AXIAL LOCATION

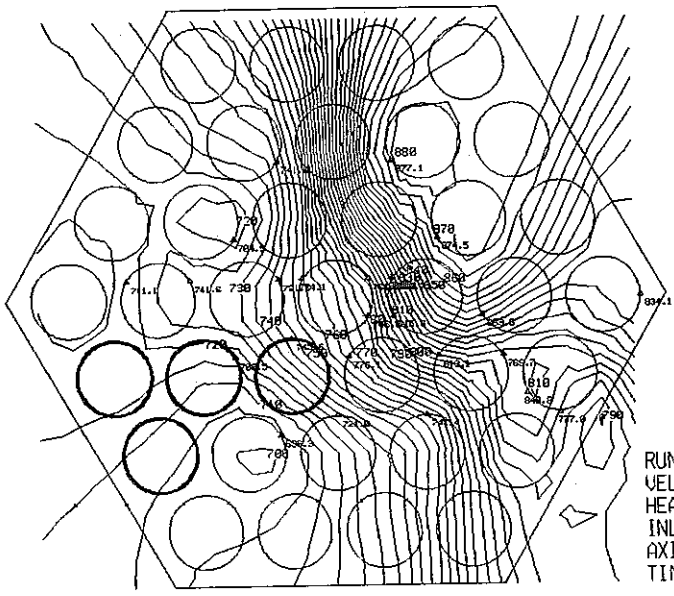

RUN NAME 37(33)LHF-247
VELOCITY 0.019 M/S
HEAT FLUX 3.63 W/CM2
INLET TEMP. 443.4 C
AXIAL 0.0 MM
TIME 16.000 SEC.

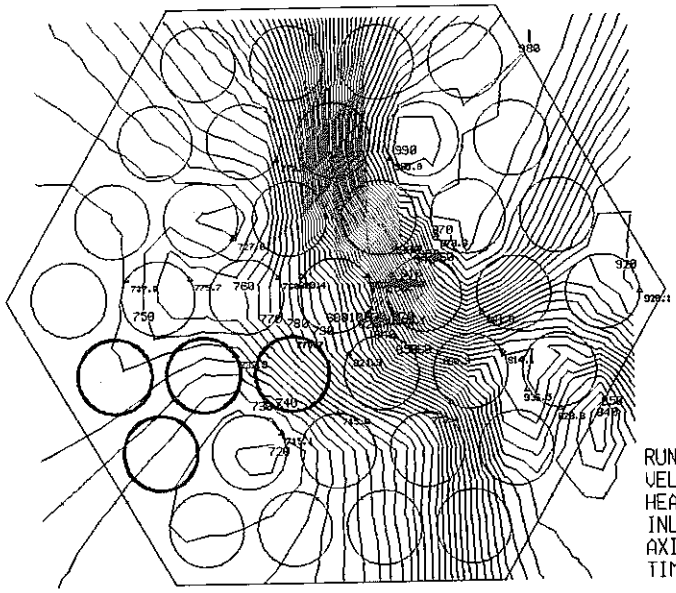

RUN NAME 37(33)LHF-247
VELOCITY 0.019 M/S
HEAT FLUX 6.67 W/CM2
INLET TEMP. 437.7 C
AXIAL 0.0 MM
TIME 136.000 SEC.

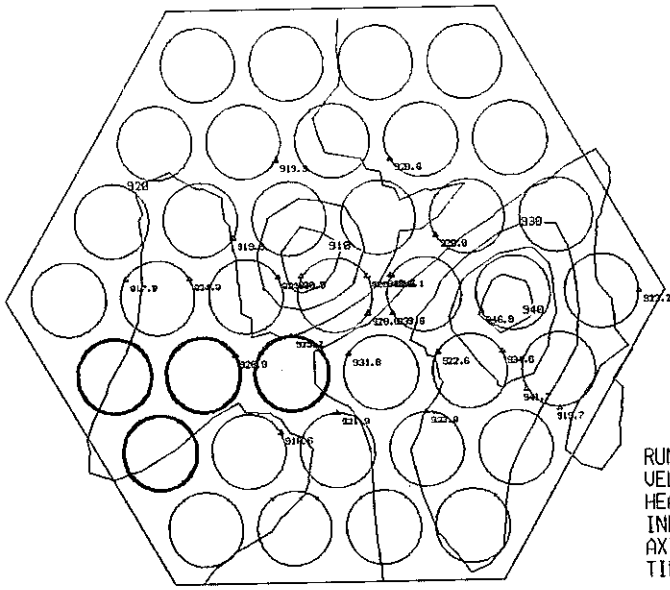

RUN NAME 37(33)LHF-247
VELOCITY 0.004 M/S
HEAT FLUX 8.99 W/CM2
INLET TEMP. 418.9 C
AXIAL 0.0 MM
TIME 870.400 SEC.

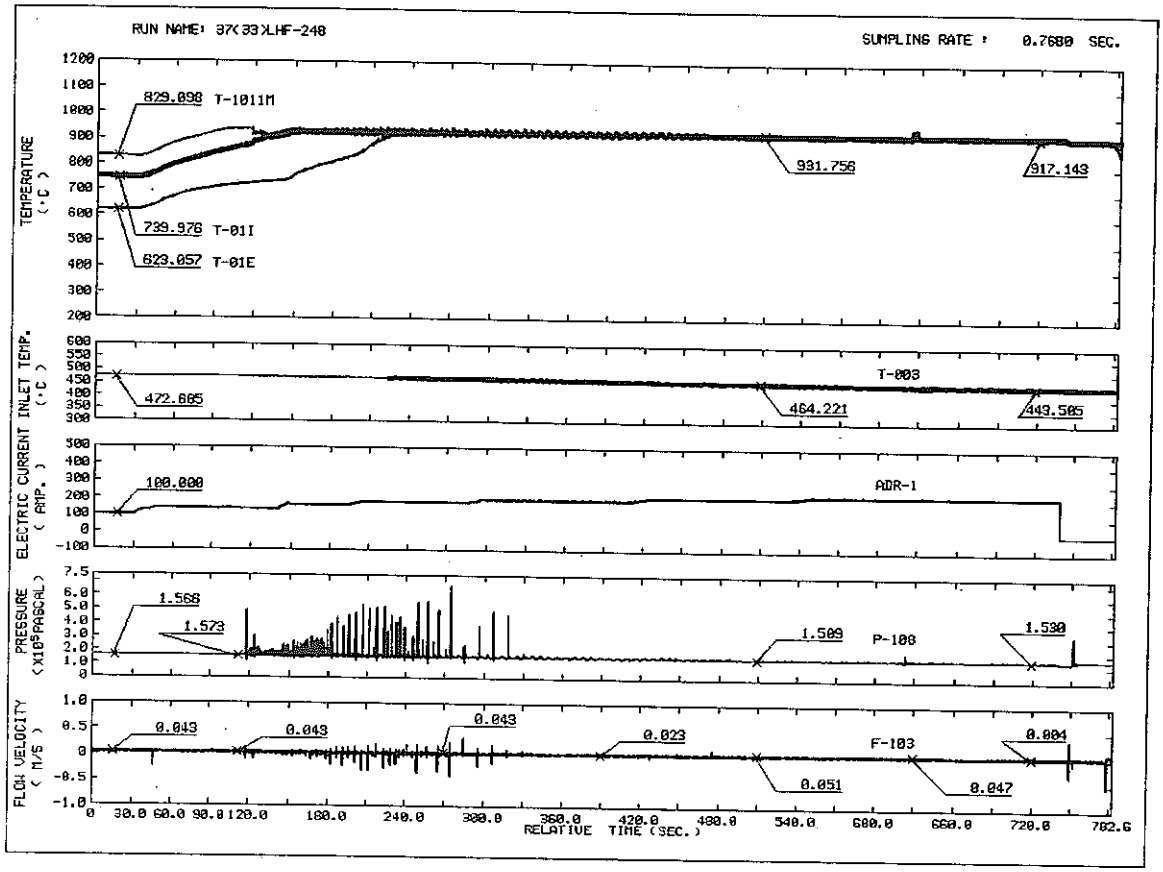
RUN NAME: 37(33)LHF-248
SUMPLING RATE : 0.7680 SEC.
TEMPERATURE ('C)
829.898 T-1011M
931.756
917.143
739.976 T-01I
623.057 T-01E
INLET TEMP. ('C)
472.665
T-003
464.221
449.505
ELECTRIC CURRENT (AMP.)
100.000
ADR-1
PRESSURE (X10⁵PASCAL)
1.568
1.573
1.509
P-100
1.530
FLOW VELOCITY (M/S)
0.043
0.043
0.043
0.023
F-103
0.004
0.051
0.047
RELATIVE TIME (SEC.)

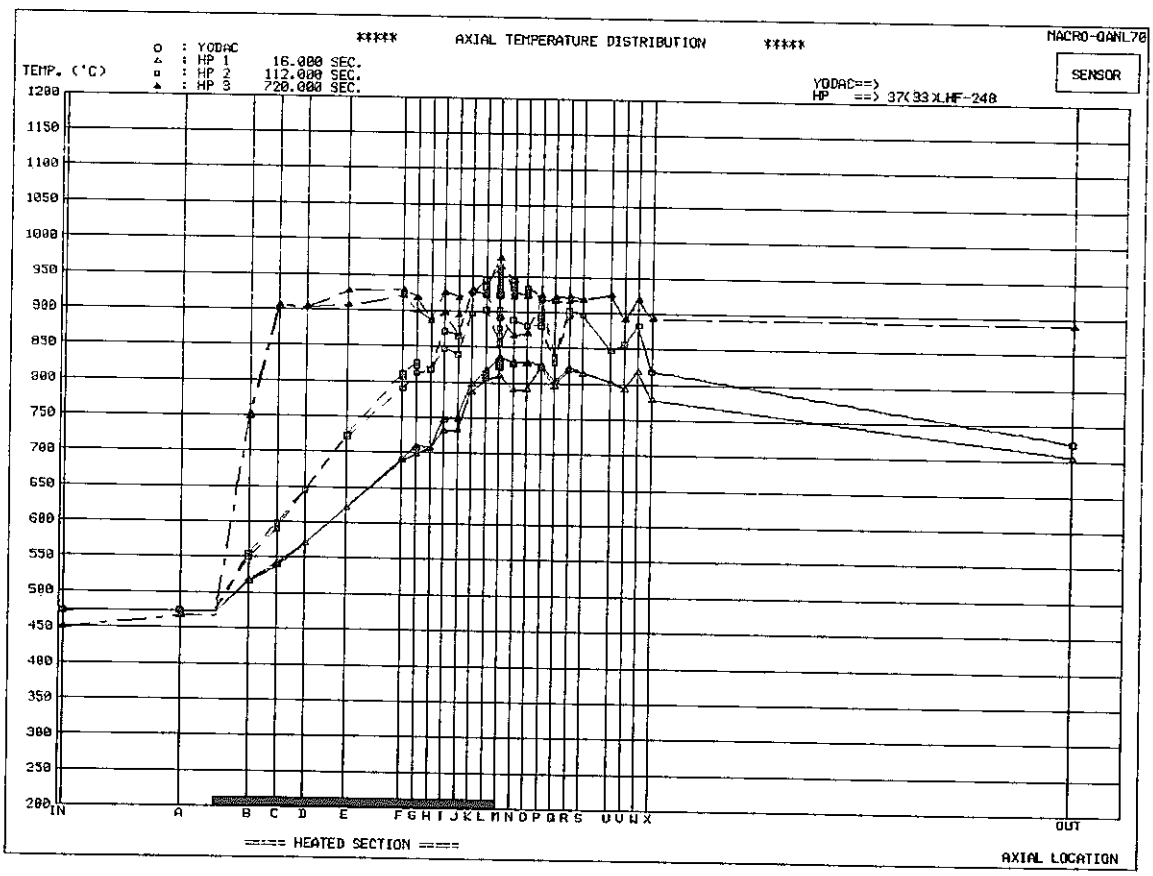
***** AXIAL TEMPERATURE DISTRIBUTION *****
MACRO-GANL70
SENSOR
O : YODAC
△ : HP 1 16.000 SEC.
□ : HP 2 112.000 SEC.
▲ : HP 3 720.000 SEC.
TEMP. ('C)
YODAC==>
HP ==> 37(33)LHF-248
IN
OUT
==== HEATED SECTION ====
AXIAL LOCATION

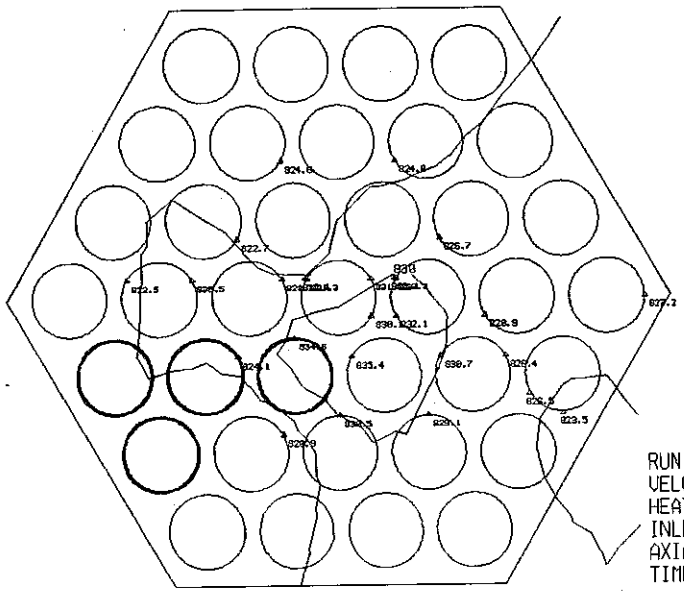

RUN NAME 37(33)LHF-248
VELOCITY 0.035 M/S
HEAT FLUX 3.92 W/CM2
INLET TEMP. 474.6 C
AXIAL 0.0 MM
TIME 16.000 SEC.

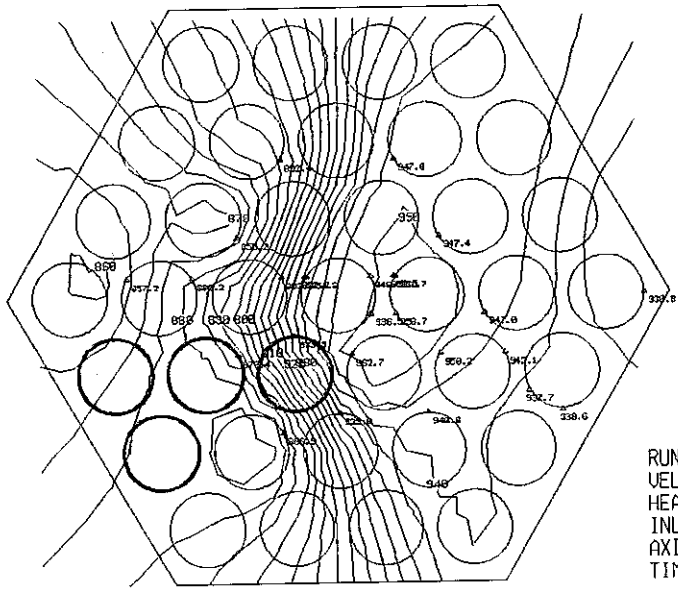

RUN NAME 37(33)LHF-248
VELOCITY 0.031 M/S
HEAT FLUX 7.79 W/CM2
INLET TEMP. 472.7 C
AXIAL 0.0 MM
TIME 112.000 SEC.

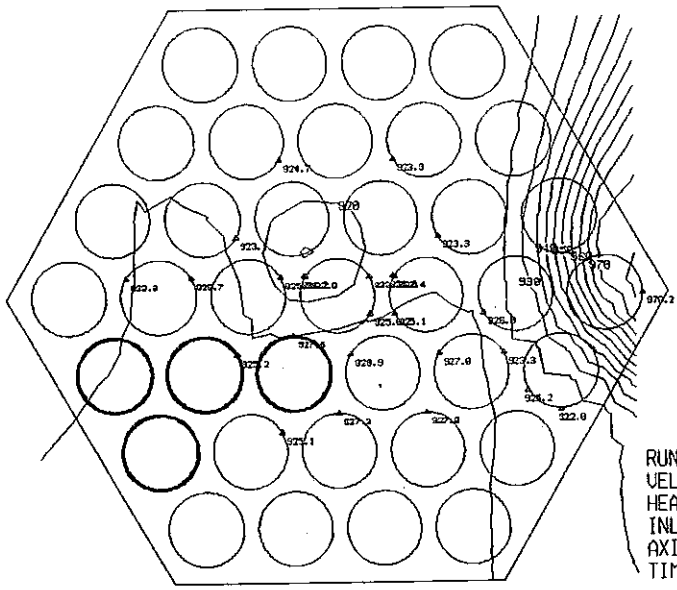

RUN NAME 37(33)LHF-248
VELOCITY 0.004 M/S
HEAT FLUX 23.58 W/CM2
INLET TEMP. 443.5 C
AXIAL 0.0 MM
TIME 720.000 SEC.

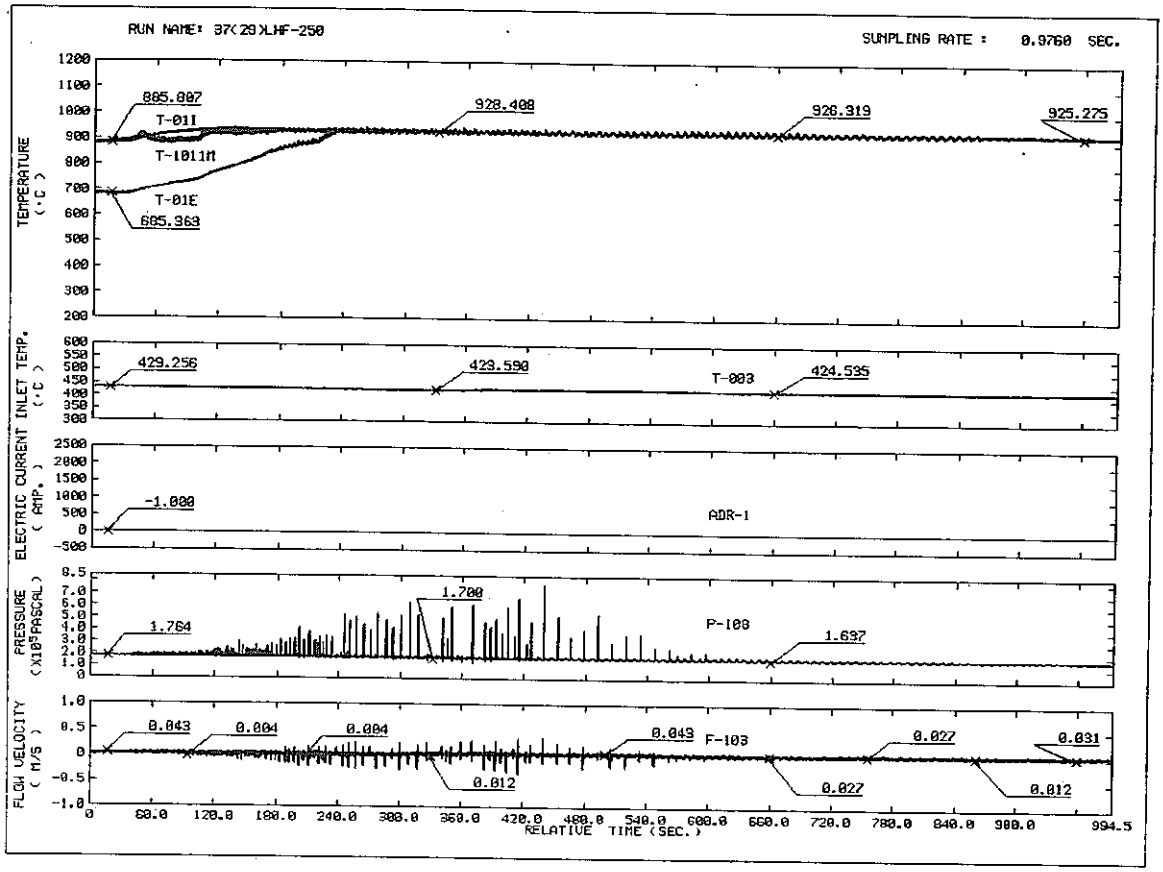
RUN NAME: 37(29)LHF-250
SUMPLING RATE : 0.9760 SEC.
TEMPERATURE (°C)
885.807
T-01I
928.408
926.319
925.275
T-1011M
T-01E
685.363
INLET TEMP. (°C)
429.256
423.590
T-003
424.535
ELECTRIC CURRENT (AMP.)
-1.000
ADR-1
PRESSURE (X10⁵PASCAL)
1.764
1.700
P-108
1.697
FLOW VELOCITY (M/S)
0.043
0.004
0.004
0.049
F-103
0.027
0.031
0.012
0.027
0.012
RELATIVE TIME (SEC.)

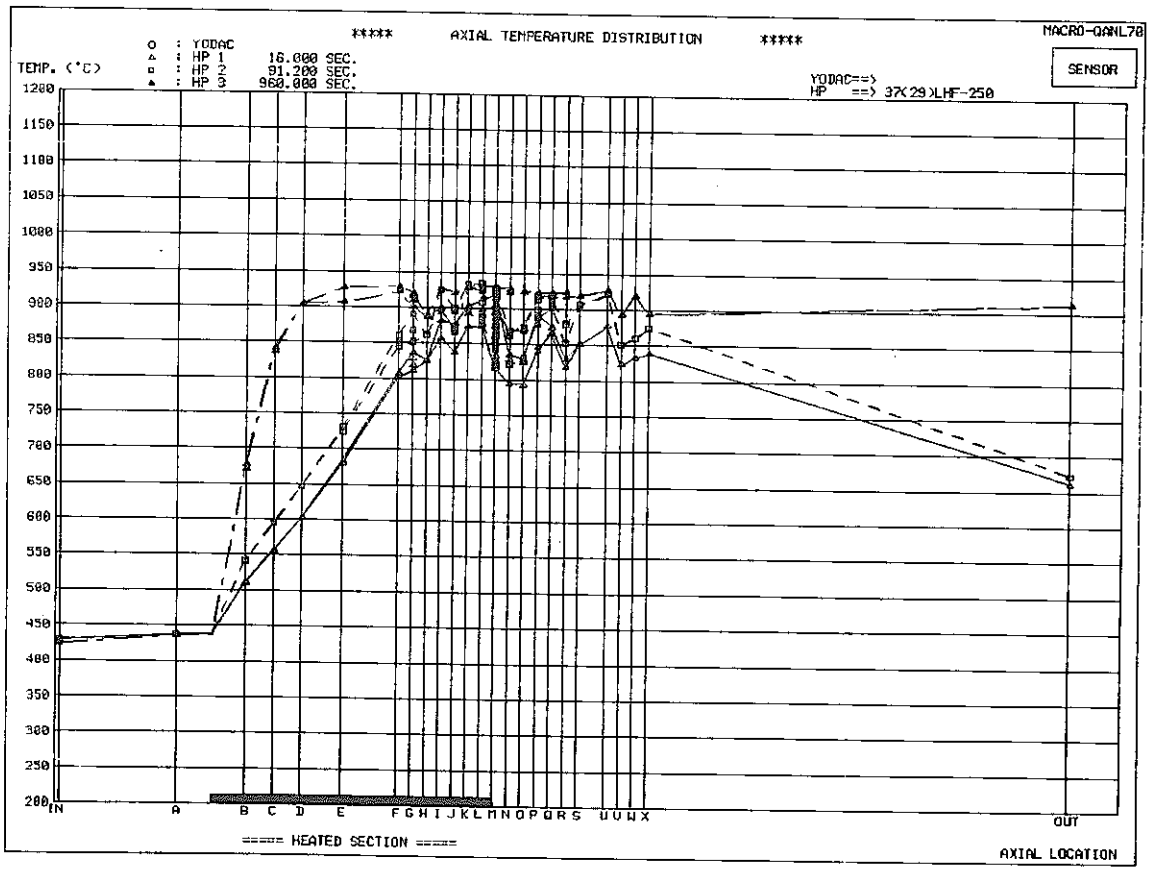
***** AXIAL TEMPERATURE DISTRIBUTION *****
MACRO-GANL70
SENSOR
O : YODAC
Δ : HP 1 16.000 SEC.
□ : HP 2 91.200 SEC.
▲ : HP 3 960.000 SEC.
TEMP. (°C)
YODAC==>
HP ==> 37(29)LHF-250
IN
A B C D E F G H I J K L M N O P Q R S U V W X
OUT
===== HEATED SECTION =====
AXIAL LOCATION

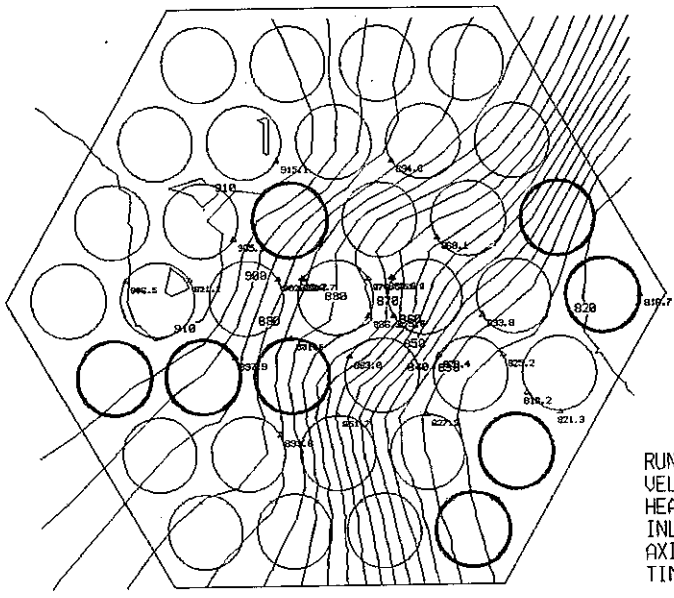

RUN NAME 37(29)LHF-250
VELOCITY 0.012 M/S
HEAT FLUX 3.64 W/CM2
INLET TEMP. 430.2 C
AXIAL 0.0 MM
TIME 16.000 SEC.

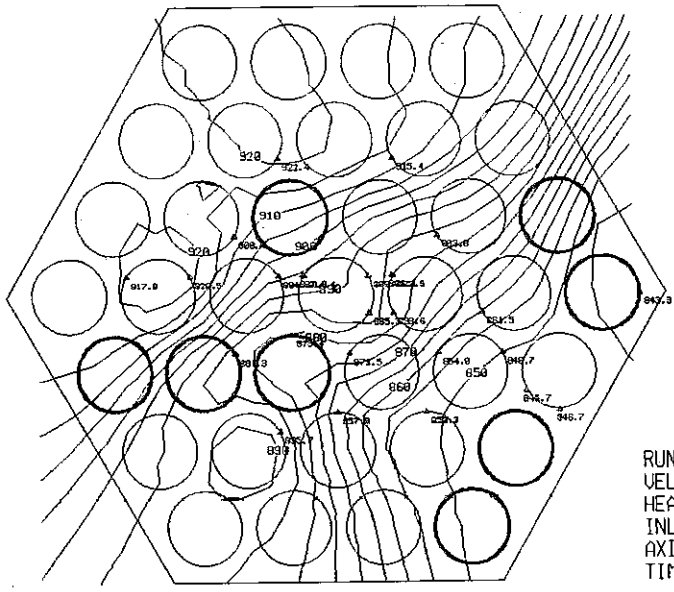

RUN NAME 37(29)LHF-250
VELOCITY 0.012 M/S
HEAT FLUX 5.83 W/CM2
INLET TEMP. 429.3 C
AXIAL 0.0 MM
TIME 91.200 SEC.

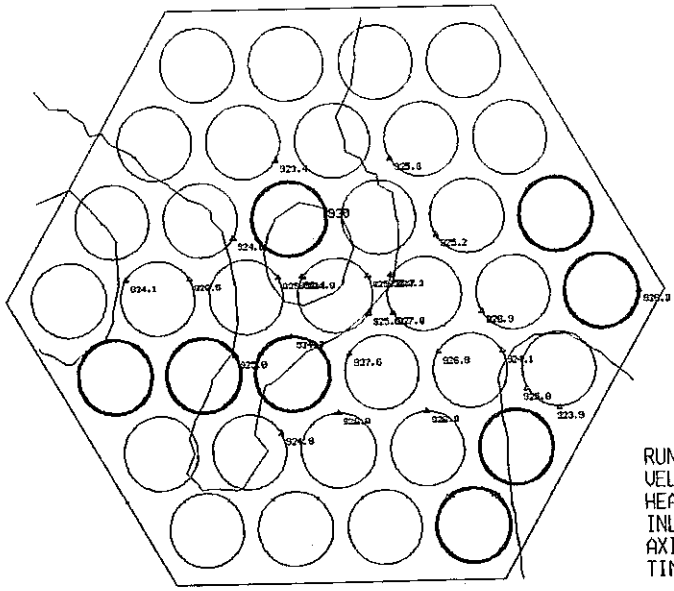

RUN NAME 37(29)LHF-250
VELOCITY 0.055 M/S
HEAT FLUX 12.39 W/CM2
INLET TEMP. 423.6 C
AXIAL 0.0 MM
TIME 960.000 SEC.

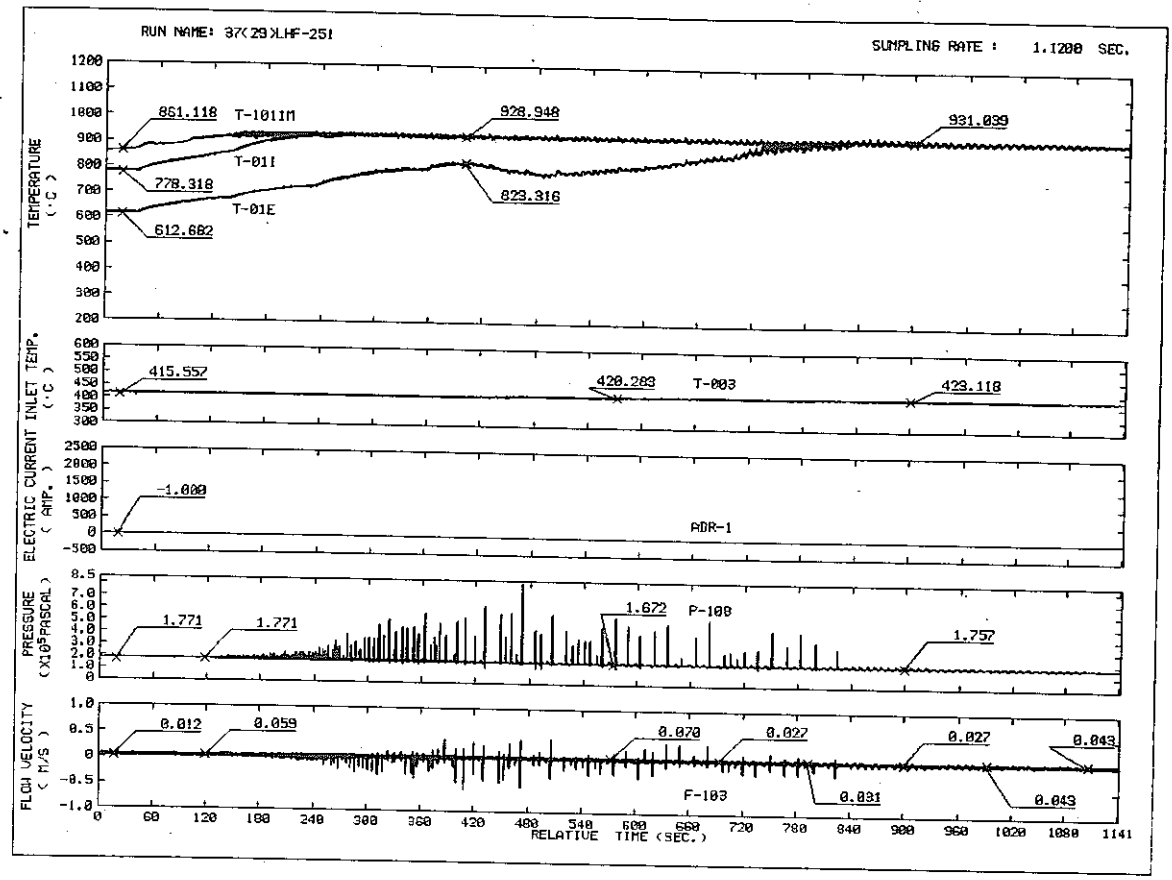
RUN NAME: 37(29)LHF-251
SUMPLING RATE : 1.1200 SEC.
TEMPERATURE (°C)
851.118
T-101M
928.948
931.039
T-011
778.318
823.316
T-01E
612.682
ELECTRIC CURRENT INLET TEMP. (°C)
415.552
420.283
T-003
423.118
ELECTRIC CURRENT (AMP.)
-1.000
ADR-1
PRESSURE (X10⁵PASCAL)
1.771
1.771
1.672
P-100
1.757
FLOW VELOCITY (M/S)
0.012
0.059
0.070
0.027
0.027
0.043
F-103
0.031
0.043
RELATIVE TIME (SEC.)

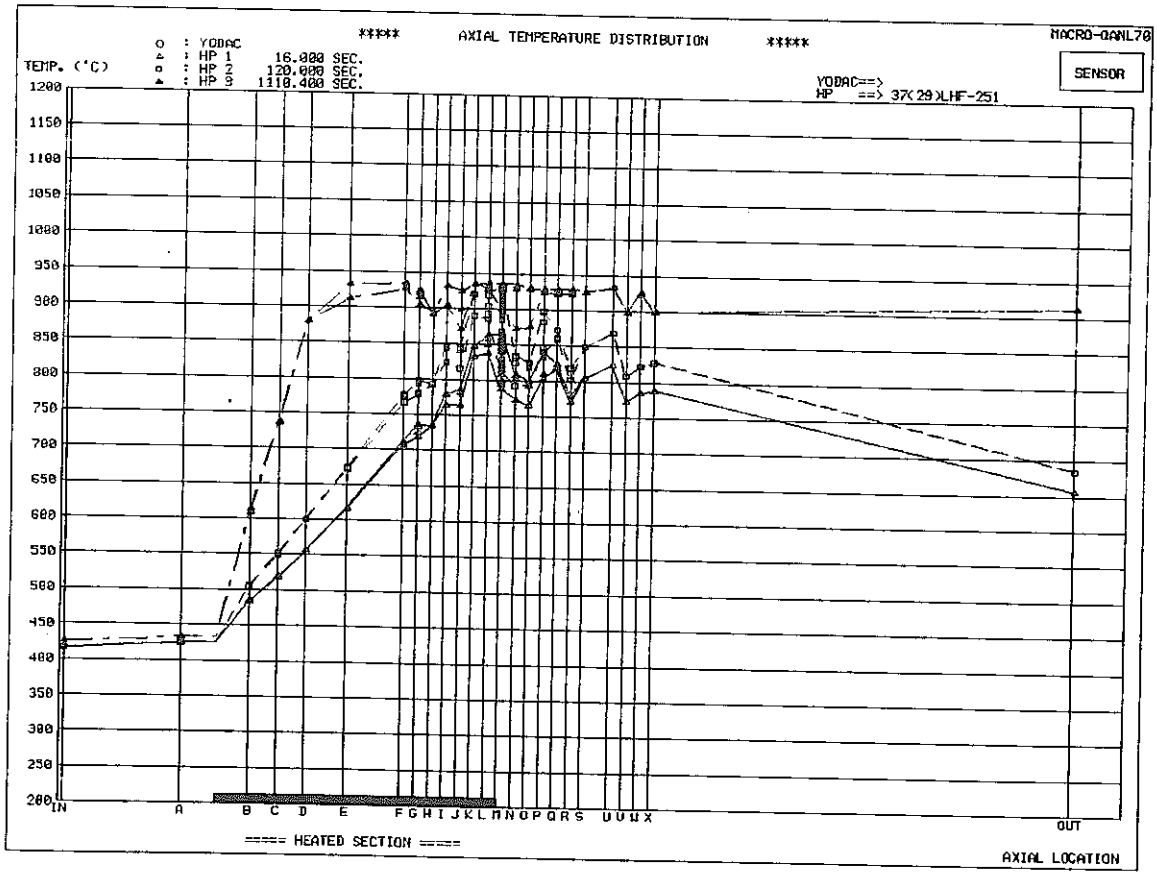
***** AXIAL TEMPERATURE DISTRIBUTION *****
MACRO-GANL70
SENSOR
o : YODAC
Δ : HP 1 16.000 SEC.
□ : HP 2 120.000 SEC.
▲ : HP 3 1110.400 SEC.
TEMP. (°C)
YODAC==>
HP ==> 37(29)LHF-251
IN
A
B C D E
F G H I J K L M N O P Q R S
U V W X
OUT
==== HEATED SECTION ====
AXIAL LOCATION

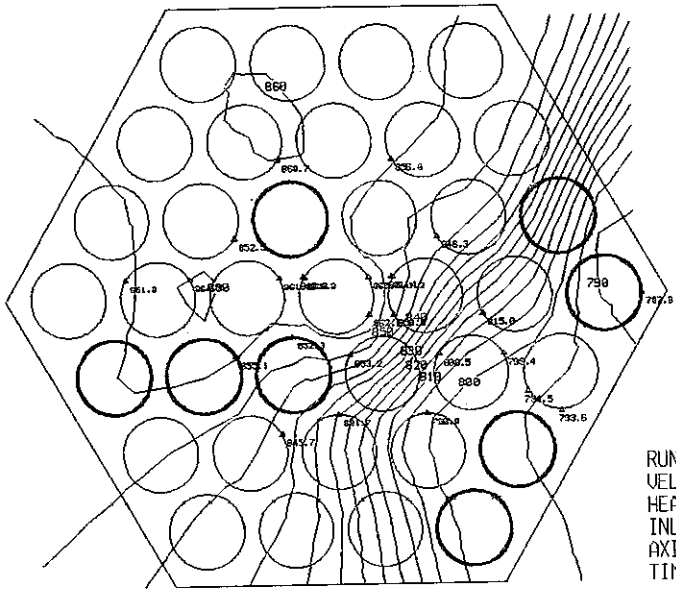

RUN NAME 37(29)LHF-251
VELOCITY 0.039 M/S
HEAT FLUX 4.50 W/CM2
INLET TEMP. 417.4 C
AXIAL 0.0 MM
TIME 16.000 SEC.

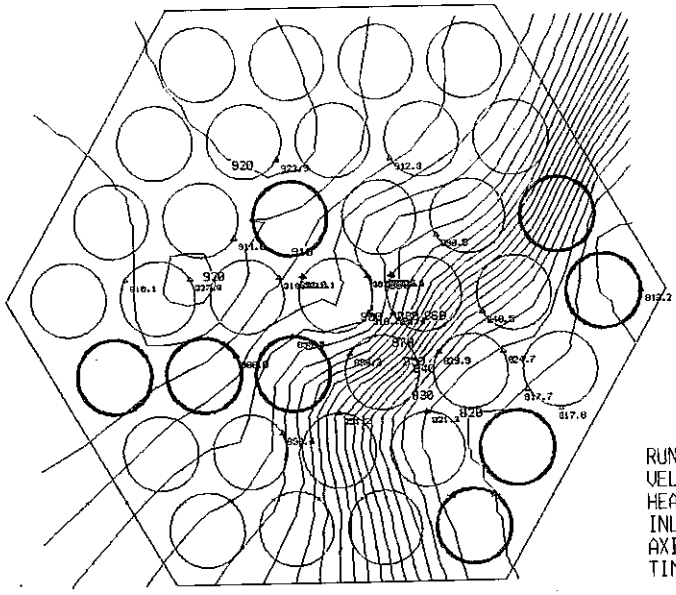

RUN NAME 37(29)LHF-251
VELOCITY 0.035 M/S
HEAT FLUX 6.38 W/CM2
INLET TEMP. 416.5 C
AXIAL 0.0 MM
TIME 120.000 SEC.

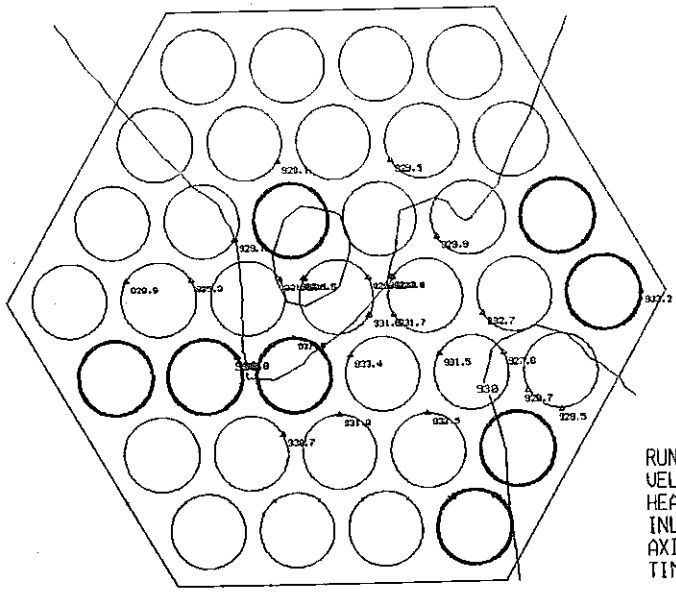

RUN NAME 37(29)LHF-251
VELOCITY 0.039 M/S
HEAT FLUX 12.22 W/CM2
INLET TEMP. 424.1 C
AXIAL 0.0 MM
TIME 1110.400 SEC.

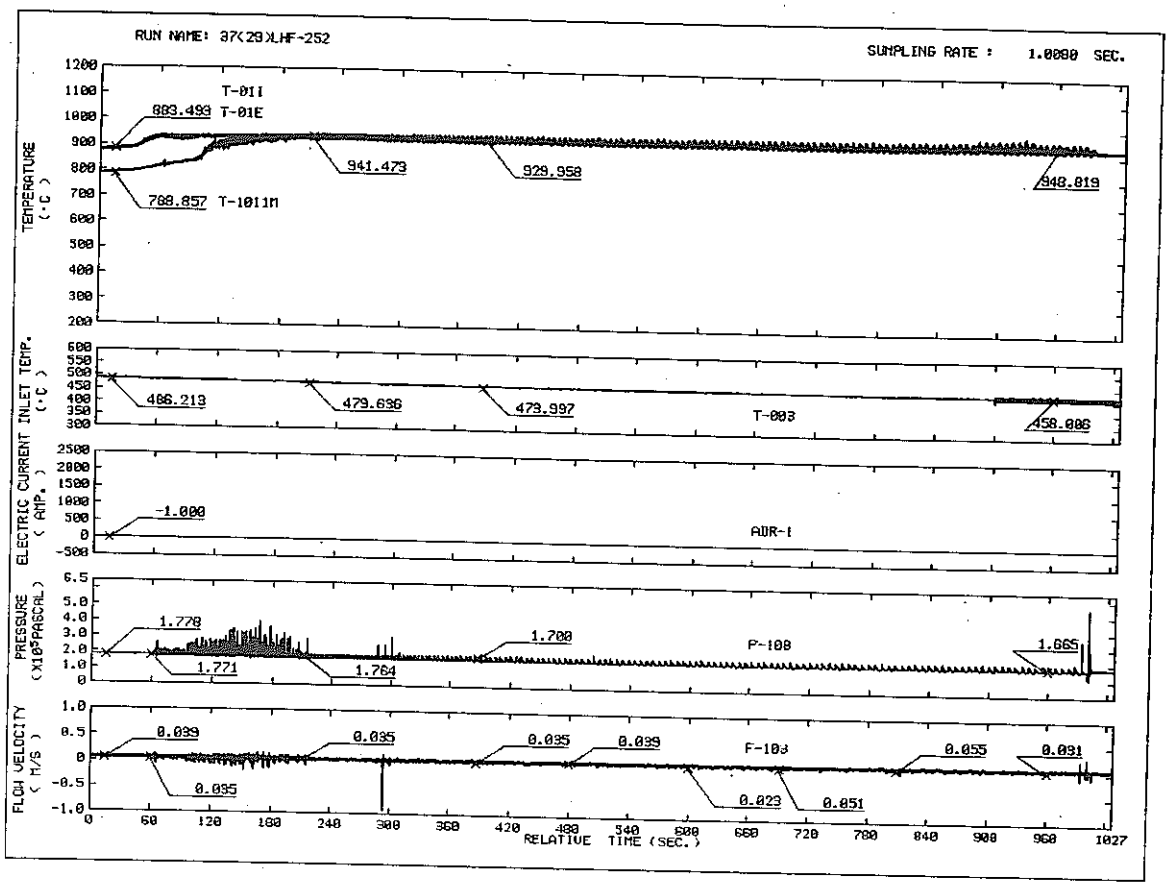
RUN NAME: 37(29)LHF-252
SUMPLING RATE : 1.0000 SEC.
TEMPERATURE (°C)
T-011
883.499 T-01E
941.473
929.958
948.819
788.857 T-1011M
INLET TEMP. (°C)
486.213
479.696
473.997
T-003
458.006
ELECTRIC CURRENT (AMP.)
-1.000
ADR-1
PRESSURE (X10⁵PASCAL)
1.778
1.700
P-108
1.865
1.771
1.764
FLOW VELOCITY (M/S)
0.039
0.035
0.035
0.039
F-103
0.055
0.031
0.095
0.023
0.051
RELATIVE TIME (SEC.)

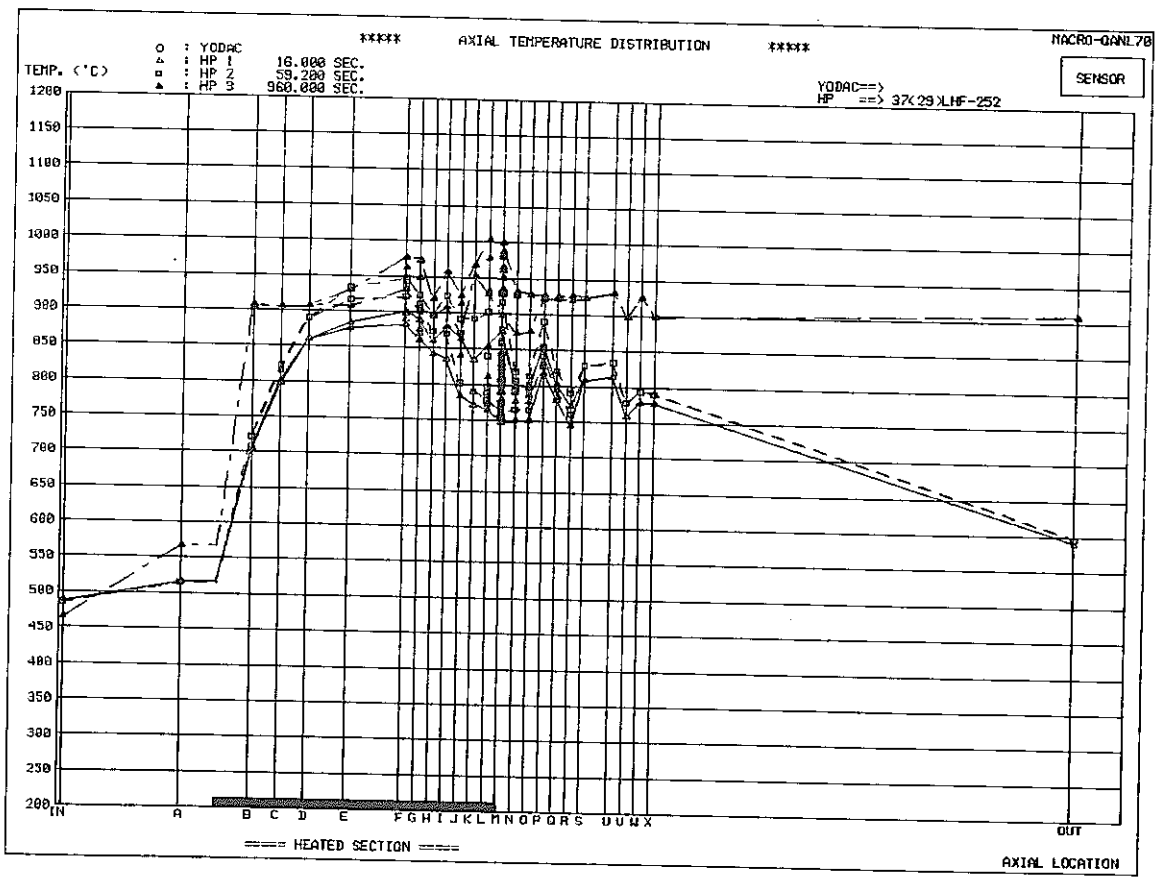
***** AXIAL TEMPERATURE DISTRIBUTION *****
MACRO-QANL78
SENSOR
○ : YODAC
△ : HP 1 16.000 SEC.
□ : HP 2 59.200 SEC.
▲ : HP 3 960.000 SEC.
YODAC==>
HP ==> 37(29)LHF-252
TEMP. (°C)
IN
A B C D E F G H I J K L M N O P Q R S U U W X
OUT
==== HEATED SECTION ====
AXIAL LOCATION

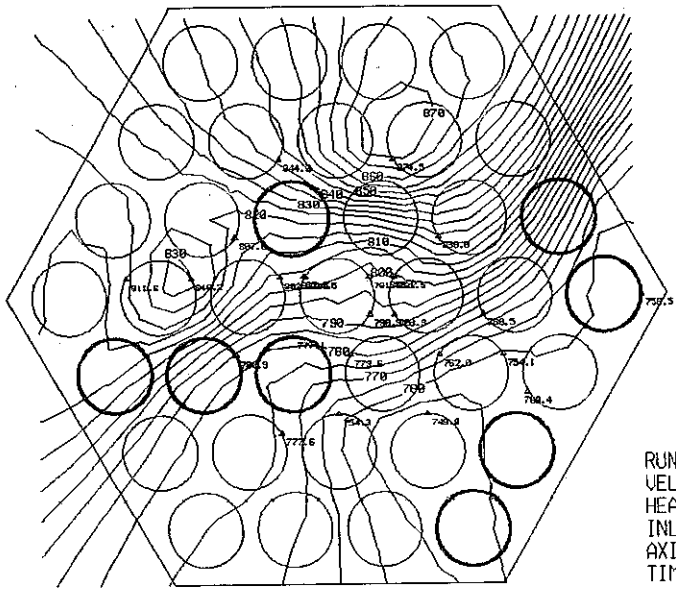

RUN NAME 37(29)LHF-252
VELOCITY 0.055 M/S
HEAT FLUX 2.82 W/CM2
INLET TEMP. 488.1 C
AXIAL 0.0 MM
TIME 16.000 SEC.

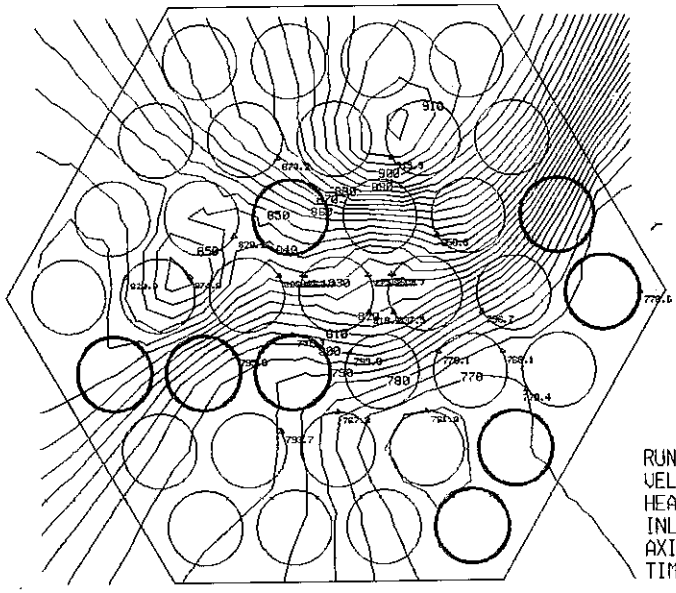

RUN NAME 37(29)LHF-252
VELOCITY 0.063 M/S
HEAT FLUX 4.82 W/CM2
INLET TEMP. 486.2 C
AXIAL 0.0 MM
TIME 59.200 SEC.

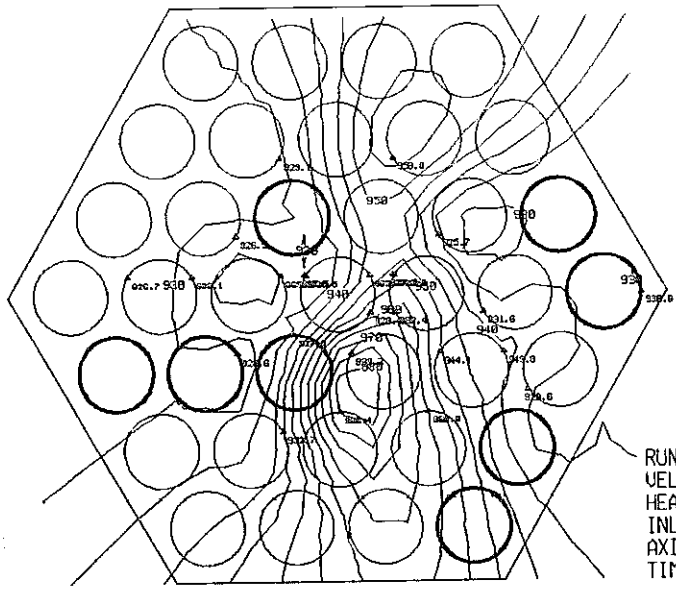

RUN NAME 37(29)LHF-252
VELOCITY 0.070 M/S
HEAT FLUX 12.42 W/CM2
INLET TEMP. 460.8 C
AXIAL 0.0 MM
TIME 960.000 SEC.

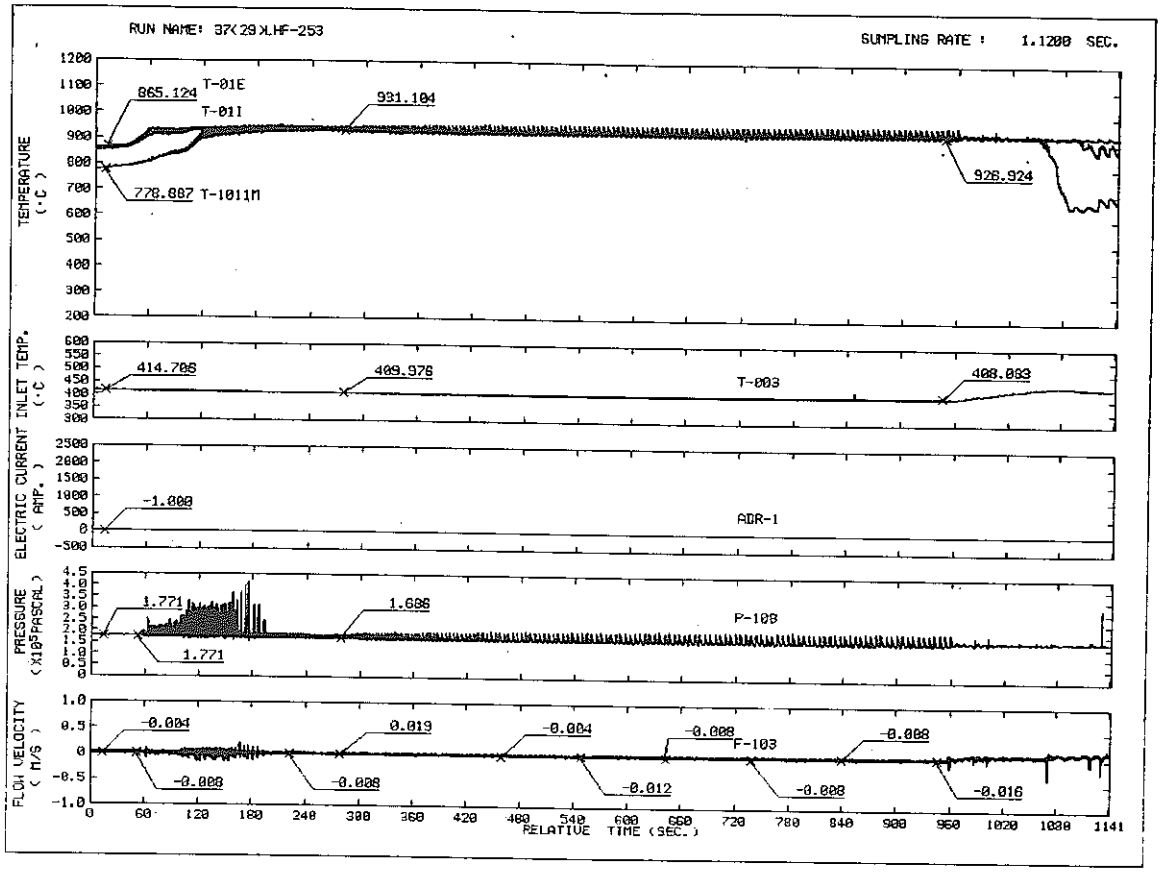
RUN NAME: 37(29)LHF-253
SAMPLING RATE : 1.1200 SEC.
TEMPERATURE (°C)
865.124 T-01E
T-011
931.104
926.924
778.887 T-1011M
ELECTRIC CURRENT INLET TEMP. (°C)
414.708
409.976
T-003
408.083
(AMP.)
-1.000
ADR-1
PRESSURE (X10⁵PASCAL)
1.771
1.686
P-108
1.771
FLOW VELOCITY (M/S)
-0.004
0.019
-0.004
-0.008
F-103
-0.008
-0.008
-0.008
-0.012
-0.008
-0.016
RELATIVE TIME (SEC.)

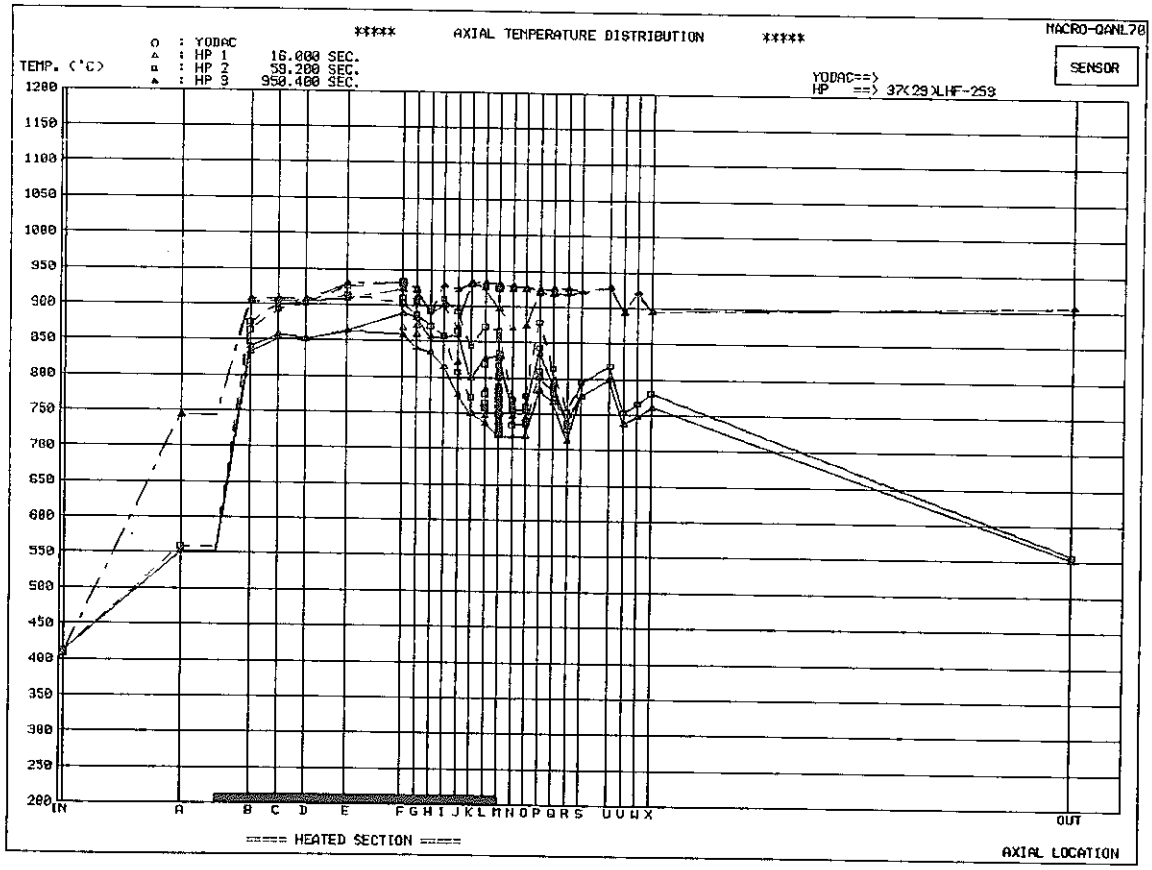
***** AXIAL TEMPERATURE DISTRIBUTION *****
MACRO-QANL70
SENSOR
O : YODAC
Δ : HP 1 16.000 SEC.
□ : HP 2 58.200 SEC.
▲ : HP 3 950.400 SEC.
YODAC==>
HP ==> 37(29)LHF-253
TEMP. (°C)
IN
OUT
==== HEATED SECTION ====
AXIAL LOCATION

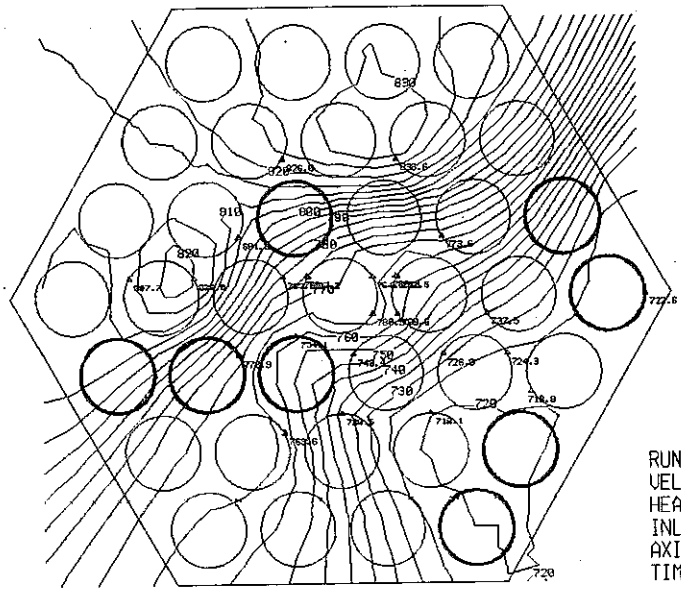

RUN NAME 37(29)LHF-253
VELOCITY 0.004 M/S
HEAT FLUX 3.00 W/CM2
INLET TEMP. 412.8 C
AXIAL 0.0 MM
TIME 16.000 SEC.

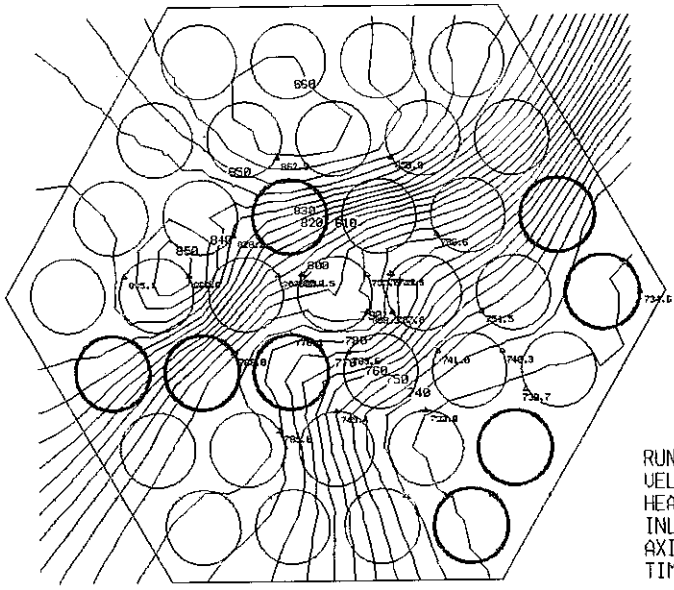

RUN NAME 37(29)LHF-253
VELOCITY 0.012 M/S
HEAT FLUX 5.45 W/CM2
INLET TEMP. 413.8 C
AXIAL 0.0 MM
TIME 59.200 SEC.

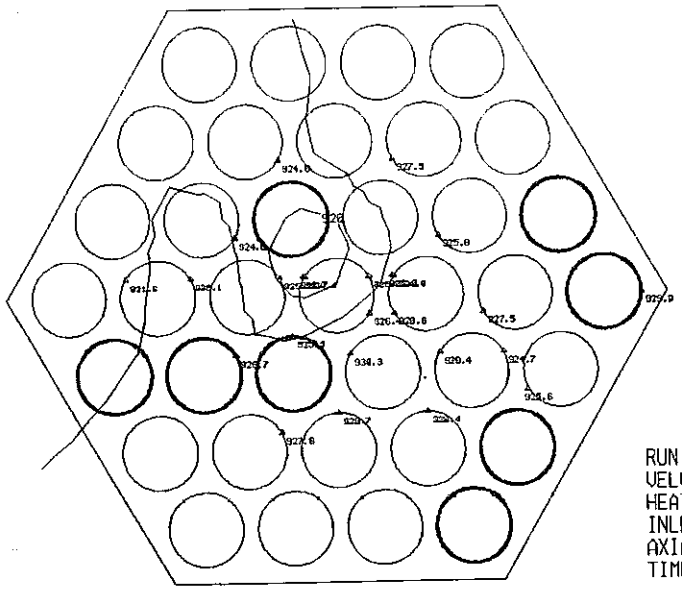

RUN NAME 37(29)LHF-253
VELOCITY 0.004 M/S
HEAT FLUX 12.43 W/CM2
INLET TEMP. 407.1 C
AXIAL 0.0 MM
TIME 950.400 SEC.

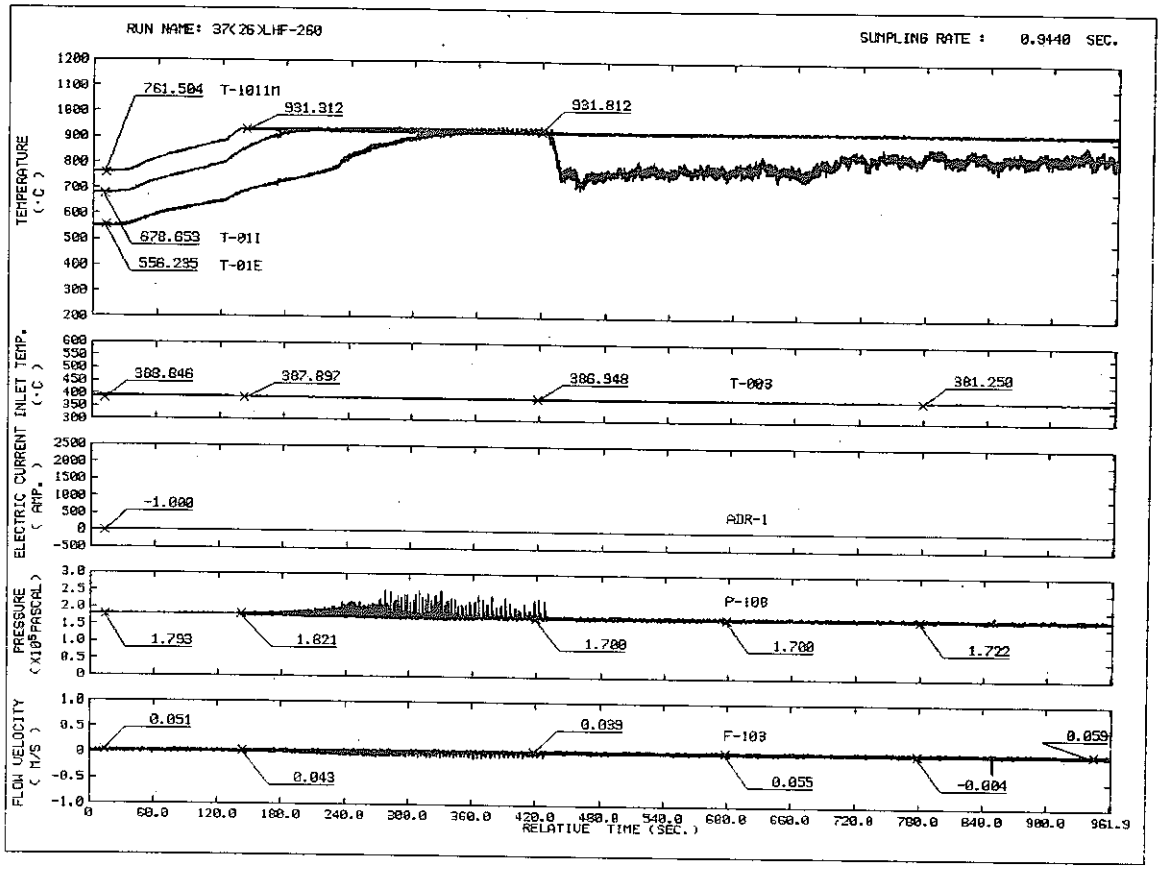
RUN NAME: 37(26)LHF-260
SUMPLING RATE : 0.9440 SEC.
TEMPERATURE (°C)
761.504 T-1011M
931.312
931.812
878.659 T-01I
556.295 T-01E
INLET TEMP. (°C)
388.846
387.897
386.948
T-003
381.250
ELECTRIC CURRENT (AMP.)
-1.000
ADR-1
PRESSURE (X10⁵PASCAL)
P-108
1.793
1.821
1.700
1.700
1.722
FLOW VELOCITY (M/S)
0.051
0.039
F-103
0.059
0.043
0.055
-0.004
RELATIVE TIME (SEC.)

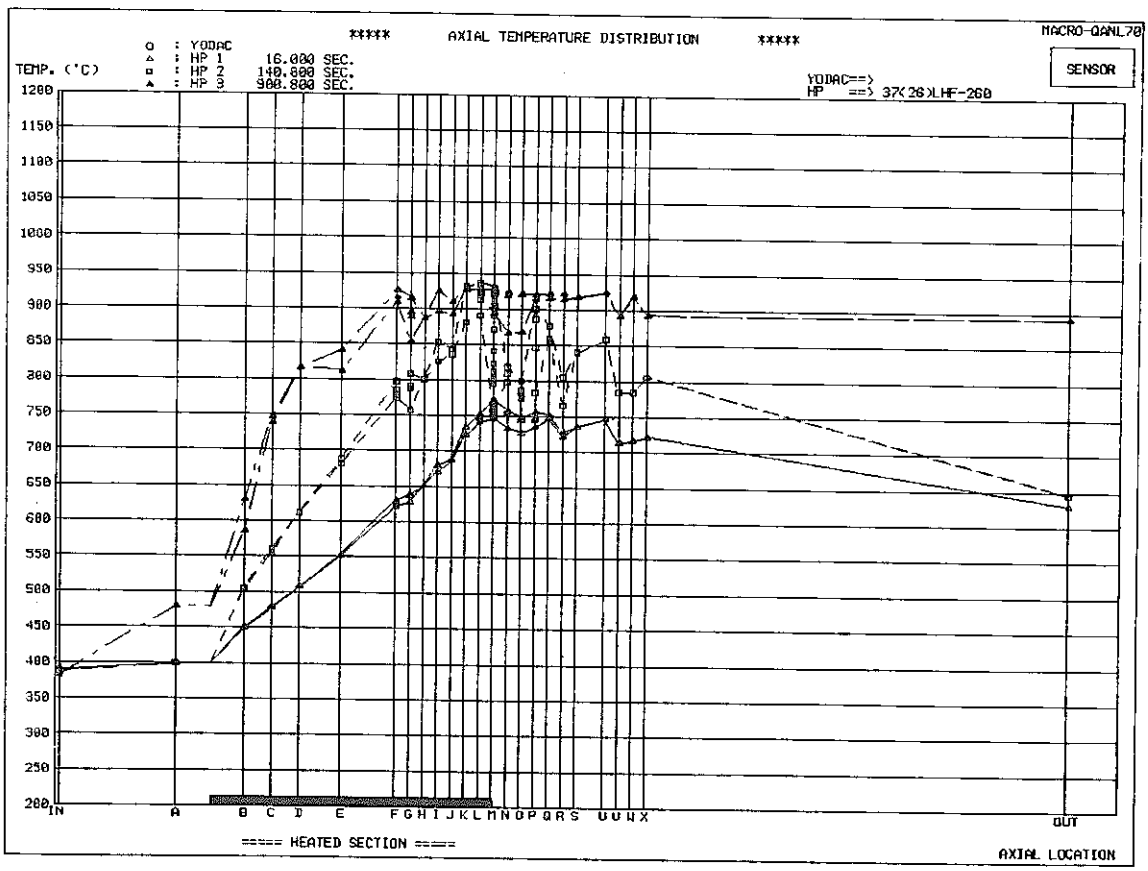
MACRO-QANL70
SENSOR
***** AXIAL TEMPERATURE DISTRIBUTION *****
○ : YODAC
△ : HP 1 16.000 SEC.
□ : HP 2 140.800 SEC.
▲ : HP 3 908.800 SEC.
TEMP. (°C)
YODAC==>
HP ==> 37(26)LHF-260
IN A B C D E F G H I J K L M N O P Q R S U U W X OUT
===== HEATED SECTION =====
AXIAL LOCATION

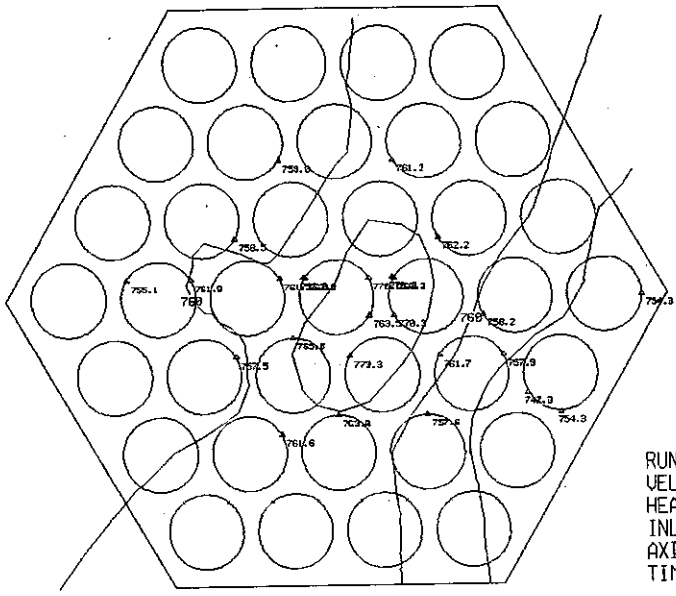

RUN NAME 37(26)LHF-260
VELOCITY 0.023 M/S
HEAT FLUX 4.44 W/CM2
INLET TEMP. 391.7 C
AXIAL 0.0 MM
TIME 16.000 SEC.

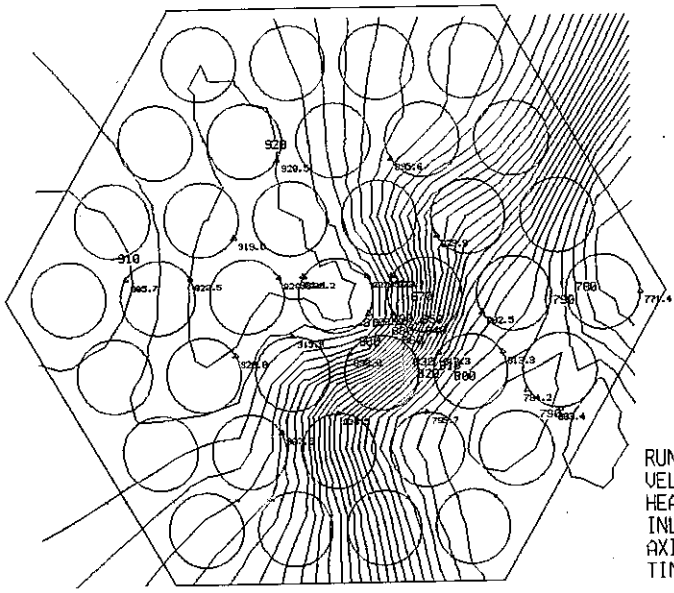

RUN NAME 37(26)LHF-260
VELOCITY 0.023 M/S
HEAT FLUX 11.21 W/CM2
INLET TEMP. 387.9 C
AXIAL 0.0 MM
TIME 140.800 SEC.

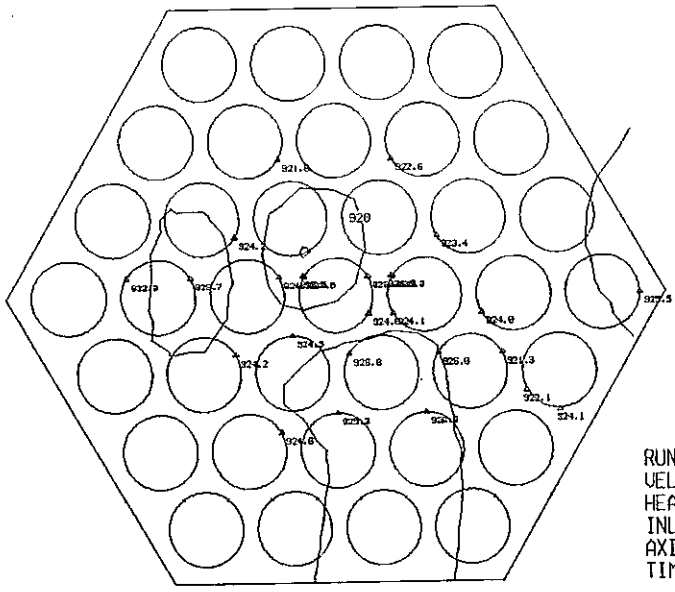

RUN NAME 37(26)LHF-260
VELOCITY 0.035 M/S
HEAT FLUX 16.48 W/CM2
INLET TEMP. 383.1 C
AXIAL 0.0 MM
TIME 900.800 SEC.

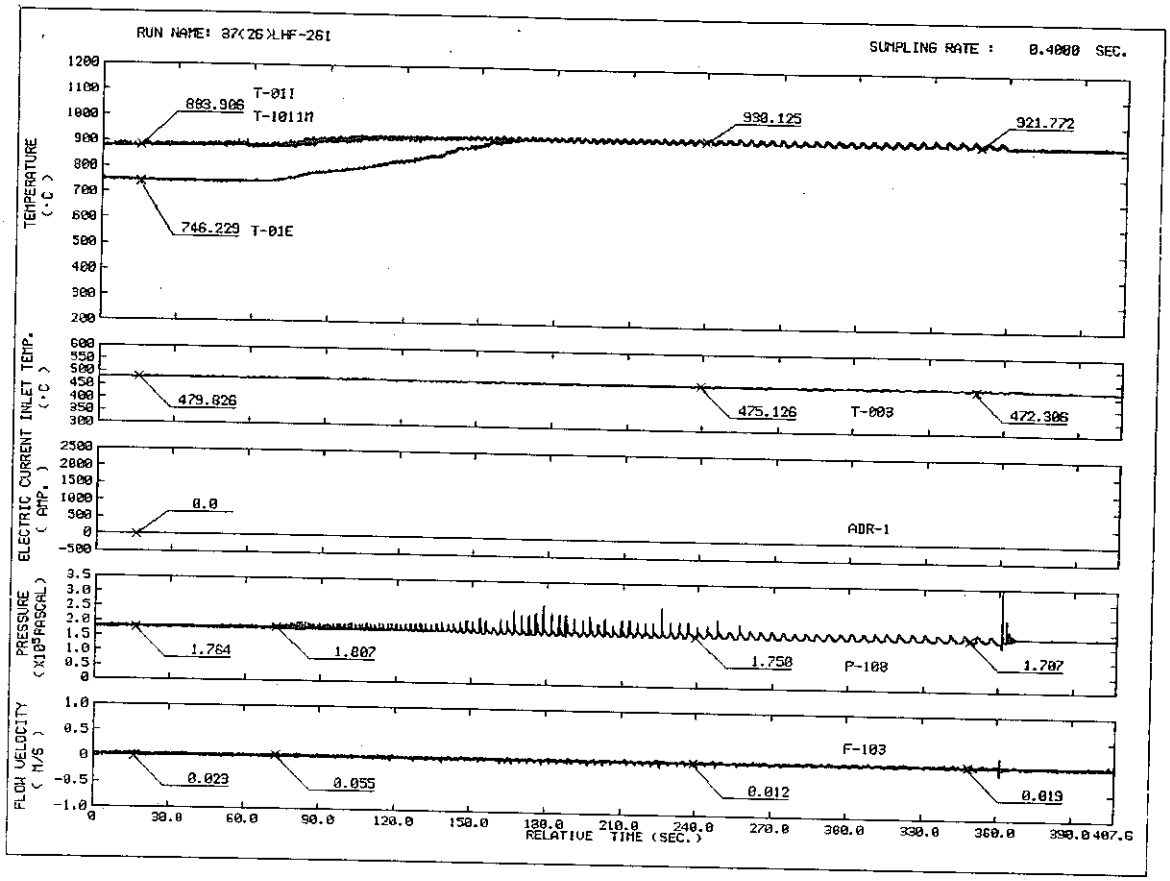
RUN NAME: 37(26)LHF-261
SUMPLING RATE : 0.4000 SEC.
TEMPERATURE (°C)
883.906 T-011
T-1011M
930.125
921.772
746.229 T-01E
ELECTRIC CURRENT INLET TEMP. (°C)
479.826
475.126 T-003
472.306
(AMP.)
0.0
ADR-1
PRESSURE (X10⁵PASCAL)
1.764
1.807
1.750 P-108
1.707
FLOW VELOCITY (M/S)
F-103
0.023
0.055
0.012
0.019
RELATIVE TIME (SEC.)

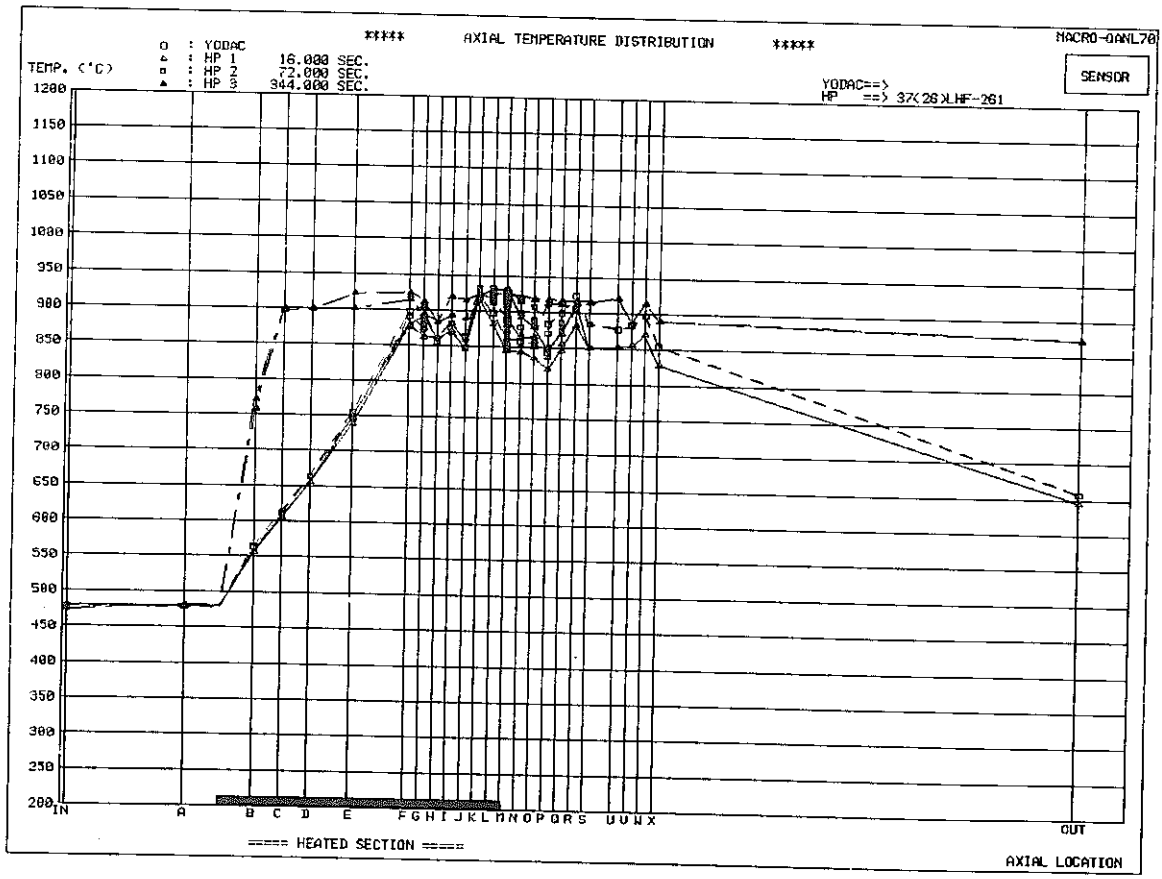
O : YODAC
Δ : HP 1 16.000 SEC.
□ : HP 2 72.000 SEC.
▲ : HP 3 344.000 SEC.
***** AXIAL TEMPERATURE DISTRIBUTION *****
MACRO-GANL70
SENSOR
TEMP. (°C)
YODAC==>
HP ==> 37(26)LHF-261
IN
OUT
===== HEATED SECTION =====
AXIAL LOCATION

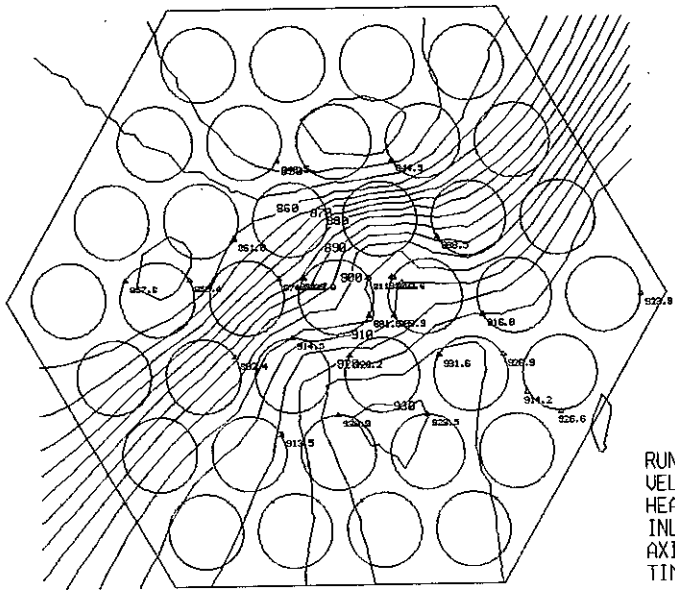

RUN NAME 37(26)LHF-261
VELOCITY 0.035 M/S
HEAT FLUX 3.80 W/CM2
INLET TEMP. 478.9 C
AXIAL 0.0 MM
TIME 16.000 SEC.

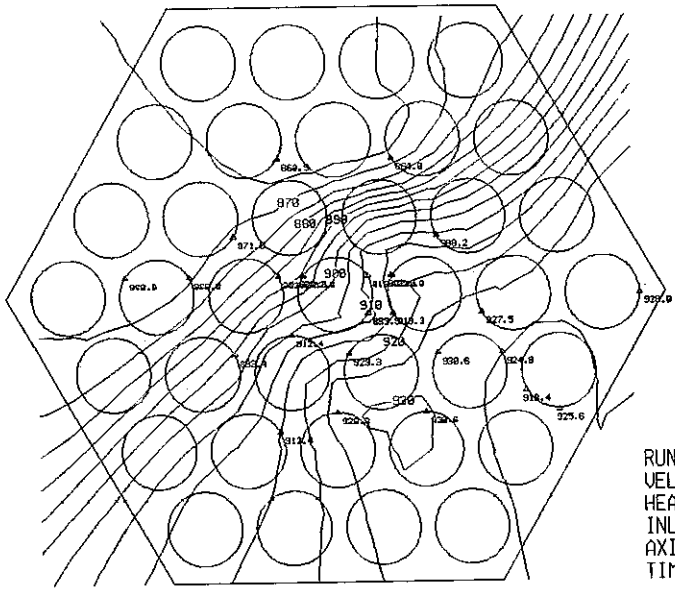

RUN NAME 37(26)LHF-261
VELOCITY 0.019 M/S
HEAT FLUX 7.63 W/CM2
INLET TEMP. 478.9 C
AXIAL 0.0 MM
TIME 72.000 SEC.

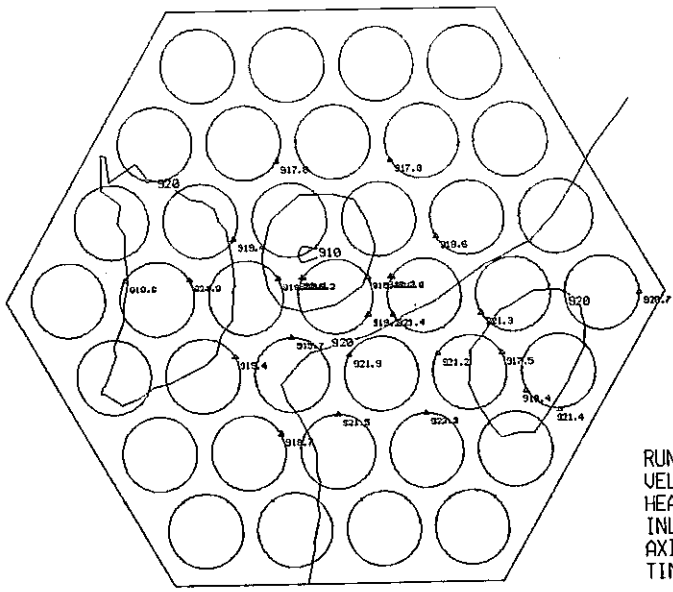

RUN NAME 37(26)LHF-261
VELOCITY -0.008 M/S
HEAT FLUX 15.68 W/CM2
INLET TEMP. 475.1 C
AXIAL 0.0 MM
TIME 344.000 SEC.

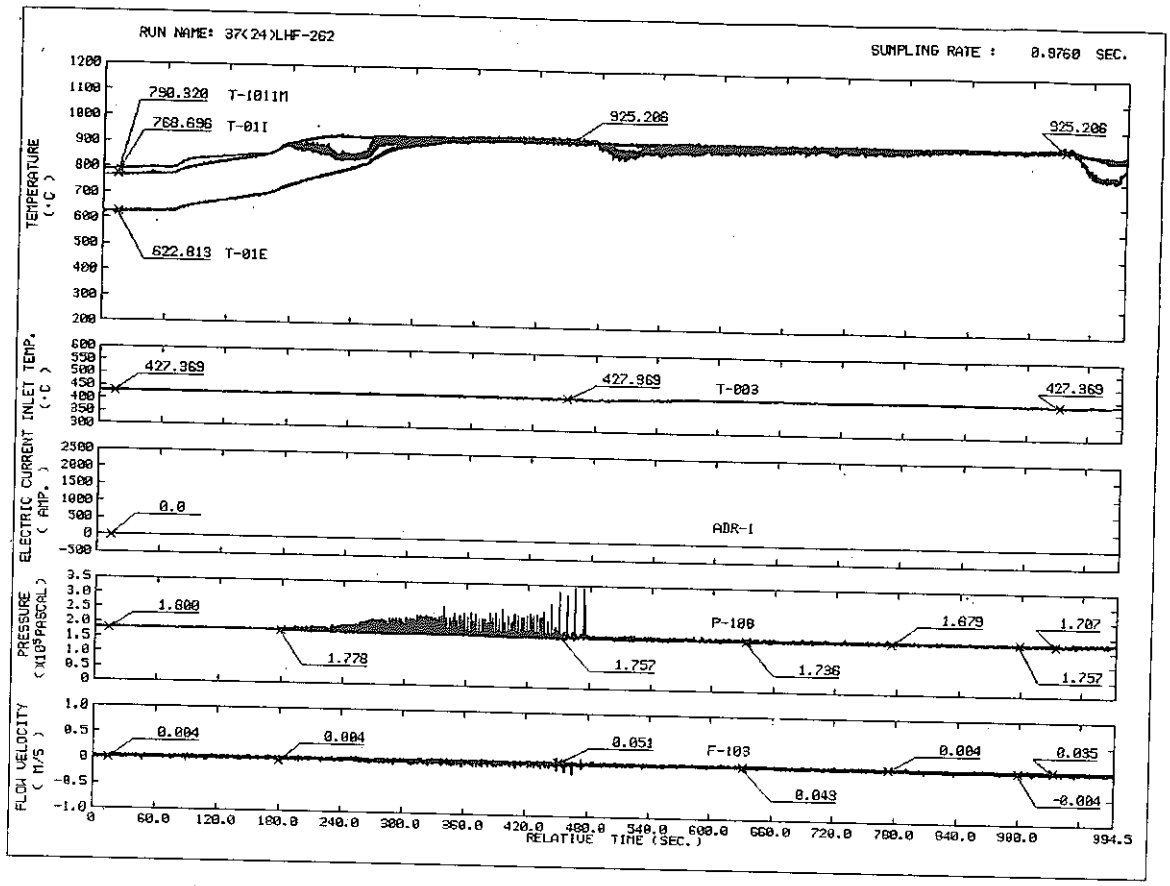
RUN NAME: 37(24)LHF-262
SAMPLING RATE : 0.9760 SEC.
TEMPERATURE ('C)
790.320 T-101M
768.696 T-01I
925.206
622.813 T-01E
ELECTRIC CURRENT INLET TEMP. ('C)
427.969
T-003
ELECTRIC CURRENT (AMP.)
0.0
ADR-I
PRESSURE (X10³PASCAL)
1.800
1.778
1.757
P-108
1.679
1.736
1.707
FLOW VELOCITY (M/S)
0.004
0.051
F-103
0.043
0.035
-0.004
RELATIVE TIME (SEC.)

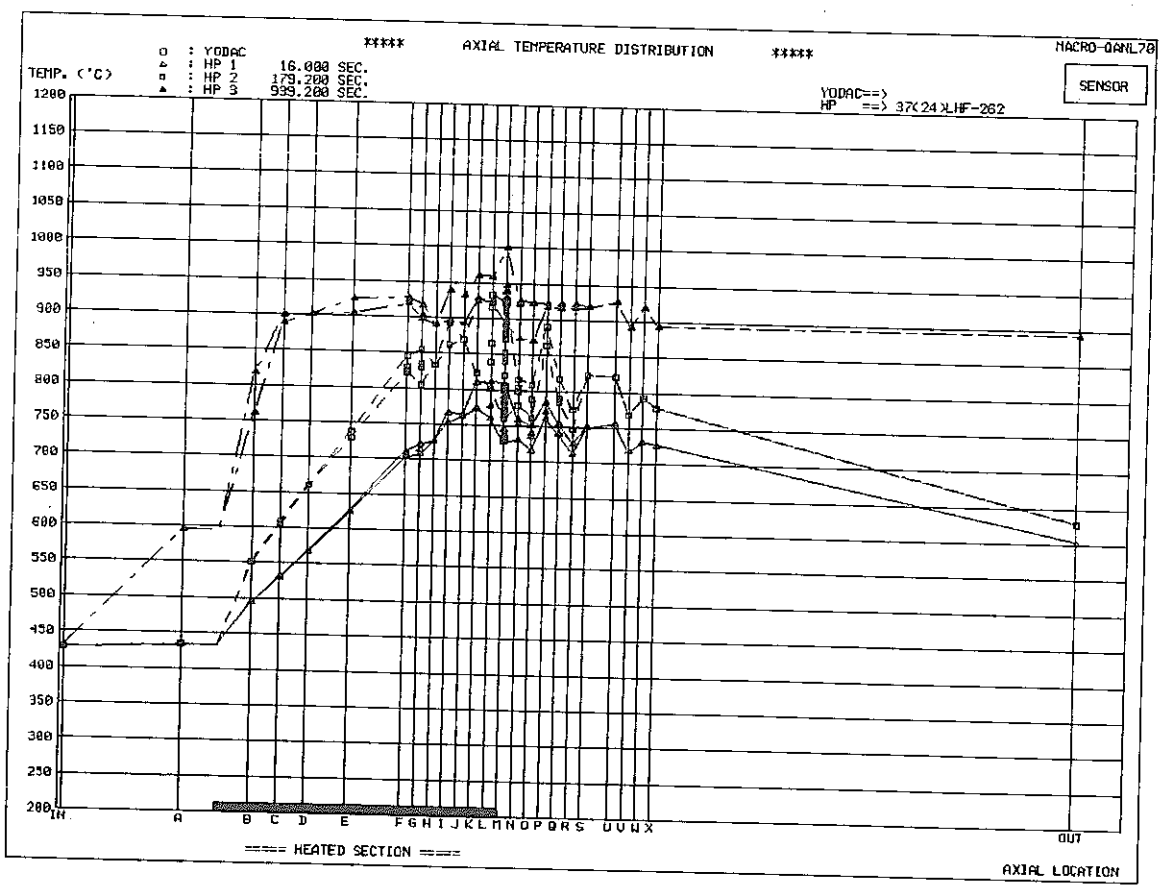
AXIAL TEMPERATURE DISTRIBUTION
MACRO-GANL70
SENSOR
TEMP. ('C)
: YODAC
: HP 1 16.000 SEC.
: HP 2 179.200 SEC.
: HP 3 939.200 SEC.
YODAC==>
HP ==> 37(24)LHF-262
IN
OUT
==== HEATED SECTION ====
AXIAL LOCATION

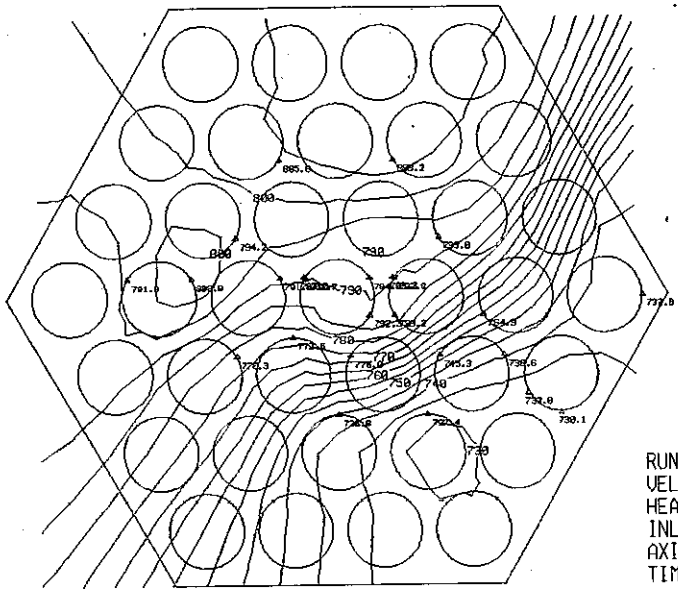

RUN NAME 37(24)LHF-262
VELOCITY 0.031 M/S
HEAT FLUX 3.49 W/CM2
INLET TEMP. 430.2 C
AXIAL 0.0 MM
TIME 16.000 SEC.

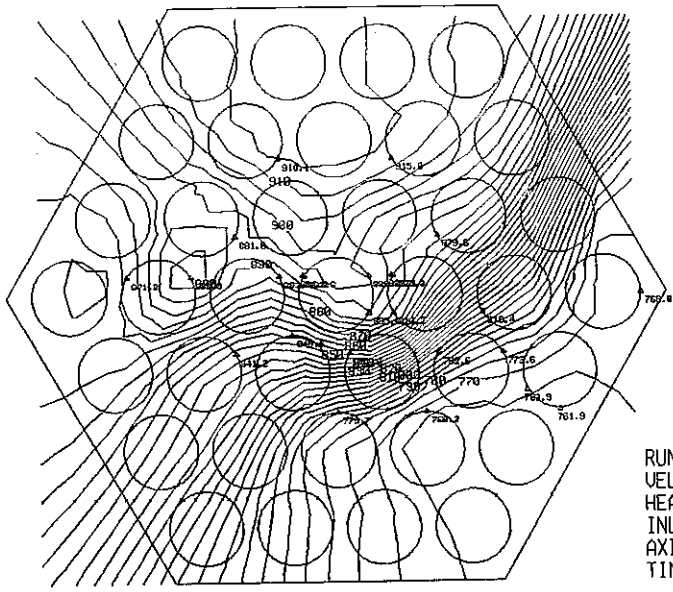

RUN NAME 37(24)LHF-262
VELOCITY 0.004 M/S
HEAT FLUX 8.59 W/CM2
INLET TEMP. 427.4 C
AXIAL 0.0 MM
TIME 179.200 SEC.

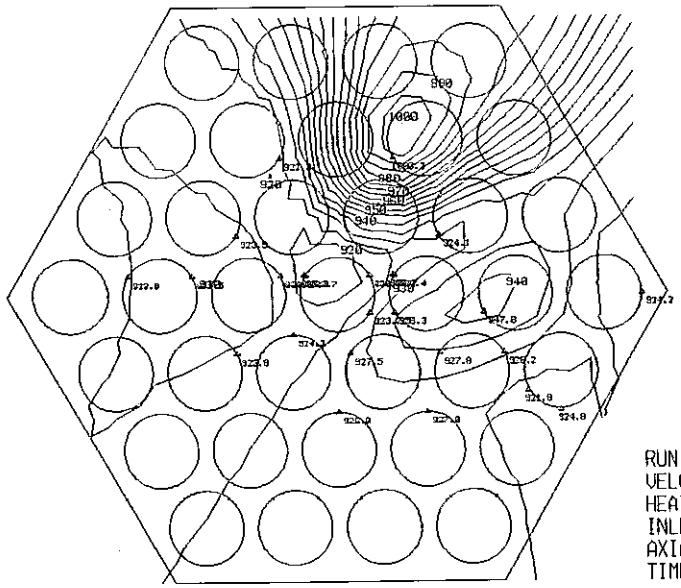

RUN NAME 37(24)LHF-262
VELOCITY 0.016 M/S
HEAT FLUX 12.66 W/CM2
INLET TEMP. 431.1 C
AXIAL 0.0 MM
TIME 939.200 SEC.

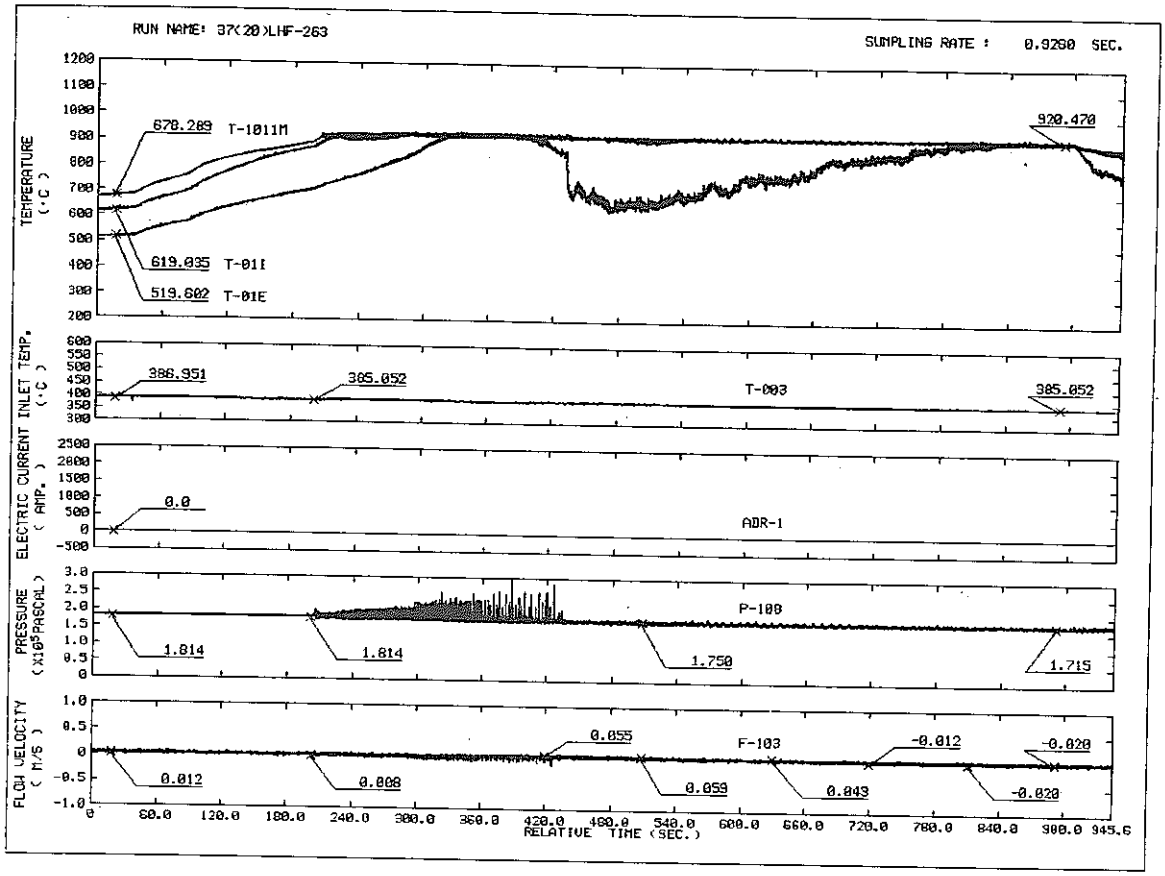
RUN NAME: 37(20)LHF-263
SAMPLING RATE : 0.9290 SEC.
TEMPERATURE (°C)
670.289 T-1011M
920.470
619.035 T-011
519.602 T-01E
ELECTRIC CURRENT INLET TEMP. (°C)
386.951
385.052
T-003
385.052
(AMP.)
0.0
ADR-1
PRESSURE (X10⁵PASCAL)
P-100
1.814
1.814
1.750
1.715
FLOW VELOCITY (M/S)
0.055
F-103
-0.012
-0.020
0.012
0.008
0.059
0.043
-0.020
RELATIVE TIME (SEC.)

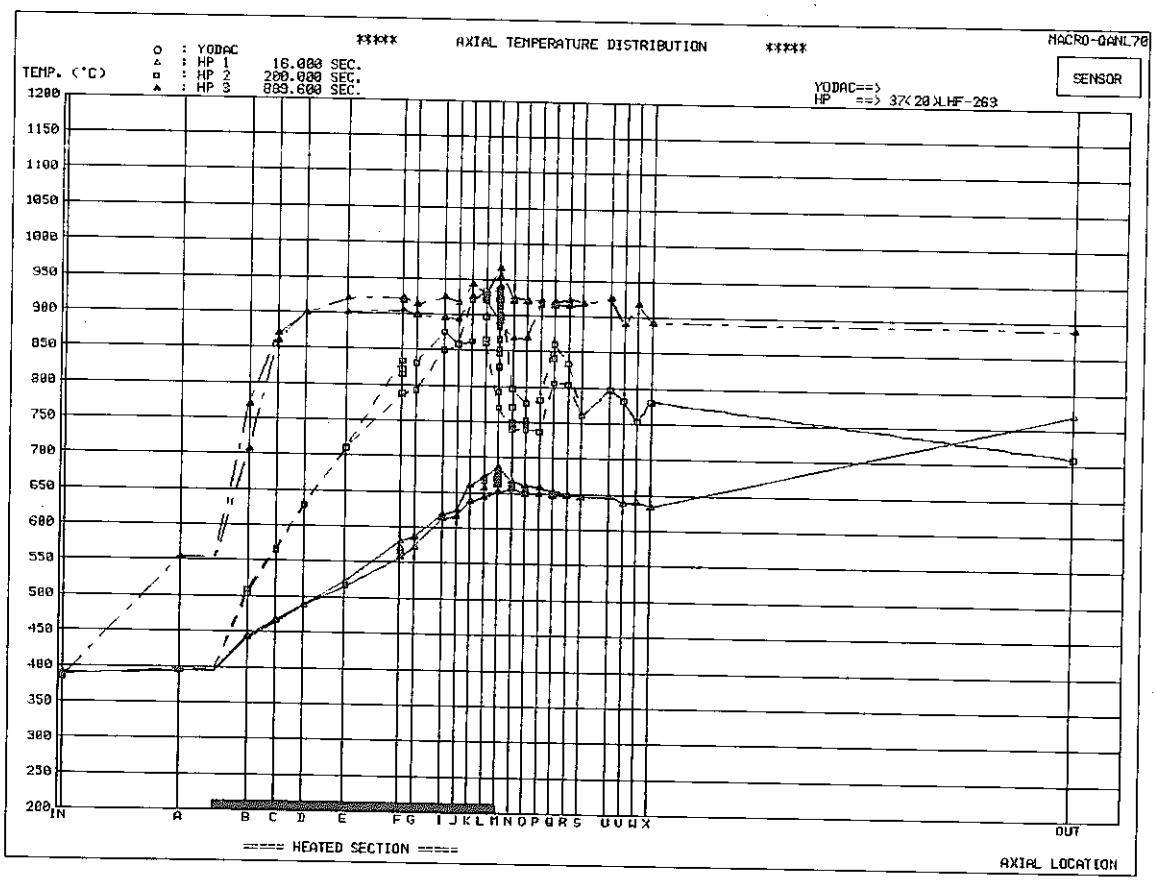
O : YODAC
Δ : HP 1 16.000 SEC.
□ : HP 2 200.000 SEC.
▲ : HP 3 889.600 SEC.
***** AXIAL TEMPERATURE DISTRIBUTION *****
MACRO-GANL70
SENSOR
TEMP. (°C)
YODAC==>
HP ==> 37(20)LHF-263
IN
A B C D E FG I J K L M N O P Q R S U U W X
OUT
==== HEATED SECTION ====
AXIAL LOCATION

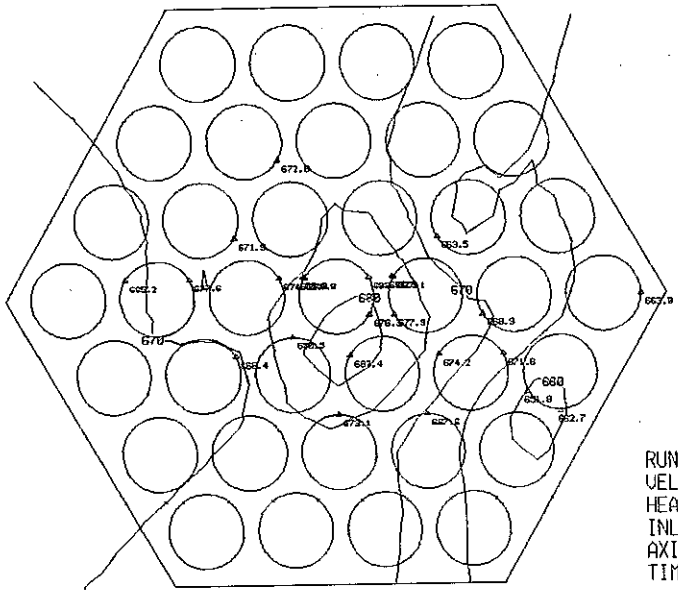

RUN NAME 37(20)LHF-263
VELOCITY 0.027 M/S
HEAT-FLUX 5.00 W/CM2
INLET TEMP. 388.8 C
AXIAL 0.0 MM
TIME 16.000 SEC.

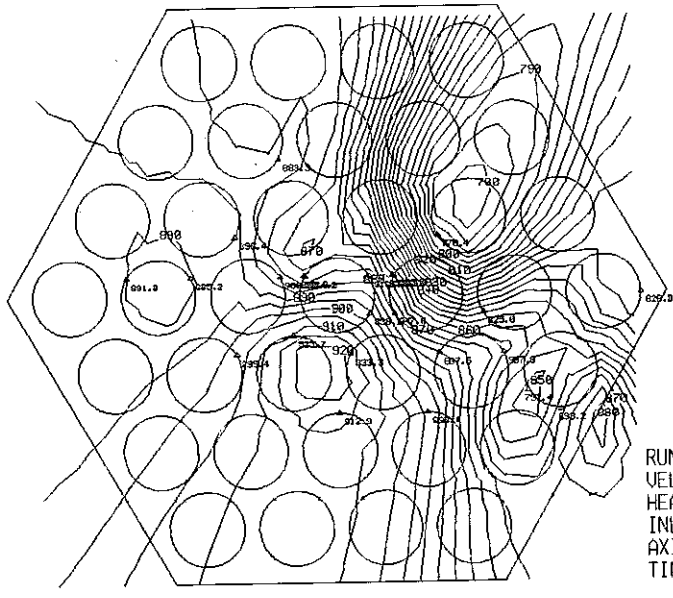

RUN NAME 37(20)LHF-263
VELOCITY 0.027 M/S
HEAT FLUX 13.57 W/CM2
INLET TEMP. 387.9 C
AXIAL 0.0 MM
TIME 200.000 SEC.

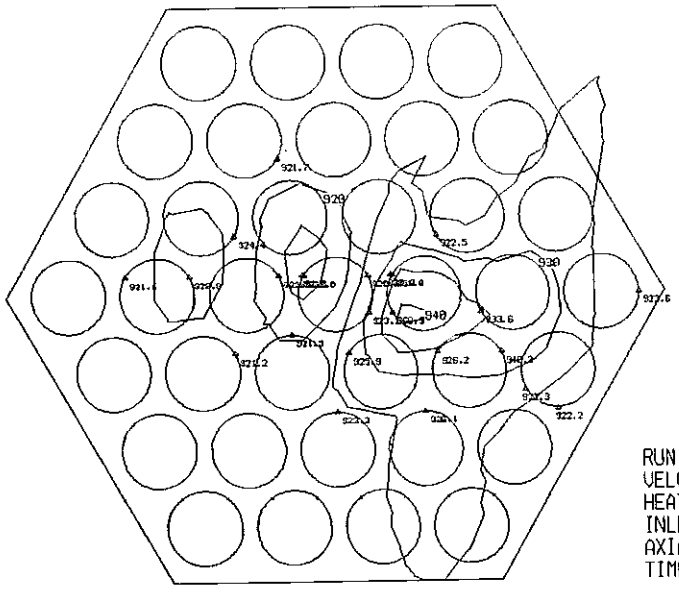

RUN NAME 37(20)LHF-263
VELOCITY 0.019 M/S
HEAT FLUX 15.52 W/CM2
INLET TEMP. 384.1 C
AXIAL 0.0 MM
TIME 889.600 SEC.